



GRID 2014

UNIVERSITY OF NOVI SAD
FACULTY OF TECHNICAL SCIENCES
DEPARTMENT OF GRAPHIC ENGINEERING AND DESIGN

7TH INTERNATIONAL SYMPOSIUM ON
GRAPHIC ENGINEERING AND DESIGN

PROCEEDINGS

November 13-14, 2014
Novi Sad, Serbia



University of Novi Sad
Faculty of Technical Sciences

DEPARTMENT OF GRAPHIC
ENGINEERING AND DESIGN



7TH INTERNATIONAL SYMPOSIUM ON
GRAPHIC ENGINEERING AND DESIGN

<http://www.grid.uns.ac.rs/symposium/enpocetna.html>

Proceedings – The Seventh International Symposium GRID 2014

PUBLISHER:

FACULTY OF TECHNICAL SCIENCES
DEPARTMENT OF GRAPHIC ENGINEERING AND DESIGN
21 000 Novi Sad, Trg Dositeja Obradovića 6

EDITORIAL COMMITTEE:

PhD Dragoljub Novaković
PhD Igor Karlović
PhD Sandra Dedijer

TECHNICAL SECRETARY:

MSc Ivana Jurič

EDITOR:

PhD Dragoljub Novaković

LAYOUT AND PRODUCTION:

GRID team

PRINT:

Grafički centar GRID, Trg Dositeja Obradovića 6, Novi Sad

CIRCULATION:

300 copies

CIP - Каталогизacija у публикацији
Библиотека Матице српске, Нови Сад

655 (082)
7.05 : 655 (082)

INTERNATIONAL Symposium on Graphic Engineering and Design GRID (7 ; 2014 ; Novi Sad)

Proceedings [Elektronski izvor] / 7th International Symposium on Graphic Engineering and Design GRID 2014, November 13-14, 2014, Novi Sad ; [organizer] Faculty of Technical Sciences, Department of Graphic Engineering and Design ; [co-organizers Faculty of Graphic Arts, Zagreb and Óbuda University, Institute of Media Technology, Budapest ; editor Dragoljub Novaković]. - Novi Sad : Faculty of Technical Sciences, Department of Graphic Engineering and Design, 2014

Način pristupa (URL): <http://www.grid.uns.ac.rs/symposium/zbornici.html> - Nasl. sa naslovnog ekrana. - Opis zasnovan na stanju na dan: 21.11.2014.
- Bibliografija uz svaki rad.

ISBN 978-86-7892-647-1

a) Графичка индустрија - Зборници b) Графички дизајн - Зборници
COBISS.SR - ID 291408135

SCIENTIFIC COMMITTEE

President Prof.PhD Dragoljub Novaković, Faculty of Technical Sciences, Novi Sad (SRB)
Prof.PhD Wolfgang Faigle, HDM, Stuttgart (GER)
Prof.PhD Thomas Hoffman-Walbeck, HDM, Stuttgart (GER)
Prof.PhD Malferd Verfel, IFRA, Darmstadt (GER)
Prof.PhD Lidija Mandić, Faculty of Graphic Arts, Zagreb (CRO)
Prof.PhD Miroslav Gojo, Faculty of Graphic Arts, Zagreb (CRO)
Prof.PhD Diana Milčić, Faculty of Graphic Arts, Zagreb (CRO)
Prof.PhD Diana Gregor – Svetec, Faculty of Natural Sciences and Engineering, Ljubljana (SLO)
Prof.PhD Aleš Hladnik, Faculty of Natural Sciences and Engineering, Ljubljana (SLO)
Prof.PhD Tadeja Muck, Faculty of Natural Sciences and Engineering, Ljubljana (SLO)
Prof.PhD Marie Kaplanova, Faculty of Chemical Technology, Pardubice (CZE)
Prof.PhD Georgij Petriaszwili, Warsaw University of Technology, Warsaw (POL)
Doc.PhD Erzsébet Novotny, Faculty of Light Industry and Environmental Engineering, Budapest (HUN)
Prof.PhD Csaba Horváth, Faculty of Light Industry and Environmental Engineering, Budapest (HUN)
Prof.PhD Slobodan Nedeljković, Academy of Arts, Novi Sad (SRB)
Prof. Boško Ševo, Academy of Arts, Novi Sad (SRB)
Prof.PhD Katarina Gerić, Faculty of Technical Sciences, Novi Sad (SRB)
Prof.PhD Branko Milosavljević, Faculty of Technical Sciences, Novi Sad (SRB)
Prof.PhD Siniša Kuzmanović, Faculty of Technical Sciences, Novi Sad (SRB)
PhD Rossitza Velkova, Printing Industry Union of Bulgaria, Sofia (BUL)
Doc.PhD Igor Karlović, Faculty of Technical Sciences, Novi Sad (SRB)
Prof.PhD Rafael Huertas, Department of Optics, Faculty of Science, University of Granada (ESP)
Prof.PhD Miloš Sorak, Technical Faculty, Banja Luka (BIH)
Prof.PhD Ilija Ćosić, Faculty of Technical Sciences, Novi Sad (SRB)
Prof.PhD Miljana Prica, Faculty of Technical Sciences, Novi Sad (SRB)

ORGANIZATIONAL COMMITTEE

President, Igor Karlović, Faculty of Technical Sciences, Novi Sad (SRB)
Dragoljub Novaković, Faculty of Technical Sciences, Novi Sad (SRB)
Živko Pavlović, Faculty of Technical Sciences, Novi Sad (SRB)
Željko Zeljković, Faculty of Technical Sciences, Novi Sad (SRB)
Sandra Dedijer, Faculty of Technical Sciences, Novi Sad (SRB)
Magdolna Pal, Faculty of Technical Sciences, Novi Sad (SRB)
Nemanja Kašiković, Faculty of Technical Sciences, Novi Sad (SRB)
Uroš Nedeljković, Faculty of Technical Sciences, Novi Sad (SRB)
Ivan Pinčjer, Faculty of Technical Sciences, Novi Sad (SRB)
Ivana Tomić, Faculty of Technical Sciences, Novi Sad (SRB)
Neda Milić, Faculty of Technical Sciences, Novi Sad (SRB)
Vladimir Zorić, Faculty of Technical Sciences, Novi Sad (SRB)
Srđan Draganov, Faculty of Technical Sciences, Novi Sad (SRB)

Gojko Vladić, *Faculty of Technical Sciences, Novi Sad (SRB)*
Bojan Banjanin, *Faculty of Technical Sciences, Novi Sad (SRB)*
Irma Puškarević, *Faculty of Technical Sciences, Novi Sad (SRB)*
Rastko Milošević, *Faculty of Technical Sciences, Novi Sad (SRB)*
Jelena Vladušić, *Faculty of Technical Sciences, Novi Sad (SRB)*
Stefan Đurđević, *Faculty of Technical Sciences, Novi Sad (SRB)*
Darko Avramović, *Faculty of Technical Sciences, Novi Sad (SRB)*
Jelena Vladušić, *Faculty of Technical Sciences, Novi Sad (SRB)*
Jelena Novaković, *Faculty of Technical Sciences, Novi Sad (SRB)*
Marko Brkić, *Faculty of Technical Sciences, Novi Sad (SRB)*
Miljana Prica, *Faculty of Technical Sciences, Novi Sad (SRB)*

TECHNICAL SECRETARY

Ivana Jurič, *Faculty of Technical Sciences, Novi Sad (SRB)*

REVIEWING COMMITTEE

Prof.PhD Miroslav Gojo, *Faculty of Graphic Arts, Zagreb (CRO)*
Prof.PhD Csaba Horváth, *Faculty of Light Industry and Environmental Engineering, Budapest (HUN)*
Prof.PhD Diana Gregor - Svetec, *Faculty of Natural Sciences and Engineering, Ljubljana (SLO)*
Prof.PhD Tadeja Muck, *Faculty of Natural Sciences and Engineering, Ljubljana (SLO)*
Prof.PhD Marie Kaplanova, *Faculty of Chemical Technology, Pardubice (CZE)*
Prof.PhD Dragoljub Novaković, *Faculty of Technical Sciences, Novi Sad (SRB)*
Prof. PhD Rafael Huertas, *Department of Optics, Faculty of Science, University of Granada (ESP)*
Prof.PhD Klementina Možina, *Faculty of Natural Sciences and Engineering, Ljubljana (SLO)*
Prof. PhD Rozália Szentgyörgyvölgyi, *Faculty of Light Industry and Environmental Engineering, Budapest, (HUN)*
Doc.PhD Igor Karlović, *Faculty of Technical Sciences, Novi Sad (SRB)*
Doc.PhD Sandra Dedijer, *Faculty of Technical Sciences, Novi Sad (SRB)*
Doc.PhD Živko Pavlović, *Faculty of Technical Sciences, Novi Sad (SRB)*
Doc.PhD Nemanja Kašiković, *Faculty of Technical Sciences, Novi Sad (SRB)*
Doc.PhD Gojko Vladić, *Faculty of Technical Sciences, Novi Sad (SRB)*
Prof.PhD Miljana Prica, *Faculty of Technical Sciences, Novi Sad (SRB)*

WITH SUPPORT OF:

Ministry of Education, Science and Technological Development,
Republic of Serbia

Provincial Secretariat for Science and Technological Development,
Vojvodina, Republic of Serbia

Faculty of Technical Sciences, Novi Sad, Republic of Serbia

CEEPUS III RS-0704-03-1415

CO - ORGANISER:

Faculty of Graphic Arts, Zagreb, Croatia

Óbuda University, Institute of Media Technology, Budapest, Hungary

EQUIPMENT AND MATERIAL DONORS:

KBA, Germany

Alois Carmine KG, Austria

Horizon, Germany

Perfecta, Germany

Flint Group, Germany

Foliant, Czech Republic

Dalim Software, Germany

StudioRIP, England

Merus, Slovenia

Rotografika, Subotica, Serbia

Systemic, Belgrade, Serbia

Centropapir, Sremski Karlovci, Serbia

TABLE OF CONTENTS

FOREWORD	13
INTRODUCTORY LECTURES	
1. Huertas R.: AN OVERVIEW OF RECENT COLOR-DIFFERENCE FORMULAE	15
2. Novaković D., Karlović I., Đurđević S.: GRAPHIC TECHNOLOGIES IN TIMES OF CHANGE	29
SPECIAL PRINTING APPLICATIONS AND MATERIALS	
3. Vilko Ž., Agić D., Politis A., Pap K.: "INFRAREDGRAPHIC"® SECURITY PRINTING TECHNOLOGY MERGING V AND Z SPECTRUM.	45
4. Urbas R., Pavlović Ž., Stanković Elesini U., Draganov S.: OFFSET PRINTING BY THE MICROCAPSULES – INFLUENCE ON THE PROPERTIES OF PAPER SUBSTRATE	51
5. Škola O., Jašúrek B., Vališ J., Němec P.: THE STUDY OF POLYMERIZATION OF HYBRID SYSTEMS	59
6. Pavlović Ž., Dedijer S., Stanković E.U., Urbas R.: STRUCTURE OF MICROCAPSULES AND IT'S USE IN THE INDUSTRY– OVERVIEW.	65
7. Cigula T., Pavlović Ž., Fuchs G.R., Risović D.: INFLUENCE OF SODIUM METASILICATE SOLUTION'S CHARACTERISTICS ON THE DEVELOPING OF THE OFFSET PRINTING PLATE	71
8. Dedijer S., Pal M.: COMPARATIVE STUDY OF LINE AND DOT ELEMENTS REPRODUCTION ON FLEXO PRINTING PLATES USING DIFFERENT FILM MAKING TECHNOLOGIES	77
9. Cigula T., Mahović Poljaček S., Tomašegović T., Gojo M.: DYNAMIC CONTACT ANGLE AS A METHOD IN GRAPHIC MATERIALS CHARACTERIZATION.	87
10. Držková M., Ptáčková M.: EXTENDING THE FUNCTIONALITY OF PRINTED PRODUCTS USING AUGMENTED REALITY	93
11. Đokić M., Kavčič U., Pivar M., Mraović M., Radonić V., Pleteršek A., Muck T.: PRINTED ANTENNA FOR NEAR FIELD COMMUNICATION TAG	105
12. Syrový T., Milec M., Pretl S., Syrová L., Kuberský P.: PRINTED PRIMARY ZN/MNO ₂ BATTERIES FOR SMART PACKAGE APPLICATION	113
13. Kašiković N., Pál M., Milošević R., Milić N., Jurišić B.: INFLUENCE OF TEXTILE WASHING TREATMENT ON READABILITY OF QR CODES	119
14. Jančovičová V., Štromajer Z., Krivošová B., Machatová Z.: THE STABILITY OF PRINTED POLYOLEFIN FOILS	127
15. Panák O., Halenkovič T., Holická H.: ACCELERATED AGEING OF SAMPLES IMITATING HISTORICAL PRINTS.	133

16. Stančić M., Grujić D., Geršak J.:
INFLUENCE OF PARAMETERS OF DIGITAL PRINTING
ON THERMO- PHYSIOLOGICAL PROPERTIES OF TEXTILE MATERIALS 139
17. Vukić N., Ristić I., Simendić B, Teofilović V., Budinski-Simendić J.:
THE INFLUENCE OF AGING ON OPTICAL, MECHANICAL AND
THERMAL PROPERTIES OF PRINTED POLYLACTIDE FILMS 149

APPLIED MEASUREMENT METHODS IN GRAPHIC ARTS

18. Machatová Z., Jančovičová V., Ozimová L.:
THE IDENTIFICATION OF HISTORICAL PHOTOGRAPHIC PROCESSES
BY OPTICAL MICROSCOPY AND FT-IR SPECTROSCOPY 157
19. Dvonka V., Reháková M., Čeppan M., Gál L., Belányiová E., Gemeiner P.:
IMAGE ANALYSIS OF WRITING MEANS AND ITS FORENSIC ANALYSIS 165
20. Donevski D., Miličić D., Banić D.:
THE USE OF SHOCK RESPONSE SPECTRUM IN PROTECTIVE PACKAGING 171
21. Dvonka V., Čeppan M., Belovičová M., Gál L., Reháková M., Gemeiner P.:
GRAPHICAL DOCUMENTS EXAMINATION USING MOLECULAR
SPECTROSCOPY AND CHEMOMETRY 175
22. Pál M., Koltai L., Dedijer S., Draganov S., Đokić M.:
INSTRUMENTAL INVESTIGATION
OF FOLD-CRACK RESISTANCE OF COATED PAPERS 183
23. Novotny E.:
EFFECT OF THE APPLICATION OF METAL PRINTING INKS ON
LAMINATION QUALITY OF PLASTIC LAYERS 191

PRINT QUALITY

24. Tsigonias A., Siarampalou K., Politou G., Gamprellis G., Politis A., Tsigonias M.:
HEXACHROME SYSTEM MODIFICATION FOR A PROTOTYPE
SCREEN PRINTING REPRODUCTION. 203
25. Majnarić I., Slugić A., Puhalo M., Bolanča Mirković I.:
THE POSSIBILITY OF USING INKJET FOR
PRINTING ON METAL PACKAGING. 211
26. Golob G., Gerl I., Bobnar M., Pivar M.:
COLOUR DIFFERENCES RESULTING FROM DRYING PROCESS OF CONVENTIONAL
PRINTED AND IN-LINE UV VARNISHED CARDBOARD SAMPLES 219
27. Bota J., Brozović M., Hrnjak-Murgić Z.:
INFLUENCE OF SILICA NANOPARTICLES IN PCL OVERPRINT COATING
ON THE COLOR CHANGE OF OFFSET PRINT 225
28. Plazonić I., Bates I., Barbarić-Mikočević Ž.:
ANALYSIS OF PRINTED DOT FIDELITY ON PAPER SUBSTRATES
MADE OF TRITICALE STRAW FIBRES 233
29. Ružičić B., Stančić M., Milošević R., Sadžakov M.:
INFLUENCE OF SUBSTRATE THICKNESS ON THE REPRODUCTION
QUALITY OF SCREEN-PRINTED POLYMER MATERIALS. 239
30. Gazibarić Z., Živković P.:
PARAMETERS OF REPRODUCTION AND THEIR INFLUENCE TO
APPEARANCE OF MOIRE PATTERN IN LITHOGRAPHIC OFFSET PRINTING. 247

31. Milošević R., Kašiković N., Stančić M., Ružičić B.: UV LIGHT EXPOSURE EFFECTS ON PRINT MOTTLE OF INK-JET PRINTED TEXTILE MATERIAL	253
32. Karlović I., Tomić I., Jurić I., Ranđelović D.: DETERMINATION OF SUBSTRATE AND HALFTONE DOT SHAPE INFLUENCE ON IMAGE REPRODUCTION WITH IMAGE DIFFERENCE METRIC	261
33. Jurić I., Karlović I., Tomić I., Zdravković S.: VISUAL EXPERIENCE OF GRAININESS	267
34. Sadžakov M., Banjanin B., Ružičić B., Adamović B.: THE SURFACE COVERAGE ANALYSIS OF METAL SUBSTRATE PRINTED WITH UV INKJET INK	273
COLOUR RESEARCH AND APPLICATION	
35. Molek I., Muck T., Javoršek D.: WHERE ARE THE STANDARDS FOR DIGITAL PROJECTION?	281
36. Vujić J., Agić A., Stanimirović I.Ž., Nassirzadeh M.: THEORY OF TWIN COLORANTS RESPONSE IN VISUAL AND INFRARED SPECTRUM	289
37. Smejkalová H., Dzyk P., Veselý M.: LIGHTFASTNESS EVALUATION OF PRINTS USING GAMUT VOLUME AND VOLGA SOFTWARE	295
38. Hladnik A., Palanjuk I.: CLASSIFICATION AND CLUSTERING: TWO MACHINE LEARNING TOOLS FOR COLOR IMAGE SEGMENTATION	301
39. Tomić I., Huertas R., Jurić I.: COLOUR TO TEXTURE FUSION IN HSI COLOUR SPACE	309
40. Milić N., Novaković D., Kašiković N., Dedijer S.: THE INFLUENCE OF VIEWING CONDITIONS ON COLOUR GAMUT OF RED-GREEN VISION DEFICIENCIES	317
PRINT MANAGEMENT AND SIMULATION	
41. Koltai L., Horváth C.: PRINCIPAL QUESTIONS OF THE FUTURE'S PRINTING SALES	327
42. Ribeiro A. de S., Souto P., Mihorko B.: MIS TOOLS TO INCREASE SUSTAINABILITY	331
43. Zeljković Ž., Novaković D., Avramović D., Đurđević S.: THE DEVELOPMENT OF KNOWLEDGE BASE SYSTEM FOR THE IDENTIFICATION OF THE PARAMETERS OF THE PRINTING PROCESS	335
ENVIRONMENTAL PROTECTION IN GRAPHIC ARTS	
44. Szentgyörgyvölgy R., Angeli E.: CELLULOSE BASED CARTONBOARD ESTER RETENTION	343
45. Vukoje M., Plazonić I., Barbarić-Mikočević Ž.: EFFLUENT CHARACTERISTICS FROM NEWSPAPER CHEMICAL FLOTATION DEINKING	351
46. Bečelić-Tomin M., Kerkez Đ., Prica M., Dalmacija B., Tomašević D., Pucar G.: APPLICATION OF BENTONITE BASED FENTON CATALYST IN THE PROCESS OF REACTIVE DYE DEGRADATION	357
47. Simendić B., Marinković V., Teofilović V., Vukić N.:	

THE AMOUNTS AND PROPERTIES OF DUST RELEASED FROM LASER PRINTERS	363
48. Kerkez Đ., Bečelić-Tomin M., Prica M., Tomašević D., Pucar G., Dalmacija B., Rončević S.: DECOLOURIZATION OF REACTIVE RED 120 BY AN ADVANCED FENTON PROCESS IN CONJUNCTION WITH ULTRASOUND	369
49. Adamović S., Prica M., Radonić J., Turk Sekulić M., Adamović D., Maletić S.: THE LEACHING OF ZINC FROM PRINTED GRAPHIC PRODUCT WASTE.	375
DIGITAL AND WEB MEDIA	
50. Gabrijelčić Tomec H., Bratuž N., Javoršek D., Javoršek A.: COMPARISON OF IMAGE PROCESSING OPERATIONS FOR ADJUSTMENT AND EVALUATION OF RENDERINGS GENERATED WITH DIFFERENT RENDERING ENGINES.	381
51. Pinčer I., Nedeljković S., Puškarević I., Zeljković Ž.: GRAPHICAL SYSTEM VISUALIZATION IN A VIRTUAL SPATIAL ENVIRONMENT AS A LEARNING METHOD	389
52. Bratuž N., Jerman T., Gabrijelčić Tomc, H. Javoršek D.: INFLUENCE OF RENDERING ENGINES ON COLOUR REPRODUCTION.	395
53. Đurđević S., Zeljković Ž.: THE INTEGRATION OF TTI SENSOR OF SMART PACKAGING AND MODERN PERSONAL PORTABLE DEVICES	401
54. Avramović D., Vladić G., Zorić V.: ANALYSIS OF THE MESSAGE TRANSPORT SYSTEMS IN AJAX APPLICATIONS USING IMAGES	411
DESIGN, TYPOGRAPHY AND USER EXPERIENCE	
55. Mandić L., Poljičak A., Strgar Kurečić M.: THE USE OF COLOR IN VISUAL PRODUCT MESSAGE REDESIGN	423
56. Puškarević I., Pinčer I., Banjanin B.: VISUAL ANALYSIS OF THE TYPEFACE MANAGEMENT IN BRAND IDENTITY	427
57. Tamás-Nyitrai C., Hegedűs E.: LINEWORK ON CONSUMER PACKAGING CAN HELP TO IMPROVE THE IMAGE OF PORT WINES.	435
58. Banjanin B., Nedeljković U.: COMPARING DIFFERENT LETTER SPACING METHODS IN SANS-SERIF TYPEFACE DESIGN	441
59. Pinčer I., Nedeljković U., Draganov S.: SUBJECTIVE ANALYSIS OF IMAGE QUALITY: EXPERTS AND NAĬVE.	449
60. Mandić L., Trojko D., Pibernik J., Dolić J.: THE INFLUENCE OF COLOR IN DIGITAL MEDIA IN USER EXPERIENCE.	457
61. Vladić G., Avramović D., Sadžakov M., Milić N., Kecman M.: THE INFLUENCE OF PACKAGING SHAPE ON PERCEIVED PRODUCT VALUE AND CONSUMER NICHE.	461
62. Kuzmanović S., Vladić G., Rackov M.: NEW AND CREATIVE PRODUCT IDEA GENERATION ASSOCIATION METHOD	467
63. Rajčetić Z.: ECONOMIC DESIGN OF VOJVODINA (1945-1985): INTRODUCTION TO THE ONE STUDY	473

Foreword

Dear readers,

It is my great pleasure to introduce You the research papers of the Seventh Symposium on Graphic Engineering and Design. With this proceeding we continue the works of previous symposiums which have been held biennial since year 2002.

We're delighted that this international symposium has again a great number of the papers and participants coming from many countries.

The papers include the achievements of researches in the field of technology and scientific areas relevant to graphic technology and graphic design. Through the work of the symposium GRID we continued significant scientific cooperation with educational institutions all over the world, especially with the neighbouring countries in the region. With them we are continuing good cooperation which is the driving force for the creation and display of new developments, both individual and common.

I want to thank everyone who participated with their paper and presentation in the symposium. Your contribution is significant for the improvement of the Symposium on Graphic Engineering and Design GRID 14. The research achievements here presented are also valuable to the scientific and professional community and are highly appreciated.

Prof. PhD Dragoljub Novaković

AN OVERVIEW OF RECENT COLOR-DIFFERENCE FORMULAE

Rafael Huertas, University of Granada, Faculty of Science, Department of Optics, Spain

Abstract: This paper does not intend to be an exhaustive state of the art in the field of color differences. From the main concepts used in color-difference evaluation, this work tries to provide the reader critical information about the current status in this specific field of Colorimetry, which could be used as a guide for people working in different aspect of color but are not expert in the topic. In the paper, mainly written in a chronological order, a revision of both, some historically important and recent, color-difference formulae can be found. Since the recommendation of CIELAB, together with CIELUV, by the Commission International of Illumination (CIE) in 1978, many color difference formulae have been proposed. The last recommendations on industrial color-difference formulas by CIE, (i.e. the CIE94 and CIEDE2000 color-difference formulas) are considered. However, after the proposal of CIEDE2000 by the Technical Committee 1-47, in 2001, research and development of new equations continue, not only in CIELAB color space, as DIN99 formulas, but others as OSA-UCS color space, where OSA-GP color-difference formula. In the very last years, color differences and color appearance models have converged. Then, in the base of CIECAM02 have appeared color difference formulas with quite good performance.

Key words: CIELAB, CIE94, CIEDE2000, OSA-UCS, CIECAM02.

1. INTRODUCTION

Colorimetry has been widely used in three main application areas: color specification, color difference evaluation and color appearance prediction. Research has conventionally been conducted independently in each area, although in fact they are closely related. Historically, color specification was outlined first, followed by color difference evaluation and lastly color appearance.

Particularly, color difference is not a new topic, and it is of great interest in industrial applications: food, artworks, automobiles, etc. The definition of a color-difference formula for small-medium color differences is a highly debated problem in color science during the past few decades and is still open today. Historically, since the MacAdam threshold chromatic discrimination (MacAdam, 1942) for 25 color centers, many works have been published about color differences (Brown, 1957; Wyszecki, 1971; Witt, 1990; Hita, 1986). A glance at MacAdam's ellipses shows clearly that the CIE 1931 xy chromaticity diagram is absolutely unsuitable for color differences representations. Then color difference formulas in other color spaces begun to appear. In the early 1970s, there were as many as 20 different formulas being used to calculate color differences (Robertson, 1977). An open issue, even today, is that the results from different formulas are not comparable, which can results in a communication problem between industries. In 1976, to promote uniformity of practice pending the development of a better formula, the CIE recommended two color spaces, CIE 1976 $L^*a^*b^*$ (CIELAB) and $L^*u^*v^*$ (CIELUV) (Robertson, 1977; Robertson 1990), to be used for the specification of color differences. The Euclidean distance between two points in these spaces is taken to be a measure of their color difference (ΔE^*_{ab} or ΔE^*_{uv}). At that time there was not any evidence of better performance of one over the other. However, eventually CIELAB was preferred over CIELUV, which became relegated to particular applications, as lighting, monitors and displays. The reason is that CIELUV has a chromaticity diagram, very useful for additive mixings. Nowadays CIELAB has prevailed over CIELUV, as demonstrated by the fact that the following recommendations of the CIE about color difference are based on the CIELAB color space. Alman et al. (Alman et al., 1989) provide experimental evidence for the poor performance of CIELUV as a color difference equation. Additional comparisons between CIELUV and CIELAB have been made by Robertson (Robertson, 1990). Effectively the main goal in the recommendation of CIELAB and CIELUV, the uniformity of use, was achieved; in 1990 a survey in 114 USA industries showed that 92% employed CIELAB (Kuehni, 1990). In 1994 the CIE recommended a single better formula for color difference measurement, based on the CIELAB space, known as ΔE^*_{94} (Berns 1993a, CIE 1995). CIE94 corrects the most important deficiencies of CIELAB: the tolerance in chroma increases with chroma, the tolerance in hue also increases with chroma.

New experimental data, allowed that the CIE TC 1-47 developed a new formula, CIEDE2000, in 2001 [CIE, 2001; Luo et al., 2001]. It used a combined experimental dataset (designed as COM dataset), compiled from four independent experiments: BFD-P (Luo et al, 1986), Leeds (Kim et al., 1997), RIT-DuPont (Berns et al., 1991) and Witt (Witt, 1999b). These data have been widely employed later in the field of color differences. CIEDE2000 tunes the corrections introduced in CIE94 and adds three additional ones: the dependency of lightness tolerances with lightness, a rotation term that accounts for the interaction between chroma and hue differences in the blue region, and a correction for achromatic stimuli.

After the proposal of CIEDE2000, research and development of new equations continue. New technical committees of division 1 of the CIE have been created in this sense. Examples are, the TC 1-55 Uniform Colour Space for Industrial Colour Difference Evaluation (To derive a new uniform colour space for industrial colour difference evaluation using existing experimental data), TC 1-63 Validity of the Range of CIE DE2000 (To investigate the application of the CIE DE2000 equation at threshold, up to CIELAB colour differences greater than 5), TC 1-81 Validity of Formulae for Predicting Small Colour Differences (To evaluate available formulae for small colour differences), TC 1-85 Update CIE Publication 15:2004 Colorimetry (To update CIE Publication 15:2004 taking into consideration the current CIE/ISO standards on colorimetry and the work of TC1-36 Fundamental Chromaticity Diagram with Physiologically Significant Axes).

Alternatively, modern color difference formulae have appeared in other context, different from CIELAB color space. Some examples are DIN99d and OSA-UCS based formulas.

On the other hand, color appearance, although closely joint to color differences, has followed a different way. Anyway, it is not by chance that CIELAB, developed as a color space which Euclidean distance representing color difference and the basic for next color-difference formulas, is at the same time a color appearance model. In the very last years, color-difference formulae and color appearance models have converged. In the basics of CIECAM02, Luo et al. (Luo et al., 2006) have developed color-difference formulas with quite good performance, called CAM02-SCD, CAM02-LCD and CAM02-UCS.

Then, attending to the former historical review, most of color difference formulae can be classified in the following four groups:

- Color difference formulae based on direct transformation from XYZ tristimulus values: many formulas are in this group (Wyszecki et al., 1982), as FMC I and FMC II, NBS (Judd Hunter formula), Hunter Lab in 1948, CIELAB and CIELUV, and many others.
- Color difference formulae based on CIELAB: the wide acceptance of CIELAB made it the base of a generation of formulas called "advanced color difference formulae".
- Color difference formulae based on Color Order Systems: some of old formulas (Wyszecki et al., 1982), as Balikin in 1936 or Godlove in 1951, also Adams-Nickerson (Adams, 1942), OSA-GP (Huertas et al., 2006), OSA_GPE (Oleari et al., 2009) and GLAB (Guan et al., 1999) for large color differences.
- Color difference formulae based on Color Appearance Models: CAM02-SCD, CAM02-LCD, CAM02-UCS (Luo et al., 2006) are examples of this group.

In the next section some of the formulae inside these groups are analyzed.

2. THRESHOLD, SUPRA-THRESHOLD AND LARGE COLOR DIFFERENCES

Usually the thresholds around color centers have been represented by ellipses/ellipsoids, although some authors contest it. Anyhow, according to the size of the color difference three cases can be considered [CIE, 1995]:

- Threshold color differences or just noticeable differences (jnd).
- Supra-threshold color differences or color tolerances.
- Large color differences, as the ones in the color atlas (Munsell Book of Color, NCS, Pantone, etc.).

While threshold color differences are very interesting in research, in many applications supra-threshold color differences, or even large color differences, are important, as jnd are too severe in real viewing conditions.

The size of a threshold color difference (hence the supra-threshold and large color differences) depends on the observation conditions and the color center considered, because of the non-uniformity of the color spaces. Then, it is impossible to give a fixed value for each of the three cases. Anyway averaging over the complete color space, from experimental results of different authors [Melgosa, 1992], an estimation about the size of color differences is obtained, summarized in Table 1, which shows estimations about thresholds, supra-threshold and large color differences.

Table 1: Averaged color differences over the color space, in CIELAB units, from different experimental dataset. Table from [Melgosa et al., 2001]

Author (reference)	Number of centers or pairs	ΔE^*_{ab}
MacAdam, 1942	24	0.73
Brown et al., 1949	34	0.57
	33	0.55
Brown, 1957	21	0.90
	21	0.71
Wyszecki et al., 1971	28	1.04
	28	1.00
	28	1.12
Witt, 1990	5	0.38
Luo et al., 1986	131	1.14
Cheung et al., 1986	5	1.79
RIT-Dupont (Berns et al., 1991)	19	1.75
Munsell Book of Color, 1976 (gloss finish)	350	10.24
	365	8.45
	53	10.86

From Table 1 could be deduced that a color difference in the range 0.38 to 0.73 CIELAB units correspond to jnd, while supra-threshold color differences are around 1.75 CIELAB units [Melgosa et al., 1997]. Above 5 CIELAB units can be considered large color differences [CIE, 1995]. Nevertheless, from an industrial point of view [Lozano, 1978], a strict color tolerance corresponds to the range 1.1 to 2.8 CIELAB units; a normal color tolerance to the range 2.8 to 5.6 and above 5.6 CIELAB units a generous color tolerance.

3. ADVANCED COLOR-DIFFERENCE FORMULAE

Since its proposal, CIELAB was considered as an “approximately uniform” color space, as was indicated in a note in its publication report [CIE, 1986; CIE, 2004]: “In different practical applications it may be necessary to use different weightings for ΔL^* , ΔC^* and ΔH^* ”. This non-uniformity of CIELAB space can be seen in Figure 1, which shows plots of constant perceived hue lines from Hung and Berns [Hung et al., 1995]. It is clear that red and blue hues are not represented properly.

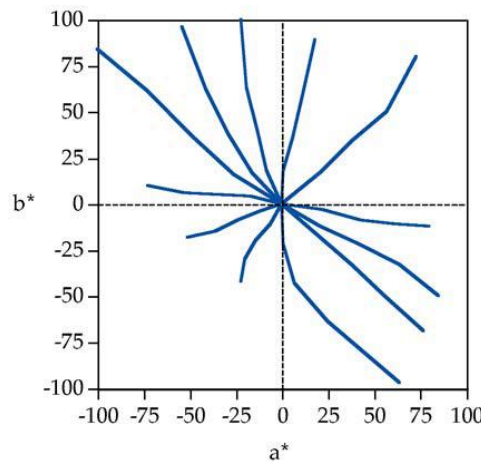


Figure 1: Contours of constant perceived hue from plotted in the CIELAB a^*b^* plane. Figure from [Fairchild, 1998].

In addition, the perceptual unique hues (red, green, yellow and blue) do not align directly with the CIELAB a^*b^* axes. Under daylight illumination the unique hues lie approximately at hue angles of 24° (red), 90° (yellow), 162° (green), and 246° (blue) [Fairchild, 1996]. Other limitations of CIELAB are caused by the implementation of a von Kries-type chromatic adaptation transform using CIE XYZ tristimulus values rather than cone responsivities. This has been called a wrong von Kries transform [Terstiege, 1972].

However, the wide acceptance of CIELAB made it the base of a generation of formulae, called advanced color-difference formulae. These formulas, in chronological order, were JPC79 [McDonald, 1980], CMC [Clarke et al., 1984], BFD [Luo et al., 1987], CIE94 [CIE, 1995] and CIEDE2000 [CIE, 2001], which have improved CIELAB in different ways for particular experimental dataset. In particular, CIEDE2000 is the currently recommended formula by the CIE. The advanced color-difference formulae follow the format shown below:

$$\Delta E^*(k_L : k_C : k_H) = \sqrt{\left(\frac{\Delta L^*}{k_L W_L}\right)^2 + \left(\frac{\Delta C^*}{k_C W_C}\right)^2 + \left(\frac{\Delta H^*}{k_H W_H}\right)^2 + R_T \left(\frac{\Delta C^*}{k_C W_C}\right)^2 \left(\frac{\Delta H^*}{k_H W_H}\right)^2} \quad (1)$$

where ΔL^* , ΔC^* y ΔH^* are lightness, chroma and hue differences respectively, in CIELAB units; W_L , W_C and W_H are weighting functions to improve the uniformity of CIELAB space; k_L , k_C and k_H are the parametric factors; R_T is called rotation term and is included only in some formulae as BFD and CIEDE2000.

The parametric factors, k_L , k_C , k_H are correction terms for variation in experimental conditions. Under reference conditions they are all set at 1. For other choices see [CIE, 1993]. These factors are intended to get better agreement between computed and perceived differences under specific viewing conditions, which are interesting in some industrial application. For example, the CIE suggests [CIE, 1995] that in textile industry it is usual to take $k_L=2.0$, $k_C=1.0$ and $k_H=1.0$, indicating that the experimental conditions for that situation are unknown.

3.1 CIE94

In 1994 the CIE recommended a single better formula for color difference measurement based on the CIELAB space, known as ΔE^*_{94} [Berns 1993a, CIE 1995]. CIE94 was developed by the Technical Committee 1-29 of the CIE [CIE, 1995] on the basis of CMC [Clarke et al., 1984], which was employed mainly by textile industries. Three dataset, obtained by Witt [Witt et al., 1983; Witt, 1987], Berns et al. [Berns et al., 1991] and Luo et al. [Luo et al., 1986] were considered in the development of CIE94 to fit the weighing functions to corrects the most important deficiencies of CIELAB. These weighing functions of CIE94 are given below:

$$S_L = 1.0 \quad (2)$$

$$S_C = 1 + 0.045 C^*_{ab} \quad (3)$$

$$S_H = 1 + 0.015 C^*_{ab} \quad (4)$$

where C^*_{ab} is the geometric mean of the chroma in CIELAB. Finally, CIE94 is given by:

$$\Delta E^*_{94} = \sqrt{\left(\frac{\Delta L^*}{k_L S_L}\right)^2 + \left(\frac{\Delta C^*}{k_C S_C}\right)^2 + \left(\frac{\Delta H^*}{k_H S_H}\right)^2} \quad (5)$$

where ΔL^* , ΔC^* , ΔH^* are computed from CIELAB; k_L , k_C , k_H are the parametric factors, equal to 1 under the reference conditions for CIE94, which are [CIE, 1995]:

- Illumination: source simulating the spectral relative irradiance of CIE standard illuminant D65.
- Illuminance: 1000 lx.
- Observer: normal colour vision.
- Background field: uniform, neutral grey with $L^* = 50$.

- Viewing mode: object.
- Sample size: greater than 4 degrees subtended visual angle.
- Sample separation: minimum sample separation achieved by placing the sample pair in direct edge contact.
- Sample color difference magnitude: 0 to 5 CIELAB units.
- Sample structure: homogeneous color without visually apparent pattern or non-uniformity.

3.2 CIEDE2000

The philosophy in the development of CIE94 was to propose a versatile model for future corrections, with the maximum simplicity. Then, based on CIELAB, CIE94 incorporated, by the weighting functions, only the most important corrections, which were the most consistent with the different dataset used. It could be though that CIE94 was a little conservative, discarding some effects included in CMC and BFD at those times. This was the reason why some years later CIEDE2000 appeared, incorporating those effects tested with new experimental data (Luo et al., 2001).

After the recommendation of CIE94, a new technical committee (CIE TC 1-47) begun to study some effects not completely understood in CIE94. These effects were: the dependency of the difference in lightness with the lightness, the dependency of the difference in hue with the hue and the possible interaction between chroma and hue. New experimental data allowed study these effects and another one: a correction for achromatic stimuli. Some papers describe very well the work of the technical committee (CIE, 2001; Luo et al., 2001). The following is a description of the formula. As advanced formulae, CIEDE2000 are based on CIELAB (CIE, 1986), but before compute the differences in chroma and hue a transformation over a^* is performed according to:

$$L' = L^* \quad (6)$$

$$a' = (1 + G)a^* \quad (7)$$

$$b' = b^* \quad (8)$$

$$C' = \sqrt{a'^2 + b'^2} \quad (9)$$

$$h' = \arctg\left(\frac{b'}{a'}\right) \quad (10)$$

where G is function of the chroma and approaches to unit out of achromatic stimuli region:

$$G = 0.5 \left(1 - \sqrt{\frac{\overline{C_{ab}^{*7}}}{\overline{C_{ab}^{*7}} + 25^7}} \right) \quad (11)$$

where, the bar over the variable indicates arithmetic mean over the two samples, 'batch' (b) and 'standard' (s).

Following, the differences in lightness, chroma and hue are computed.

$$\Delta L' = L'_b - L'_s \quad (12)$$

$$\Delta C' = C'_b - C'_s \quad (13)$$

$$\Delta H' = 2\sqrt{C'_b C'_s} \sin\left(\frac{\Delta h'}{2}\right) \quad (14)$$

where

$$\Delta h' = h'_b - h'_s \quad (15)$$

Finally, CIEDE2000 is given by the expression:

$$\Delta E_{00} = \sqrt{\left(\frac{\Delta L'}{K_L S_L}\right)^2 + \left(\frac{\Delta C'}{K_C S_C}\right)^2 + \left(\frac{\Delta H'}{K_H S_H}\right)^2 + R_T \left(\frac{\Delta C'}{K_C S_C}\right) \left(\frac{\Delta H'}{K_H S_H}\right)} \quad (16)$$

where the weighting functions are:

$$S_L = 1 + \frac{0.015(\overline{L'} - 50)^2}{\sqrt{20 + (\overline{L'} - 50)^2}} \quad (17)$$

$$S_C = 1 + 0.045 \overline{C'} \quad (18)$$

$$S_H = 1 + 0.015 \overline{C'} T \quad (19)$$

And T is a factor depending on hue tolerance according to:

$$T = 1 - 0.17 \cos(\overline{h'} - 30^\circ) + 0.24 \cos(2\overline{h'}) + 0.32 \cos(3\overline{h'} + 6^\circ) - 0.20 \cos(4\overline{h'} - 63^\circ) \quad (20)$$

Again, the bar over the variable indicates arithmetic mean over the two samples, 'b' y 's'. Lastly, the rotation term, which operates in the blue region, is given by:

$$R_T = -\sin(2\Delta\theta)R_C \quad (21)$$

where

$$\Delta\theta = 30e^{-[(\overline{h'} - 275^\circ)/25]^2} \quad (22)$$

$$R_C = 2\sqrt{\frac{\overline{C'}^7}{\overline{C'}^7 + 25^7}} \quad (23)$$

The parametric factors, k_L, k_C, k_H are equal to 1 under the same reference condition that CIE94. As can be seen, only the chroma weighting function is equal to the one in CIE94, which was the most important correction in both CIE94 and CIEDE2000. With an arbitrary value of 100 assigned to this correction, the score of the hue-difference correction in CIE94 was 21, and the scores of the four remaining corrections in CIEDE2000 were as follows: hue difference, 29; rotation term, 8; lightness difference, 8; and gray correction, 6. At 95% confidence level each of the corrections introduced in CIEDE2000 or CIE94 was statistically significant for the whole combined dataset, in agreement with the results reported by CIE TC 1-47 and 1-29 [Melgosa, 2004]. However, CIEDE2000 cannot be considered the last step in research in this area [Kuehni, 2002; Kuehni, 2008].

4. OTHER COLOR DIFFERENCE FORMULAE

In the last years color difference formulae not based on CIELAB have appeared, in competition with the CIELAB based ones. Among others, the following stand out: OSA-GP (Huertas et al., 2006), OSA_GPE (Oleari et al., 2009), and DIN99d (Cui et al., 2002). OSA-GPE is the Euclidean version of OSA-GP, achieving a Euclidian space based on OSA-GPE, hence it will be considered further on.

4.1 OSA-GPE

The starting point was to consider the CIELAB space inadequate to represent small-medium color differences, as shows by the complexity of the CIEDE2000 formula. If a uniform, Euclidean color space exists, then a color difference or threshold is represented by the equation for the surface of a sphere. The huge effort to realize an empirical uniform color space for large color differences has shown that the best space obtained, i.e., the OSA-UCS (MacAdam, 1974; MacAdam, 1978; MacAdam, 1985) (Uniform Color Space) one, has non-uniform scales. OSA-UCS is an empirical color system for large color differences developed in 1974 by the Optical Society of America's committee on Uniform Color Scales. In this space, although non-uniform, the straight lines radiating from any color sample are geodesic lines, each with a uniform scale.

The OSA-GPE formula is based on the OSA-UCS (Uniform Color Space), for the CIE 64 Supplementary Standard Observer and the illuminant D65. The formula was fitted with the BFD (Bradford University) ellipses at constant luminance (Luo et al., 1986) and the so-called COMData set (Luo et al., 2001) (combined data set used for the development of the CIEDE2000 formula) to extend the color-difference formula to sample pairs with a different luminance factor. The formula is given by Equation (24):

$$\Delta E_{GP} = 10 \sqrt{\left(\frac{\Delta L_{OSA}}{k_L S_L} \right)^2 + \left(\frac{\Delta C_{OSA}}{k_C S_C} \right)^2 + \left(\frac{\Delta H_{OSA}}{k_H S_H} \right)^2} \quad (24)$$

where the factor 10 was introduced because the OSA-UCS unit of distance is equal to 10 just-noticeable differences [jnds]; the parametric factors, k_L , k_C , and k_H , introduced as correction terms for variation in experimental conditions, are all set equal to 1 under reference conditions; S_L , S_C and S_H are linear functions of the average coordinates lightness L_{OSA} and chroma C_{OSA} of the two color samples of any pair, defined as follow:

$$S_L = 2.499 + 0.007(10x\bar{L}_{OSA}) \quad (25)$$

$$S_C = 1.235 + 0.058(10x\bar{C}_{OSA}) \quad (26)$$

$$S_H = 1.392 + 0.017(10x\bar{C}_{OSA}) \quad (27)$$

where the bar over the variable indicates arithmetic mean over the two samples.

ΔL_{OSA} , ΔC_{OSA} , and ΔH_{OSA} are independent color differences in the OSA-UCS space related to differences of lightness, chroma, and hue, respectively. The transformation from tristimulus values are given below:

$$L_{OSA} = \frac{5.9 \left[\left(Y_0^{1/3} - \frac{2}{3} \right) + 0.042(Y_0 - 30)^{1/3} \right] - 14.4}{\sqrt{2}} \quad (28)$$

with

$$Y_0 = Y_{10} (4.4934 x_{10}^2 + 4.3034 y_{10}^2 - 4.2760 x_{10} y_{10} - 1.3744 x_{10} - 2.5643 y_{10} + 1.8103) \quad (29)$$

It is worth noting that the OSA-UCS lightness, L_{OSA} , takes account of the Helmholtz-Kohlrausch effect. The chroma is defined as follow:

$$C_{OSA} = \sqrt{J^2 + G^2} \quad (30)$$

And the difference in hue, is defined indirectly by Equations [31] and [32]:

$$(\Delta H_{OSA})^2 = (\Delta E_0)^2 - (\Delta L_{OSA})^2 - (\Delta C_{OSA})^2 \quad (31)$$

where

$$(\Delta E_0)^2 = (L_{OSA,s} - L_{OSA,b})^2 + (J_s - J_b)^2 + (G_s - G_b)^2 \quad (32)$$

where subscripts 's' and 'b' refer to 'standard' and 'batch'.

The coordinates J and G , which correspond to the empirical j and g of the OSA-UCS system, are obtained by a sequence of linear transformations from tristimulus values with a logarithmic compression.

$$\begin{pmatrix} J \\ G \end{pmatrix} = \begin{pmatrix} 2(0.5735 L_{OSA} + 7.0892) & 0 \\ 0 & -2(0.7640 L_{OSA} + 9.2521) \end{pmatrix}^x \begin{pmatrix} 0.1792 & 0.9837 \\ 0.9482 & -0.3175 \end{pmatrix} \begin{pmatrix} \ln\left(\frac{A/B}{0.9366}\right) \\ \ln\left(\frac{B/C}{0.9807}\right) \end{pmatrix} \quad (33)$$

$$\begin{pmatrix} A \\ B \\ C \end{pmatrix} = \begin{pmatrix} 0.6597 & 0.4492 & -0.1089 \\ -0.3053 & 1.2126 & 0.0927 \\ -0.0374 & 0.4795 & 0.5579 \end{pmatrix} \begin{pmatrix} X_{10} \\ Y_{10} \\ Z_{10} \end{pmatrix} \quad (34)$$

The value of the performance factor PF/3 for the proposed OSA-UCS-based formula shows that the formula performs like the more complex CIEDE2000 formula for small–medium color differences [Huertas et al., 2006].

4.2 DIN99d

In 1999, K. Witt proposed the DIN99 color-difference formula [Witt, 1999a], later adopted as the German Standard DIN6176 [DIN6176, 2000]. Then DIN99 color space applies a logarithmic transformation on the CIELAB lightness L^* , and a rotation and stretch on the chroma plane a^*b^* , followed by a chroma compression inspired in the CIE94 weighting function for chroma. The DIN99 color-difference formula is just the Euclidean distance in the DIN99 color space. In 2002, Cui et al. [Cui et al., 2002] proposed different uniform color spaces based on DIN99, the DIN99d being the one with the best performance [Fernandez-Maloigne, 2013]. In DIN99d space the tristimulus value X is modified by subtracting a portion of Z to improve the performance in the blue region, as suggested by Kuehni [Kuehni, 1999]. Equations defining the DIN99d color-difference formula are as follow:

$$\Delta E_{99d} = \sqrt{\Delta L_{99d}^2 + \Delta a_{99d}^2 + \Delta b_{99d}^2} \quad (35)$$

where

$$\begin{pmatrix} X' \\ Y' \\ Z' \end{pmatrix} = \begin{pmatrix} 1.12 & 0 & -0.12 \\ 0 & 1 & 0 \\ 0 & 0 & 1 \end{pmatrix} \begin{pmatrix} X \\ Y \\ Z \end{pmatrix} \quad (36)$$

Next, usual computation of CIELAB coordinates L^*, a^*, b^* from tristimulus values is performed, but using X', Y', Z' and X'_o, Y'_o, Z'_o . It is clear that the transformation of Equation (36) will only affects to the coordinate a^* , which will be renamed as $a^{*'}_o$.

$$L_{99d} = 325.22 \ln(1 + 0.0036 L^*) \quad (37)$$

$$C_{99d} = 22.5 \ln(1 + 0.006 G) \quad (38)$$

where the chroma C_{99d} is a compression of CIELAB chroma C^*_{ab} .

$$G = (e^2 + f^2)^{1/2} \quad (39)$$

$$e = a^{*'}_o \cos(50^\circ) + b^* \sin(50^\circ) \quad (40)$$

$$f = 1.14 [-a^{*'}_o \sin(50^\circ) + b^* \cos(50^\circ)] \quad (41)$$

Finally, h_{99d} , a_{99d} and b_{99d} are computing according to:

$$h_{99d} = \arctan\left(\frac{f}{e}\right) + 50^\circ \quad (42)$$

$$a_{99d} = C_{99d} \cos(h_{99d}) \quad (43)$$

$$b_{99d} = C_{99d} \sin(h_{99d}) \quad (44)$$

The formula performed satisfactorily in predicting a combined small-color-difference data set, predicting small color differences more accurately than did the CIELAB, CMC, and CIE94 formulas. Most important, they were found to have uniform color spaces with attributes similar to those of the CIELAB formula [Cui et al., 2002].

5. CIECAM02 BASED COLOR DIFFERENCE FORMULAS

According to Wyszecki [Wyszecki et al., 1982] the domain of advanced colorimetry includes methods of assessing the appearance of color stimuli presented to the observer in complicated surroundings as they may occur in everyday life. He stated that outstanding examples of the domain of advanced colorimetry are the measurement of color differences, whiteness, and chromatic adaptation.

While color differences underwent a considerable development in the last half-century, in the last decade it is true for Color Appearance Models [CAM]. However, color differences and color appearance are close one to the other. The CIE 1976 $L^*a^*b^*$ color space [CIELAB] and CIE 1976 $L^*u^*v^*$ color space [CIELUV] could be considered color appearance models, because they include simple chromatic adaptation transforms and predictors of lightness, chroma, and hue. The CIE constructed a color space [CIELAB or CIELUV] with some predictors of color appearance

attributes to create a color-difference formula. It is not surprising that the best way to describe the difference in color of two stimuli is to first describe the appearance of each (Fairchild, 1998). But, as stated above, CIELAB and CIELUV are inappropriate as CAM. In a CIE expert symposium on “Colour Standard for Image Technology” held in Vienna in 1996, the need for the establishment of a color appearance model for general use arose. This model could be used throughout the industry to promote uniformity of practice and compatibility between various components in modern open imaging systems. The TC1-34 completed this work publishing a technical report on the first CIE color appearance model, CIECAM97s (CIE, 1998). Nowadays CIECAM97s can be considered as an interim CAM, which allowed researchers to focus their efforts on a single model. This quickly led to suggestions for the improvements of CIECAM97s and ultimately to the formulation of a simpler and more effective model called CIECAM02 (CIE, 2004). CIECAM02 represents a significant advance in color appearance models and it is currently the model recommended by the CIE. The time between CIECAM02 and the next CIE color appearance model will be significantly longer than the time between CIECAM97s and CIECAM02 (Fairchild, 1998). Next step could be consider if a single color model can be used for all colorimetric applications, i.e. color differences and color appearance under different viewing conditions. As uniform color spaces are embedded in color appearance models, Euclidean distance could lead to a worthy color difference formula. In addition, color differences could be computed under different viewing conditions, for example under illuminants different from daylight, as is recommended by the CIE for color-difference formulas. Luo et al. (Luo et al., 2006) on the basis of the CIECAM02 color appearance model, derived three uniform color spaces for small (CAM02-SCD), large (CAM02-LCD), and all color differences (CAM02-UCS). The Euclidean color-difference formulas were obtained fitting, through the PF/3 index (Guan et al., 1999), three types of data sets: SCD (small color differences), LCD (large color differences) and the combined LCD and SCD data sets. In these CAM02 formulas a non-linear transformation to CIECAM02 lightness J , and a logarithmic compression to the CIECAM02 colorfulness M is applied. The general format of the CAM02 color-difference formulas is given in Equation (45):

$$\Delta E' = \sqrt{\left(\frac{\Delta J'}{K_L}\right)^2 + \Delta a'^2 + \Delta b'^2} \quad (45)$$

where the lightness, J' , is computed according to:

$$J' = \frac{(1+100c_1)J}{1+c_1J} \quad (46)$$

and the coordinates a' , b' in the way:

$$\begin{aligned} a' &= M' \cos(h) \\ b' &= M' \sin(h) \end{aligned} \quad (47)$$

where the colorfulness, M' , is calculated by Equation (48):

$$M' = \frac{1}{c_2} \ln(1+c_2M) \quad (48)$$

where J , M , and h are the CIECAM02 lightness, colourfulness, and hue angle values, respectively. The $\Delta J'$, $\Delta a'$, and $\Delta b'$ are the J' , a' , and b' differences between the “standard” and “batch” in a pair. The K_L , c_1 , and c_2 coefficients for the CAM02-LCD, CAM02-SCD, and CAM02-UCS, respectively, are given in Table 2.

Table 2: The coefficients for each version of UCS based upon CIECAM02. Table from (Luo et al., 2006).

	CAM02-LCD	CAM02-SCD	CAM02-UCS
k_L	0.77	1.24	1.00
c_1	0.007	0.007	0.007
c_2	0.0053	0.0363	0.0228

The performance of the developed spaces compared with former ones and color difference formulae are shown in Table 3.

Table 3: PF/3 values for different uniform color spaces and color difference formulae in three dataset: LCD, SCD and BFA. Lowest values are marked bold. Table from (Luo et al., 2006).

	LCD (daylight)	SCD (daylight)	BFA (Illuminant A)
CIELAB	26	52	52
CMC	-	38	37
CIE94	-	37	35
BFD	-	33	35
CIEDE2000	-	33	35
DIN99d	-	35	34
Kuehni	26	-	-
OSA	24	-	-
GLAB	24	-	-
IPT	26	52	-
CIECAM02	25	47	43
CIECAM02-LCD	23	41	37
CIECAM02-SCD	27	34	32
CIECAM02-UCS	25	35	32

The results showed that compared with the other formulae and spaces, CAM02-LCD and CAM02-SCD performed either the best or close to the best model at predicting the LCD and SCD data, respectively. It is encouraging that CAM02-UCS (developed to fit both LCD and SCD data sets) gave a satisfactory performance, i.e., only slightly poorer than the CAM02-LCD and CAM02-SCD for the LCD and SCD data, respectively. Most importantly, it can be used for applications including color differences ranging from small to large magnitudes such as the color reproduction in the graphic arts industry (Luo et al., 2006).

4. Performance of color-difference formulas

Different index have been employed to check the performance of a color-difference formula. Basically they consist in a comparison between the result of the formula, ΔE , and the answer of the observer, ΔV , over a pair of color with a color difference. Obviously the number of pairs is increased and the answer of the observer average over an important number of them.

Recently two indexes, PF/3 (Guan et al., 1999) and STRESS (Melgosa, 2008), have been widely employed. Table 4 shows the STRESS values for recent advanced color-difference formulae using the experimental COM dataset (Luo et al., 2001) and its four individual datasets: BFD-P (Luo et al, 1986), Leeds (Kim et al., 1997), RIT-DuPont (Berns et al., 1991) and Witt (Witt, 1999b).

Table 4: STRESS values for recent color-difference formulae for COM dataset and its four components. Lowest values are marked bold. Table from (Melgosa, 2008).

	COM	BFD-P	Leeds	RIT-DuPont	Witt
CIELAB	43.93	42.46	40.09	33.42	51.71
CIE94	32.07	33.88	30.57	20.31	31.94
CIEDE2000	27.49	29.55	19.25	19.47	30.22
DIN99d	29.24	31.70	22.76	20.91	30.06
CAM02-SCD	28.46	29.93	22.13	24.42	30.27
CAM02-UCS	29.08	30.96	24.59	21.27	30.46
OSA-GP	29.72	30.14	27.41	24.29	32.19

Table 5 shows the PF/3 values computed for recent advanced color-difference formulae using the experimental COM dataset (Luo et al., 2001) and its four individual datasets: BFD-P (Luo et al., 1986), Leeds (Kim et al., 1997), RIT-DuPont (Berns et al., 1991) and Witt (Witt, 1999b).

Table 5: PF/3 values for recent color-difference formulae for COM dataset and its four components. Lowest values are marked bold. Table from (Melgosa, 2008).

	COM	BFD-P	Leeds	RIT-DuPont	Witt
CIELAB	55.71	56.31	47.23	33.79	70.94
CIE94	37.72	42.96	33.35	20.98	42.33
CIEDE2000	32.11	37.31	22.02	19.56	38.78
DIN99d	34.31	39.34	26.07	21.54	40.10
CAM02-SCD	33.67	38.05	25.46	24.85	39.09
CAM02-UCS	34.30	39.27	27.92	21.90	39.52
OSA-GP	35.32	38.09	30.09	24.19	41.76

As expected CIEDE2000 achieves the best results, as it was fitted to the data set employed in the analysis. Besides, a good agreement appears between STRESS and PF/3.

It can be noted that the four datasets composing the COM give very different results, what could indicate inconsistencies between them.

Besides the different performance and characteristic of the different formulas, the color differences computed by them are not comparable directly because scale factors do not exist all over the color space, which lead to a problem for communication between industries. However, the ratios between the different formulas can be estimated, as appear in Table 6, considering the above mentioned COM dataset and the ratio over CIELAB.

Table 6: Average and standard deviation (in bracket) over the COM dataset and its four components. First row color color difference in CIELAB units. Other rows the ratio between a color difference formula and CIELAB.

	COM	BFD-P	Leeds	RIT-DuPont	Witt
CIELAB	2.64 (2.26)	2.62 (1.91)	1.63 (0.67)	1.44 (0.51)	1.87 (1.42)
CIELUV/CIELAB	1.25 (0.26)	1.26 (0.26)	1.24 (0.24)	1.24 (0.24)	1.29 (0.23)
CMC/CIELAB	0.774 (0.285)	0.770 (0.275)	0.846 (0.271)	0.866 (0.30)	0.768 (0.328)
BFD/CIELAB	0.940 (0.339)	0.960 (0.331)	0.974 (0.341)	1.03 (0.30)	0.923 (0.415)
CIE94/CIELAB	0.676 (0.213)	0.672 (0.205)	0.783 (0.226)	0.747 (0.179)	0.665 (0.233)
CIEDE2000/CIELAB	0.670 (0.243)	0.683 (0.242)	0.739 (0.234)	0.735 (0.206)	0.654 (0.292)
DIN99d/CIELAB	0.783 (0.287)	0.790 (0.280)	0.881 (0.273)	0.869 (0.252)	0.779 (0.341)
ΔE -GP/CIELAB	0.637 (0.248)	0.649 (0.250)	0.712 (0.239)	0.710 (0.196)	0.638 (0.290)

6. CONCLUSIONS

Color difference is an active research field, of great interest in industry. Important advances have been achieved in the last 25 years, but new challenges appears, especially unifying the color difference and color appearance topics, which until very recently have followed separate paths. Transitions from plain color difference to color difference in images could be also the next stage. Nowadays, color images deserve a great interest in industrial applications. In additions, new reliable experimental data are required both to test current formulae and to develop new ones.

It can be notice that, historically, the uniformity of practice has been very important to focus research and effort in one way and ease communication between practitioners. However, also the diversity of models and proposals are enriching and necessary for the progress of the color differences. These two tendencies come and go alternatively.

7. ACKNOWLEDGMENTS

This work was supported by the research project FIS2013-45952-P ("Ministerio de Ciencia e Innovación", Spain). Special thanks to Ivana Tomić and Prof. Igor Karlović for their support and help.

8. LITERATURE

- [1] Adams, E.Q.: "x-z plans in the 1931 ICI system of colorimetry", J. Opt. Soc. Am. 32, 168-173, 1942.
- [2] Alman, D.H., Berns, R.S., Snyder, G.D., Larson, W.A.: "Performance testing of color difference metrics using a color tolerance dataset", Color Res. Appl. 14, 139-151, 1989.
- [3] Brown, W.R.J., MacAdam, D.L.: "Visual sensitivities to combined chromaticity and luminance differences", J. Opt. Soc. Am. 39, 808-834, 1949.
- [4] Brown, W.R.J.: "Color discrimination of twelve observers", J. Opt. Soc. Am. 47, 137-143, 1957.
- [5] Berns, R.S., Alman, D.H., Reniff, L., Snyder, G.D., Balonon-Rosen, M.R.: "Visual determination of suprathreshold color-difference tolerances using probit analysis", Col. Res. Appl. 16, 297-316, 1991.
- [6] Berns, R.S., Motta, R.J., Gorzynski, M.E.: "CRT colorimetry, part I: Theory and practice", Color Res. Appl. 18, 299-314, 1993.
- [7] Cheung, M., Rigg, B.: "Colour-difference ellipsoids for five CIE colour centres", Col. Res. Appl. 11, 185-195, 1986.
- [8] CIE Publication 15-2: "Colorimetry", (CIE Central Bureau, Vienna, 1986).
- [9] CIE Publication 101: "Parametric Effects in Colour-Difference Evaluation", (CIE Central Bureau, Vienna, 1993)
- [10] CIE Publication 116: "Industrial colour-difference evaluation", (CIE Central Bureau, Vienna, 1995).
- [11] CIE Publication 131: "The CIE 1997 Interim Colour Appearance Model, Simple Version: CIECAM97s", (CIE Central Bureau, Vienna, 1998).
- [12] CIE Publication 142: "Improvement to Industrial Colour-Difference Evaluation", (CIE Central Bureau, Vienna, 2001)
- [13] CIE Publication 15: "Colorimetry", (CIE Central Bureau, Vienna, 2004).
- [14] CIE Publication 159: "A Colour Appearance Model for Colour Management System: CIECAM02", (CIE Central Bureau, Vienna, 2004).
- [15] Clarke, F.J.J., McDonald, R., Rigg, B.: "Modification to the JPC79 colour-difference formula", J. Soc. Dyers Colour. 100, 128-132, 1984.
- [16] Cui, G., Luo, M.R., Rigg, B., Roesler, G., Witt, K.: "Uniform colour spaces based on the DIN99 colour-difference formula", Color Res. Appl., 27, 282-290, 2002.
- [17] DIN 6176: "Farbmetrische Bestimmung von Farbabständen bei Körperfarben nach der DIN99-Formel". Berlin: DIN Deutsche Institut für Normung e.V., 2000.
- [18] Fairchild, M.D.: "Refinement of the RLAB color space", Color Res. Appl. 21, 338-346, 1996.
- [19] Fairchild, M. D.: "Color Appearance Models", (Addison-Wesley, 1998).
- [20] Fernandez-Maloigne, C.: "Advanced Color Image Processing and Analysis", (Springer, New York, 2013).
- [21] Guan, S.S., Luo, M.R.: "Investigation of parametric effects using large colour differences", Col. Res. Appl. 24, 356-368, 1999.
- [22] Hita, E., Jimenez del Barco, L., Romero, J.: "Differential color thresholds from metameric matches: experimental results concerning failures of colorimetric additivity", J. Opt. Soc. Am. A 3, 1203-1209, 1986.
- [23] Huertas, R., Melgosa, M., Oleari, C.: "Performance of a Color-Difference Formula Based on OSA-UCS Space Using Small-Medium Color Differences", J. Opt. Soc. Am. A 23 (9), 2077-2084, 2006.
- [24] Hung P.-C., Berns, R.S.: "Determination of constant hue loci for a CRT gamut and their predictions using color appearance spaces", Color Res. Appl. 20, 285-295, 1995.
- [25] Kim, D.H., Nobbs, J.H.: "New weighting functions for the weighted CIELAB colour difference formula", Proceedings of AIC Colour 97, (AIC: Kyoto, 1997), Vol. 1, pages 446-449.
- [26] Kuehni, R.G.: "Industrial color-difference: progress and problems", Col. Res. Appl. 15, 261-265, 1990.
- [27] Kuehni G.: "Towards an improved uniform color space", Color Res Appl. 24, 253-265 , 1999.

- [28] Kuehni, R.G.: "CIEDE2000, milestone or final answer?", *Color Res. Appl.* 27, 126–127, 2002.
- [29] Kuehni, R.G.: "Color difference formulas: An unsatisfactory state of affairs", *Color Res. Appl.* 33, 324–326, 2008.
- [30] Lozano, R.D.: "El color y su medición" (Ed. Americalee, Buenos Aires, 1978), Cap.VI, pages 276–277.
- [31] Luo, M.R., Rigg, B.: "Chromaticity-discrimination ellipses for surface colours", *Color Res. Appl.* 11, 25–42, 1986.
- [32] Luo, M.R., Rigg, B.: "BFD(l:c) colour-difference formula. Part 1 – Development of the formula", *J. Soc. Dyers Colour.* 103, 86–94, 1987.
- [33] Luo, M.R., Cui, G., Rigg, B.: "The development of the CIE 2000 colour-difference formula: CIEDE2000", *Col. Res. Appl.* 26, 340–350, 2001.
- [34] Luo, M.R., Cui, G., Li, C.: "Uniform Colour Spaces Based on CIECAM02 Colour Appearance Model", *Col. Res. Appl.* 31 (4), 320–330, 2006.
- [35] MacAdam, D.L.: "Visual sensitivities to color differences in daylight", *J. Opt. Soc. Am.*, 32, 247–274, 1942.
- [36] MacAdam, D.L.: "Uniform color scales," *J. Opt. Soc. Am.* 64, 1691–1702, 1974.
- [37] MacAdam, D.L.: "Colorimetric data for samples of OSA uniform color scales," *J. Opt. Soc. Am.* 68, 121–130, 1978.
- [38] MacAdam, D.L.: "Color Measurement" (Springer-Verlag, 1985), pages 165–177.
- [39] McDonald, R.: "Industrial pass/fail colour matching, Part 3: colour-matching formulas", *J. Soc. Dyers Colour.* 96, 486–497, 1980.
- [40] Melgosa, M., Hita, E., Romero, J., Jimenez del Barco, L.: "Some classical color differences calculated with new formulas", *J. Opt. Soc. Am. A* 9, 1247–1254, 1992.
- [41] Melgosa, M., Hita, E., Poza, A.J., Alman, D.H., Berns, R.S.: "Suprathreshold color-difference ellipsoids for surface colors", *Col. Res. Appl.* 22, 148–155, 1997.
- [42] Melgosa, M., Perez, M.M., Yebra, A., Huertas, R., Hita, E.: "Some reflections and recent international recommendations on color-difference evaluation", *Optica Pura y Aplicada* 34, 1–10, 2001.
- [43] Melgosa, M., Huertas, R.: "Relative significance of the terms in the CIEDE2000 and CIE94 color-difference formulas", *J. Opt. Soc. Am. A* 21 (12), 2269–2275, 2004.
- [44] Melgosa, M., Huertas, R., Berns, R. S.: "Performance of recent advanced color-difference formulas using the standardized residual sum of squares index", *J. Opt. Soc. Am. A* 25 (7), 1828–1834, 2008.
- [45] Melgosa, M., Huertas, R., Garcia, P.A.: "Analysis of color-differences with different magnitudes using the visual data employed at CIEDE2000 development", *Proceeding of AIC 2008*, (AIC, Stockholm, Sweden, 2008), pages 279–280.
- [46] "Munsell Book of Color, glossy finish collection" (Macbeth Kollmorgen. Baltimore, MD, 1976).
- [47] Oleari, C., Melgosa, M., Huertas, R.: "Euclidean color-difference formula for small-medium color differences in log-compressed OSA-UCS space", *J. Opt. Soc. Am. A* 26, 121–134, 2009.
- [48] Pointer, M.R.: "On the number of discernable colours", *Col. Res. Appl.* 23, 337, 1998.
- [49] Robertson, A.R.: "The CIE 1976 color-difference formulae", *Col. Res. Appl.* 2, 7–11, 1977.
- [50] Robertson, A.R.: "Historical development of CIE recommended color difference equations", *Color Res. Appl.* 15, 167–170, 1990.
- [51] Terstiege, H.: "Chromatic adaptation: A state-of-the-art report", *J. Col. & Appear.* 1, 19–23, 1972.
- [52] Witt, K., Döring, G.: "Parametric variations in a threshold colour-difference ellipsoid for green painted samples", *Col. Res. Appl.* 8, 153–163, 1983.
- [53] Witt, K.: "Three-dimensional threshold of colour-difference perceptibility in painted samples: variability of observers in four CIE colour regions", *Col. Res. Appl.* 12, 128–134, 1987.
- [54] Witt, K.: "Parametric effects on surface color-difference evaluation at threshold", *Col. Res. Appl.* 15, 189–199, 1990.
- [55] Witt, K.: "DIN99 color-difference formula, a Euclidean model", Private communication, 1999a.
- [56] Witt, K.: "Geometric relations between scales of small colour differences", *Color Res. Appl.* 24, 78–92, 1999b.
- [57] Wyszecki, G., Fielder, G.: "New color matching ellipses", *J. Opt. Soc. Am.* 61, 1135–1152, 1971.
- [58] Wyszecki, G., Stiles, W.S.: "Color Science: Concepts and Methods, Quantitative Data and Formulae", 2nd Edition, (John Wiley & Sons Inc., 1982), pages 825–830.

GRAPHIC TECHNOLOGIES IN TIMES OF CHANGE

*Dragoljub Novaković, Igor Karlović, Stefan Đurđević
University of Novi Sad, Faculty of Technical Sciences,
Department of Graphic Engineering and Design, Serbia*

Abstract: Intensive changes in the development of information technology are an important generator of changes in various aspects of the human society and directly influences businesses. A pervasive technology and trend changes across the economy influences also the graphic arts industry. In the area of graphics technology the Drupa world fair is a four year milestone which outlines the future development trends. We are currently in the middle of this time interval which points out to certain financial and technological development trends and their impact. This paper tries to point out on important topics for the graphic engineering and design research area. The financial changes on the market induces structural changes in the leading manufacturers of printing equipment and the restructuring of media products. The number of classic printers has a decreasing trend while printing is more and more applied as an industrial manufacturing process of electronic and other digital device. New opportunities are opening with functional printing, 3D printing, multichannel publishing, green printing with the combination of innovations in packaging sector. Graphic arts companies have to broaden their scope and from production driven business model to adopt a more complex service based products with continual investment primarily in innovation and knowledge.

Keywords: graphic industry, trends and changes, intelligent packaging

1. INTRODUCTION

Social media, mobile, wearables, Internet of Things, real-time — these are just some of the technologies that are disrupting markets. Changes in how people communicate, connect, and discover are carrying incredible implications for businesses and just about anything where people are involved. The real threat and opportunity in technology's disruption lies in the evolution of customer and employee behavior, values, and expectations. Companies are faced with a quandary as they invest resources and budgets in current technology and business strategies (business as usual) versus that of the unknown in how those investments align, or don't, with market and behavior shifts. Technological advances matter because they play a fundamental role in the creation of wealth, improve the quality of life, have an impact on economic growth, and can even transform societies. Also recesses ion and economic crisis proved that guaranteed revenue streams are diminishing and so companies need to continuously innovate and experimenting, and nothing is risk-free. Finally, technology is evolving really quickly and consumer and business strategies need to keep up. This is a time of Digital Darwinism — an era where technology and society are evolving faster than businesses can naturally adapt. This sets the stage for a new era of leadership, a new generation of business models, charging behind a mantra of "adapt or die." (Solis, 2014). EU and the USA as the leaders of technological revolution are facing similar challenges in the graphic arts industries. While the profit margins in USA are in expected range according to Quarterly Financial Report which implicates that the industry continues to generate profits despite declining volume of shipments, meaning that weak companies are exiting or being forced out of the business, and that the efficiencies of consolidation are being realized. This remains a challenging environment that tests the management and marketing skills of industry owners and executives. Maintaining this general range of profits for the last four years despite having about 4,000 fewer establishments and approximately 45,000 fewer employees shows the tenacity and adaptability of print businesses that is not often recognized. (Webb, 2014). In EU where 95% print business are small and middle sized companies which employ less than 20 workers is very prone to closure in such cutthroat environment. At recent figures the graphic arts industry in EU had 134.000 companies with 850.000 employees (Integraf, 2012) with Italy, Germany, UK having the highest number of companies. If we look at recent data in Figure 1 there is a linear steady decline in investments and companies in graphic arts in Germany which is often associated with the flagship country for the printing industry (MMB, 2013).

Figure 1: Number of companies in the printing industry

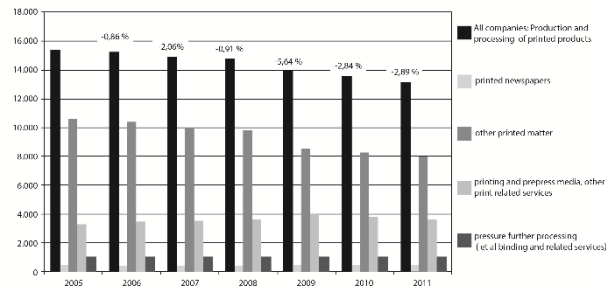


Figure 1: Turnover in the printing industry

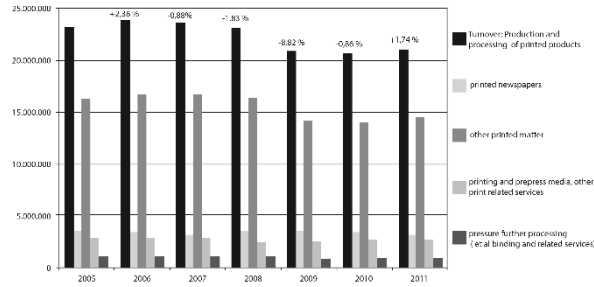


Figure 1: Gross investment in the printing industry

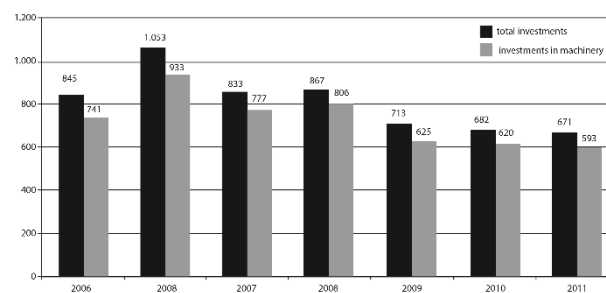


Figure 1: Economic trends in the German printing industry (MMB, 2013)

Some of the problems which influences these trends are the economic crisis, change of the behavior of the customers, decline in print advertising spending and overcapacity which is seen by many companies as the largest problem. Previously published figures show the scale of the issue. Between 2006 and 2009, the European print industry's productive capacity increased by 30%, but aggregate demand for the product by only 1%. This means that investment and productivity cycles are out of synchronization. The offset printing sector alone is estimated to have excess capacity of some 15-20%, while for the web offset and rotogravure sector analysts have recently indicated an overcapacity of 25-30%. Other threats and their perception by the industry is presented in Figure 2 (Intergraf, 2011)

Factors impacting on companies

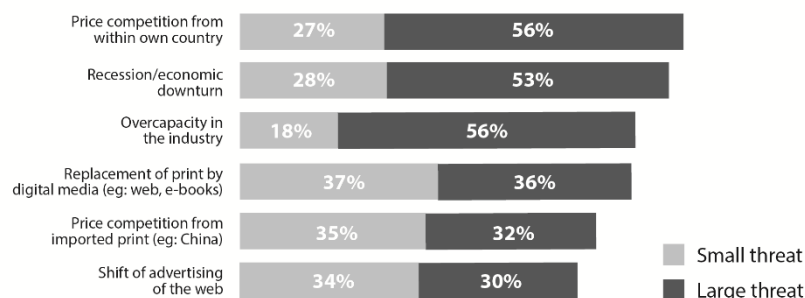


Figure 2: Factors impacting companies

The strategies to overcome these threats is to cut costs, invest in new technologies/alternative technologies and in new printing equipment. All surveyed companies and other industry partners agreed that the main investment needs to be put in new knowledge.

Strategies being considered in the short/long term

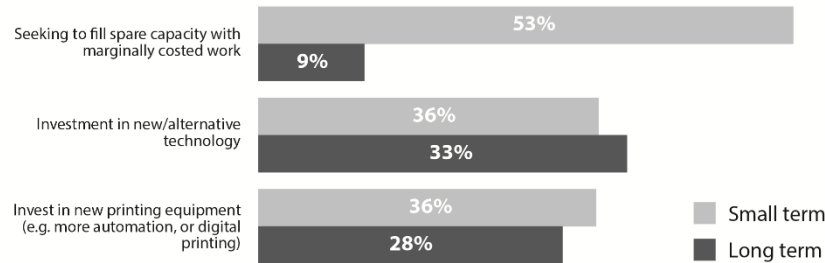


Figure 3: Strategies being considered to overcome threats to graphic arts business

2. NEW TRENDS AND OPPORTUNITIES

The question arises which are these new technologies or knowledge which can help graphic arts companies to survive structural problems and also the digital darwinism of the 21st century. Drupa as the pinnacle of new technology showcase which is held every 4 years already published the main topics on their website (Figure 4)



Figure 4: Trends and topics forwarded by the Drupa fair (Drupa, 2014)

As we can see the topics are: print, functional printing, packaging production, multichannel, 3D printing and green printing. In the next section we shall give a small overview of the current state in all these areas with some representative examples.

2.1 Print

The prepress part of the conventional and digital printing still moves into more workflow automation with smart templates which separates content from design and using maximum potential of multichannel distribution. These trends underline the need for a very flexible, highly personalizable technologies which can print very short runs on wide range of different substrates. Digital print is growing because it allows print suppliers to improve the levels of service they offer to customers, as well as opening new opportunities and helping them to make money. Increasing versioning and personalization helps make print more targeted to end users which is increasingly important as the digital world continues to become more and more connected. In a study by Pira (2013) "The Future of Digital Printing to 2024". In 2013, the digital print market was worth \$120.9 billion in constant 2012 dollar values, or \$131.0 billion in current dollar terms that

take into account inflation and currency exchange rate fluctuations. This is the equivalent of 1.13 trillion A4 size prints manufactured by print-for-profit service providers and packaging converters. The total digital market will reach 225% of the 2013 value by 2024. The segmentation between different technologies is presented in Figure 5.

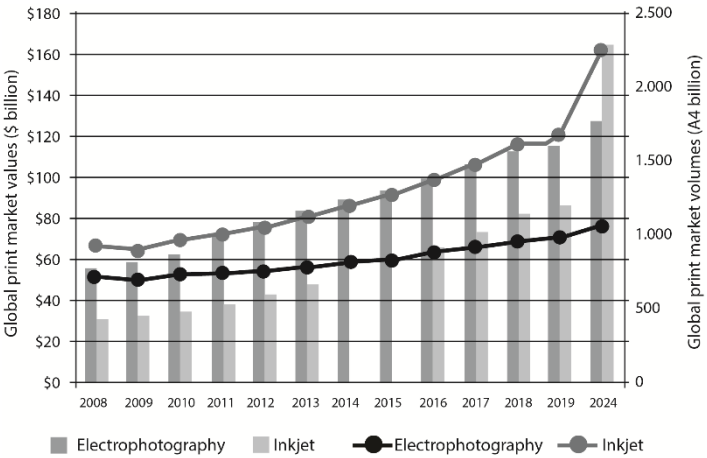


Figure 5: Trends in digital printing rise to 2024

In terms of future forecasts, the report states that over the next ten years or so, the most dynamic area for change will be in the fields of packaging. Cartons, rigids, flexibles, metal and corrugated are sectors that will take up digital production methods. Future growth predictions for printed packaging are all positive with increases in volume and value, with no substitution for electronic versions. Digital print is being used even beyond the graphics and packaging sectors. These applications include textiles, ceramic tiles, flat and round glass, decorative laminates, automotive applications, electronic and photovoltaic products, bio-medical and many other promotional/miscellaneous items. The other printing technology which has a rise in volumes and profits is the flexography printing process. This rise is mainly driven by the packaging sector with transition from rigid to flexible packaging which suits flexography the most. Already in 2011 presented in Pira report (Pira, 2011) this trend was noticeable which can be seen in Figure 6. The global flexo printing and converting market reached \$136 billion for the full year 2011, projected to grow steadily over the next five years at a growth rate of 3.8% in current terms and by 2.1% growth per annum in real terms from 2011 to 2016.

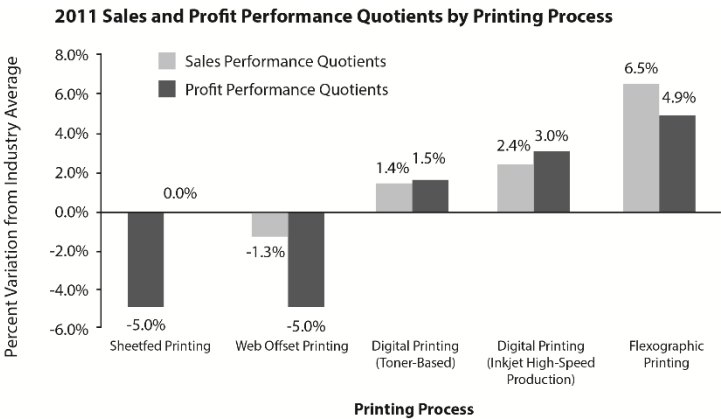


Figure 6: Smithers Pira estimation of Sales and Profit Performance by Printing Processes (Pira, 2011)

2.2 Functional printing

Some of the common applications of functional printing are 3D printer, printed electronics and RFID. Other application of functional printing may include production of sensors, solar cells or QR

or bar code, OLED displays, OLED lightening and batteries. The printing can be visible or invisible depending upon the nature or type but it should have some common functional characteristics of functional printing. One of the key driver of the functional printing market is the field is very diverse and new. Due to this fact there is no real market leader of the market. In other words, functional printing is a type of production process which controls and deposits the selective patterns upon the material. The technology employed presently is limited to printing of graphics but functional printing is the extension of the printing. Last decade, lighting and display markets have been witnessing major development in regard to functional printing technology. This can also be seen as the biggest driver for the market. According to a report by IDTechEx (IDTechEx, 2014) the total market for printed, flexible and organic electronics will grow from \$23.97 billion in 2014 to \$70.39 billion in 2024. The majority of that is OLEDs (organic but not printed) and conductive ink used for a wide range of applications. On the other hand, stretchable electronics, logic and memory, thin film sensors are much smaller segments but with huge growth potential as they emerge from R&D.

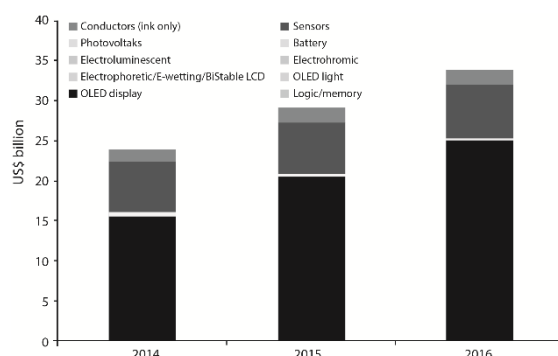


Figure 7: Market forecast by component type in US\$ billions* (IDTechEx)

OLED lighting is an emerging solid-state lighting technology. It potentially provides a route into the large and growing global lighting market. The lighting market is however complex as it is a highly fragmented space thanks to the existence of a broad technology mix and a diversity of customer needs. IDTechEx forecast that the market will grow to 1.9 billion USD in 2025 (optimistic scenario). The market growth will however be very slow until 2019 where the overall sales at panel level will remain below 200 million USD globally. Other printed electronics products also reported by separate IDTechEx (IDTechEx, 2014) reports find that in 2014, the total RFID market is worth \$8.89 billion, up from \$7.77 billion in 2013 and \$6.96 billion in 2012. This includes tags, readers and software/services for RFID cards, labels, fobs and all other form factors. IDTechEx forecast that to rise to \$27.31 billion in 2024. In retail, RFID is seeing rapid growth for apparel tagging – that application alone demands 3 billion RFID labels in 2014 – which still has some way to go with RFID penetrating about 7% of the total addressable market for apparel in 2014. RFID in the form of tickets used for transit will demand 700 million tags in 2014. The tagging of animals (such as pigs, sheep and pets) is now substantial as it becomes a legal requirement in many more territories, with 425 million tags being used for this sector in 2014. This is happening in regions such as China and Australasia. In total, 6.9 billion tags will be sold in 2014 versus 5.8 billion in 2013. Most of that growth is from passive UHF RFID labels, with UHF tag sales overtaking HF and LF tag sales by volume in 2012. However, in 2013 UHF tag sales by value will only be 11% of the value of HF tag sales. Form factor is becoming a major driver shaping innovation and transforming the energy storage industry globally. This is fueled by the emergence of new market categories such as wearable electronic devices and Internet of Things, which demand thinness and flexibility. These new market categories will help the market for thin and flexible batteries reach \$300 million in 2024. Thin, flexible or printed batteries have commercially existed for more than ten years. Traditionally, the micro-power thin and printed batteries were used in skin patches, RFID tags and smart cards. Today, however, the composition of the target market is undergoing drastic change driven by the emergence of new addressable market categories. This trend has enticed many large players to enter the foray, starting to transform a business landscape that was once populated predominantly by small firms. The change in target markets is inevitably driving change in the technology landscape too. (IDTechEx, 2014) The market and technology landscape is complex. There are no black-and-white and clear

technology winners and the definition of market requirements is in a constant state of flux. Indeed, on the technology side, there are many solutions that fall within the broad category of thin film, flexible or printed batteries. These include thin lithium batteries, thin film lithium polymer batteries, curved lithium ion batteries, flexible supercapacitors, and printed zinc-based batteries. It is therefore confusing technology landscape to navigate and betting on the right technology is not straightforward. On the market side, many applications are still emerging and the requirements are fast evolving. The target markets are also very diverse and not overlapping, each with different requirements for power, lifetime, thinness, cost, charging cycles, fits-all solution. In general, wearable electronics is a major growth area for thin film and flexible batteries. Conventional secondary batteries may meet the energy requirements of wearable devices, but they struggle to achieve flexibility, thinness and light weight. These new market requirements open up the space for energy storage solutions with novel form factors. Indeed, the majority of thin film battery companies tell us that they have on-going projects in the wearable technology field. High-energy thin film batteries have the highest potential here followed by printed rechargeable zinc battery provided the latter can improve. Some of the applications of thin printed batteries are presented in Figure 8. This diversity of requirements means that no thin film battery solution offers a one-size.

Thin, Flexible, Printed Batteries



Figure 8: Application fields of printed batteries

2.3 Packaging production

Three main trends in packaging development according to FAO (FAO, 2014) are: bio-packaging, high-performance materials, and intelligent/functional packaging. Often these trends can merge into enhanced bio-packaging, supporting its gradual mainstreaming (through e.g. bio-replacement/drop-in bio-plastics). They are different driving forces for different segmentations in the packaging production. Major manufacturers of packaging are now looking to differentiate their products from those of their competitors by providing best possible biodegradable packaging products as per consumer demands. The demand for biodegradable packaging is increasing and will continue to increase as the companies utilize packaging like a medium to protect and promote the safety of the environment along with their products. Other factors influences the fast development and rapid growth of electronic smart packaging are:

- Ageing population
- Consumers are more demanding
- Consumers are more wealthy

- Changing lifestyles
- Tougher legislation
- Concern about crime and the new terrorism

Electronics and electrics are already used in packaging, from winking rum bottles and talking pizza boxes to aerosols that emit electrically charged insecticide that chases the bug. Electronic medication packs record how much is taken and when and prompts the user. Reprogrammable phone decoration has arrived. But that is just a warm up. The key enabling technology - printed electronics - often used with other conventional electronics - can make new packaging and product features feasible. Consequently, many leading brand owners have recently put multidisciplinary teams onto the adoption of the new paper thin electronics on their high volume packaging. It will provide a host of consumer benefits and make competition look very tired indeed. This is mainly about modern merchandising - progressing way beyond static print - and dramatically better consumer propositions. In a report by IDTechEx (2014) it has been revealed that the global demand for electronic smart packaging devices is currently at a tipping point and will grow rapidly to \$1.45 billion within 10 years. The electronic packaging (e-packaging) market will remain primarily in consumer packaged goods (CPG) reaching 14.5 billion units that have electronic functionality within a decade. Concerning biodegradable packaging a report by (ReportLinker, 2014) is now predicting that this market will grow at 18.05% CAGR to 2019 - a considerable about-turn from about a decade ago, when biodegradable packaging market was not considered to be one of any real significance. The report, "Biodegradable Packaging Market by Packaging Type (Plastic and Paper), by Applications (Food Packaging, Beverage Packaging, Pharmaceuticals Packaging, Personal & Home Care Packaging, and Others), and by Geography (North America, Europe, Asia-Pacific, and ROW) - Global Trends & Forecast to 2019", defines and segments the global biodegradable packaging market with an analysis and forecast for biodegradable plastic and paper packaging by types, applications, and geography by value as well as volume. The global biodegradable plastic packaging market is expected to grow at a CAGR of 18.05% from 2013 to 2019 to reach a value of \$8,415.20million. Due to increasing degree of consumer awareness, and generic and contract manufacturing activities in Europe and North America, the developed geographies are expected to register maximum growth. Country wise, the U.S. is the top consumer of biodegradable packaging product globally, and is also the largest market growing at a CAGR lower than the global average till 2019. Member countries of EU, Sweden, Switzerland, U.K., and Germany are the key markets in European biodegradable packaging market and constitute majority of the market size. While food packaging takes the topmost position in the biodegradable packaging market, with more than 70% share by value of biodegradable plastic packaging and more than 40% share by value of biodegradable paper packaging, maximum growth in the future is expected from the beverage packaging application segment. Plastics and polymers are the largest consumed raw material for the beverage packaging products and are being fast replaced by their biodegradable substitutes such as PLA, starch-based Plastics, PHA, and so on due to its ease in design, excellent barriers properties, and cost-effectiveness. The biodegradable packaging market is expected to witness fastest growth from biodegradable plastic packaging market, as it is a relatively new market with a great potential to capture existing market share from non-degradable conventional plastic packaging. Lack of interest of governments of many developed regions to provide incentives to promote the use of biodegradable packaging and price difference in conventional versus biodegradable packaging materials are primary factors curbing the growth of this market

2.4 Multichannel

Multichannel publishing is also developing fast gaining new grounds in combining versatile digital printing possibilities with other electronic devices. The main channel enablers are among others:

- Traditional web: Web sites, landing pages, micro sites, etc.
- Mobile: Mobile/Touch Web sites, web apps, native apps, etc.
- Social media: Facebook, Twitter, Google+, Flickr, Instagram, Foursquare, LinkedIn, etc.
- Traditional media: Print, Smart TV, digital signage

Digital contents and assets can be flexible re-used in multiple different mediums, whether in traditional websites, landing pages, e-mail newsletters or mobile apps, social-media channels or

even in print, TV or digital signage. Due to high segmentation and multichannel synergy many of multichannel marketing campaigns rely on combining different approaches. In one survey conducted by WoodWing Survey (2014) many of the users of multichannel printing still see printing as a very important part of the multichannel strategy.

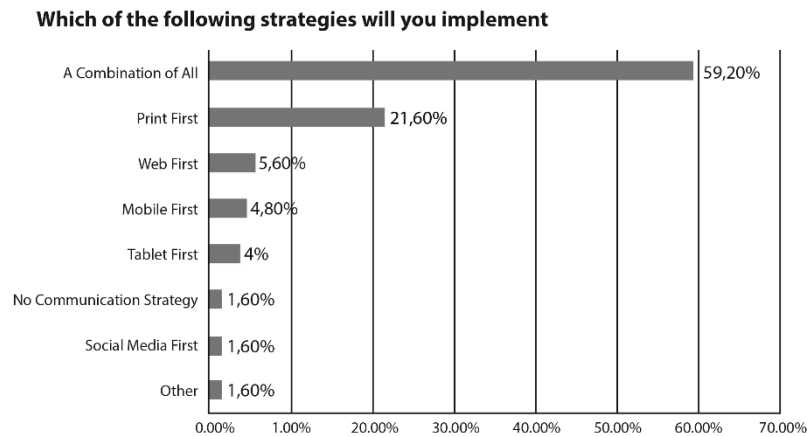


Figure 9: Multichannel segmentation from a survey by WoodWing

The drivers for multichannel market are listed as network and technological advancements, growing trends in digital marketing, emergence of advanced mobility options such as smartphones, tablets, and other hand-held devices and growing mobile marketing trend. The restraint for this market is changing dynamics of marketing channels, technological constraints of compatibility and customer privacy concerns. Proximity marketing and customer-centric solutions have been acknowledged as the opportunities in this market. Whereas, competitive rivalry in the digital marketing industry is the major challenge, companies are facing today. As digital media channel have a harsh competition between channels printing seems remains as a standalone channel which will have some future growth mostly based on variable data printing.

2.5 Printing

3D printing is on the brink of revolutionizing manufacturing. Also known as additive manufacturing, 3D printing uses digital models and special material deposition devices to build physical objects one layer at a time. Although they are nowhere near having the capabilities of a science fiction replicator, today's 3D printing machines have progressed leaps and bounds in a short time and are capable of fabricating complex components out of a variety of materials, including steel, aluminum, titanium, and different types of plastics. 3D printing is quietly crossing the chasm from interesting concept to legitimate production technology (PWC, 2014). Figures on sales and profit are going up just like the "hype" around this manufacturing technologies and makes 3D printing a primary emergent technology in 2014. The Gartner report predicted worldwide shipments of sub-\$100,000 3D printers grew 49% last year, reaching a total of 56,507 units. That rate of growth is forecast to rise to 75% in 2014, fuelling shipments of 98,065 units. It's the first time Gartner has put together a forecast for the sub-\$100,000 3D printer market so that's something of a rite of passage for the technology too. Gartner's forecast shows enterprises continuing to dominate 3D printer purchases over the next few years, with enterprises spending more than \$325 million in 2013 vs \$87 million in the consumer segment; and \$536 million in 2014 vs consumer spending of \$133 million. Combined end-user spending on 3D printers is predicted to hit \$412 million this year, up 43% from spending of \$288 million in 2012. While the analysis expects spending to increase 62% next year, reaching \$669 million. The 3D printing industry's traditional prime report, The Wohlers Report, 2013 edition, stated the following important developments in 3D printing applications, processes, manufacturers, and materials: "The market for 3D printing in 2012, consisting of all products and services worldwide, grew 28.6% (CAGR) to \$2.204 billion. This is up from \$1.714 billion in 2011, when it grew 29.4%. Growth in 2010 was 24.1%. The average annual growth (CAGR) of the industry over the past 25 years is an impressive 25.4% including CAGR 2010 – 2012 of 27.4%." (Taylor, 2014) According to research by Wohlers Associates growth of the low-cost (under \$5,000) "personal" 3D printer market segment averaged a

phenomenal 346% each year from 2008 through 2011. In 2012, the increase cooled significantly to an estimated 46.3%. Wohlers Associates believes the 3D printing industry will continue strong double-digit growth in forthcoming years, and the sale of 3D-printing products and services will approach \$6 billion worldwide. By 2021, Wohlers Associates forecasts the industry to reach \$10.8 billion. 3D printing is not just a huge so called disruptive technology but a strong synergy driver for other technologies like functional printing. Forbes predicts that electronics will be one of 7 industries most disrupted by 3D printing. According to Forbes (2013) "Designing and 3D printing electronics with optimal shape and styling properties will be common. 3D printing is ideal for the complex geometric features needed in small, compact electronic circuit boards that use multiple materials ranging from low conductivity plastics to high conductivity metal materials." There are substantive advantages of 3D printed electronics vs. traditional manufacturing technology that will drive the market's growth for these printers. Due to these factors, IDTechEx Market Research estimates the market for printed electronics (which equaled under \$5 billion in 2012) will grow rapidly to \$35 billion in 2020 and an astounding \$300 billion by 2030. As this chart indicates, the lion's share of growth in 3D printed electronics according to IDTechEx Market research will be in printing of OLED displays. This is a huge segment that Ceradrop has early mover advantage in (IDTechEx, 2014).

IDTechEx 2011-2021 Forecast

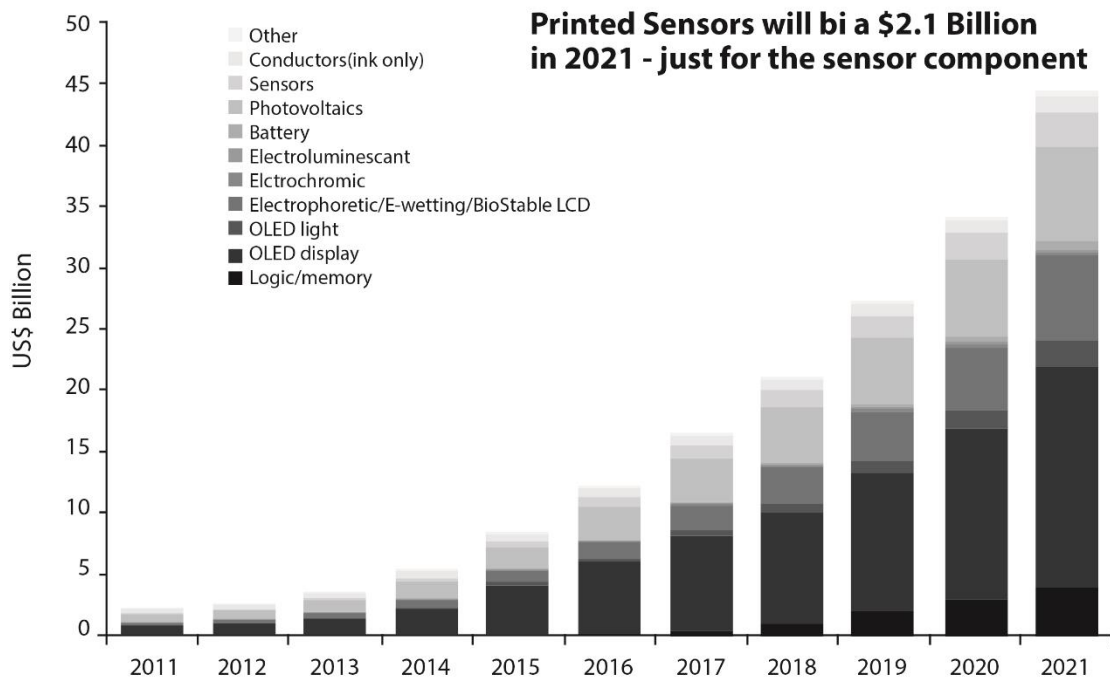


Figure 10: The Growth of 3D printed electronics

Some interesting blending of classical CMYK printing and 3D printing can be found in some specific product solutions and technologies. Selective Deposition Lamination (SDL) or paper 3D printing brings together the 3D technology paper and ink. This technology starts like any other with a 3D model in basic data formats with an additional software for applying colour to the 3D sliced model. The production process is explained in Figure 11. Paper sheets are deposited with selective application of adhesive (high density where the parts are and low density for the waste part). A new sheet of paper is fed into the printer from the paper feed mechanism and placed precisely on top of the freshly applied adhesive. The build plate is moved up to a heat plate and pressure is applied. This pressure ensures a positive bond between the two sheets of paper. When the build plate returns to the build height, an adjustable Tungsten carbide blade cuts one sheet of paper at a time, tracing the object outline to create the edges of the part. When this cutting sequence is complete, the machine starts to deposit the next layer of adhesive and the whole process continues until all the sheets of paper are stuck together and cut and the model is finished (Mcor, 2014). The printing part and the colour component is done by preprinting the colour outline of the

part on each page in the appropriate colour combinations using a modified 2D colour inkjet printer with water-based ink which permeates the paper, preventing any white edges on the part. A barcode is also printed on each page to ensure the pages are in the right sequence. The pre-printed stack is then inserted into the 3D printer, which initiates the process described above. Some examples of the printed full colour 3D products are presented in Figure 12.

How SDL Works

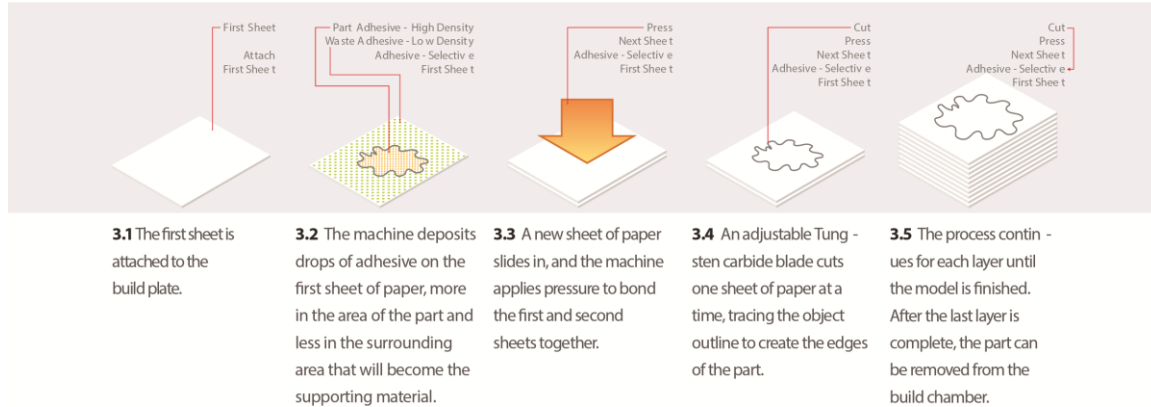


Figure 11: Selective Deposition Lamination process



Figure 12: Photorealistic 3D model printed by Mcor Iris 3D Color printer technology

Another crossover application of classical 2D printing with 3D printing technology is the hydrographics process. Hydrographics or HydroGraphics, also known as immersion printing, water transfer printing, water transfer imaging, or cubic printing, is a method of applying printed designs to three-dimensional surfaces. The hydrographic process can be used on metal, plastic, glass, hard woods, and various other materials. The Water Transfer Printing process is extensively used to decorate items that range from entire all-terrain vehicles and car dashboards, to small items like bike helmets or other automotive trim. Films can be applied to all types of substrates including plastic, fiberglass, wood, ceramics, and metal. For the most part, if the item can be dipped in water and can be painted using traditional techniques then the hydrographic printing process can be used. In the process, the substrate piece to be printed is pre-treated and a base coat material is applied. A polyvinyl alcohol film is gravure or ink jet printed with the graphic image to be transferred, and is then floated on the surface of a vat of water. After removing the piece from the water, a top coat is applied to protect the design. With multiple prints, hydrographics printing can achieve full 360° coverage of the part surface, including small crevices. Compared with airbrushing as an example the hydroprinting process is much quicker and far more complex and detailed designs can be applied. These examples show some niche possibilities of using classic printing equipment in conjunction with new 3D models and technology.

2.6 Green printing

The green industry focuses on making a profit while having a negligible (or even a beneficial) impact on the environment. Leaders make sustainability a key consideration in decision-making throughout the organization as they work to minimize both use and production of harmful chemicals, excess materials, and waste byproducts in the delivery of their goods and services. Going green is becoming increasingly attractive as a business strategy. As headlines scream of pollution and dwindling natural resources, green industry practices not only enjoy benevolent public sentiment and the psychic income of a lower carbon footprint, but increased cost savings, supportive government policies, and ever-increasing profitability as well. Trends in consumption, government policy, and costs all point towards even more green industry business opportunities in the years ahead (Franchise Help, 2014). Packaging producers, ink and substrate manufacturers and printers are also involved in this trend. Overall 54% of paper in Europe is made out of recovered used paper. The European paper business is at the vanguard of industrial recycling and two tons of wastepaper are recycled in the EU every second. In 2010 the paper recycling rate in the EU reached 68.8% percent and 90% of newspapers and corrugated boxes are made from recycled fiber (Intergraf, 2012). Beyond the simple elimination of heavy metals like lead, cadmium and mercury, which is mandatory in many markets, eco-friendly inks can come in a number of forms. The most common is the reduction or removal of volatile organic compounds (VOCs), a by-product of traditional solvent-based inks, which are a potential hazard for both the environment and human health.

As a result, the eco-friendly ink market has experienced a sustained period of growth over the last few years, a winning streak which is expected to continue for the foreseeable future. A 2010 study by Smithers Pira (Smithers Pira, 2010) estimated that the eco-friendly ink market will grow from €5.8bn in 2009 to nearly €7.2bn in 2014, with a strong compound annual growth rate (CAGR) of 4.5%. The use of eco-friendly inks and printing techniques is on the rise as the packaging world continues its drive to reduce its environmental impact. National and international governments are now adopting environmental regulations which specifically address the content of ink, like the European Union's EN 134323 standard on packaging compostability. Advances made in ink chemistry and printing technology over the last decade have yielded a host of solutions to the technical challenge of developing high-performance and eco-friendly printing techniques. As such, the challenge is not to create eco-friendly printing methods, but to achieve environmental goals while maintaining an uncompromising level of quality (Lo, 2012).

3. CONCLUSION

The figures and facts again strongly indicates that the ICT sector is having a huge impact on restructuring not just business models and technologies, but also human behavioral patterns. The classic printing of words, sentences and images formed in books, newspapers and other paper products are under constant pressure by internal (overcapacity, dumping prices) and external (technological change, government regulations) which induce a strong investment in new technologies. The new directions already on the horizon are not to transfer words, ideas on paper or other substrates but pass an electron from one point to another or build 3D structure from polymer particles. But how much of the new "printing" technologies can really be implemented in the classic print shop is still unclear. While the low cost of 3D printers just like the DTP in 80's move a large amount of work from the print shops or companies to fragmented singular customers or independent agencies and designers some other new technologies like functional printing require more substantial investments. We cannot forget that 3D printing inherently comes from rapid prototyping with deep roots in mechanical engineering. Also the "printing" of biological materials will not be printed in print shops but laboratories with sterile environments. The graphic art printers will have to compete with these parts of the industry for the "printing" part. Also in functional printing the question remains how much of the "printing" will be adopted and transferred to printers and how much of the volume share will be directly implemented on the production lines of large companies. Or we can say there is a change from manufacturing to serve industry. Package printing (bio and intelligent) and customized interactivity enhanced printed products (brochures, direct mail, magazines) remain a secure ground for some time. There are numerous possibilities for the printers to implement new technologies into their business models. It requires investments mostly in new knowledge which indicates that it will be the greatest asset in the future which bring new revolutionized industry. Investment in this new knowledge

and innovations models which can help them to survive the Digital Darwinism. As Heraclitus said "Everything changes and nothing stands still".

4. ACKNOWLEDGMENTS

This work was supported by the Serbian Ministry of Science and Technological Development, Grant No.:35027 "The development of software model for improvement of knowledge and production in graphic arts industry".

5. REFERENCES

- [1] Boucher, B.: Pellow Predicts: 2013 Top 10 Trends for the Printing Industry, The Digital Nirvana, URL <http://thedigitalnirvana.com/2013/02/pellow-predicts-2013-top-10-trends-for-the-printing-industry/> (last request 15-8-2014)
- [2] FAO: Tackling food loss and waste with bio-based packaging, URL <http://www.fao.org/forestry/trade/86447/en/> (last request 21-8-2014)
- [3] Forbes: Our Future With 3D Printers: 7 Disrupted Industries, URL <http://www.forbes.com/sites/ehrllichfu/2013/10/29/our-future-with-3-d-printers-7-disrupted-industries/> (last request 23-8-2014)
- [4] Franchise Help: Green Industry Analysis 2014 - Cost & Trends, URL <https://www.franchisehelp.com/industry-reports/green-industry-report/> (last request 22-8-2014)
- [5] IDTechEx: Smart Packaging Comes To Market: Brand Enhancement with Electronics 2014-2024, URL: <http://www.idtechex.com/research/reports/smart-packaging-comes-to-market-brand-enhancement-with-electronics-2014-2024-000360.asp> (last request 22-8-2014)
- [6] IDTechEx: Flexible, Printed and Thin Film Batteries 2015-2025 URL <http://www.idtechex.com/research/reports/flexible-printed-and-thin-film-batteries-2015-2025-000410.asp> (last request 15-9-2014)
- [7] IDTechEx: Printed, Organic & Flexible Electronics Forecasts, Players & Opportunities 2014-2024, URL <http://www.idtechex.com/research/reports/printed-organic-and-flexible-electronics-forecasts-players-and-opportunities-2014-2024-000404.asp> (last request 25-8-2014)
- [8] IDTechEx: RFID Forecasts, Players and Opportunities 2014-2024, URL Read more at: <http://www.idtechex.com/research/reports/rfid-forecasts-players-and-opportunities-2014-2024-000368.asp> (last request 24-8-2014)
- [9] IDTechEx: Applications of 3D Printing 2014-2024: Forecasts, Markets, Players URL <http://www.idtechex.com/research/reports/applications-of-3d-printing-2014-2024-forecasts-markets-players-000385.asp?viewopt=desc> (last request 23-8-2014)
- [10] IDTechEx: The impending surge in e-packaging and intelligent packaging with printed and flexible electronics, URL <http://www.idtechex.com/research/reports/smart-packaging-comes-to-market-brand-enhancement-with-electronics-2014-2024-000360.asp?viewopt=showall> (last request 11-8-2014)
- [11] Intergraf: Print Media in Times of change, URL http://www.intergraf.eu/images/PMG_WEB.pdf (last request 24-8-2014)
- [12] Intergraf: The Future of the European printing industry – in our own hands, what the industry says, URL http://www.intergraf.eu/dwl/SociallyResponsible_Study_ENG.pdf (last request 24-8-2014)
- [13] Lo Chris: Supporting eco-friendly packaging: green inks, URL <http://www.packaging-gateway.com/features/featureeco-friendly-ink-uv-flexo-biodegradable-ink/> (last request 25-8-2014)
- [14] Mccor Technologies: How paper-based 3d printing works, URL <http://mccor technologies.com/resources-white-paper/> (last request 1-9-2014)
- [15] MMB-Institut für Medien- und Kompetenzforschung: „Strukturwandel in der Druckindustrie – Eine Branchenanalyse zur Ermittlung der strukturellen Veränderungen in beschäftigungsintensiven Teilbranchen der Druckindustrie“, MMB-Institut für Medien- und Kompetenzforschung, page 3–11, [2013].
- [16] Pricewaterhouse Coopers LLP: 2014 10 Technology Trends for Business, , URL <http://www.pwc.com/us/en/advisory/10-business-technology-trends.jhtml> (last request 12-9-2014)

- [17] PWC: Digital IQ 2014 10 Technology Trends for Business, URL <http://www.pwc.com/us/en/advisory/assets/pwc10technologytrends2014.pdf> (last request 29-8-2014)
- [18] Report Linker: Biodegradable Packaging Market by Packaging Type (Plastic and Paper), Applications (Food Packaging, Beverage Packaging, Pharmaceuticals Packaging, Personal & Home Care Packaging) & by Geography (North America, Europe, Asia-Pacific, and ROW) - Global <http://www.reportlinker.com/p02107862-summary/Biodegradable-Packaging-Market-by-Packaging-Type-Plastic-and-Paper-Applications-Food-Packaging-Beverage-Packaging-Pharmaceuticals-Packaging-Personal-Home-Care-Packaging-by-Geography-North-America-Europe-Asia-Pacific-and-ROW-Global-Trend.html> (last request 22-8-2014)
- [19] Smithers Pira: The Future of Digital Printing to 2024, URL <https://www.smitherspira.com/market-reports/printing/digital-printing-industry-future-mThe-Future-of-Digital-Printing-to-2024arket-analysis.aspx> (last request:10-9-2014)
- [20] Smithers Pira: Global Environmentally Friendly Inks Market Poised to Reach almost €7.2 billion by 2014, URL <https://www.smitherspira.com/market-reports/global-environment-friendly-inks-market-poised-to-reach-almost-eur7-billion-by-2014.aspx> (last request 23-8-2014)
- [21] Smithers Pira : The Future of Flexographic Printing to 2016, URL <https://www.smitherspira.com/market-reports/printing/flexographic-printing-industry-future.aspx> (last request5-9-2014)
- [22] Solis, B.: Digital Darwinism: How Disruptive Technology Is Changing Business for Good, Wired online magazine , URL <http://www.wired.com/2014/04/digital-darwinism-disruptive-technology-changing-business-good/> (last request: 6-8-2014)
- [23] Taylor S.: Trend Evolution: 3D Printing Trends (Part 1), URL <http://3dprintingindustry.com/2014/02/24/trend-evolution-3d-printing-trends-part-1/> (last request 23-8-2014)
- [24] Webb, J.: Industry Profits Remain Rangebound but Positive, Show Effects of Consolidation and Market Adaptation, WhatTheyThink Economics & Research, URL <http://blogs.whattheythink.com/economics/2014/09/industry-profits-remain-rangebound-but-positive-show-effects-of-consolidation-and-market-adaptation/> (last request: <10.09.2014.>).
- [25] WoodWing: WoodWing Survey "Trends 2014": Multi-channel top of the agenda – print to survive, URL <http://www.woodwing.com/en/Newsflashes/20140129-woodwing-survey-trends2014-multi-channel-top-of-the-agenda%E2%80%93print-to-survive> (last request 20-8-2014)

Special Printing Applications and Materials

"INFRAREDGRAPHIC"® SECURITY PRINTING TECHNOLOGY MERGING V AND Z SPECTRUM

Žiljak Vilko¹, Agić Darko², Politis Anastasios³, Pap Klaudio⁴

¹Fotosoft, Zagreb, Croatia

²Croatian Academy of Engineering, Zagreb, Croatia

³Graphic Arts Technology, Athens TEI, Greece,

⁴Faculty of Graphic Arts, Zagreb, Croatia

Abstract: Graphic products containing information that can be recognized with infrared camera are introduced. Multicolor infrared printing that camouflages planned hidden graphics is developed. A hidden image that exists in reproduction is added, but can be visualized with the aim of ZRGB camera, and is scanned into Z record (Žiljak V. et al, 2012) (Žiljak V. 2013). Reproduction containing two images for two spectral domains can not be copied or altered, while today's scanning technique does not accept collectiveness of visual and infrared spectrum (Uglješić et al, 2014). Conventional banknotes and valuables as first and top rate graphic product contain only one infrared dye. INFRAREDGRAPHIC® makes possible a large number of tones on the same document in two set-up conditions: V-visual, and Z- infrared. The work approves merging of two graphics, where Z graphic is halftoned with new individualized stochastic screens, that are in function of high quality stealthy information in printing procedures. The proof for merging possibilities of two independent images is demonstrated in two extreme areas. First: camouflage military uniform with hidden graphics. Second example is micro infrared image containing textual information in invisible QR-code mode. Results of double security images are based on "twins theory" of colors. The work displays spectrograms of some twin colors that allowed successful appliance of investigations results of light absorption in visual and infrared spectrum.

Key words: security printing, IRDMark, hidden image, camouflage uniform

1. INTRODUCTION

Marking out an graphic product containing information recognised with infrared camera is introduced. An multicolor infrared printing is developed that camouflages an planned hidden graphics. Visual and Z domains are combined to develop IRG marking. With complete collate V and Z design, we have two graphics, V and Z, that have not any common connection.

A hidden image is added, existing in reproduction, but observed only with ZRGB camera, scanned as Z record. Reproduction carrying two images for two spectral domains can not be copied or rearranged, while up to date scanning technique does not connect collectiveness visual and infrared spectra. Conventional banknotes as a top valuable graphic product are carrying only one IR dye. INFRAREDGRAPHICS® enables infinite number of color hues on the same document in two stages: V-visual and Z-infrared. This work displays merging two graphics, where Z-graphic is halftoned with new individualised stochastic screens, that are in function of better information hiding with printing procedures. The proof on merging possibility of two independent images is demonstrated in two extreme fields: first camouflage military uniform with a hidden graphics, and second: infrared micro image carrying a textual information in a QR invisible shape. The results of double securing images are based on 'twins color' theory. References on spectrograms of dual defined colors that facilitated efficacy of investigations about light absorption characteristics in visual and infrared spectrum are presented.

Security printing of valuables always used dyes with characteristic out of human visual response. Dedicated instrument aided observations for any forensic purpose were used. Today we are surrounded with security cameras with a useful response to discover dye properties on our cloths and other surrounding materials or media in visual and infrared spectrum.

Double monitoring of circulation, especially people, field of computer aided instrumental detecting everything surrounding us is widened. Statements about truth determining got new tools. Software development for visual and infrared spectra in various fields of detection and reproduction is foreseen.



Figure 1: four security cameras on elementary school entrance

2. STANDARD DYES SYSTEM BROADENING

Flora, fauna and variety of natural objects have its specific dyes, possess specific absorption abilities in ultraviolet and infrared solar irradiation. Our neighborhood is more and more surrounded with cameras detecting UV, Visual and IR reflection. We measure colorate properties in nature for purpose of creating clothes with dyes that respond in the same way. We investigate radiance impact in range from 200 to 1300 nm for vegetative, animal and synthetic produced dyes. For this investigation purposes, selected floral examples are chosen, with direct measuring of their spectra.

Figure 2 shows dandelion, clover leaf, clover bloom spectra, integrating domain from visible begin till NIR-900 nm. Clover leaf appears 'as white' in NIR domain, while dandelion and clover bloom render some more absorption, and slightly appear in Z point of NIR spectra. InfraredGraphics starts its designers activity at the same spectra we got from flora, fauna and printing inks. Common fact is continuous spectral curves in visual and infrared domain. Floras very complex structure continues its specific absorption in NIR spectrum. There is no break, as it is in human vision system. We do not 'see' above 700 nm, and that fact is used for developing a new graphic security system. For conventional printing we prepare prepress settings that is carrying separated data for RGB and Z-spectrum.

Our goal is to find printing inks that will have the same spectral characteristics as matter and substances in nature. That is the ground of introducing 'new color management' that respects light absorption in visual and near infrared spectra. Colors are described with three dimension values, such as computer applications device dependent RGB (red, green, blue) or HSB (hue, saturation, brightness), or colorimetric models such as XYZ, $L^*a^*b^*$, $L^*u^*v^*$, etc. Similar to such kind of description, human visual system also employs three separate receptors for color experience, while forming ultimate colors and tones perception. Light absorption measurement in near infrared domain is interpreted as 'gray scale', while that the way that it can be instrumentally registered: Z-camera, monitoring camera, infrared camera. Z-value that describes light absorption from analysed matter at 1000nm is the fourth value in broadened color dyes system. The 700 nm limit, where visible part terminates, is ideal to establish a new graphic security method in printing procedures, enigmatics, non-visible textile marking, books, leather, etc. Graphic will be 'seen' with instruments adjusted for recognising and recording of Z-value. Characteristic of human eye-vision, that we term as '700 nm break', inspired a new designers creation system of generating, disengaging, recognizing and combining of two images that exist on the print.

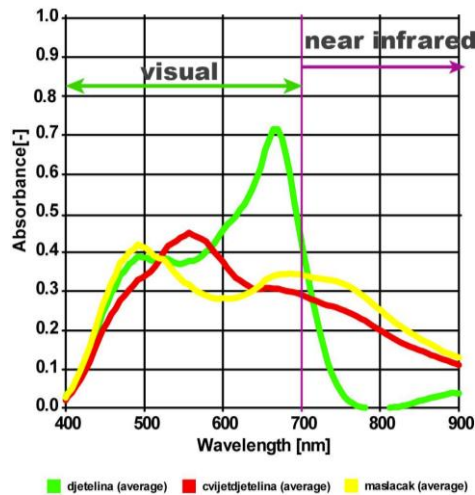


Figure 2: V and IR spectra from natural examples: dandelion, clover lief, clover bloom

3. OPERATIONALISATION OF BROADENED VISION AND VISUALISATION SYSTEM

Marking and camouflage imply observing with visual and infrared Z-RGB camera. System of double or twin color pairs is established for textile printing, fulfilling the same visual response, but different in NIR response. This task is to solve problem of equality of colors in visual, but planned diversity in infrared spectrum.

Present camouflage clothing dealt only visual equalising of dyes and nature. We intend to widen knowledge on light reflexion and absorption forming 'new color/colorant management' (Vujić et al, 2014). Clothing marked with IRGraphics acquire new function. Recognizing and differing these that wear such cloths will find various examples. For instance, pupils who will be on a different way recorded while entering and getting out from school, will be examined in a way that existing camera system offers (Vujić et al, 2014), Figure 1.

Into the informations system we are introducing collectiveness of color vision and material properties, so we can equalise the space where non-natural (artificial) dyes are applied, with the space coming from nature.

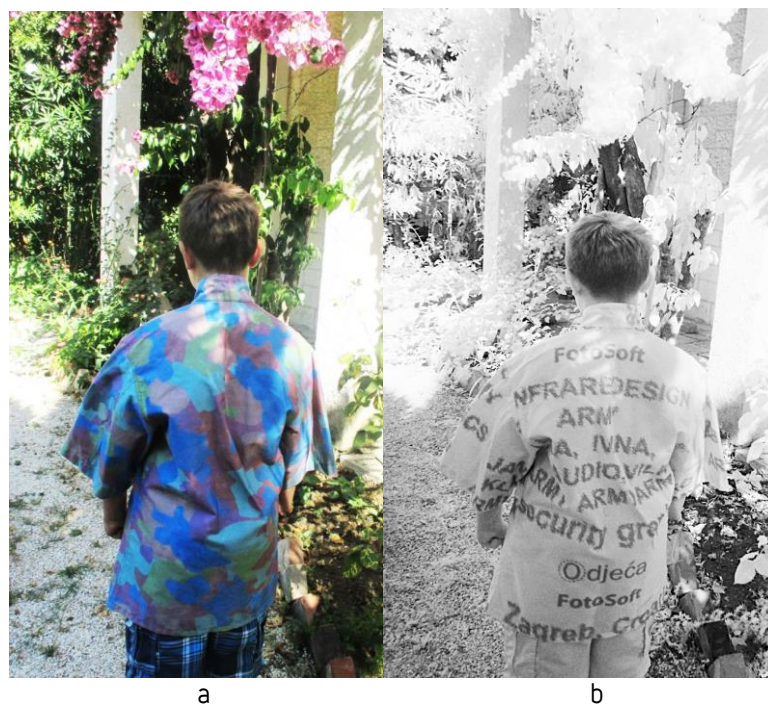


Figure 3: Visual (a) and infrared recording with ZRGB camera (b) (Žiljak et al 2011).

CMY+K printing inks combinations do not always fit all needable color combinations of twin dyes, so introducing extra dyes is necessary. In such combinations careful adjusting of spectral curves is required, so desired visual outfit of 'equal' colors is achieved.

Twin pairs are dedicated pairs of colors that in visual domain have the same color response and (mostly) identical spectral curves, where colorimetric yield is ΔE criteria. In near Infrared spectrum their spectral curves differ. Z-camera detects the difference, and Z-value analysis quantifies it. Such twins are achieved with process dyes mixtures, and especially with spot dyes developed for further mixtures. Depending on type and composition of mixed component, different responses for visual and IR spectra are achieved.

4. STOCHASTIC HALFTONING

According that double graphics appear in both systems, visual and infrared, in this case – printing on textile, applying dedicated screening system, additional security elements and printing effects can be achieved. Various examples of merging text, portrait, sketch, with personalized and needle-effect screening are performed (Vujić, 2014). Realisation was on textile fabric, Figure 4, with a colorful masking design, containing QR code.

For spectral shift demonstration, barrier scanning of canvas, QR code in camouflage design is presented. The selected camouflage dyes are closest to floral dyes that surround us. Each dye includes two different material compositions. Their spectra differ in near infrared spectrum. For all dyes the same light absorption value at 1000 nm was defined.



Figure 4: Camouflage design on fabric, with hidden text and QR code

The aim is to equalize Z-image on the whole camouflage design. All letters parts and QR code are of the same Z-intensity. QR code can not be seen with bare eye. Only IR camera (ZRGB camera) with adequate QR reading software can detect the hidden text, Figure 6.



Figure 5: Camouflage design with barrier scanning at 570 (a) and 715 nm (b)

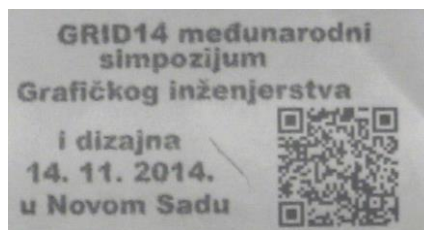


Figure 6: Camouflage design (fig. 5) with Z-barrier scanning at 1000 nm

In example (Figure 5) barrier at 570 nm cut off the yellow component. That is already enough for graphics appearance, that will fully appear at 1000 nm. 715 nm barrier stopped magenta experience. Till 770 nm only cyan vision left. Barrier scanning was performed with Projektina 4500 Model.

5. MATHEMATICAL MODELS

For each combination of materials and corresponding twin pairs of dyes, new, updated algorithm is needed. Several algorithms are developed during last six years, that with more or less success accomplish mutual two graphics hiding. On that 'hiding test' a new way of judgement for planned colors is established. An error in color twins manifests as appearance of a opposite non-wanted image, in visual as well as in infrared spectrum.

Mathematical models of individualised screens are presented in book: (Vujić, 2014) (Žiljak et al, 2009). Supplementary methods are developed, dealing with additional human eye visual features. Screening, item and methods of displaying various shades according to its coverage, but the same ink hue, is known for more than 200 years. It uses human visual system ability not to distinguish screen elements smaller than 1/40 of a centimeter. Opposite, infrared design implements low ruling systems, but with individualised approach, indented shapes, till to needle shaped elements.

Recent INFRAREDESIGN mathematical models are proposed in articles that deal with printing on polymers, transparent and opaque media with two different solutions. (Frišić et al, 2013) (Vujić et al, 2013). First solution includes three independent variables so that each value of C_{40} , M_{40} i Y_{40} depends on starting C_0 , M_0 , Y_0 values. Second solution comprehends six independent variables, where additional differences between starting process dyes values combinations: $C_0/M_0 + C_0/Y_0$; $Y_0/M_0 + Y_0/C_0$; $M_0/C_0 + M_0/Y_0$. For each material and belonging dyes experimentally matrix with parameters from regression equations are solved, including extended correlation model of dependence $[C_{40}, M_{40} \text{ i } Y_{40}]$ o $[C_0, M_0, Y_0]$.

Models are published, where appliance of INFRAREDESIGN for military uniform, documents and valuables. Detailed description and references for mathematical models are presented in the work for Croatian Academy of Engineering (Žiljak, 2013).

6. CONCLUSION

Security printing is broadened with procedures defined with INFRAREDESIGN® theory (Žiljak I, 2008), and two graphics merging. Appliance does not use special dyes. In each dyes set components that will generate effect that will be detected in infrared domain. For all procurable dyes spectral analysis in domain from 700 to 1000 nm has to be performed, so the starting point for recipes for twin color pairs formation can be set. In that experimental work we distinguish spectral domain in three parts: visual, transient (700-800 nm) and Z spectrum (800-1000 nm). Z measurement ensures controlled content of intensive INFRA color. In the case of broadened approach, that dye can be also a UV dye that would correspond to spectrum domain from 200-400 nm. Nevertheless, many dyes have astonishing properties in the eight octave of the sun spectrum. Defining spectral curves is important, while that is starting phase of dual pairs defining, described as 'twin pairs, twins'. Z measurement system and Z camera will quantize the system and define separate relations between twins, so needable intensities between double images can be performed. Application is in design of military uniforms that need camouflage in visual and infrared spectrum. A new new value is added, marked as 'Infrared uniform annotation', with graphics in inner or outer side of the uniform. A invisible QR code for Z spectrum purposes can be added. For decoding a dedicated camera with appropriate text recognition ability after scanning is needed.

7. REFERENCES

- [1] Friščić, M., Međugorac, O., Tepeš, L., Jurečić, D.: "INVISIBLE INFORMATION ON THE TRANSPARENT POLYMER FOOD PACKAGING WITH INFRA V/Z TECHNOLOGY", TTEM volume 8 (4), pages 1512 -1519., [2013].
- [2] Uglješić, V., Žiljak Stanimirović, I., Koprivnjak, S., Žiljak Vujić, J., Bernašek, A.: "THE TWEENS DYES PRINCIPLE ON THE CAMOUFLAGE UNIFORM", Međunarodna konferencija tiskarstva, dizajna i grafičkih komunikacija Blaž Baromić, [Senj, 2014].
- [3] Žiljak, I., Pap, K., Žiljak-Vujić, J.: "INFRARED SECURITY GRAPHICS", Zagreb: FotoSoft, 2009 [monografija]. ISBN 978-953-7064-11-2, Zagreb, 2009
- [4] Žiljak, I., Pap, K., Žiljak-Vujić, J.: "INFRAREDESIGN", Zagreb: Fotosoft, 2008 (monografija), ISBN 978-953-7064-09-9, Zagreb, 2008
- [5] Žiljak, V.: "COLLECTIVENESS OF VISUAL AND Z-INFRARED SPECTRUM IN THE SECURITY PRINTING" Annual 2013 of the Croatian Academy of Engineering [Zagreb, 2013], pages 373- 396.
- [7] Žiljak Vujić, J.: "SIGURNOSNA GRAFIKA, INDIVIDUALIZACIJA VRIJEDNOSNIH PAPIRA I RASTERSKI MODELI", Tehničko veleučilište u Zagrebu, page 180., [2014].
- [8] Žiljak-Vujić, J., Agić, A., Agić, D., Politis, A. E.: "EXPANDING DOUBLE HIDDEN INFORMATION WITH INFRARED DYES", 46 Annual International conference on graphic Arts and media Technology Management and Education, [Athens, Greece, 2014].
- [9] Žiljak, V., Pap, K., Stanimirović, I., Vujić, J.: "MANAGING DUAL COLOR PROPERTIES WITH THE Z- PARAMETER IN THE VISUAL AND NIR SPECTRUM, Infrared Physics & Technology, volume 55 (4), [2012].
- [11] Žiljak, V., Pap, K., Žiljak-Stanimirović, I.: "DEVELOPMENT OF A PROTOTYPE FOR ZRGB INFRAREDESIGN DEVICE", Technical Gazette, volume 18 (2), pages 153-159., [2011].
- [12] Žiljak Vujić, J., Žiljak Stanimirović, I., Bjelovučić kopilović, S., Friščić, M.: "ZAŠTITA PROZIRNE SAVITLJIVE PLASTIČNE AMBALAŽE POSTUPKOM INFRAREDESIGN®", POLIMERI, volume 34 (2-3), pages 42-46., [2013].

OFFSET PRINTING BY THE MICROCAPSULES – INFLUENCE ON THE PROPERTIES OF PAPER SUBSTRATE

Raša Urbas¹, Živko Pavlović², Srđan Draganov² and Urška Stankovič Elesini¹

*¹University of Ljubljana, Faculty of Natural Sciences and Engineering,
Department of Textile, Ljubljana, Slovenia*

*²University of Novi Sad, Faculty of Technical Sciences,
Department of Graphic Engineering and Design, Novi Sad, Serbia*

Abstract: Microcapsules have been for many years successfully used in the graphic technology – printing processes. Their use has different purposes, depending on the type and structure, as well as filling. Many times microcapsules are added on the surface of different materials with simple padding or spraying techniques but we must not forget that printing is also one of the application possibilities.

Regardless of their aim, microcapsules have been mainly applied to the surface of printing materials with flexo or screen printing, being mixed into the printing ink or varnish. The reason lies in the printing technology, which causes no damages to the microcapsules in the printing ink. Because other printing technologies have rarely been used, we wanted to conduct a research, which would include one of the most widely used printing technologies – offset. This technology applies inks or varnishes to the surface of paper substrates with rather high pressures between the printing rollers, which can cause damages to the microcapsules.

This research presents the influence of microcapsule application in printing varnish and the results of structural and mechanical properties of printed paper substrates.

Key words: offset printing, varnish, microcapsules, printing

1. INTRODUCTION

Microcapsules are small containers for various substances, which can be used for different purposes. Structural properties of microcapsules enable efficient packaging of liquids, gases and even solids, thus providing different effects. The inner substance is being released after the application of low pressure to the surface or by changing pH value, temperature etc. of their environment. Thanks to their small size (even in nano level), solid shell and relative thermal stability, microcapsules can be added into different material during its production or they can be applied on to its surface with several distinguished techniques. (Kumar Ghosh, 2006; Bensode et al, 2010; Bone et al, 2011).

Graphic technology has been one of the first technologies, which has successfully used microcapsules for the production of carbonless copy paper (Kipphan, 2001). Microcapsules are usually added into the printing ink or into varnish, depending of the purpose and technology. When screen printing, microcapsules are most often added directly into the printing ink where their small size doesn't impede the printing procedure – due to the small size of microcapsules they don't tend to stay on the surface of screen printing mesh (Stankovič Elesini et al, 2014). Some problems can occur during squeegee passage, though if the right pressure is used, microcapsules don't crack and they withstand the shear forces caused by the squeegee. Many times microcapsules are also printed with flexo printing technique, added into very low viscosity inks. Flexo rollers enable easy transmission of microcapsules on to the surface of printing substrate. Where, similar as in screen printing technique, the procedure itself doesn't damage the microcapsules.

The aim of this research was to try to print very small microcapsules (1–10µm) with offset printing technique, which due to the technology consists of many printing rollers, among which relatively high pressures occur. Different studies have been made on how preparation of printing ink can influence the quality and stability as well as durability of prints (Rose, 2014; Kim, 2013; Sorvari, Parola, 2014), but there are no known researches on microcapsules printed with this technology. For that purpose we have decided to perform a simple preliminary research, which would give us an idea how this additive influences the process of printing and how it influences the quality and properties of prints.

2. MATERIALS AND METHODS

2.1 Materials

Paper substrate

Structure and properties of paper substrate play an important role in quality of prints. For this research two types of paper substrates were selected – Kunstdruck matt (in this research indicated as **KDM**) and Kunstdruck gloss (in this research indicated as **KDG**). Both paper substrates were coated – one with matt and other with gloss coating (Figure 2). Paper substrate with gloss coating KDG had higher grammage ($\text{KDM}=130\text{g/m}^2 \pm 3\%$, $\text{KDG}=150\text{g/m}^2 \pm 3\%$) and it was thinner than KDM ($\text{KDM}=124\mu\text{m}$, $\text{KDG}=110\mu\text{m}$). Also glossy coated paper substrate sample had higher ISO Brightness ($\text{KDM}=90\%$ ISO, $\text{KDG}=104\% \pm 2\%$ ISO) and gloss ($\text{KDM}=30\%$, $\text{KDG}=73\% \pm 10\%$), respectively. The opacity of both paper samples was almost the same ($\text{KDM}=96\%$, $\text{KDG}=95\% \pm 2\%$).

Printing ink – varnish

For the purpose of this research only printing varnish was used instead of printing ink. In this varnish microcapsules were added. Selected paper samples (e.g. KDM and KDG) were firstly printed only with varnish and secondly with the mixture of varnish and microcapsules. An offset printing varnish c378 Gloss (Cinkarna Grafika, Slovenia), on the basis of mineral oils, with high gloss, was chosen. This varnish can be printed directly on the surface of printing material without the addition of water. According to the manufacturer this type of varnish easily dries, but the speed of drying can be stimulated with IR. In our case all samples were dried on air.

Microcapsules

Commercially prepared microcapsules in dry state, with the essential oil of basil, were used. Microcapsules, in the form of white powder, were directly mixed into the varnish in 10% mass concentration. Selected microcapsules with distinguished fragrance were chosen with a reason. Namely, confirming the presence of microcapsules in the varnish, even after some time after printing (e.g. one month), can be achieved not only with image analyses but also with application of gentle pressure (e.g. rubbing) on the printed surface, where if microcapsules are present, added pressure causes cracking of the microcapsule thus revealing the fragrance.

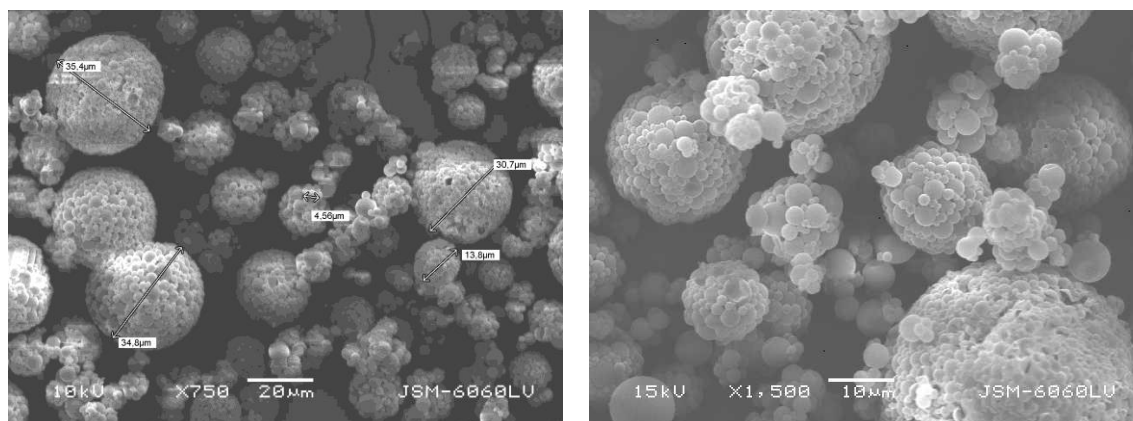


Figure 1: SEM image of dry microcapsules
(SEM, 750x (left) and 1500x (right) magnification)

SEM (scanning electron microscope) image analyses showed that selected microcapsules differed in size (Figure 1), from $1\mu\text{m}$ to $10\mu\text{m}$, respectively. Image analyses also showed that microcapsules tended to join into clusters. Size of these clusters varied from $10\mu\text{m}$ to $40\mu\text{m}$. Some smaller clusters were present in smaller amount in the mixture with varnish (Figure 2) and also on the printed samples as will be seen in the continuation.

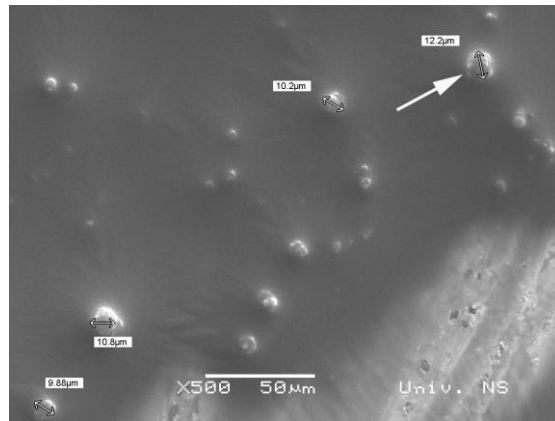


Figure 2: Mixture of microcapsules in the varnish; white arrow indicates microcapsule cluster (SEM; 500x magnification)

Printing procedure

Samples were printed using offset printing machine Rapida 75 (KBA – Koenig & Bauer Group, Germany) with the printing speed 5500 prints/h. Prints were made on sheets of both selected paper substrate with the pressure between the printing rollers 460-530N/cm³. The pressure was defined and measured on five points with the help of LP101 roller Nip Control aperture.

Samples

The aim of this research was to investigate how the addition of microcapsules influences on properties of selected printed paper substrates. Therefore, six different samples were compared – two samples of chosen paper substrates (KDM and KDG), two samples of chosen paper substrates printed with varnish (KDM-V and KDG-V) and two samples of paper substrates printed with mixture of varnish and microcapsules (KDM-V-MC and KDG-V-MC), respectively.

2.2 Methods

The following measurements were performed on samples (unprinted and printed paper substrates): **Grammage** was measured according to the method described in standard EN ISO 536:2012. (ISO, 2012) **Thickness** was measured on apparatus Mitutoyo, No: 2050 F-10 with load 500cN/cm² on the sample area of measurement 1cm² and according to the standard ISO 534:2011. (ISO, 2011) **ISO Brightness** of samples was measured according to ISO 2470-1:2009 standard. (ISO, 2009) **Roughness** of samples according to Bendtsen method was determined in accordance with ISO 5636-3:2013 standard. (ISO, 2013) **Tear resistance (Elmendorf Tear)** was measured according to ISO 1974:2012. ISO, 2012) **Maximal force and elongation at rupture** (Universal dynamometer Instron 5567) was measured according to SIST EN ISO 13934-1:2013. (ISO, 2013) **Image analyses** of samples and morphological properties of selected materials were performed on scanning electron microscope JSM 6060 LV, Jeol (Spain).

3. RESULT AND DISCUSSION

3.1 Properties of paper substrates

The surface of two selected paper substrates was first examined by scanning electron microscope (SEM). Figure 3 shows that surface of KDM paper substrate sample was rougher than and not as smooth as the surface of KDG sample. Results in Table 1 also confirm these observations.

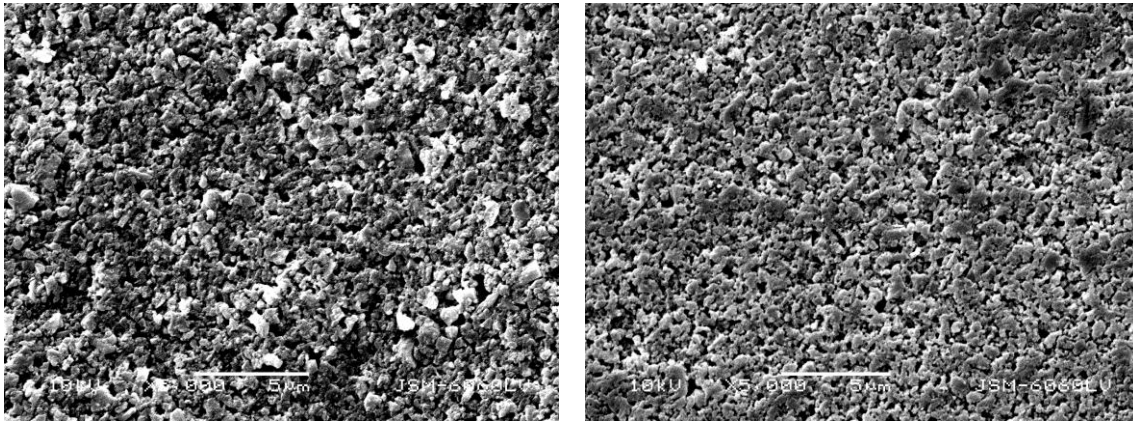


Figure 3: Surface image of KDM (left) and KDG (right) paper substrate
(SEM, 5000x magnification)
(author of photography: Mirjam Leskovšek, MSc)

Measured basic paper substrate properties are presented in Table 1. They have shown that paper substrate KDG with gloss coating had higher grammage, lower thickness, higher ISO brightness and lower roughness compared with paper substrate KDM. The results are slightly different as declared values, probably because of the measuring conditions. However, they are all in the range of declared deviation.

Roughness is much higher for KDM paper substrate in comparison to KDG. The reason is smoother surface of KDG paper substrate.

The analyses have shown that paper substrate KDM had similar force to rupture and elongation in both directions – longitudinal and lateral (transverse), however paper substrate KDG was stronger in longitudinal direction (but lower elongation), which meant that it probably had slightly different structure than paper substrate KDM e.g. fibre orientation in longitudinal direction.

Consequently, paper substrate KDM also had lower tear resistance in longitudinal direction but higher in lateral direction. The difference between lateral and longitudinal tear resistance of paper substrate KDM was not major, since strength was in both direction similar, as well as probably the morphological structure of sample.

Table 1: Properties of paper substrates KDM and KDG

Property \ Sample	KDM			KDG		
	value	Std. dev.	CV (%)	value	Std. dev.	CV (%)
Grammage (g/m²)	126.27	0.002	0.01	148.05	0.006	1.61
Thickness (µm)	115.9	0.001	0.76	109.1	0.003	2.34
ISO Brightness (%)	88.54	0.271	0.31	94.59	0.308	0.33
Roughness (ml/min)	17.20	2.049	11.92	6.60	0.548	8.30
Tensile strain						
lateral (MD)						
max load (N)	105.53	2.659	2.52	104.10	2.123	2.04
elongation at max load (%)	2.80	0.141	5.05	9.77	0.530	5.42
longitudinal (CD)						
max load (N)	105.86	0.458	0.43	162.05	0.593	0.37
elongation at max load (%)	2.90	0.070	2.44	4.45	0.141	3.18
Tear resistance						
lateral (MD) (cN)	240.35	1.587	0.25	225.63	0.029	1.54
longitudinal (CD) (cN)	225.63	2.459	2.48	186.39	0.154	0.98

3.2 Properties of printed samples

As mentioned above, paper substrates were firstly printed only with varnish and secondly with the combination of varnish and microcapsules. Results of measurements are presented in Table 2.

Table 2: Measured properties of unprinted (paper substrates) and printed samples

Properties	Samples	KDM			KDG		
		KDM	KDM-V	KDM-V-MC	KDG	KDG-V	KDG-V-MC
Grammage (g/m ²)		126.27	127.58	129.20	148.05	149.52	150.40
Thickness (μm)		115.90	114.00	118.80	109.10	107.70	110.60
ISO Brightness (%)		88.54	84.13	86.51	94.59	90.33	91.53
Roughness (ml/min)		17.20	20.60	24.40	6.60	7.00	8.20
Tensile strain							
lateral (MD)							
max load (N)		105.53	47.486	50.25	104.10	104.30	104.48
elongation at max load (%)		2.80	4.35	6.50	9.77	10.13	10.15
longitudinal (CD)							
max load (N)		105.86	108.09	121.46	162.05	159.83	163.08
elongation at max load (%)		2.90	2.63	3.03	4.45	4.05	4.20
Tear resistance							
lateral (MD) (cN)		240.35	279.59	255.06	225.6318	269.78	245.25
longitudinal (CD) (cN)		225.63	255.06	235.44	6.39	245.25	225.63

According to the expectations the grammage of both paper substrates increased with the printing of varnish (samples KDM-V and KDG-V) and also when a mixture of varnish and microcapsules was printed (samples KDM-V-MC and KDG-V-MC).

Thickness of paper substrates slightly decreased after the printing of varnish probably because the samples are during the printing procedure exposed to the pressure of printing rollers. Additionally, printing of varnish probably also caused filling of small uneven surface gaps (Figure 4).

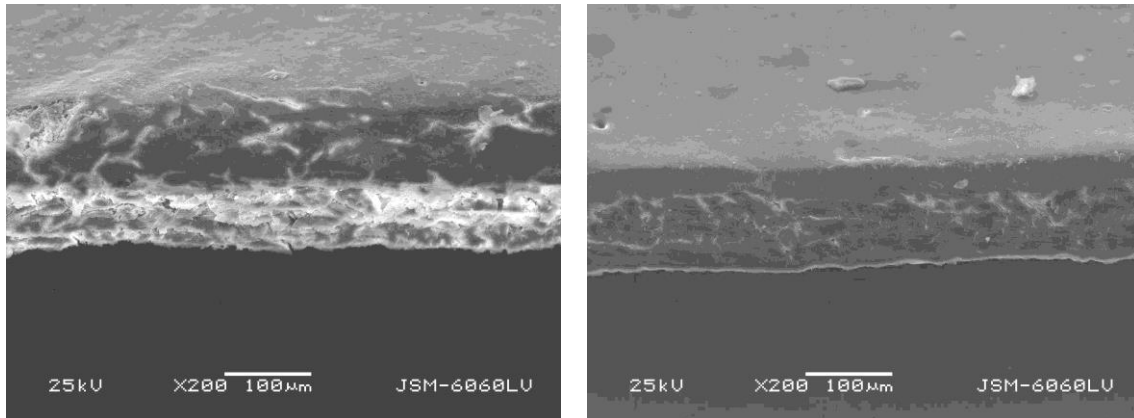


Figure 4: Surface and cross-section image of KDM-V (left) and KDG-V (right) paper substrate printed with varnish (SEM, 200x magnification)
(author of photography: Mirjam Leskovšek, MSc)

Thickness of samples printed with varnish and microcapsules (KDM-V-MC and KDG-V-MC) was higher than the initial thickness; it was presumed that higher thickness of these samples could be contributed to the presence of microcapsules especially clusters, which prevent filling the surface gaps and attribute to the loading of varnish just to the surface of paper (Figure 5).

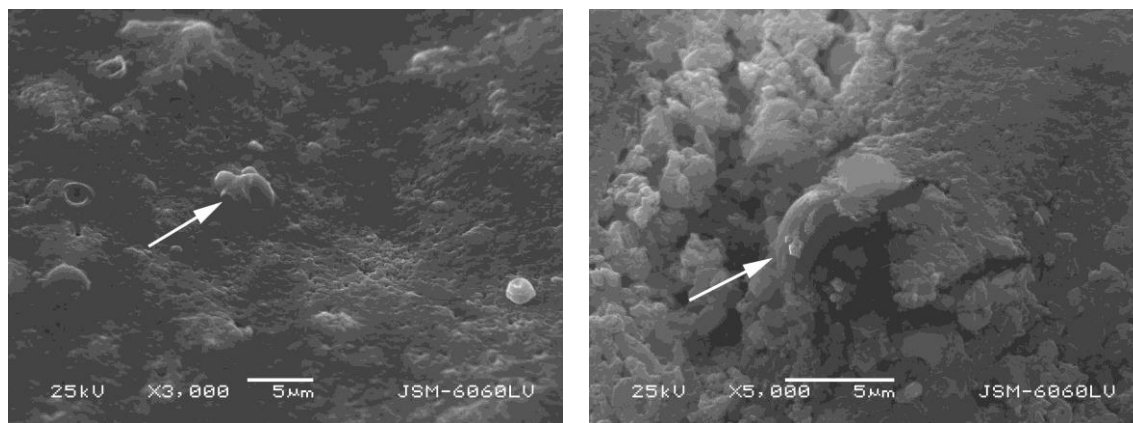


Figure 5: Surface image of KDM-V-MC (left, SEM, 3000x magnification) and KDG-V-MC (right, SEM, 5000x magnification) paper substrate printed with varnish and microcapsules; arrows point the microcapsules
(author of photography: Mirjam Leskovšek, MSc)

Brightness of KDM-V and KDG-V decreased after the printing of varnish. Varnish, which has a slightly “milky” color, expectedly decreased values of brightness. The addition of white powder of microcapsules in printing varnish (printed samples KDM-V-MC and KDG-V-MC) increased these results, though the values of brightness did not achieve the initial ones.

Roughness, measured according to Bendtsen method, increased with the addition of varnish, though it could be presumed that varnish would increase the smoothness of the surface. This value increased with the printing of mixture varnish and microcapsules (printed samples KDM-V-MC and KDG-V-MC), which confirms the presence of microcapsules on the surface of varnish.

Measurements of force and elongation at rupture for all samples showed interesting results.

Measurements of force and elongation at rupture of unprinted KDM paper substrate in both directions were almost the same. After the printing of varnish (KDM-V) and varnish with microcapsules (KDM-V-MC) on the paper substrate, force to rupture in both samples significantly decreased (for almost 50%), but only in lateral direction, while in longitudinal direction force to rupture slightly increased. On the other side, elongation at rupture increased, which meant that paper substrate with varnish obtained more “elastic” properties. Those results coincided with the results of tear resistant of KDM paper substrate since more force was needed for tearing the samples with varnish (KDM-V) and with varnish with added microcapsules (KDM-V-MC).

Measurements of force and elongation at rupture of unprinted KDG paper substrate in both directions were significantly different (significantly higher in longitudinal direction). However, those values remained almost the same after the varnish (KDG-V) and varnish with added microcapsules (KDM-V-MC) were printed to the paper substrate KDG. Although the values for force and elongation at rupture remained almost the same, the tear resistance was significantly higher. According to the results, varnish alone or with microcapsules had significant impact on the properties of KDM paper substrate and on contrary, almost no impact on paper substrate KDG. The reason could be found in the morphological structure and properties of surface of both paper substrates. Paper substrate KDM had probably less oriented structure than KDG, and rougher surface with higher adhesion to varnish or varnish with added microcapsules. On contrary, paper substrate KDG had more oriented structure and smoother surface, which had lower adhesion to printed varnish or varnish with added microcapsules. Consequently, on paper substrate KDM with higher adhesion, influence of printed varnish or varnish with microcapsules was more obvious than on paper substrate KDG.

Image analyses have shown that microcapsules are present in the layer of varnish with some microcapsules partially emerging from the surface (Figure 5). This fact contributes to better durability of microcapsules, which content is additionally protected by varnish layer. From the images on Figure 6 and 7 it can be seen that smaller microcapsules remain intact while clusters are damaged because of the pressure of printing rollers in printing process. Present of basil fragrance, after application of slight rub force (rubbing with the tip of finger) even after one month, assured us of the presence of microcapsules and confirmed that the initial presence of fragrance wasn't the consequence of cracked microcapsules directly after printing.

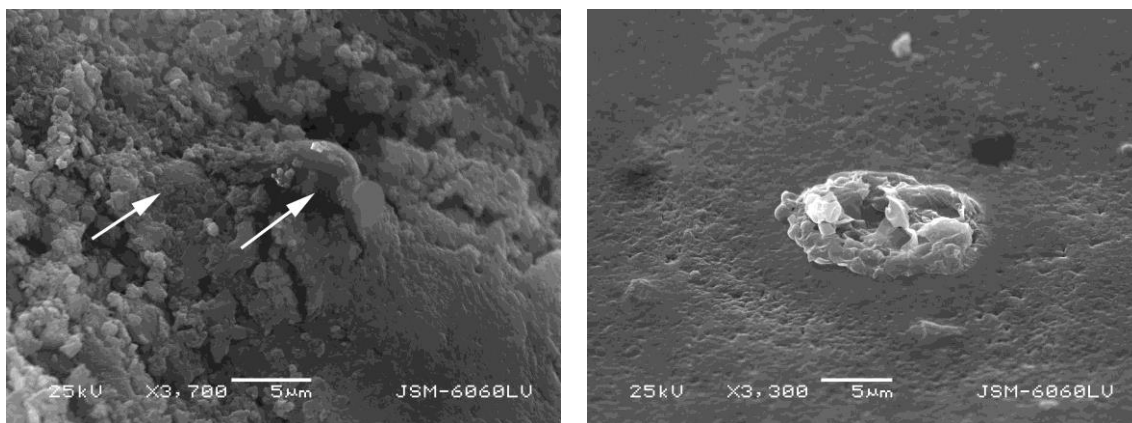


Figure 6: Microcapsules under the surface of KDM-V-MC (left, SEM, 3700x magnification) and cluster of microcapsules immersing from the varnish of KDG-V-MC (right, SEM, 3300x magnification); arrows point the microcapsules
[author of photography: Mirjam Leskovšek, MSc]

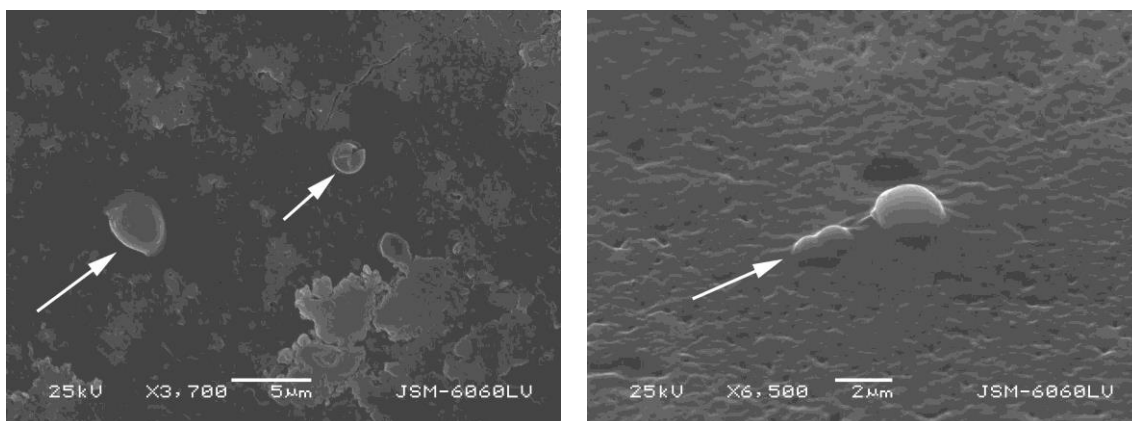


Figure 7: Microcapsules under the surface of KDM-V-MC (left, SEM, 3700x magnification) and KDG-V-MC (right, SEM, 6500x magnification); arrows point the microcapsules
[author of photography: Mirjam Leskovšek, MSc]

4. CONCLUSION

Research has shown that microcapsules can be successfully printed with offset printing technique. Thus they have to be adequate size e.g. max 10µm otherwise they tend to crack before the printing procedure is over. Addition of microcapsules effects the properties of printed samples – it increases the thickness, brightness and roughness. They also increase the tear resistance and tensile strain. The bigger effect was recognized on rougher surface of the paper substrate which became a bit stiffer but still not so much that its structural properties would dramatically change. This research has also proved that microcapsules stay undamaged in the printing varnish, thus providing even distribution through the printing material. Higher concentration of microcapsules within the varnish layer offers better durability and protection of microcapsule core.

5. REFERENCES

- [1] Bensode S. S., Banarjee S. K., Gaikward D. D., Jadhav S. I. in Thorat R. M. Microencapsulation: a review. Vishal Institute of Pharmaceutical Education and Research, 2010, Vol. 1, Issue 2, Article 008, pp. 38-43.
- [2] Bone S., Vautrin C., Berbesant V., Truchon S. in Harrison Geffroy C. Microencapsulated fragrances in melamine formaldehyde resins. Chimia 2011, Vol. 65, No. 3, pp. 177-181.
- [3] Kumar Ghosh S. Functional coatings: By Polymer Microencapsulation, Published Online: 29 june 2006, Copyright© 2006 Wiley-VCH Verlag GmbH & Co. KGaA.

- [4] ISO 536:2012 Paper and board – Determination of grammage.
- [5] ISO 534:2011 Paper and Board – Determination of thickness, density and specific volume.
- [6] ISO 2470-1:2009 Paper, board and pulps – Measurement of diffuse blue reflectance factor – Part 1: Indoor daylight conditions (ISO brightness).
- [7] ISO 5636-3:2013 Paper and board – Determination of air permeance (medium range) – Part 3: Bendtsen method.
- [8] ISO 1974:2012 Paper – Determination of tearing resistance – Elmendorf method.
- [9] ISO 13934-1:2013 Tensile Properties of fabrics: Maximum Force and Elongation at Maximum Force Using the Strip Method.
- [10] Kim I., Kwak S. W., Kim K. S., Lee T. M. Effect of ink cohesive force on gravure offset printing, 2012, *Microelectronic Engineering*, Vol. 98, pp. 587–589.
- [11] Kipphan H. *Handbook of Print Media*; Springer – Verlag, New York, 2001.
- [12] Rose H. Scent Encapsulated Printed Products, 2007, available online: https://projekt.beuth-hochschule.de/fileadmin/projekt/sprachen/sprachenpreis/erfolgreiche_beitraege_2007/1._Preis_07_-_Scent_Encapsulated_in_Printed_Products_-_Heike_Rose.pdf (accessed: 26.9.2014), p. 16.
- [13] Sorvari J., Parola M. Feeding and rolling contact of layered printing cylinders, *International Journal of Mechanical Sciences*, Vol. 88, 2014, pp. 82–92.
- [14] Stankovič Elesini U., Šumiga B., Manojlović S., Urbas R. Raised printing with screen printing technique. In: 7th Symposium of Information and Graphic Arts Technology, Ljubljana, 5–6 June 2014, Urbas R. (editor), *Proceedings*, pp. 187–192.

THE STUDY OF THE POLYMERIZATION OF HYBRID SYSTEMS

Ondřej Škola, Bohumil Jašůrek, Jan Vališ, Petr Němec
 University of Pardubice, Faculty of Chemical Technology,
 Department of Graphic Arts and Photophysics, Pardubice, Czech Republic

Abstract: Nowadays, UV curable systems (inks, varnishes) are frequently used in printing industry. These systems can be classified according to the type of polymerization reactions as free radical and cationic. In the majority, UV inks and varnishes are based on free radical polymerization. This type of polymerization is characterized by very fast curing (fraction of seconds). On the other hand, the inhibition by atmospheric oxygen and worse adhesion of cured films to polymeric or metallic foils are the main disadvantages of free radical polymerizations. Cationic polymerization is not as fast as free radical polymerization and the final properties of cured film are obtainable approximately after 24 hours. Cationic systems are not inhibited by atmospheric oxygen and cured films have very good adhesion to various substrates. Disadvantage of cationic systems is their inhibition by air humidity and alkaline substances. Hybrid UV systems are simultaneously cured by free radical and cationic polymerization. Hybrid systems have lower sensitivity to inhibition by atmospheric oxygen and air humidity, thus the final film properties could be much better than those of systems cured by only free radical or cationic polymerization.

The aim of this work was to study the polymerization reaction of hybrid systems and to compare them with systems polymerizing by only free radical or cationic polymerization. Hybrid systems were prepared from photoinitiators: Darocure 1173 (free radical photoinitiator) and Irgacure 250 (cationic photoinitiator), and monomers: pentaerythritol triacrylate (free radical polymerization) and Uvacure 1500 (epoxyde monomer, cationic polymerization). The molar ratio of monomers in hybrid systems was 1:1, 1:3 and 3:1. Concentration of photoinitiator was 3 mol% in all cases. The degree of conversion was evaluated based on results obtained from FTIR spectroscopy. The polymerization reaction of samples was observed for various UV doses (medium pressure mercury lamp as UV source) and the optimal UV dose was estimated from FTIR spectra.

The results show that hybrid polymerization systems reached higher overall degree of conversion. For example, pure pentaerythritol triacrylate reached 51 % degree of conversion pure epoxyde monomer Uvacure 1500 reached 91 %. In hybrid system (1:1 molar ratio), pentaerythritol triacrylate reached 63 % degree of conversion and Uvacure 1500 reached degree of conversion of 85 %.

Key words: radical polymerization, cationic polymerization, hybrid polymerization

1. INTRODUCTION

UV curable systems (inks, varnishes) are frequently used in printing industry. These systems can be classified according to the type of polymerization reactions as free radical, cationic and hybrid. Radical polymerization is special case of chain reactions. Polymeric chain is growing by the consecutive reactions of an active centre with a monomer or oligomer molecule. Free radical active centres are created by decomposition of photoinitiators. Derivatives of aromatic ketones are frequently used as the photoinitiators for free radical polymerization. For free radical reactions, acrylic monomers and oligomers are mainly used (Webster, 1997). Main advantage of free radical polymerization is very fast curing (fractions of seconds). On the other hand, their main disadvantages are inhibition by air oxygen and large change of volume (contraction of cured film) which arises during the curing (in case of acrylate systems the change can reach up to 10–15 %) (Decker, 2002). Large volume change results in worse adhesion of cured films to polymeric substrates or metallic foils.

In case of cationic polymerization, active centre has a positive charge. Cationic polymerization can be used for curing monomers and oligomers as an epoxides, vinyl ethers and propenyl ethers. Cationic polymerizations are not inhibited by air oxygen and volume changes proceeding during polymerization are lower (for example polymerization of epoxides leads to 5 % change of volume); therefore cured films have better adhesion to polymeric or metallic foils. On the other hand, cationic polymerization is not as fast as free radical polymerization (the final properties of a cured film are obtainable approximately after 24 hours) and is inhibited by the air humidity and alkaline substances (Lin, Stransbury, 2003).

Hybrid polymers are created from monomers and oligomers with different reactive groups which are polymerized by different reaction mechanisms. Monomers combine free radically and cationically polymerizable groups (for example acrylic, epoxy and vinyl ether groups). For initiation of the polymerization, mixture of free radical and cationic photoinitiators can be used. Initiators can be activated simultaneously or consecutively by a selective excitation. As a result, free radical and cationic polymerization can proceed simultaneously or consecutively [Crivello, Dietliker, 1998]. Main advantages of hybrid polymer systems consist of often synergistic combination of the properties of the constituent polymers, increased curing speed, faster development of the final properties of cured films, lower sensitivity to the inhibition of air oxygen, humidity and other inhibitors and improved properties of fabricated films [Lin, Stransbury, 2003].

2. USED MATERIALS AND EQUIPMENT

2.1 Free radical system

As a monomer for free radical system, pentaerythritol triacrylate was used. As a photoinitiator for free radical polymerization, 2-hydroxy-2-methyl-1-phenyl-propan-1-one (commercially available photoinitiator Darocure 1173) was employed. Free radical systems contained 3 mol. % of photoinitiator and 97 mol. % of monomer. Free radical system was labelled as R1.

2.2 Cationic system

As a monomer for cationic system, 3,4-epoxycyclohexylmethyl-3,4-epoxycyclohexane carboxylate (commercially available epoxide monomer – Uvacure 1500) was exploited. As a photoinitiator for cationic system, iodonium, [4-methylphenyl][4-(2-methylpropyl) phenyl]-, hexafluorophosphate(1-) (commercially available photoinitiator Irgacure 250) was used. Cationic systems consisted of 3 mol. % of photoinitiator and 97 mol. % of monomer. Cationic system was labelled as C1.

2.3 Hybrid system

Three hybrid systems were prepared from the substances listed above. Hybrid systems contained free radical and cationic polymerizable monomers in molar ratio 1:1, 1:3 and 3:1, 3 mol % of Irgacure 250 and 3 mol % of Darocure 1173. Hybrid systems were labelled as H1:1, H1:3, H3:1.

2.4 Equipment

UV tunnel Miniterm UV 220 Q Super (medium pressure mercury lamp) was used for curing of samples. UV dose was measured by radiometer UV-integrator (uv-technik). FTIR spectrometer Avatar 320 (Nicolet) was used for IR spectra measurements. For measured spectra evaluation, Omnic software and Peak resolve tool were employed.

3. RESULTS AND DISCUSSION

All prepared samples were coated on aluminium foil. Thickness of fabricated films was between 10–15 µm. Degree of conversion was calculated by equation:

$$X(\%) = [(S_0 - S_t) / S_0] \cdot 100 \quad (1)$$

where S_0 is area of measured band (acrylate double bond or epoxide group) before UV exposure and S_t is area of measured band in different time lags after UV exposure.

3.1 Polymerization of R1 samples

IR spectrum before and after irradiation with UV dose about 150 mJ/cm² (one pass through the UV tunnel Miniterm UV 220 Q super) was measured for each sample. Samples were irradiated ten times. Polymerization of samples was monitored by the decrease of absorption bands corresponding to deformation vibration of acrylate double bond (1600–1649 cm⁻¹). Mean degree of conversion of R1 samples is shown in Figure 1. Degree of conversion of free radical system

achieved 51.8 % (UV dose 468 mJ/cm²) and 58.4 % (UV dose 1514 mJ/cm²). For next measurement of cationic and hybrid samples was used UV dose around 468 mJ/cm².

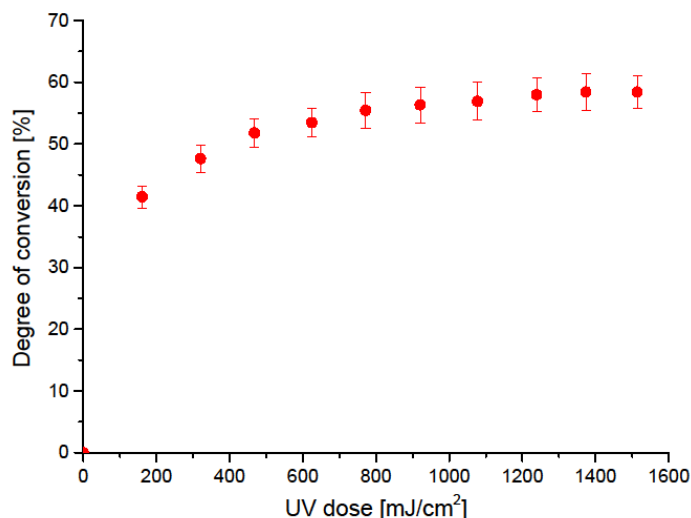


Figure 1: Mean degree of conversion of R1 samples

3.2 Polymerization of C1 samples

IR spectra were measured before and after irradiation of sample in UV tunnel (one pass with UV dose between 450–480 mJ/cm²). After irradiation, IR spectrum was measured every two minutes for 2 hours and one more spectrum after 24 hours. Polymerization of samples was monitored by the decrease of absorption triple band (776–815 cm⁻¹) with maxima at 788, 798 and 808 cm⁻¹ and also by only fraction of this band with maximum at ~788 cm⁻¹ (deconvolution done by Peak resolve tool). Mean degree of conversion of C1 samples is shown in Figure 2. Degree of conversion achieved 81.6 % in the case of entire absorption band and 81.4 % in case of fragment band (1 hour after irradiation). In case of 24 hours after irradiation, the degree of conversion achieved 93.4 % in the case of entire absorption band and 90.8 % in case of fragment band. In Table 1 are summarized degree of conversions of free radical, cationic systems and overall degree of conversion. Overall⁽¹⁾ is sum of degree of conversion of free radical polymerization (UV dose 468 mJ/cm²) and degree of conversion of cationic system 1 hour after irradiation. Overall⁽²⁾ is sum of degree of conversion of free radical polymerization (UV dose 468 mJ/cm²) and degree of conversion of cationic system 24 hours after irradiation.

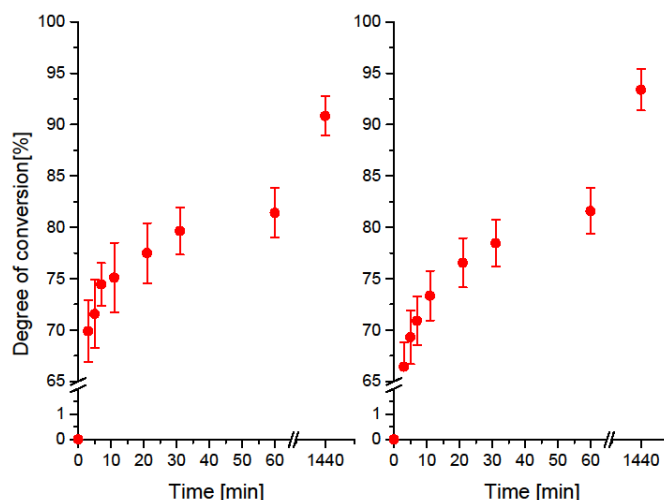


Figure 2: Mean degree of conversion of C1 samples (left panel – using fragment of absorption band at 788 cm⁻¹, right panel – using entire absorption band).

Table 1: Mean degree of conversion of free radical, cationic systems and overall degree of conversion

Degree of conversion [%]					
R1		Time after irradiation [hour]	C1		overall
UV dose [mJ/cm ²]			Entire band	Fragment of band	
468	51.8±2.2	1	81.6±2.2	81.4±2.4	133.2 ⁽¹⁾
1514	58.4±2.6	24	93.4±2.0	90.8±1.9	149.2 ⁽²⁾

3.3 Polymerization of hybrid samples

IR spectra were measured before and after irradiation of sample in UV tunnel (one pass with UV dose between 450–480 mJ/cm²). After irradiation, IR spectrum was measured every two minutes for 2 hours and one more spectrum after 24 hours. Degree of conversion of free radical part of hybrid systems was monitored by the same procedure as in 4.1. Degree of conversion of cationic part of hybrid systems was monitored by only of fraction of absorption triple band with maximum at ~788 cm⁻¹. This fraction of absorption triple band was used because the other two absorption bands overlap with absorption band belonging free radical polymerization (deformation vibrations of acrylate double bond). Mean degree of conversion of hybrid samples is showed in Figure 3. In Table 2, degrees of conversion (after 1 and 24 hours) of free radical and cationic part of hybrid systems and overall degree of conversion are summarized. Overall degree of conversion is a sum of free radical and cationic part. Large differences in achieved degree of conversions of various components of hybrid samples were observed for radically polymerizable monomer, where differences were around 30 % compared to cationically polymerizable monomer with differences only around 5 %

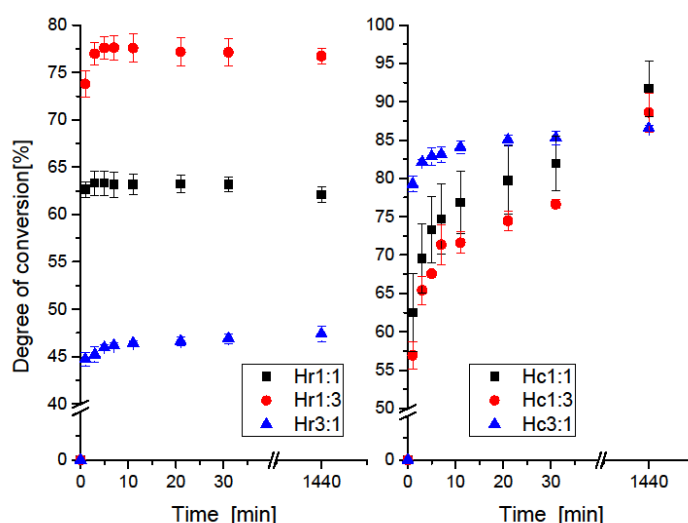


Figure 3: Mean degree of conversion in hybrid systems (left panel – free radical part, right panel – cationic part).

Table 2: Mean degree of conversion of free radical, cationic part and overall degree of conversion in hybrid systems 1 and 24 hours after irradiation.

Sample	Degree of conversion of hybrid systems					
	1 hour after irradiation			24 hours after irradiation		
	Radical part	Cationic part	Overall	Radical part	Cationic part	Overall
H1:1	63.3±	83.9±3.6	147.2	62.1±0.8	91.7±3.4	153.8
H1:3	76.9±1.4	79.4±1.2	156.7	76.7±0.8	88.6±2.5	165.3
H3:1	47.2±0.7	85.7±0.6	132.82	47.4±0.9	86.5±0.4	133.9

4. CONCLUSIONS

The results show that two from three hybrid systems reached higher overall degree of conversion (samples H1:1, H1:3) than systems that polymerize by only free radical or cationic polymerization. Overall degree of conversion of separately polymerizable free radical and cationic system 24 hours after irradiation was 149.2 %. Hybrid sample H1:3 reached 165.3 %, H1:1 153.8 % and H3:1 133.9 %. This increased of overall degree of conversion can be explained by lower viscosity of hybrid systems containing higher amount of cationically polymerizable monomer (cationic polymerization is slower than free radical) and lower influence of oxygen inhibition on free radical polymerization.

5. REFERENCES

- [1] Crivello, J., Dietliker, K., "Chemistry and Technology of UV & EB Formulation for Coatings, Inks & Paints", volume III: Photoinitiators for Free Radical, Cationic & Anionic Photopolymerization, 2nd Edition, (John Wiley & Sons and Sita Technology, London, 1998).
- [2] Decker, C.: "Kinetic Study and New Applications of UV Radiation Curing", Macromolecular Rapid Communications, volume 23 (18), page 1067., (2002).
- [3] Lin, Y., Stransbury J. W.: "Kinetics studies of hybrid structure formation by controlled photopolymerization", Polymer, volume 44 (17), page 7481, (2003).
- [4] Webster G.: "Chemistry & Technology of UV & EB Formulation for Coatings, Inks & Paints", 2nd Edition, (John Willey & Sons and SitaTechnology, London,1997)

STRUCTURE OF MICROCAPSULES AND ITS USE IN THE INDUSTRY – OVERVIEW

Živko Pavlović¹, Sandra Dedijer¹, Urška Stanković Elesini², Raša Urbas²

¹University of Novi Sad, Faculty of Technical Sciences,

Department of Graphic Engineering and Design, Novi Sad, Serbia

²University of Ljubljana, Faculty of Natural Sciences and Engineering,

Department of Textiles, Ljubljana, Slovenia

Abstract: Microencapsulation technology has been initially used in the paper industry for the production of carbonless copy paper (with encapsulation of leuco dyes) and its use has been later transferred from its basic application purpose to other areas of use: microencapsulated perfumes in cosmetics, special coatings in textile industry and versatile application possibilities in graphic and printing industry, medicine, pharmacy, food industry, agriculture and even in construction, biotechnology etc.

Various conditions of microencapsulation procedure have impact on the size, proportion of particles size, thickness and structure of walls and properties of microcapsules. Size and material used for the microencapsulation determine field of the application.

The aim of this paper is to give a general introduction and overview on microcapsules and its use in industry with emphasis on graphic industry.

Key words: microcapsules, paper and graphic industry

1. INTRODUCTION

Encapsulation is a process where certain selected compound is captured into a coating material (Thies, 2003). This procedure is currently used in several industrial fields as a scientific advanced methodology of application. It offers numerous possibilities of applications which can improve industrial commercial products, such as: immobilization, isolation, protection and control of the rate of transfer of many substances like metals, acids, drugs, nutrients, pesticides and herbicides, perfumes, flame retardants, etc. Mainly, encapsulation is used to extend the shelf life of unstable compounds. The encapsulated compounds, from an industrial point of view, are easy to handle as they preserve their properties and stay safe in the meaning of prolonged storage. This stabilization is enabled by the coating material, which acts as a protective physical barrier (Peña et al., 2012).

Microcapsules are usually prepared with one of the three technological possibilities (Arshady, 1999):

- *mechanical methods* (e.g. spray drying, pan coating, extrusion, deposition in vacuum, solvent evaporation from emulsions) where the microcapsule wall is mechanically applied or condensed around the microcapsule core;
- *coacervation*, a phenomenon taking place in colloid systems where macromolecular colloid rich coacervate droplets surround dispersed microcapsule cores and form a viscous microcapsule wall, which is solidified with cross-linking agents, and
- *polymerisation methods* where monomers polymerise around the droplets of an emulsion and form a solid polymeric wall. In the in situ polymerisation, monomers or precondensates are added only to the aqueous phase of emulsion, while in interfacial polymerisation, one of the monomers is dissolved in the aqueous phase and the other in a lipophilic solvent.

Capsules can be defined as spherical membranes with an empty core (Thies, 2003; Peña, 2009; Gumí et al, 2009). They can be classified, according to their diameter size, in nanocapsules (with diameter smaller than 1µm), microcapsules (with diameter between 1 and 1000µm) and macrocapsules (with diameter larger than 1000µm).

A long list of different materials can be used for preparation of capsules, among which polymeric materials are frequently used (Rodrigues, 2009). In the latter case, phase inversion precipitation is

one of the most commonly used techniques for their preparation (Peña, 2009; Tona, Jiménez, Bojarski, 2008; Van den Berg et al., 2009; Juanjuan et al., 2010; Gong et al., 2009; Yang et al., 2007; Gumí et al. 2009; Gong et al., 2006; Ghen et al., 2005; Wang et al., 2006; Mulder, 2003). Preparation of capsules is based on the separation (by precipitation) of the polymeric phase from a mixture that contains a solvent and a polymer, by means of thermodynamic processes. The precipitation of the polymeric phase occurs by a diffusion process in which the polymeric solution is immersed into a non-solvent (immersion precipitation) (Mulder, 2003). The controlled release of fragrances is a challenge for the industries, which use perfumes in their products, due to the fact that the consumers are attracted by articles with a long-lasting fragrance perception. Perfumes present compounds that may be lost due to their highly volatility (Ternat et al., 2008; Herrmann et al., 2000; Jacquemond et al., 2009) but, by encapsulation, they can be protected during storage and until the final use of the product (Rodrigues et al., 2009; Tona, Jiménez and Bojarski, 2008; Peña et al., 2009; Wang et al. 2008; Jacquemond et al., 2009; Nelson, 2002).

2. MORPHOLOGY OF MICROCAPSULES

Microcapsules can be divided into two parts, namely the core and the shell. The core (intrinsic part) contains an active ingredient (e.g. hardener), while the shell (extrinsic part) protects the core permanently or temporarily from the external atmosphere (Figure 1).

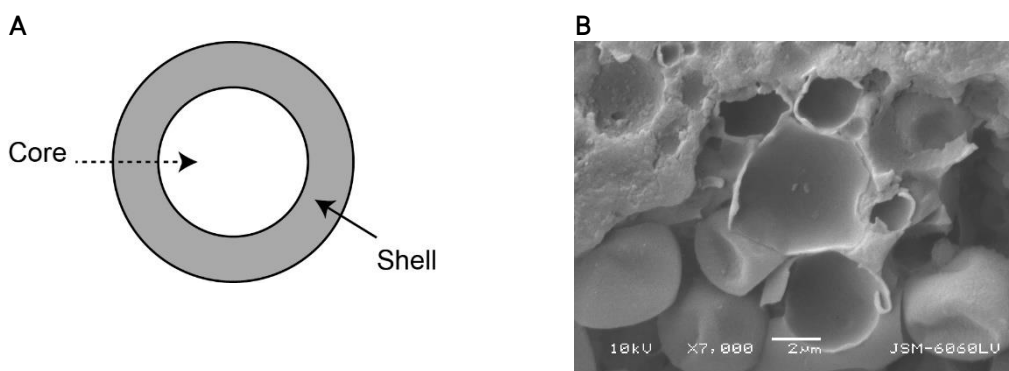


Figure 1: A - Schematic view of microcapsule; B – Shell and core of microcapsule (SEM; 7.000x magnification; author: Mirjam Leskovšek)

Core materials in microcapsules may exist in the form of either solid, liquid or gas. The core materials are mainly used in the form of a solution, dispersion or emulsion. Compatibility of the core material with the shell presents an important criterion for enhancing the efficiency of microencapsulation; the pre-treatment of the core material is very often carried out for improving such compatibility.

Type and morphology of shell also plays an important role for diffusion, permeability or controlled-release applications. Depending on applications, a wide variety of core materials can be encapsulated, including pigments, dyes, monomers, and catalyst, curing agents, flame-retardants, plasticizers and nanoparticles.

The abundance of natural and man-made polymers provides a wider scope for the choice of shell material, which may be made permeable, semi-permeable or impermeable. Permeable shells are used for prolonged release of active components in the environment, while semi-permeable capsules are usually impermeable to the core material but permeable to low molecular-weight liquids. Thus, these capsules can be used to absorb substances from the environment and to release them again when brought into another medium. The impermeable shell encloses the core material and protects it from the external environment (for example: separation of reactive component, protection of sensitive substances against environmental effects, taste and odour masking, toxicity reduction etc.). To release the content of the core material the shell must be ruptured by outside pressure, melted, and dried out, dissolved in solvent or degraded under the influence of light. Release of the core material through the permeable shell is mainly controlled by the thickness of shall wall and its pore size. The dimension of a microcapsule is an important criterion for industrial application (Figure 2) (Kumar Ghosh, 2006).

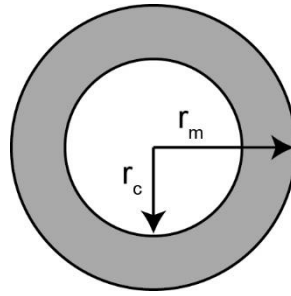


Figure 2: Cross-section of an idealized microcapsule

The morphology of microcapsules depends mainly on the core material and the deposition process of the shell. Microcapsules may have regular or irregular shapes and, on the basis of their morphology, can be classified as mononuclear, poly-nuclear and matrix type (Figure 3).

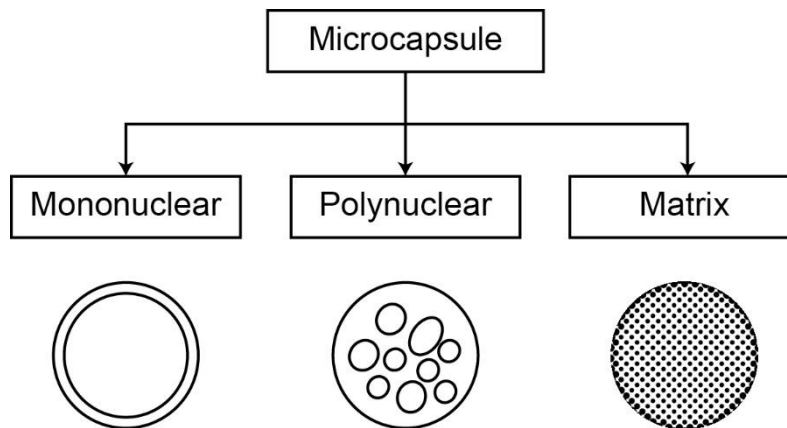


Figure 3: Morphology of microcapsules

Mononuclear (core-shell) microcapsules contain the shell around the core, while poly-nuclear capsules have many cores enclosed within the shell. In matrix encapsulation, the core material is distributed homogeneously into the shell material. In addition to these three basic morphologies, microcapsules can also be mononuclear with multiple shells, or they may form clusters of microcapsules (Kumar Ghosh, 2006).

3. APPLICATION OF MICROCAPSULES IN THE INDUSTRY

Microencapsulation has several interesting advantages, and the main reasons for microencapsulation can be summarized as follows:

- protection of unstable, sensitive materials from their environments prior to use,
- better process ability (improving solubility, dispersibility, flowability),
- self-life enhancement by preventing degradative reactions (oxidation, dehydration),
- controlled, sustained, or timed release,
- safe and convenient handling of toxic materials,
- masking of odour or taste,
- enzyme and microorganism immobilization,
- controlled and targeted drug delivery,
- handling liquids as solids, ...

Many producers of microcapsules developed their own field of applications. Some are in the early stages and others have been widely marketed for some time now. The main markets involve areas of cosmetics, cosmetotextiles, paper and non-woven materials, graphic arts, odour maskers and deodorants, food products, detergent-phytosanitary products, biotechnology, photography, electronics etc.

3.1 Microcapsules for the cosmetics industry

Microcapsules, with shell made of silicone copolymers, were specifically designed for cosmetics industry. Tests performed by a well-known laboratory on the cationic microcapsules containing a caffeine organic solution (the hardest-to-use form) showed excellent skin acceptance and flawless toxicology, which lead to the conclusion that these microcapsules can be considered as hypoallergenic. They can have an anionic (type S and IS) or cationic (type SK and ISK) charge; also in their dry form they can easily be admixed to makeup formulations (Microcapsules-technologies, 2014).

3.2 Microcapsules for the textile industry

By microencapsulation technologies the properties of textiles are improved or even obtained completely new functions. Typical examples of patented microcapsule applications in textile products include microencapsulated dyes and pigments, thermochromic and photochromic effects, microencapsulated catalysts and enzymes for special textile treatment, agents for textile sizing, adhesive bonding, softener and antistatic compositions, ingredients in textile detergents, microencapsulated textile fragrances, perfumes, and special functional textiles with microencapsulated insect repellents, antimicrobial, disinfectant and deodorant components, bioactive medical and cosmetic textiles and textiles for active thermal control with microencapsulated phase change materials (PCMs). Microcapsules can be added to the textiles by spraying or impregnating textiles or prior integration into the fibers.

Since the beginning mainly melamine-based microcapsules, containing perfumes and essential oils, as well as cationic gelatine-containing microcapsules for the needs of cosmetotextiles have been in use in the textile industry. Substantial recent advances in encapsulation for the cosmetics industry have resulted in the development of functionalized silicone microcapsules (patent filed) specially suited to, so called cosmetotextiles due to their perfect chemical compatibility with the skin. Cationic microcapsules (SK) show superior affinity to textile fibres, allowing almost 100% fixation rate and good wash resistance. Binders are available to further increase this resistance for even higher requirements. The IS and ISK forms allow fixation of aqueous actives to textiles.

In collaboration with the cosmetics industry, several companies have developed a wide range of microcapsules for textile applications, that contain actives formulated for tights, panties, socks and underwear, with efficiency been proven by tests carried out according to strictly controlled protocols applied according to the accepted practice (Microcapsules-technologies, 2014).

3.3 Odor maskers and deodorants

A whole range of mechanically breakable or permeation microcapsules was developed for these uses. Spray formulas are available for public and private areas. 8G microcapsules, which are entirely transparent and of the permeation type, are particularly attractive as they only, require two applications per week for a permanent effect.

3.4 Detergents

Microcapsules adapted to the various environments in which they are used, such as cleaners, detergents, textile softeners, are available. The cationic forms allow efficient fixation to textiles, thus providing remarkable effects when they contain perfumes (Microcapsules-technologies, 2014).

3.5 Phitosanitary

Many specific industrial applications have been developed for infected countries, such as permeating and biodegradable gelatine-based microcapsules, insecticides, repellents and disinfectants.

3.6 Food-grade products

Some of the producers have developed a line of food-grade gelatine-based microcapsules ranging from 0.3 to 1.5mm in diameter, which can be dried and offered as a coloured or colourless flowing powder. This type of microcapsules is mainly intended for encapsulation of brittle or volatile

ingredients, such as essential oils, highly unsaturated oils, aromas and food adjuncts (Microcapsules-technologies, 2014).

3.7 Microcapsules for papers and nonwoven materials

Microcapsules are generally surface-deposited through coating or spraying. Once they are functionalized they develop strong affinity to paper fibres and therefore, can be incorporated within the paper or nonwoven batch materials. Based on these various techniques producers can manufacture:

- cleaning, polishing, disinfecting dry towelettes, ...
- scented, hydrating or decongestant tissues,
- hygienic products (pH or moisture-activated microcapsules),
- safety papers (such as the EDICODE form produced with the LATA Company) etc.

3.8 Graphic arts

Some of the the microcapsules, produced by several companies, can be applied on paper, cardboard or plastic substrates through various printing techniques, such as:

- screen printing,
- offset printing, and
- flexography.

Microcapsules are usually added into water-based inks, as well as UV and plastisol printing inks. Sometimes microcapsules can also be integrated in the printing varnish, depending on the printing technique. The application technique has a significant impact on the amount of microcapsules, which can be applied on paper surface. With the thicker layer of the printed ink the amount of microcapsules can be higher (Kipphan, 2001).

Besides printing technique printing material also plays an important role. Paper and cardboard are two of the most widely used substrates. Absorbency of the material defines the amount of bonded ink or varnish deposit on the surface. Depending on the structure and grammage of the printing material/substrate good or bad absorption of the varnish or printing ink is defined by which drying process are also directly affected (Jayashree et al., 2013).

The printing method has a crucial influence on the activity level as it can be expected, given that the amount – thickness of varnish or printing ink transferred on paper surface will be undoubtedly affected on the microcapsule activity (Savolainen et al., 2011).

4. ACKNOWLEDGEMENT

This work was supported by the Serbian Ministry of Science and Technological Development, Grant No.: 35027 "The development of software model for improvement of knowledge and production in graphic arts industry".

5. REFERENCES

- [1] Du Y. Z., Wang L., Dong Y., Yuan H., Hu F. Q. Carbohydr. Polym. 2010, 79, pp.1034.
- [2] Ghen F., Luo G., Yang, W., Wang Y. Preparation and adsorption ability of polysulfone microcapsules containing modified chitosan gel, Tsinghua Science and Technology, 10, 2005, pp. 535–541.
- [3] Gong X., Lu Y., Xiang Z., Luo G. Preparation of polysulfone microcapsules containing 1-octanol for the recovery of caprolactam, Journal of Microencapsulation, 26, 2009, pp. 104–110.
- [4] Gong X., Luo G., Yang W., Wu F. Separation of organic acids by newly developed polysulfone microcapsules containing triethylamine, Separation and Purification Technology, 48, 2006, pp. 235–243.
- [5] Gumí T., Gascón S., Torras C., Garcia-Valls R. Vanillin release from macrocapsules, Desalination, 245, 2009, pp.769–775.

- [6] Herrmann A., Debonneville C., Laubscher V., Aymard L. Dynamic headspace analysis of the light-induced controlled release of perfumery aldehydes and ketones from keto esters in bodycare and household applications, *Flavour and Fragrance Journal*, 15, 2000, pp. 415–420.
- [7] Jacquemond M., Jackelmann N., Ouali L., Haeffliger O. Perfume-containing polyurea microcapsules with undetectable levels of free isocyanates, *Journal of Applied Polymers Science*, 114, 2009, pp. 3074–3080.
- [8] Jayashree K., Satya Priya A., Sugumar. S., Arul Vanishwari M. Vishnuvarthanan M., Rajeswari N. Encapsulated Fragrance in Overprint Coatings, *Journal of Applied Sciences Research*, 9 (1), 2013, pp. 141–148.
- [9] Juanjuan Y., Rui C., Yongsheng J., Chuande Z., Guanghui Z., Haixia Z. Adsorption of phenols by magnetic polysulfone microcapsules containing tributyl phosphate, *Chemical Engineering Journal*, 157, 2010, pp. 466–474.
- [10] Kipphan, H. *Handbook of Print Media*; Springer-Verlag: New York, 2001.
- [11] Kumar Ghosh S. *Functional Coatings: By Polymer Microencapsulation*, Published Online: 29 JUN 2006, Copyright © 2006 Wiley-VCH Verlag GmbH & Co. KGaA.
- [12] *Microcapsules-technologies* (2014) <http://www.microcapsules-technologies.com/an/applications.php> (Accessed: 26.09.2014.)
- [13] Mulder M. *Basic Principles of Membrane Technology*, 2nd ed., Kluwer Academic, Dordrecht, 2003 [copyright 1996].
- [14] Nelson G. Application of microencapsulation in textiles, *International Journal of Pharmaceutics*, 242, 2002, pp. 55–62.
- [15] Peña B., Panisello C., Aresté G., Garcia-Valls R., Gumí T. Preparation and characterization of polysulfone microcapsules for perfume release, *Chemical Engineering Journal*, 179, 2012, pp. 394–403.
- [16] Peña B., Casals M., Torras C., Gumí T., Garcia-Valls R. Vanillin release from polysulfone macrocapsules, *Industrial & Engineering Chemistry Research*, 48, 2009, pp. 1562–1565.
- [17] Poncet D. *Surf. Chem. Biomed. Environ. Sci.* 2006, 228, pp. 23.
- [18] Rodrigues S., Martins I., Fernandes I., Gomes P., Mata V., Barreiro M., Rodrigues A. Scentfashion: microencapsulated perfumes for textile application, *Chemical Engineering Journal*, 149, 2009, pp. 463–472.
- [19] Savolainen A., Zhang Y., Rochefort D., Holopainen U., Erho T., Virtanen J., Smolander M. Printing of Polymer Microcapsules for Enzyme Immobilization on Paper Substrate, *Biomacromolecules*, 2011, 12, pp. 2008–2015.
- [20] Thies C. *Microcapsules*, *Encyclopedia of Food Sciences and Nutrition*, 2nd ed., Academic Press, Oxford, 2003, pp. 3892–3903.
- [21] Ternat C., Ouali L., Sommer H., Fieber W., Velazco M., Plummer C., Kreutzer G., Klok H., Manson J., Herrmann A. Investigation of the release of bioactive volatiles from amphiphilic multiarm star-block copolymers by thermogravimetry and dynamic headspace analysis, *Macromolecules*, 41, 2008, pp. 7079–7089.
- [22] Tona R., Jiménez L., Bojarski A. Multiscale modeling approach for production of perfume microcapsules, *Chemical Engineering & Technology*, 8, 2008, pp. 1216–1222.
- [23] Van den Berg C., Roelands C., Bussmann P., Goether E., Verdoes D., Van der Wielen L. Preparation and analysis of high capacity polysulfone capsules, *Reactive and Functional Polymers*, 69, 2009, pp. 766–770.
- [24] Wang P., Zhu Y., Yand X., Chen A. Prolonged-release performance of perfume encapsulated by tailoring mesoporous silica spheres, *Flavour and Fragrance Journal*, 23, 2008, pp. 29–34.
- [25] Wang G., Chu L., Zhou M., Chen W. Effects of preparation conditions on the microstructure of porous microcapsule membranes with straight open pores, *Journal of Membrane Science*, 284, 2006, pp. 301–312.
- [26] Yang W., Lu Y., Xiang Z., Luo G. Monodispersed microcapsules enclosing ionic liquid of 1-butyl-3-methylimidazolium hexafluorophosphate, *Reactive and Functional Polymers*, 67, 2007, pp. 81–86.

INFLUENCE OF SODIUM METASILICATE SOLUTION'S CHARACTERISTICS ON THE DEVELOPING OF THE OFFSET PRINTING PLATE

Tomislav Cigula¹, Živko Pavlović², Regina Fuchs Godec³, Dubravko Risovic⁴,

¹ University of Zagreb, Faculty of Graphic Arts, Zagreb, Croatia

² University of Novi Sad, Faculty of Technical Sciences,

Department of Graphic Engineering and Design, Novi Sad

³ University of Maribor, Faculty of Chemistry and Chemical Engineering, Maribor, Slovenia

⁴ Molecular Physics Laboratory, Ruder Boskovic Institute, Zagreb, Croatia

Abstract: Lithographic printing is characterized by the fact that the selective ink adsorption in the printing process is achieved by opposite physical-chemical properties of printing and nonprinting areas on the printing plate. The majority of the printing plates used in the offset printing are built from aluminium foil, which is chemically and electrochemically processed in order to form rough and porous aluminium-oxide film and in the end coated by a photoactive coating. The rough aluminium-oxide film will form nonprinting areas, and the photoactive coating forms printing areas. In the plate making process the plate is exposed to an electromagnetic radiation with certain wavelength and subsequently developed to remove parts of the photoactive coating and open the aluminium-oxide layer. The developing solutions are often highly alkaline and could as well dissolve the aluminium oxide layer, thus deteriorating its wetting characteristics. The aim of this paper is to determine influence of the developer saturation and developing time on the characteristics of a printing plate. For that purpose, printing plate samples were made by varying the investigated parameters. To evaluate the influence of considered parameters, contact angle measurements and determination of roughness parameters were performed. Results of the investigation showed that both, developer saturation and the developing time influence surface properties of the made printing plate. It could be concluded that for the investigated range of process parameters increase of the developer saturation and of the developing time increases the wetting characteristics of printing plate. In addition, future research is needed to investigate range of the developer saturation in which the noticed behaviour is occurring i.e. which developer saturation results in unacceptable printing plate's surface properties.

Key words: printing plate, wetting, developing process, sodium metasilicate

1. INTRODUCTION

Lithography is a complex printing technique in which the selective absorption of the printing ink is achieved by opposite surface properties of the image and nonimage areas on the printing plate. Image areas are built of the organic coating which makes them oleophilic and hydrophobic while non-image areas are most often built of aluminium-oxide which makes them hydrophilic and enables good adsorption of water based fountain solution (Wilson, 2005). Main representative of lithography is offset. It is characterized by indirect transfer of the printing ink. The printing ink is transferred from the printing plate on the rubber coated cylinder and then on the printing substrate (Wilson, 2005).

As mentioned, majority of the printing plates used today in lithography are made of aluminium foils. The aluminium foil is mechanically, chemically and electrochemically processed in order to make surface with desired properties. The surface processing is done to improve adhesion of the fountain solution and photoactive coating in the printing process (Limbach et al, 2003; Lin et al, 2001). Besides electrochemical roughening (graining), in the next step anodic oxidation is performed in order to build a thin aluminium-oxide layer which consists of a compact layer (barrier layer) and outer porous layer (Nishino et al, 2004). The printing performance and durability of the printing plate are highly influenced by the formed surface structure of the aluminium foil (Rivett et al, 2011). In the plate making process one distinguishes two processes, exposure to a defined electromagnetic radiation and developing process. The electromagnetic irradiation should induce a chemical reaction in the photoactive layer which will make it soluble (positive working) or insoluble (negative working) in defined solution (developer). The developing process must completely remove parts of the photoactive layer thus opening surface of the aluminium foil creating non-image areas.

Although considerable effort is put into development of the chemistry-free printing plates, which are developed in the printing machine, they still lack durability and are not widely spread in the print-shops. On the other hand, majority of the chemically developed plates use as a developer a high alkaline solution (pH \approx 13). This makes determination of the processing parameters highly important as the developing process, due to the amphoteric character of the aluminium-oxide, could induce unwanted changes of the aluminium-oxide topography. In addition, determination of adequate developer composition could lead to lowering usage of chemical resulting in environmentally friendlier developing process.

2. MATERIALS AND METHODS

The samples used in this study were made of conventional and CtCP (Computer to Conventional Plate) diazo positive printing plate. Regardless of the plate making process (conventional or CtCP) the developing process is the same.

All samples of the printing plate were exposed by PlurimetEXPO74 exposure unit equipped with a metal-halide lamp with power of 3.5 kW. The exposure for the plate samples was 60 pulses. Samples were developed in the developers of different saturations. The saturation s is calculated using (1).

$$s = \frac{A_p}{V_d} \left[\frac{\text{cm}^2}{\text{cm}^3} \right] \quad (1)$$

where A_p is area of the processed plate and V_d is the volume of the developer.

Developers were prepared by dissolving Na_2SiO_3 p.a. crystals in distilled water (INA, ISO 9001, ISO 14001, OHSAS 18001) in concentration of 0.2 mol dm^{-3} [Cigula et al, 2012] and then saturated by dissolving defined area of a plate. Three sets of four plate samples were prepared by alternating the developing time ($t_1 = 10 \text{ s}$, $t_2 = 30 \text{ s}$, $t_3 = 60 \text{ s}$) and the developer saturation ($0 - 0.9 \text{ cm}^{-1}$ with a step of 0.3 cm^{-1}). All samples were developed at temperature of $25 \pm 0.1^\circ\text{C}$. After developing process all samples were washed in distilled water and dried at room temperature.

Profilometric roughness parameters – R_a , R_z , R_p and R_v were measured by the Portable Surface Roughness Tester TR200. The unit is compatible with ISO 4287, DIN 4768, ANSI B 46.1 and JIS B601 standards. The selected profilometric parameters were chosen among others as they were previously used in the lithographic printing plate's surface characterization [Pavlovic et al, 2012; Risovic et al, 2009]. In order to determine influence of the developing process on the functionality of the printing plate, measurements of the contact angle were performed. The contact angle measurements were performed by Dataphysics's OCA30 goniometer. Contact angle was determined using Sessile drop method. Analysis of the liquid drop was performed by Dataphysics' SCA20 software using ellipse/Laplace-Young fitting depending on the drop shape [Dataphysics, 2006]. The volume of the applied liquid drop was $1 \mu\text{l}$. The measurements were performed using commercial alcohol based fountain solution, prepared by adding 2.5 %vol buffer, 1 %vol additive for conductivity correction and 11 %vol propan-2-ol in demineralised water.

3. RESULTS AND DISCUSSION

Figure 1 shows value of the roughness parameter R_a depending on developer saturation and developing time.

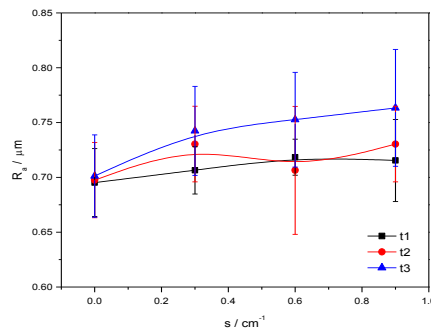


Figure 1: R_a depending on the developer saturation and developing time

One can see that the value of the R_a increases with increase of developing parameters i.e. the developer saturation and the developing time. The value of R_a measured on sample developed in developer with saturation of 0.6 cm^{-1} for 30 s is not as high as expected, but as the standard deviation corresponding to that value is very high it could be assumed that this is due to sample preparation.

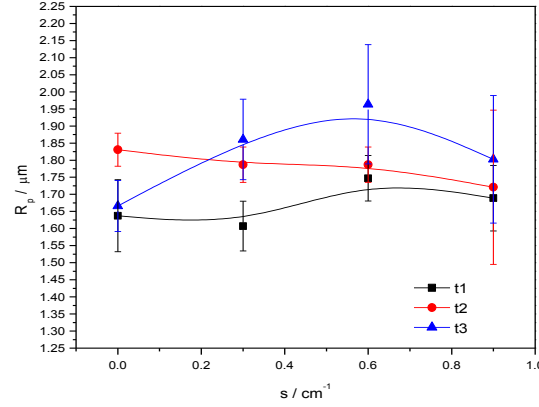


Figure 2: R_p depending on the developer saturation and developing time

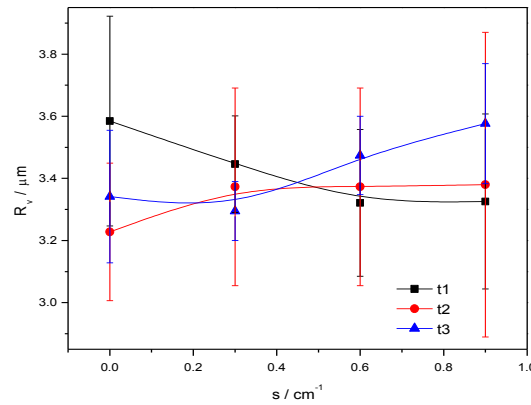


Figure 3: R_v depending on the developer saturation and developing time

In Figure 2 and Figure 3 one can see the influence of the developing parameters on the peaks (roughness parameter R_p) and valleys (roughness parameter R_v) of the aluminium oxide layer. One can see that both roughness parameters have higher values when a printing plate is developed with more saturated developer. The highest value of the parameter R_p is measured on the sample developed at developer's saturation of 0.6 cm^{-1} and developing time of 30 s, while highest value of the parameter R_v is measured on the printing plate sample developed in the most saturated developer ($s = 0.9 \text{ cm}^{-1}$) and with highest developing time (60 s). One can also notice a high standard deviation in results obtained for roughness parameter R_v , which could be the consequence of the aluminium oxide structure with different size of the valleys from which the photoactive coating must be chemically dissolved and removed. Increasing developing time enables complete removal of the photoactive coating and therefore increasing roughness of the nonimage areas, but on the other hand longer developing time causes dissolving of the aluminium oxide layer. As the developer saturation decreases the speed of the chemical reaction, it reduces time in which alkaline developer dissolves aluminium oxide causing increase of the roughness parameters.

Observing Figure 4, one can see that shortest developing time causes decrease of the R_z value and longest developing time causes increase of the R_z by the increase of the developer saturation. Figure 5 shows values of contact angles, representing wetting characteristics of the printing plate samples developed at different developing parameters.

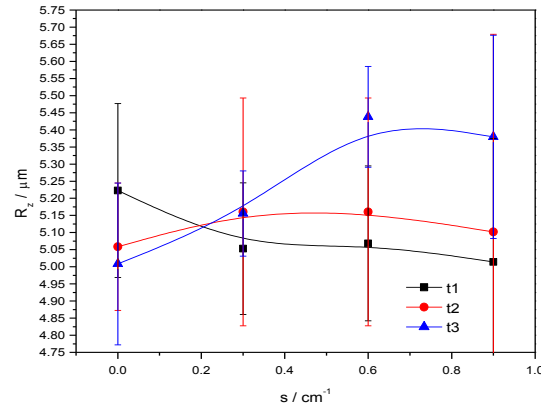


Figure 4: R_z depending on the developer saturation and developing time

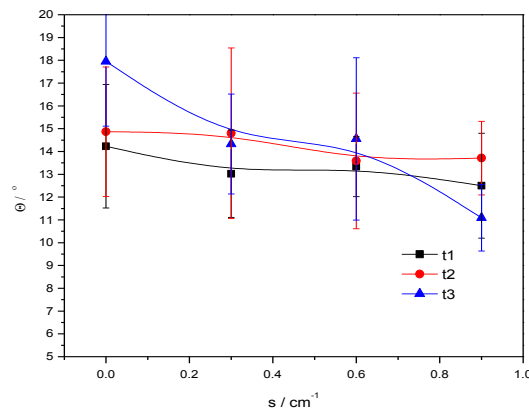


Figure 5: Contact angle value vs. developer saturation and developing time

One can see that best wetting (smallest contact angle) is achieved on the printing plates developed in developer of highest saturation ($s = 0.9 \text{ cm}^{-1}$) for all developing times. Although, one could expect that longest time would result in best removal of the photoactive layer and consequently lead to the best wetting characteristics, the dissolution of the aluminium oxide layer is higher if a less saturated developer is used which then causes decrease of the wetting properties. The smallest value of the contact angle (best wetting properties) was measured on the sample developed using highest values of both investigated parameters ($s = 0.9 \text{ cm}^{-1}$, $t_3 = 60 \text{ s}$).

4. CONCLUSIONS

This research was conducted in order to determine influence of the developer saturation (s) and the developing time on the surface properties of the CtCP positive working printing plate. To that purpose three sets of samples were prepared by using developers of four saturations, fresh developer ($s = 0 \text{ cm}^{-1}$), saturation of 0.3 cm^{-1} , 0.6 cm^{-1} and 0.9 cm^{-1} and developing times of 10 s, 30 s and 60 s. Measurements of various roughness parameters and contact angles were conducted in order to examine the influence of considered parameters of the developing process. The results of the investigation showed that both parameters influence observed surface characteristics of the printing plate, in particular those of the nonimage areas. The increase of the developer saturation causes increase of the average roughness (parameter R_a) and enhances wetting characteristics.

For the investigated process parameters range the increase of both parameters, the developer saturation and the developing time enhances wetting properties. These results must be taken into account in selection of process parameters in order to make printing plates with needed surface properties. However, the results also indicate that a future research is needed to investigate range of the developer saturation in which the noticed behaviour occurs i.e. which saturation will results in unacceptable printing plate's surface properties.

5. REFERENCES

- [1] Cigula, T., Poljak, J., Peko, V., Tomašegović, T.: "Sodium metasilicate solution as a developer for the CtCP offset printing plates", Proceedings - The Sixth International Symposium GRID 2012, (GRID, Novi Sad, Serbia, 2012), pages 115-120.
- [2] Data Physics Instruments GmbH. Operating manual OCA, 2006.
- [3] Limbach, P. K. F., Amor, M. P., Ball, J.: "Aluminium Sheet with Rough Surface", Patent No.: US 6,524,768 B1, date of patent February 25, 2003.
- [4] Lin, C. S., Chang, C. C., Fu, H. M.: "AC electrograining of aluminum plate in hydrochloric acid", Materials Chemistry and Physics, 68, pages 217-224, 2001.
- [5] Nishino, A., Masuda, Y., Sawada, H., Uesugi, A.: "Process for Producing Aluminum Support for Lithographic Printing Plate", Patent No.: US 6,682,645 B2, January 27, 2004.
- [6] Pavlovic, Z., Novakovic, D., Cigula, T.: "Wear analysis of the offset printing plate's non-printing areas depending on exploitation", Technical gazette, 19, pages 543-548, 2012.
- [7] Risovic, D., Mahovic Poljacek, S. Gojo, M.: "On correlation between fractal dimension and profilometric parameters in characterization of surface topographies", Applied Surface Science, 255, pages 4283-4288, 2009.
- [8] Rivett, B., Koroleva, E.V., Garcia-Garcia, F.J., Armstrong, J., Thompson, G.E., Skeldon, P.: "Surface topography evolution through production of aluminium offset lithographic plates", Wear, 270, pages 204-217, 2011.
- [9] Wilson, D. G.: "Lithography primer", (Pittsburg, USA, GATFPRESS, 2005.), pages 79-82

COMPARATIVE STUDY OF LINE AND DOT ELEMENTS REPRODUCTION ON FLEXO PRINTING PLATES USING DIFFERENT FILM MAKING TECHNOLOGIES

Sandra Dedijer, Magdolna Pal
University of Novi Sad, Faculty of Technical Sciences,
Department of Graphic Engineering and Design, Novi Sad, Serbia

Abstract: Flexography today is printing process widely used in packaging domain. Due to its high printing speed and ability to print on variety of substrates, including flexible and nonporous printing materials, it found its place on highly demanding printing market, having tendency to become leading printing process in packaging industry, leaving behind gravure and offset printing. The technological improvements made in domain of anilox rollers, photopolymer plates and ink development has led to predictable and stable print quality, ready to answer almost any quality demands. One of the main advantages of flexo printing process is its flexible printing plate. But on the other hand, its advantage is at the same time one of the leading threats to insufficient final imprint quality. Being flexible, it influences printing image deformation caused by plate mounting and the pressure during printing. Thus proper and controlled printing plate reproduction is one of key factors which verily influence print quality. Although today CtP flexo plate making process is well known, the conventional plate making process, which evolves usage of negative film, is still frequently used. It is usually economically driven choice and it still gives satisfactory results concerning tone value reproduction. Regardless of used technology, the control over the plate making procedure is essential for stable, repeatable and satisfactory platemaking production in terms of aimed, high quality final printing product. The plate making procedure affects the final area and profile of the halftone dots and consequently, the amount of ink transferred to the substrate. Thus the research in domain of flexo printing plates is mostly aimed on defining tone value reproduction, dot shape, dot profile, dot shoulder angle and dot surface. In conventional flexo plate making process where negative film is used, these parameters are highly influenced by the characteristic of used film.

The purpose of this study was to determine the effect of using different negative films on line and dot elements reproduction on conventional flexo printing plates. Beside different film making technology, two different screen rulings were applied. Three different negative films were used (ink-jet, matte and non-matte negative film), two different screen rulings (120 lpi and 150 lpi) and two flexo printing plates (Nyloflex Ace and Nyloflex FAR, both 1.14 and 2.84 mm thick).

Key words: film making technologies, conventional flexo plates, line and dot reproduction

1. INTRODUCTION

Flexographic printing today stands for stable and predictable printing process which certainly evidence major positive economical growth and technological enhancements. Shoulder to shoulder with other printing processes, conventional as well as digital, it testifies a clear indication of the positive sales and profit potential contrasted to low, sheetfed offset and web offset sales and profit performance quotients (Multimediaman, 2012). The imprint quality is improved mostly in accordance with technical and technological innovations in the field of photopolymer plates, printing inks and anilox rollers.

Flexography is a high speed printing process mostly used for packaging printing due to its ability to print on various, flexible and nonporous substrates (Bould et al, 2014; Valdec, Zjakić & Milković, 2013; Hershey, 2010). It is accomplished by virtue of the main characteristic of its printing plate – its flexibility. But still, its main advantage could be at the same time the drawback. Namely, the improper plate production, plate mounting or printing conditions (in the first place printing pressure) can lead to deformation of printing image (Mahović Poljaček et al, 2013; Tomašegović, Mahović Poljaček & Cigula, 2013). Also, printing pressures required to print solids and halftones are different and image distortion may occur, especially when printing is conducted on uneven substrates (Bould et al, 2014). But still, when printing plates are in question, several key parameters can be abstracted that can largely affect the quality produced by flexographic printing: line ruling, dot geometry, plate thickness, film making process and plate making

parameters. The control over the plate making procedure affects the final area and profile of the halftone dots, line and single dot elements and textual elements. Apropos, the research in domain of flexo printing plates includes research in tone value (TV) reproduction, single dot area, shape and profile, line reproduction in terms of line width and line profile, as well as reproduction of text elements, mostly aimed on determining the smallest font size which is going to be clearly transferred and readable on printing substrate. The stable thin line reproduction on flexo plates which is going to be, without cease, transferred to the printing substrate has become more of an interest with involving flexo printing process in production process of printed electronics (Lunt, 2013; Feu & Lara, 2013; Embury, 2010). Since the conventional flexo plate making process involves film, these parameters are certainly influenced by its characteristic. Flexo plates, conventional or digital, are produced using photopolymer compounds (photosensitive monomers and additives like photo initiators and plasticizers) which harden when exposed to UV radiation, due to photo polymerization process (Bould et al, 2014; Mahović Poljaček et al, 2013; Tomašegović, Mahović Poljaček & Cigula, 2013; Liu & Guthrie, 2003; Liu, Guthrie & Bryant, 2002). Although digital plate processing has altered the landscape in flexography, the conventional systems are still in use (Kenny, 2007). Conventional photo-polymer flexographic plates need high-contrast film negative that is essential for the main exposure process (Bould et al, 2014; Liu, Guthrie & Bryant, 2002; Gilbert & Lee, 2008). The reproduction of the future printing elements on the film primarily determine these on a processed printing plate (Hamblyn et al., 2005; Bould et al, 2004). Also, other processing phases such as exposure and washout can affect the final printing element reproduction (Liu, Guthrie & Bryant, 2002; Hamblyn et al., 2005; Novaković, Dedijer & Mahović Poljaček, 2010). Today on a free market are available a variety of graphic films from different producers which can be used in conventional flexo platemaking process. According to technological specifications, they can be divided as follows: standard matte negative film, non-matte negative film and film made by ink-jet technology.

The purpose of this investigation was to examine the effect of different negative films used on line and dot elements reproduction on conventional flexo printing plates. Beside different film making technology, two different screen rulings were also applied.

2. METHODS AND MATERIALS

The imaging of flexo plates used in this experiment was done using three different negative films: non-matte (A), ink - jet (B) and matte film (C). The applied screen rulings were 120 lpi and 150 lpi. During film making process, no compensation curves were applied. The film processing was done according to the standard procedure of the manufacturer. Optical density of films used (Table 1) was controlled by means of transmission densitometer Viptronic Vipdens 150. The optical density of the clear film is noted as D_{min} and is recommended to be below 0.04. Maximum optical density of the fully exposed film is noted as D_{max} and it should be over 4.00 (FFTA, 1999). Used flexo plates were: Nyloflex Ace, 1.14 mm and 2.84 mm thick (Plate Ia and Plate Ib) and Nyloflex FAR, 1.14 mm and 2.84 mm thick (Plate IIa and Plate IIb). The processing was done on Nyloflex Combi FISuper device. The processing parameters, according to manufacturers' recommendations (Flint Group, 2014a; Flint Group, 2014b) are listed in Table 2.

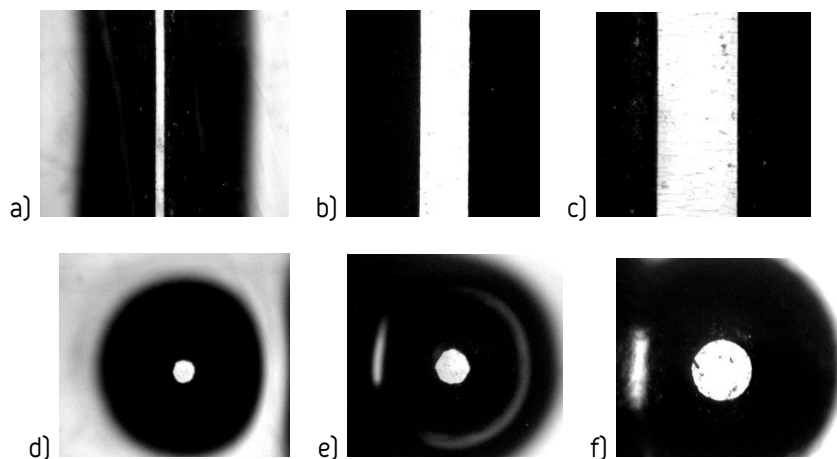


Figure 1: Examples of microscopic images of line (a, b and c) and dot (d, e and f) elements

The measurements of reproduced line and dot elements on film as well on printing plate, were done on microscopic images (Figure 1) gained using measuring device Viptronic Vipflex 334 and corresponding functions of PerfectEye v. 4.0 software. The elements of interest were solid lines initially 0.05, 0.1, 0.2, 0.3, 0.4 and 0.5 mm wide (later on graphs named as I,II,III,IV,V and VI, respectively) and single dots of initial diameter 0.05, 0.1, 0.2, 0.3, 0.4 and 0.5 mm (later on graphs named as I,II,III,IV,V and VI, respectively). Two replicas of each plate/screen ruling/film combinations were made and each element was measured four times. The presented results are average values of eight measurements.

Table 1: Optical density of used films

Film	D _{min}	D _{max}	D _{min}	D _{max}
	120 lpi		150 lpi	
Film A	0.05	3.85	3.05	3.89
Film B	0.01	4.82	0.01	4.61
Film C	0.05	3.21	0.05	3.19

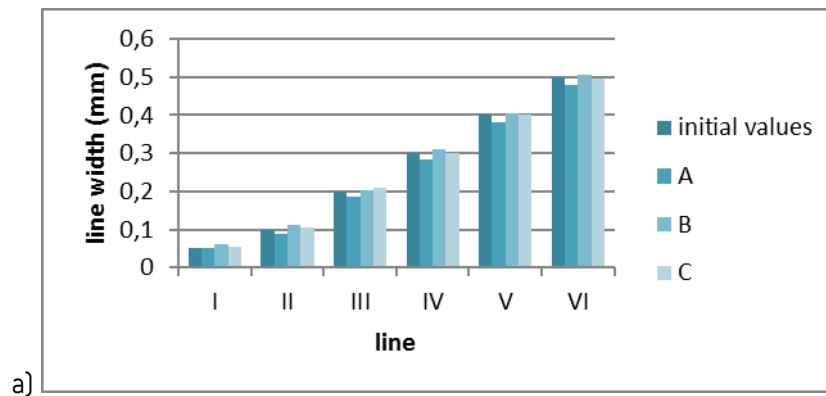
Table 2: Plate processing parameters

Plate	Back exposure (sec)	Main exposure (min)	Developing speed (mm/min)	Drying time (h)	Post exposure (min)	Light finishing (min)
Plate Ia	30	20	200	2	10	10
Plate IIb	110	20	180	2	10	15
Plate IIa	15	17	200	2	10	15
Plate IIb	60	22	150	3	10	15

3. RESULTS AND DISCUSSION

First step in conducted experiment involved line width and dot area measurements on used films. The gained results are presented on Figures 2 and 3. Having in mind the initially defined line width (Figure 2), the one can see that, regardless of screen ruling used, the lowest width values for the whole range of lines were measured on film A. On contrary, the highest ones were gained on film B. As it was expected, the same trend was seen in case of dot reproduction (Figure 3), whereas rather poor reproduction of dot I was noted.

On Figure 4 are graphically presented results of line width measurements on printing plates obtained using film A (120 and 150 lpi). Regardless of screen ruling as well as initial line width, higher values were noted in case of printing plate type I. In comparison to line width obtained on film (120 lpi), the reproduced lines on printing plates are wider than those on film. The exception is reproduction on plate IIa, with the narrowest lines reproduced. From the graph on figure 4b, it can be seen that on printing plate type I lines are slightly wider than those on film, while in case of printing plate type II, the trend is opposite.



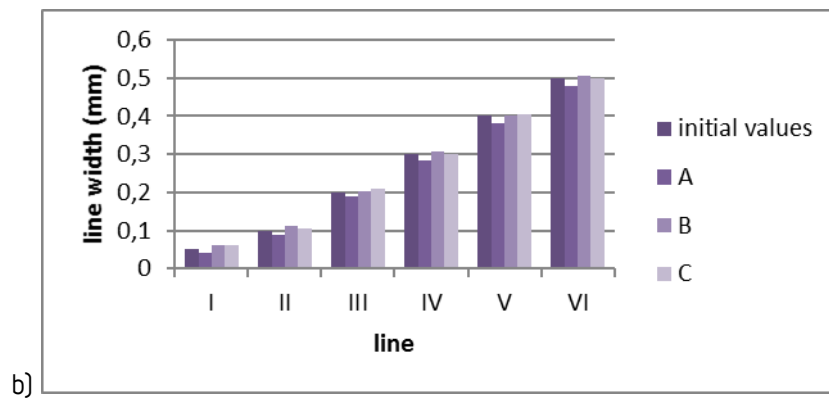


Figure 2: Line element width on films: a) 120 lpi and b) 150 lpi

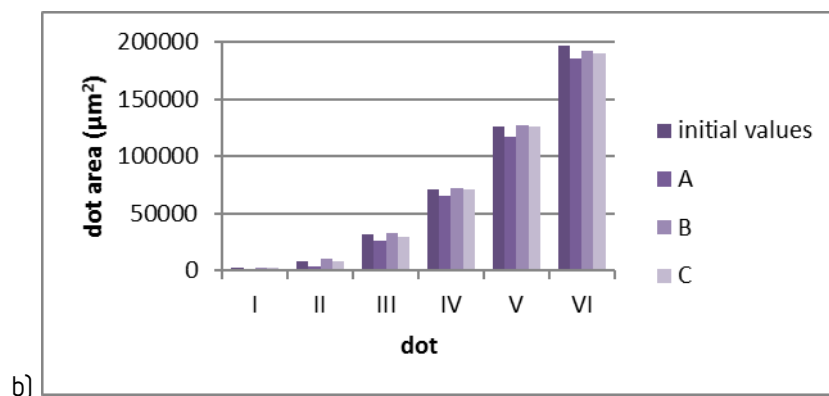
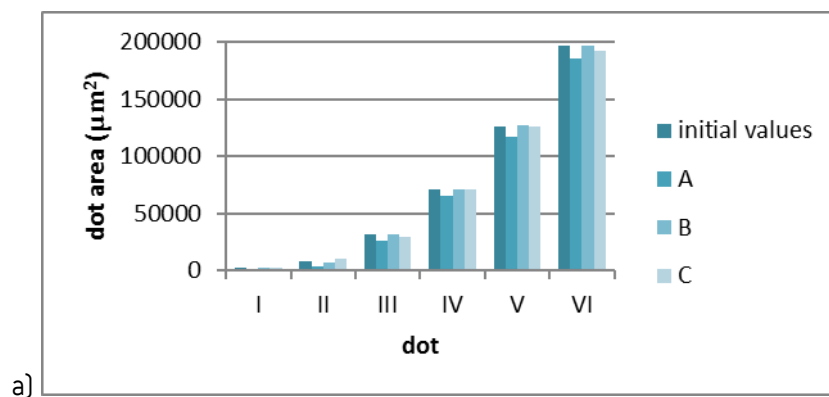
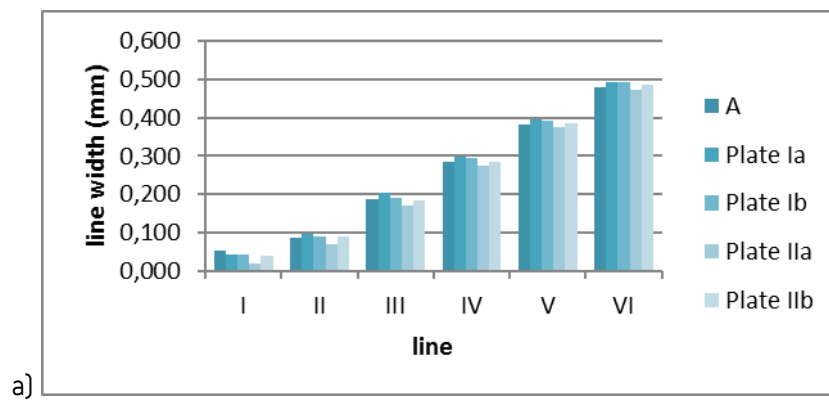


Figure 3: Dot area on films: a) 120 lpi and b) 150 lpi



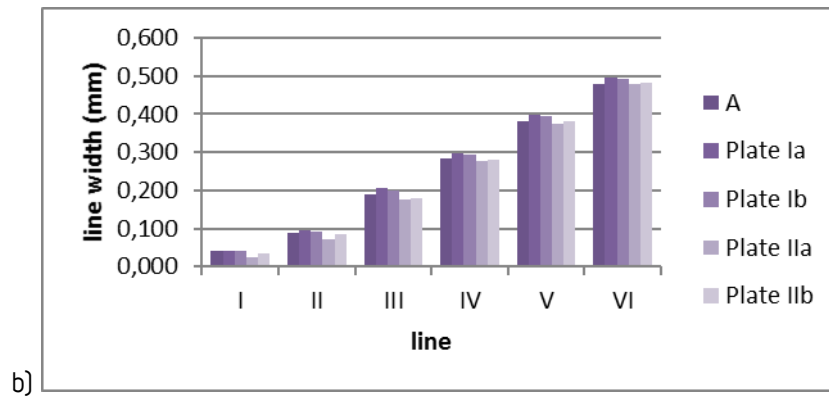


Figure 4: Line element width on printing plates (using film A): a) 120 lpi and b) 150 lpi

On Figure 5 are graphically presented results of dot area measurements on printing plates obtained using film A (120 and 150 lpi). From the graphs presented, it can be seen that reproduction of dots I and II was unsuccessful. It is the fact that dot II was reproduced on printing plate Ia (150 lpi) but with dot area which is almost half of the size of these on film, assuming that it cannot be sustained on printing plate during printing process.

Dots with larger dot area, regardless of initial diameter and film used, are noted on plate type I compared to plate II. In comparison to values reproduced on film (120 and 150 lpi), the enlargement of dot area is observed with printing plate type I, while opposite trend is remarked for printing plate type II. Overall, the highest values are measured on plate Ia, while the lowest ones were on printing plate IIa.

On Figure 6 the one can see the results of line width measurements on printing plates type I and II achieved using film B (120 and 150 lpi). Regardless of screen ruling as well as initial line width, lines reproduced on printing plates are narrower than those on film, with the exception of line VI. Independently from values on film and screen ruling, the lowest line widths are measured on printing plate Ia.

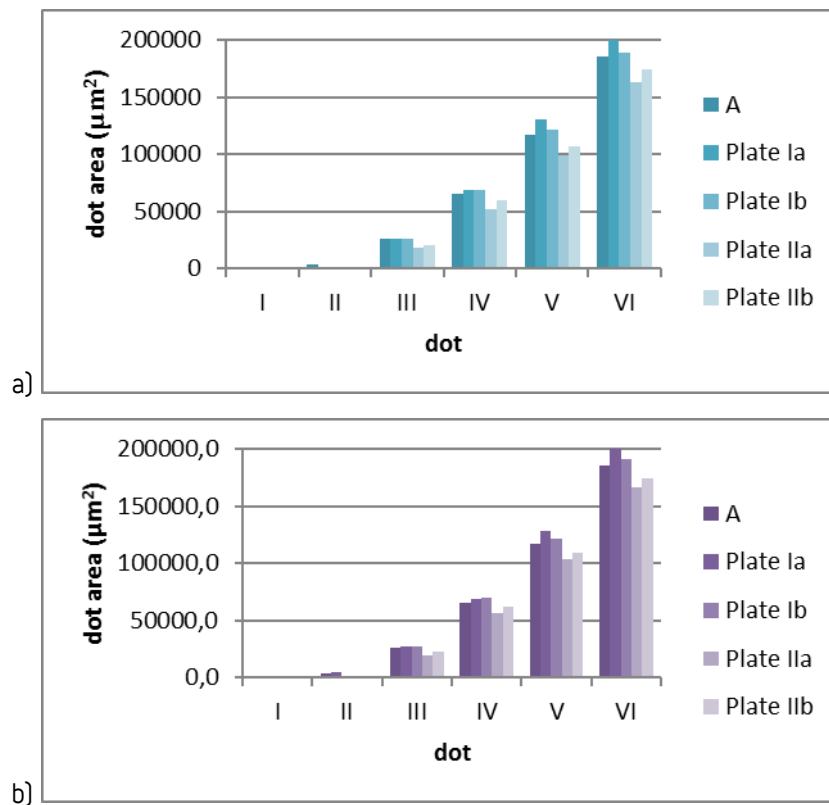


Figure 5: Dot area on printing plates (using film A): a) 120 lpi and b) 150 lpi

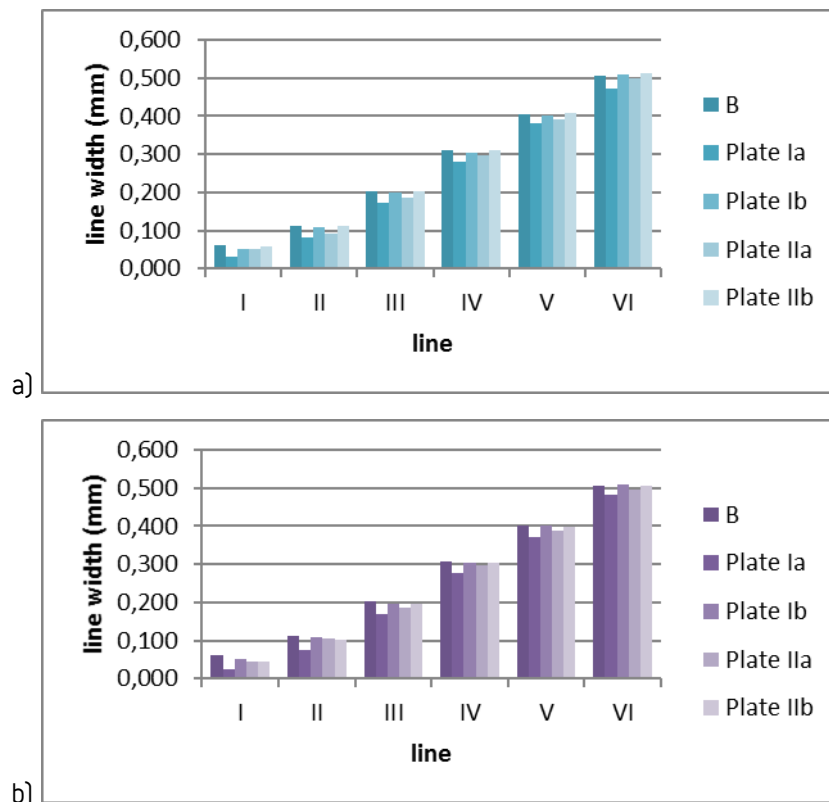


Figure 6: Line element width on printing plates (using film B): a) 120 lpi and b) 150 lpi

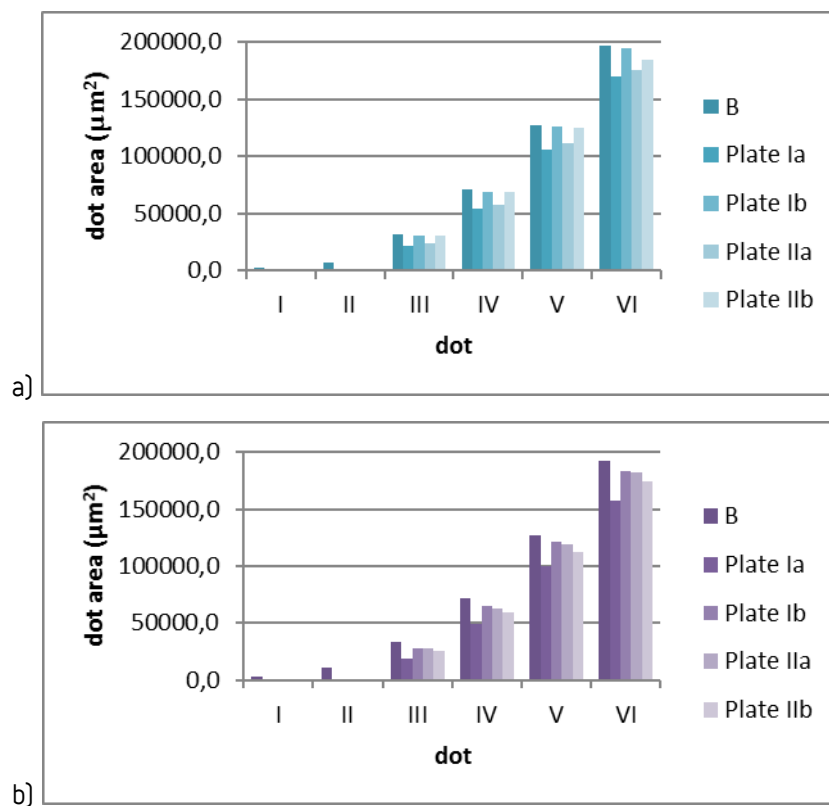


Figure 7: Dot area on printing plates (using film B): a) 120 lpi and b) 150 lpi

On Figure 7 are graphically presented results of dot area measurements on printing plates used, obtained with film B (120 and 150 lpi). It is apparent that dots I and II could not be reproduced on

any printing plate. Also, apart from screen ruling and dot area on film, dots reproduced on plates are of lower area. Comparing dot reproduction between plates used, the lowest values are achieved on plate Ia, while the highest ones are on Ib.

The results of line width measurements on printing plates obtained using film C (120 and 150 lpi) are presented on Figure 8. It can be seen that when screen ruling of 120 lpi was used, wider lines were reproduced on plates than on film (excluding line I and II on plates IIa and IIb). Comparing between the plates, the lowest values were measured on plate IIb, while the highest were on plate Ib. In case of screen ruling of 150 lpi, the lines reproduced on plates were wider than those on film, with the exception of plate Ia. Consequently, observing among plates, the narrowest lines are measured on plate Ia, while the widest were on plate Ib.

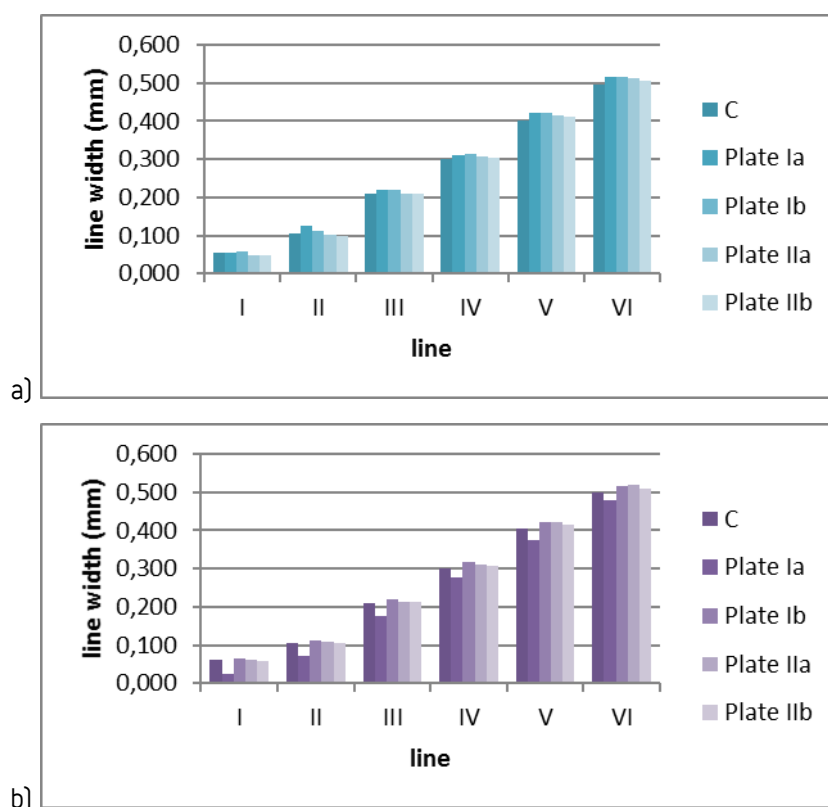
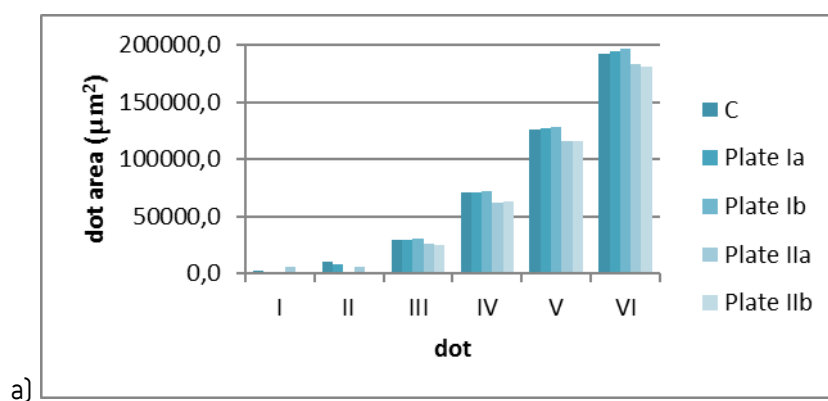


Figure 8: Line element width on printing plates (using film C): a) 120 lpi and b) 150 lpi

On Figure 9 are graphically presented results of dot area measurements on printing plates, obtained with film C (120 and 150 lpi). For both screen rulings, larger dots were reproduced on plate type I than on plate II. In comparison to those reproduced on films, larger dots are measured on plate type I (screen rulings of 120 and 150 lpi) and IIa (screen ruling of 150 lpi), while smaller ones were on plate type II (screen ruling of 120 lpi) and IIb (screen ruling of 150 lpi).



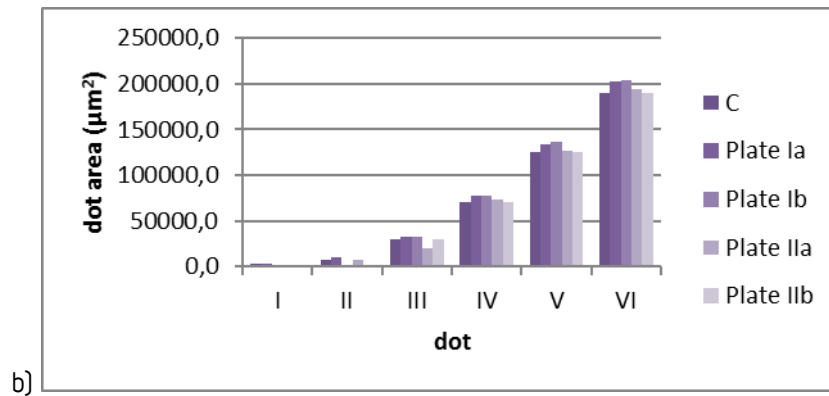


Figure 9: Dot area on printing plates (using film C): a) 120 lpi and b) 150 lpi

4. CONCLUSIONS

This study was aimed to define how does the using of different negative films affect line and dot elements reproduction on conventional flexo printing plates. Three different negative films were involved in experiment: non-matte (A), ink – jet (B) and matte (C), two different screen rulings (120 lpi and 150 lpi) and two flexo printing plates (Nyloflex Ace and Nyloflex FAR, both 1.14 and 2.84 mm thick).

Gained results were influenced by elements' reproduction on films in terms of initial line width and dot area. Having in mind that conventional flexo platemaking process was used, it was expected that reproduction on plates will be heading towards incensement of line width ad dot area. But, this was not noted in all cases, where the line and dot reproduction using ink – jet film (B) particularly stands out. Namely, measurements indicate that using ink – jet film results in smaller dots and narrower lines reproduced on printing plates, although having the best solid density values among tested films. This might lead to the conclusion that when ink – jet film is in question, in order to gain closer reproduction to those on film, the one must enhance main exposure time. Nevertheless, the reproduction of all line elements was enabled using all three film types. But, the reproduction of dot elements I and II (initial diameter of 0.05 and 0.1 mm) was not successful, with the exception of matte film (applied on thinner plates). This should be taken with certain caution since, according to microscopic images and dot area values, their sustainability during printing is jet to be tested. From the results presented, it can also be concluded that the screen ruling has less significant influence on line and single dot reproduction. This was expected, since the screen ruling affects tone value reproduction rather than solid/full tone. Also it was noted that plate thickness has less influence on elements reproduction in comparison to plate type.

From presented research, it is shown that all three films (film produced using ink – jet technology, non-matte as well as conventional matte film), with certain improvements in film and platemaking process, can be used for satisfying reproduction of line and dot elements on plate. Nevertheless, in order to get a more precise insight in film/plate correspondence further investigations are inevitable. They should be aimed towards testing of TV reproduction, dot structure, dot circularity, single dot profile and overall consistency and productivity.

5. ACKNOWLEDGMENTS

This work was supported by the Serbian Ministry of Science and Technological Development, Grant No.: 35027 "The development of software model for improvement of knowledge and production in graphic arts industry".

6. REFERENCES

- [1] Bould, D.C., Claypole, T.C., Bohan, M.F.J.: "An experimental investigation into Flexographic printing plates", TAGA Journal of Graphic Technology, 1(4), (2004)
- [2] Bould, D. C., Claypole, T. C., Bohan, M. F. J., Gethin, D. T.: "Deformation of Flexographic Printing Plates", (2004) URL <http://www.printing.org/page/8623#>, [last request: 20.09.2010.]

- [3] Embury, L. "Presentation on Flexographic Printing Techniques", (2010), URL <http://www.gwent.org/presentations/Simtech2.pdf>, [last request: 08.09.2014.]
- [4] Feu, M., Lara, E. "Printed electronics: more than promising Printed Intelligence", (2013), URL <http://thegreatproject.com/printed-electronics-more-than-promising-printed-intelligence/>, [last request: 08.09.2014.]
- [5] FFTA - Foundation of Flexographic Technical Association: "Flexography: Principles And Practices" Flexographic Technical Association, (Inc., USA, 1999), page 110
- [6] Flint Group "Nyloflex ACE", (2014a), URL http://www.scorpio.com.pl/Portals/1/Files/PDFY/Fleksografia/nyloflex_ACE_NEW_EN.pdf, [last request: 25.08.2014.]
- [7] Flint Group "Nyloflex FAR", (2014b), URL http://www.flintgrp.com/en/documents/Printing-Plates/nyloflex/nyloflex_FAH_EN.pdf, [last request: 25.08.2014.]
- [8] Gilbert, D., Lee, L.: "Flexographic Plate Technology: Conventional Solvent Plates versus Digital Solvent Plates", *Journal of Industrial Technology*, 24(3), 2-7, (2008)
- [9] Hamblyn, S. M., Bould, D. C., Bohan, M. F. J., Claypole, T. C., Gethin, D. T.: "Consistency of Flexographic Platemaking", (2005), URL <http://www.printing.org/page/8669#>, [last request: 20.09.2010.]
- [10] Hershey, J.: "Dots Do It Right", (2010), URL http://printing.macdermid.com/pdf/Dots_Do_It_Right_Nov2010_PackagePrinting.pdf, [last request: 20.05.2013.]
- [11] Kenny, J.: "Flexo plate evolution" Label & Narrow Web. (2007), URL <http://shows.labelandnarrowweb.com/articles/2007/04/flexo-plate-evolution>, [last request: 08.07.2014.]
- [12] Liu, X., Guthrie, J. T.: "A review of flexographic printing plate development", *Surface Coatings International Part B: Coatings Transactions*, 86(2), 91-168, (2003)
- [13] Liu, X., Guthrie, J. T., Bryant, C.: "A study of the processing of flexographic solid-sheet photopolymer printing plates", *Surface Coatings International Part B: Coatings Transactions*, 85(4), 313-319, (2002)
- [14] Lunt, T.: "The Future of Printing Electronics with Flexography", (2013), URL http://www2.dupont.com/Packaging_Graphics/en_US/assets/downloads/pdf/Future-of-Printing-Electronics-with_Flexography-Lunt-2013.pdf, [last request: 08.09.2014.]
- [15] Mahović Poljacek, S., Cigula, T., Tomasegović, T., Brajnović, O.: "Meeting the Quality Requirements in the Flexographic Plate Making Process", *International Circular of Graphic Education and Research*, 6. 62-69, (2013)
- [16] Multimediaman: "PIA forecast for printers: Industry transition in a slow-growth economy, Sales vs. profitability", (2012), URL <http://multimediaman.wordpress.com/2013/04/13/pia-forecast-for-printers-industrytransition-in-a-slow-growth-economy/>, [last request: 23.06.2014.]
- [17] Novaković, D., Dedijer, S., Mahović Poljaček, S.: "A model for improving the flexographic printing plate making process" *Technical Gazette*, 17(4), 403 – 410, (2010)
- [18] Tomašegović, T., Mahović Poljaček, S., Cigula, T.: "Impact of Screen Ruling on the Formation of the Printing Elements on the Flexographic Printing Plate", *Acta Graphica*, 24(1-2), 1-12, (2013)
- [19] Valdec, D., Zjakić, I., Milković, M.: "The influence of variable parameters of flexographic printing on dot geometry of pre-printed printing substrate", *Tehnički vjesnik*, 20(4), 659-667, (2013)

DYNAMIC CONTACT ANGLE AS A METHOD IN GRAPHIC MATERIALS CHARACTERIZATION

*Tomislav Cigula, Sanja Mahović Poljaček, Tamara Tomašegović, Miroslav Gojo,
University of Zagreb, Faculty of Graphic Arts, Zagreb, Croatia*

Abstract: Surface properties of the materials play very important role in their usability in many industries. The best example in graphic arts industry is lithographic printing where printing process is based on the opposite surface properties of the printing and nonprinting areas on the printing plate. Another aspect of the surface phenomena could be seen in the ink acceptance on the printing substrates in conventional and digital printing techniques. This makes determination of the surface properties and wetting characteristics of the solid materials and properties of the liquids very significant.

Contact angle is the value which determines wetting characteristics between observed solid and liquid as liquid drop forms different shapes depending on the solid surface. It is known that formation of the liquid drop's shape is a dynamic process. One differentiates two contact angle values, static one, measured when the drops shape is stable and dynamic one, where measurement of the contact angle is varying in time from applying the liquid on the solid surface. But beside time variation, one could measure advancing and receding contact angle when liquid is added and sucked back from the surface, respectively.

The aim of this paper is to perform evaluation of the applicability of dynamic contact angle determination in characterization of the surface properties of graphic materials. For that purpose a set of the offset printing plate was prepared by immersing them into developing solution made of sodium metasilicate. Measurements of the time dependant and advancing and receding contact angle were performed by applying redistilled water on the image areas of the prepared printing plate samples.

Results of the investigation showed that the time dependant contact angle is similar on all printing plate samples and is not depending on the value of the contact angle. The value of the contact angle hysteresis is smallest on the unprocessed printing plate, but it decreases by increasing the developing time.

Obtained results showed that observing time dependant contact angle one could not detect all changes of the printing plate's surface due to the chemical processing. The value of the contact angle hysteresis is implying the change of the surface roughness and therefore could be useful tool for the surface analysis of the printing plate. But to confirm that results, one should take further research including performing other methods for surface characterization to confirm usability of the dynamic contact angle in graphic materials characterization.

Key words: wetting, dynamic contact angle, printing plate, material characterization

1. INTRODUCTION

Surface properties of the materials play a very important role in their usability in industrial applications. Graphic industry is not an exception. Throughout the reproduction process one could see many solid-liquid interfaces, for example in lithography printing ink and printing plate, printing ink and offset rubber, printing ink and printing substrate, fountain solution and printing plate and fountain solution and offset rubber. Therefore, defining the wetting characteristics of both, liquids and solids, is very important. One of the methods to determine wetting properties is to observe the shape of the liquid drop when applied on the solid surface.

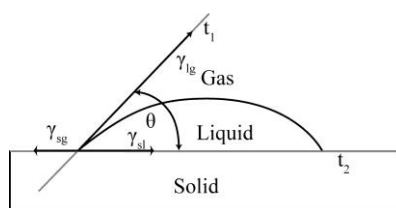


Figure 1: Contact angle between liquid and solid surface

Contact angle is the angle between the solid surface and liquid–gas interface, measured through the liquid phase (Cigula, 2011), i.e. it is the angle between tangent on the liquid drop (t1) and the tangent on the solid surface (t2) in the point where all three phases (solid, liquid and gas) meet (Figure 1) (Cigula, 2010).

The contact angle of a liquid drop on an ideal solid surface is defined by the mechanical equilibrium of the drop under the action of three interfacial tensions:

$$\gamma_{lv} \cos \theta = \gamma_{sv} - \gamma_{sl} \quad (1)$$

where γ_{lv} is the liquid–vapour interface tension, θ is the contact angle, γ_{sv} is the solid–vapour interface tension and γ_{sl} is the solid–liquid interface.

Beside Young's description of the contact angle, one must keep in mind that the phenomenon of wetting is more on only a static state. The liquid moves to expose its fresh surface and to wet the fresh surface of the solid in turn. Therefore, the measurement of a single static contact angle to characterize wetting behaviour is no longer adequate in the material's surface characterization. If the point in which three phases meet is in motion, the contact angle produced is called a "dynamic" contact angle. In particular, the contact angles formed by expanding and contracting the liquid are referred to as the advancing contact angle θ_a and the receding contact angle θ_r , respectively (Figure 2).

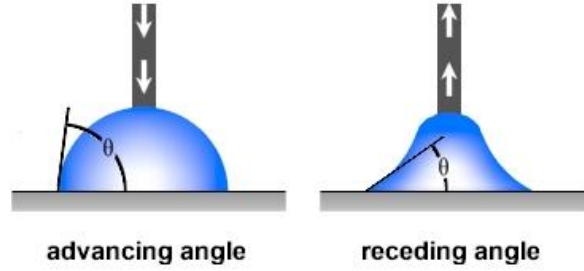


Figure 2: Advancing and receding contact angle (Farshid, 2011)

The difference between the advancing angle and the receding angle is called the contact angle hysteresis (H) (Gao, 2006):

$$H = \theta_a - \theta_r \quad (2)$$

The significance of contact angle hysteresis has been extensively investigated (Krumpfer, 2010; Gao, 2006), and the general conclusion is that it arises from surface roughness and/or heterogeneity.

On the other side, the value of the contact angle is also depending on the time of the measurement, i.e. time passed from the liquid's application on the solid surface until the measurement is performed (Yuan, 2013).

The speed of spreading depends on a combination of several factors, and can be understood from variations in the contact angle over time (Figure 3).

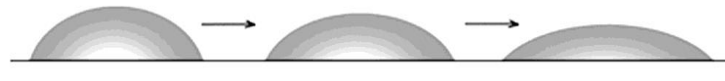


Figure 3: Changes of the contact angle with time function

2. EXPERIMENTAL

The samples of the lithographic printing plates were made by immersing them into a developing solution. The solution was made by dissolving sodium metasilicate crystals in distilled water in concentration of 0.2 mol dm^{-3} . Sample 1 was printing plate without immersion in the developing

solution, Sample 2 was immersed for 30 s, Sample 3 immersed for 60 s and Sample 4 immersed for 90 s. The developing solution temperature was for all samples the same, $25 \pm 0,5^{\circ}\text{C}$. The samples were afterwards washed with distilled water and dried at room temperature. Contact angle measurement was made with Dataphysics' OCA 30 measuring unit. This measuring unit is computer controlled and enables high precision measurement. The unit is equipped automatic dosing unit that enables measurement with defined volume of fluid. Measurement starts with putting sample of solid plate on a working table. After a drop is defined and left hanging on the end of syringe, one starts recording with CCD camera while computer controlled working table with sample increases its altitude until sample comes in contact with fluid. The recorded movie is later computer processed to perform measurements in the defined time period. Measurement of the time depending contact angle was made in the time period of 0 – 5 s, where 0 s means time in which drop has formed on the solid surface. The measurements were made using Sessile drop measuring method and drop shape fitting with the Laplace-Young fitting method. The advancing and receding contact angle was measured using Sessile drop with needle in method and using Tangent fitting.

3. RESULTS

In Figure 4 one can see the value of the time dependent contact angle on the printing plate samples. The contact angle is decreasing as the processing time of the plate increases. The stabilization time (in which equilibrium state is reached) is decreasing as the processing time increases, as it can be noted that on the Sample 1 the contact angle decreases all the time, but on Sample 4 it is stable after 1,5 seconds.

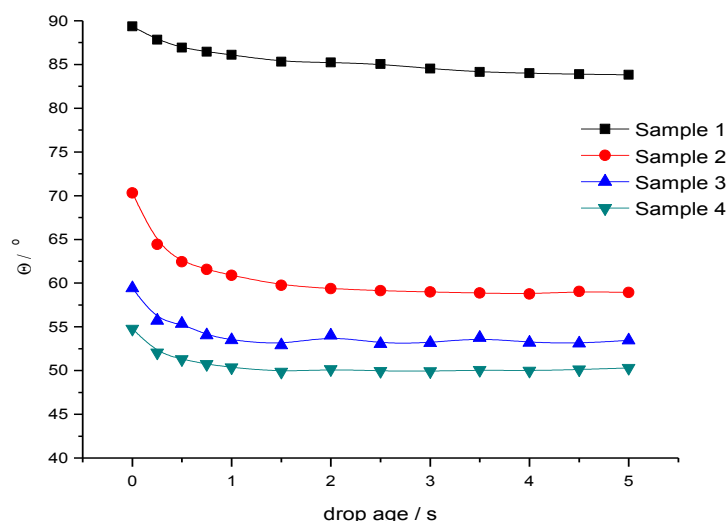


Figure 4: Time dependant contact angle

The decrease of the contact angle in the observed time period is nearly the same on all printing plate samples, round 5° . Only on the Sample 2 the first contact angle (at the time $t = 0$ s) is higher so the difference is round 12° .

The noticed behavior of the contact angle value is meaning that developing solution is influencing the wetting properties of the image areas of the printing plate. This behavior is not expected as without exposure, diazo photoactive layer should not be soluble in the alkaline solutions. Furthermore, better wetting with water could mean problem with absorption of the printing ink in the printing process and the decrease of the printing quality.

In Figure 3 one can see that both advancing and receding contact angle decreases with the increase of the time in which printing plate sample was immersed in the developing solution.

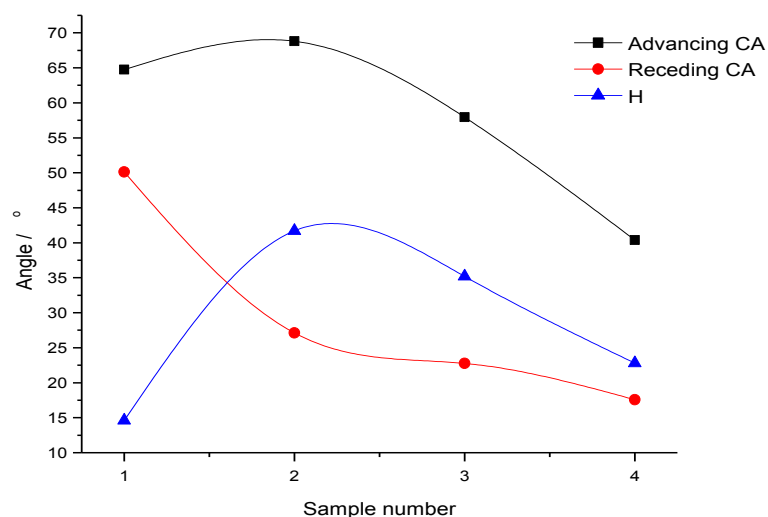


Figure 5: Advancing and receding CA depending on the sample preparation

The value of the contact angle hysteresis is smallest on the Sample 1 (the one which was not immersed in the developing solution), largest on the Sample 2 and decreases on the Samples 3 and 4. These results indicate that increase of the contact between developing solution and diazo positive layer causes partial dissolving of the layer and increasing the surface roughness [8] and/or homogeneity of the observed surface.

4. CONCLUSIONS

This research was made by assumption that dynamic contact angle could be a tool in the graphic materials characterization.

For the purpose of the research a set of lithographic plates were prepared by immersing plate samples in the developing solution. Four printing plate samples were prepared, Sample 1 without immersion in the developing solution, Sample 2 immersed for 30 s, Sample 3 immersed for 60 s and Sample 4 immersed for 90 s. Measurements of the time dependent and dynamic contact angle were conducted in order to detect surface properties of the prepared samples. Measurements were performed on the image areas as they should not be significantly influenced by the developing solution and therefore could enable evaluation of the proposed measuring methods. Results have shown that both measuring methods detected change of the surface properties of the investigated printing plate samples. The contact angle is decreasing with the increase of the time in which plates were immersed in the developing solution. In the same time, decrease of the contact angle was not affected by it' value, on all plate samples the decrease in the examined time period (0 – 5 s) was nearly the same although values were different. As time dependent contact angle showed surface properties change, and decrease of the image area's hydrophobic properties, the value of the contact angle hysteresis implies that developing solution is causing surface roughness and/or homogeneity of the image areas.

Therefore, dynamic contact angle could be useful tool for the surface analysis of the printing plate, but to confirm that, one should take further research including performing other methods for surface characterization to confirm usability of the dynamic contact angle in graphic materials characterization.

5. REFERENCES

- [1] Cigula, T., Gojo, M., Novaković, D., Pavlović, Ž.: "Influence of Various Concentrates on Quality of Printing Plates' Wetting Process", *Machine Design*, 325-330, 2010.
- [2] Cigula, T., Mahović Poljaček, S., Gojo, M.: "Influence of Drop Volume on Time-dependant Contact Angle", in "DAAAM International Scientific Book 2010", DAAAM International Vienna, Vienna, 195-202, 2010.

- [3] Farshid Chini, S., Amirfazli, A.: "A method for measuring contact angle of asymmetric and symmetric drops", *Colloids and Surfaces A: Physicochemical and Engineering Aspects*, 388, 29– 37, 2011.
- [4] Gao, L., McCarthy, T.J.: „Contact Angle Hysteresis Explained“ *Langmuir* 22 (14), 6234 – 6237, 2006.
- [5] Krumpfer, J.W., McCarthy, T.J.: „Contact angle hysteresis: a different view and a trivial recipe for low hysteresis hydrophobic surfaces“ *Faraday Discuss.* 146, 103 195–215, 2010.
- [6] *Surface and Interfacial Aspects of Biomedical Polymers* (Vol. 1), (Andrade, J. D. ed., Plenum Press, NY, 1985.), pages. 249–292
- [7] Yuan, Y., Randall Lee, T.: „Contact Angle and Wetting Properties“ (*Surface Science Techniques*, Bracco, G., Holst, B. ed., Springer, Berlin, 2013.) pages 3 – 34

EXTENDING THE FUNCTIONALITY OF PRINTED PRODUCTS USING AUGMENTED REALITY

*Markéta Držková, Markéta Ptáčková,
University of Pardubice, Faculty of Chemical Technology,
Department of Graphic Arts and Photophysics, Czech Republic*

Abstract: Due to the global economic situation and growing competition, both within the graphic arts industry as well as between print and other media, many printers are at present forced to look for the new markets beyond the traditional product types. Thanks to the recent intensive research and development, extending the functionality of printed products using digital technologies seems to be a promising way. A number of various products are on their way to customers, moving from scientific laboratories to the production. However, many of them are difficult to implement for a common printer, as they require investments into advanced technologies, special materials, and qualified staff. This work briefly summarizes the main options how to utilize digital features in printed products and their potential use in the near future with respect to their demands. Based on this comparison, the experiment was focused on the possibility to extend the functionality of printed matter by adding a marker for augmented reality (AR) and supplementary information in form of the common quick response (QR) code. The preparation and use of a model printed product featuring the AR markers for three freely accessible applications and QR code was examined to verify the required functionality at different conditions. Namely, the influence of marker size on the distance and angle of reading device needed for proper response was investigated. For all AR applications, the significant effect of the movement direction of both tablet and mobile phone was observed. The results are discussed with the respect to the anticipated end user requirements. Further, the attitude of printers in Central and Eastern Europe towards production of digital features or their employment in printed products was surveyed within the printing industry companies. The findings of the survey form the base for the planned aggregate study in European countries in scope of the European Cooperation in Science and Technology (COST) Action named New Possibilities for Print Media and Packaging – Combining Print with Digital.

Key words: augmented reality, marker, printed product

1. INTRODUCTION

There are many various ways of extending the functionality of printed products beyond their common features. As an example, different security features can be mentioned. Technology behind these extensions may be relatively simple. It can comprise, e.g., the use of special prepress settings or materials offering some special effect. For many years, digital technologies are widely used at all steps in printing production, both for content creation and for automation and control. Recently they started to appear also directly as integral part of printed products themselves; in other cases, printed products are utilized by digital devices in novel ways. Digital devices are becoming “smart”, i.e., besides their original functions they bring internet connectivity and a possibility to install plenty of different applications, often making use of built-in sensors. For example, mobile phones enable to create new kinds of advertising campaigns, games and educational content and thus became a strong marketing platform.

This work aimed to deal with practical usability of selected class of products. First, the present and near future perspectives of the main options of utilizing digital features in printed products were discussed, taking into account the implementation difficulty. Based on this pre-analysis, adding a marker for augmented reality (AR) and supplementary information in form of the common quick response (QR) code has been chosen for the experiment. There is a lot of research work going on for the technological issues of printed electronics. On the other hand, AR markers and QR codes generally don't have special demands on print production and the difficulty lies in the creation of applications and related content. However, the knowledge of technical limits for proper functionality essential for the customer contentment is still important, especially during the design and prepress steps. Reliable rendering of the content is crucial not only for outdoor applications, like large-scale advertisements or prints used in poor lighting conditions, but in all

cases. The proper functionality of a model printed product featuring the AR marker and QR code was tested with respect to the influence of marker size on the distance and angle of reading device. Three freely accessible AR applications and two QR code reading applications were applied. The effect of color and gloss of the printing substrate was examined as well. Finally, the printing industry awareness of the possibilities for combining print with digital and industry's opinion on implementing the new related technologies was assessed in three Central and Eastern Europe countries.

2. DIGITAL FEATURES IN PRINTED PRODUCTS

The large group of products which combine print with digital falls into the category of printed electronics or, more generally, printed functionalities (O-EA, 2013). They may be self-contained or functional in combination with other device or system. This group comprises printed products like organic photovoltaics, batteries, light sources and displays, audio devices, memories, sensors or features for RFID (Radio Frequency Identification). For their production, various printing techniques can be used, and often it is beneficial to combine more techniques to achieve optimal quality of all features. The key challenge is the proper design of the functional elements or of the whole device, and the right formulation of printing inks. Except the most basic and well established functional elements, both of these tasks are complex and require either an intensive development, or a purchase of suitable license – if there is some available. From the perspective of common printers, it is connected with a substantial investment with quite high risks, because the markets for these products seem to emerge more slowly than was predicted. At the same time, the character of production as well as qualitative requirements significantly differs from those of conventional prints. Another type of utilizing digital features in printed products is represented mainly by 2D bar codes and augmented reality markers or similar tags. In this case, the functionality is always dependent on an external device or system, and for the success, a good marketing idea is the key factor. On the other hand, these features are printable with common equipment using normal printing materials.

Looking closer at 2D codes like QR or Data Matrix, they enable coding of more data bits compared to 1D bar codes, thus offering more application possibilities. Even more opportunities bring the related technologies (Lumby, 2012), like Mobile Visual Search (MVS), where the code is replaced by any captured picture, which is matched with the database of the service provider, or AR applications. The technology of AR, which allows to merge the real world or its image with virtual reality, is gaining more attention recently. A large group of AR applications is marker-based (Siltanen, 2012), with a wide range of possible applications within printed products. As an example, the enhanced instruction manual available through AR marker on packaging or the product itself can be mentioned. A lot of possibilities arise in advertising campaigns (Blippar Channel, 2014), catalogues (IKEA, 2014; GServis, 2014), textbooks (iTunes, 2014; iTunes, 2014; Whittlejam, 2014; Arloon, 2014) and books generally (iTunes, 2014). The basic AR process consists of capturing an image, detection of the marker, evaluation of the distance and orientation of the camera, rendering a virtual content in the right size, location and perspective (so called pose), and displaying it, commonly on the screen of a smart device.

A readability of QR codes has been assessed by several authors; according to the recent analysis (Tarjan et al., 2014), QR code readability is directly influenced only by the size of modules that constitute the code, not by the number of coded characters or by the error correction level. Also, the base material affects the code readability. Another author (Zvonar, 2012) showed that the QR code color has minor effect, with the exception of yellow significantly limiting the readability. In case of the other mentioned technologies, more factors have influence on a proper function, nevertheless, the same rules apply for the basic properties connected to a readability – in general, sufficient contrast and line thickness or element size combined with functional, reasonably simple design are the key prerequisites.

3. METHODS

3.1 A model printed product

Combination of a poster and a leaflet with a cinema program has been chosen as a model printing job. Through the AR, movie trailers could be available, ready to help a customer with a choice. This model situation avoids the need to create the content, as only the integration of

existing trailers into an AR application would be necessary. Once established, this could be a periodical printing job, profitable for the printer as well as the customer. Besides pictorial AR markers, the QR code was included. In a model situation, it can provide the link to the AR application, or it can be utilized as an AR marker itself.

Three freely available AR applications with distinct AR markers were selected: SRG United Solutions AR (further marked as application A) (SRG United Solutions, 2013; Anon, 2014), Logie T.Rex Augmented Reality (application B) (Logie, 2013; Anon, 2014), and SubmARiner (application C) (EligoVision, 2012; EligoVision, 2014). A QR code was generated by a free QR code generator [21] using a simple text "goqr.me". The AR markers and QR code are shown in Figure 1. For QR code reading, two applications were used: Google Goggles (application D) (Google Inc., 2013), requiring an internet connection, and Norton Snap (application E) (NortonMobile, 2013), working offline.



Figure 1: Markers for tested AR applications (A, B, C) and QR code (QR)

The poster in A2 format (42 × 59.4 cm) and the leaflet in A5 format (14.8 × 21 cm) were considered, enabling to use the same graphics, only scaled to a proper size. Typical reading distances of more than 75 cm for customer standing in front of the poster and above 25 cm for holding the leaflet in customer's hand or reading the leaflet laid on the table before the customer were assumed. The experiment utilized AR markers and QR code in several sizes (Table 1) to find the correct size for each version (poster and leaflet).

Another parameter influencing the readability is the viewing angle, as the reading device often is not held in a parallel position either due to space limitations, or intentionally – when the user wants to see the content from various sides. Therefore, the experimental setup enabled to change reading distance up to 95 cm by a movement of a device holder along optical bench and also to change viewing angle by a side-to-side ($\pm 90^\circ$) or upward rotation (90°) of a holder with the sample, as illustrates Figure 2. In addition, the influence of color and gloss of the printing substrate was studied (Table 2). The parameters of printing substrates were measured by a gloss-meter Viptronic VipGloss-I (gloss according DIN 16537), and a spectrophotometer X-Rite i1 (CIE $L^*a^*b^*$ values).

AR markers and QR code in all tested sizes were placed on A3 page and printed by black process ink on all tested substrates by Heidelberg Quickmaster QM 46-2 sheet-fed offset press.

Quite different lighting conditions can occur when using model prints, from direct sunlight to relatively dark environments with dimmed lights. For the experiment, the lighting conditions on the low end of assumed illuminance scale were chosen and measured using a light meter Lutron LX-105. Similarly, the low-cost tablet and mobile phone were used as reading devices: Sencor Element 10.1 V2 (2 Mpx) and Sony Xperia tipo (3.2 Mpx), respectively. It is expected that the results in better lighting conditions and with reading devices of higher quality would be better, while the aim of the experiment was to test the limits for the most general use.

All measurements were repeated three times and averaged. First, the distance between the sample and reading device placed in parallel position was changed. The optimal reading distance for assessment of the influence of side-to-side and upward rotation was derived from ranges of correct function determined for forward and backward movement as illustrated in Figure 3. For wider ranges of correct function, the measurement of rotation was also done in minimal and maximal distances. This way, the limits for watching the AR from various angles at given distances were examined. In case of QR code, the working range is not influenced by the direction of movement or rotation; once in the feasible range, the code was read.

Table 1: AR markers and QR code sizes

Marker for AR application A			Marker for AR application B		
Sample	Height (cm)	Width (cm)	Sample	Height (cm)	Width (cm)
A1	18.5	13.0	B1	7.5	15.3
A2	9.1	6.4	B2	3.8	7.6
A3	4.6	3.2	B3	2.8	5.7
A4	3.4	2.4	B4	1.8	3.8
A5	2.6	1.8	B5	1.4	2.8
—	—	—	B6	1.0	2.1
—	—	—	B7	0.8	1.6
Marker for AR application C			QR code		
Sample	Height (cm)	Width (cm)	Sample	Height (cm)	Width (cm)
C1	12.5	11.4	QR1	13.0	13.0
C2	6.0	5.7	QR2	6.5	6.5
C3	4.5	4.3	QR3	3.2	3.2
C4	3.0	2.8	QR4	1.6	1.6
C5	2.2	2.1	QR5	1.2	1.2
C6	1.7	1.6	QR6	1.0	1.0
C7	1.3	1.2	QR7	0.6	0.6

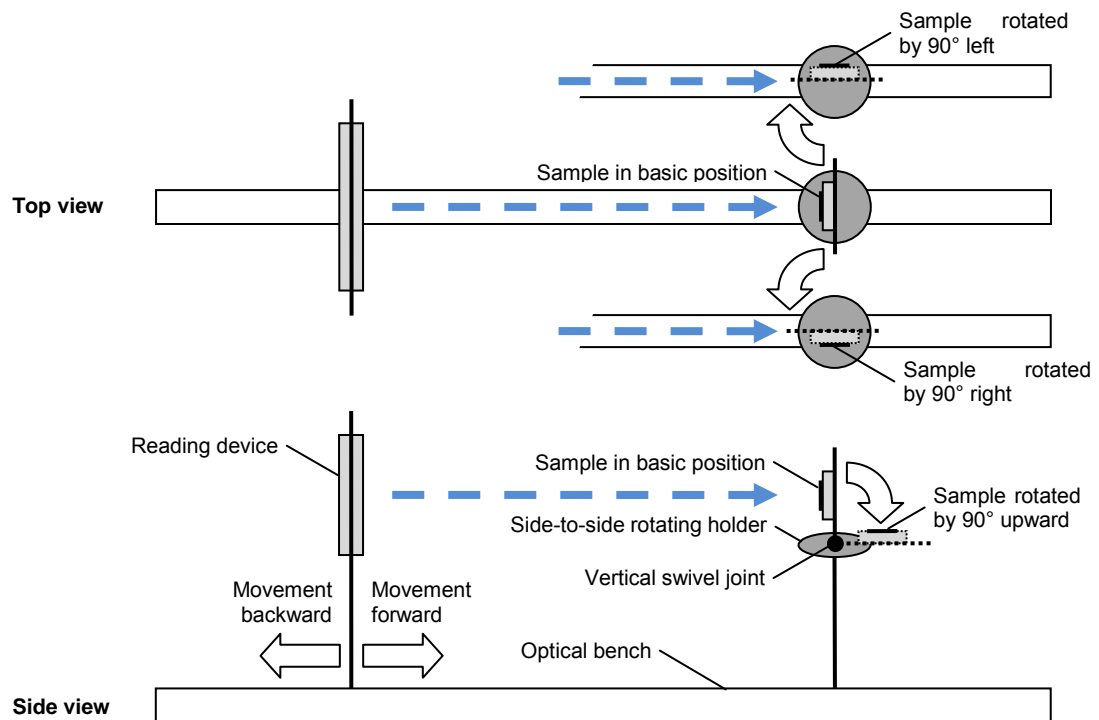


Figure 2: Markers for tested AR applications (A, B, C) and QR code (QR)

Table 2: Parameters of printing substrates

Substrate	Type	Grammage (g/m ²)	Gloss ¹	L*	a*	b*
S1	coated gloss paper	130	6,87	93,35	1,14	-4,58
S2	coated silk paper	130	3,23	94,06	0,93	-3,67
S3	silk ² paper	160	3,33	94,81	1,23	4,78
S4	uncoated offset paper	120	3,97	93,70	1,07	-7,34
S5	uncoated light yellow paper	80	4,20	92,10	1,15	18,10
S6	uncoated yellow paper	80	3,90	85,12	-2,29	65,48
S7	uncoated light green paper	80	3,97	87,64	-15,43	10,27
S8	uncoated recycled paper	80	4,03	82,65	0,34	1,59

¹ DIN 16537; ² Conqueror CX22, finish specification unavailable

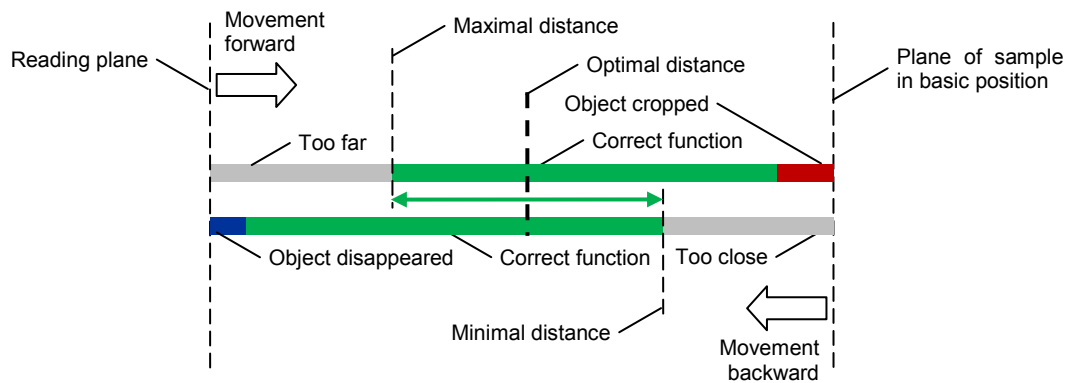


Figure 3: Markers for tested AR applications (A, B, C) and QR code (QR)

3.2 Printing industry attitude survey

The aggregate study of printing industry opinion on innovative printing in European countries is planned in scope of the European Cooperation in Science and Technology (COST) Action named New Possibilities for Print Media and Packaging – Combining Print with Digital. Within presented work, the printing industry awareness of the possibilities for combining print with digital and industry's attitude to accomplishment of related technologies was assessed in three Central and Eastern Europe countries. The questionnaire composed in English was translated into Slovak, Czech and Serbian language. In each country, different mode of the survey was employed to test the effectiveness of considered channels. In Slovakia, the questionnaire was presented on the Slovak web portal dedicated to printing and photography (Polygrafia-Fotografia, 2014). In Czech Republic, the questionnaire was sent by email. The selection of companies listed in (Europeans Community, 2014) in sections of printers providing sheet-fed printing, digital printing, web-offset printing, screen-printing, pad printing and other types of printing was made pseudorandomly, comprising two groups. The first group included advertised companies and the second the non-advertised ones, so as they were evenly distributed throughout the country, preferably from the districts not represented in the first group. Resulting list comprised 134 companies. First, 30 of them were selected so as 2 from each region were included, except Prague with 4 companies. Their representatives were asked by email to take part in the survey either by filling the online form or by answering the questions during phone interview. Second, remaining companies were asked by email to fill the online form. In Serbia, the personally known representatives of companies were asked to answer the questions during a phone interview.

The introductory questions assessed the type of a company (number of employees, printing techniques used in the company and its common production). The main part was focused on the

attitude of the company to various types of printed products related to digital technologies, the channels used for learning about this topic and the interest to get more information.

4. FUNCTIONALITY OF AUGMENTED REALITY MARKERS AND QUICK RESPONSE CODES

During all experiments, the measured illuminance ranged between 53 to 60 lx, being 55.5 lx on average. It corresponds to living room conditions sufficient for conversation, relaxation and entertainment. Tablet, having lower resolution, was used as a primary device for measurement of sequence of tested sizes of individual AR markers and QR code. The smallest working size was then measured also with mobile phone.

4.1 Influence of the size on reading distance and angle

The graphical summary of the experiment aimed at the effect of the size of AR markers and QR code on reading distance and angle is given in Figure 4. All samples on printing substrate S1 were measured.

The marker of application A was readable only in first three sizes. Except the biggest size, the reading distances are quite short; in farther distances the object started to disappear (was displayed only partially). There were no significant differences between a movement towards the marker (forward) and backward. The measurement of rotation in both axes has shown marked difference between rotating towards parallel position and away. As expected, the performance with respect to the range of feasible rotation angles is worse at distances close to the reading limits than in optimal reading distance. Comparing mobile phone and tablet, maximum distances were similar; mobile phone provided better reading results at shorter distances. According to the results, even a bigger marker size would be suitable for use on a poster, while for a leaflet, second size would be appropriate.

In case of application B, first four marker sizes were readable. Starting from the second size, the reading distances are again quite short when moving towards the marker. However, the working range is considerably extended to farther distances when moving back. In shortest distances, the size of the object exceeded the resolution of the display and the object was cropped. For rotation of a marker of given size in both axes, the range of feasible angles increased with decreasing distance; generally, rotating away from parallel position allows for much wider working range. Using mobile phone, the reading distances were shorter and the ranges of working rotation angles narrower than using tablet; the range was strongly limited especially for a movement towards the marker and a rotation towards parallel position. Application B provided the best results overall. First tested marker size should be sufficient for use on a poster and third size is suitable for a leaflet.

With application C, only the smallest tested marker size was not readable. This is probably thanks to less complex graphics of the marker, ensuring good readability also at reduced sizes. On the contrary, the reliability of the application itself was low with respect to stable rendering of the AR object (blinking effect) and reading reproducibility for given distances and rotation angles. This may be connected with repeated reading of the marker. As a consequence, the values measured in both directions of movement as well as of side-to-side or upward rotation are very similar. Furthermore, the influence of marker size is ambiguous for reading distances and also for reading angles. The results measured with mobile phone and tablet are comparable. Like in case of application A, the use on a poster would need marker size bigger than was tested for application C; for a leaflet, fifth size is optimal.

First four QR code sizes were readable, but for first two sizes, the maximum reading distance exceeded the limit of the experimental setup (95 cm); for smaller sizes, similar values were measured using both tested applications. However, looking at minimum reading distance, the performance of application E is much worse. This is caused by the fact that the application scans the code only in given rectangle within the display area. In comparison with AR markers, QR codes of similar size enable reading from larger distances, while at short distances, the reading is more problematic. The sensitivity to reading angle is apparently higher as well and the range of feasible angles is thus significantly limited. Second tested QR code size should be sufficient for use on a poster and fourth size is suitable for a leaflet.

To resume, QR codes with tested module configuration (21 × 21 modules) can be beneficially utilized in situations where the reading distance is higher, while all tested AR applications worked better in closer contact with the marker.

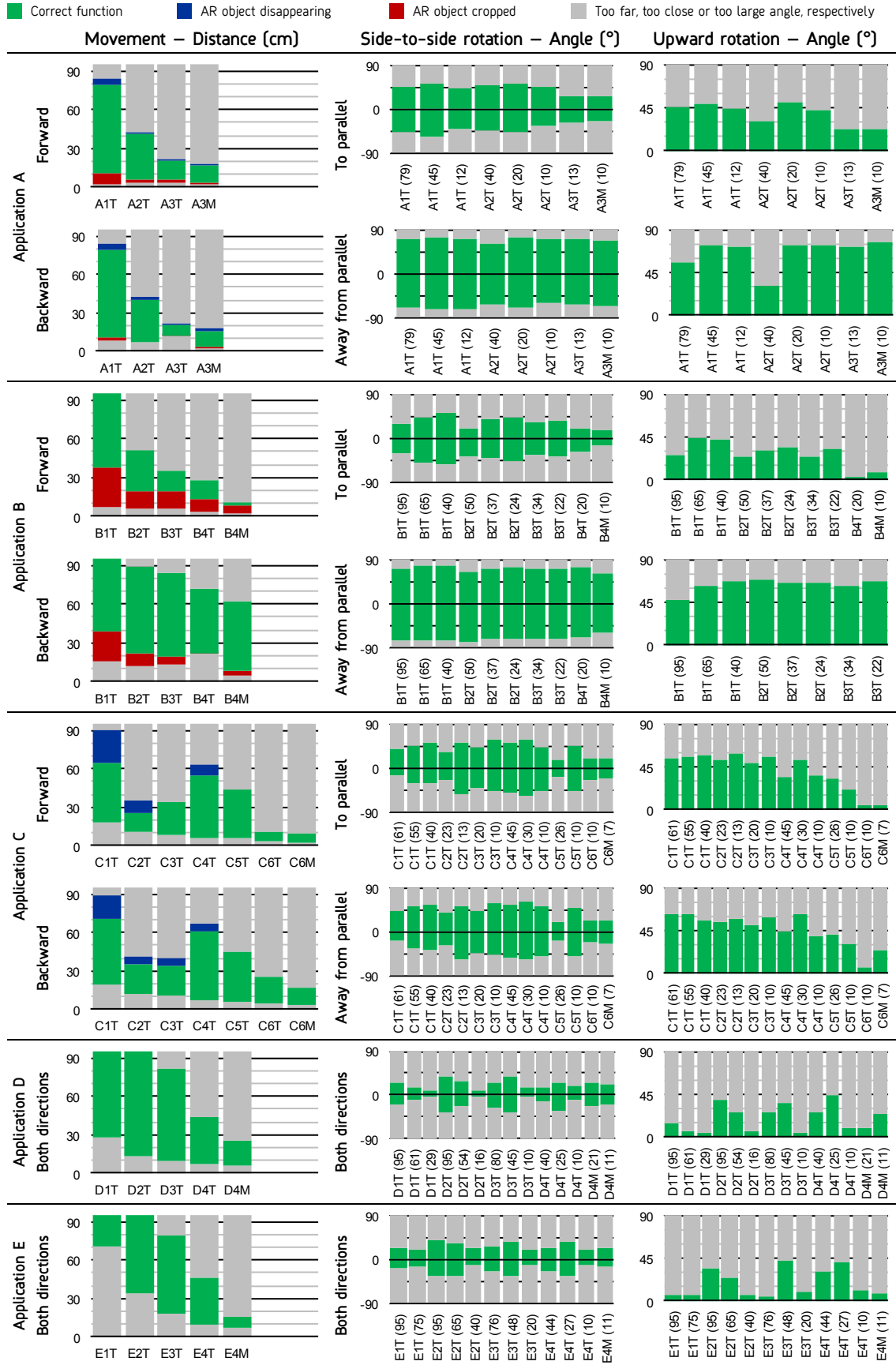


Figure 4: Influence of AR marker and QR code size on reading distance and angle for tested AR applications (A, B, C) and QR code reading applications (D, E), respectively; categories are marked with the sample designation (see Table 1) and indication of measuring device (T for tablet, M for mobile phone), and in case of rotation also with the distance given in parentheses

Figure 5 illustrates the dependence of maximum reading distance for movement towards the sample and minimum reading distance for movement away from the sample on geometric mean of dimensions of individual AR markers and QR code for corresponding tested applications. Generally, the mean dimensions of smallest samples were close to 2 cm except the marker for AR application A, which needed the dimensions of almost 4 cm to be readable. There was an assumption that the reading distance should be proportional to the size of the marker or QR code. In left part of Figure 5, a linear character can be seen for all AR applications, except three points in case of less reliable application C. The results for QR code are distorted due to space limitations of experimental setup. In right part of Figure 5, all dependencies resemble linear curves with different slopes, with the exception of first points corresponding to smallest sizes of markers for AR applications A and B.

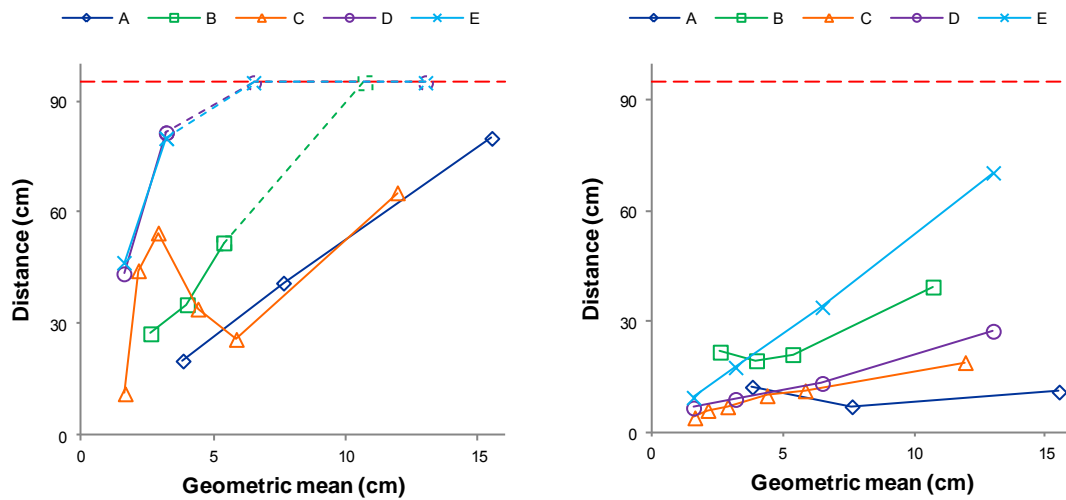


Figure 5: Dependence of maximum reading distance for forward movement (left) and minimum reading distance for backward movement (right) on geometric mean of AR marker and QR code dimensions for tested AR applications (A, B, C) and QR code reading applications (D, E), respectively; the dashed line denotes the measurement limit of 95 cm

4.2 Dependence of reading distance and angle on the printing substrate

Based on the aforementioned results discussed in section 4.1, individual markers and QR code in the corresponding smallest readable size were measured on all tested printing substrates. The reading distance for assessment of the influence of rotation was chosen at 13 cm for application A, 20 cm for application B, 10 cm for application C, and at 25 cm for applications D and E. The measured reading distances and angles are summarized in Figure 6. The variation among different printing substrates is generally low and no substrate can be classified as the most or the least suitable. Only the maximum reading distance for QR code on printing substrate S8 (recycled paper with lowest L^* value) is notably lower in comparison with other substrates for both tested applications. Neither higher gloss of printing substrate S1 nor color of substrates S5, S6, and S7 showed a marked effect on reading distances and angles.

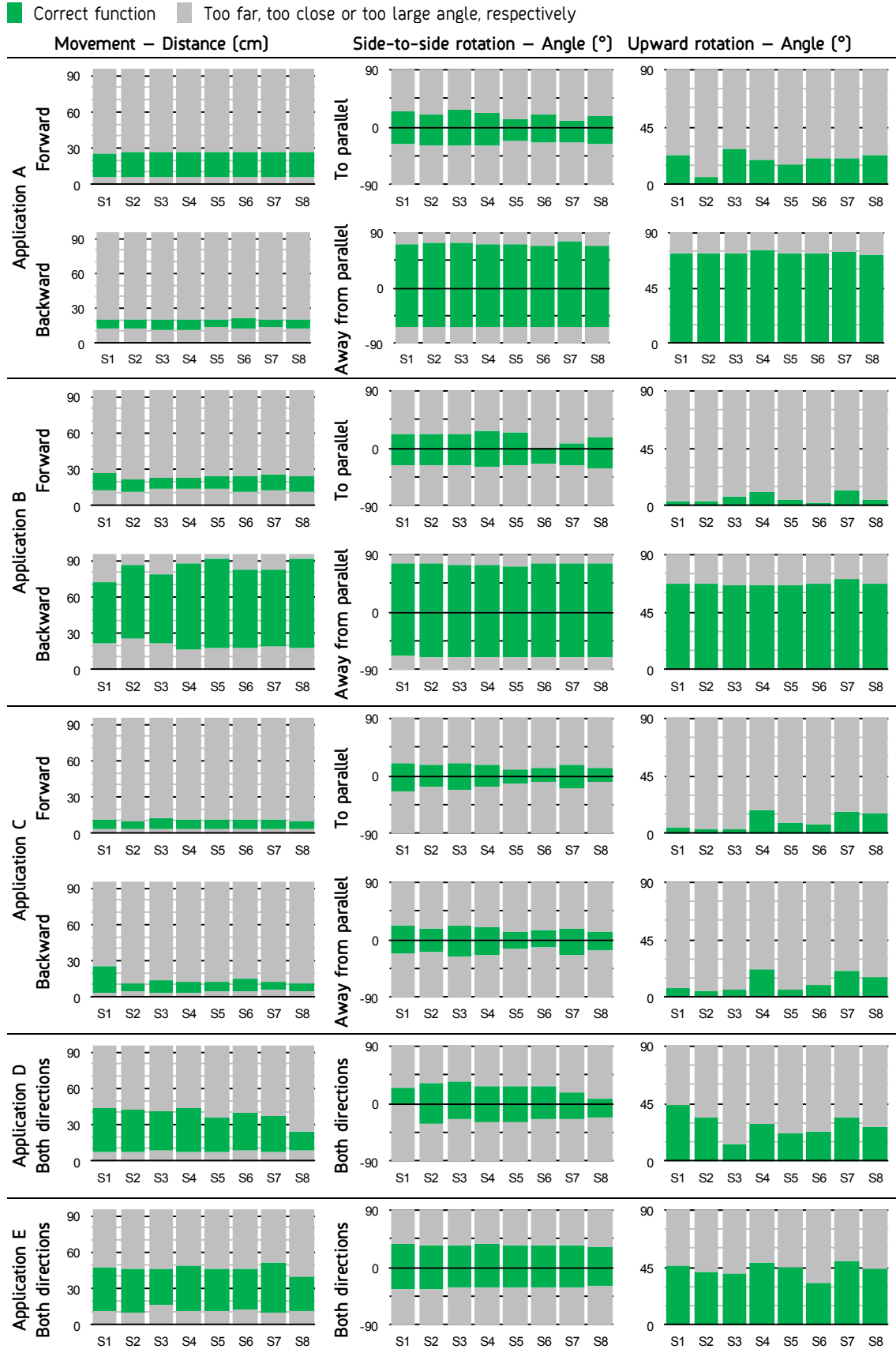


Figure 6: Effect of printing substrate on reading distance and angle for smallest readable size for tested AR applications (A, B, C) and QR code reading applications (D, E), respectively; categories are marked with the printing substrate designation (see Table 2)

5. ATTITUDE OF PRINTERS TOWARDS PRODUCTION OR EMPLOYMENT OF DIGITAL FEATURES

The answers for the online questionnaires were collected within one month. The non-addressed Slovak version published on the web portal has not yielded any response. In case of the Czech version sent by email, in total 6 % was returned as undeliverable and 8 % was answered, whereof 56 % within a first day and 38 % within one week. From 30 emails sent to specified representatives, 3 % was returned as undeliverable and 17 % was answered, which is considered a satisfactory result. In Serbian part of the survey, all personally known representatives asked by a phone answered the questions during the interview.

Following results are based on all 16 responses. As show the basic characteristics presented in Figure 7, all major printing techniques and classes of printed products are covered by the companies which answered the questionnaire, mainly representing small and medium enterprises. In general, wide range of products is offered, with only three companies being more focused (two producing labels and one security printing). Besides the products listed in individual categories (Figure 7c), personalized packaging, securities and documents, and branding were mentioned. Predominantly, offset printing is employed (listed by 75 % of respondents). About one third uses screen printing and electrophotography (often termed as digital printing) and one quarter inkjet printing, followed by flexography and gravure. Further, letterpress and pad printing were listed.

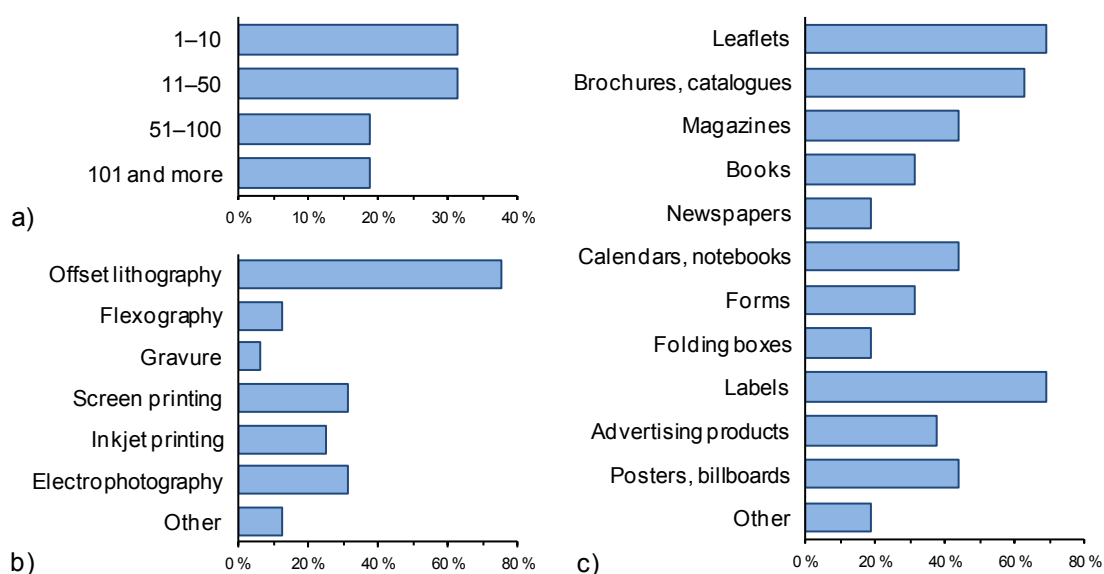


Figure 7: Characterization of companies and their production – number of employees (a), printing techniques used for production (b), and main types of products (c)

The survey has shown that the awareness of the possibilities for combining print with digital among printers is generally low, as illustrates Figure 8. Looking at individual groups of products, the answers follow similar pattern, when almost one half did not heard about the technology and another half has no plans for future production. As expected, the situation is slightly better in case of printed features for RFID and 2D bar codes with AR tags, which was the only group marked as already produced (but still, only by one respondent). The information on this topic is mostly gathered from public sources, mainly internet and magazines for printing and publishing industry (69 %), followed by industry channels, especially trade fairs (31 %). Further, product representatives, workshops, conferences, cooperation with academics and also TV were listed. On the other hand, all companies except one would like to get more information on the possibilities of combining printed products with digital technologies, which suggest possible improvement of the situation in near future.

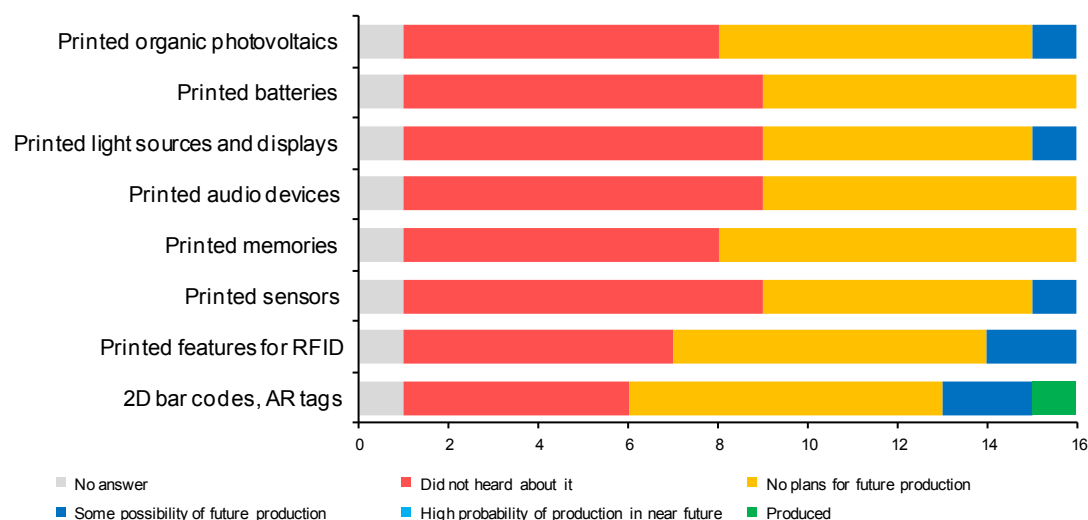


Figure 8: Attitude of companies to the listed types of products

6. CONCLUSIONS

The printing of AR markers and QR codes, considered relatively easy to implement, was investigated with respect to their correct function, namely, the influence of their size on reading distance and angle. With widely accessible devices, the size should be around 2 cm and more, depending on the planned context of use. For two AR applications, the significant effect of the movement and rotation direction was observed using both tablet and mobile phone. In case of the third AR application, the direction did not play a role; on the other hand, the reliability of its function was lower. Therefore, the importance of the quality of AR application itself was confirmed. Based on the comparison of various printing substrates, no one was recognized as more or less suitable.

The printing industry survey affirmed that prospects of extending the functionality of printed products using AR are slightly better than for other possibilities of utilization of digital features in printed products. In general, the answers of the Czech and Serbian printing companies, which took part in the survey, have shown that the knowledge in this area is low; however, there is a rather large room for improvement. As the survey modes appropriate for the planned aggregate study of printing industry opinion on innovative printing, sending the questionnaire by email directly to company representatives or asking them to answer during a phone interview can be recommended. To minimize the risk of the distortion of the results, the list of the representatives should not be limited to people with personal connections to academia.

7. ACKNOWLEDGMENTS

Cooperation within the COST Action FP1104 is gratefully acknowledged. Igor Karlović from Department of Graphic Engineering and Design, Faculty of Technical Sciences, University of Novi Sad is especially thanked for printers survey in Serbia.

8. REFERENCES

- [1] Alliban, J.: "LearnAR – eLearning with Augmented Reality", URL <http://www.youtube.com/watch?v=7G3H3ImCWIE> (last request: 2014-09-18).
- [2] Anon: "SRG United Solutions". URL <http://www.srgunitedsolutions.com/markers.pdf> (last request: 2014-09-18).
- [3] Anon: "T-Rex" URL <http://logielab.com/promotypes/docs/markers/trex-a4.pdf> (last request: 2014-05-16).
- [4] Arloon: "AR Chemistry | Augmented Reality Education | Zientia", URL <http://www.youtube.com/watch?v=IpNrWKQFq6Q> (last request: 2014-09-18).
- [5] Blippar Channel: "Heinz Tomato Ketchup recipe book in augmented reality by blippar", URL <http://www.youtube.com/watch?v=GbplSdh0lGU#t=53> (last request: 2014-09-18).

- [6] EligoVision: "SubmARiner", September 3, 2012 – Google Play, URL <https://play.google.com/store/apps/details?id=ru.eligovision.augmented.catfish> (last request: 2014-09-18).
- [7] Eligo Vision: URL http://www.eligovision.com/download/docs/August_page.pdf (last request: 2014-09-18).
- [8] Europeans Community: "Graphic Arts Industry of the Czech Republic – Complete directory of the firms of the printing industry and related fields and their suppliers", Edition 19, (Brno: ISMC Bohemia, 2014).
- [9] Google Inc.: "Google Goggles", November 22, 2013 – Google Play, URL <https://play.google.com/store/apps/details?id=com.google.android.apps.unveil> (last request: 2014-05-16).
- [10] GServis: "Domy G SERVIS" (in Czech), URL <http://www.gservis.cz/dodavane-sluzby/tisteny-katalog/mobilni-aplikace-rodinne-domy/> (last request: 2014-09-18).
- [11] IKEA: "2014 IKEA Catalogue Comes To Life with Augmented Reality", URL http://www.ikea.com/ca/en/about_ikea/newsitem/2014catalogue (last request: 2014-09-18).
- [12] iTunes: "Spacecraft 3D", Jet Propulsion Laboratory, July 30, 2014 – iTunes, URL <https://itunes.apple.com/cz/app/spacecraft-3d/id541089908?mt=8&affId=2058070> (last request: 2014-09-18).
- [13] iTunes: "Anatomy 4D", Augmented Dynamics, June 01, 2014 – iTunes, URL <https://itunes.apple.com/cz/app/anatomy-4d/id555741707?mt=8&affId=2058070> (last request: 2014-09-18).
- [14] iTunes: "Guinness World Records 2014 – Augmented Reality", Guinness World Records, April 01, 2014 – iTunes, URL <https://itunes.apple.com/au/app/guinness-world-records-2014/id686619823?mt=8> (last request: 2014-09-18).
- [15] Logie: "Logie T.Rex Augmented Reality", May 15, 2013 – Google Play, URL <https://play.google.com/store/apps/details?id=com.logie.promotypes.trex&hl=en> (last request: 2014-09-18).
- [16] Lumby, N.: "Linking physical print and digital media: opportunities and challenges of quick response codes in the face of mobile visual search technology", *Advances in Printing and Media Technology*, Vol. XXXIX, (Ed. N. Enlund and M. Lovreček, International Association of Research Organizations for the Information, Media and Graphic Arts Industries, Darmstadt, 2012), pages 303–311.
- [17] NortonMobile: "Norton Snap", October 15, 2013 – Google Play, URL <https://play.google.com/store/apps/details?id=com.symantec.norton.snap> (last request: 2014-09-18).
- [18] O-EA: "Organic and Printed Electronics – Applications, Technologies and Suppliers", 5th edition, (Frankfurt am Main: VDMA Verlag, 2013).
- [19] Polygrafia – Fotografia, URL <http://www.polygrafia-fotografia.sk/> (last request: 2014-09-18).
- [20] QR code generator, URL <http://goqr.me/> (last request: 2014-09-18).
- [21] Siltanen S.: "Theory and applications of marker-based augmented reality", VTT Science 3, (Espoo: VTT Technical Research Centre of Finland, 2012).
- [22] SRG United Solutions: "Augmented Reality", July 18, 2013 – Google Play, URL <https://play.google.com/store/apps/details?id=com.srgunitedsolutions.arshowcase> (last request: 2014-09-18).
- [23] Tarjan, L., Šenk, I., Tegeltija, S., Stankovski, S., Ostojic, G.: "A readability analysis for QR code application in a traceability system", *Computers and Electronics in Agriculture* 109, 1–11, 2014.
- [24] Whittlejam: "Augmented Reality to Learn Math – Pocket Tutor for iOS", URL <http://www.youtube.com/watch?v=tDDkSYLF3vM> (last request: 2014-09-18).
- [25] Zvonár, D.: "QR codes, the ways of use and readability at different light conditions", Bachelor thesis (in Slovak), (Pardubice: University of Pardubice, 2012).

PRINTED ANTENNA FOR NEAR FIELD COMMUNICATION TAG

Miloje Đokić¹, Urška Kavčič², Matej Pivar¹, Matija Mraović³, Vasa Radonić,
Anton Pleteršek⁵, Tadeja Muck¹

¹University of Ljubljana, Faculty of Natural Sciences and Engineering,
Ljubljana, Slovenia

²Volkarton Rakek d.o.o., Rakek, Slovenia

³Pulp and Paper Institute, Ljubljana, Slovenia

⁴University of Novi Sad, Faculty of Technical Sciences, Novi Sad, Serbia

⁵University of Ljubljana, Faculty of Electrical Engineering, Ljubljana, Slovenia

Abstract: Near Field Communication (NFC) is a standards-based technology used to provide short range wireless connectivity that carries secure two-way interactions between electronic devices. It works on the base of high frequency (HF) RFID technology. NFC has the advantage over the regular HF RFID technology because it allows wireless communication with or between common mobile devices like phones or tablets with integrated NFC chips. Present and anticipated applications of NFC technology include contactless transactions, data exchange, and simplified setup of more complex communications such as Wi-Fi. Communication is also possible between a NFC device and a passive NFC tag. Depending on the type of the NFC tag's chip it can have also a fully integrated various sensors for e.g. temperature or humidity tracking.

This paper presents process of manufacturing NFC tag with integrated temperature sensor. Antenna design and simulation, process of screen printing and final NFC tags operability are described in experimental part.

NFC tags were read by two devices, the classical reader and a mobile device – tablet. After operability testing, the tag's operating frequency, real and imagined resistance and its capacitive or inductive nature was analyzed using network analyzer. The results have enabled us to see the characteristic of printed NFC tags, their strengths and weaknesses and the possibility to what extent mobile device can replace conventional reader.

Key words: NFC, HF, RFID, printed electronics, sensors, mobile phone

1. INTRODUCTION

Printed electronics brings new products and new manufacturing processes in electronic industry. These processes enable us to manufacture different electronic components on a wide range of flexible materials, like foils, variety of different papers etc. Printed electronics is a new kind of electronics characterized by flexibility, small weight and thickness, low price, concern for the environment and possibility for new applications.

One of major parts of printed electronics is radio frequency identification (RFID) tag. RFID is an automatic identification technology that uses a wireless non-contact radio-frequency to transfer data for the purposes of automatically identifying and tracking tags attached to objects. RFID tag is consisted of antenna and integrated circuit (IC). It can be divided on the basis of various parameters like working frequency, functionality of chip and his interactivity, working distance etc. but main division is on active, semi-active and passive tags. Division based on working frequency splits RFID system on low frequency (LF: 125 – 134 kHz), high frequency (HF: 13.56 MHz) and ultra-high frequency (UHF: 840 – 960 MHz). LF and HF RFID tags are using inductive coupling to communicate with a reader, while UHF tags for communication use radiative coupling. LF and HF tags have short working distance (up to 10 cm), while UHF tags have up to several meters (Dobkin, 2008) (Zichner et al, 2011).

NFC technology is based on HF RFID technology, so it has small working distance. In this particular case that can be an advantage, because NFC technology combine different standards and safety technologies. Advantages of passive NFC tags are small price and smaller complexity of manufacturing. The operating principle of the RFID system with passive tags is as follows: the reader sends a modulated RF signal to the tag which is comprised of the chip and the antenna. The chip obtains energy through the antenna and responds by modifying its input impedance and thus modulates the signal, which is sent back to the reader. For modulating signals are often used method ASK (Amplitude Shift Keying) (Nikitin, Rao, 2006).

It is applicable in various applications, so it is possible to use it for non-contact transfer of data in tough weather conditions (water, dust...) and where is necessary to avoid electrical contacts. (Azad, Wang, 2012) NFC technology can find its application on smart packaging, access control, coupons and loyalty cards, in different kinds of paying, in health etc. (Häikiö et al, 2007) (Bravo et al, 2010) (Hardy et al, 2009) (Rainer et al, 2010). Nowadays wireless systems are increasingly popular and demands for them are increasing every day. Unlike most popular wireless technologies, like Bluetooth, Wi-Fi, RFID etc., NFC technology is characterized by low power consumption, higher stage of safety and lower possibility of interference with others radio frequency systems (Curran et al, 2012) (Cho et al, 2009). NFC has slower data transfer (up to 424 kbps), compared with others wireless technologies like WiFi (up to 250 Mbps) or Bluetooth (up to 25 Mbps). The main advantage of NFC is ability to establish connections with others wireless technology (WiFi, Bluetooth ...) that use the same standards as NFC.

Although NFC is young technology is already standardized by ISO/IEC 18092 standard (Curran et al, 2012). This technology is supporting other standards like ISO 14443, ISO 15693, ISO 18000-3, and because of that fact NFC offers a wide range of possibilities for developing applications.

Architecture of NFC technology is divided onto three parts (Riyazuddin, n.d.): Card emulation mode, Reader/Writer mode and Peer-to-Peer mode (Figure 1). Card emulation mode is passive mode where device can be used as a smart card for identification. In Reader/Writer mode NFC device is active and is used for reading/writing of NFC passive tag. Peer-to-Peer mode is used when two or more devices exchange data. In this mode initiator uses less energy than in card emulation mode, because both devices have their own power system.

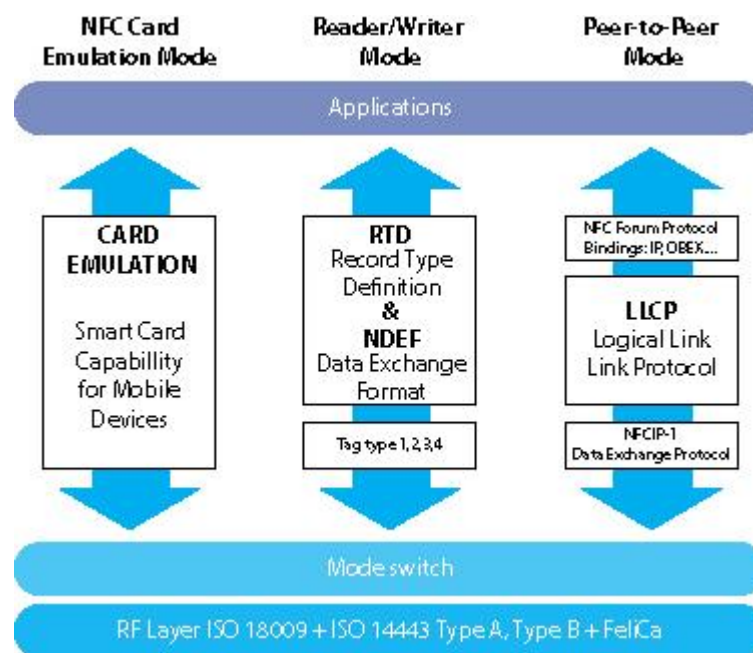


Figure 1: Architecture of NFC technology

In this paper the process of manufacturing passive printed NFC tag that contains a temperature sensor on tag's chip is presented. Tag's antenna was printed with screen printing, using conductive silver ink. In the results, tag's real and imagined resistance, his capacitive or inductive nature and his operating frequency are presented.

2. MATERIALS AND METHODS

Process of research is shown in Figure 2. Our research is consisted of four phases. The first phase started with conventional NFC tag, fabricated with process of etching. Aim of this phase was to get acquainted with the characteristics of that NFC tag. Next step, the second phase, was an attempt to fabricate conventional design by screen printing. This phase has not brought the expected results. Because of that, in the third phase, new design was presented and has made improvements primarily on the field of tag's resistance. Resistance was a major problem in the second phase, and due to high resistance values, tags did not work. Now, our researches are

stopped at the fourth phase. Aim of this phase is to present new and better design which will give us better functional and operational characteristic than previous one.

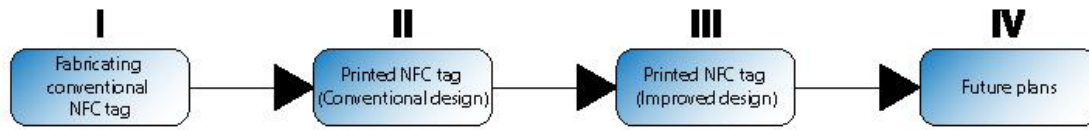


Figure 2: Process of NFC research

2.1 First phase

In our work IDS-SL13A chip was used. The mentioned chip has integrated temperature sensor and data logger designed for use in smart passive and semi-passive labels. Smart semi-passive labels are defined as thin and flexible labels that contain an integrated circuit and a power source (in this case tag can be powered by 1.5 V battery), also known as battery-assisted back-scattered passive labels, which enable enhanced functionality and superior performance over existing passive labels. Tag can also work in passive mode (without power source), but in that particular case it is not capable for temperature data logging. The IDS-SL13A is operating at 13.56 MHz and is fully ISO 15693 compliant.

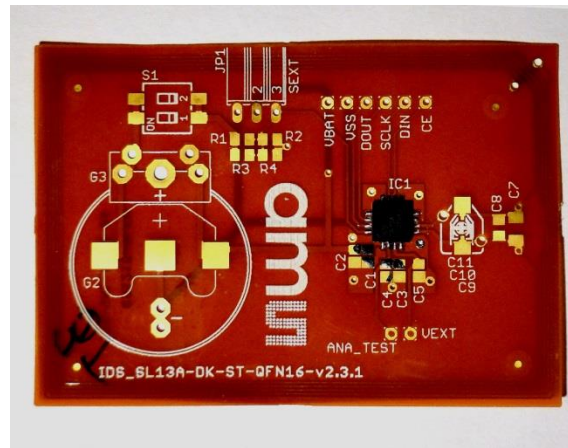


Figure 3: Conventional NFC tag

At our first phase NFC tag was fabricated by conventional process of etching. That process of fabrication is very popular in production of conventional electronics.

Tag was etched on 145 μm thick polyamide foil. This foil remains stable across a wide range of temperatures, from $-269\text{ }^{\circ}\text{C}$ to $+400\text{ }^{\circ}\text{C}$. For making conductive lines and antenna loops copper was used. For better and easier bonding every contact pad was plated with gold.

2.2 Second phase

In this phase, the same design as conventional tag was printed on PETG foil (thickness: 160 μm , roughness Ra [DIN 4768]: 0.8 – 2 μm). Despite the lack of data on the thermal resistance in specification, it was found out that the foil is tolerating high temperature up to 200 $^{\circ}\text{C}$.

Two different kinds of functional inks were used for printing. All samples were printed using the ROKU SD-05 screen printer with monofilament polyester plain weave mesh with 120 l/cm and theoretical ink volume of 16.3 cm^3/m^2 . For printing conductive lines SunChemical CRSN 2442 SunTronic Silver 280 thermal drying silver conductive ink was used. Dielectric layers were printed with SunChemical CFSN6057 SunTronic Dielectric 681 UV curing ink. Process of drying was divided to two stages. Conductive ink was dried thermally in temperature tunnel Zhejiang Dingye Machinery Co BS-B400. The best results – the lowest sheet resistance – were obtained when samples passed the IR tunnel for 225 seconds at 130 $^{\circ}\text{C}$. For UV drying Aktiprint L UV tester was used. The UV printed samples were optimally cured when passed through a UV tunnel four times

with a dose of 750 mJ/cm^2 . Printed NFC tag with design taken from conventionally fabricated tag is shown on Figure 4.

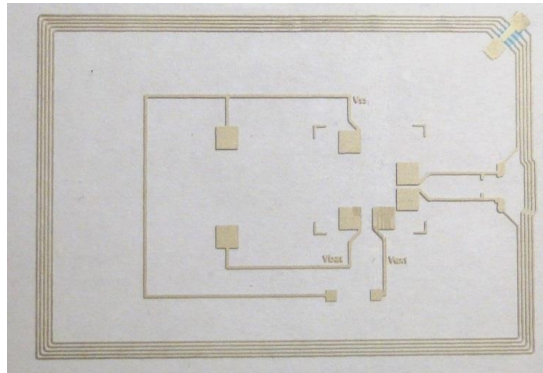


Figure 4: Printed NFC tag with conventionally fabricated tag design

After process of fabricating antennas, chip integration was performed. IDS SL13A chip was used, same one like used on conventionally fabricated tag. In our research this chip worked only in passive mode, without external battery. Previously prepared chips were assembled with isotropic conductive glue based on silver particles (Bison, Netherlands). After chip integration, tags were dried in a thermal oven at 120°C for 30 minutes. At the end of the second phase printed NFC tags were analyzed.

NFC tags fabricated with the same (conventionally fabricated) antenna design did not show their functionality. Reason for that was high resistance of antenna's loop. The resistance was measured after 24 hours of conditioning in the area with 50% relative humidity at 23°C using the Fluke 289 True-rms Industrial logging multimeter.

2.3 Third phase

New improved antenna (Figure 5) was designed and simulated using the EM simulator CST Microwave Studio.

New design has thicker conductive lines, which contributes to reducing resistance. It is smaller than previous one and it has one more layer printed on the other side of the foil. That new layer is so called "reflector", and its purpose is to increase directivity and capacitance of printed antenna. In this phase for printing and drying same equipment was used like in the second phase. When antenna samples were done chip integration was performed. Again, SL13A chip was used. The chips were assembled with isotropic conductive glue EPO-TEK P1011. This glue is one component modified polyamide with silver particles specially design for use in microelectronics. After chips assembling tags were dried in a thermal oven at 150°C for 60 minutes.

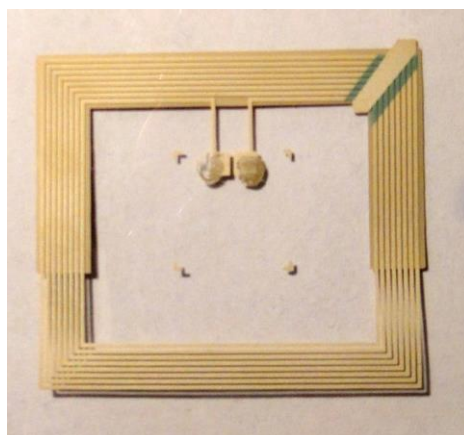


Figure 5: Printed NFC tag with new design

In the third phase process of testing was divided to three steps. A first resistance measuring was performed after 24 hours of conditioning in the area with 50% relative humidity at 23 °C with Fluke 289 True-rms Industrial logging multimeter. Then tags operability was tested with two different readers: classical reader IDS R13MP v2 (Figure 6, (a)) with appropriate software equipment and mobile device – tablet: Asus Nexus 7 (Figure 6, (b)), which is equipped with NFC chip. These measurements were done in real environment with the purpose to select working tags for final testing.

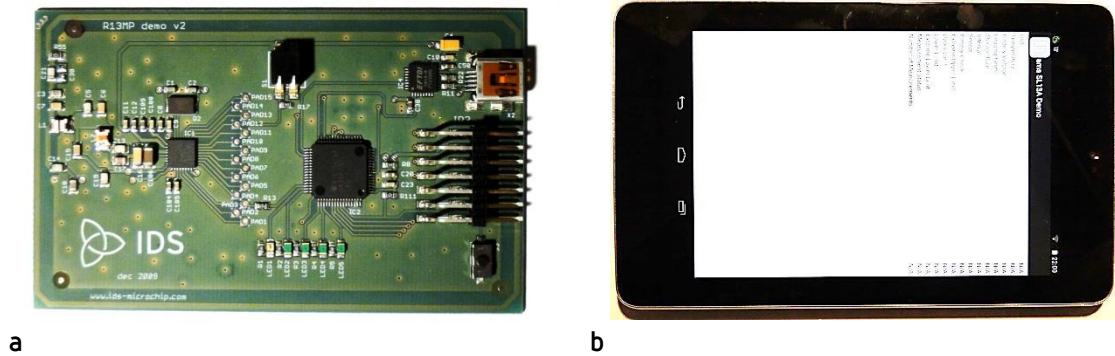


Figure 6: Classical reader IDS R13MP v2 (a); mobile device – tablet: Asus Nexus 7 (b)

Measurements of real and imaginary part of resistance, operating frequency and capacitive or inductive nature of tags were performed in final testing. For that purpose Agilent E5071C VNA Network Analyzer (Figure 7) was used. The characteristic impedance of tags was measured in the anechoic chamber. The results of those measurements help us to see characteristic of printed NFC tags.



Figure 7: Agilent E5071C ENA Network Analyzer

2.4 Fourth phase

In our further researches we are planning to create even better design which will have improved resistance characteristic and better operability.

3. RESULTS AND DISCUSSION

3.1 Characteristic of conventionally fabricated NFC tag

Resistivity of conventional NFC tags was around 2.9Ω . From the Smith chart (Figure 8) tags behavior on operating frequency of 13.56 MHz is presented. On that frequency tag has real part of impedance of 9.12Ω and imaginary part of 446.16Ω with inductance of $5.24 \mu\text{H}$. This information shows that this tag at operating frequency has inductive nature.

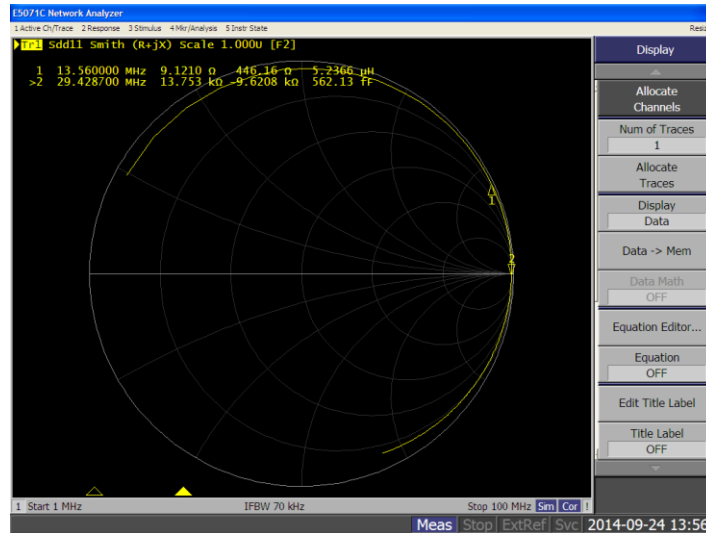


Figure 8: Smith chart of conventionally fabricated NFC tag

3.2 Resistance of printed NFC tag with same design like conventional one

Results of resistance are presented in Table 1. Five different samples with their resistivity, resistivity at operating frequency of 13.56 MHz, antenna resonant frequency and inductance were analyzed.

Table 1: Results of resistance of printed NFC tag with same design like conventional one

Sample	Resistance [Ω] (DC)	Resistance [Ω] (@ 13.56 MHz)	Antenna resonant frequency [MHz]	Inductance [μH]
V1	85	190* (@ 36.2 MHz)	244.43	0.25
V2	520	1420	25.07	2.6
V3	570	1450	26.08	2.8
V4	396	1100	28.08	3.3
V5	262	626	51.15	1.44

Samples presented in Table 1 were measured with multimeter (DC current) and Network analyzer. All samples had a high resistivity, except sample V1. That sample had short circuit on part covered with dielectric ink, and because of that current ran through a smaller number of loops. Consequently, tag has had smaller resistivity and completely different behavior than all other samples.

3.3 Resistance and characteristics of printed NFC tag with improved design

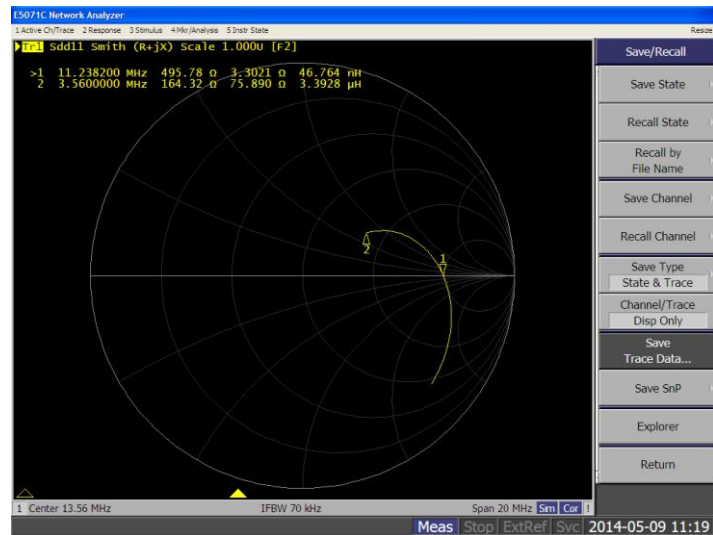
Results of resistance measurements are shown in Table 2. Resistance of test elements (before and after chips assembling) and resistance of antenna (DC) were presented. M1, M2 and M3 are working tag with new improved design.

Table 2: Results of resistance of printed NFC tag with same design like conventional one

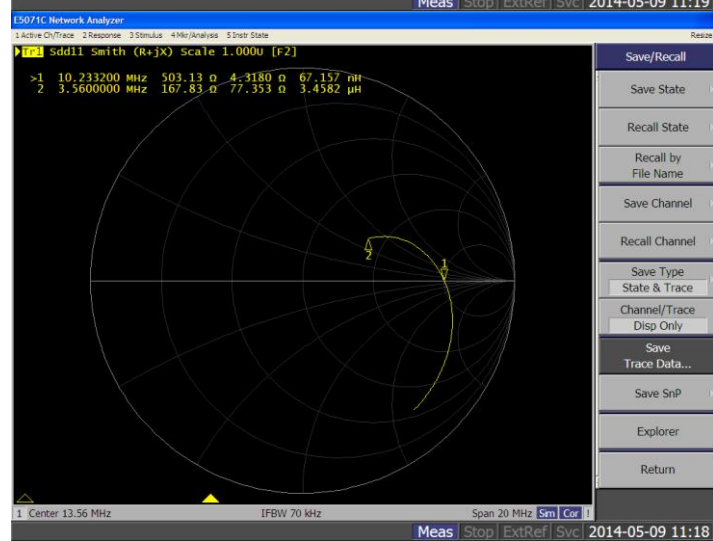
Sample	Resistance of test element [Ω]		Resistance of antenna [Ω] (DC)
	Before	After	
M1	1.424	0.880	134.82
M2	1.480	0.935	136.82
M3	1.332	0.970	146.57

In next three figures Smith charts with characteristics of tags measured by VNA network analyzer will be presented. Sequentially, characteristics for M1, M2 and M3 are shown on Figure 9.

M1



M2



M3

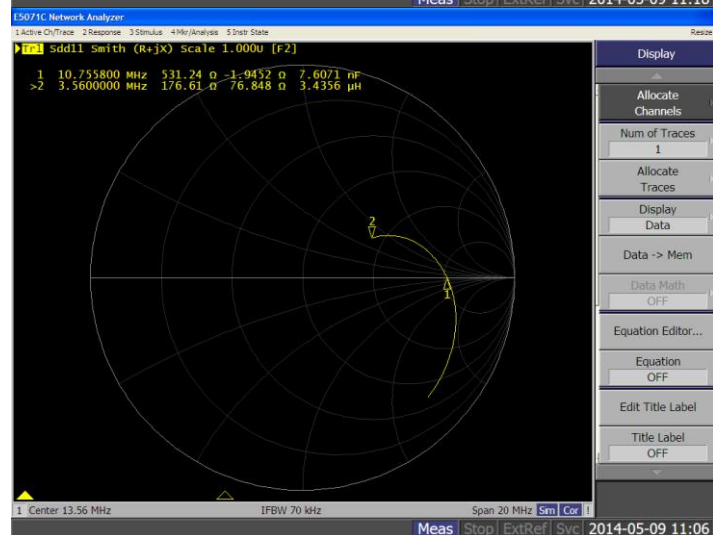


Figure 9: Smith charts for M1, M2 and M3 measured by VNA network analyzer

As can be seen, from Smith charts (Figure 9), tags at operating frequency at 13.56 MHz have similarly behavior. Real parts of impedance varies from 495 to 530 ohms, and imaginary parts are similar for M1 and M2 (3.3 and 4.32, consequently). Imaginary part of impedance for M3 was -1.95. Information about imaginary part of impedance shows us nature of tag. If imaginary part of impedance is positive, tag has an inductive nature. Otherwise, the tag has a capacitive nature.

Compared to conventionally fabricated NFC tag printed tags have worse characteristics. Antennas on printed tags have higher resistivity (DC and at particular frequency) and because of that more energy is needed for communication. That fact directly affects on decrease of reading range. Conventionally fabricated NFC tag is readable at about 6-8 cm, while printed tags are readable at 0-1.5 cm (depends of tag).

4. CONCLUSIONS

In this paper study for Near Field Communication tag's printed antenna has been proposed. Research started with conventionally fabricated NFC tags and continued with showing printed versions of tags, with the same and with improved design as conventionally fabricated one. Through optimizing the antenna design improved characteristics of tag were obtained. It was shown that higher ink conductivity impacts on tags characteristics, operability and reading range. Results of this research shows that conventionally fabricated NFC tags comparing to printed NFC tags has advantages in characteristics, reading range and repeatability. Advantages of printed NFC tags are flexibility, ecology, price etc. Future steps will be optimization of current design with aim to get better characteristics and operability with lower resistivity.

5. REFERENCES

- [1] Azad, U., Wang Y.E.: „Direct Antenna Modulation scheme for enhanced capacity performance of near-field communication link”, (IEEE International Workshop of Antenna Technology (iWAT) 2012), pages 88-91.
- [2] Bravo, J., Hervás, R., Fontecha J.: “Touch-Based Services’ Catalogs for ALL”, Current Trends in Web Engineering (Lecture Notes in Computer Science), volume 6385, pages 459-462., (2010).
- [3] Cho, J.H., Cole, P.H., Shiho K.: “An NFC transceiver using an inductive powered receiver for passive, active, RW and RFID modes”, SoC Design Conference (ISOC) (Busan, South Korea, 2009), pages 456-459.
- [4] Curran K., Millar A., Mc Garvey C.: “Near Field Communication”, IJECE, volume 2 (3), pages 371-382., (2012).
- [5] Dobkin, D. M.: “The RF in RFID: Passive UHF RFID in Practice”, (Elsevier, Boston, 2008).
- [6] Häikiö J., Wallin, A., Isomursu, M., Ailisto, H., Matinmikko, T., Huomo, T.: “Touch-based User Interface for Elderly Users”, Proceedings of Mobile HCI '07. (2007), (New York, USA, 2007), pages 289-296.
- [7] Hardy R., Rukzio, E., Wagner, M., Paolucci, M.: “Exploring Expressive NFC-Based Mobile Phone Interaction with Large Dynamic Displays”, First International Workshop on Communication, Networking & Broadcasting, pages 36-41., (2009).
- [8] Nikitin P.V., Rao, K.V.S.: “Performance limitations of passive UHF RFID systems”, Proceedings of International Symposium Antennas and Propagation Society, IEEE 2006, (Albuquerque, USA, 2006), pages 1011-1014.
- [9] Rainer, S., Preißinger, J., Schöllermann, T., Müller, A., Schnabel, I.: “Near Field Communication (NFC) in an automotive Environment”, Second International Workshop on Communication, Networking & Broadcasting, pages 15-20., (2010).
- [10] Riyazuddin M.: “NFC: A review of the technology, applications and security”, Information Technology Center, King Fahd University of Petroleum & Minerals, Saudi Arabia, URL: <http://123seminaronly.com/Seminar-Reports/023/46910687-Near-Field-Communications-Review.pdf> (last request: 2014-09-12)
- [11] Zichner, R., Siegel, F., Baumann, Reinhard, R.: “Communication Quality of printed UHF RFID transponder antennas”, Proceedings of Large-Area, Organic and Polymer Electronics Convention 2011, (Frankfurt, Germany, 2011), pages 361-363.

PRINTED PRIMARY ZN/MNO₂ BATTERIES FOR SMART PACKAGE APPLICATIONTomáš Syrový¹, Marian Milec¹, Silvan Pretl², Lucie Syrová¹, Petr Kuberský²¹ University of Pardubice, Faculty of Chemical Technology Pardubice,
Department of Graphic Arts and Photophysics, Czech Republic,² University of West Bohemia in Pilsen, Faculty of Electrical Engineering,
Department of Technologies and Measurement/RICE, Pilsen, Czech Republic

Abstract: The presented study is focused on development of primary batteries as an energy source for developed RFID based Smart Label which is intended for monitoring of climate conditions. The developed battery is based on well-known Zn/MnO₂ system, which is consisted of relatively cheap and environmentally friendly chemical substances. The energy requirements of Smart label are in interval 2 - 3 V, so experimental plan was focused on preparation of two serially connected cells. The study was oriented to development of technology where the most of the parts of battery should be fabricated by printing or coating technologies. As a main fabrication technique was used screen printing technique, because of the required layers thickness and ink viscosity, solid of ink respectively.

Key words: Printed battery, Zn, MnO₂, electrolyte, screen printing, smart label, monitoring

1. INTRODUCTION

A new trend called printed electronic has been developing recently in graphic arts industry. By using printing and coating techniques and proper new printing materials are produced several types of functional layers and structures. There are manufactured functional structures which are already known/produced for a long time, but their production by using printing/coating techniques could offer low cost, usually low end alternative for usage in everyday life. This trend could be also found in production of thin flexible primary or secondary cells. There are needs of technology process which would enable to create the current sources with the small dimensions for the reasonable prices. All these demands are possible to fulfil through the thin flexible batteries which could be produced by the printing/coating technologies. The main goal of this study is to design the composition of an individual ink formulation which is used for printing of the selected battery layers. The next task is to develop technology of preparation of printed batteries, where the order of preparation of the individual functional layers has to be designed. In order to keep the quality of encapsulation the assembling process should be optimized too.

2. METHODS

The ink formulation and other materials used for fabrication of primary battery cell were prepared from chemical substances purchased from Sigma-Aldrich. The printing/encapsulation substrate was used Fatra Tenolan OAN 50 and 125 µm.

During the preparation of collectors, electrodes and others elements of batteries, analytical balance KERN & Sohn GmbH AB 220-4 was used for the estimation of precise weight of active materials. Haake RV1 was used for measurements of rheology properties of ink formulations. Selected layers of cells were printed using screen printing machine Ever Bright S-200 HF. Drying of printed layers was performed in an oven Memert UFP400. UV curable sealing layers were cured in the UV tunnel Aerotherm MINITHERM UV 220 Super Q. The resistance of the carbon collector layers was measured using the Digital Multimeter RIGOL DMM3068. Discharging characteristics were measured by the Digital Multimeter Keithley 2700.

2.1 Preparation of MnO₂ ink formulation

The electrode material was synthesized according to equation (1). The MnSO₄ was titrated by KMnO₄ in presence of HCl. The precipitated MnO₂ was centrifuged and washed two times in demi water, then triple times in absolute ethanol.



The dried MnO_2 was grinded together with carbon black. The base of typical ink formulation was consisted of 14 % of MnO_2 /Carbon black mixture, 79 % of water based solution, 9 % of ethylene glycol. In the experiments were used modified ink formulations EPMn_1 to EPMn_3.

2.2 Preparation of Zn ink formulation

The zinc ink formulation was based on fine Zn particles with size lower than 10 μm . The typical printing paste was consisted from mixture of Zn and PVDF in ratio 60:1. The solvent system was based N-Methyl pyrrolidone. This ink formulation was named as a EPZn_1. The second ink formulation (EPZn_2) was based on the same zinc powder mixed in ratio 6.2:1 with solvent based polymer solution. The EPZn_2 delivered better printing behavior during preparation of Zn electrode and better stability of fabricated cells.

2.3 Preparation of electrolyte ink formulation

The electrolyte was based on water based solution of ZnCl_2 and NH_4Cl , where mixture of the salts was chosen because, each of them have influence for selected parameters of cells as a short current, capacity, stability, etc. Base electrolyte system was consisted from 24 wt % NH_4Cl and 8 wt % ZnCl_2 , distilled water then accounted for 68 wt %. Then was tested compatibility of base electrolyte with several rheology modifiers to obtain viscosity in order of units Pa.s, which should be suitable for screen printing process. There were tested several types of rheology modifiers as a polyethylene oxide (two different Mw), carboxymethyl cellulose, hydroxyethyl cellulose, polyvinyl pyrrolidone, poly vinyl alcohol. For all types of rheology modifiers was found that at concentration (2-3 %) which deliver suitable viscosity in range of Pa.s., the concurrency of solubility equilibria salts/rheology modifier caused precipitation of one of components. The resulted ink formulation of electrolyte was consisted from water based solution consisted from ZnCl_2 , NH_4Cl and Setix rheology modifier in mixture ratio 3:1:1.

2.4 The fabrication of printed battery and battery assembly

In presented study were made batteries, consisting of a series connection of two cells. Cells were prepared in sandwich arrangement. The collector, electrodes (Zn , MnO_2), sealing/encapsulating layers, electrolyte were printed by using screen printing technique. For each printed material was determined precise weight amount of deposited materials. The PET substrate was cut to size 105 x 148 mm. For this dimension, the different parts of battery have been allocated in the manner as shown in Figure 1. The active area of each electrode layer was 25 x 25 mm.

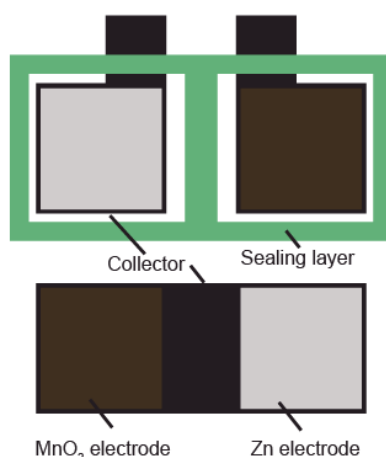


Figure 1: Layout of printed Zn/ MnO_2 battery

The battery collectors were printed by using carbon based ink formulation. The collector layers were dried in an oven at a temperature 60° C for 50 minutes. Collector layer thickness after drying was about 0.015 (0.002) mm, where in the bracket is standard deviation of parameter. The typical sheet resistance of collector was equalled 100 Ω/\square . Subsequently on the collector

electrode was printed the zinc electrode, then was dried in the oven for 50 minutes at 60 °C. The dried zinc electrode has the average thickness 0.079 (0.014) mm. After drying the zinc electrode was printed MnO₂ ink formulation and these layers were dried in oven for 40 minutes at 60 °C. After drying, the mass per unit area of the dried electrode material MnO₂ was 4.7 mg/cm². It was not possible to measure the thickness of the electrode layer, because the mechanical properties didn't allow it. The sealing layer was based on UV curable ink formulation for screen printing technique, where the cured layer was resistant to electrolyte. The UV curable layer was printed on one part of battery, on second part was deposited electrolyte. The next step was assembly of both parts of battery together, with high care to prevent electrolyte spreading into the area overprinted by UV curable ink. Assembled battery cell was cured on both sides under UV radiation source with the dose of irradiation 450 mJ/cm².

3. RESULTS AND DISCUSSION

3.1 Measurements of open circuit voltage of printed battery cells

After assembling of the battery the open circuit voltage was measured, then for selected batteries was measured short circuit current. The results of these measurements are shown in Table 1. The selected batteries mainly differ in amount of deposited electrolyte and used ink formulation for electrolyte, which was varied in rheology modification given by rheology modifier. From table is obvious, that the higher values of open circuit voltage overall exhibit cells with higher viscosity and from experiments was obvious that batteries with better encapsulation without leakage of electrolyte exhibit better characteristics and higher stability. It is obvious, that the maximum value of open circuit voltage of serial connected cells is close to typical voltage of alkaline cell.

Table 1: Open circuit voltage of printed battery cells

Battery No.	Zn Ink	MnO ₂ Ink	Electrolyte viscosity/type	Electrolyte weight [g]	V _{oc} [V]
B2	EPZn_1	EPMn_1	Low	0.2379	2.9
B3	EPZn_1	EPMn_1	Low	0.2678	2.847
B4	EPZn_1	EPMn_1	Low	0.3612	2.856
B5	EPZn_1	EPMn_1	High	0.2299	2.936
B6	EPZn_1	EPMn_1	High	0.313	2.993
B7	EPZn_1	EPMn_1	High	0.3674	2.96

3.2 Stability of battery open circuit voltage in time

For the first set of batteries, time stability was estimated. It could be concluded, that batteries with gel-like high viscosity electrolyte deliver better performance than batteries with low viscosity electrolyte. From data is clear, that the proper amount of electrolyte is important for stability of battery in time.

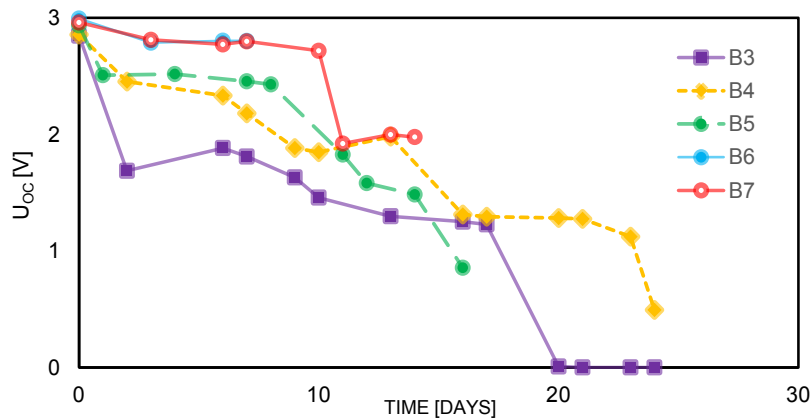


Figure 2: Stability of battery open circuit voltage in time.

3.3 Measurements of discharging characteristics of batteries

The batteries were tested under load 15 kOhm which correspond to average consumption of 66–200 μ A what is equal to level of consumption of developed Smart Labels. The sampling frequency of measurement of actual voltage was set to 120 second. The measured characteristics were compared to commercial printed battery Enfucell Reg 3.0V.

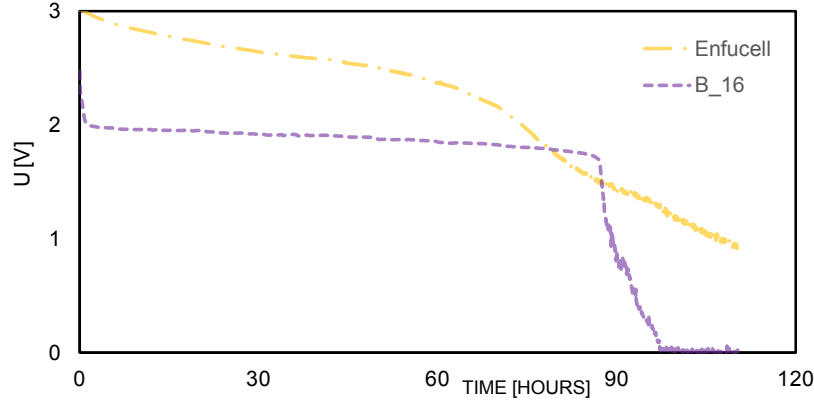


Figure 3: Discharge characteristics under 15 kOhm load.

From desired data is evident that the output voltage of fabricated battery dropped down under load. It is probably caused by high internal resistance given by relative high resistivity of collectors and by properties of electrode materials and their mechanical stability, which have an influence on efficiency of charge transferring to collectors. The others factors could be caused by self-discharging effect too, because the characteristic was measured two days after assembling. In Table 2 are calculated discharging characteristics for batteries.

Table 2: Discharging characteristics of printed batteries

Battery No.	Zn Ink	MnO ₂ Ink	Electrolyte weight [g]	$Q_{(65\%)}$ [mAh]	$Q_{(1V)}$ [mAh]	$E_{(65\%)}$ [mWh]	$E_{(1V)}$ [mWh]
B16	EPZn_2	EPMn_3	0.3714	11.18	11.15	20.99	20.96
Enfucell Reg 3.0V	-	-	-	15.76	15.91	37.68	37.84

4. CONCLUSIONS

In presented study is described development of fully printed battery based on Zn/MnO₂ system. Alongside the development of technology of fabrication process was developed screen printing ink formulation for corresponding active layers of battery cell too.

The fabricated batteries were compared to commercial one – Enfucell Reg 3.0V. At the same load (15 kOhm) the battery Enfucell Reg 3.0V from the start of discharging until the empty state (0–78 hour) deliver output voltage in range of 3 to 1.8 V. During discharging the Enfucell provided electric current from 0.2 mA to the minimum 0.12 mA. The developed battery provided, during discharging cycle, output voltage from 2.5 to 1.8 V, when the voltage dropped down to 2V within first hour. The lower output voltage of developed battery is probably given by high internal resistance and by other reasons, which have to be solved in next R&D activities.

From estimated discharge characteristics could be concluded that the areal density of energy of the developed printed battery is 1.55 mWh/cm² and the areal energy density of the battery Enfucell is 4.71 mWh/cm². The comparison of these two values shows that the developed printed battery delivered 33% of Enfucell battery capacity.

From the performed experiments is obvious, that the performance of battery is influenced by a lot of parameters, like material characteristics of collector, electrodes, etc. It was found that the one of the most important parameter is quality of assembly process and quality of encapsulation of battery itself.

5. ACKNOWLEDGMENTS

This research has been supported by Ministry of Industry and Trade, project No. FR-TI4/167.

6. REFERENCES

- [1] BLUE SPARK. Blue Spark UT (Ultra Thin) Series: Product Line Matrix. URL: <http://www.bluesparktechnologies.com/index.php/products-and-services/battery-products/ultra-thin-series> (last request 2013-11-09)
- [2] CHOI, M., G., KIM, K., M., LEE, Y., Design of 1.5 V thin and flexible primary batteries for battery-assisted passive (BAP) radio frequency identification (RFID) tag. *Current Applied Physics*. 2010 (4), vol. 10, pages 92-96. DOI: 10.1016/j.cap.2010.03.010.
- [3] CHABRE, Y., PANNETIER, J., Structural and electrochemical properties of the proton / MnO₂ systems. 1995, 130 s. Great-Britain.
- [4] IZUMI, A., SANADA, M., FURUICHI, K., TERAOKI, K., MATSUDA, T., HIRAMATSU, K., MUNAKATA, H., KANAMURA, K., Development of high capacity lithium-ion battery applying three-dimensionally patterned electrode. *Electrochimica Acta*. 2012, vol. 79, pages 218-222. DOI: 10.1016/j.electacta.2012.07.001.
- [5] GRANDE, L., CHUNDI, V., T., WEI, D., BOWER, Ch., ANDREW, P., RYHÄNEN, T., Graphene for energy harvesting/storage devices and printed electronics. *Particuology*. 2012 (1), vol. 10, pages 1-8. DOI: 10.1016/j.partic.2011.12.001.
- [6] GAIKWAD, A., M., WHITING, G., L., STEINGART, D., A., ARIAS, A., C., Highly Flexible, Printed Alkaline Batteries Based on Mesh-Embedded Electrodes. *Advanced Materials*. 2011 (29), vol. 23, pages 3251-3255. DOI: 10.1002/adma.201100894.
- [7] GOLLER, G., J., PETRAGLIA, V., J., DEWS, G., Screen printing method for making an electrochemical cell electrode [patent]. United Technologies Corporation. 1978, United States. 920,038.
- [8] PARK, M., HYUN, S., NAM, S., Mechanical and electrical properties of a LiCoO₂ cathode prepared by screen-printing for a lithium-ion micro-battery. *Electrochimica Acta*. 2007, pages 7895-7902.
- [9] PRELONIC TECHNOLOGIES. Battery Technology: Primary Cell. [online]. [cit. 2013-11-09]. <http://www.prelonic.com/Default.aspx?PageId=19>
- [10] POWER PAPER. Printable Battery Benefits, URL: <http://www.powerpaper.cn/indexfddc.html?categoryId=43873> (last request 2013-11-09)
- [11] ROCKET. Paper battery: Model & specification. URL: <http://www.rocket.co.kr/> (last request 2013-11-09)
- [12] SOUTHEE, D., HAY, G., I., EVANS P., S., A., HARRISON, D., J., Lithographically printed voltaic cells – a feasibility study. *Circuit World* . 2007, str. 31-35. Emerald Group Publishing Limited.
- [13] WENDLER, M., HÜBNER, G., KREBS, M., Development of Thin and Flexible Batterie. *Science & technology*. 2010, pages 32-41.

INFLUENCE OF TEXTILE WASHING TREATMENT ON READABILITY OF QR CODES

*Nemanja Kašiković, Magdolna Pal, Rastko Milošević,
Neda Milić, Bojan Jurišić,
University of Novi Sad, Faculty of Technical Sciences,
Department of Graphic Engineering and Design, Novi Sad, Serbia*

Abstract: The use of QR codes in textile printing is increasing because QR codes give the possibility to store greater amounts of data compared to bar codes, which insures wider possibilities for information storage. QR codes can be printed on textile using different printing techniques (screen, pad, as well as ink jet printing). Materials used in textile printing are often exposed to influence of different factors such as heat, UV light, moist, rain, washing, rubbing and etc. The aim of this paper is to examine the influence of washing treatment on readability of QR codes printed on textile materials, wherein the analyzed QR codes have different content, size, and level of data protection.

Key words: QR codes, textile printing, washing treatment

1. INTRODUCTION

More than thirty different 2D-barcodes are currently in use (Kato and Tan, 2007). At present, seven 2D-barcodes are used for camera phone applications among them. These are: QR Code (ISO/IEC 18004, 2000), VeriCode (Veritec, 2005), Data Matrix (ISO/IEC 16022, 2000), mCode (Squires and Levinger, 2006), Visual Code (Rohs, 2005), ShotCode (Madhavapeddy et al, 2004) and ColorCode (Han et al, 2006).

QR Code is capable of encoding all types of data including symbols, binary and multimedia and so forth. The maximum data capacity of numeric, alphanumeric and binary is 7,089 characters, 4,296 characters and 2,953 bytes, respectively. By applying Reed-Solomon error correction coding, up to 30% of original data can be restored even if the symbol is damaged (Kato, Tan and Chai, 2010). Quick Response (QR) Code was developed by Denso Wave (a division of Denso Co. at the time) in 1994 (DensoWave, 2008). This code is a two-dimensional matrix symbology that has position-detection patterns at three corners. As the name suggests, it was initially designed for ultra-high-speed and omnidirectional reading (ISO/IEC 18004, 2000). Thus, QR Code was developed to improve the reading speed of complex-structured 2D barcodes. It is also known for its capability of directly encoding the Japanese and Sino-Japanese Kanji-Kana character sets. Other QR Code features are massive data capacity, high data density and selectable levels for error correction ability (Bushnell and Meyers, 1999). Recently QR Code derivatives have been developed; these include Mobile Code and MS-Code.

In August 2002 in Japan, J-SH09 (the manufacturer was Sharp and the carrier was J-Phone) was released as the first mobile phone that had a reader for Japanese Article Number (JAN) code (1D barcode) and QR Code (2D barcode) as one of its functions (Saito, 2008). Many other Japanese phone companies such as DoCoMo, Vodafone (now, Softbank Mobile Co.) and KDDI au also began offering mobile phones with the ability to read QR Code (Saito, 2008).

QR codes have become popular and can be seen in advertising, in the print media, on business cards, products, websites and vending machines etc (Cook, 2010).

Screen and digital printing processes are mostly used for printing on textile substrates. The great progress is made in the field of textile materials. Materials have different characteristics; those characteristics can be influential factors in the printing process and textile materials may be describe with fabric weight, thread count and material composition.

The use of textile materials is increasing as well as printing QR codes on textile.

Textile materials printed with screen or digital printing during the exploitation can be under the influence of various treatments such as washing, heat, light, rubbing etc. (Kašiković et al, 2012).

The aim of this research is to determine influence of textile materials and washing treatment on the first read rate (FRR).

2. METHOD

QR codes were generated using the Goqr.me application (Goqr.me, 2014). We used H level of error correction (30% of codewords can be restored) with code size 10 x 10 cm, 5 x 5 cm and 2.5 x 2.5 cm. We used URL as our test data: www.grid.uns.ac.rs.

Figure 1 presents examples of QR codes use in experiment.



Figure 1: QR codes

QR codes were printed on five different textile materials. All materials were characterized by following parameters: fabric weight using standard SRPS F.S2.016 and material composition (SRPS F.S3.112). These properties are presented in Table 1.

Table 1: Characteristics of material used in testing

Material characteristic	Composition	Fabric weight (g/m ²)
Material 1	65 % polyester, 35 % cotton	216
Material 2	100 % cotton	100
Material 3	100 % viscose	120
Material 4	100 % polyester	164
Material 5	25 % cotton, 75 % polyester	136
Methods	SRPS F.S3.112	SRPS F.S2.016

Materials were printed by digital inkjet printing machine Epson 4880. Epson UltraChrome K3 ink was used. After printing process, print was fixed using Difol TP4040s (160 °C, 30 s).

First read rate (FRR) of each sample was calculated, where

$$\text{FRR} = \frac{\text{Number of successful first reads}}{\text{Number of attempted first reads}} \quad (1)$$

We calculated the FRRs by the numbers of successful first reads out of the number of attempts (i.e. 50 times).

The recommended reading time involves three periods of reading: reading is less than 2 seconds (<2), between 2 and 7 seconds (2-7) and more than 7 seconds (> 7). When reading time is longer than 7 seconds, it is unsuccessful code read. On the other hand, successful code reading time is below 7 seconds (Grover et al., 2010).

Each barcode sample was captured by Samsung N7100 with 8 megapixels camera. We captured each sample image from two distances (15 and 25 cm away from the target) under lighting conditions TL84, 4100 K using Agile Radiant CVC5-2E light cabinet.

More than one reader was available for some 2D-barcodes. We conducted the FRR experiments with QR Code Reader (Google Play, 2014).

After those analysis we determined QR codes fastness on washing treatment (40 °C, 2 h 40 min).

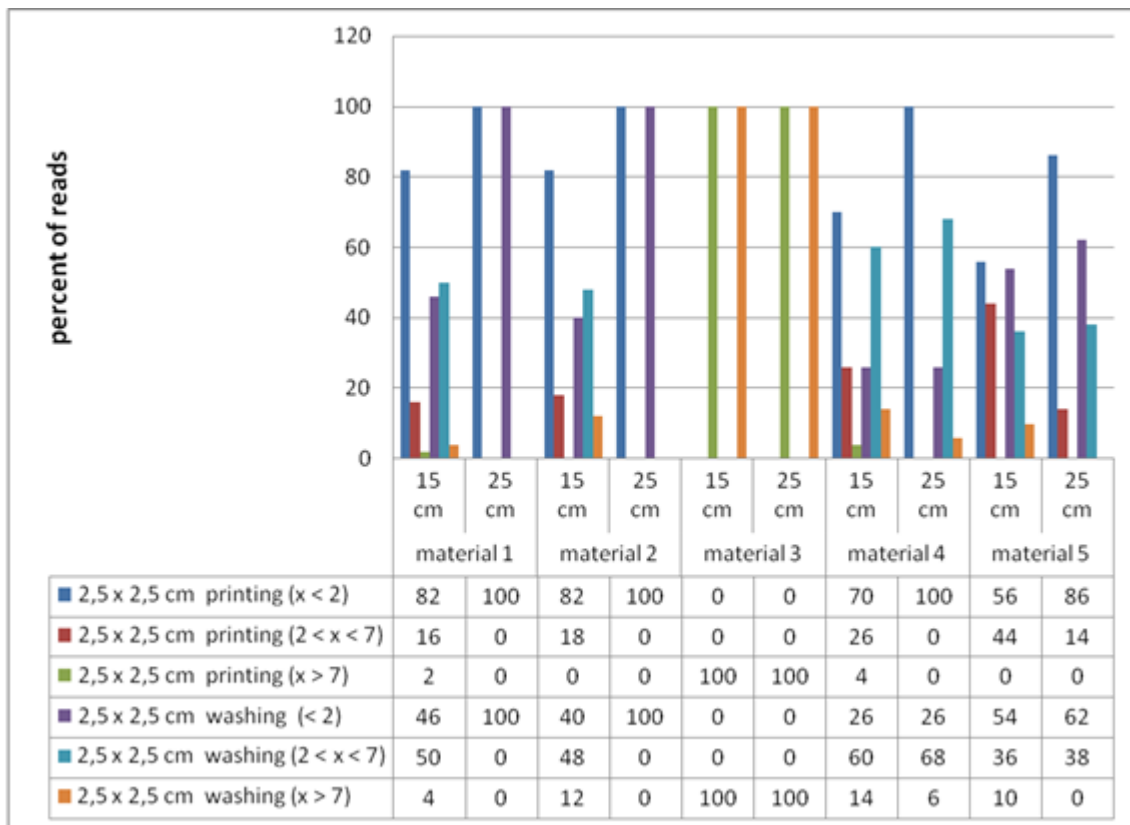
3. RESULTS

First read rate for samples after printing process and after washing treatment are presented in table 2.

Table 2: FRR - first-read rate

Sample	Read distance (cm)	QR code sizes					
		2,5 x 2,5 cm		5 x 5 cm		10 x 10 cm	
		FRR after printing (%)	FRR after washing treatment (%)	FRR after printing (%)	FRR after washing treatment (%)	FRR after printing (%)	FRR after washing treatment (%)
Material 1	15	98	96	100	100	100	100
	25	100	100	100	100	100	100
Material 2	15	100	88	100	100	100	58
	25	100	100	100	100	50	36
Material 3	15	0	0	100	98	0	0
	25	0	0	100	100	0	0
Material 4	15	96	86	100	96	72	44
	25	100	94	100	100	54	18
Material 5	15	100	90	0	0	0	0
	25	100	100	0	0	0	0

QR codes reading time are presented in Figures 2, 3 as well as 4.



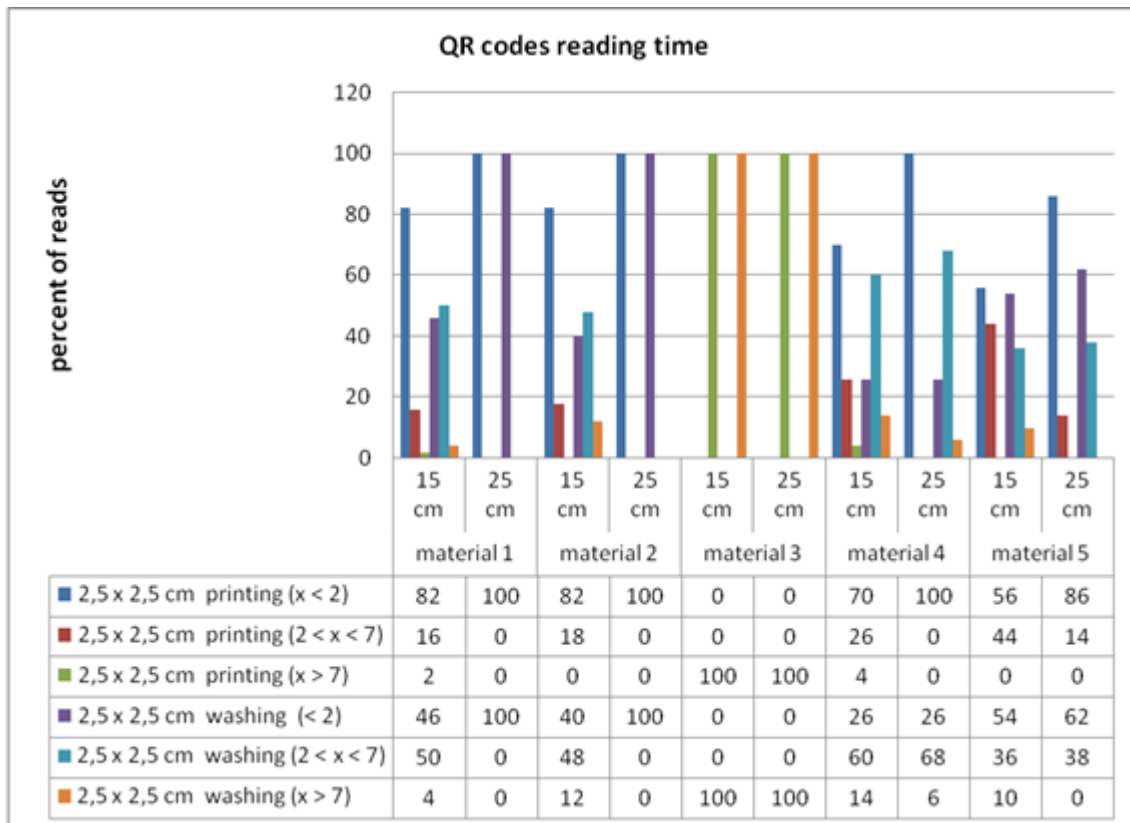
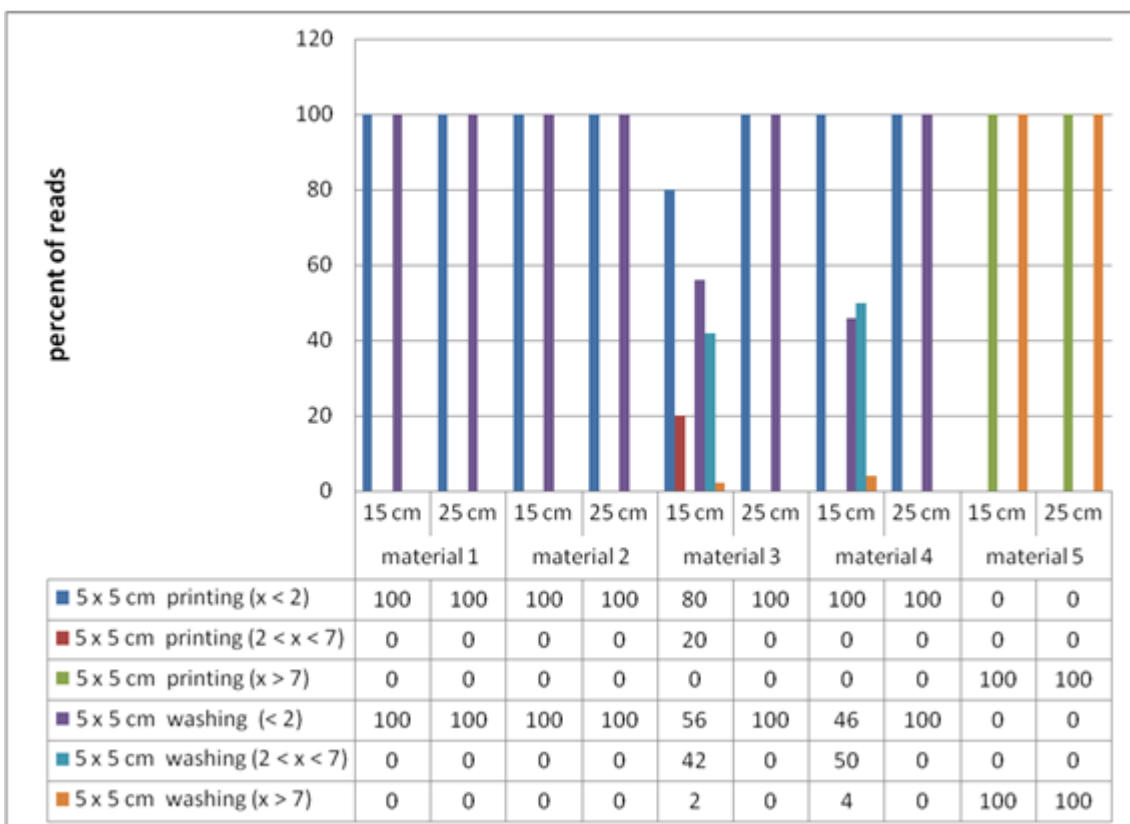


Figure 2: QR codes reading time (2,5 x 2,5 cm)



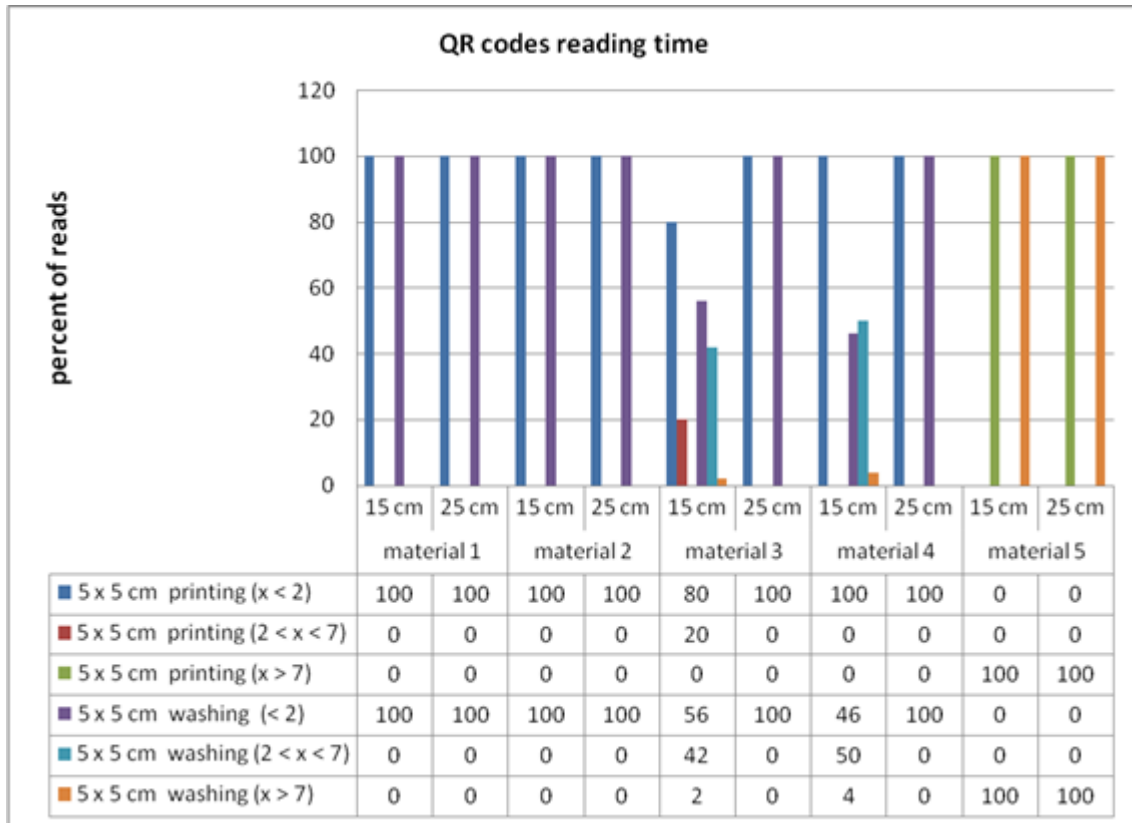
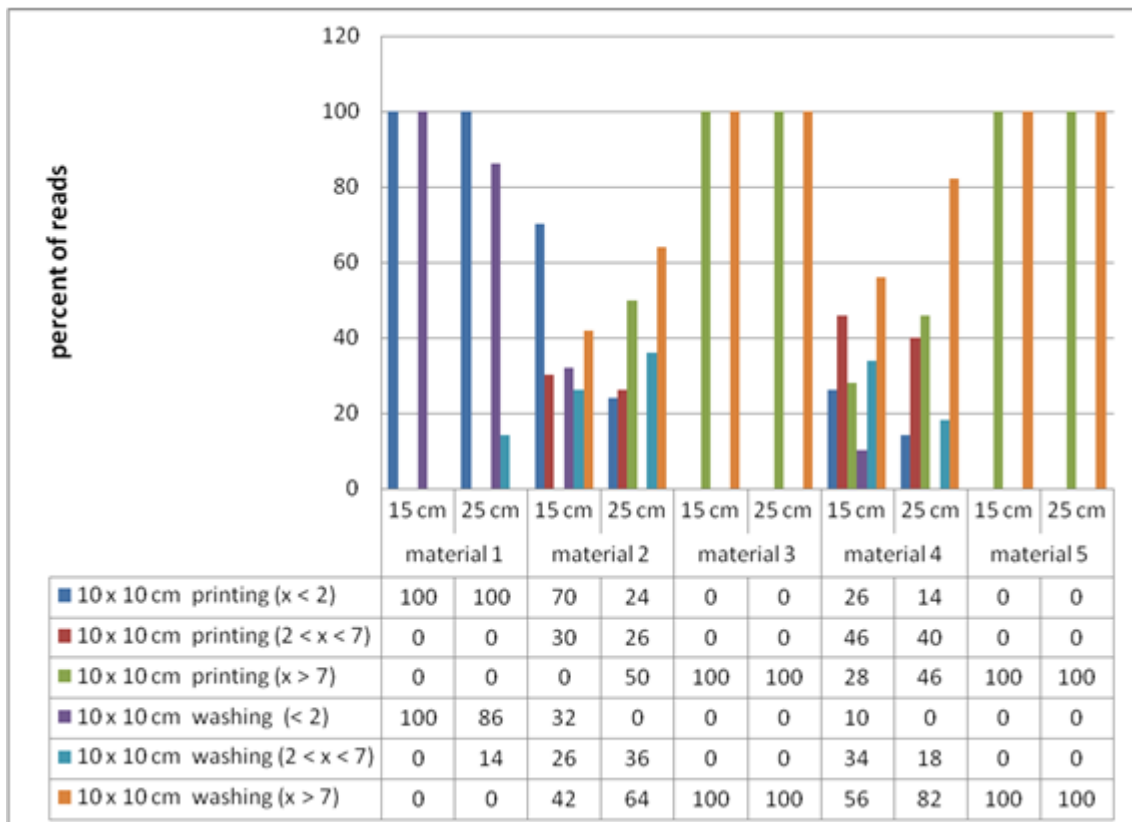


Figure 3: QR codes reading time (5 x 5 cm)



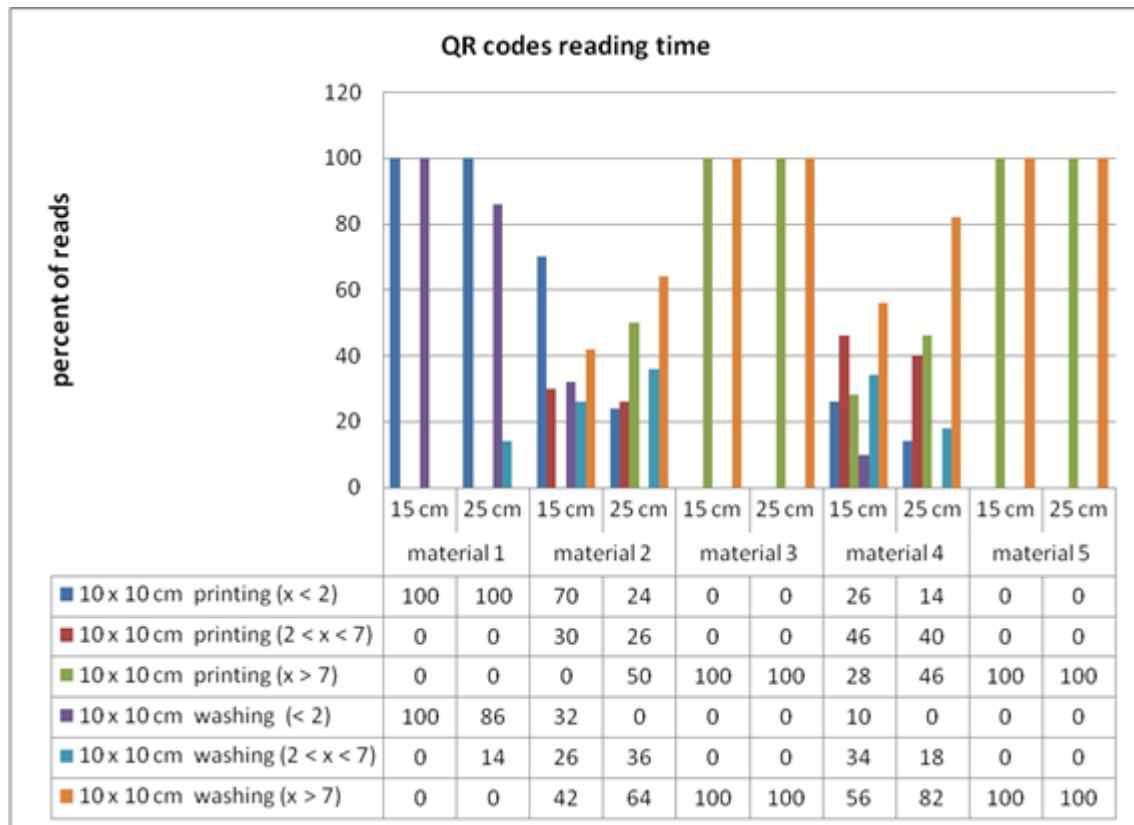


Figure 4: QR codes reading time (10 x 10 cm)

4. DISCUSSION

After the printing process we can see that all codes printed on a material 1 had good value of FRR. The lowest value was 98% for reading the code size of 2.5 x 2.5 cm from a distance of 15 cm. Material 2 also had a 100% value almost in all cases, except when we read code 10 x 10 cm (25 cm). We found problems with code reading in codes printed on material 3, specially in codes 2.5 x 2.5 cm as well as 10 x 10 cm (0%). Codes printed on material 4 have shown good FRR results. The lowest value of FRR was of code size 10 x 10 cm; 72% (15 cm) and 54% (25 cm). Influence of material on FFR was found when we analyzed QR codes printed on material 5. FRR for codes 5 x 5 as well as 10 x 10 cm were 0%.

Washing treatment changed FRR in some cases, especially for codes printed on material 4 (10 x 10 cm) and material 2 (10 x 10 cm). For those codes FRR decreased 28% (15 cm) and 36% (25 cm) – material 4 as well as 42% (15 cm) and 14% (25 cm) – material 2.

Although, FRR values were high after washing treatment, in Figures 2, 3 and 4, we can see that washing treatment influenced the read time. Figure 2 shows that the most reading times is in period between 2 and 7 seconds (2.5 x 2.5 cm). In Figure 3 (5 x 5 cm) reading time is longer for codes printed on material 3 and 4 (15 cm) as well as for material 2 and 4 (10 x 10 cm), Figure 4.

5. CONCLUSIONS

Based on the results we can conclude that textile materials are significant parameters for FRR. Use of suitable combination of inks and textile materials is recommended in order to achieve good quality print and readable QR codes..

Code size and read distance are in correlation with FRR. We can improve results for FRR with bigger code size as well as longer read distance.

In the end, we can say, that washing treatment is influenced on readability of QR codes (FRR has not changed much, but read time is longer).

In the future research, we can analyze different level of error correction ([L(7%) M(15%) Q(25%) H(30%)]) as well as the influence of increasing number of washing process.

6. ACKNOWLEDGMENTS

This paper was supported by the Serbian Ministry of Science and Technological Development, Grant No.: 35027 "The development of knowledge and production in graphic arts industry"

7. REFERENCES

- [1] Bushnell, R. D. Meyers, R. B.: "Getting Started with Bar Codes: A Systematic Guide", 5th edn (Pennsylvania, USA: QuadII, Inc., 1999).
- [2] Cook, H.: "Promoting Informal Learning Using a Context-Sensitive Recommendation Algorithm For a QR Code-based Visual Tagging System", <https://www.dur.ac.uk/resources/education/research/Thesis-Cook-01-01-2011.pdf> (last request: 2014-09-30)
- [3] DensoWave Inc.: "QR Code.Com" <http://www.denso-wave.com/qrcode/index-e.html>. (last request: 2008-03-17)
- [4] Google Play (2014): QR code reader: <<https://play.google.com/store/apps/details?id=me.scan.android.client>> (last request: 2014-08-30)
- [5] Goqr.me.: "QR code generator". <http://goqr.me/> (last request: 2014-07-01)
- [6] Grover, A., Braeckel, P., Lindgren, K., Berghel, H., Cobb, D.: "Parametres Effecting 2D Barcode Scanning Reliability": <http://www.berghel.net/publications/2d-bar/2d-bar.pdf> (last request: 2014-09-21)
- [7] Han, T-D, Cheong, C-H., Lee, N-K., Shin, ED.: "Machine readable code image and method of encoding and decoding the same," US Patent 7,020,327, US Patent and Trademark Office, March 28, 2006.
- [8] International Organization for Standardization: Information technology - Automatic identification and data capture techniques - Bar code symbology - QR Code. ISO/IEC 18004, 2000.
- [9] International Organization for Standardization: Information technology - International symbology specification - Data Matrix. ISO/IEC 16022, 2000.
- [10] Kašiković, N., Novaković, D., Vladić, G., Avramović, D.: "Influence of ink layers on the colourfastness to rubbing of printed textile materials" *Tekstilna industrija* 60 (2), 28-32, 2012.
- [11] Kato, H., Tan, K.T.: "First read rate analysis of 2D-barcode for camera phone applications as a ubiquitous computing tool", *TENCON 2007 - 2007 IEEE Region 10 Conference*, (IEEE, Taipei, 2007), pages 1-4.
- [12] Kato, H., Tan, K., Chai, D.: „Barcodes for Mobile Devices”, (Cambridge University Press 2010)
- [13] Madhavapeddy, A., Scott, D., Sharp, R., Upton, E.: "Using camera-phone to enhance human-computer interaction", <http://www.ubicomp.org/ubicomp2004/adjunct/demos/madhavapeddy.pdf> (last request: 2014-09-21)
- [14] Rohs, M. C.: "Real-world interaction with camera-phones", *Proc. 2nd Int. Symp. On Ubiquitous Computing Systems (UCS 2004)*, LNCS 3598, Springer-Verlag, 2005, pages 74-89.
- [15] Saito, K.: "J-SH09 - a camera becomes a bridge between virtual world and real world" <http://plusd.itmedia.co.jp/mobile/0208/01/barcode.html> (last request: 2008-03-20)
- [16] Squires, S. R. and Levinger, J. K. Efficient finder patterns and methods for application to 2D machine vision problems, United States Patent application 20060269136 A1. 2006-11-30.
- [17] Veritec Inc. Benefits of Veritec's 2D Codes - VeriCode® and VSCode® <http://www.veritecinc.com/vericode.html>. (last request: 2008-04-12)

THE STABILITY OF PRINTED POLYOLEFIN FOILS

Viera Jančovičová¹, Zuzana Štromajer², Blažena Krivošová², Zuzana Machatová¹,

¹ University of Technology in Bratislava, Faculty of Chemical and Food Technology,
Department of Graphic Arts Technology and Applied Photochemistry,
Bratislava, Slovak Republic

² Chemosvit Folie, a.s., Svit, Slovak Republic

Abstract: Printing on polyethylene foils is a long-term studied issue. In case the foil is used as a package for aggressive materials such as peat substrate, it begins to degrade, the optical properties change and often a significant reduction in the adhesion of the ink layer to a substrate occurs, which can result into abrasion due to handling of the packaged goods.

The aim of this work is to investigate the effect of light and thermal aging on the colour stability of the ink layer and the degradation processes in LDPE foils (monolayer and multilayer) and their possible correlation with poor adhesion of the ink to the substrate.

Key words: LDPE foil, flexographic inks, accelerated ageing, peat substrate

1. INTRODUCTION

Packaging industry is an inseparable part of plastics manufacturing and printing industry. Raw materials or finished goods, almost everything is being packed. Various properties are expected to be provided by a package, protection of material, easy handling, providing information and many more. Last but not least a package is an effective weapon on competitive market. It has to be able to draw consumer's attention at first sight. Also in recent years, another important property is being considered – ecological aspects of packaging, altogether at an acceptable price.

The answer to these requirements is a constant improvement in manufacturing, not only by using various material combinations creating multilayer packages, but also intelligent and active components incorporated. Although majority of packages are supposed to protect its inner content from degradation, sometimes the opposite is required, thus to protect the environment and consumer from aggressive material packed. Either way it is often necessary to pick a material with low surface energy providing good chemical resistance, low water vapor permeability, static electricity resistance, harmless and without volatile organic compounds included (Štromajer, 2014). Considering these requirements what seems to be a best choice is polyolefin materials. Easy to process, cheap and highly resistant they are providing great properties. However due to their low surface energy printing is often difficult and requires previous surface treatment, or significant reduction in the adhesion of the ink layer to a substrate occurs, which can result into abrasion when handling the packed goods.

The aim of this work is studying a possible link between insufficient flexographic ink adhesion on polyolefin foil, packed good, in this case peat substrate, light aging and adverse climatic conditions. Soon after filling the packages with peat substrate and storing them outside, the reduction of ink adhesion in corners of a package occurs, this causes difficulties in handling and unnecessary customer claims (Štromajer, 2014).

2. EXPERIMENTAL

Three types of foils supplied by Chemosvit Folie, a.s. were used:

- **AGB 300** – Polyten AGW 300, LDPE foil consisting of white obverse side containing TiO₂ pigment and black reverse side. Thickness of the foil was 60 µm (foil 1).
- **AGB 300/2** – Polyten AGW 300, LDPE foil consisting of transparent polyethylene obverse side, middle white layer containing TiO₂ pigment and black reverse side. Thickness of the foil was 60 µm (foil 2).
- **Polyten HP** – HP transparent, LDPE monofoil, width 35 µm (foil 3).

Polyethylene foils were printed with flexographic inks manufactured by Sun Chemical Corporation, series Truweather. These inks are designed for materials stored in exterior; manufacturer declares their high chemical and light stability together with heat resistance up to 180 °C.

All samples, both printed and not printed, were exposed to three types of accelerated aging:

- Accelerated weathering in exterior on a 5th floor window of Faculty of chemical and food technology in Bratislava. Samples were exposed to weathering for 20 weeks, from 16. 12. 2013 to 5. 5. 2014.
- Accelerated light aging on the same window in the same time as accelerated weathering, but inside.
- Thermal aging in closed glass containers in 80 °C and 80 % relative humidity in dark (Multifunctional dryer APT Line series), some of the samples with peat substrate present.

During aging, the samples were monitored by FTIR spectroscopy (FTIR spectrophotometer Excalibur Digilab FTS 3000MX, USA, using the ATR adapter with diamond window), the adhesion was evaluated using TESA test.

The colorimetric coordinates of samples (L^* , a^* , b^*) were obtained by means of Spectrophotometer Spectrodens (Techkon, illumination D50, standard observer 2°). CIE $L^*a^*b^*$ system was used to evaluate the colour changes. Value L^* represents lightness of colour spot, chromatic coordinates a^* and b^* range from green to red and from blue to yellow colours, respectively.

The total colour difference ΔE_{ab}^* was calculated from Eq. (1) [2],

$$\Delta E_{ab}^* = \sqrt{(\Delta L^*)^2 + (\Delta a^*)^2 + (\Delta b^*)^2} \quad (1)$$

where values L^* , a^* and b^* are the differences between relevant values attributed to aged and non-aged samples.

3. RESULTS AND DISCUSSION

In this work we used three types of polyethylene foils (exact composition in part 2). All three foils were made of LDPE, while samples **AGB 300** (foil 1) and **AGB 300/2** (foil 2) also contained a layer with TiO_2 , which is overlaminated with transparent polyethylene foil in sample 2. **Polyten HP** (foil 3) is a transparent monofilm made of polyethylene containing high amount of non specified additives ensuring stability, required sliding properties and static electricity prevention. Surface corona treatment was used on all foils directly after manufacturing (Štormajer, 2014).

3.1 Influence of the external conditions on the foil degradation

To study light and thermal stability of used samples FTIR spectroscopy was used. The mechanism of polyethylene degradation is a very complex process associated with wide range of side products formation. Because these reaction products keep forming and decomposing, interpretation of results is quite difficult. Using multilayer materials containing many additives made results evaluating even more complicated. Both printed and non printed foils were subjected to light and thermal accelerated aging, what allowed us to acquire some results about their light and thermal stability.

After **aging in exterior** there was a wide band found in FTIR spectrum with maximum absorbance at 1660 cm^{-1} . This band probably corresponds to ketones forming during polyethylene photooxidation (Gardette et al., 2013; Milata et al., 2008). In the next phase of degradation ketones transformed into carboxylic acids by Norris I mechanism, what occurred in FTIR spectrum as disappearing bands at 1660 cm^{-1} and creation of a new band at 1715 cm^{-1} . (Figure 1a). The same process was detected in sample 2 and 3, but in a considerably slower rate. After 12 weeks a wide band at $3100 - 3685 \text{ cm}^{-1}$ appeared in the spectrum. This band is typical for $-\text{OH}$ groups in polymer chain. Also there were secondary alcohols (Figure 1b) detected in the spectrum at $1260 - 1310 \text{ cm}^{-1}$ and 1100 cm^{-1} . These were most significant in sample 2 after 12 weeks aging and disappeared in following reactions.

Foils exposed to **interior light aging** (on window behind glass) were degrading slower than samples in exterior. This phenomenon was caused by different spectral distribution of the light, which, in interior, is depleted mainly of ultraviolet content. Also indoor samples were exposed to

different climate conditions. In case of sample 1 (Figure 2a) a small band at 1714 cm^{-1} occurred in FTIR spectrum showing carboxylic acids formation after 20 weeks exposition. Sample 2 did not show any changes in FTIR spectrum and sample 3 (Figure 2b) showed changes very similar to the same foil type aging in exterior.

During **thermal aging** ($80\text{ }^{\circ}\text{C}$, 80% relative humidity) there was increase in absorbance at $3110 - 3600\text{ cm}^{-1}$ in every sample. This is caused by variously bound hydroxyl groups. Together with band occurring at 1100 cm^{-1} and $1260 - 1350\text{ cm}^{-1}$ we assume secondary alcohols were created. These are typically created during thermal degradation of polyethylene (Figure 3a). In all samples there was a band at 1740 cm^{-1} detected in the spectrum, what showed creation of carbonyls (probably aldehydes) as a product of thermal degradation (Gardette et al., 2013).

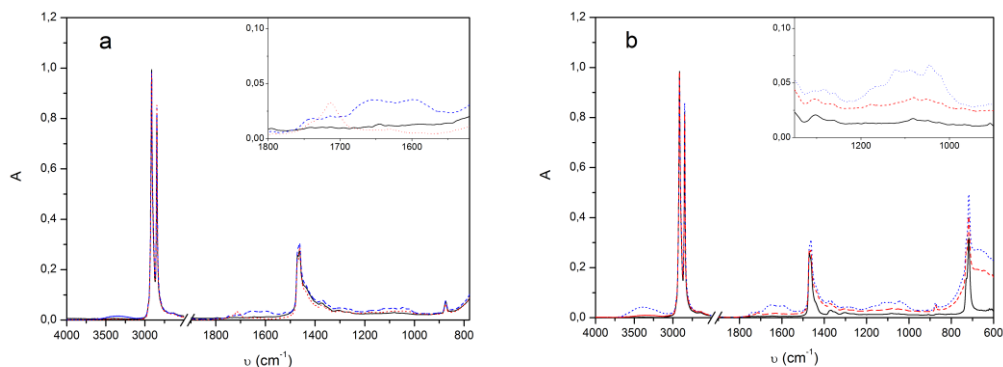


Figure 1: FTIR spectrum of foil 1 (Figure a) and foil 2 (Figure b) after exterior aging: unaged foil (solid line), foil exposed for 12 weeks (dashed line), foil exposed for 20 weeks (dotted line) (Štromajer, 2014)

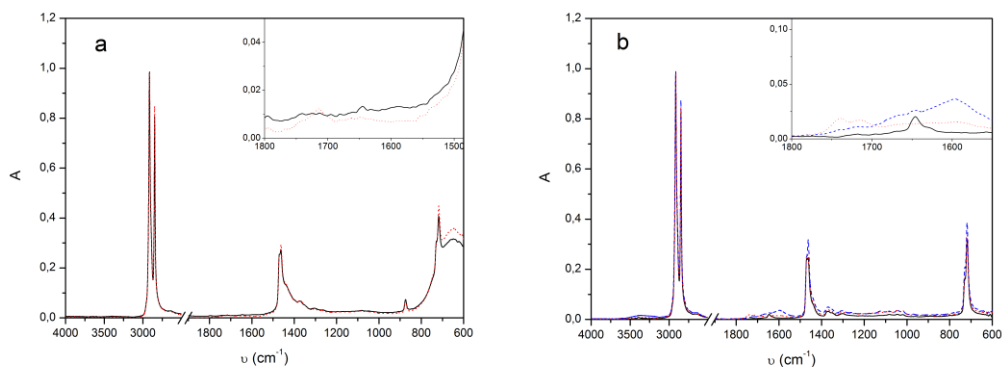


Figure 2: FTIR spectrum of foil 1 (Figure a) and foil 2 (Figure b) after interior aging: unaged foil (solid line), foil exposed for 12 weeks (dashed line), foil exposed for 20 weeks (dotted line) (Štromajer, 2014)

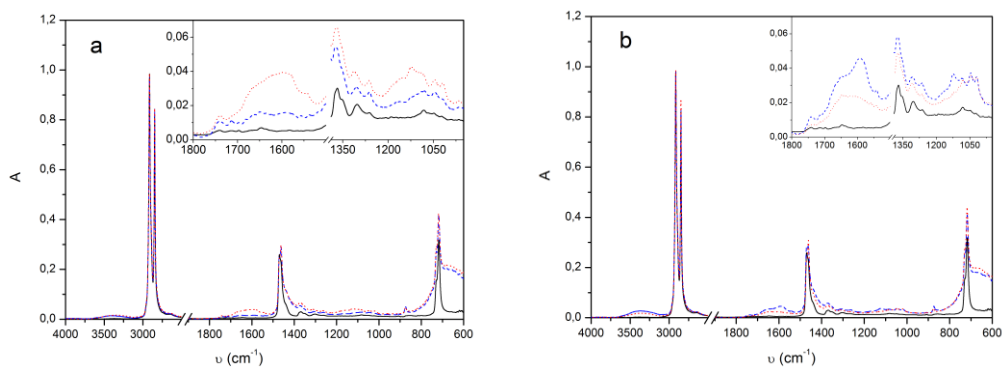


Figure: 3: FTIR spectrum of foil 2 after thermal aging ($80\text{ }^{\circ}\text{C}$ a 80% relative humidity): unaged foil (solid line), foil aged for 7 days (dashed line), foil aged for 28 days (dotted line) (Štromajer, 2014)

FTIR spectra of all foils have shown similar changes after thermal aging with and without peat substrate (Figure 3b). Differences in spectrum with peat substrate at 1500–1600 cm⁻¹ were caused by organic compounds of nitrogen. From FTIR spectra we assume that polyethylene degradation during light aging and thermal aging have different mechanisms and are similar to those listed in thesis (Hunt, 1995).

3.2 Light and thermal stability of flexographic inks

Colorimetric measurements (Table 1 and Table 2) have shown that not every flexographic ink was equally light resistant. The biggest differences were detected in the samples exposed to exterior conditions. This behaviour is probably caused by UV light supporting ink degradation. The biggest colour difference was found in yellow ink (Table 2), where changes in coordinate b^* towards blue occurred (Table 1). Though inks printed on film 3 (Polyten HP) have shown the biggest differences in colour ΔE_{ab}^* , we assume that the light stability of ink is not related with substrate (Table 2), but with the type of ink and degradation. The least light resistant inks were magenta and yellow, on the contrary cyan and black were quite colour stable and have shown only minor changes in colour. From the colour differences measured it is apparent that films submitted to thermal aging in presence of peat substrate degraded more rapidly than those aged without peat. We have found possible the peat substrate acts as a catalyst in the process of ink degradation, although samples stored with substrate in the dark were colour stable.

Table 1: Changes in colour coordinates L^* , a^* , b^* in cyan, magenta and yellow printed on film 1 during exterior weathering

	Weathering period [days]		ΔL^*	a^*	Δa^*	b^*	Δb^*	ΔE_{ab}^*
Cyan	0	52.1	0	-32.4	0	-44.0	0	
	28	52.6	0.5	-32.9	0.5	-43.7	0.3	0.8
	56	52.8	0.7	-32.8	0.4	-43.6	0.4	0.9
	84	52.8	0.7	-32.9	0.5	-43.6	0.4	0.9
	112	53.1	1.0	-33.0	0.6	-43.5	0.5	1.5
	140	53.5	1.4	-33.6	1.2	-43.0	1.0	2.1
Magenta	0	48.5	0	60.7	0	3.8	0	
	28	47.9	0.6	60.5	0.2	3.4	0.4	0.7
	56	48.0	0.5	59.7	1.0	2.9	0.9	1.4
	84	48.3	0.2	58.9	1.8	2.2	1.6	2.4
	112	47.8	0.7	58.2	2.5	1.6	2.2	3.4
	140	48.1	0.4	56.9	3.8	0.9	3.9	5.4
Yellow	0	79.4	0	-10.8	0	69.2	0	
	28	80.1	0.7	-11.4	0.6	70.1	0.9	1.3
	56	80.3	0.9	-12.0	1.2	69.8	0.6	1.6
	84	80.2	0.8	-12.3	1.5	68.4	0.8	1.9
	112	80.2	0.8	-12.2	1.4	64.7	4.5	4.8
	140	80.4	1.0	-12.3	1.5	57.6	11.6	11.9

Table 2: Colour difference ΔE_{ob}^* of CMYK inks during different types of aging [1]

	Film 1	Film 2	Film 3
Weathering in exterior (20 weeks)			
Cyan	2.1	1.3	2.7
Magenta	5.4	3.4	4.9
Yellow	11.9	10.9	12.1
Black	1.3	1.1	1.3
Interior aging behind glass (20 weeks)			
Cyan	0.8	0.7	1.5
Magenta	2.3	1.8	2.8
Yellow	3.8	3.9	4.7
Black	0.3	0.4	1.3
Thermal aging (80 °C, 80 % RH) (28 days)			
Cyan	1.4	1.3	1.5
Magenta	2.9	3.0	2.4
Thermal aging (80 °C, 80 % RH) with peat substrate (28 days)			
Cyan	3.5	3.1	2.3
Magenta	2.8	2.8	4.5
Aging in dark with peat substrate (laboratory temperature)			
Cyan	0.2	0.2	0.3
Magenta	0.4	0.2	0.3

3.3 Ink adhesion to the substrate

During aging we assessed ink adhesion using TESA test on all foils (Table 3). The higher the value in the table, the better adhesion was detected. Number 3 means the best adhesion without any ink torn down by TESA tape. Every flexographic ink used in tests achieved this value before aging.

Table 3: Ink film adhesion on polyethylene foils (3 – no ink torn down, 2 – small areas torn down, 1 – bigger areas torn down, 0 – large areas torn down) [1]

	Foil 1	Foil 2	Foil 3
Weathering in exterior (20 weeks)			
Cyan	3	3	3
Magenta	3	3	2
Yellow	3	3	3
Red	3	3	1/2
Violet	3	3	2
Interior aging behind glass (20 weeks)			
Cyan	3	3	3
Magenta	3	3	3
Yellow	3	3	3
Red	3	3	2/3
Violet	3	3	2
Thermal aging (80 °C, 80 % RH) (28 days)			
Cyan	3	3	3
Magenta	3	2/3	2/3
Red	3	3	2
Thermal aging (80 °C, 80 % RH) with peat substrate (28 days)			
Cyan	3	2/3	3
Magenta	2	2	0/1
Red	2	2	1
Aging in dark with peat substrate (laboratory temperature)			
Cyan	3	3	3
Magenta	3	3	3
Red	3	3	3

During light degradation, the ink adhesion was slightly worse, in the case of exterior aging only foil 3 showed significantly worse results in magenta, red and purple. Interior aging behind glass did not seem to reduce adhesion, slight decrease was recorded in foil 3 (red and purple). The most significant ink adhesion reduction occurred in the samples after thermal aging in the presence of peat substrate, especially magenta and red on foil 3. From the results of the TESA test is therefore obvious that light aging had minimal effect on the adhesion of the ink. Variables that

seemed to worsen the results were peat substrate, high temperature and relative humidity. The worst result was detected in foil 3 (Polyten HP mono foil), conversely the best adhesion was recorded in foil 1 (Polyten AGW 300) containing TiO₂ on obverse side.

4. CONCLUSIONS

Changes in the infrared spectrum showed the degradation of the polyethylene occurs due to light and thermal aging and is accelerated by the presence of peat. Formation of degradation products (ketones, carboxylic acids, secondary alcohols) was observed, the overall amount and form depend on the aging method used and the LDPE foil specimen, as well. Thermal aging was accelerated by the presence of peat substrate.

The results of the light aging procedure show that not all flexographic inks exhibit the necessary light stability, especially when light ageing with a higher proportion of UV component is used, in yellow colour samples exceeded the total colour difference the value of 10. On the other hand, cyan and black inks are stable.

In all of printed samples the colour layer adhesion test was performed using an adhesive tape TESA. The results showed only a slight deterioration of the adhesion due to light aging, but there was a significant decrease in the samples exposed to accelerated thermal aging at high humidity in the presence of peat substrate. We assume that in the presence of peat at elevated temperature and relative humidity, unspecified reactions take place which lead to the deterioration of adhesion and subsequently wiping the paint off the foil. Among the inks, the worst adhesion showed the magenta and the red, which contains magenta as well.

In practice, the peat packages are perforated, stored in stacks and wrapped in stretch foil, resulting in extreme conditions formation, effecting the packaging and detrition of the color layer.

5. ACKNOWLEDGMENTS

This work has been supported by the Scientific Grant Agency of the Slovak Republic (project 1/0818/13) and by the Slovak Research and Development Agency under contract No. APVV-0324-10.

6. REFERENCES

- [1] Gardette, M., Perthue, A., Gardette, J., Janecska, T., Földes, E., Pukánszky, B., Therias, S.: "Photo- and thermal-oxidation of polyethylene: Comparison of mechanisms and influence of unsaturation content", *Polymer Degradation and Stability*, 2383–2390, 2013.
- [2] Hunt R.W.G., *Measuring Colour*, Ellis Horwood Limited, London, United Kingdom, 1995.
- [3] Milata, V., Segl'a, P., Brezová, V., Gatiaľ, A., Kováčik, V., Miglierini, M., Stankovský, Š., Šíma, J.: "Aplikovaná molekulová spektroskopia" (Bratislava, Slovak Republic; STU, 2008), pages 546 – 550.
- [4] Štromajer, Z.: "Stabilita potlačených obalových materiáľov", Diploma work (Bratislava, Slovak Republic, 2014).

ACCELERATED AGEING OF SAMPLES IMITATING HISTORICAL PRINTS

Ondrej Panák, Hana Holická, Tomáš Halenkovič, Anna Sochová, Anna Pácaltová
 University of Pardubice, Faculty of Chemical Technology,
 Department of Graphic Arts and Photophysics, Pardubice, Czech Republic

Abstract: This paper deals with accelerated ageing of imitations of historical prints using black ink on paper substrates. Two types of black printing inks, containing bone black and lamp black, were used to print onto a handmade paper and machine made grand wood paper. The samples were exposed to heat, light and NO₂ pollutions. Infrared spectroscopy using ATR technique, VIS reflectance spectroscopy and electron microscopy were used in sample analyses.

Results shows, that the wet heat has the largest influence on colour changes of unprinted paper and paper imprinted by linseed oil, the clear binder. Infrared spectroscopy also shows changes in characteristic peaks of linseed oil, especially on samples exposed to wet heat.

Key words: black ink, heat ageing, light ageing, NO₂ pollutions

1. INTRODUCTION

Ageing of prints is one of problematic issues considered in documents archiving. Aged documents are treated by several procedures, like disinfection and neutralization (Ďurovič, 2002). Artificial ageing serves as a tool to specify changes in materials due to atmospheric influences and conditions are normalized for paper samples (ISO 5630/1,1991; ISO 5630/2,1996; ISO 5630/6,2009; ISO 5630/1,1991). The restoration procedures are applied to the document, which contains the information imprinted on paper substrate. The changes of imprinted ink and its consequent treatment by restoration processes remains an open question. The aim of this paper is to investigate, how accelerated ageing influences the layer of black printing ink printed on paper substrates.

In the past, black printing inks used boiled linseed oil as a binder, and several types of black printing inks (Savage, 1832; Mills et al, 1994; Friend, 1917). Linseed oil is a triglyceride of higher unsaturated fatty acids, concretely linoleic acid (14–16 %), oleic acid (20–25 %) and linolenic acid (50–56%) and small percentage of other fatty acids (Lazzari et al, 1999, Bayrak 2010). The leading drying mechanism in linseed oil based inks is oxypolymerisation (Mills et al, 1994; Lazzari et al, 1999; Wicks, 2000). The first step of oxypolymerization is formation of free radical at methylene group, initialized by light or temperature. This radical reacts with air oxygen and forms labile peroxy radical. The reaction continues by forming hydroxyl peroxides, which are consequently falling apart forming free radicals. Propagation of the reaction continues by reaction of free radicals. By recombination of free radicals, C–C bond C–O–C bond or C–O–O–C bond is formed. The oxidative drying process is influenced by several factors like temperature, dryers, light and pigments (Bonaduce et al, 2011; Lazzari et al, 1999).

Widely used black pigments are carbon black particles, obtained by several techniques (Šalda, 1983; Stijnman, 2000). Lamp black pigments are obtained from the soot of burned fat plant oil, mineral oil or resin with limited presence of oxygen. They are deep in colour and have very strong covering power. Other black pigments can be produced by charring organic materials, like bones, grapevine and seeds. Bone black pigment contain except of carbon also some amount of ash. The main chemical components of ash are calcium phosphates, carbonates and small amount of sulfate and sulfide. (Buxbaum, 2006; Šalda, 1983). Inks made of bone black are deep in colour. Disadvantage of bone black pigment is their poor wetting and they might slow down the drying process.

2. METHODS

Two substrates were used in our investigation. The custom made handmade paper (grammage 120 g/m²) containing textile fibers, concretely 60 % of cotton and 40 % linen. The additive was 2 % of technical gelatin with alum (4 % of gelatin weight). Second paper was machine made of ground wood and pulp with grammage of 58,5g/m² and pH 5.3. Two printing inks were prepared. As a binder, polymerized linseed oil (by Umtonbarvy) was used. One ink contained 40 weight % of bone

black pigment „Beinschwarz 47100“ (by Kremer pigmente) and another contained 20 weight % of lampblack pigment „Flammruß: Lampenschwarz 47250“ (by Kremer pigmente).

All samples were printed on a laboratory print tester IGT C1 by using rubber printing cylinder. The ink transfer of all samples varied between 8,7–9,9 g/m². After the prints dried, they were stored in a room with temperature 23 °C and 50% relative humidity.

The prints with two black inks, with print of clear linseed oil and also unprinted paper were aged by four methods. The accelerated ageing by wet heat was done by using Sanyo Gallenkamp PLCchamber at 80 °C and 65% relative humidity for 30 days (720 hours). Ageing chamber Sanyo Gallenkamp OMT OVEN was used for accelerated ageing by dry heat at 105 °C for 12 days. Accelerated ageing by light was done using QSUN Xe-1-B chamber with xenon lamp and day filter for 120 hours at temperature 60 °C. Chamber CTS C +10/600-SG was used to age the samples in atmosphere with concentration of NO₂ pollutions about 25 ppm at temperature 23 °C and 50 % relative humidity for 360 hours.

Colorimetric parameters of aged samples were obtained by Gretag SpectroEye spectrometer with reflectance measurement from 380 to 730 nm with 10 nm steps, using D50 standard source and two degree observer. Infrared spectra were scanned using Nicolet Avatar 320 spectrometer by ATR technique with ZnSe crystal in interval 4000–650 cm⁻¹ with 4 cm⁻¹ step and 64 scans. The Surface of aged samples was also analysed by SEM electron microscopy using Mira3 LMU device.

3. RESULTS AND DISCUSSION

3.1 Colorimetric analyses

Figure 1 shows colour difference measured on all samples after ageing by four methods described above. All ageing methods caused large colour difference of ground wood paper without any applied layer. This difference increases by application of linseed oil. The handmade paper is very stable against light and NO₂ pollutions. However the ageing by wet heat caused large colour difference of paper its self. Samples with applied linseed oil show much larger increase in colour difference comparing to increase in colour difference on ground wood paper. Samples of printing ink containing bone black printed on ground wood paper show slightly higher colour difference, which can be attributed to lower colour density comparing to lamp black.

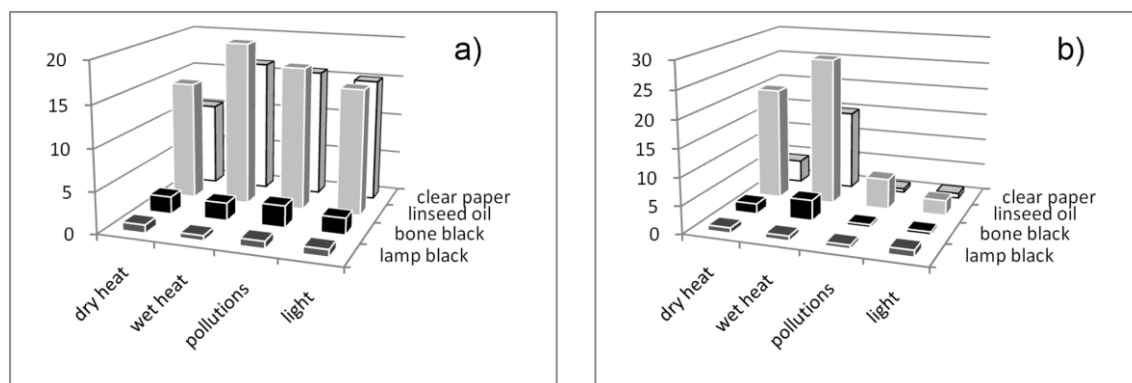


Figure 1: Colour differences of aged samples printed on ground wood paper (a) and handmade paper (b)

3.2 Infrared spectroscopy

The evaluation of infrared spectra was carried out by analysing characteristic groups, using literature (Derrick et al, 1999; Meilunas et al, 1990; Gullén et al, 2003). Analysed spectra show large signal from the substrate, and therefore only small intensities of the ink could be observed (see Figure 2 and 3). In spectra of ground wood papers weak vibrations at 3710 cm⁻¹ corresponding to kaolin vibrations can be observed. At 1512 cm⁻¹ a slightly stronger vibration can be observed and it is attributed to presence of lignin. On samples printed by linseed oil and printing inks a peak at 2920 cm⁻¹ is appearing and it can be attributed to asymmetric vibration of methylene groups of dried oil and peak at 2850 cm⁻¹ is characteristic to symmetric methylene vibration.

The peak observed at 1750–1700 cm^{-1} corresponds to ketone and ester vibrations according to [Derrick et al, 1999; Meilunas et al, 1990; Gullén et al, 2003].

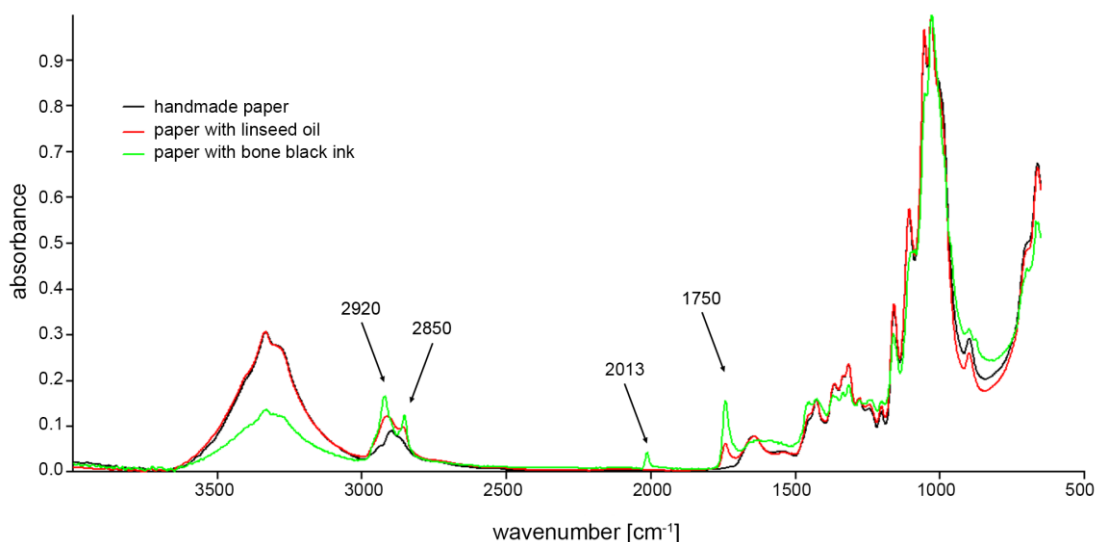


Figure 2: Infrared of not aged samples printed on handmade paper

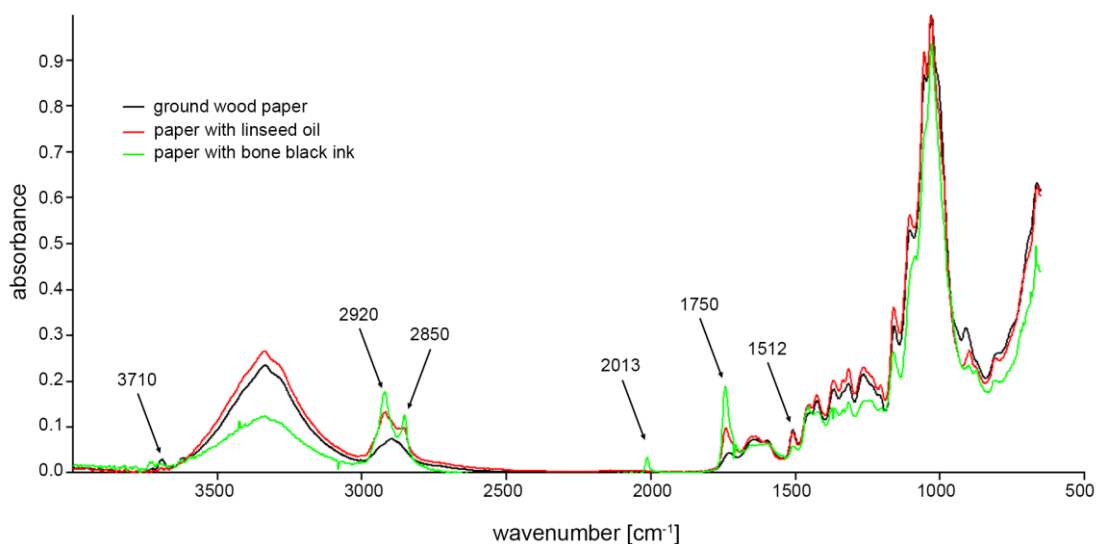


Figure 3: Infrared of not aged samples printed on ground wood paper

In case of imprinted samples the intensity of these peaks increase, which is due to larger concentration of ester groups of linseed oil. In case of samples imprinted by inks containing bone black vibrations at 2013 cm^{-1} are attributed according to [Derrick et al, 1999; Villa et al, 2007] to vibrations of hydroxyapatite. The analyses of aged processes show only changes in methylene and ester peaks of linseed oil exposed to heat ageing, especially wet heat. In samples aged by NO_2 pollutions a small peak at 1628 cm^{-1} appears, what can be attributed to some nitrate compound appearing on surface of the samples. Other significant changes in infrared spectra were not observed. Samples with lamp black could not be analysed due problematic signal, which is in agreement with [Villa et al, 2007].

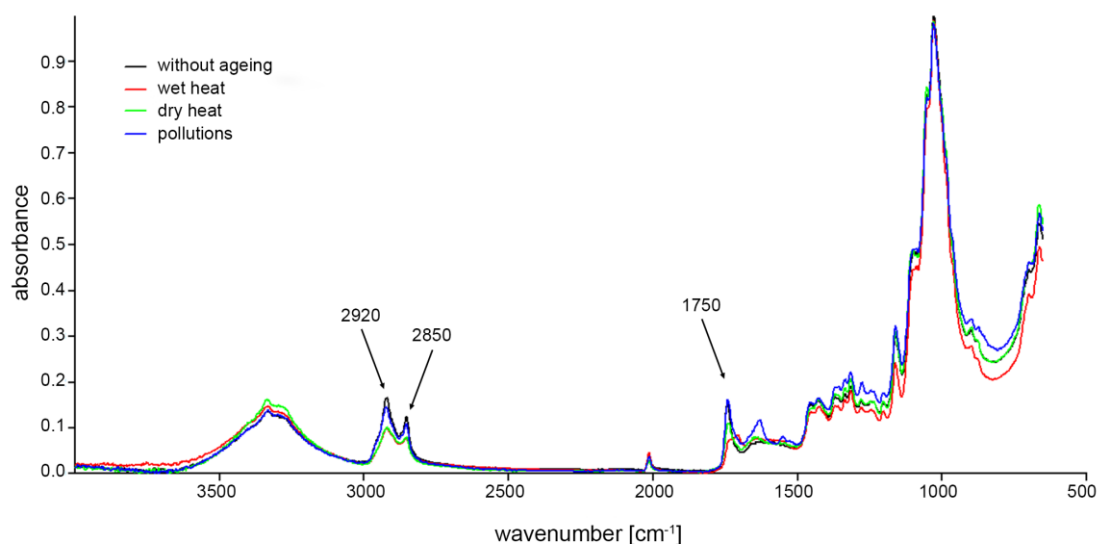


Figure 4: Infrared of aged samples of bone black ink imprinted on ground wood paper

3.3 Electron microscopy

The electron microscopy does not show any significant changes in surface of aged samples except of samples with lamp black. In Figure 5 and 6 the samples aged by wet and dry heat show a bit more porous surface.

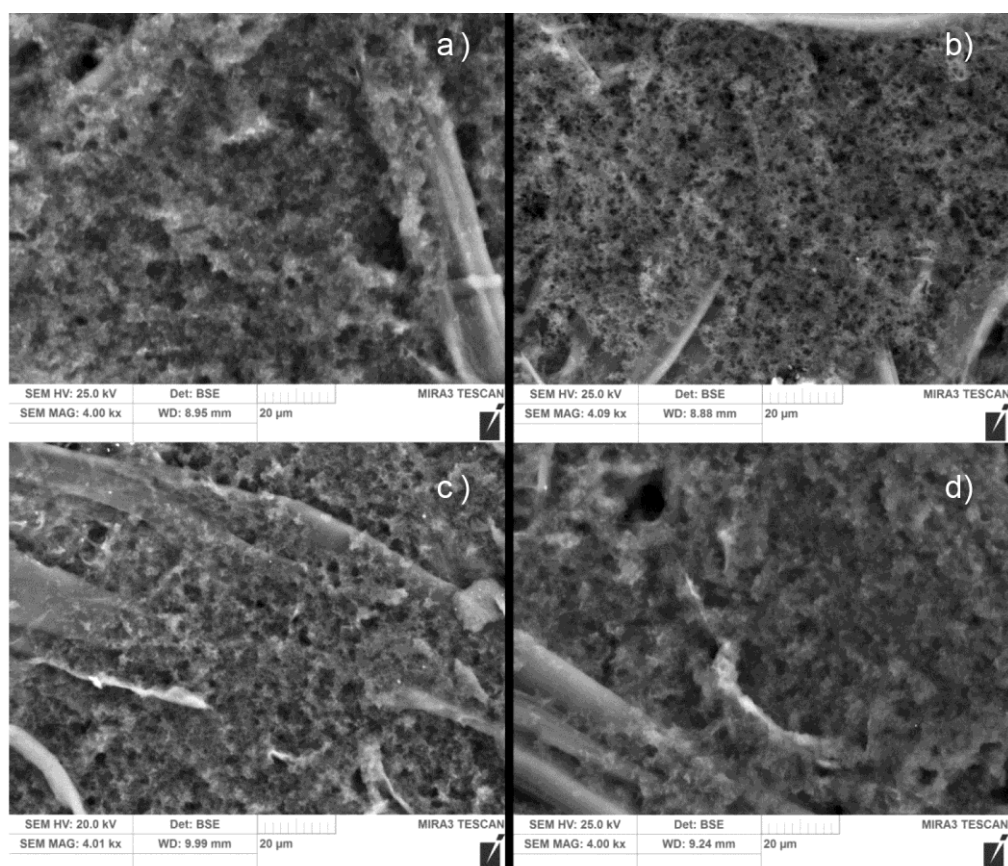


Figure 5: SEM images of lamp black ink imprinted on ground wood paper without ageing (a), wet heat (b), dry heat (c) and NO₂ pollutions (d)

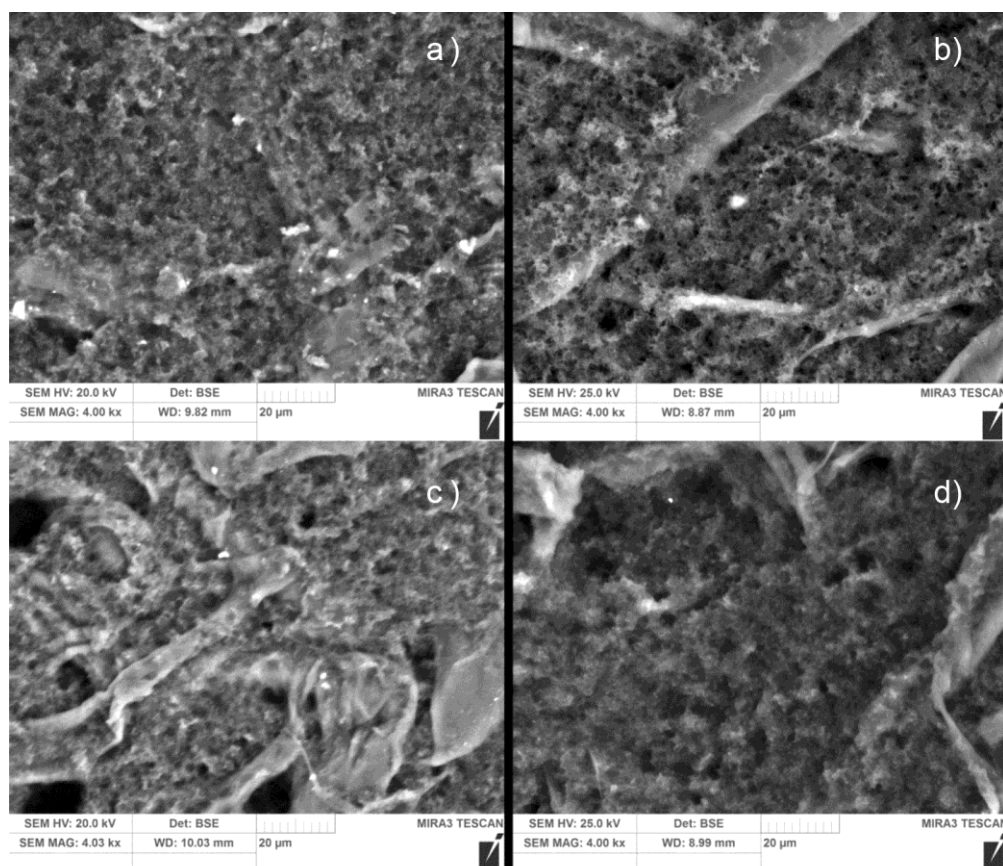


Figure 6: SEM images of lamp black ink imprinted on handmade paper without ageing (a), wet heat (b), dry heat (c) and NO₂ pollutions (d)

4. CONCLUSIONS

The ageing of black printing inks on paper substrates was performed. Ground wood paper its self is very sensitive to all methods of ageing. Handmade paper was resistant to light and NO₂ pollutions. The wet heat seemed to have the largest influence on appearance and also infrared spectra of samples with linseed oil and bone black. It seems, that Infrared spectroscopy is not sufficient to obtain reliable data. Other methods should be used to analyse prepared samples, like gas chromatography. Aged samples are now prepared for treatment by neutralization and disinfection procedures, to analyse the influence of these restoration techniques.

5. ACKNOWLEDGMENTS

Research was co-financed by the European Social Fund and the state budget of the Czech Republic within the project VEPA – Science for paper artefacts, Reg. No. CZ.1.07/2.3.00/20.0236.

6. REFERENCES

- [1] Bayrak, A., M. Kiralan, A. Ipek, N. Arslan, B. Cosge A. K. M. Khawar. Fatty Acid Compositions of Linseed (*Linum Usitatissimum* L.) Genotypes of Different Origin Cultivated in Turkey. *Biotechnology*. 2010, No. 24, Vol. 2], pp. 1836–1842. ISSN 1310–2818.
- [2] Bonaduce, Ilaria, Leslie Carlyle, Maria Perla Colombini, Celia Duce, Carlo Ferrari, Erika Ribecchini, Paola Selleri a Maria Rosaria Tiné. A multi-analytical approach to studying binding media in oil paintings: Characterisation of differently pre-treated linseed oil by De-ms, TG and GC/MS. 2011. DOI: 10.1007/s10973-011-1586-6.
- [3] Buxbaum, Gunter a Gerhard Pfaff. *Industrial Inorganic Pigments*. 3. vyd. John Wiley & Sons, 2006, pp. 163–184. ISBN 3527604030.

- [4] Derrick, Michele R., Dusan Stulik a James M. Landry. Infrared spectroscopy in conservation science. Los Angeles: Getty Conservation Institute, 1999, 235 p. ISBN 08-923-6469-6.
- [5] Ďurovič, Michal. Restaurování a konzervování archiválií a knih. 1. vyd. Praha: Paseka, 2002, 517 s. ISBN 80-718-5383-6.
- [6] Friend, John Newton. The Chemistry of Linseed Oil. London: Gurney & Jackson, 1917.
- [7] Guillén, María D., Ainhoa Ruiz, Nerea Cabo, Rosana Chirinos a Gloria Pascual. Characterization of sachá inchi (*Plukenetia volubilis* L.) oil by FTIR spectroscopy and ¹H NMR. Comparison with linseed oil. Journal of the American Oil Chemists Society. 2003, 80(8), 755-762. ISSN 0003-021X.
- [8] ISO 5630/1. Paper and board-accelerated ageing: Part 1: Dry heat treatment. 1991
- [9] ISO 5630/3. Paper and board-accelerated ageing: Part 3: Moist heat treatment at 80 °C and 65 relative humidity. 1996
- [10] ISO 5630/6. Paper and board-accelerated ageing: Part 6: Exposure to atmospheric pollution (nitrogen dioxide). 2009
- [11] ISO 5630/7. Paper and board-accelerated ageing: Part 7: Exposure to light. 2014
- [12] Lazzari, Massimo and Oscar Chiantore. Drying and oxidative degradation of linseed oil. Polymer Degradation and Stability. 1999, No. 65, pp. 303-313.
- [13] Meilunas, Raymond J., James G. Bentsen and Arthur Steinberg. Analysis of aged paint binders by FTIR spectroscopy. Studies in conservation. 1990, 35(1), pp. 33-51. ISSN 0039-3630.
- [14] Mills, John S. a Raymond White. The organic chemistry of museum objects. 2. vyd. Boston: Butterworth-Heinemann. 1994, 206 p. ISBN 07-506-1693-8.
- [15] Šalda, Jaroslav. Od rukopisu ke knize a časopisu. 4. vyd. Praha: Nakladatelství technické literatury, 1983. ISBN 04-606-83.
- [16] Savage, William. On the preparation of printing ink: both black and coloured. London: Samuel Bentley, 1832, 185 p.
- [17] Stijnman, Ad. Oil-based printing ink on paper: Bleeding, browning, blanching and peroxides. Papier Restaurierung. 2000, No. 1, pp. 61-68.
- [18] Villa, Anna, Núria Ferrer a Jose F. Garcia. Chemical composition of contemporary black printing inks based on infrared spectroscopy: Basic information for the characterization and discrimination of artistic prints. Analytica Chimica Acta. 2007, 591(1), pp. 97-105. ISSN 0003-2670.
- [19] Wicks JR., Zeno W. Drying Oils. Kirk-Othmer Encyclopedia of Chemical Technology. 2000, No. 9, pp.142-155

INFLUENCE OF PARAMETERS OF DIGITAL PRINTING ON THERMO- PHYSIOLOGICAL PROPERTIES OF TEXTILE MATERIALS

Mladen Stančić¹, Dragana Grujić², Jelka Geršak³

¹ University of Banja Luka, Faculty of Technology,
Graphic engineering, Banja Luka, Bosnia and Herzegovina

² University of Banja Luka, Faculty of Technology,
Textile engineering, Banja Luka, Bosnia and Herzegovina

³ University of Maribor, Faculty of Mechanical Engineering,
Textile Materials and Design, Maribor, Slovenia

Abstract: Manufacturers today are using different textile materials for making clothes. Those materials can look the same, but in the same time, they can have significantly different characteristics. The material and its characteristics should allow clothes making that will meet the aesthetic, ergonomic and physiological requirements. Increase of the aesthetic value of clothing, nowadays, is often carried out with the process of printing. This paper presents the influence of parameters of digital printing, such as the number of passes and tone value, on thermo-physiological properties of different material composition. For research were used fabric made of 100% cotton fiber (100% CO), 100% polyester fibers (100% PES) and their mixture (50% CO / 50% PES). The influence of printing parameters on thermo-physiological properties of the material is evaluated through thermal resistance of textiles and textile resistance to the flow of water vapor as a parameter of a thermo-physiological comfort of clothing. The results showed that in addition to the process and printing parameters, a material composition also has a major influence on thermo-physiological properties of textile materials.

Key words: digital printing, textile materials, material composition, thermal resistance of textiles, textile resistance to the flow of water vapor

1. INTRODUCTION

The development of technology every day poses new demands on manufacturers. Rise of life standards demand increasingly high criteria for products that meet the basic needs of man. To that end, manufacturers are investing more and more resources in developing products adapted to the needs of men and which meet the personal needs of every individual (Grujić, 2010). So the clothes today should satisfy three functions: aesthetic, ergonomic and physiological. (Mechels, 1992). Increase of the aesthetic value of textile materials, and therefore the clothes, is more often carried out with printing process. Textile printing can be best described as the art and science of decorating a fabric with a colorful pattern or design (Tippett, 2002). Some estimates indicate that more than 27 billion m² of textile material substrates are printed every year (Provost, 2009). Also, it is considered that printing of textile materials has annual growth of 2% (Momin, 2008). Printing on the textile substrates can be achieved using variety of different techniques and machines (Novaković et al, 2010). The most suitable printing techniques for textile substrates are: screen printing, digital ink-jet printing and thermal transfer printing (Stančić et al, 2014).

In recent years, in the technique of digital ink-jet printing have been implemented numerous innovations, enabling digital printing of textile materials. This technique of textile materials printing has an annual growth of 1%. The efficacy of ink jet printing as a flexible ink transfer method is primarily based on its cost and time saving for small print runs (Kašiković et al, 2012). What more, this printing technique enables achieving better visual effects, far more flexible formats, besides with the repeated printing process better reproducibility and consistent quality is achieved (Owen, 2003; Xue et al, 2006). The world of textile printing is rapidly changing and digital textile printing technology supports the industrial trends: integration in a digital workflow, qualitative and short runs, fast turnaround orders, reduced stock risks, exclusive, unique designs and personalized textile, demanding an ability to supply rapidly (Onar Çatal et al, 2012). Also, digital printing technologies are considerably cleaner than conventional ways of applying color to textiles (Tyler, 2005). In addition to the aesthetic, clothing needs to fulfill the ergonomic and physiological requirements. Modern consumers are interested in clothing that not only looks good but also feels great. Studies have shown the importance of clothing comfort in deciding customer

satisfaction (Vivekanadan et al, 2011). During clothes wearing, heat and humidity produced by the body stop as layers of air before passing into the environment, resulting in characteristic microclimate between the skin and clothing, which is defined as a feeling of comfort (Yoo et al, 2000; Grujic et al, 2010). Essentially, clothing prevents evaporation of sweat from the skin surface and often when wearing clothes this insufficient evaporation creates a sense of discomfort (Kim, 1999). Comfort in clothes is the result of a balanced process of heat transfer between the body, clothes and environment and its dependent on the specific thermal characteristics of clothes, which represent ability of clothes to transfer heat and moisture from the surface of the human body to the environment. Comfort in wearing clothes is dependent on climatic conditions, physical activity of people, clothes cut, the number of clothing layers, as well as the properties of the material of which it is made. Some of the material properties, such as air permeability, thermal conductivity and resistance to water vapor flow are very important to define the thermal comfort of clothes (Grujic, 2012).

Previous studies of the authors (Stancic et al, 2014) showed that the print parameters have a significant effect on warm or cold feeling and the heat retention ability of printed knitwear. It was also needed to expand this research on fabrics, as well as other parameters of thermo-physiological comfort. In order to further knowledge in this paper was analyzed the influence of print process, as a means of achieving aesthetic function of clothes, on the thermal characteristics of printed fabrics. To that end, it was analyzed dependence of thermal resistance and resistance to water vapor flow from the print parameters: the tone value and the different number of passes.

2. METHODS AND MATERIALS

Research of the effect of tone value and a different number of passes on thermal resistance and resistance to water vapor flow was performed on three types of textile knitwear, of approximately the same surface mass and surface structures but different material composition. Material characterization was done according to following parameters: material composition (ISO 1833), fabric weight (ISO 3801) and thread count (ISO 7211-2). Characteristics of the materials are presented in Table 1.

Table 1: Basic characteristics of fabrics used in research

Code of fabrics	Type of materials	Type of weaves	Raw material composition (%)	Mass per unit weight (g/m ²)	Density (cm ⁻³)	
					Warp	Weft
TCO	Fabric	Plain weave	Cotton 100 %	177.68	20	20
TPES	Fabric	Plain weave	Polyester 100 %	153.73	18	20
TCO/PES	Fabric	Plain weave	Cotton 50 % Polyester 50 %	166.32	18	20
Method			ISO 1833	ISO 3801	ISO 7211-2	

For this study it was created a special test image using Adobe Illustrator CS5 software. Test image contained 200 x 200 mm patches, with 10 %, 50 % and 100 % tone values of black process color. Samples were printed by ink-jet printing system Polyprint TexJet. Samples were printed in one, three and five passes, resolution 720 x 720 dpi. It was printed with water-based inks (Artisti Pigment Ink- P5400 Black). Because of a need for a low viscosity, inks contain demineralised water (51%), the appropriate pigment (1-5%), poly(oxyethylene) (14%), ethane-1,2-diol (12%), 1-methyl-2-pyrrolidone (15%), poly(1-hydroxyethylene) (3%), tris(2-hydroxyethyl)amine (1%), biocide (0.1%) and buffer (0.3%). Ink fixation was performed at a temperature of 130 °C for 120 seconds.

Examination of thermal resistance and resistance to water vapor flow of knitwear is performed with KES-F7 (Thermo Labo II) measuring device. Measuring device Thermo Labo II for analyzing thermal properties is consisted of next components (Figure 1.): Measuring body T, used for measuring warm or cold feeling; Measuring body BT, used for measuring constant thermal conductivity; Larger measuring body BT, used to measure heat loss, to determine the thermal resistance, resistance to the flow of water vapor and to determine the ability to retain heat;

Measuring body with water VT, used to maintain a constant temperature while measuring warm or cold feeling and the coefficient of thermal conductivity; and Wind column, where was constant air flow rate of 1 ms^{-1} at a constant air temperature of $20^\circ\text{C} \pm 2^\circ\text{C}$. The wind column measures heat loss i.e. heat flow, which is used for the determination of heat retention ability, heat resistance and resistance to the flow of water vapor.

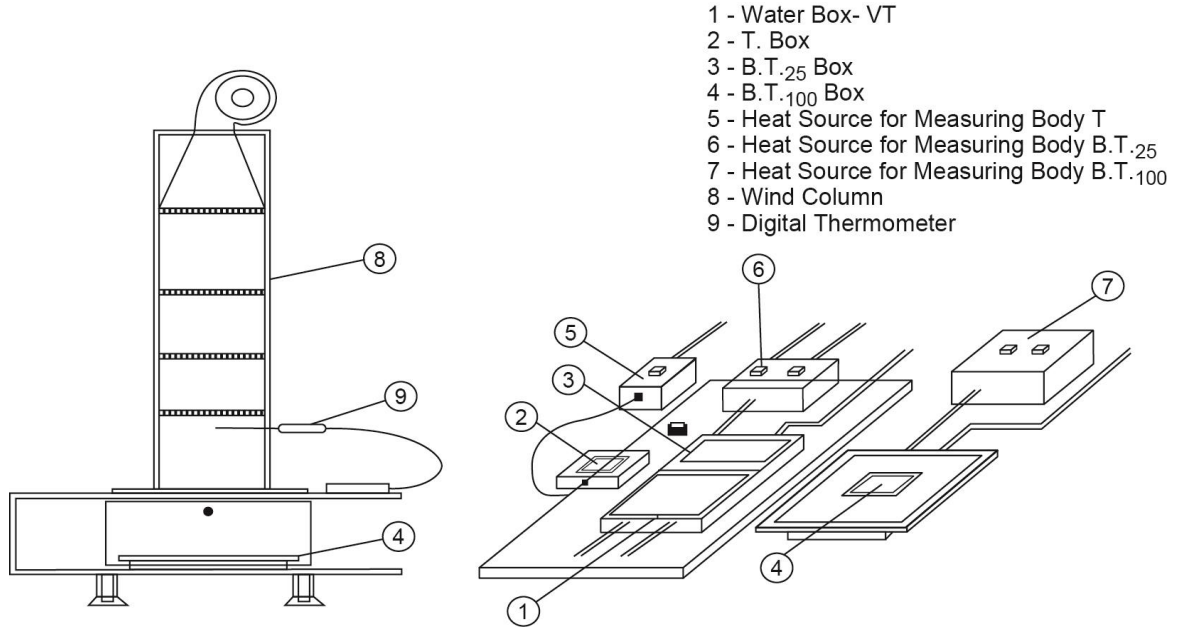


Figure 1: Components of measuring device KES-F7 Thermo Labo II

Thermal resistance of textile was determined according to the formula:

$$R_c = \frac{(T_s - T_a) \cdot A}{H_{ct}} \quad (1)$$

where:

R_c – thermal resistance of textile [$\text{m}^2\text{K/W}$],
 H_{ct} – dry heat transmission, which flow through material [W],
 A – BT board area [m^2],
 T_s –BT board temperature (skin temperature) [$^\circ\text{C}$],
 T_a – air temperature in wind column (air temperature) [$^\circ\text{C}$].

When the water evaporates, i.e. when a man sweats, sweat is conducted through clothes in the environment. Sweat evaporation rate will depend greatly from clothes as a barrier for the evaporation process. That evaporation rate affects the comfort that one feels when wearing clothes.

Thermal resistance of textiles to water vapor flow is determined according to the following formula:

$$R_e = \frac{(p_s - p_a) \cdot A}{H_{et}} \quad (2)$$

where:

R_e – resistance to water vapor flow [$\text{Pa m}^2/\text{W}$],
 H_{et} – vaporized thermal flow [W],
 A – BT board area [m^2],
 p_s – partial pressure on BT board area [Pa],
 p_a – partial air pressure in wind column [Pa].

3. RESULTS AND DISCUSSION

3.1 Thermal resistance analysis

Test results of thermal resistance of selected printed cotton fabrics are shown in Figure 2.

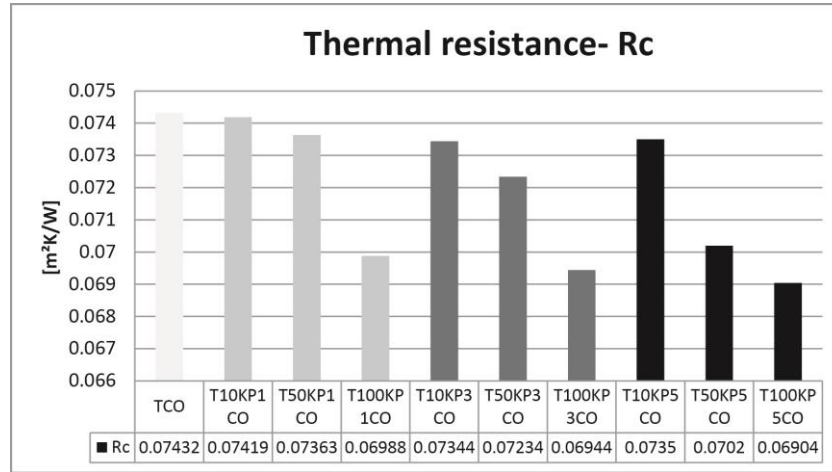


Figure 2: Thermal resistance of cotton fabrics subjected to the printing process (Note: T mark indicates fabrics, 10, 50 and 100 denote a print with 10%, 50% and 100% of tonal values, K is a black ink mark, P1, P3 and P5 are the marks of the print with 1, 3 and 5 passes, CO stands for cotton)

By analyzing the values of thermal resistance of printed cotton fabric (Figure 2) it can be noticed that with increasing the tonal values, there is decline in the value of thermal resistance. This trend holds true for the number of passes also, i.e. increasing number of passes leads to reduced values of thermal resistance. When comparing equal tonal value printed with different number of passes, it can be noted that increasing the number of passes also leads to a decline in the value of thermal resistance. From the above it can be concluded that increasing the amount of ink decreases the value of thermal resistance.

In addition, it can be noted that a sample of 10% tone value printed with five passes have almost identical value of the thermal resistance as the sample of 50% tone values printed with a single pass. This is consistent with previous finding, because these two samples have the approximately same amount of applied ink.

Test results of thermal resistance of selected printed polyester fabrics are shown in Figure 3.

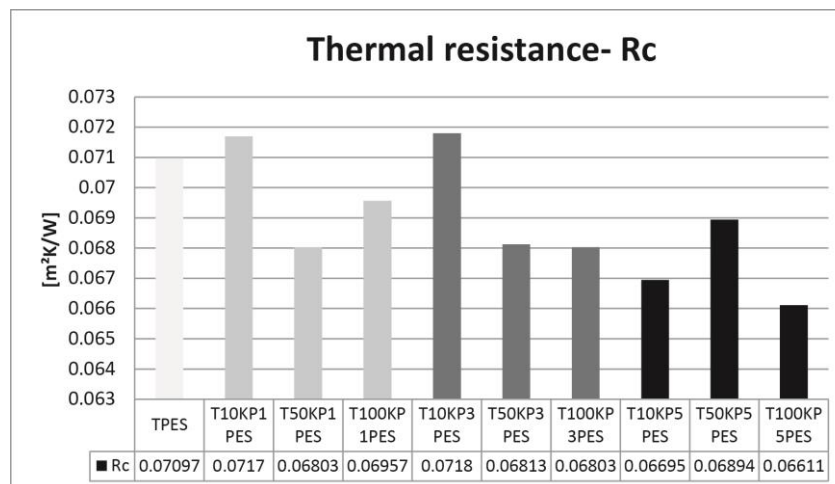


Figure 3: Thermal resistance of polyester fabrics subjected to the printing process (Note: T mark indicates fabrics, 10, 50 and 100 denote a print with 10%, 50% and 100% of tonal values, K is a black ink mark, P1, P3 and P5 are the marks of the print with 1, 3 and 5 passes, PES stands for polyester)

Observing samples printed with 10% tone value can be noticed that the values of thermal resistance are equal in the print with a single and three runs (Figure 3). Increasing number of passes to 5 shows a drop in the value of thermal resistance. For samples with 50% tonal value thermal resistance values are also equal in print with one and three passes. However, in this case, further increasing the number of passes leads to the growth in the value of thermal resistance. For samples with 100% tonal value increasing the number of passes leads to the decrease in the value of thermal resistance. Also, it should be noted that the smallest variation in relation to the unprinted sample are appearing in print of 10% tone value with one and three passes. Values of thermal resistance of printed fabrics from fiber mixtures of CO/PES are shown in Figure 4.

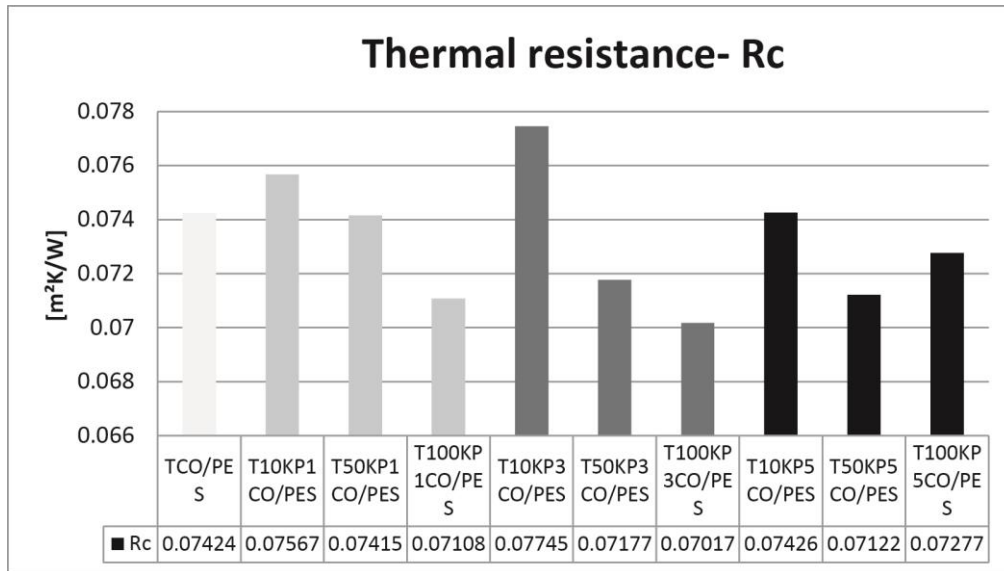


Figure 4: Thermal resistance of CO/PES fabrics subjected to the printing process (Note: T mark indicates fabrics, 10, 50 and 100 denote a print with 10%, 50% and 100% of tonal values, K is a black ink mark, P1, P3 and P5 are the marks of the print with 1, 3 and 5 passes, CO/PES stands for fiber mixture of cotton and polyester)

Analysis of the results of the thermal resistance of CO/PES fabric (Figure 4) shows that in print with single and three passes increasing of tonal values results in a decline in thermal resistance value. Print with five passes shows that the highest value was achieved on the sample printed with 10% tone value. The values of samples printed with 50% and 100% tone values are lower than with the sample printed with 10% tone values. However, the measured thermal resistance on sample printed with 50% tone values is lower in relation to the sample printed with 100% tone value. Also, it can be noticed that thermal resistance values on unprinted sample, on sample printed with 50% tone value with one pass and sample printed with 10% tone value with five passes are equal. Equal values of thermal resistance also have samples with 100% tone values printed with single pass and 50% tone value printed with five passes.

3.2 Water vapor flow resistance analysis

Test results of water vapor flow resistance of selected printed cotton fabrics are shown in Figure 5.

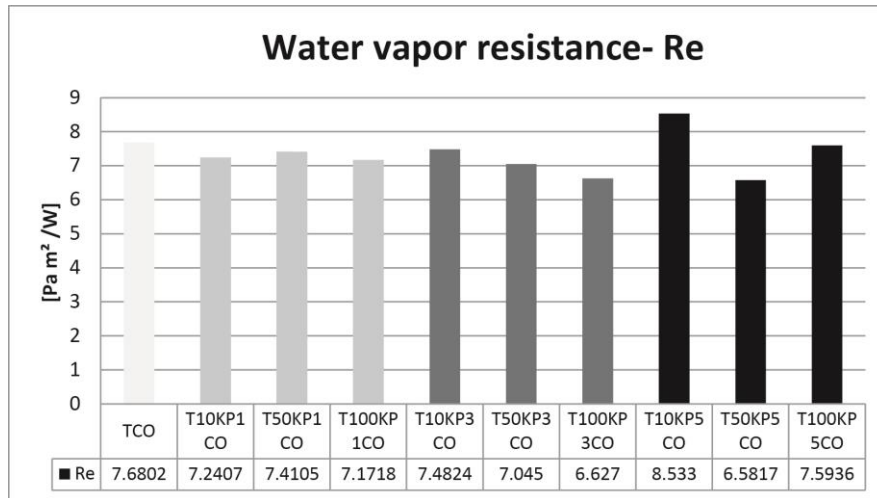


Figure 5: Water vapor flow resistance of cotton fabrics subjected to the printing process (Note: T mark indicates fabrics, 10, 50 and 100 denote a print with 10%, 50% and 100% of tonal values, K is a black ink mark, P1, P3 and P5 are the marks of the print with 1, 3 and 5 passes, CO stands for cotton)

From Figure 5 it can be noticed that the water vapor flow resistance values, on the samples with 10% tone value, increase with the increasing number of passes. Resistance to water vapor on sample printed with 50% tone value behaves the opposite, i.e. on these samples increasing the number of passes reduces the water vapor flow resistance values. For samples printed with 100% tone value the highest water vapor flow resistance values are achieved in print with five passes, while the lowest recorded values are in print with three passes. This may be associated with the measured value of the printed material thickness, which is also the lowest on a sample printed with three passes.

Test results of water vapor flow resistance of selected printed polyester fabrics are shown in Figure 6.

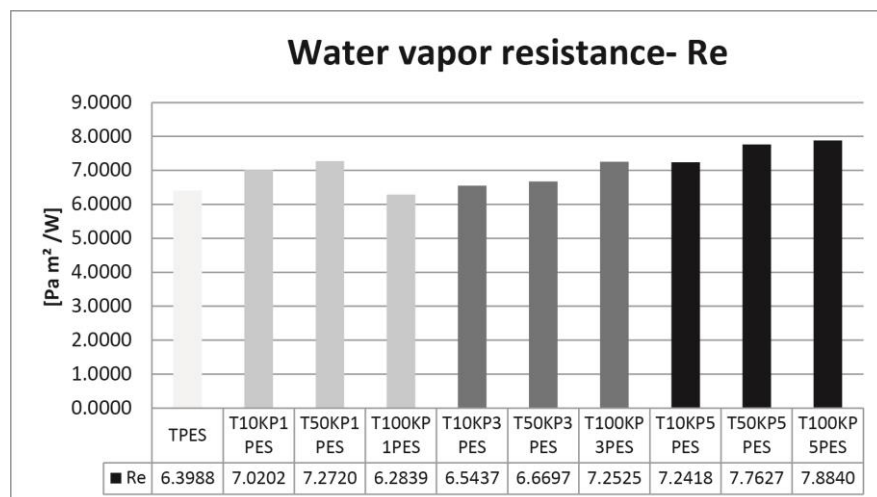


Figure 6: Water vapor flow resistance of polyester fabrics subjected to the printing process (Note: T mark indicates fabrics, 10, 50 and 100 denote a print with 10%, 50% and 100% of tonal values, K is a black ink mark, P1, P3 and P5 are the marks of the print with 1, 3 and 5 passes, PES stands for polyester)

By analyzing the results on Figure 6 it can be noticed that the water vapor flow resistance of the samples printed with 10% and 50% tone values are the highest in print with five passes, and the lowest in print with three passes. For samples printed with 100% tone value increasing the number of passes leads to the growth of water vapor flow resistance value.

Test results of water vapor flow resistance of selected printed fiber mixtures of CO/PES are shown in Figure 7.

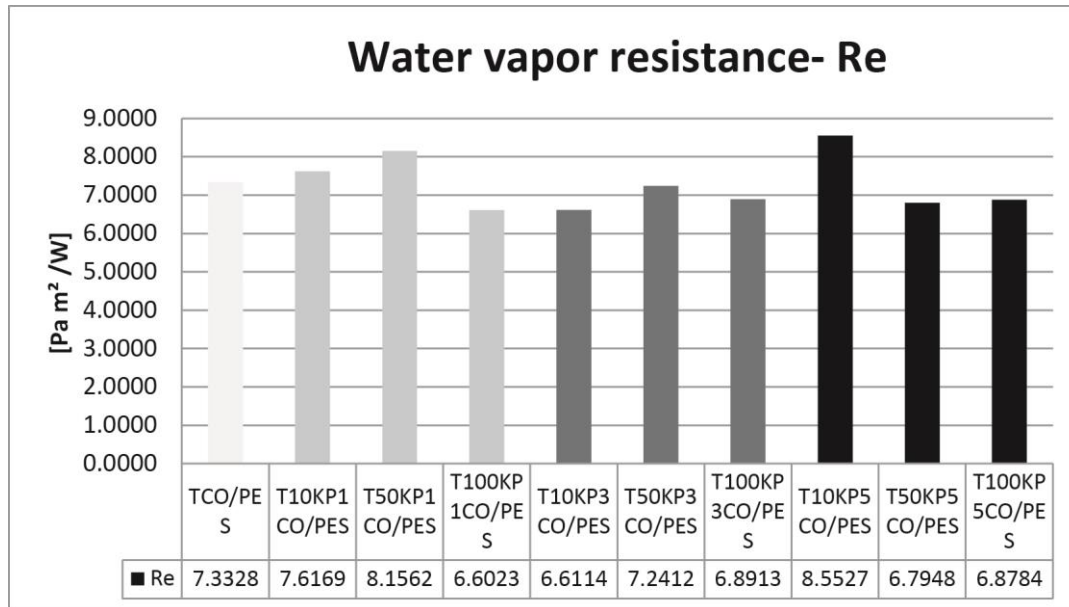


Figure 7: Water vapor flow resistance of CO/PES fabrics subjected to the printing process (Note: T mark indicates fabrics, 10, 50 and 100 denote a print with 10%, 50% and 100% of tonal values, K is a black ink mark, P1, P3 and P5 are the marks of the print with 1, 3 and 5 passes, CO/PES stands for fiber mixture of cotton and polyester)

Obtained water vapor flow resistance values of CO/PES fabrics (Figure 6) indicate that in print with 50% tone values increasing the number of passes decrease the water vapor flow resistance values. In the case of printing samples with 100% tone values the increasing of passes leads to the growth of water vapor resistance values. And at printing of samples with 10% tone values the highest water vapor flow resistance values are obtained on samples printed with five passes, and the lowest on samples printed with three passes.

4. CONCLUSION

Textile materials are increasingly being subjected to the process of printing. In this paper the impact of digital printing parameters on the thermal characteristics of printed fabrics were analyzed. For this purpose, the influence of the tonal value and different numbers of passes in print on thermal resistance and water vapor flow resistance for three types of fabrics.

While observing the CO and CO/PES fabrics it can be noticed that by increasing of tone value as well as the increasing of number of passes leads to decrease in thermal resistance values. At PES fabrics change of tone values and the number of passes also leads to changes in thermal resistance. In fact, in the light and dark tones increasing the number of passes leads to lower values of thermal resistance, while in the midtones increasing the number of passes leads to the growth of thermal resistance value. On this basis, it can be concluded that the change in thermal resistance can be influenced by changing the tonal value or number of passes, as digital printing parameters. Thus, the parameters of the press should be adjusted according to the later purpose of the printed textile materials, in order to obtain lower or higher thermal resistance values.

Analysis of water vapor flow resistance indicates that this parameter also may be affected with the print parameters. The study noted that in light tones of CO fabrics increasing the number of passes leads to growth of resistance values, and in midtones decrease the value of water vapor flow resistance. The highest values of the dark tones are achieved in print with five passes, and

the lowest in print with three passes. When you print dark tones of the PES fabric increase of the number of passes leads to the growth of the water vapor flow resistance. In medium and light tones highest values are also achieved in print with five passes. And the lowest values were obtained in print with three passes. For fabrics made from fabric mixture of cotton and polyester fibers has been noticed that in printing of midtones increasing the number of passes leads to a drop of the water vapor flow resistance. At the same time, in print of dark tones increasing the number of passes leads to the growth of water vapor flow resistance value. At print of light tones values of water vapor flow resistance behaved in the same way as the PES fabric.

Summarizing the results obtained, it can be concluded that the print parameters have a significant impact on thermal resistance and water vapor flow resistance of printed fabric. In addition to the print parameters significant affect also have their material characteristics. In order to further knowledge, the research carried out should be taken also on other process colors. Also, research is needed to expand to other parameters of materials thermal properties, which are important for thermo-physiological comfort of clothing.

5. ACKNOWLEDGEMENTS

The research is supported by bilateral project between the Republic of Srpska and Republic of Slovenia "Research of effects of high performance textiles on comfort of sportswear" and project CEEPUS CIII-SI-0217-07-1314 „Ars-Techne: Design and Development of Multifunctional Products“.

6. REFERENCES

- [1] Grujić, D.: "Dependency of a temperature and a skin moisture from the thermal features of a sports clothing materials", Proceedings of 4rd scientific-professional conference Textile science and economy, November 06-07th, 2012, Zrenjanin, Serbia, pages 139-145.
- [2] Grujić, D.: "Influence of fabric properties of thermal physiological comfort of clothing", PhD thesis, Maribor, Faculty of Mechanical Engineering, University of Maribor, 2010.
- [3] Kašiković, N., Novaković, D., Karlović, I., Vladić, G.: "Influence of ink layers on the quality of ink jet printed textile materials", *Tekstil ve Konfeksiyon* 22 (2), 115-124, 2012.
- [4] Kim J.O.: "Dynamic Moisture Vapour Transfer Through Textiles, Part III: Effect of Film Characteristics on Microclimate Moisture and Temperature Changes", *Textile Research Journal* 69 (3), 193-202, 1999.
- [5] Mecheels, J.: "Anforderungsprofile für funktionsgerechte Bekleidung", Aachen, DWI-Deutschen Wollforschungsinstitut, 1992.
- [6] Momin, N. H.: "Chitosan and improved pigment ink jet printing on textiles", PhD thesis, Melbourne, RMIT University, 2009.
- [7] Novaković D., Kašiković N., Vladić G.: "Integrating internet application in to the workflow for costumisation of textile products", Proceedings of International Joint Conference on Environmental and Light Industry Technologies, November 18-19th, 2010, Budapest, Hungary, pages 471-476.
- [8] OnarÇatal, D., Özgüney, A. T., Akçakoca Kumbasar, E. P.: "The influence of rheological properties of the pretreatment thickeners on ink-jet printing quality", *Tekstil ve Konfeksiyon* 22 (4), 309-316, 2012.
- [9] Owen, P.: "Digital printing: A world of opportunity from design to production", *AATCC Review* 3 (9), 10-17, 2003.
- [10] Provost, J. (2009) Ink Jet Printing on Textiles. [Online] Available from: <http://provost-inkjet.com/resources/Ink+Jet+Printing+on+Textiles.pdf> (last request: 2014-09-10).
- [11] Stančić, M., Grujić, D., Novaković, D., Kašiković, N., Ružičić, B., Geršak, J.: "Dependence of warm or cold feeling and heat retention ability of knitwear from digital print parameters", *Journal of Graphic Engineering and Design* 5 (1), 25-32, 2014.
- [12] Stančić, M., Kašiković, N., Novaković, D., Dojčinović, I., Vladić, G., Dragić, M.: "The influence of washing treatment on screen printed textile substrates", *Tekstil ve Konfeksiyon* 24 (1), 96-104, 2014.
- [13] Tippet, B. G. (2002) The Evolution and Progression Of Digital Textile Printing. [Online] Available from: <http://www.brookstippett.com/docs/Print2002-BGT.pdf> (last request: 2014-09-08).
- [14] Tyler, D.J.: "Textile Digital Printing Technologies", *Textile Progress*, 37 (4), 1-65, 2005.

- [15] Vivekanadan, M.V., Sheela Raj, Sreenivasan, S., Nachane, R.P.: "Parameters affecting warm-cool feeling in cotton denim fabrics", *Indian Journal of Fibre & Textile Research* 36, 117-121, 2011.
- [16] Xue, C.H., Shi, M.M., Chen, H.Z.: "Preparation and application of nanoscale micro emulsion as binder for fabric inkjet printing", *Colloids and Surfaces A: Physicochemical. Eng. Aspects* 287 (1-3), 147-152, 2006.
- [17] Yoo, H.S.; Hu, Y.S., Kim, E.A.: "Effect of Heat and Moisture Transport in Fabrics and Garments Determined with a Vertical Plate Sweating Skin Model", *Textile Research Journal* 70 (6), 542-549, 2000.

THE INFLUENCE OF AGING ON OPTICAL, MECHANICAL AND THERMAL PROPERTIES OF PRINTED POLYLACTIDE FILMS

Nevena Vukić, Ivan Ristić, Borislav Simendić, Vesna Teofilović,
Jaroslava Budinski-Simendić

¹University of Novi Sad, Faculty of Technology, Novi Sad, Serbia

²Higher Technical School of Professional Education, Novi Sad, Serbia

Abstract: Due to the ecological concerns and difficulty in the treatment of packaging waste, biodegradable polymers can be good alternative to traditional polymer materials. Nowadays there are a lot of biodegradable materials on the market which have different properties and polylactide (PLA) is one of the most important. PLA as a thermoplastic aliphatic polyester derived from renewable resources (such as corn starch or sugarcane) is printable with all conventional printing techniques and has high optical density, good scratch resistance and high dyne level without surface treatment. These properties position this material as a replacement for traditional petroleum-based polymers used in the packaging industry. PLA contains a methyl group as polypropylene (PP) and has the same carbonyl function group as polyethylene terephthalate (PET), these similarities may contribute to similar printing properties. The main purpose of this study was to observe the influence of aging on optical, mechanical and thermal properties of printed polylactide films. PLA films were printed and subjected to aging. Tensile strength and elongation at break tests were measured on a universal tensile testing machine before and after aging. After mechanical properties testing, surface of printed PLA films and the breaking area of printed samples were analysed in order to determine the degree of cracking and disordering of surface morphology. The optical microscopy was used for this purpose. The interaction between printing ink and PLA film was observed by scratch resistance and abrasion resistance tests. Spectrophotometric parameters were measured to determine how the optical properties of PLA films change with time do. Thermal properties of aged and unaged printed PLA films were obtained using a differential scanning calorimeter (DSC).

Key words: polylactide, mechanical properties, thermal properties.

1. INTRODUCTION

The collection rate of the most commonly used traditional petroleum-based polymers in many developing and developed countries is very low, so they accumulate in the environment contaminating vital natural resources, including terrestrial, freshwater and marine habitats (Thompson et al, 2009). Also, traditional petroleum-based polymers are produced from the deficit fossil raw materials. Biodegradable polymers can be the most suitable alternatives for many applications. Polylactide (PLA), as a synthetic biopolymer derived from agricultural feedstock, is a promising material because of its mechanical and biodegradable properties (Krochta et al, 1996, Datta et al, 1995). Polylactide has the potential to replace some of the most commonly used polymer films used in the packaging industry, but it is long and difficult process to introduce new material to already positioned market.

Polylactide films can be rigid and transparent with good barrier properties to aromas and the permeability to carbon dioxide, oxygen and water vapour. Some of the most common polymer films which are used nowadays in the food industry, may be replaced with this biodegradable polymer material. Because of many advantages, PLA is a promising candidate for the fabrication of biaxial oriented films, thermoformed containers and stretch-blown bottles. Printability and runnability of PLA films are comparable to standard petroleum based flexible packaging materials. Ink layers applied over short lifetime polymer packaging, after the curing process, have various functions: making the product more attractive to the consumer, supplying information about the product contents, and also offering protection against physical and chemical agents (Marcelo et al, 2014). Once the solid ink layer is obtained, the cross-linked network cannot be easily undone, offering considerably high chemical and physical resistance and stability (Roy et al, 2010). But, aging is a natural phenomenon that affects the properties of the amorphous phase in glassy or partly glassy polymers. The effect of aging could be detected in the temperature interval around glass transition temperature (T_g) and can be noticed by shrinkage of specific

volume, decreases in specific enthalpy and entropy, and a decrease in molecular mobility. These effects are associated with decrease of free volume, which controls the mobility of large segments of the polymer chains and affects the mechanical properties of polymers [McGonigle et al, 2000]. The importance of the quality of the material and its properties and the quality of printing may change with storage time. The changes in materials mostly depend on temperature, humidity, and light, especially in the UV region, as well as the action of gases. The aim of this study was to characterize the optical, mechanical and thermal properties and to report the effect of aging on printed PLA films made by the screen printing technique. The samples were aged in fluctuating relative humidity and temperature conditions that simulates the uncontrolled warehouse and usage situations.

2. MATERIALS AND METHODS

For this investigation screen printing ink *Polyplast PY206 deep blue* was used, producer Sericol (UK). This ink is dried by solvent evaporation and tack-free time at room temperature is achieved in 8-15 min. *Polyplast PY206 deep blue* is formulated free from lead and other heavy metals and is tested to comply with the EN71-3:1995 Toy Safety Standard and do not contain ozone depleting chemicals as described in the Montreal Convention. The dark blue color was selected for testing because of the assumption that the pigment would possess quite good resistance to ageing in comparison with yellow or magenta [Halínová et al, 2002].

PLA films were kindly supplied by Sidaplast (UK) and they were used as the polymer substrate for printing the ink. These films are made from NatureWorks Ingeo™ resin and their technical properties are shown in Table 1.

Table 1: Technical properties (laboratory averages) of PLA films*

Properties	Unit	Typical values	Test method
Thickness	μm	50	ASTM D 4321
Yield	m ² /kg	15.3	ASTM D 4321
Optical Density	O.D.	0.5	X-Rite 301
Gloss at 60°	Gloss units	30	ASTM D 523
Surface tension untreated	dynes/cm	38	ASTM D 5946
Coefficient of Friction COF (static)	-	0.4	ASTM D 1894

*Provisional technical data *EARTHFIRST@PLA TWL*

For the purpose of this study, screen printing technique was found out to be the most convenient for printing on PLA films. In comparison with other printing techniques, screen printing has the most varied range of applications, and it can be used for printing on a wide variety of substrates. Used screen printing mesh was density of 120 threads per centimetre.

The ageing of printed PLA samples was performed to simulate normal conditions of storage and usage of this material. Samples were stored at 5 to 40 °C and relative humidity fluctuating between 90 and 30%, from 2 to 365 days, with periodically exposure to the sunlight.

Tensile strength and elongation at break tests were measured on a universal tensile testing machine Instron 1122 according to the specifications of SRPS G. S2. 612 standard (ASTM D882) at 25 °C. The sample sizes were measured by micrometre, and the crosshead speed was set at 10 mm/min. The surface morphology of the aged and unaged printed PLA films and their breaking area were characterized with an optical microscope (Bresser, Germany). A difference between the samples was also analysed by scratch resistance and abrasion resistance tests.

Thermal properties of the samples were investigated by differential scanning calorimetry using DSC Q20 instrument (TA Instruments, USA). Hermetically sealed aluminium pans containing around 5 mg of samples were prepared. Samples were exposed to temperature cycles consisting of heating from room temperature to 180 °C at heating rate 10 °C min⁻¹, cooling down to the room temperature at a cooling rate of 20 °C min⁻¹, and reheating up to 180 °C. Data for melting temperature (T_m), crystallization temperature (T_c) and glass transition (T_g) were recorded and are reported. Spectrophotometric measurements were done with a Spectro Eye spectrophotometer (GretagMacbeth, Switzerland). Measurements of colorimetric values L^* , a^* , b^* of the aged and unaged printed PLA films were carried out with illuminant D65 for 2° observer. The reported $L^*a^*b^*$ coordinates are the average of measurements from three different positions for each sample.

3. RESULTS AND DISCUSSION

3.1 Mechanical properties

Mechanical characteristic measurements of aged and unaged printed PLA films were carried out at 25 °C, according to the specifications of standard. This involved standard tube for investigation and measuring of five samples for each data point. Tensile strength and elongation at break were calculated according to following equations:

$$\sigma_m = F_m / A_0 \quad (1)$$

$$\varepsilon, \% = (\Delta l / l_0) \times 100\% \quad (2)$$

where are: F_m – force measured at break, A_0 – cross section area (mm²), l_0 the original length of an extension sample, Δl change in length.

The results of mechanical testing of aged and unaged printed PLA films are shown in Table 2. From the obtained results it can be seen that ageing increased tensile strength of printed PLA films. This can be explained by decreasing of the printed film flexibility, due to the additional curing. Value of elongation at break of aged printed PLA films significantly decreased compared to the value before the ageing process, which indicates that printed PLA films becomes brittle, because of the ink structure disordering.

Table 2: Mechanical properties of unaged and aged printed PLA films

Sample name	Tensile Strength σ (MPa)	Elongation at break (%)
Printed PLA	25.42	154
Aged printed PLA	40.42	23

After mechanical testing, breaking area of the aged and unaged printed PLA films was analyzed by microscopy in order to determine the degree of cracking and disordering of surface morphology. As shown in the Figure 1a, after mechanical testing, unaged printed PLA film retains almost unchanged morphology. On the sample which was subjected to ageing, the high level of surface damage was observed, what was expected (Figure 1b). A visual assessment in the difference between scratch resistance and abrasion resistance of the aged and unaged samples was also observed, but the it was not significant.

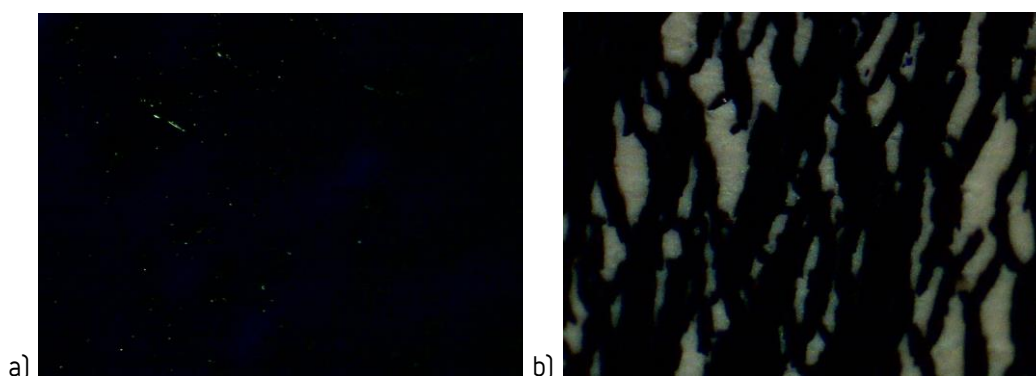


Figure 1: Surface morphology at the breaking area of the a) printed PLA film and b) aged printed PLA film

3.2 Thermal properties

From the results obtained from DSC analysis (Figure 2, Table 3) it can be seen that the glass transition temperature (T_g) and melting temperature (T_m) of printed polylactide films, did not significantly changed with a time, in the tested conditions. As expected, compared to the unaged

printed PLA, aged printed PLA films showed crystallization peak at a temperature of 94.19 °C, implying that the aging caused formation of crystalline domains in the printing ink.

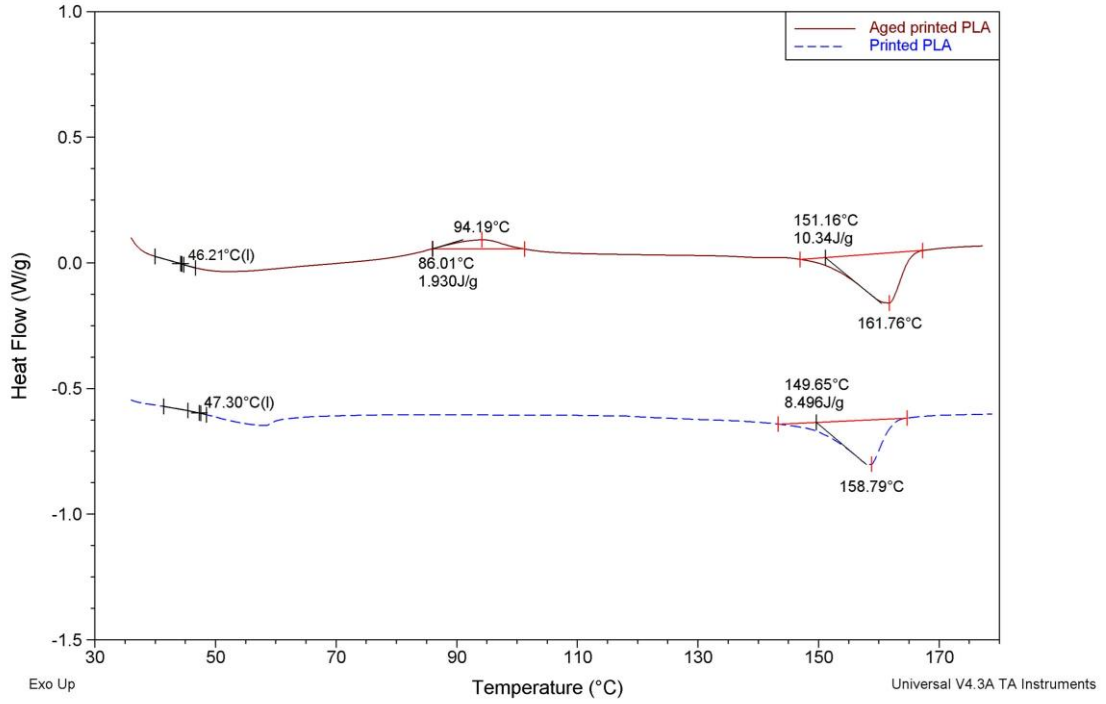


Figure 2: DSC curves of aged and unaged printed PLA films

Table 3: Thermal properties of the unaged and aged printed PLA films obtained by DSC analyses

Sample name	Glass transition temperature T_g (°C)	Crystallization temperature T_c (°C)	Melting temperature T_m (°C)
Printed PLA	47.30	-	158.79
Aged printed PLA	46.21	94.19	161.76

Normal conditions of storage and usage of printed PLA films, humidity between 90 and 30% and temperatures of 5 to 40 °C with periodically exposure to the sunlight, did not have an significant effect on the transition temperatures of aged printed PLA samples. This can be explained by PLA low water sorption values and with minor influence of printing ink on thermal properties of printed PLA films.

3.3 Evaluation of color difference

The aging can cause visible changes in the appearance and quality of printed PLA films. Color difference (ΔE) of aged and unaged printed polylactide films was calculated from formulas:

$$\Delta E^* = [\Delta L^{*2} + \Delta a^{*2} + \Delta b^{*2}]^{1/2} \quad (3)$$

$$\Delta L^* = L - L_0; \Delta a^* = a^* - a_0^*; \Delta b^* = b^* - b_0^* \quad (4)$$

where ΔL^* , Δa^* and Δb^* are the differences between parameter values of samples measured before and after ageing. L^* values indicate lightness (the higher the value indicates the lighter sample); positive or negative a^* values indicate a reddish or greener colour sample, respectively; and positive or negative b^* values indicate a yellowish and bluish colour sample, respectively.

Table 4 presents the average values for CIE $L^*a^*b^*$ coordinates, of unaged and aged printed PLA films.

Table 4. CIE $L^*a^*b^*$ colour coordinates of the unaged and aged printed PLA films (CIE76)

Sample name	CIE L^*	CIE a^*	CIE b^*
Printed PLA	8.07	6.80	-17.59
Aged printed PLA	11.22	12.39	-24.30

The aging causes significantly visible changes in the appearance of the printed PLA films. This is evidenced by quite high values of color difference ($\Delta E=9.28$). For aged printed PLA films the L^* and a^* average values increase with decreasing average values of b^* color coordinate. These differences in color of unaged and aged printed PLA films are mainly caused by the chemical composition of the printing ink and its resistance to the sunlight.

4. CONCLUSIONS

Aging may be factor that cause decreases in properties of printed biopolymer films. The aim of this paper was to point out importance of biopolymers and to provide valuable information for selection of material, prediction of product performance, and product quality. Under normal conditions of storage and usage of printed polylactide films, deterioration processes are slow; however, they eventually and inevitably still lead to the ageing effects. Moreover, exposure to light can cause fading and can shorten the use-life of printed polylactide films. In this paper polylactide films were printed by a screen printing technique and subjected to aging. Particular consideration was given to the mechanical and thermal stability of printed samples. Also optical properties on the printed PLA film surface were observed. From the results of mechanical testing it can be seen that ageing increased tensile strength of printed PLA films, which can be explained by decreasing of the printed film flexibility, due to the additional curing of printing ink. Value of elongation at break of aged printed polylactide films significantly decreased compared to the value before the ageing process. This can indicate that printed PLA films becomes brittle, because of the ink structure disordering, what was also confirmed by the optical microscopy, by observing the breaking area surface of the obtained printed PLA films. Aged printed PLA films showed the slightly lower glass transition temperature and the slightly higher melting temperature than the unaged PLA films. Also, aged printed PLA films showed crystallization peak, implying that the aging caused formation of crystalline domains in the printing ink. After aging the colour changes on the printed PLA films are significantly visible. The presented results are useful to answer the question of whether in the storage or usage conditions biodegradable printed materials will change their properties with time, which can be noticeable by the user. If we ignore change in colour of printed PLA films, which is probably due to the chemical composition of printing ink, we can conclude that aged printed polylactide films showed considerable stability.

5. ACKNOWLEDGEMENT

Authors wish to express the gratitude to the Ministry of Education, Science and Technological Development of Republic of Serbia, Project No. III 45022 for financial support.

6. REFERENCES

- [1] Datta R., Tsai S., Bonsignore P., Moon S., and Frank J.R., FEMS Microbiol. Rev., 16, 221 (1995).
- [2] Halínová B. et al., Dyes and Pigments, 54, 173-188 (2002).
- [3] Krochta J.M. and De Mulder-Johnston C.L.C., "Biodegradable polymers from agricultural products," in Agricultural Materials as Renewable Resources: Nonfood and Industrial Applications, G. Fuller, K.A. Mckeon, and D.D. Bill, Eds., Washington, DC, 120 (1996).
- [4] Marcelo A.G. Bardi, Mara M.L. Munhoz, Rafael A. Auras, Luci D.B. Machado, Assessment of UV exposure and aerobic biodegradation of poly(butylene adipate-co-terephthalate)/starch blend films coated with radiation-curable print inks containing degradation-promoting additives, Industrial Crops and Products, 60, 326-334 (2014).
- [5] McGonigle E.A., Daly J.H., Jenkins S.D., Liggat J.J., and Pethrick R.A., Macromolecules, 33, 480 (2000).
- [6] Thompson, R.C., Moore, C.J., vom Saal, F.S., Swan, S.H., Plastics, the environment and human health: current consensus and future trends. Phil. Trans. R. Soc. B 364, 2153-2156 (2009).

Applied measurement methods in graphic arts

THE IDENTIFICATION OF HISTORICAL PHOTOGRAPHIC PROCESSES BY OPTICAL MICROSCOPY AND FTIR SPECTROSCOPY

Zuzana Machatová, Viera Jančovičová, Ľubica Ozimýová

*Slovak University of Technology in Bratislava, Faculty of Chemical and Food Technology,
Department of Graphic Arts Technology and Applied Photochemistry,
Bratislava, Slovak Republic*

Abstract: Situated on the crossroad of various artistic and technical interests, photography represents an important part of everyday life for over 160 years. Its importance is accentuated by documentary character of the records, which increases steeply with time. To preserve the recorded information for the future, detailed knowledge of constitution of the numerous photographic processes is needed. The relevance of this topic is further emphasized by inherent quality of all photographic materials – low photostability.

The aim of this work is to study spectral characteristics of original historical salted paper, albumen silver print, cyanotype and silver gelatin photographs from reference collection of the Academy of Fine Arts and Design in Bratislava by means of Fourier transform infrared spectroscopy and optical microscopy. Features of the original photographs were compared to the properties of model system samples, prepared according to instructions in historical photographic literature, a good correlation in infrared spectra between original and model samples was found. Although the diversity of photographic processes prevents from postulating an exact microscopy-based identification method, optical microscopy represents rapid, informative and low-cost method for basic categorization and evaluation of the state of preservation.

Key words: historical photography, infrared spectroscopy, identification

1. INTRODUCTION

The first 30 years of photographic history were a period of intense exploration of the possibilities of photographic materials. The discoveries, improvements and mystifications, were printed in journals and freely circulated. Taken into account the amount of recipes published, the overall experimentation must have been great. In the 20th century, as photography became fully commercialized and set firmly on the silver gelatin technology, further technical development, including additives influencing the stability has been held as commercial secret. However, both approaches mentioned introduce the conservator concerned, as well as the conservation scientist into a difficult situation. Proper identification of photographic processes is a determining factor for appropriate deposition, housing, exhibition and treatment of historic photographs. Furthermore, basic identification is necessary for understanding historical and artistic values of individual photographs, as well as for collection cataloguing associated with digitization project. As photographic collections are usually large and diversified, rapid and sufficiently accurate identification methods should be used.

In this study we present a brief summary of identification keys of some photographic processes by means of digital microscopy and Fourier transformed infrared spectroscopy (FTIR) in their historic context.

2. EXPERIMENT

2.1 Instrumentation

For FTIR measurements FTIR spectrophotometer EXCALIBUR Series DIGILAB USA, FTS 3000 MX with ATR adapter with single reflection diamond crystal (resolution 4 cm⁻¹; 30 scans; standard ATR correction of data) and evaluated using Origin (version 6.0) software. The spectra were measured at D_{max} , D_{min} and medium photographic density values, averaged from 3 measurements and normalized [0, 1]. For optical microscopy Olympus SZ61 with Olympus C7070 camera and Olympus KL 1500 LCD light source (correlated color temperature 3200 K) was used.

2.2 Photographic material

Any photographic material, in general, consists of photosensitive layer and supportive layer. In the processed photographic material, *image layer* is frequently specified as a layer constituting the image (silver clusters, pigment particles). The *support layer* was traditionally high quality paper, glass, metal sheets, textile, ceramic surfaces or jewelry. In 1880s, when machine coating of photographic materials became widespread, *substrate layer* was coated on paper support/ under light-sensitive layer to cover the rough paper surface and brighten the highlights. This layer was first featured for collodion and aristotype papers and is not to be found in earlier types of prints. However, as the concept can be traced to the year 1826, exceptions are theoretically possible. The substrate or baryta layer is formed by barium sulfate, barium chloride or hydroxide and gelatin, coated on preprocessed paper creating a chemically inert barrier. Dyes, pigments and since the 1955 optical brightening agents were added to the substrate layer (Messier, 2011).

As photographic technique progressed, more complex and multi layered materials were put on the market, in this study, we will focus on selected studio-produced or early commercially available positive photographic materials.

3. RESULTS AND DISCUSSION

3.1 Salted paper

The concept of salt print process had been investigated as early as in the beginning of the 19th century by Sir Thomas Wedgwood (1771–1805) and Joseph Nicéphore Niépce (1765–1833), but it was not until 1832–34 when Hercules Florence was able to permanently fix photographic images (Stulik, 2013a). In 1834–35 William Henry Fox Talbot (1800–1877) developed an advanced concept of photography on paper and a method of stabilization of prints using a solution of sodium chloride. Positive impact of sizing on paper surface structure and subsequently image quality was soon recognized and exploited. Among the very first materials to be tried were gelatin and albumen (1850), starch (1854) and whey. After 1855 most of the salted paper prints were processed with sizing step. This technical complication was swiftly capitalized by newly opening commercial sphere, dedicated manufacturers were selling pre-sized and sensitized papers.

In 1841 Talbot patented the *calotype* negative process, based on chemical development of the latent photographic image (Reilly, 1980, Stulik 2013a).

The salted paper prints are prepared by contact printing in a copy frame, thus belong to *printing out paper* (POP) family of photographic techniques. This principle, though simpler and advantageous in many ways, requires considerable higher levels of light energy – 10^5 times more, in some cases (Reilly, 1980). The colloidal silver particles are dispersed in organic matrices and their refraction indices influence the final color tonality of the print.

Under low magnification (20x – 50x) the mesh of paper fibers is clearly visible. Retouching of print as seen on *Figure 1* was a common practice and was usually coupled with retouching of the glass negative by etching or abrading the emulsion layer.



Figure 1: Microphotography of salted paper print (magnification 20x)

Spectra of salted paper (*Figure 2*) formulated in conventional manner are virtually identical to that of the paper support – cellulose. These the in-plane (COC) vibration at 895 cm^{-1} , vibrations of the primary and secondary alcohols at 1025 and 1050 cm^{-1} , the vibration glycosidic bond at 1105

cm^{-1} , [CC] vibration of the aromatic ring at 1155 cm^{-1} , the [CH] vibration at 1315 and 1429 cm^{-1} . Band at 1630 cm^{-1} corresponding to the signal of bound water may be present as well. Band at app. $1429\text{--}1430\text{ cm}^{-1}$ is generally assigned to CH_2 bending (C_6 position), band at $1457\text{--}1462\text{ cm}^{-1}$ corresponds to in-plane OH bending. Band at 1453 cm^{-1} refers to bending vibrations and CH_3 band in 2900 and 2850 cm^{-1} corresponding to symmetric and asymmetric vibrations CH_2 and CH_3 groups respectively. At 3330 cm^{-1} a broad band of OH stretching vibrations may be observed (Calvini et al 2002). In the Figure 3. an example of varnished salted paper print is given. Varnishing of photographs had been considered a suitable preventive conservation method, or a preparatory step before hand-coloring. Generally, the signal of the varnish layer usually obscures bands of the light-sensitive layer and makes the identification process more complex. In the spectra on the Figure 3, the bands at 2928 , 2916 and 2860 cm^{-1} which may be attributed to signal of [CH] functional groups of long aliphatic hydrocarbons together with band at 1705 cm^{-1} and [C-C] stretching bands at $1660\text{--}1600\text{ cm}^{-1}$ and [C-H] bending bands at $1480\text{--}1300$ is corresponding to the vibration of ester group indicate the presence of dammar varnish (Derrick 1999).

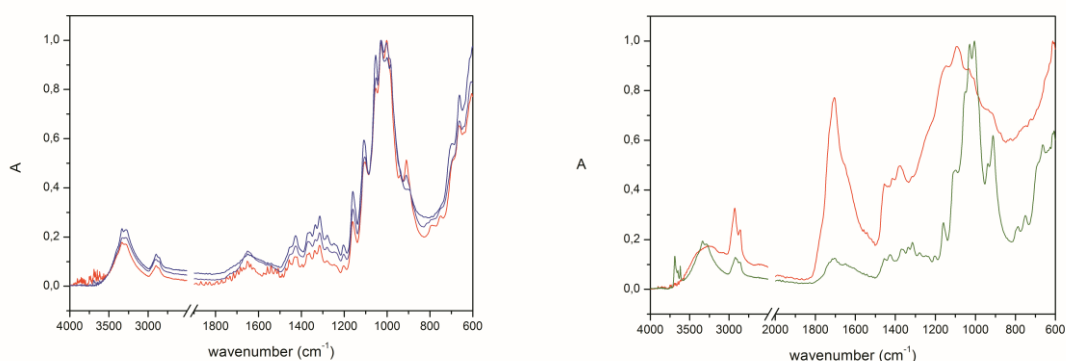


Figure 2: FTIR spectra of salted paper print (historical salted paper prints – violet and blue line, salted paper dated 2012 – red) and FTIR spectra of central (red) and marginal part (green line) of varnished salted paper print. The marginal part, covered by mat, remained unvarnished.

3.2 Albumen print

The albumen silver print was a dominant positive photographic process of the 19th century. During this relatively long period, starting from 1850s and culminating in 1890s (with some echoes till the 1920s) the albumen print underwent several modifications.

Frist published notice about using albumen in photography comes from *The Athenaeum* journal [11.5.1839] by anonymous author. Several formulas employing albumen were published subsequently, however, Louis Desiré Blaquant-Evrard (1850) is considered to be the inventor of the albumen silver print, including sodium chloride in his preparation. In spite of major improvement in speed and useful density range of the material, pure albumen formulations (free of halogen salts) were reinvented several times after that (1865 Schultner, 1866 Schnauss). Their main advantage was to be lower concentration of silver nitrate needed and thus lower price. Special class of the early albumen silver prints are so called *albumenized prints*, where albumen was strongly diluted with water. The resulting print is matte, resembling optical properties of the salt prints. The characteristic signs of albumen silver print degradation are oxidation of image forming silver clusters, most readily visible on suppression of detail, and overall yellowing of albumen matrix. The yellowing is accelerated by the exposure to light and the discoloration is the most evident on the D_{\min} areas (Stulik, 2013b, Ali et al. 2012). Numerous articles in 19th century specialized literature prove this problem was prominent as early as in the golden age of albumen printing. (Stulik, 2013b). This situation created new possibilities for albumen paper manufacturers as new products, dye toned albumen papers, were put on the market. Probably a large percentage of the albumen paper produced 1870 – 1900 was toned by aniline dyes before coating.

The first tinted paper appeared of the market as soon as in the 1863 and was awarded immediate commercial success. Various shades of pink, cyan, purple became very popular for portrait photography. Light stability of these dyes was, however, lower than predicted and often faded when exposed to light during display.

Characteristic microscopic feature of albumen silver prints is cracking of the albumen layer (Figure 3). Cracking is caused by shrinking and curling of the drying albumen layer. It is exacerbated by humidity changes, as well as by contact with moisture during surface cleaning as well or even water immersion. This feature is common for the majority of albumen prints, with some exception of the later double coated and burnished prints. As no substrate layer is present, mesh of paper fibres is clearly visible under the image layer (Stulik, 2013b)



Figure 3: Original albumen print and microphotography showing cracking of light-sensitive layer

Gloss of the paper depends on concentration of albumen used, on the number of layers and of course, on the finishes of the print. The evolving aesthetic opinions and expectations strongly influenced the technology of photography. The earliest albumen prints (created before about 1870) were usually less glossy corresponding to qualities of well-established salt print, whereas in the period 1870 – 1890 were usually more glossy than older prints, because of use of burnishing and rolling machines. Using partially putrefied albumen or drying of papers at elevated temperature (to 50°C) resulted into glossier finish as well.

Varnishing was a frequent practice, though hardly affected the yellowing in a positive way. Collodion, as well as shellac, beeswax and resinous varnishes were widely used. All these substances have marked analytical signatures in infrared spectra and make the identification process more complex.

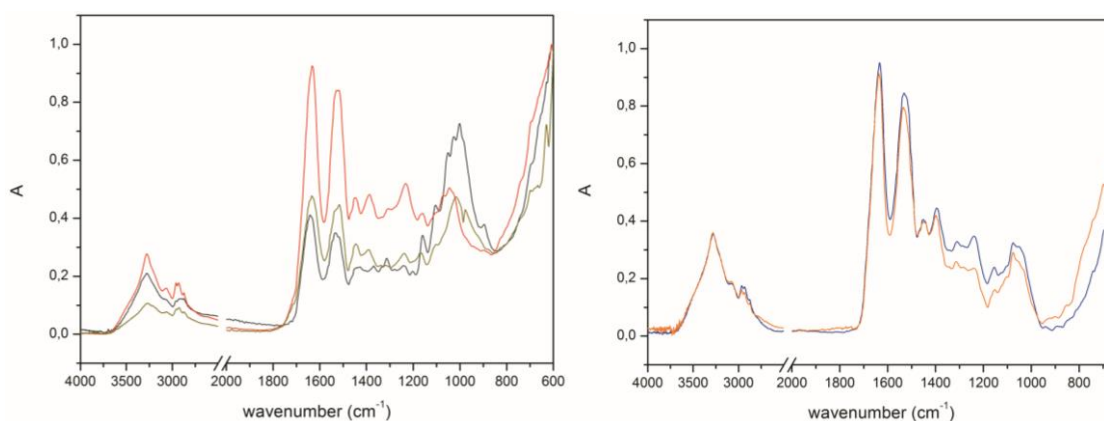


Figure 4: infrared spectra of hot pressed glossy double coated albumen silver print 1890s (red), albumen silver print from 1880s (yellow) and matte, probably single coated albumen silver print (grey). Right – infrared spectra of pure albumen and double coated modern albumen print (2012)

The most important structures of infrared spectra of the light sensitive layer of the amide I and II bands at 1636 ν (C = O) and 1534 cm^{-1} δ (CNH) respectively (Ali et al. 2012). The spectra of the silver gelatin layers are very similar, and special attention must be paid when distinguishing between these two techniques is in question (Figure 7). The spectra of the albumin layer on the paper support also containing bands of cellulose – 3340, 1160, 1100, 1060 and 1030 cm^{-1} (Figure 4).

3.3 Cyanotype

The cyanotype process was invented by the English astronomer and chemist J. F. W. Herschel (1792–1871). Easy to produce, low cost and fairly permanent, it soon became the first commercially successful non-silver printing process. In 1843 Anna Atkins produced her book on British algae, illustrated with cyanotype photograms, which was the first book with a body of photographic illustrations. Variations of the original formula involve different ratios of potassium ferricyanide and ferric ammonium citrate (green), the resulting image layer is formed by insoluble iron(III) hexacyanoferrate(II).

Under low magnification (20x – 50x) the mesh of paper fibers is clearly visible, with colloidal particles of iron(III) hexacyanoprussiate (II) distributed on the top of the fibres, and in the nodes of the paper mesh. If Pellets process was applied, glossy layer of gum Arabic may be observed.

The characteristic feature in the FT-IR spectra of cyanotype is the $\nu(\text{C}\equiv\text{N})$ band at 2070 cm^{-1} as well as absence of strong amide bands and bands of inorganic sulfates associated with substrate layer. Analytical signatures of cellulose ($1400\text{--}900\text{ cm}^{-1}$) when printed on cellulosic material (paper, fabric) as mentioned above, are present as well (Figure 5).

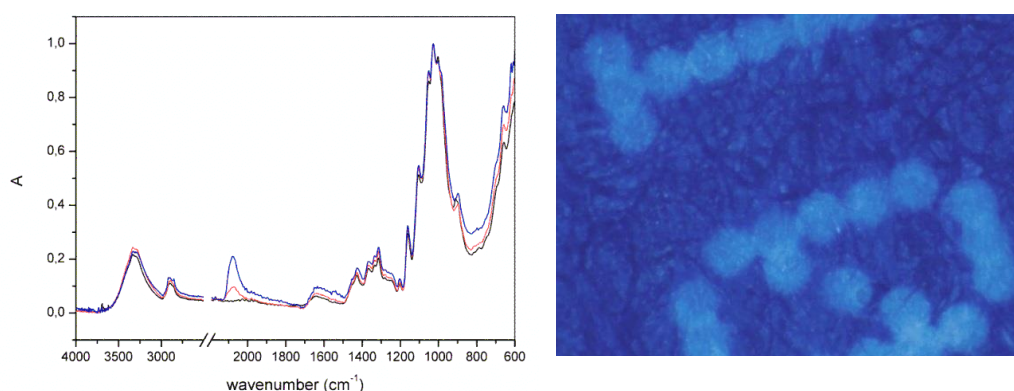


Figure 5: FTIR of the cyanotype print: D_{\max} (blue), D_{\min} (orange), verso (black) and microphotography thereof (magnification 20x)

Characteristic position of the band significantly reduces the probability of misinterpretation, however, there are other techniques that may show similar optical, and more importantly, also structural properties under the circumstances – eg. blue carbon or pigment prints, Woodburytypes and blue dyed silver gelatin DOP [Stulik, 2013c]. Comparison of infrared spectra of cyanotype (2013) and tinted DOP photography (1940) are shown in the Figure 6.

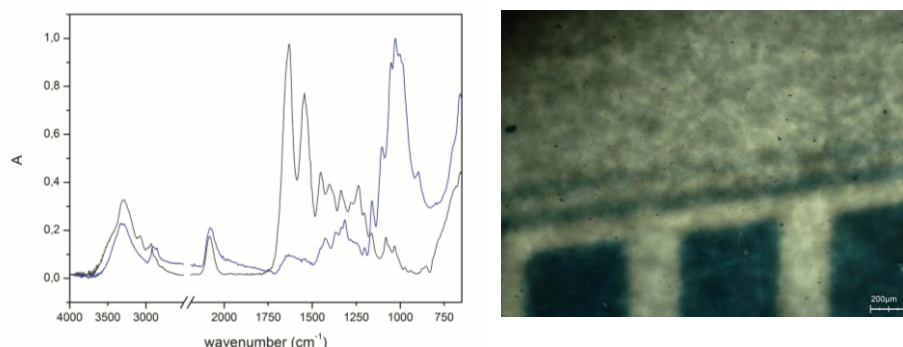


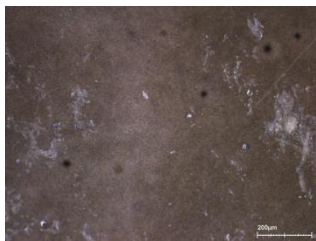

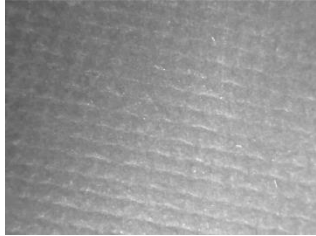
Figure 6: Cyanotype D_{\max} (blue) and silver-gelatin developed out paper dyed blue by toner containing cyano- group (grey) and microphotography of thereof showing clusters of dye dispersed in the image layer

Detection of weak signal of gum Arabic may indicate Pellet's cyanotype process had been used to prepare the studied print, signal of complex carbohydrates (starch), proteins (gelatin) or resins may refer to sizing of the paper support. As varnishing of cyanotypes was not a common practice, coatings do not usually interfere with the identification process.

3.4 Silver gelatin process

The first experiments with making silver-gelatin light-sensitive layers were conducted as early as 1853 by Marc Gaudin. However, the first working solution for gelatin dry plates was published almost 15 years later in the British Journal of Photography (January 17th 1868) by W.H. Harrison. In 1871 Dr. Richard Leach Maddox introduced the idea that gelatin emulsions should contain silver bromide, rather than silver iodide; the basis of modern gelatin emulsions for development. Improvements, such as washing the emulsion (J. Johnson 1873) and ripening by heat to increase sensitivity (C.E. Bennett, 1874) were further major contributions to the evolution of the medium. By the early 1930's the dominance of silver gelatin developing out papers as a photographic printing medium was firmly established and assured. Competition among numerous manufacturers promoted a tremendous diversity as papers the combinations of paper color, weight, texture and sheen. In the 1940's, these stylistic achievements were overshadowed by wartime shortages and new requirements for prints made quickly and cheaply. Following the war, the attention was gradually shifted to color print materials (Messier ,2011).

Table 1: Comparison of microscopic characteristics of DOP photographic papers (magnification 20x) and possible correlations with FTIR analytical signatures

		Matte DOP with thick structured substrate layer (1940) and matte DOP with thin substrate layer (1910) - presence of matting agents (starch, inorganic matting agents) or strong signal of cellulose
		Glossy DOP 1940s and glossy DOP 1970s - presence of protective coating -> celluloid or gelatin overcoat
		Silk - embossed DOP 1950s and 1970s - formed in paper-making process -> regular FTIR spectra of DOP

Band at 1633 cm^{-1} is corresponding to stretching vibration ν ($\text{C}=\text{O}$) of the coil structure of gelatin and may be obscured by the band of bound water [18]. Amide II band ($\sim 1531\text{ cm}^{-1}$) corresponding to the vibration $\nu(-\text{CN})$ and $\delta(-\text{CN}-\text{H})$, is less sensitive to changes in secondary structure as the amide I, but is strongly influenced by hydration as well. Amide III band ($\sim 1446\text{ cm}^{-1}$) corresponds to the deformation vibration $\delta(\text{CH})$ and its intensity is lower than the intensity of the bands I and amide II. Following bands at 1395 and 1330 cm^{-1} are of decreasing, or approximately the same intensity.

The substrate layer is characterized by amide band at app. 1540 cm^{-1} and the bands associated with the presence of barium sulfate. Band attributed to stretching vibrations of inorganic sulfates ($\text{S}-\text{O}$) can be detected at $1179 - 1083\text{ cm}^{-1}$, the band centered at $1190 - 1072$ and shoulder at 982 cm^{-1} correspond to asymmetric vibrations of the sulfate group. Bands at 608 and 637 cm^{-1} belong to out-of-plane vibrations - $\delta(\text{SO}_4)$.

Infrared spectroscopy can help to distinguish between gelatin and albumen light sensitive layers. Although shape, position and intensity of Amid I and Amid II bands is very similar, a significant differences in the 1470 – 1250 cm^{-1} region can be observed (Stulik, 2013d). In the albumen layers, two bands at 1448 and 1385 cm^{-1} are present, whereas in the silver gelatin layers, three or more bands at 1449, 1399 and 1332 (1278) cm^{-1} are observed (Figure 7).

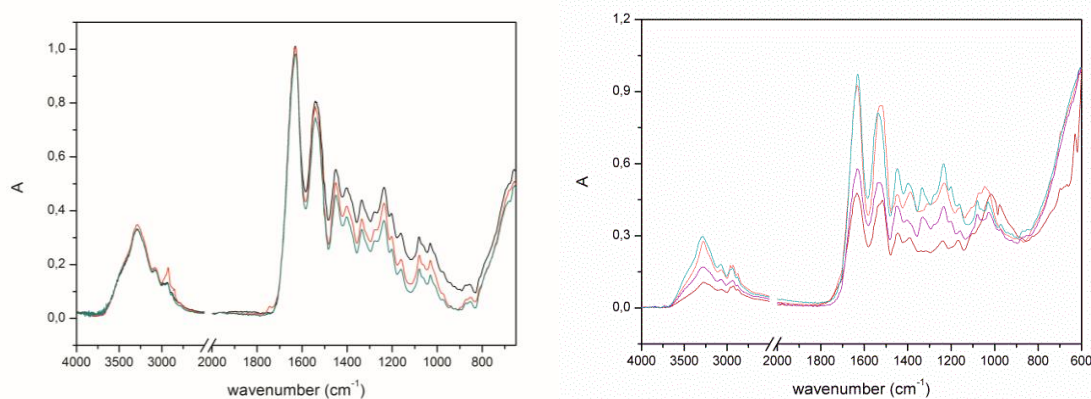


Figure 7: FTIR spectra of silver gelatin developed out paper Gevaert (1954) and comparison of gelatin (cyan and magenta) and albumen silver prints (orange and red line)

4. CONCLUSION

ATR-FTIR measurement is a quick, reliable and nondestructive way to confirm the presence of organic binder in photosensitive layer. Moreover, it provides the information about the state of preservation and enables to identify secondary protective. Digital or optical microscopy represents low-cost and facile method of obtaining data about surface structure and grain pattern. However, supplementary elemental analysis measurements are necessary, because many photographic processes or process variants (kallitype, Van Dyke print, platinotype) may exhibit similar visual features and infrared spectra closely resembling those of support, most frequently cellulose, pure or seized. FTIR spectroscopy with optical microscopy are useful tools for identification and study of stability of historical photographic documents, however, nondestructive elemental analysis is necessary for specification of certain important properties, such as toning with noble metal compounds, or supporting the hypothesis of image layer constitution, if questioned

This methodology has been published and widely applied by Photography research department of the Getty conservation institute as well as other individual researchers (Stulik 2013a – 2013d, Reilly 2001). The authors tried to apply and adapt the methodology for the research and educational needs of the department of restoration (Academy of Fine Arts and Design in Bratislava) and Department of graphic arts technology and applied photochemistry (Slovak University of Technology), as systematic approach to identification of photographic techniques with the use of nondestructive instrumental analysis has not yet been applied in Slovakia. The multitude and largeness of photographic collections, as well as their diversity stress the importance of accurate and validated.

5. ACKNOWLEDGEMENTS

This work has been supported by the Scientific Grant Agency of the Slovak Republic (project 1/0818/13) and by the Slovak Research and Development Agency under contract No. APVV-0324-10.

6. REFERENCES

- [1] Ali, M. A., Ali, M. F. et al. "Investigations on the chemical degradation of silver gelatin prints. "International Journal o Conservation Science 3 (2), 93-106. 2012
- [2] Calvini, P.; Gorassini, A. "FTIR– Deconvolution Spectra of Paper Documents" Restaurator Vol. 23 (1) 2002. URL <www.viks.sk/chk/res_1_02_48_66.doc> (last request < 5-14-2014>)

- [3] Derrick, M. R., Stulik, D., Landry J. M. "Infrared Spectroscopy in Conservation Science." (The Getty Conservation institute, Los Angeles USA, 1999)
- [4] Messier, Paul. Photographic Papers in the 20th Century: Methodologies for Research, Authentication and Dating. Paper originally submitted to the post print publication of Fotoconservación 2011 Logroño, Spain, June 2011.
URL<www.paulmessier.com/pm/papers.html> (last request <20.8.2014>)
- [5] Reilly, J. M. The albumen & Salted Paper Book. The history and practice of photographic printing, 1840 – 1895. Light Impressions Corporation. Rochester, 1980.
- [6] Reilly J.: Albumen Prints: A Summary of New Research about their Preservation. Picturescope Vol. 30 (1). 1982. pp. 34–37. URL <<http://albumen.conservation-us.org/library/c20/reilly1982b.html>> (last request <5.12.2014>)
- [7] Reilly, James M. Care and Identification of 19th Century Photographic Prints, Eastman Kodak Company; Reissue edition ISBN: 0-87985-365-4. 2001
- [8] Ricci, C., Bloxham, S., Kazarian, S. G. "ATR-FTIR imaging of albumen photographic prints." Journal of Cultural Heritage. Vol. 8, Issue 4, s. 387–395. 2007
- [9] Stulik, D., Kaplan, A. "The Atlas of Analytical Signatures of Photographic Processes, Albumen." URL<http://www.getty.edu/conservation/publications_resources/pdf_publications/pdf/atlas_saltprint.pdf> (last request 20.9.2014) ISBN number: 978-1-937433-12-3. 2013 (a)
- [10] Stulik, D., Kaplan, A. "The Atlas of Analytical Signatures of Photographic Processes, Albumen." <http://www.getty.edu/conservation/publications_resources/pdf_publications/pdf/atlas_albumen.pdf> (last request 20.8.2014) ISBN: 978-1-937433-04-8 (online resource). 2013 (b)
- [11] Stulik, D.; Kaplan, A. "The Atlas of Analytical Signatures of Photographic Processes, Cyanotype."<http://www.getty.edu/conservation/publications_resources/pdf_publications/pdf/atlas_cyanotype.pdf> (last request 1.9.2014) ISBN: 978-1-937433-08-6 (online resource). 2013 (c)
- [12] Stulik, D.; Kaplan, A. "The Atlas of Analytical Signatures of Photographic Processes, Silver Gelatin." <http://www.getty.edu/conservation/publications_resources/pdf_publications/pdf/atlas_silver_gelatin.pdf> (last request 20.9.2014), ISBN: 978-1-937433-13-0 (online resource). 2013 (d)

IMAGE ANALYSIS OF WRITING MEANS AND ITS FORENSIC ANALYSIS

Vladimír Dvorka, Milena Reháková, Michal Čepčan,
 Lukáš Gál, Eva Belányiová, Pavol Gemeiner
 Slovak University of Technology in Bratislava,
 Faculty of Chemical and Food Technology,
 Department of Graphic Arts Technology and Applied Photochemistry,
 Institute of Natural and Synthetic Polymers
 Bratislava, Slovak Republic

Abstract: Forensic analysis of writing means is useful to classify documents if they are originals or forgeries. Material analysis is very important in this field, not only for writing means as well as for paper substrate. In this paper is introduced image analysis technique of writing means samples as a non-destructive analyzing methods against destructive analysis methods. The samples consist of three type of writing means: ball pens with paste, gel pens and ink pens. Image analysis methods consist of modulation transfer function, analysis of line spread function (line width), color coordinate calculation and analysis of fluorescence. Modulation transfer function (MTF) of the ink line edge gives information about its deformation based on paper quality and ink bleeding. Line spread function (LSF) describes line width and its deformation based on ink and paper quality. Color coordinates CIE $L^*a^*b^*$ calculation presents information about color of ink and ink variability on paper surface. The samples consist of micro lines and were digitized using microscopy. All image analyzing methods and colorimetry will be evaluated by Principal Component Analysis (PCA), which is able transform too much variables to only a few variables (2 or 3 principal components) to identify the sample. Reduced variable space is than represented into 2D or 3D space for better visual identification of the samples.

Key words: forensic analysis, fluorescence, colorimetry, modulation transfer function

1. INSTRUMENTS AND SAMPLES

1.1 Measurement instruments

Microscope: Leica metallographic microscope DM2700 M with CMOS digital camera DMC2900 (working internal in CIE $L^*a^*b^*$ color space, 10 bit, max. 3.1 Mpix physical resolution, pixel size $3.2 \times 3.2 \mu\text{m}$), objective 5 \times enlarge (215 \times total image enlarge), LED illumination system with 4500 K color temperature. Picture sample size 2048×1536 pixels ($2382 \times 1786 \mu\text{m}$).

1.2 Sample type

The same paper type from one producer was used, only the type of pen was various. The filling was for samples B1–B10 paste, for samples G1–G5 gel and for samples R1–R4 ink. Writing means generally consist of resin (ketones, esters, aldehydes, phenolic...), solvent (water, glycols or benzyl alcohol), lubricant (oil acid) and dye (monoazo-, diazo-, ftalo-cyanine or arylmetane).

2. MEASURING METHODS AND RESULTS

2.1 Modulation transfer function (MTF)

The calculation of modulation transfer function is presented on Figure 1. Modulation transfer function was calculated from pen line edge in Matlab (Figure 2).

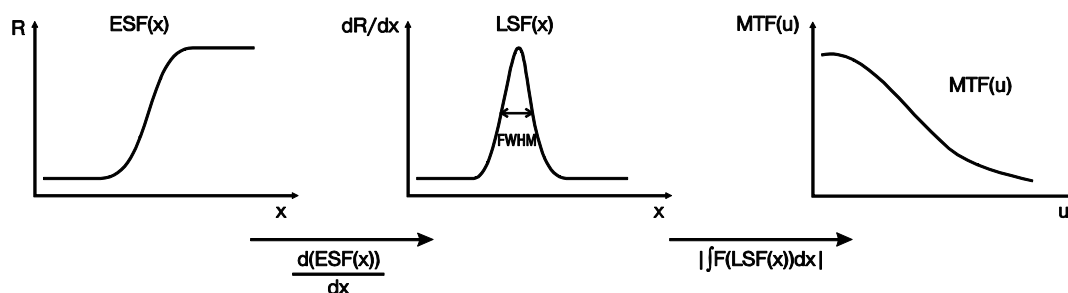


Figure 1: Calculation of modulation transfer function (MTF).
ESF – Edge spread function, LSF – Line spread function.

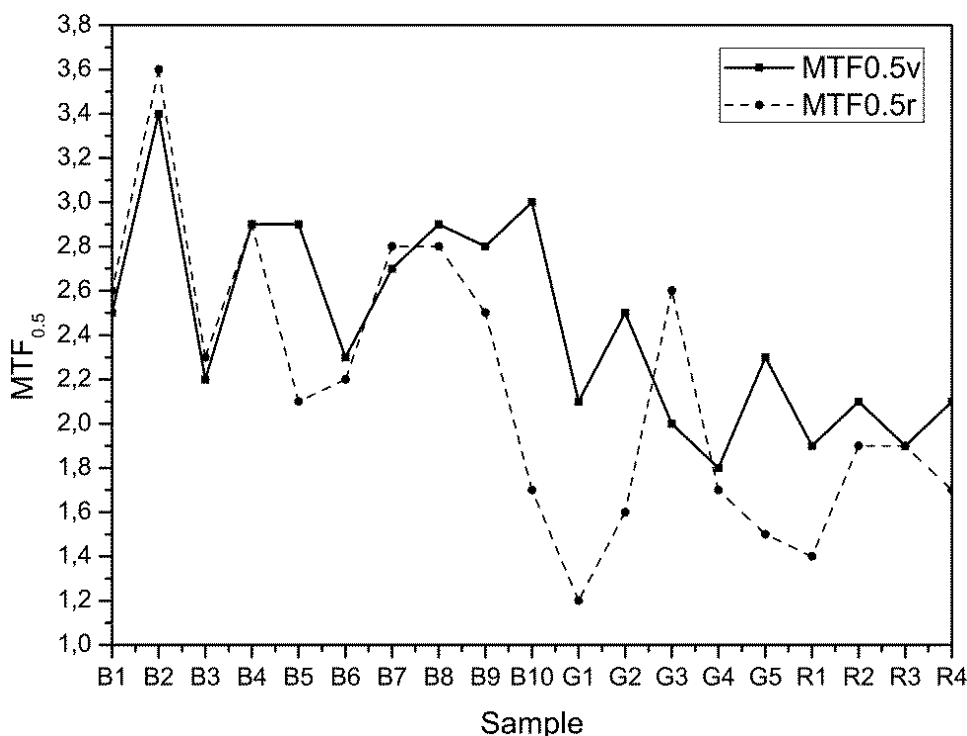


Figure 2: Modulation transfer function of samples ($MTF_{0.5}$).
V – smoothed dependence, R – real dependence.

The samples were separated into 5 groups based on $MTF_{0.5, v}$:

- Group 1 – samples R1, R2, R3, R4, G1, G3 and G4 ($MTF_{0.5} = 1.81\text{--}2.07$).
- Group 2 – sample B3 ($MTF_{0.5} = 2.19$).
- Group 3 – samples B1, B6, G2 ($MTF_{0.5} = 2.33\text{--}2.52$).
- Group 4 – samples B4, B5, B7, B8, B9, B10 ($MTF_{0.5} = 2.72\text{--}2.99$).
- Group 5 – sample B2 ($MTF_{0.5} = 3.41$).

Modulation transfer function is dependent on paper substrate too, because the roughness of the substrate influences the quality of written pen line.

2.2 Line width measurement

The line width deformation was not the same for all samples. In all cases was measured line width lower as declared pen tip diameter, mostly less than half of declared size (Table 1). Only pens of G and R sets were with higher line width as half of declared size (except sample G1) caused by ink bleeding and better wetting of surface (viscosity was lower as at B set). This table can be used for line width prediction for unknown sample if the sample was classified in to group (B/G/R) by other methods.

Table 1: Line pen width of the samples

Sample	B1	B2	B3	B4	B5	B6	B7	B8	B9	B10	G1	G2	G3	G4	G5	R1	R2	R3	R4
Line width [m]	287	244	236	249	359	331	230	302	274	361	759	465	251	390	433	499	458	359	407
Standard deviation [m]	16	11	10	34	19	30	35	47	27	25	44	13	32	16	25	13	19	36	54
Tip diameter [m]	–	–	–	–	800	–	700	1000	–	1000	1600	700	400	700	700	700	300	500	700

2.3 Color coordinates

Modern measurement instruments allow to measure color coordinates from color captured sample. The CIE $L^*a^*b^*$ coordinates were computed as average value from 31×31 pixels matrix in 30–45 different positions of written line (approximately 200 pixels total line width). Color coordinates L^* , a^* , b^* were calculated from R, G, B color values using Adobe RGB color space and D_{50} light source (Figure 3).

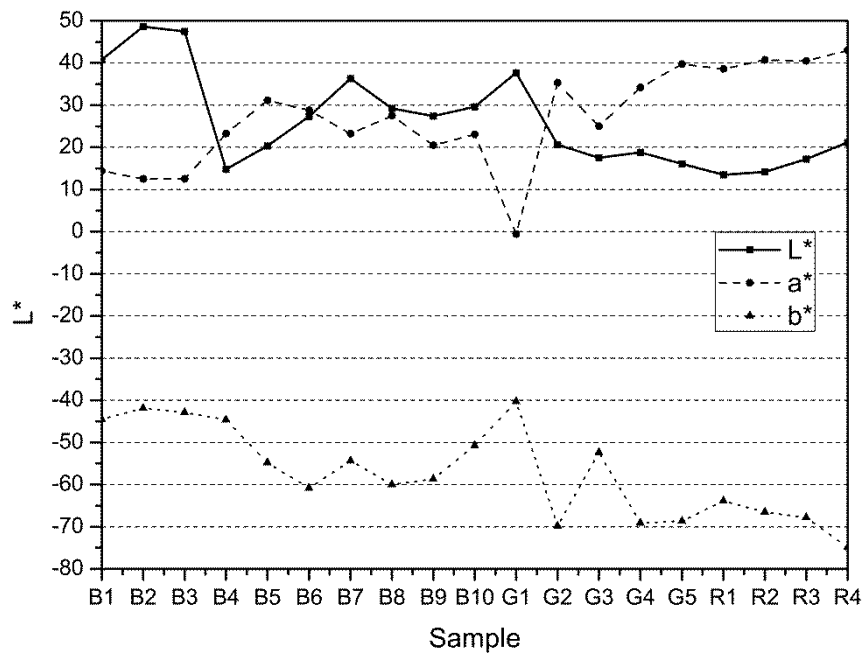


Figure 3: Average color coordinates L^* , a^* , b^* of micro measured pen lines.

Calculating E^*_{ab} was made against average paper color coordinates ($L^* = 73.6$, $a^* = 1.9$, $b^* = -4.6$). We can sample divide into 5 groups R1–R4/G2/G4/G5, B4–B6/B8/B9/G3, B7/B10, B1/G1 and B2/B3 (Table 2).

Table 2: Color difference E^*_{ab} of samples.

Sample	B1	B2	B3	B4	B5	B6	B7	B8	B9	B10	G1	G2	G3	G4	G5	R1	R2	R3	R4
E^*_{ab}	53	46	48	74	79	78	66	75	74	67	51	90	77	91	94	92	94	93	97

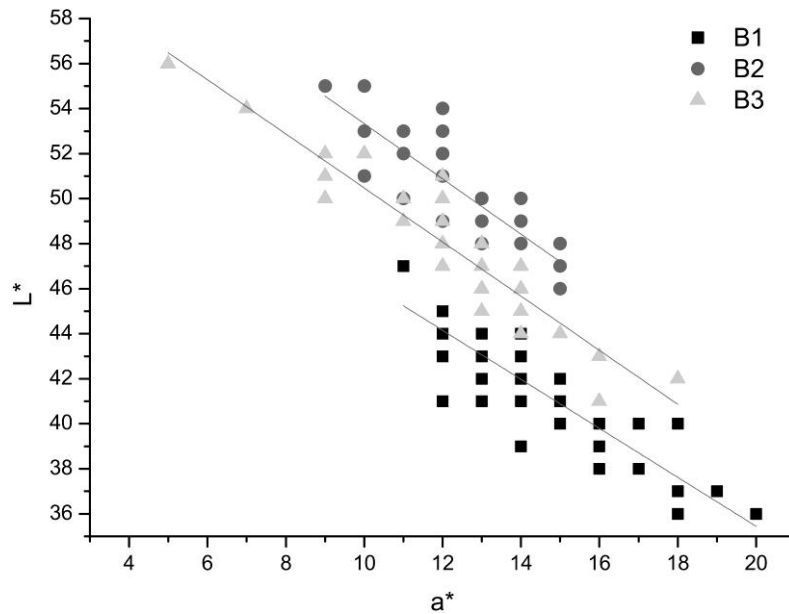


Figure 4: Color coordinates L^* , a^* , b^* of micro measured pen lines – linear dependences

Color coordinates are not the same on different place along the pen line. Based on Figure 4 the group of color coordinates have a tendency be a part of a linear regression in L^*b^* or L^*a^* dependence (with 85 up to 93 % correlation).

2.4 Fluorescence

For measuring fluorescence was used Leica microscope with fluorescence filter cube TX2 (Excitation range: green “visible”, excitation filter: bandpass filter 560/40, dichromatic mirror 595, suppression filter: bandpass filter 645/75). As a light source was used 100 W mercury lamp (ebq 100-04, Hg 100). The sample B2 show forced fluorescence of the paper caused by ink (Figure 5). On the Figure 5 the samples B1, B4 and B5 show only fluorescence of the paper substrate, ink is without fluorescence.

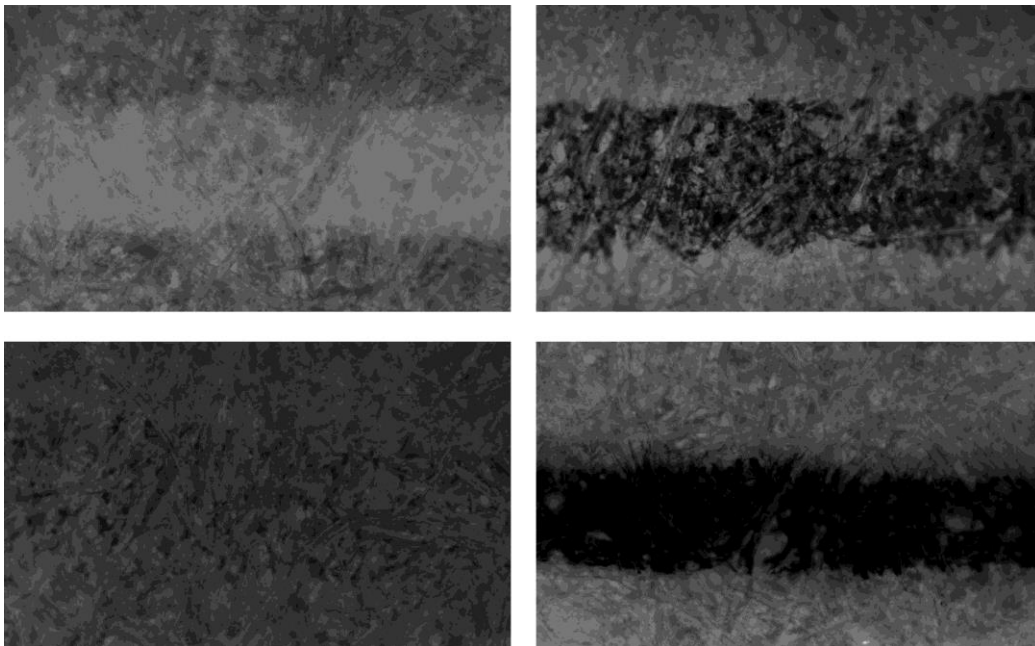


Figure 5: Fluorescence (TX2 filter) of sample B2 (left up), B5 (right up), B1 (left down) and B4 (right down).

The samples R1, R2, R3 and R4 had fluorescence similar to sample B2, but the forced fluorescence was more visible. The sample G2, G4 and G5 were similar to sample B5 with more background fluorescence (as a part of ink line). Sample G1 and G3 were similar to sample B4. The sample B6, B7, B8, B10 were similar to sample B5, sample B9 was similar to sample B4 and sample B3 was similar to sample B1 (Table 3).

Table 3: Fluorescence of samples as an average intensity of R color channel.

Sample	B1	B2	B3	B4	B5	B6	B7	B8	B9	B10	G1	G2	G3	G4	G5	R1	R2	R3	R4
Fluorescence	113	215	160	23	106	70	127	72	23	112	15	180	17	142	180	239	249	248	248

We tested second fluorescence filter cube D (Excitation range: UV, violet “visible”, excitation filter: bandpass filter 355–425, dichromatic mirror 455, suppression filter: longpass filter 470), but the result was without identification visible difference.

2.5 Principal component analysis

The variable data for all measured dependences were first normalized. Principal component analysis dependence (Figure 6) was calculated from average CIE $L^*a^*b^*$ color coordinates, modulation transfer function ($MTF_{0.5}$) and fluorescence. The maximal influence on results caused color coordinates and fluorescence, the influence of $MTF_{0.5}$ was lower.

From the principal component analysis the samples were separated for individual sample B2, B3, B5, B1, G4, G1, B7, B10 and for small groups R1/R2/R3/R4, G2/G5, B6/B8 and B4/B9/G3 (Figure 6).

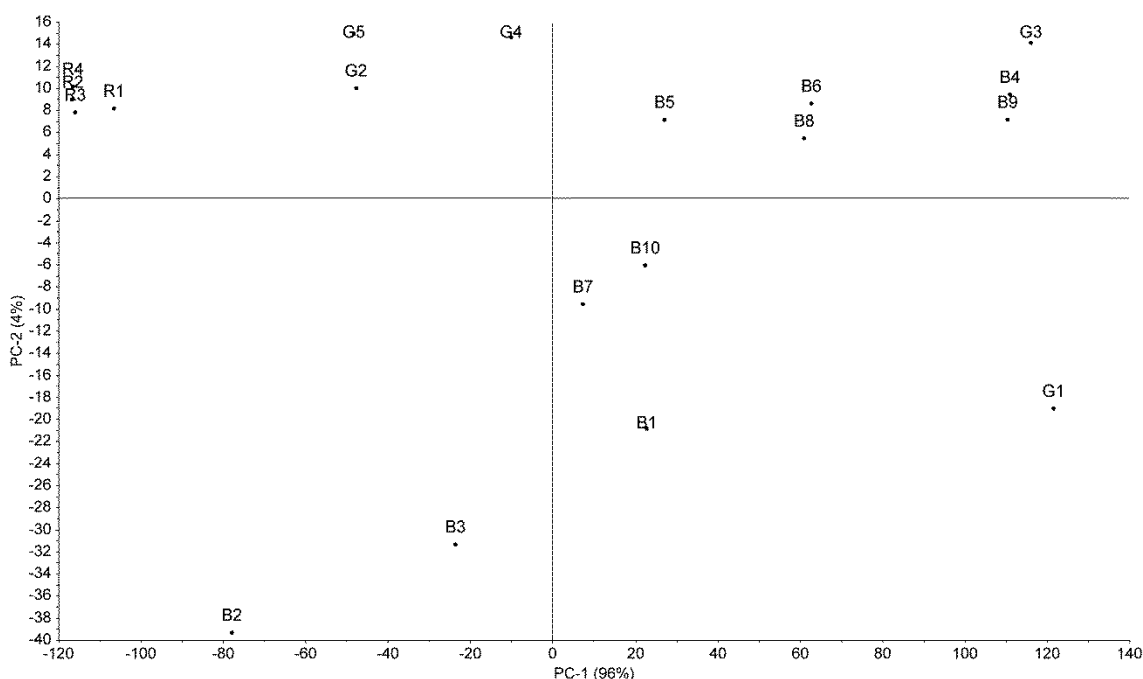


Figure 6: Score of principal component analysis computed from CIE $L^*a^*b^*$ color coordinates, fluorescence and $MTF_{0.5}$.

3. DISCUSSION AND CONCLUSIONS

In our case we need to identify chemical compounds of the samples, if they are not with the same ink composition (for example samples B4 and B9...). Fluorescence was the best individually evaluating method for separating samples to smaller groups (9 groups) and the principal component analysis enlarge the number of different groups (12 groups). Samples of B and G sets were separated to more groups, only the samples of R set were not separated, probably are with the same ink composition (only sample R1 is slightly different).

To assign precise results, the sample database and unknown sample have to be measured by the similar conditions (camera, light source, lens, filters, fluorescence filters...) to obtain similar exposure conditions.

The UV-VIS and FTIR spectra of samples will be inspected in the future in principal component analysis with image analysis results. Individual principal component analysis of UV-VIS and FTIR spectra was without separating samples to groups for their identification.

The identification more smaller group was possible by FTIR spectroscopy comparing spectra of samples (13 groups).

4. ACKNOWLEDGEMENTS

This work was supported by the Slovak Research and Development Agency under the contract No. APVV-0324-10 and Scientific grant agency of Ministry of Education... of Slovak Republic project No. VEGA 1-0818-13. This publication is the result of the project implementation: Centrum excelentnosti bezpečnostného výskumu (Center of Excellence for Security Research) ITMS code: 26240120034 supported by the Research & Development Operational Program funded by the ERDF.

5. REFERENCES

- [1] Adam, C. D., Sherratt, S. L., Zholobenko, V. L.: "Classification and individualisation of black ballpoint pen inks using principal component analysis of UV-vis absorption spectra". *Forensic Science International*, Elsevier, Vol. 174, 1, page 16–25, (2008).
- [2] Brunelle, R. L.: "Ink Analysis. Document analysis", Brunelle Forensic Laboratories, Fredericksburg, VA, USA, Academica Press, doi: 10.1006/rwfs.2000.0479, (2010).
- [3] Djozan, D., Baheri, T., Karimian, G., Shahidi, M.: "Forensic discrimination of blue ballpoint pen inks based on thin layer chromatography and image analysis". *Forensic Science International*, Elsevier, Vol. 179, 2–3, page 199–205, (2008).
- [4] Kher, A., Mulholland, M., Green, E., Reedy, B.: "Forensic classification of ballpoint pen inks using high performance liquid chromatography and infrared spectroscopy with principal components analysis and linear discriminant analysis". *Vibrational Spectroscopy*, Elsevier, Vol. 40, 2, page 270–277, (2006).
- [5] Koopipat, C., Tsumura, N., Fujino, M., Miyata, K., Miyake, Y.: "Image Evaluation and Analysis of Ink Jet Printing System (I) – MTF Measurement and Analysis of Ink Jet Images", *J. Imag. Sci. Technol.* 45, 6, page 591–597, (2001).
- [6] Lavine, B. K., Rayens, W. S.: "3.16 – Statistical Discriminant Analysis. Comprehensive Chemometrics", *Chemical and Biochemical Data Analysis*, Elsevier, Vol. 3, page 517–540, (2009).
- [7] Neumann, C., Mazzella, W. D.: "Questioned Documents. FORENSIC SCIENCES", University of Lausanne, Lausanne, Switzerland, Elsevier (2005).
- [8] Roux, C., Novotny, M., Evans, I., Lennard, Ch.: "A study to investigate the evidential value of blue and black ballpoint pen inks in Australia". *Forensic Science International*, Elsevier, Vol. 101, 3, page 167–176, (1999).
- [9] Silva, C. S., Borba, F. de S. L., Pimentel, M. F., Pontes, M. J. C., Honorato, R. S., Pasquini, C.: "Classification of blue pen ink using infrared spectroscopy and linear discriminant analysis." *Microchemical Journal* (2012). URL <http://www.sciencedirect.com/science/article/pii/S0026265X12000719>, (last request: [30. 3. 2012])
- [10] Solčáni, J.: "Riešenie problému krížených ťahov pomocou techník počítačového videnia" (diplomová práca), vedúci: doc. RNDr. Milan Ftáčnik, CSc.). Katedra informatiky, Fakulta matematiky, fyziky a informatiky Univerzity Komenského, Bratislava (2007).

THE USE OF SHOCK RESPONSE SPECTRUM IN PROTECTIVE PACKAGING DESIGN

*Davor Donevski, Diana Milčić, Dubravko Banić
University of Zagreb, Faculty of Graphic Arts, Zagreb, Croatia*

Abstract: Protective packaging design and development have to take multiple considerations into account. These are the product's requirements for protection, the protective properties of the designed package, as well as the balance between the cost of packaging and the product value. A variety of testing methods were developed in order to test for protection performance of packages with respect to shocks and vibrations. These require the making of test specimens and the use of vibration tables which are limited in the ability of reproducing shock pulses and vibrations encountered in the transport environment. On the other hand, there exist mathematical models capable of predicting protective performance of a package at fair accuracy. This paper gives an overview of such models and clarifies common misconceptions on their use. In particular, it clarifies the use of the SRS (Shock Response Spectrum) in the context of protective packaging and points out the distinction between its proper use for this purpose and the purpose it was originally developed for.

Key words: protective packaging, shock response spectrum

1. INTRODUCTION

A variety of products, either those commonly found in retail stores, or those made for special purposes such as spacecraft components require protective packaging in order to reach their destination undamaged. As various as the products and their value are, so are their protection requirements. Therefore, packaging engineers have to consider multiple factors during the protective packaging design and development. First are the product's characteristics, i.e. the fragility of the product and its components. This is normally assessed by performing laboratory tests on shock tables and developing the damage boundary curves from test results (Burgess, 1988). Once the product's fragility is known, its protection requirements have to be determined. These depend on the product's cost and the hazards of the distribution environment. Methods of estimating the distribution environment risks and damage occurrence probabilities have been developed (Ostrem and Godshall, 1979) and are used to select optimal protection level depending on product's value. Here the optimal means that the cost of packaging should not exceed some limit depending on the product's value. A certain proportion of products are expected and allowed to get damaged if a higher protection level which would ensure their safety would increase packaging costs for an amount greater than the value of those products. The packaging engineers have to design the package in such way that it serves the purpose of protecting the products in an economically justifiable way. Packages usually consist of corrugated paperboard boxes with some protective materials inserted. There is a variety of protective materials from crimped paper, honeycomb board, inflatable and bubble plastics to synthetic foams. As much as they may vary in cost and properties, they all serve the same purpose and are characterized by the same physical characteristics (Burgess, 1990; 1999; Guo and Zgang, 2004). Their purpose is cushioning, i.e. transforming high amplitude and short period waves (pulses) to which the package is exposed to lower amplitude and longer period waves to which the product is exposed within the package. Important physical characteristics of protective materials are their spring constant k , and their cushioning properties, expressed either through the cushioning curves or the damping constant c . Those characteristics influence the motion of the product – package system (product and package with cushioning) when exposed to some external force. In particular, they affect the natural frequency f_n of the system and its motion depending on the amount of damping. This is typically modelled as a simple mass-spring system. A protective package is well designed for a particular distribution environment if it is not in resonance with the external forces (shocks and vibrations) from that environment and if the damping is such that it minimizes package's motion. In addition to that, it has to take into account the product's fragility. The standard method consists of determining the product's fragility in terms of critical acceleration level A_c resulting with product's damage and then performing the Shock Response Spectrum (SRS) analysis. Once the critical SRS plot S_c is obtained, the protective package cushioning is designed to transmit shock

pulses with an SRS less than S_c at every frequency of the SRS plot (ASTM D3332-99, 2010; Goodwyn and Young, 2011). This paper gives an overview of the SRS method theory (Irvine, 2012) and presents its proper use in the protective packaging development process.

2. METHODS

This paper is focused on the use of Shock Response Spectrum (SRS) analysis for protective packaging. The SRS analysis is used to predict the responses $x_1'' \dots x_L''$ of a series of mass-spring systems with different natural frequencies f_n to an input shock pulse y'' (Figure 1). Here the second derivatives denote accelerations as they are the second derivatives of displacements x , y with respect to time.

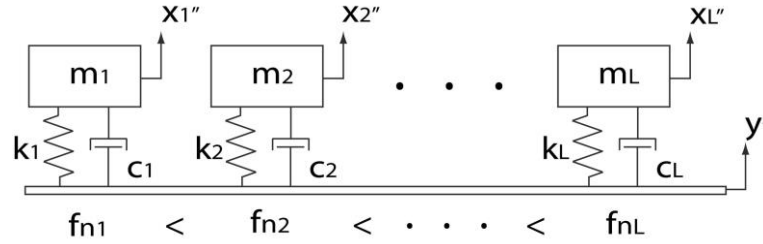


Figure 1: Shock Response Spectrum Model

In this paper, the product is not specified, but is viewed as a general case. The SRS was used to predict responses of product's components with different natural frequencies f_n to a half-sine wave with amplitude 50G and duration 3 milliseconds (Figure 2). A damping ratio $\xi = 5\%$ was used in the SRS analysis.

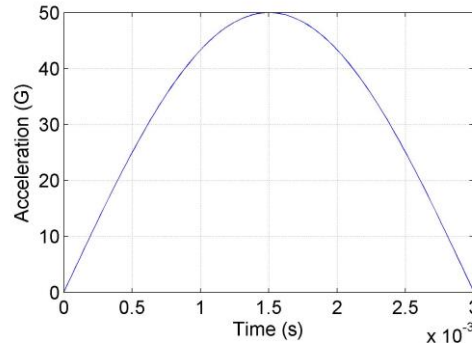


Figure 2: Half-sine shock pulse applied in SRS and package calculations

Note that this gives us predictions for the unprotected product. In order to predict responses of product's components to the same half-sine pulse when the product is protected inside a package, we view the package as a single damped mass-spring system and determine its response to a half-sine pulse. For this purpose, let's say that the product's mass is $m = 10$ kg and the cushion's spring constant $k = 600$ kg / m = 600×9.81 N / m. By (1), the critical damping of this system $C_c = 485.22$. For our example, we will suppose the system is critically damped.

$$C_c = 2\sqrt{mk} \quad (1)$$

Now the general equation (2) of a damped mass-spring system is used to model our package. Here $r(t)$ is the external, driving force, in our case the half-sine wave.

$$my'' + cy' + ky = r(t) \quad (2)$$

Plugging the values into (2), we obtain (3):

$$10y'' + 485,22y' + 5886y = 4905 \sin(333,3\pi t) [u(t) - u(t - 0,003)] \quad (3)$$

where $u(t-a)$ is a unit-step function used to define the half-sine wave, and the amplitude of 4905 was derived from Newton's Second Law for $m = 10$ kg and wave's peak acceleration 50G.

The solution to this equation is $y(t)$, the equation of motion of a damped mass-spring system, i.e. the product inside the package (4). Figure 3a is the graph of (4), showing product's motion inside the package as the response to the half-sine shock pulse (Figure 2).

$$y(t) = e^{-24,26t} (-0,0015 + 0,97t) \quad (4)$$

Since the SRS model predicts responses to acceleration inputs, we take the second derivative of motion equation (4) and obtain acceleration equation (5). The graph of (5) divided by acceleration of gravity ($g = 9,81 \text{ m/s}^2$) to obtain accelerations expressed in G units, is displayed in Figure 3b. Equation (5) is now our input for the SRS analysis of the protected product.

$$a(t) = y''(t) = -47,15 * e^{-24,26t} + 588,6 * e^{-24,26t} (-0,0015 + 0,97t) \quad (5)$$

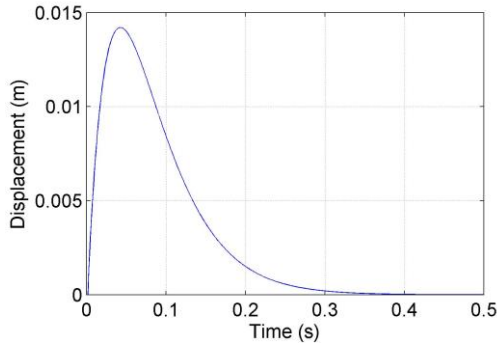
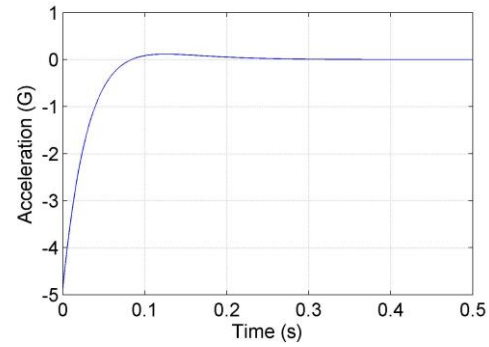


Figure 3a: Motion of product inside package



3b: Acceleration of product inside package

3. RESULTS AND DISCUSSION

In this section, we compare the results of the two conducted SRS analyses, namely of the unprotected and of the protected product. When analyzing the SRS of the unprotected product, the input to the SRS model was the 3 millisecond long half-sine shock pulse with amplitude 50G (Figure 2). Figure 4a shows the SRS to that pulse, i.e. how the unprotected product's components respond to it. Although this may not be visible clearly because of the image size, peak acceleration in this case occurs at frequency of $\approx 270\text{Hz}$ and is $\approx 83\text{G}$. When analyzing the SRS of the protected product, the half-sine shock pulse was first used as external input $r(t)$ to the package modelled by equation (2). The solution was the equation of motion of product inside the package (occurring when the whole package is exposed to half-sine pulse), and its second derivative the accelerations to which the product is exposed inside the package, equation (5). With equation (5) used as input to the SRS analysis, we obtained the SRS of the protected product, i.e. when the package is exposed to the half-sine pulse, and the accelerations transmitted to the product inside the package are modelled by equation (5). Figure 4b shows the SRS in this case. The maximum acceleration occurs at frequency of $\approx 128\text{Hz}$ and is $\approx 8,66\text{G}$. The direction of those changes was expected as the purpose of the cushioning inside the package is to transform high amplitude short period waves to lower amplitude longer period waves. This was the case if we compare Figure 2 to Figure 3b and their corresponding Figure 4a and 4b.

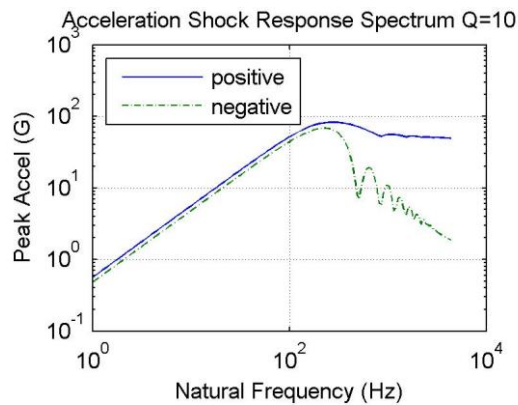
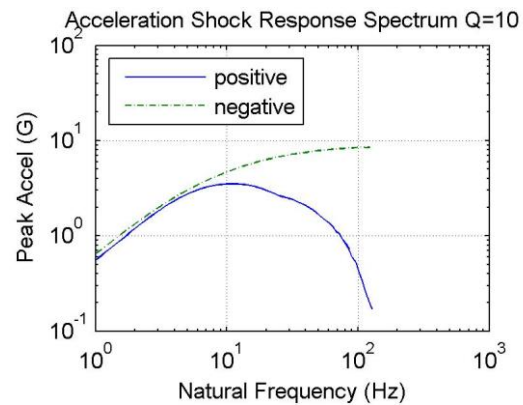


Figure 4a: SRS of unprotected product



4b: SRS of protected product

4. CONCLUSIONS

The shock response spectrum analysis is useful for predicting how the product's components with different natural frequencies would respond to some input. The method is capable of predicting responses to simple inputs like the half-sine wave shown in this paper, but also to complex vibrations. When this method was adopted for protective packaging development, the procedure of its use had to be adapted. When it is used to predict the protective properties of a package, the input to the model is not the wave or shock to which the package is exposed, but the shock or wave to which the product is exposed within the package, i.e. the one transmitted through the package. The purpose of this paper was to clarify this procedure of applying SRS to protective packaging development as it often causes confusion and isn't explained clearly in textbooks.

5. REFERENCES

- [1] ASTM D3332-99 Standard Test Methods for Mechanical Shock Fragility of Products, ASTM International, 2010.
- [2] Burgess, G.: "Consolidation of Cushion Curves", Packaging Technology and Science 3 (4), 0894-3214, 1990.
- [3] Burgess, G.: "Cushioning Properties of Convuluted Foam", Packaging Technology and Science 12 (3), 0894-3214, 1999.
- [4] Burgess, G.: "Product Fragility and Damage Boundary Theory", Packaging Technology and Science 1 (1), 0894-3214, 1988.
- [5] Goodwyn, D., Young, D.: "Protective Packaging for Distribution: Design and Development", (Lancaster PA, USA: DEStech Publications), pages 67-75, 2011
- [6] Shock and Vibration Characteristics and Vibration Transmissibility of Honeycomb Paperboard", Shock and Vibration 11 (5-6), 1070-9622, 2004.
- [7] Irwine, T. "An Introduction to the Shock Response Spectrum", URL: http://www.vibrationdata.com/tutorials2/srs_intr.pdf (last request: 2014-10-07).
- [8] Ostrem, F., Godshall, W.: "An Assessment of the Common Carrier Shipping Environment", (Madison WI, USA: U.S. Department of Agriculture 1979).

GRAPHICAL DOCUMENTS EXAMINATION USING MOLECULAR SPECTROSCOPY AND CHEMOMETRY

Vladimír Dvonka, Michal Čeppan, Michaela Belovičová, Lukáš Gál,
Milena Reháková, Pavol Gemeiner
Slovak University of Technology in Bratislava,
Faculty of Chemical and Food Technology,
Department of Graphic Arts Technology and Applied Photochemistry,
Institute of Natural and Synthetic Polymers
Radlinského 9, 812 37 Bratislava, Slovak Republic
vladimir.dvonka@stuba.sk

Abstract: The aim of this paper is to review methods of molecular spectroscopy in studying the properties of graphical documents on paper support and basis and potential of chemometric methods, esp. factor analysis methods in processing of spectral data. The reflectance FTIR spectroscopy, Vis and NIR spectroscopy is discussed. Examples of applications of combination of spectroscopy methods with chemometric processing of spectral data are presented.

Key words: molecular spectroscopy, chemometry, graphical documents, iron gal inks

1. INTRODUCTION

Graphical documents constitute a system of support and material structure of actual graphical information (inks, dyes, pigments toners, and other writing means) with complex mutual interactions. There are several ways of approach to examination of structure graphical documents. A full range of the recent physical and chemical methods is used to study and clarify the structure and conditions of graphical documents. Taking into account the nature and frequently uniqueness of the examined objects, the non-destructive methods are of superior importance. Among them methods of molecular spectroscopy and other optical methods are extensively used [Bacc, 2000; Zuieba-Palus, 2006; Kher, 2001; Trzinciska, 1993]. Combinations of the potential of spectral method (UV-Vis-NIR, FTIR) with the capability of chemometric methods and multivariate statistical methods have proven as useful in many applications fields [Pelikan et al, 1994]. Methods of absorption molecular spectroscopy utilize interaction of electromagnetic radiation with the matter to explore qualitative and quantitative nature of studied material. Generally, the whole spectrum of electromagnetic radiation is used; however the most common are absorption spectroscopies in the UV-Vis (ultraviolet and visible, 180–800 nm), NIR (near infrared, 800–2700 nm) and IR (infrared, mostly mid infrared 4000–600 cm^{-1}) region. UV-Vis absorption molecular spectra [Perkampus, 2012] originate from electron transition from ground to excited state and reflect electronic structure of the matter. In the visible region (380–800 nm) these absorption are related to the color of the material. IR absorption molecular spectra [Stuart, 2004] are related to the vibrations of molecular groups while NIR absorption spectra are based on molecular overtone and combination vibrations. One advantage is that NIR can typically penetrate much farther into a sample than mid infrared radiation [Burns and Ciurczak, 2001]. These methods can be used in transmission mode, when the radiation passing the layer of translucent sample, usually liquid, is analysed, or in reflection mode, when the radiation reflecting from the surface layer is analysed. For research of graphical documents the reflection methods are of most importance.

2. BACKGROUND OF FACTOR ANALYSIS METHODS FOR PROCESSING OF SPECTRAL DATA

Factor analysis is generally preferred for its ability to determine the number of components or factors creating the given spectra set and for its ability to classify and characterize these factors [Pelikan et al, 1994; Malinowski, 2002]. In the factor analysis the spectra are represented by a vectors (i.e. amplitudes of spectrum at individual wavelengths are elements of a vector). The set of spectra then creates a matrix consisting of column or row spectral vectors. Generally, for processing of a matrix, as a structure of linear algebra, various multivariate methods of linear algebra can be employed. If the \mathbf{R} is a spectral matrix consists of n_s spectral vector (i.e. spectra), the first step of factor analysis, principal component analysis (PCA), is diagonalization of square

symmetrical matrix Z ($Z = RR^T$; also called the scatter matrix). Orthonormal matrix of eigenvectors Q (with single eigenvectors q_k in its columns) ordered according to the descending values of corresponding eigenvalues is obtained. Matrix R can be now expressed as

$$R = Q U \quad (1)$$

where

$$U = Q^T R \quad (2)$$

A set of eigenvectors Q forms the orthonormal basis of a space of spectral data R . As was shown by Malinowski [9] the set of eigenvectors can be divided into the group of the primary eigenvectors Q_k , which is directly related to the chemical information contained in a spectral data, and the group of the secondary eigenvalues related exclusively to the experimental error in spectra data. Using the set of primary eigenvectors in following procedures would eliminate a significant portion of experimental noise in spectral data and leads to the best results.

The decomposition of the matrix R (1) is used in various multivariate methods for processing of spectral data (Pelikan et al, 1994; Malinowski, 2002). If the spectral matrix is the set of calibration spectra (i.e. spectra corresponding to the systems with known compositions), the set of primary eigenvectors can be used for construction of regression model for quantitative analysis utilizing the experimental noise reduction in factor analysis. The most used methods of this family are Principal Components Regression (PCR) and Partial Least Squares (PLS). Below two examples of spectroscopy methods with factor analysis processing of spectral data for identification of components in graphical structures are given.

3. IDENTIFICATION OF IRON-GALL INKS IN HISTORICAL DRAWING

Vast amount of historical documents and drawings contain grey-brown inks, among which the iron-gall inks were extensively used from the end of antiquity till the half of the previous century. However, these inks contain transitional metals compounds (particularly iron and copper), which accelerate degradation of paper or parchment support. After certain period the creation of cracks and mechanical damage and deterioration of documents occur. Taking into account the content of these documents, the corrosion caused by iron gall inks is consider being a serious problem endangering valuable cultural heritage (Kolar and Strlic, 2006).

The method of Fiber Optics Reflection Spectroscopy (FORS) in Vis and NIR region (500–1050 nm) with chemometric tool was developed to identify the dangerous corrosive iron-gall inks in documents and to distinguish them from other, potentially less corrosive inks (Gal et al, 2013). Chemometric tool is based on the testing of correspondence of studied individual spectrum with the database. This testing was performed by the method of the Factor Analysis – namely Target Factor Analysis (Pelikan et al, 1994; Malinowski, 2002) was used. This method projects a test spectral vector r_t (the spectrum of the tested ink in this work) on to the primary factors of the spectral space (a set of reference spectra in this work):

$$r_t^* = Q Q^T r_t \quad (3)$$

where r_t^* is a resulting projection-reconstruction of the test vector and Q is an orthonormal matrix of the axis of primary factor space. The AET (apparent error of the target vector) is the measure of the difference between the test vector and its projection. TFA and the AET enable one to test individually whether the particular spectrum (test vector) falls into the primary factor space, i.e. whether this spectrum belongs to the set of reference spectra. Great value of AET parameter indicates that the tested spectrum does not correspond to the database. On the other hand, low value of AET parameter indicates, that the tested spectrum corresponds to the spectra of databases.

Detector was tested on the spectra of other model of iron gall inks and model bistre and sepia inks – both fresh and aged. It was found, that the detector in the spectral region 500–1050 nm is capable to identify iron gall inks spectra, as well as distinguish the sepia spectra. The values of AET of bistre inks were greater than selected threshold value, however, the resolution is not so clear in some cases, as it is in the case of sepia inks, and parameters AET are close to the

threshold. With the aim to overcome the above mentioned drawback of low resolution of iron gall and bistre spectra in the region 500–1050 nm we studied the same method, i.e. detector based on target factor analysis, in the spectral range 1200–2300 nm.

3.1 Experimental

To obtain spectral properties of a wide set of iron gall inks, the model iron gall inks systems covering various mixing ratio of basic components (iron, copper and tannin) were prepared and applied on the paper. The samples were submitted to various time period of accelerated aging. Database consisted of 120 spectra measured in the spectra range 1200–2300 nm. Spectra were measured with the fibre optics spectrophotometer system Ocean Optics consisting of spectrometer NIR256-2.5, light source MAL-2000-FHSA and the standard reflectance accessory with 45°/45° geometry. This geometry assures, that the specular portion of light reflected from the surface is prevented from entering the detector. Original reflectance spectra were transformed into the spectra of optical densities ($D = 1/\log_{10}R$) and normalized in the interval 0–1 (Figure 1).

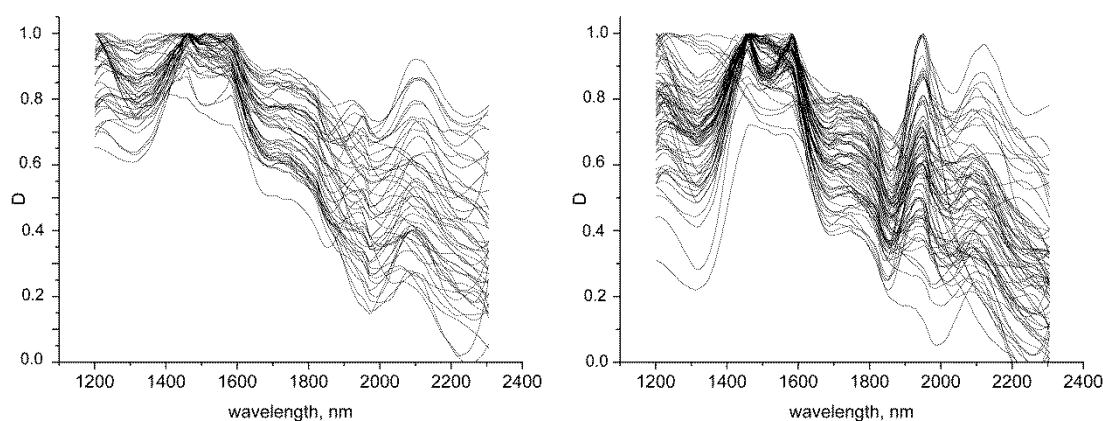


Figure 1: Database spectra of model iron gall inks, without Cu (left) and with Cu (right).

As a reference bistre ink for validation commercial ink TU 450 Bister Tusche (Kremer PIGMENTE) was used. Sample of bistre inks were applied on the paper and submitted to accelerated ageing. Similarly, sample of sepia ink prepared from sepia concentrate was applied on the paper and submitted to accelerated ageing. Reference spectra of bistre inks and sepia inks are on the Figure 2.

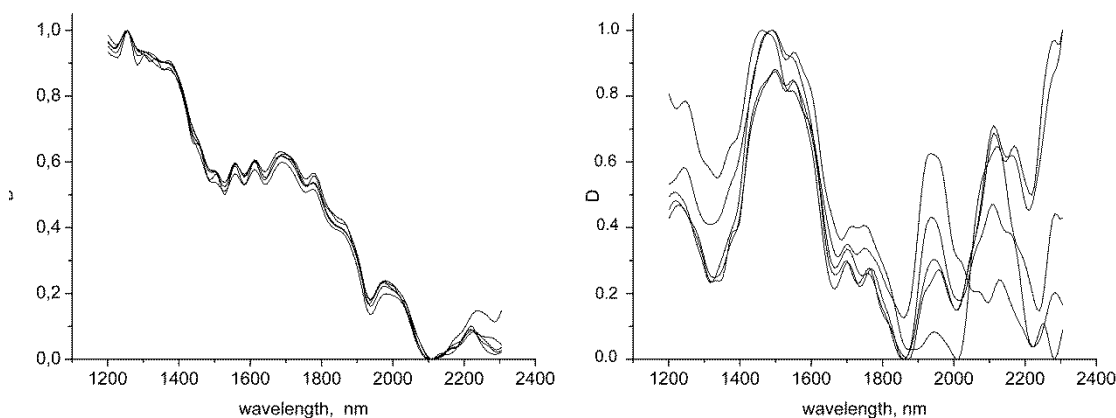


Figure 2: Spectra of model bistre inks (left) and sepia inks (right), non-aged and aged.

3.2 Results and discussion

The results of validation of chemometric tool based on the target factor analysis in the database of spectra of model iron gall inks in the range 1200–2300 nm are in the Table 1. As a threshold

value of AET parameter for judging, whether the spectrum corresponds to the spectra of database value of 0.01 was chosen (statistically determined reproducibility of spectral data of database).

Table 1: Results of Target Factor Analysis testing of model spectra in the region 1200–2300 nm (NA – non-aged samples, A – aged samples)

Inks	AET						
	NA	A	A	A	NA	A	A
Iron Gall	0.006	0.006	0.005	0.006	0.006	0.005	0.006
Sepia	NA	A	A	A	A		
	0.030	0.034	0.038	0.041	0.031		
Bister	NA	A	A	A	A		
	0.018	0.019	0.019	0.022	0.020		

The AET values all of the reference iron gall inks are lower than the threshold value, what suggest, that the chemometric tool in this spectral range is able to identify the iron gall inks. On the other hand, the AET values of the reference sepia and bistre spectra are clearly greater than threshold value, what reliably indicate, that the chemometric tool in this spectral region is able to distinguish sepia and bistre inks from corrosive iron gall inks. The resolution of spectra of bistre inks is more reliable in this region comparing to the resolution in the spectral region 500–1000 nm. Figure 3 shows the results of the survey of the drawing from 17th century using FORS NIR spectra in the region 1200–2300 nm. Spectra were measured in 2 locations. The obtained AET values of 0.008 and 0.007 indicate that the iron gall ink was used.

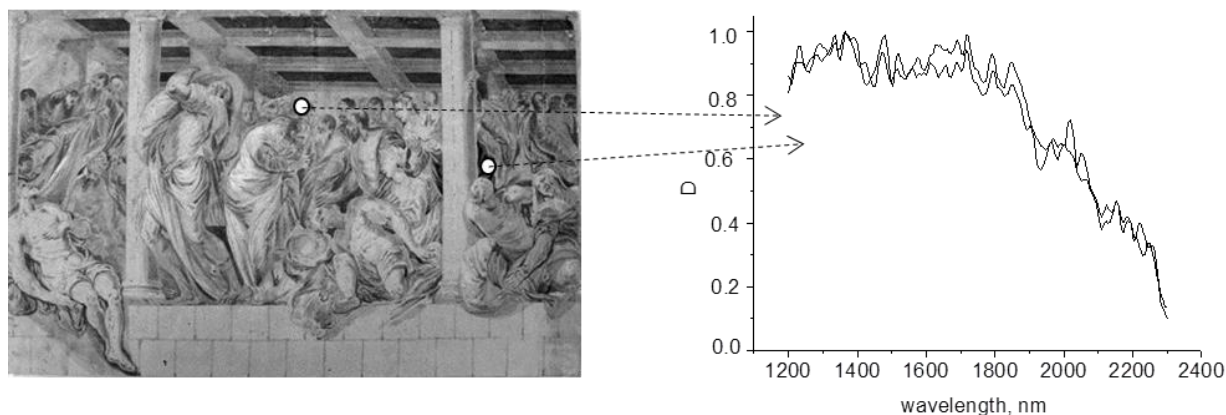


Figure 3: Figural Composition, Unknown Italian Master, 18th Cent., Slovak National Gallery, Bratislava, Slovak Republic, Inventory No. K 1067.

4. PRINCIPAL COMPONENT ANALYSIS OF IR SPECTRA OF LASER PRINTS

Laser printers are commonly used means for preparation of wide range of documents, and hence they are used for forging and illegal modification of various documents. Identification of toners of laser prints is of interest in examination of questioned documents in forensic analysis. One of the possible approaches to the classification of spectra of these documents into classes is Principal Component Analysis (PCA) [Esbensen et al, 2002]. Principal component analysis (PCA) is a method commonly applied which enables the visualization of sources of natural variability within the data in the form of 2-D or 3-D plots of different principal component (PC) combinations. In addition to data visualization, PCA as a method based on the factor analysis scheme is also used to reduce data dimensionality. In this example the application of PCA for distinguishing different laser printers used for printing one document is shown.

4.1 Experimental

Three pages of model document were prepared on three different laser printers. It was not possible to distinguish the origin of these prints by simple visual comparison, nor microscopic examination.

The IR spectra of laser prints were acquired on Excalibur FTS 3000MX (Digilab, USA) FTIR spectrometer with ATR adapter with diamond crystal. The spectra of each sample were measured three times and were averaged. To reduce noise in spectra Gaussian smoothing was applied. To eliminate the differences in intensity the baseline correction and area normalization were applied.

4.2 Results and discussion

Based on the -FTIR spectra it is possible to distinguish, that one page (middle gray) was printed on the different printer. However, the resolution of the other two pages is not evident (Figure 4). For PCA analysis the regions 700–1850 cm^{-1} and 2280–3800 cm^{-1} was selected, because the other regions contained no relevant spectral information.

The set of spectra was submitted to the Principal Component Analysis. This method utilizes the decomposition of the spectral matrix using the few first primary eigenvectors (= principal components)

$$\mathbf{D} = \mathbf{Q}_{1,2}^{\#} \mathbf{U}^{\#} \quad [4]$$

and the corresponding reduction of the number of variables to describe the spectra of studied samples in reduced space, usually two dimensional space of the first two most significant principal components, which can be represented graphically in a plane. This graph is called the scatter plot.

The visual inspection of the scatter plot of spectra (Figure 5) of our prints reveals three different groups of spectra, i.e. three different printers. Although the light gray and dark gray groups seems to be different, the sizes of the corresponding clusters in the two dimensional space allow for some doubts.

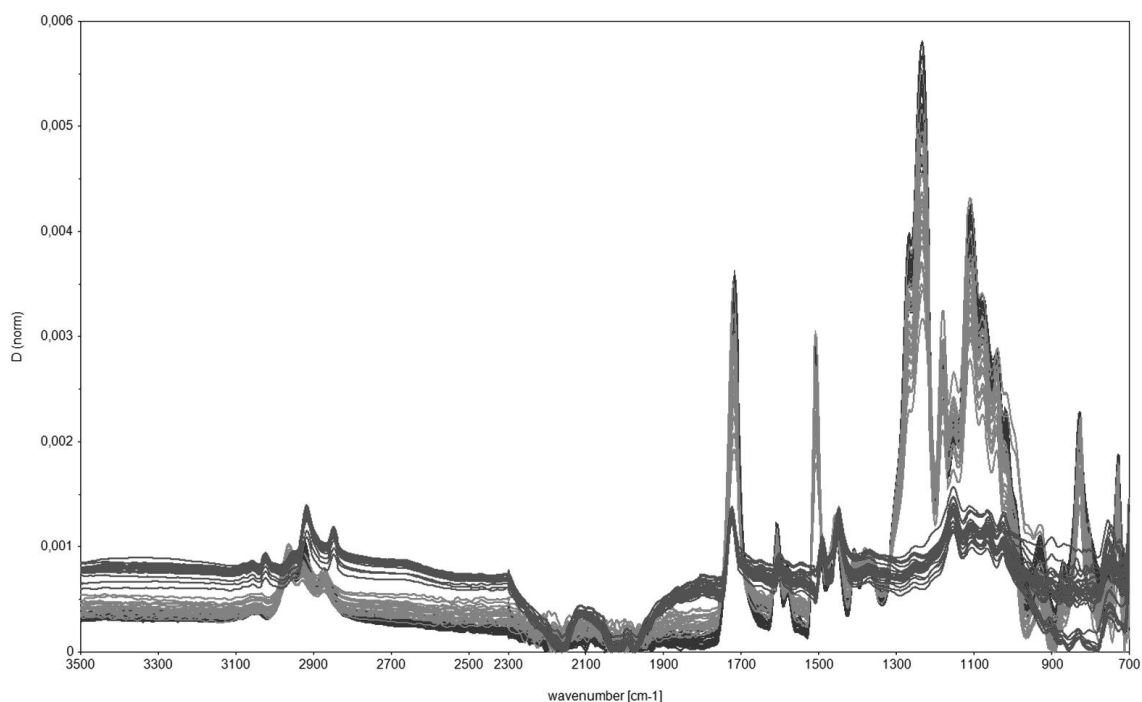


Figure 4: FTIR spectra of set of laser prints.
Sample 1 – dark gray, Sample 2 – light gray, Sample 3 – middle gray.

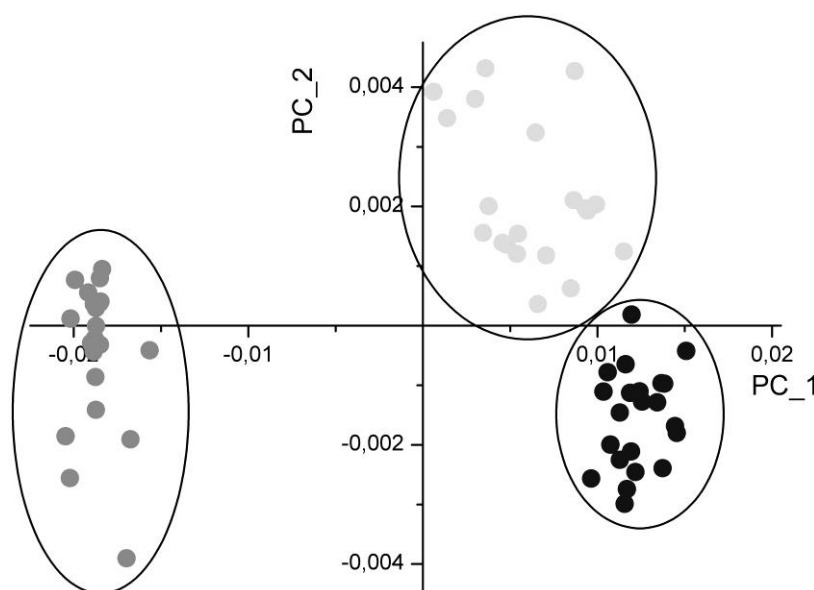


Figure 5: PCA scores plot (PC1 vs. PC2) of FTIR-ATR spectra of laser prints.
Sample 1 – dark gray, Sample 2 – light gray, Sample 3 – middle gray.

We tested the statistical difference of this groups in the two dimensional PCA space by Multivariate (two dimensional) Analysis of Variance (MANOVA). We tested H_0 (zero hypotheses): the mean vectors of the groups are statistically not different against H_1 (alternative hypotheses): the mean vectors of the groups are statistically different. Very low value of p (5×10^{-15}) suggests that the zero hypotheses can be rejected on a very low level of significance $\alpha \ll 0.01$, so this test affirms, that the clusters of dark grey and light grey spectra are different and that the model documents were printed on three different printers.

5. CONCLUSION

The presented examples demonstrate the possibility and potential of the combination of methods of molecular absorption spectroscopy with chemometric-factor analysis processing. The developed chemometric tool for identification of iron gal inks in historical drawings and documents based on FORS NIR spectra proved to be useful in survey of historical artefacts. The classification of leaser prints based on PCA analysis of their FTIR-ATR spectra are suitable for recognition of different printers used to print one questioned document.

6. ACKNOWLEDGEMENT

This work was supported by the Slovak Research and Development Agency under the contract No. APVV-0324-10 and Scientific grant agency project No. VEGA 1-0818-13. This publication is the result of the project implementation: Centrum excelentnosti bezpečnostného výskumu [Center of Excellence for Security Research] ITMS code: 26240120034 supported by the Research & Development Operational Program funded by the ERDF.

7. REFERENCES

- [1] Bacc, M.: UV-VIS-NIR, FT-IR, FORS Spectroscopies, in *Modern Analytical Methods in Art and Archaeology*, Ed. By E. Ciliberto and G. Spoto, Chemical Analysis Series, Vol. 155, Chapter 12, ISBN: 047129361X, John Wiley and Sons, New York (2000), pp. 321–361
- [2] Burns D. A., Ciurczak E. W.: *Handbook of Near – Infrared Analysis: Second Edition, Revised and Expanded*, Marcel Dekker, ISBN 0-8247-0534-3 (2001)
- [3] Esbensen K. et all: *Multivariate Data Analysis – In Practice*, 5th edition, CAMO Process AS, ISBN 978-956-8504-59-5, Oslo (2002)

- [4] Gál L. et al: Chemometric tool for identification of iron–gall inks by use of visible–near infrared fibre optic reflection spectroscopy, *J. Anal. Bioanal. Chem.*, Vol. 405 (2013), 9085–9090, ISSN 1618–2642
- [5] Kher A. et al: Classification of documents papers by infrared spectroscopy and multivariate statistical techniques, *Appl. Spectrosc.*, Vol. 55 (2001), pp. 1192–1198, ISSN 0166–1280
- [6] Kolar J., Strlic M.: *Iron Gall Inks: On Manufacture, Characterization, Degradation and Stabilization*, Narodna i univerzitetna knjižnica, ISBN 961–6551–19–1, Ljubljana (2006)
- [7] Malinowski E. R.: *Factor Analysis in Chemistry (Third Edition)*, Wiley, ISBN 978–0471134794, New York (2002)
- [8] Pelikan P., Ceppan M., Liska M.: *Applications of Numerical Methods in Molecular Spectroscopy*, CRC Press, ISBN 0–8493–7322–0, Boca Raton (1994)
- [9] Perkampus H.-H.: *UV-VIS Spectroscopy and Its Applications*, Springer, ISBN 9783642774799, London (2012)
- [10] Stuart B. H.: *Infrared Spectroscopy: Fundamentals and Applications*. Wiley, ISBN: 978–0–470–85428–0, Chichester (2004)
- [11] Trzicinska B.: Writing materials examination in criminalistic research by FTIR spectroscopy, *J. Mol. Structure* Vol. 294 (1993), pp. 259–262, ISSN 0166–1280
- [12] Zuieba-palus J., Kunicki M.: Applications of the micro_FTIR spectroscopy, Raman spectroscopy and XRF method examination of inks, *Forensic Sci. Int.*, Vol. 158 (2006), p. 164–172, ISSN: 0379–0738

INSTRUMENTAL INVESTIGATION OF FOLD-CRACK RESISTANCE OF COATED PAPERS

Magdolna Pál¹, László Koltai², Sandra Dedijer¹, Srđan Draganov¹, Miloje Đokić³

¹ *University of Novi Sad, Faculty of Technical Sciences,*

Department of Graphic Engineering and Design, Novi Sad, Serbia

² *Rejtő Sándor, Faculty of Light Industry and Environmental Protection Engineering,
Óbuda University, Budapest, Hungary*

³ *University of Ljubljana, Faculty of Natural Sciences and Engineering, Slovenia*

Abstract: The folding process is one of the basic converting operations in graphic production and essentially it represents an extreme bending mechanism resulting in high and localized surface strains. If the surface layers become strained beyond their yield points, characteristic surface damages appear in form of crack lines along the folded edge of the paper which can lead to decreased aesthetic appearance of printed products or even to complete loss of functionality. Since the surface cracking of coated papers can have significant economic and environmental effects, the improvement of the fold cracking resistance of coated papers has become an important field of research. This study presents an instrumental analysis of fold-crack resistance of commercially available glossy coated paper conducted in order to determine the referent fold-crack measurements for the needs of developing a computer aided fold-crack evaluation method. The investigated papers are characterized by basis weight, thickness, ash content, surface roughness, tensile strength, tensile index and burst strength. For the fold-crack resistance evaluation methods based on residual tensile and burst strength of unfolded samples have been used. The obtained results showed that the residual tensile strength, as a commonly used fold-crack resistance assessment method can be employed for determination of overall surface damage amount, and due to the specific mechanism of Mullen-burst strength test it can derive relevant information about the structure of surface damages.

Key words: fold-cracking, coating, tensile strength, burst strength

1. INTRODUCTION

During the folding process papers and paperboards are subjected to extreme bending mechanism which is resulting in high-localized tension stresses on the outer side of the folded line (Sappi, 2006). Because the coating layer is not as flexible as the base paper, coated papers are more sensitive to surface cracking than uncoated (Eklund et al, 2002). Once formed, surface coating cracks usually propagate through the cross section of the folded paper resulting in notable loss of mechanical strength and jeopardizing not only the aesthetic feature of graphic product, but its functionality too (Salminen et al, 2009). The fold-crack resistance has become an important coated paper quality driven by constant raw material and production cost optimisation in paper industry and waste reduction in graphic industry (Alam et al, 2009). Along the mechanical characteristics in the last decades the visual appearance of folded coated papers were also evaluated, in the beginning by human experts, but by the time via computer aided image analysis (Barbier et al, 2003; Kim et al, 2010; Rättö et al, 2011; Yang and Xie, 2011; Sim et al, 2012). The positive features of this method are more than obvious, however significant deficiencies are noticed in its application (different sample preparation, digitalisation techniques and evaluation process) as well as in the used parameters for the quality assessment (basically just the overall amount of damage has been used in different form). The aim of this study was to gather results which can act as a kind of material-information and aid the development of a standardised and more sophisticated computer aided fold crack analyses.

2. MATERIALS AND METHODS

In order to simulate the increasing tendency of the surface damages according to Barbier et al. (2002), the coated paper samples were chosen with the same base paper fibre and coating composition, coating weight and applying technique (double and triple blade coating), but five different basis weights: 90, 115, 130, 150 and 170 g/m² (Symbol Freelifa Gloss, Fedrigoni). To achieve

better contrast between damaged and undamaged areas and to simplify image analysis procedure later on, the selected coated papers were printed with cyan ink in full tone coverage (100%). Printing process was done on KBA Rapida 75 offset machine with process ink World Series Cyan, Sun Chemical. 48 hours after the printing process, samples were folded in both paper fibre directions on Horizon AFC 544 AKT folding machine using one buckle folding unit with standard rollers and gap adjustment at standard climate conditions (temp. 23°C, RH 55%). The specimens prepared for this investigation split into three groups: not folded, folded along (MD) and perpendicular to (CD) the paper fibre orientation.

The basic properties of paper samples were measured on unfolded specimens according to the corresponding ISO and TAPPI standards. The basic information about the equipment used in this investigation are given in Table 1.

Table 1- Basic properties of used equipment

Characteristics	Used equipment
Basis weight	Mettler Toledo AE 200, measurement range of 50 mg up to 205 g, resolution: 0,1 mg
Thickness	Metrimpex, type 6-12-1/B, sample surface of 2 cm ² , load of 2 kg
Bendtsen roughness	PTA Group Paper Testing Association, Type Bendtsen Manual, N3500, sample surface of 10 cm ²
Ash content	Degetherm Easy 6, temperature of 525°C
Mullen burst strength	Lorentzen & Wettre Burst-o-matic, pressure range: 8-12 kp/cm ² , sample break detection within 10s
Tensile strength	Frank tensile testing machine, type 800A, No. 10, Karl Frank GMBH, at room temperature and standard RH, constant speed of traction displacement (30 and 40 mm/min), sample break detection within 20s ± 5s

According to Holik (2013) the fracture toughness can be determined by tensile and bursting strength test performed on intentionally damaged samples. Surface crack lines which arose during the folding process can be interpreted as intentionally damage on the specimens under controlled conditions and the obtained results of these strength tests can deliver useful information about the nature and behaviour of folded samples. The fold-crack evaluation, based on intentionally damaged specimens, was done on folded coated papers in both fibre orientations (MD and CD) by determining the residual tensile strength and Mullen burst strength.

The residual tensile strength is defined as the ratio of tensile break-up-strength of paper samples before and after folding according to the following equation (Barbier et al, 2003; Salminen et al, 2009; Yang and Xie, 2011):

$$RTS = FTS / UTS * 100 (\%) \quad (1)$$

where: RTS – residual tensile strength,
 FTS – folded tensile stress at break,
 UTS – unfolded tensile stress at break.

Mullen burst strength test of the folded papers did not require specific sample preparation or data processing. The burst strength is closely related to tensile strength (Ek et al, 2009) but more sensitive to paper structure compactness than tensile strength, therefore it can be a useful method to get insights of the folded paper structure and provide information about the changes (e.g. delamination) and damages in the base paper and coating layer caused by folding.

3. RESULTS AND DISCUSSION

The obtained results of basis weight, thickness, surface roughness, ash content and tensile strength with tensile index are first presented (Figure 1-6, respectively), followed by the gathered results of two fold-cracking assessment methods (Figure 7 and 8). Since the burst strength of unfolded and folded samples cannot be analysed separately, they are shown on the same graph. While the

number of specimens for all standard test methods was according the corresponding standards, the fold-cracking assessments were performed on 15 specimens per fiber grain directions (MD and CD), and the average values were calculated after the extreme values were eliminated. Although the deviations of basis weight of 150 g/m² and 170 g/m² were above the tolerance limit defined by the relevant standard, the measured basis weights (Figure 1) of selected papers have linear trend with the nominal basis weight with high coefficient of determination ($R^2=0.999$). The very low values of standard deviations indicate high consistency of measured values (the corresponding coefficients of variations are 1.59%, 0.87%, 1.40%, 1.01% and 1.07%, respectively for the nominal basis weights).

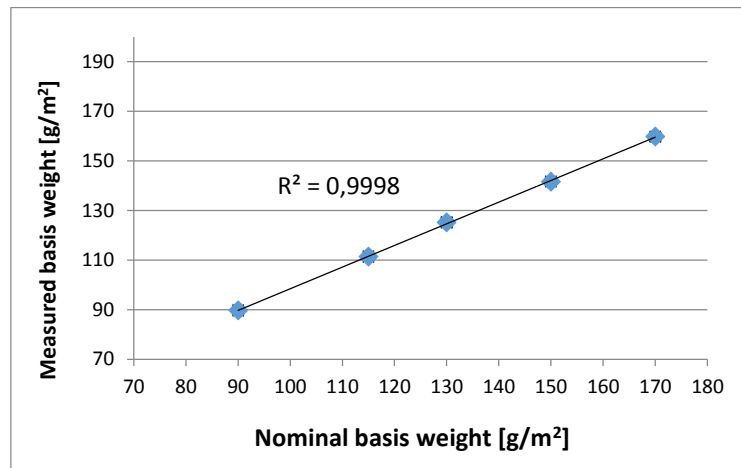


Figure 1: Nominal basis weight compared to measured basis weight of selected paper samples

According to Barbier et al. [2002] the amount of surface damages is expected to increase with the increase of sample thickness, therefore the thickness of the paper samples is an important characteristic for fold-cracking assessment. The obtained results of paper sample thickness (Figure 2) are also linearly correlated with the measured basis weights (with coefficient of determination $R^2=0.983$) with minor deviation for 150 g/m² paper, which is thicker than expected based on the rest of the samples. Deviations, even the small ones need to be taken into consideration at the analysis of the fold-crack assessment results.

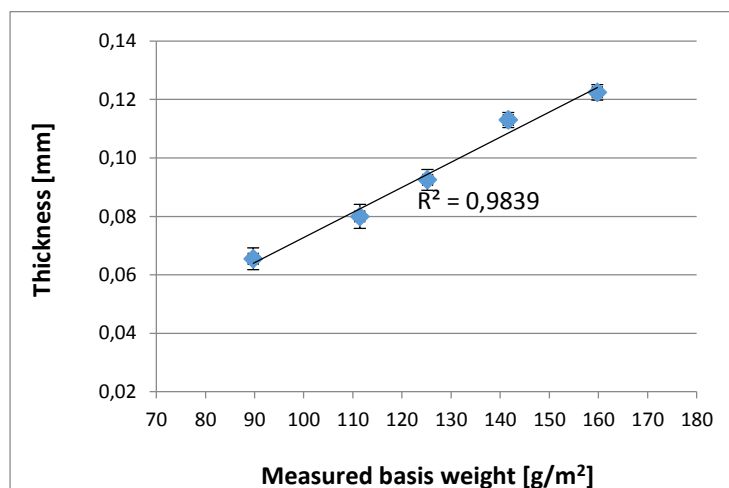


Figure 2: Thickness compared to measured basis weight of selected paper samples

The ash content of the selected papers shows their inorganic filler and coating content. It is usually expressed as a percentage (%) of the original oven dried weight of samples, but for the adequate graphic representation (Figure 3) in this investigation the ash content is expressed in grams, calculated from the ash content in % and measured basis weight of samples. Although the ash content does not have to grow with the increase of basis weight, but for the selected set of coated papers it can be seen that there is a strong correlation with the basis weight (coefficient of

determination $R^2=0.927$). The obtained results for 130 g/m² paper are significantly higher than for the other papers (45.63%, 5% higher than the rest of the paper samples). Increased ash content indicates thicker coating layer on samples with 130 g/m² and it is expected to have lower tensile strength and surface roughness.

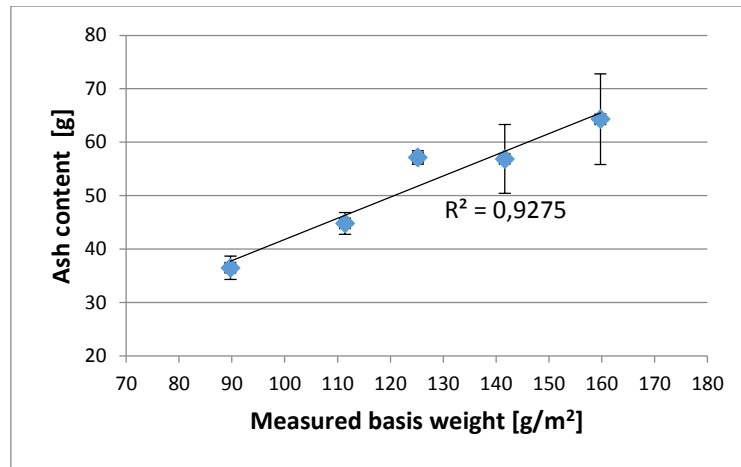


Figure 3: Ash content compared to measured basis weight of selected paper samples

The obtained results for surface roughness presented on Figure 4 are corresponding with the manufacturers' specification. Although the selected coated papers have identical base paper composition, coating weight and composition, application techniques as well as the number of the applied coating layers could not be the same for the whole group due to technical limitations (applying three coating layers for low basis weight). Therefore, the samples with 90 g/m² have just two coating layers which have resulted in significantly higher surface roughness compared to the other samples. The higher surface roughness may cause more noticeable mottling effect on the printed samples of coating paper, which can increase the false positive detection of surface damages during the fold-cracking assessment by digital image analysis.

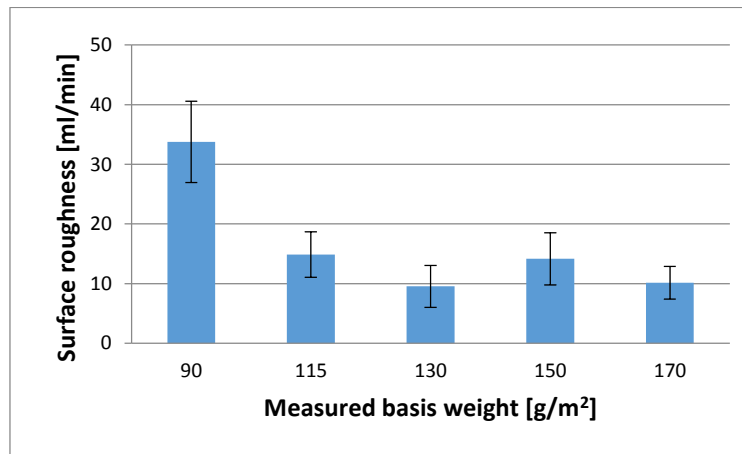


Figure 4: Surface roughness compared to measured basis weight of selected paper samples

The obtained results for the tensile strength of the coated papers presented on Figure 5 are in line with the referent values given by the manufacturer, but there are minor deviations. The low values of standard deviations measured values (all values of coefficient variation are less than 9%) indicate an uniform structure of the examined sample set. The lower value of coefficient of determination for samples in MD ($R^2=0.914$) can be explained by notable deviations for samples 90 g/m² (20% higher than reference values) and 130 g/m² (6.6% lower than reference values). Higher coefficient of determination can be seen for samples in CD ($R^2=0.944$) with minor deviations for 90 g/m² paper.

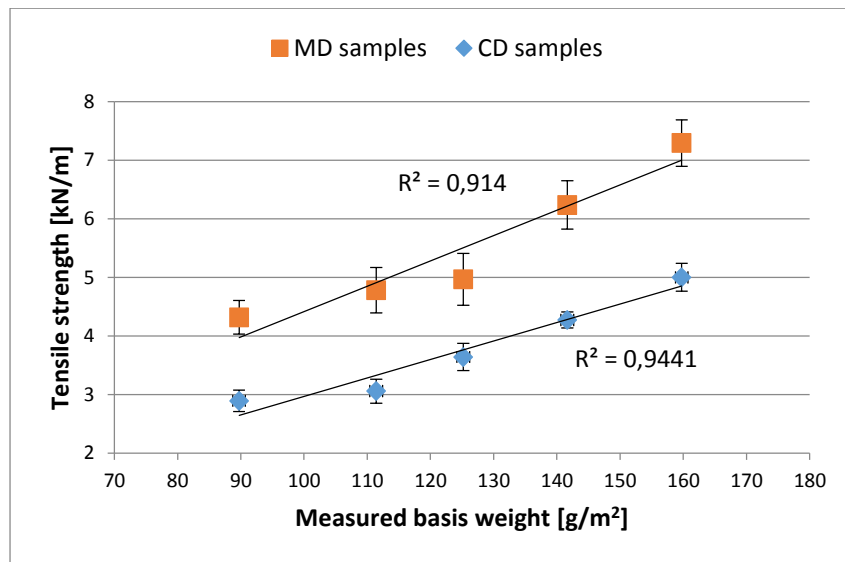


Figure 5: Tensile strength vs. measured basis weight of selected paper samples

Tensile index is a useful measure for comparing tensile strength of samples with different basis weight. The higher values of tensile strength for 90 g/m² papers are reflected on the tensile index values too, as it can be seen on Figure 6. The lower value of tensile index in MD for 130 g/m², driven by lower tensile strength for this group of samples, is also noticeable.

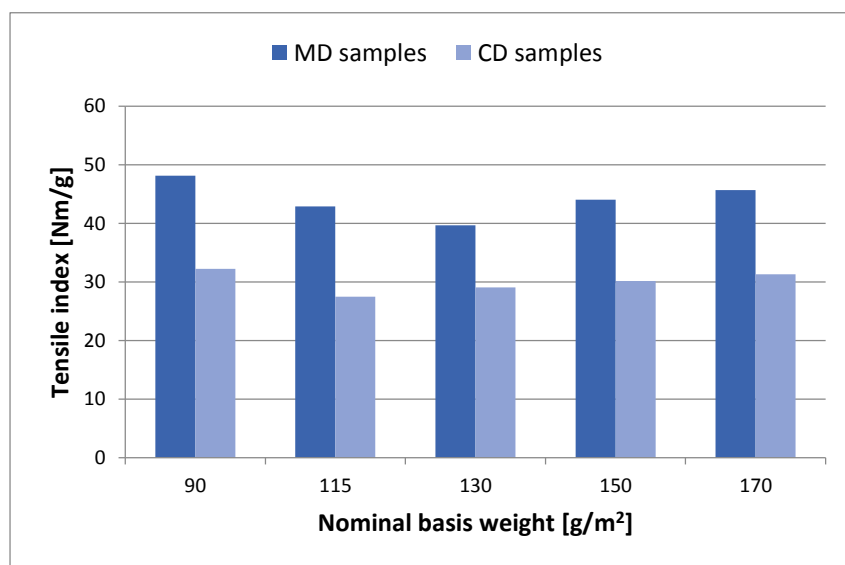


Figure 6: Tensile index by nominal basis weight of selected paper samples

Figure 7 presents the results of residual tensile strength which are in line with the literature findings and their mutual relation coincides with the conclusions presented in (Barbier et al, 2003; UPM, 2008; Yang and Xie, 2011; Sim et al, 2012). The decreasing tendency of residual tensile strength is more pronounced for CD-folded samples, than for the MD-folded ones. These differences in strength loss are governed by anisotropy behaviour of base paper during the folding process. By folding a coated paper in cross direction the localised surface stresses introduce more defects and damages than by folding along the paper grain (MD-folding), including not just the surface cracking of the coated layer, but the inter-fiber bond weakening and fiber damages in the base paper. The lower surface stresses, registered during MD folding, cause less damage in the fiber structure and the coating layer as well, so the overall strength loss for papers with MD folded line is less significant.

By analysing the obtained results and considering the fiber direction of selected coated papers, it can be seen that CD folded samples show a more unified tendency of tensile strength loss ($R^2=0.948$) than MD folded samples ($R^2=0.651$). As it can be seen on Figure 6, the 90 g/m² paper has much higher tensile index then the rest of the samples, which may cause higher residual tensile strength. On the presented graph it can be noticed also, that the residual tensile strength for samples of 150 g/m² and 170 g/m² are very close, indicating a similar surface damage level. This can be explained by the 150 g/m² paper is being thicker than it was expected based on its basis weight (see Figure 2), resulting almost the same amount of damages and strength loss as the 170 g/m² paper.

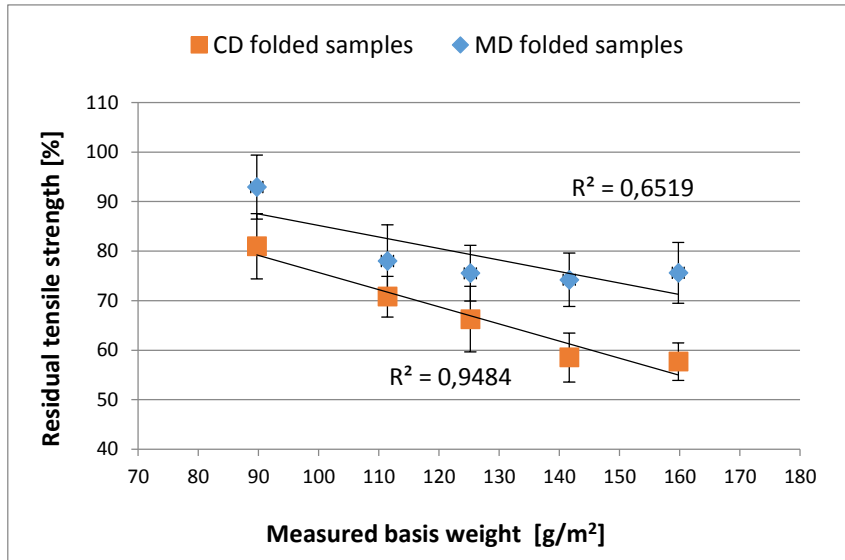
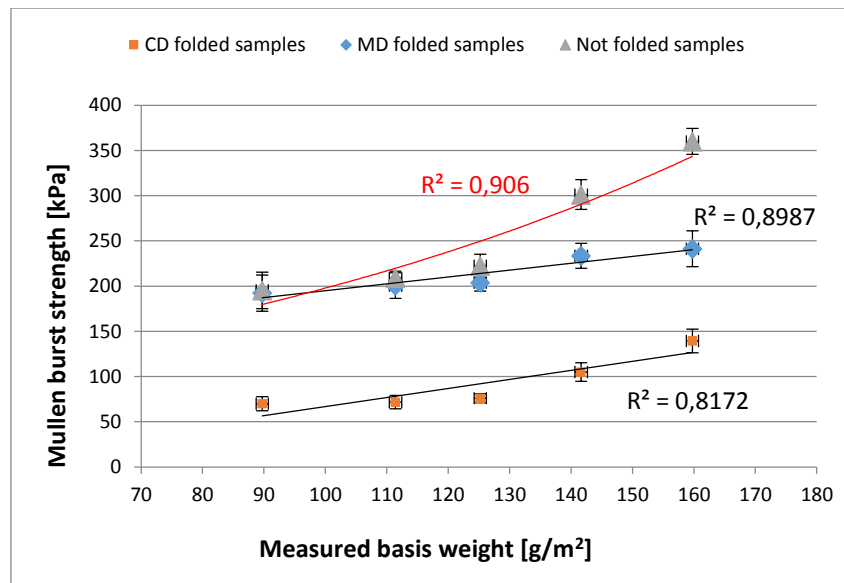


Figure 7: Residual tensile strength compared to measured basis weight of selected paper samples

The results of Mullen burst strength of all three types of paper specimens (unfolded, MD-folded and CD-folded) are graphically presented on Figure 8.



Figures 8: Mullen burst strength of unfolded and folded samples vs. measured basis weight of selected paper samples

According to the results of Mullen burst strength for unfolded samples, the influence of basis weight increase on the measured values of pressure at break is significant. These results were expected, since with the increasing basis weight of selected papers, the thickness of base paper has

also increasing tendency (but not linear) resulting in higher burst strength for the papers with higher basis weight. The range of measured burst strength corresponds to literature findings (Holik, 2013) and has a high correlation coefficient ($R^2=0.979$) for second order polynomial function. Minor deviation can be seen for the 130 g/m² samples, which was expected, since that paper has higher mineral content with thinner base paper (compared to other paper samples).

The burst strength of folded samples displays a similar pattern of decreasing as for the tensile strength regarding to the basis weight: samples with higher basis weight lost more in burst strength during the folding process than samples with lower basis weight. However, the strength loss tendency and ratio are different than for tensile strength. According to (Barbier et al, 2012) the shear stresses in the folded substrate can lead to delamination of the base paper, i.e. to weaken the internal bonds which directly affects the decrease in resistance to bursting. In addition, the coating cracks size and their distribution on the specimen's surface could have influence on the burst strength decrease, since one larger crack or few smaller concentrated on a certain segment of folded line could represent the weakest point in the specimen structure.

Differences in results derived from MD and CD folded samples (Figure 8) indicate that the fiber orientation during the folding process has great influence on the remaining burst strength: by parallel folding (MD samples) there is less burst strength compared with cross folding (CD samples). Based on the presented results it can be supposed that the damages on the MD samples with lower basis weight (90 and 115 g/m²) are mostly aesthetic defects including just minor surface cracks occurred only in the coating layer. For higher basis weight, along the coating cracks, delamination of base paper, minor fiber splits and fractures appear, resulting in mayor strength loss. Damages on CD folded samples pointed out more significant material destruction due to surface cracking and fiber fracture already for the papers with lower basis weights which are just emphasised by delamination for higher basis weight.

The obtained results follow linear trend of increasing the burst strength by the basis weight, with high values of coefficient of determination ($R^2=0.898$ for MD folded and $R^2=0.817$ for CD folded samples).

4. CONCLUSIONS

The presented investigation was aimed to material characterisation and instrumental investigation of fold-crack resistance of coated papers. For the needs of objective fold-crack assessment method improvement, the precise material characterization and referent fold-cracking assessment have great importance. The material characterisation included the basis weight, thickness, surface roughness, ash content, tensile strength, tensile index and burst strength determination. As referent fold-crack evaluation methods the residual tensile strength and the Mullen burst strength of folded samples were applied. Based on the obtained results, as a conclusion it can be conducted, that the damages occurred on the coated papers during the folding process can be assessed by tensile and burst strength testing, but their correspondence with the nature of damage are different. By tensile testing the obtained results could be used as referent measures for overall surface crack amount, while the burst strength is more appropriate for describing structure damages due to its sensitivity to the compactness of the base paper. Although the size of the coating cracks and their distribution on the folded line supposedly have influence on burst strength decrease tendency, based on the obtained result it could not be determined for sure.

5. ACKNOWLEDGMENTS

This work was supported by the Serbian Ministry of Science and Technological Development, Grant No.: 35027 "The development of software model for improvement of knowledge and production in graphic arts industry".

6. REFERENCES

- [1] Alam, P., Toivakka, M., Carlsson, R., Salminen, P., Sandås, S.: "Balancing between Fold-crack Resistance and Stiffness", *Journal of Composite Materials*, 43 (11), pages 1265–1283, 2009.
- [2] Barbier, C., Larsson, P.-L., Östlund, S.: "Experimental investigation of damage at folding of coated papers", *Nordic Pulp and Paper Research Journal*, 17 (1), pages 34–38, 2002.

- [3] Barbier, C., Larsson, P.-L., Östlund, S.: "Folding of printed papers: experiments and numerical analysis", Proceedings of International Paper Physics Conference 2003 (IPPC, Victoria, BC, Canada, 2003), pages 193-196.
- [4] Ek, M., Gellerstedt, G., Henriksson, G.: „Paper Products Physics and Technology, Pulp and Paper Chemistry and Technology“ (Vol. 4, de Gruyter, Berlin, 2009)
- [5] Eklund, J., Österberg, B., Eriksson, L., Eindenvall, L.: „Finishing of digital prints – a failure mapping“, Proceedings of the International Congress on Digital Printing Technologies 2002 (IS&T NIP 18, San Diego, California, USA, 2002), pages 712-715.
- [6] Holik, H.: „Handbook of Paper and Board“, Volume 1-2, Second, Revised and Enlarged Edition (Wiley-VCH, Weinheim, 2013), chapter 24.
- [7] Kim, C.-K., Lim, W.-S., Lee, Y. K.: "Studies on the fold-ability of coated paperboard (i): influence of latex on fold-ability during creasing/folding coated paperboard", Journal of industrial and engineering chemistry, 16 (5), pages 842-847, 2010.
- [8] Rättö, P., Hornatowska, J., Changhong, X. Terasaki, O.: "Cracking mechanisms of clay-based and GCC-based coatings", Nordic Pulp and Paper Research Journal, 26 (4), pages 485-492, 2011.
- [9] Salminen, P., Carlsson, R., Sandas, S., Toivakka, M., Alam, P., Roper, J.: "Combined Modeling and Experimental Studies to Optimize the Balance Between Fold Crack Resistance and Stiffness for Multilayered Paper Coatings – Part 2: Pilot Coater Experimental Studies", Proceedings of PaperCon 2008, (Tappi, Dallas, TX, USA, 2008), pages 2267-2303.
- [10] Sappi: "Folding and creasing", Sappi's Technical brochures, 2nd, revised edition, 2006. URL <http://www.na.sappi.com/documents/10165/13508/Folding+and+Creasing.pdf> (last request: 10th September 2014).
- [11] Sim, K., Youn, H. J., Oh, K.-D. Lee, H. L., Han, C. S., Yeu, S. U., Lee, Y. M.: "Fold cracking of coated paper: the effect of pulp fiber composition and beating", Nordic Pulp and Paper Research Journal, 27 (2), pages 445 – 450, 2012.
- [12] UPM: "Testing and selecting papers, Printing and Paper Fact Book – Sheet-fed offset press", Technical brochures, Edition 1, 2008.
- [13] Yang, A., Xie, Y.: "From Theory to Practice: Improving the Foldcrack Resistance in Industrially Produced Tripple Coated Paper", Proceedings of PaperCon 2011, (Tappi, Covington, Kentucky, USA, 2011), pages 1845-1858.

EFFECT OF THE APPLICATION OF METAL PRINTING INKS ON LAMINATION QUALITY OF PLASTIC LAYERS

*Erzsébet Novotny,
ANY Security Printing Company, Budapest, Hungary*

Abstract: In this study we made tests suitable for identifying potential problems related to lamination plastic layers that might occur when applying different metal inks and the results may provide assistance when choosing different types of ink that can be used in manufacturing of plastic cards in a reliable manner. Qualification analysis of processability of six screen inks of different colour and metallic outlook was carried out. Our examinations were primarily focused to screen printing inks, but as in the industrial practice it may happen that offset printing ink is applied on the screen printing ink layer, we carried out offset printing of a spot colour on the plastic foils screen printed previously. Based on measurement results of layer peel strength, layer adhesion, dynamic bending and torsion tests, it was established that out of the selected metal printing inks, the best laminating level can be achieved by using the gold coloured, UV curing two-component ink of Engler Company. It was also established that adhesion force between the layers of samples printed with screen inks only is higher than the adhesion force between the layers printed also with offset printing inks. Cause of this effect may be the ink layer applied during the wet offset printing process that interferes with fusing of the core and cover foils to a certain extent. This effect can be observed mainly at darker shades where tone value of the print elements is higher.

Key words: screen printing, metal printing inks, plastic cards

1. INTRODUCTION

Both customer requirements and technological opportunities justify the introduction of solutions, representing higher added value in the area of plastic cards as well. One of the solutions representing higher added value could be applying metal printing inks on print carriers. Thanks to technological developments and continuous improvements, different types of metal printing inks and newer and newer compositions have been appearing in the market and their testing and examination are essential if we would like to keep up with the changing market demand by outpacing our competitors. Screen printing process is one of the most versatile printing technologies that has almost unlimited area of application and variety of materials.

In accordance with the goal of the printing, printing inks should meet very diverse requirements. Each of the different print carriers requires inks that are suitable for them, so the ink should be selected in the knowledge of features of the material to be printed on. When using a specific ink, particle size of the pigments should be known; they should be minimum 25 times smaller than mesh count of the applied screen printing fabric. With the development of the packaging industry, textile manufacturing, and advertising industry, a very wide range of plastic print carriers is available and their quantity required by the market is getting higher and higher every year. Accordingly, in order to meet the requirements appearing in that area of screen printing, quick-drying, well-adhering inks with proper abrasion resistance had to be developed. Different polymer based (e.g., PVC based) inks meet the aforementioned requirements and they are readily used for printing other materials as well. In these inks, bonding agent of the pigments is pre-polymerized plastic and their drying and curing takes place on the printed surface through chemical or photochemical (UV radiation) reactions; for the purpose of achieving better ink spreading, these inks also contain a small quantity of solvent that evaporates from the layer after printing within a short period of time. Knowledge of the print carrier material is also important because the more similar of the bonding agent of the ink to the carrier, the higher the quality of products are. For example, abrasion resistance of a PVC foil printed with PVC based ink is good, while applying the ink on other types of carriers the abrasion resistance might decrease.

Screen printing inks containing metal particles are well processable with screen printing. Metallic effect appearing on the surface of the print is created by pigments forming a coating because they reflect incident light illuminating them in the same angle as the angle of incidence in an orderly manner.

Metallic pigments (e.g., planar aluminium particles) can also be considered as small mirrors. When mixing these mirrors into the ink and preparing the print, a large mirror is created. The more successful of the creation of ordered arrangement of these particles parallel to the surface of the of the carrier so that they cover approximately 100 % of the surface, the more perfect of the achieved metallic effect is. Magnified prints of the six used metal particles containing printing inks are shown in Figure 1.

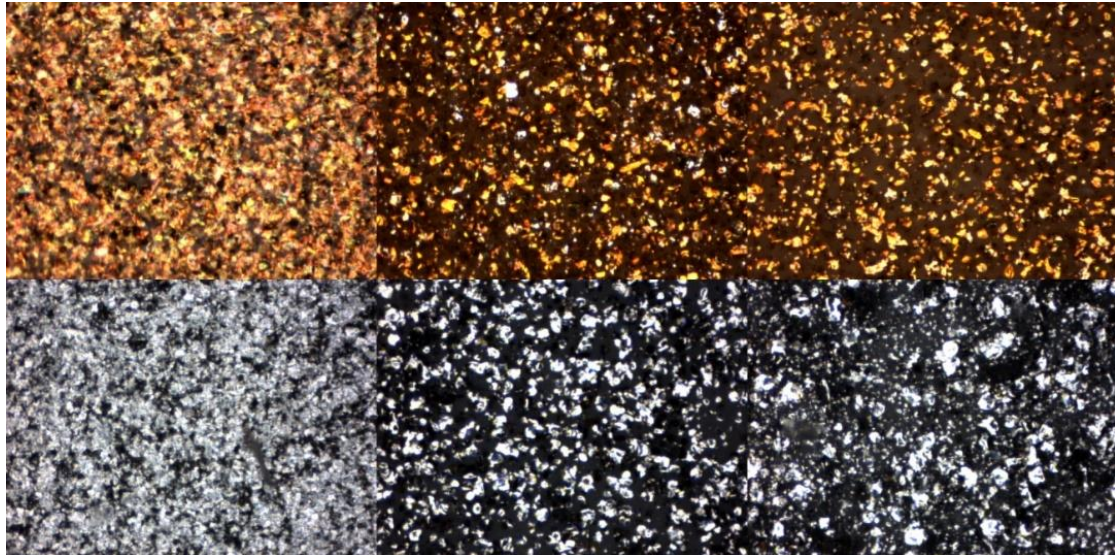


Figure 1: Print samples of the tested metal screen printing inks (magnification: 190x)

2. TEST PRINTING

2.1 Raw materials used for test printing

During the tests, every effort was made to obtain results that can be used in practice directly, so the most widely used plastic foils were included in the examination. We would like to find metal particles containing screen printing inks that can be used together with these foils in a reliable manner. Raw materials used in the tests and their features are shown in Table 1.

Table 1: Foils used in printing

	Cover foil	Core foil (front side)	Core foil (back side)
Manufacturer	Klöckner	Klöckner	Klöckner
Thickness	80 µm	310 µm	350 µm
Type	CCM 278/01-51/8800-494-SB6-80	CC-M230/56-04/0130-493-COP-310	CC-M230/56-04/0130-493-COP-350

2.2 Inks used in printing tests

When choosing the screen printing inks, graphical trends, foreseeable market requirements, printer carriers to be used and characteristics of our screen printing machine were taken into consideration. Description and features of the selected silver and gold screen printing inks are summarized in Table 2.

Table 2: Types of screen printing inks and mesh-fiber amounts applied in the printing

Colour an No of ink	Manufacturer	Type	Curing mode	Mesh-fiber/cm
Gold 1	Apollo	S.3616 Laminating M/C Gold	By solvent	48
Gold 2	Sun Chemical	JS9MM00076: SSM8655 Special Gold: DK 02	UV curing	90
Gold 3	Engler	UV Card Effect Gold AN-MC D007999 + Gold Powder	Two-component, UV curing	90
Silver 4	Apollo	S.2494 Laminating Silver	By solvent	48
Silver 5	Card Effect	UV Silver 205	UV száradású	77
Silver 6	Engler	UV Card Ink Base Metallics D006005 + Powder Preparation C007203x - Silver 203	Two-component, UV curing	77

Primarily, our tests were aimed at testing the suitability of the screen printing inks but, as in practice, screen printing is not the exclusive method when manufacturing plastic cards, a Pantone® colour was also printed on each foils by using offset printing technology (Table 3).

Table 3: Offset printing inks used in the examination

Colour and No of ink	Manufacturer	Type	Curing mode
Pantone 4625 (for gold plastic cards)	Siegwerk	UV Sicura Plast 3.770	UV curing
Process Black (for silver plastic cards)	Siegwerk	UV Sicura Plast 3.770	UV curing

2.3 The manufacturing process of test cards

When applying screen printing, the sheets of 500 x 300 mm were used similarly to manufacturing of plastic cards. Printing operation was completed on a screen printing machine of SPS G1+ type at and speed of 550-2200 sheets/hour by using the amount of fiber of screen mesh matched to the sizes of pigment particle sizes of the used inks, in accordance with the recommendations of the ink manufacturers (Table 2), (Figure 2).



Figure 2: SPS G1+ Type Screen Printing Machine

In accordance with the graphical image to be printed on the test cards, first the full colour surface suitable to the card dimensions was printed to the print carrier then the graphical image was printed to some of these prints by offset printing.

Colours Pantone® 4625 and Pantone® Process Black were used for overprinting the gold and silver cards, respectively; these colours were prepared by mixing the inks of the same type and originating from the same manufacturer. Printing machine used was a sheet-fed offset printing machine of Heidelberg Speedmaster SM 52-4+L type.

After the printing phases, core and cover foils were collated in proper sequence and positions. The resulted four-layered sheet structures were laminated by a laminating machine of Bürkle CHK100/200 under laminating conditions shown in Table 5.

As type tests have not been carried out yet in the area of overprinting layers of metal screen printing inks by offset printing under similar conditions, laminating the printed sheets were performed at two different temperatures (140°C and 150°C) while using the same pressure force.

Table 4: Parameters of the laminating process

Parameters	Pre-heating/heat pressure	Heat-pressure main phase	Pre-cooling	Cold-pressure main phase
Time (minutes)	3	18	3	15
Temperature (°C)	140	140	50	21
Pressure (N/cm ²)	80	160	50	240

After completing the lamination, plastic cards of standard sizes (85,6 x 53,98 mm) were punched out from the laminated sheets with a step punching machine of Mühlbauer CP 2021/M type. Finally the punched plastic cards were equipped with holograms, signature panels and chips. (Figure 3)



Figure 3: Completed overprinted plastic cards with added, applied materials

3. EXAMINING THE TEST CARDS, MEASUREMENT RESULTS

3.1 Layer strength/layer adhesion measurement

After lamination, test specimens were punched from the laminated test sheets by types in accordance with the specifications included in Point 5.3.2. of the Standard No. ISO/IEC 10373-1:2006(E), then the layer strength/layer adhesion measurements were carried out using Zwick/Roell BDO-FBO 0.5 TS Tensile strength measuring device (Figure 4). The test specimens were an approximately 10 cm long strip, width of which was 10.0 ± 0.2 mm that was punched from the laminated sheet. (Before the lamination, a foil of 3 x 6 cm was placed between the layers to be tested that prevented fusing, so that we could clamp the cover foil in the pulling unit of the equipment.)

Measuring parameters of the instrument were set to the values specified in the relevant standard. Rate was 300 mm/min. Evaluation of the results was done by following the procedure specified in Point 5.3.3. of the Standard No. ISO/IEC 10373-1:2006(E). A result that is below 3.5 N/cm, which is a value is determined in the Standard, was qualified as "not acceptable".



Figure 4: Zwick/Roell BDO-FBO 0.5 TS Tensile strength measuring device

A comparative diagram was prepared from the test results in order to make the differences of adhesion forces existing between layers of the sheets manufactured with different parameters easier to survey. Evaluation of the results measured at different types of card specimen is summarized in Table 5.

Table 5: Summary of results of the layer adhesion tests

Colour and No of inks	Manufacturing mode	Peel/tensile strenght [N/cm]				Adequate > 3.5 N/cm ()
		#1	#2	#3	Mean	Inadequate < 3.5 N/cm ()
Gold 1	Screen print only	7.28	7.21	6.56	7.02	
	Screen and offset print (with 140°C laminating temperature)	6.10	6.05	7.05	6.40	
	Screen and offset print (with 150°C laminating temperature)	5.75	5.03	3.44	4.74	
Gold 2	Screen print only	7.84	7.62	7.13	7.53	
	Screen and offset print (with 140°C laminating temperature)	9.72	12.15	8.47	10.11	
	Screen and offset print (with 150°C laminating temperature)	9.72	14.70	11.36	11.93	
Gold 3	Screen print only	11.11	10.50	10.46	10.69	
	Screen and offset print (with 140°C laminating temperature)	3.43	4.52	4.37	4.11	
	Screen and offset print (with 150°C laminating temperature)	6.80	10.84	11.02	9.55	
Silver 4	Screen print only	7.33	8.01	6.68	7.34	
	Screen and offset print (with 140°C laminating temperature)	6.18	3.60	6.00	5.26	
	Screen and offset print (with 150°C laminating temperature)	4.61	5.39	6.46	5.49	
Silver 5	Screen print only	4.55	5.63	5.35	5.18	
	Screen and offset print (with 140°C laminating temperature)	4.01	3.72	4.18	3.97	
	Screen and offset print (with 150°C laminating temperature)	5.41	4.28	5.61	5.10	
Silver 6	Screen print only	8.47	8.17	8.05	8.23	
	Screen and offset print (with 140°C laminating temperature)	4.61	5.15	4.52	4.76	
	Screen and offset print (with 150°C laminating temperature)	2.65	3.98	4.38	3.67	

It can be established clearly from our diagrams, that adhesion force existing between the layers of the samples printed by screen printing only are higher than the force between the layers of sheets overprinted by offset technology (Figures 5-7). This can also be seen from the fact that all of the adhesive force levels measured at screen printed and offset printed cards laminated at different temperatures are lower than the respective results measured at the cards prepared by screen printing only. Cause of this effect may be the ink layer applied during a wet offset printing process that interferes with the level of fusing the core and cover foils to a certain extent. This effect can be observed mainly at darker shades as it was confirmed by the results of our former studies.

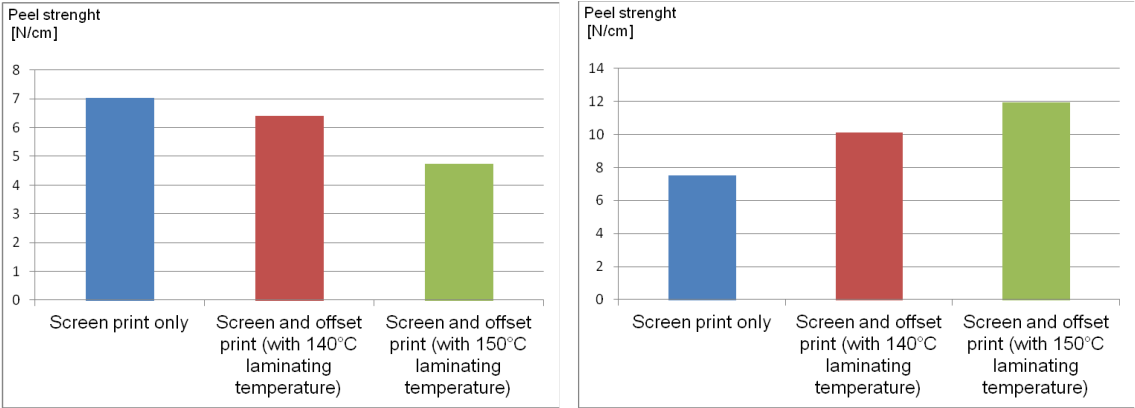


Figure 5: Diagram of peel/tensile strength results of Gold 1 (left) and Gold 2 (right) samples

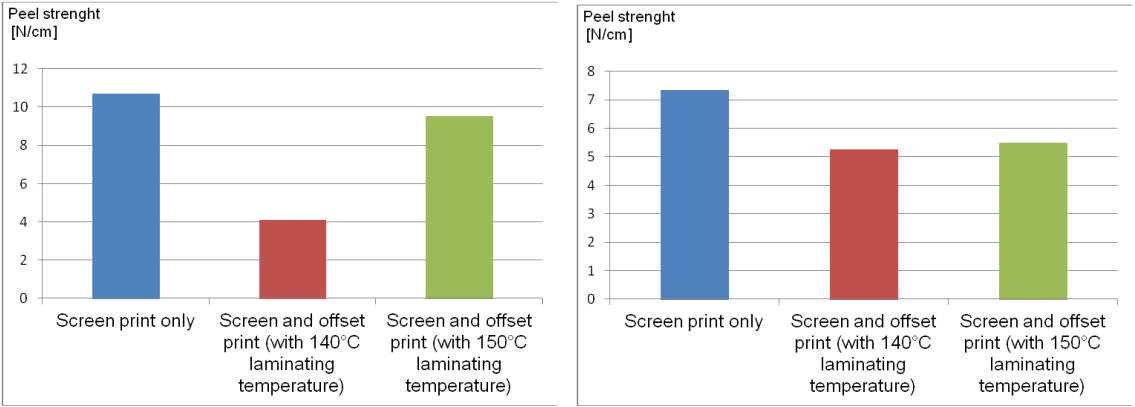


Figure 6: Diagram of peel/tensile strength results of Gold 3 (left) and Silver 4 (right) samples

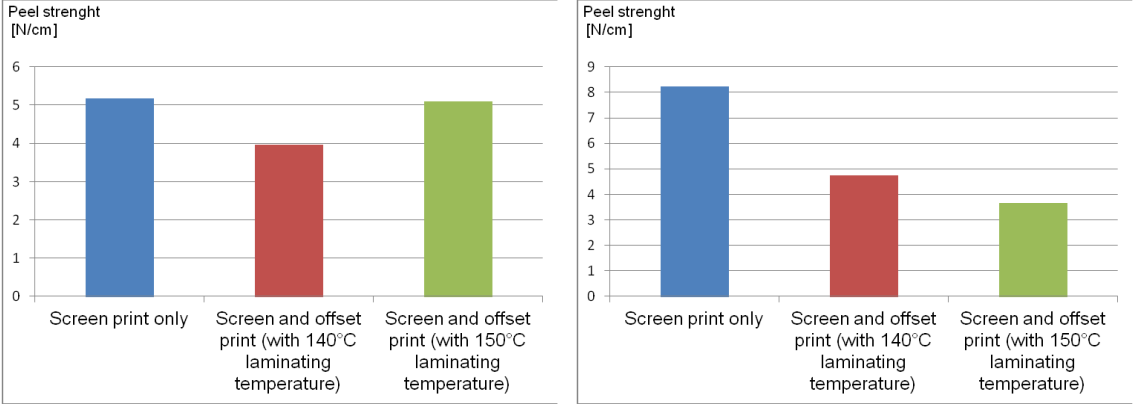


Figure 7: Diagram of peel/tensile strength results of Silver 5 (left) and Silver 6 (right) samples

Specimens punched from the sheet Gold 2, prepared by using screen printing ink of Sun Chemical Company are exceptions to this rule; in the case of these samples the adhesion result of samples printed by offset printing were higher. This was observed because of a special additive used by the manufacturer in this screen printing ink that improves fusing.

Based on our experience, the highest adhesive force was found at the Gold 3 card that is the best level of laminating level can be achieved by using the gold coloured, UV curing binary ink of Engler Company. Minimum adhesion value of 3.5 N/cm, specified in the Standard ISO 7810:2003 is met by all the specimens that were printed by screen printing technology only.

It can be concluded from the above, that the UV curing ink used in offset printing has more significant adhesion reducing effect than of the screen printing inks constituting the basis of the tested sample cards.

3.2 Dynamic bending test

The test was carried out in accordance with the procedure specified in Point 5.8.2. of the Standard No. ISO/IEC 10373-1:2006(E) by Mühlbauer SCF 2300 dynamic bending equipment at a frequency of 0.5 Hz. The whole test, which consisted of 4000 cycles, was executed in four phases in which bending directions and positions of the card were modified. According to the Standard, at the end of the test the card should not be broken and the chip should work in the ATR test. Results are shown in Table 6.

Table 6: Summary of the results of dynamic bending tests

Colour and No of inks	Card position				Number of cycles	Fracture, material separation	ATR test result
	Chip position		Bending direction				
	Up	Down	Longitudinal	Transverse			
Gold 1	x		x		1000	-	OK
		x	x		1000		
	x			x	1000	x	OK
		x		x	1000		
Gold 2	x		x		1000	-	OK
		x	x		1000		
	x			x	1000	x	OK
		x		x	1000		
Gold 3	x		x		1000	-	OK
		x	x		1000		
	x			x	1000	x	OK
		x		x	1000		
Silver 4	x		x		1000	-	OK
		x	x		1000		
	x			x	1000	x	OK
		x		x	1000		
Silver 5	x		x		1000	-	OK
		x	x		1000		
	x			x	1000	x	OK
		x		x	1000		
Silver 6	x		x		1000	-	OK
		x	x		1000		
	x			x	1000	x	OK
		x		x	1000		

The tested cards resisted to bending in longitudinal direction, no breaking or flaking off any material was observed. Cards exposed to transversal bending cracked or, in some cases, broke at the lower part of the chip. Visible cracks were more apparent on the backsides of the cards than on their front sides. Proper operation of the chip was not affected by these cracks. Based on the results found it was concluded that resistance of the basic cards are not, or only hardly, affected by the screen printing inks, and cracks and breaks are usually occur because of improper quality of the print carrier or the cover foil.

3.3 Dynamic torsion test

The test was carried out by using a dynamic torsion equipment of Mühlbauer SCT 2400 in accordance with Point 5.9.1. of the Standard No. ISO/IEC 10373-1:2006(E). The test was carried out in accordance with the procedure specified in Point 5.9.2. of the Standard No. ISO/IEC 10373-1:2006(E) at a frequency of 0.5 Hz and it consisted of 1000 cycles. At the end of the test, the card should not be broken and the chip should work in the ATR test.

When choosing the samples to be tested, the first sample was taken when punching the first sheet, the second, third and fourth samples were taken during the manufacturing process at the same intervals and the fifth sample was taken when punching the last sheet. Comparisons of the measurement results by card types are shown in Table 7.

Table 7: Summary of the results of dynamic torsion tests

Colour and No of inks	Number of cycles	ATR test result	Fracture, material separation
Gold 1	1000	OK	Not observed
Gold 2	1000	OK	Not observed
Gold 3	1000	OK	Not observed
Silver 1	1000	OK	Not observed
Silver 2	1000	OK	Not observed
Silver 3	1000	OK	Not observed

Based on the data shown in the table, it can be established that none of the cards cracked or broke and the chip operated properly during the ATR test after this stress as well. Based on the results found it was concluded that resistance of the basic cards are not, or only hardly, affected by the screen printing inks.

4. SUMMARY OF THE RESULTS

Qualification analysis of workability of six screen inks of different colour and metallic impression were carried out. We have made sure that the inks are applicable and we got an overall picture of the possible problems that may occur during the manufacturing process. Due to the customer demand we printed graphic design by offset printing process as well. The results obtained when testing card laminates also contained offset printed layers. They were compared to the results of laminated layers that consisted of screen printed ones only. Based on the tests carried out, it was established that these tests are suitable for identifying potential problems related to the fusing of plastic layers that might occur when applying different metal inks and can provide assistance when choosing different types of ink that can be used in reliable manufacturing of plastic cards. Based on the results of the completed layer strength, layer adhesion, dynamic bending and torsion tests, it was established that out of the selected metal printing inks, the best fusing level can be achieved by using the gold coloured, UV curing two-component ink of Engler type. It was also established that adhesion force between the layers of samples printed with screen inks only is higher than the force between the layers printed also with offset printing inks. Cause of this effect may be the ink layer applied during a wet offset printing process that interferes with fusing the core and cover foils to a certain extent. This effect can be observed mainly at darker shades where the tone value of the print elements is higher.

5. ACKNOWLEDGEMENTS

Thanks my colleagues Krisztián Nagy and Panna Filóci for measurements and taking part in examinations.

6. REFERENCES

- [1] Aestor: "Festékbevonat vizsgálatok" http://www.atestor.hu/Festek_bevonat_vizsgalat.html [last request: 08. 04. 2014]
- [2] CQM: Infrastructure Quality Requirements 1.9D, 2004
- [3] CQM MasterCard: "System certification" http://www.telefication.com/index.php?option=com_content&view=article&id=132:mastercard&catid=56:system-certification&Itemid=159 [last request: 08. 05. 2014.]
- [4] ISO/IEC 10373-1:2006 Identification cards – Test methods – Part1: General characteristics, 2006
- [5] ISO/IEC 7810:2003 Identification cards – Physical characteristics, 2003
- [6] SEFAR AG: "Szitakönyv – Kézikönyv szitanyomók számára" Magyar Szitanyomók Szövetsége, Budapest, 2001

Print Quality

HEXACHROME SYSTEM MODIFICATION FOR A PROTOTYPE SCREENPRINTING REPRODUCTION

Antonios Tsigonias¹, Konstantina Siarampalou¹, Georgia Politou¹, George Gamprellis¹,
Anastasios Politis^{1,2} & Marios Tsigonias^{1,2,3}

¹ TEI of Athens, Department of Graphic Arts Technology, Egaleo, Greece

² Hellenic Open University, School of Applied Arts, Patra, Greece

³ National Center of Scientific Research "DEMOKRITOS", Athens, Greece

Abstract: In this paper we present the first results of the research, attempted to enhance the basic CMYK colour gamut by adding two more colours (Orange and Green) for the accurate reproduction of Artwork material with the screen printing method. In fact, the basic principles of the Hexachrome™ (Pantone Trademark) were used for offset reproduction (CMYKOG).

The addition of the two inks provides better visual effect versus CMYK reproduction. The same observation could be stated by comparing the two colour spaces that were produced. The enlargement of the colour gamut by adding green (G) and bright orange (O) is obvious and the reproduction produces more bright and light colours compared to the CMYK colour gamut.

The whole procedure included three basic challenges which are Ink formulation, Colour standardization and Moiré settlement in order to yield some fruitful results.

For the ink preparation, the basic CMYK inks were used in order to be modified for the final production of the $C_hM_hY_hK_h$ inks. It is obvious that Hexachrome™ inks do not have the same colour characteristics with the CMYK inks that are used in common separations. For the modification of the 4 basic inks and the formulation of the orange (O) and green (G) inks that were finally used, some basic colour inks were used combined with some basic pigments such as Rodamine Red, Rubine Red and fluorescent pigments.

In the six-colour separation procedure the first technical issues occurred: raster angle, mesh angle, mesh count, undercutting effect were some of the problems that had to be considered. In the preliminary study many techniques were tested in order to reduce or to eliminate the moiré phenomenon. Finally a modified single angle printing technique was suggested and the moiré phenomenon was reduced, almost eliminated, in acceptable limits.

For the colour standardization of the produced inks a Gretag MacBeth SpectroEye was used in order to depict the spectra and to measure the $L^*a^*b^*$ values of the produced inks. A colour differentiation (ΔE) between the Hexachrome™ prototype targets and the screen printing formulated inks below 3,0 was defined as the acceptable colour error limit.

The results of this study were encouraging and gave us the opportunity to standardize the screen printing reproduction of an Artwork without taking into account the Artwork itself but the methodology that was developed. As it was shown most Artworks could be reproduced with high colour accuracy depending on the methodology but not the Prototype material that was used. The colour gamut of the Artwork that was reproduced was satisfactory extended in comparison to the classical four colour screen printing reproduction.

Key words: Hexachrome™, Screen printing, Artwork reproduction, Ink formulation, Accurate colour reproduction

1. INTRODUCTION – STATE OF THE ART

1.1 Hexachrome™ and offset printing

In 1995 Pantone has presented Hexachrome™ that is a six-colour colour separation and printing process in which additional to the custom CMYK inks, orange and green inks are used to expand the colour gamut, for better and more accurate colour reproduction. Hexachrome™ is also referred as the CMYKOG process. It provides dramatically improved colour range and accuracy over four colour process printing.

The special ink set developed by Pantone, is purer than traditional ink sets and consists of enhanced versions of the subtractive primaries yellow, magenta and cyan, along with black, vivid orange and green. In addition to utilizing the six-colour set to print in Hexachrome™, the CMYK components can be utilized for four-colour jobs with enhanced results (Jeffrey, 1995).

Hexachrome™ is capable to reproduce over 90% of solid Pantone Matching System Colours, almost twice the gamut that could be obtained by using conventional four-colour process printing. By the use of only six basic colours, Hexachrome™ generally eliminates the necessity of printing additional spot colours.

Hexachrome™ has been used with great success on sheetfed offset presses since its inception in 1995 for a variety of projects including packaging and posters, and since 1998 it is used on high-volume webfed offset presses for projects such as catalogues (www.pantone.com).

1.2 Stochastic Screening

For the last 100 years or more, the typical method for creating halftones and process screens was to modulate the screen area by changing the size of halftone dots that are in an ordered pattern in a given area. This method is known as Amplitude Modulated (AM) screening.

Stochastic Screening or else Frequency Modulated (FM) screening was developed in an attempt to solve quality issues such as moiré associated with conventional screens. In stochastic screening, the screened image is created by dots (20 micron, 10 micron) placed according to a *pseudo-random* distribution of halftone dots, using frequency modulation (FM) to change the density of dots according to the gray level desire. (Johansson et al, 2007)

With the stochastic screening technology, four-colour screening is no longer conducted with determined angle axis per colour as with the traditional screening, therefore it eliminates screening moiré. Also, rosette patterns are no longer created. Due to the very small size of the halftone dots the quality of the printed product can be compared to that of photographic prints and eco-fonts can be easily used. (Tsigonias, 2002; Johansson et al, 2007)

Many printers assume that stochastic screening is used exclusively for hi-fi but this is not the case of Hexachrome™ which repeats two of the screen angles to eliminate a moiré pattern that is observed with conventional screenings. Orange is printed at the same angle as cyan and green is printed at the same angle as magenta. (Fry, 1999).

The use of Hexachrome™ separations has been proposed in the past for high quality packaging printings in combination with Stochastic Screening. Stochastic Screening is used in order to solve the moiré phenomena that occur in the AM separation methods especially for printing techniques that involve more than 4 axis settlements of the printed ink dots (gravure cell orientation, anilox engraving, screenprinting mesh). (Tsigonias, 2001)

1.3 Single Angle Screening

An alternative way to avoid moiré and rosette patterns, that are common to the multi-angle screening is to print all of the halftones at the same angle with the dots printed on top of each other. This technique is known as dot-on-dot method and was introduced in the market in 1980 by Chemco Photoproducts as a separation method for newspapers. Dot-on-dot method offered improved colour reproduction, produced smoother colour reproduction on newsprint and gave the appearance of using a finer line screen. The main disadvantage of using dot-on-dot method is quite obvious: high risk of misregistration. Another disadvantage is that with the dots on top of each other, a much lighter tone would be reproduced cause of the larger area of unprinted white paper (spare white space). This fact is explained satisfactory since light absorption of two inks overprinted is less than the sum of the light absorptions of the ink individually. However the colour variations were much less noticeable on newsprint paper than fine papers cause of the high dot gain level of the printing method that leads to dot edge blurring. In dot-on-dot screening all colour dots are addressed in an angle of 45 degrees (or any other direction depending on the printing method). (Latanision, 1992)

Another halftone screening method which is similar to the dot-on-dot method, is the Staggered Position One-Angle technique. The staggered position technique is a modification of dot-on-dot method in which its advantages are maintained and its shortcomings are eliminated. Staggered technique uses a 45 degrees angle for all four separations and slight offsets in the horizontal and vertical dimensions to cause the dots to be arranged at the corners of squares with a different colour at each corner. The staggered position technique was reported to have several advantages over both the dot-on-dot and multi-angle halftone screening methods since it has the same advantages as dot-on-dot printing, preserves colour better in the shadows than both dot-on-dot and conventional angling cause black ink does not overprint the other colours so much, works with any dot shape and is requires less code than alternative screening methods. (Latanision, 1992)

Another advantage of the staggered position technique is that the order in which colours are laid down has little or no effect on the appearance of the colour. (Kang, 1999). The most reported disadvantage of the staggered position technique is the same colour variations due to misregistration (Latanision, 1992). Furthermore, it has limited applications in printing cause dot overlap occurs when the area coverage of the combined inks is greater than 100%. (Kang, 1999) Finally Flamenco is a modified form of staggered position technique. Flamenco is somewhere between the dot-on-dot and the dot-off-dot method (staggered position). The idea behind flamenco screening is to keep the same angle but shift screens by a certain distance. All four grids are laid right next to each other, offset by some number of pixels. Flamenco screening is sensitive to position errors, such us dot misregistration and shifting of halftone grids. (Kang, 1999)

2. PURPOSE OF THE CURRENT STUDY - METHODOLOGICAL APPROACH

The purpose of this study is to transfer expertise from offset printing reproduction to screen printing technique in order to solve the problems that are presented during the accurate reproduction of an artwork or the high quality commercial reproduction of multicolour screenprints. The methodological approach for this study included a literature review among the past efforts to transfer technology from offset printing to screen printing process colour reproduction. In the next phase a deep and comprehensive analysis of the capacities of the Pantone Hexachrome™ system led us to the conclusion that through this system the principal silkscreen printing problems could be arranged. The principal moiré problem is growing for screen printing technique cause of the existence of an additional mesh axis parameter. Two possible solutions where examined: Stochastic Screening and Single Angle Screening. The second solution was preferred to be used in the experimental printings of the study cause of the limitation of the screen printing technique to deposit too small dots on the substrate without losing details or show a strong dot loss effect.

3. INK FORMULATION

For the formulation of screen printing inks that were used in the Hexachrome™ experimental reproduction a high accuracy balance was used in order to achieve a satisfactory repeatability. For the formulation of the screen printing CMYKOG inks, pigments and basic inks of many different industries were added to the basic Unico Transparent Base. Finally the basic colour characteristics and a ΔE below 3,0 were achieved for most inks as mentioned in the paragraph 5 of the current study.

Table 1: Ink Formulation for the repeatable Hexachrome™ Screen printing reproduction

Cyan Hexachrome™	Magenta Hexachrome™
53,39 % Transparent Base Unico	56,31 % Transparent Base Unico
40,77 % Cyan 4c Process Unico	40,77 % Magenta 4c Proc Unico
3,88 % Magenta 4c Process 397 Kian	1,95 % Yellow 4 c Process Unico
0,98 % Yellow 4 c Process Unico	0,97 % Rubine Red 47 Pigment Engler
0,64 % Rubine Red Pigment Engler	
0,34 % Rosa Pigment Engler	
Yellow Hexachrome™	Black Hexachrome™
25,64 % Transparent Base Unico	67,15 % Transparent Base Unico
66,69 % Yellow 4 c Process Unico	22,45 % Black 4c Process Unico
3,75 % Fluo Yellow Pigment Engler	6,85 % Cyan 4c Process Unico
2,05 % Magenta 4c Proc 397 Kian	2,22 % Magenta 4c Process Unico
1,53 % Giallo No 112 Sirpi	1,33 % Green Basic 623 Apollo
0,34 % Rosa Pigment Engler	
Orange Hexachrome™	Green Hexachrome™
41,96 % Transparent Base Unico	79,21 % Transparent Base Unico
10,56 % Transparent Base Kian	9,31 % Green No 60 Engler
23,01 % Yellow 4 c Process Unico	8,39 % Green Basic 623 Apollo
19,22 % Orange 300 Pms Engler	2,79% Yellow 4c Process Unico
5,25% Fire Orange 312 (fluo) Kian	0,30% Rubine Red 47 Pigment Engler

4. SOLVING MOIRÉ PROBLEMS

4.1 Stochastic Screening Vs Single Angle Screening

As it is referred in the Introduction of this study both techniques Stochastic and Single Angle Screening could be used in order to solve the moiré phenomenon. Moiré occurs of the sequential overprint of six inks at different angles to each other, and the contribution of the direction of the mesh threats to the phenomenon. (Abbott, 2008) The study of the performance of these different screening techniques and their capacities is a very interesting issue but it is a matter of future study. Our choice to use Hybrid Single Angle Screening as an effort to minimize moiré phenomena was based on the simple thought that even Stochastic Screening was an attractive solution we would have to work with very small dots in large areas which poses a serious risk to have major dot loss on highlights and dot gain on Shadows (Hippopotamus Effect).

4.2 Technical Information about mesh and screen ruling selection

For this project a Yellow mesh was chosen for all the printing screens. Yellow meshes prevent from the optical noise (undercutting effect) that could infect the photosensitive emulsion during exposure. A yellow mesh is able to absorb the parasitic lighting that occurs as a result of diffraction, reflection or total reflection that could be noticed during exposure in contrary with a white mesh that is not capable to do it. (Dennings, 1998)

Regarding the geometrical characteristics a 120-30, Y, PW, 20 N mesh was used. This mesh was recommended for high quality printing since it could provide satisfactory image details and a good behaviour during printing process. The 120 threats per linear cm frequency combined with the 30 microns threat diameter are providing a 40% open area percentage that leads to 18 cm³/m² ink volume capacity. All meshes were tensed on the frames with a tension of 20 N/cm measured with a tensiometer (Sieboruck-Technik Serimeter) in 9 points regional near the frames with an accuracy of ± 1 N/cm. The direction of the mesh threats (filaments) was ordered in parallel to the screen frames. (Murakami Screen, USA)

For the exposure, a single point halogen light source (Silvania multispectral – 2000 W) with a parabolic reflector was used in order to transfer satisfactory all the details of the interlayer film onto the screen. (Dennings, 1998)

According to the screen specifications the screening rule that is optimum for the experimental separation and printing is 72 lpi for all film positives. Orange and cyan were both separated at 22,5 degrees, green and magenta were both separated at 82,5 degrees, black was separated at 52,5 degrees and yellow was separated at 7,5 degrees. For this experimental separation it was used a Hybrid single angle (per two colours) and multi-angle (two colours and two single-angle sets) separation. This technique is better described as Hybrid Flamenco Hexachrome Screening.

For the accurate reproduction of an Artwork we have chosen a painting of Silvia Pelissero (a painter best known as Agnes Cecile). The choice of "La nostra infinita abnegazione" – "Our endless abnegation" 45cm x 30cm was made cause of the many painting techniques that were involved in its creation (Watercolor, pencil, charcoal, acrylic and pen on paper).

5. COLOUR STANDARDIZATION

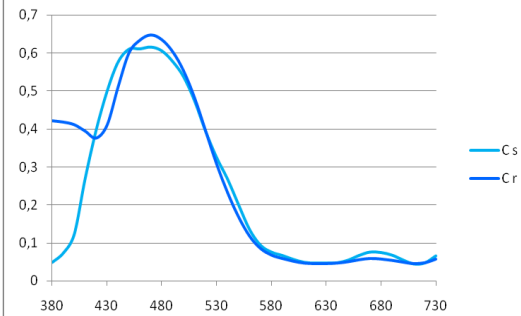
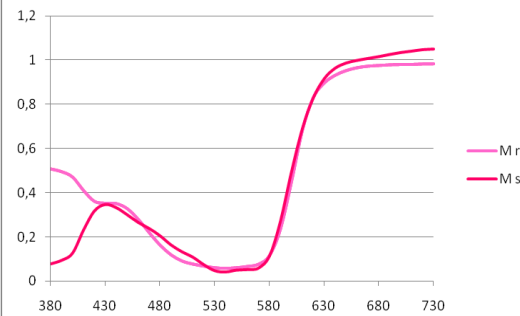
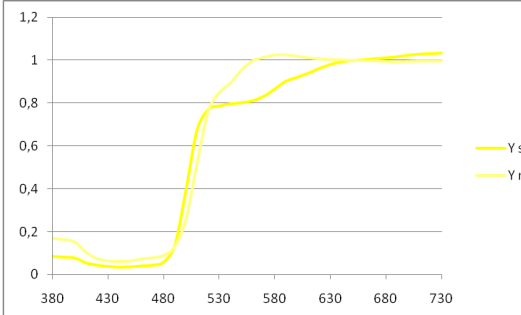
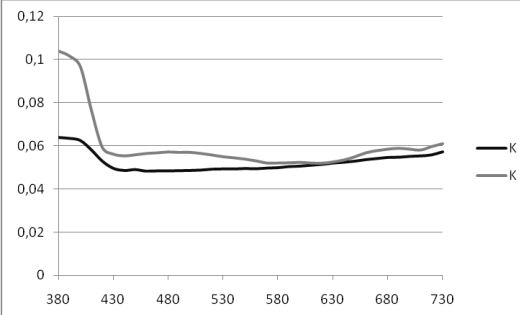
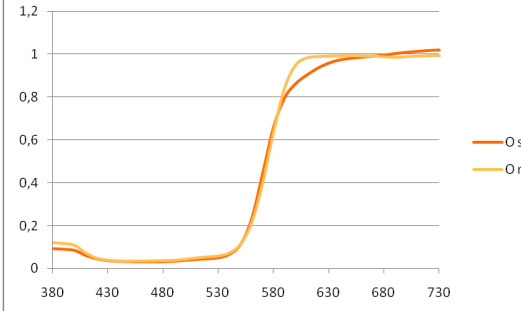
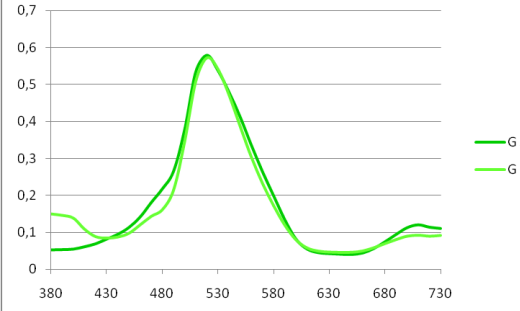
5.1 Colorimetry

In order to standardize the colour of the formulated inks a SpectroEye Gretag-Magbeth spectrophotometer was used. The conditions of the measurements were determined strictly in order to succeed the proper repeatability. The angle of light beam incidence was 2 degrees and a polar filter was used to avoid possible undesired reflections derived by the glossy of the ink. Colour characteristics of the inks that were used in the experimental screenprinting process are presented in the Table 2 opposed those that are used in the Offset Hexachrome™ process. A very low ΔE between the reference offset printing Hexachrome™ inks and the experimental (sample) screenprinting Hexachrome™ was achieved. All inks were formulated with a ΔE below 2,5 with an exception of the yellow ink which exhibited a slightly increased ΔE equal to 3,86. The colour differentiation of this ink is very difficult to be observed cause yellow is the lighter colour and human eye is not capable to notice differences much higher than 3,0.

5.2 Spectrometry

In the same Table 2 detailed spectra of the experimental Hexachrome™ screen printing inks are provided versus the measured spectra of the common Hexachrome™ inks that are used in offset printing. Both techniques colorimetry and spectrometry could provide us a significant ID of the produced inks. In combination with the ink formulation that was provided in the paragraph 3 of this study could ensure the required reproducibility of the process.

Table 2: Colour Characteristics of Screen printing (s) opposed to Offset Hexachrome™ (r) inks

CYAN					MAGENTA				
	C _r	C _s	Δ	ΔE		M _r	M _s	Δ	ΔE
L	53,00	54,01	0,99	1,53	L	52,45	52,98	0,53	2,44
a	-19,52	-19,10	-0,42		a	73,80	73,24	-0,56	
b	-45,69	-44,60	-1,09		b	-12,80	-10,48	2,32	
									
YELLOW					BLACK				
	Y _r	Y _s	Δ	ΔE		K _r	K _s	Δ	ΔE
L	94,18	90,58	-3,60	3,86	L	27,85	26,66	-1,19	2,35
a	-6,45	-7,77	-1,32		a	-0,29	0,78	1,07	
b	98,61	99,03	0,42		b	-1,42	0,29	1,72	
									
ORANGE					GREEN				
	O _r	O _s	Δ	ΔE		G _r	G _s	Δ	ΔE
L	67,13	66,50	-0,63	2,30	L	61,55	62,96	1,41	2,47
a	58,98	56,78	-2,20		a	-68,23	-67,96	0,27	
b	75,65	75,88	0,22		b	31,42	29,41	-2,01	
									

6. RESULTS

As a result of the current study, a new colour gamut (for screen printing) was reproduced. As it is obvious in the Figure 3 the new colour gamut that is reproduced with Hexachrome™ Screen printing technique is equal and slightly expanded to the Reference Offset Hexachrome™ colour gamut.

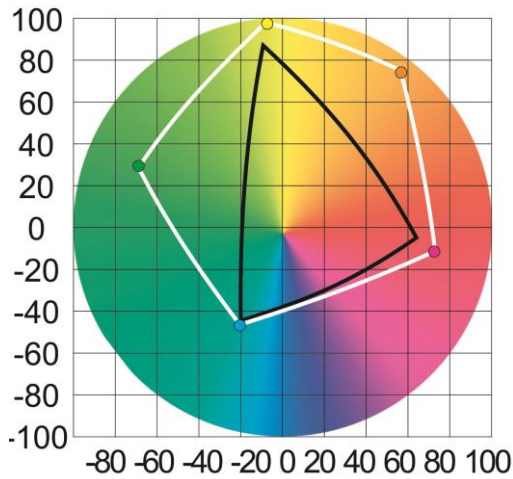


Figure 1: Hexachrome™ enhanced colour gamut vs common CMYK reproduction

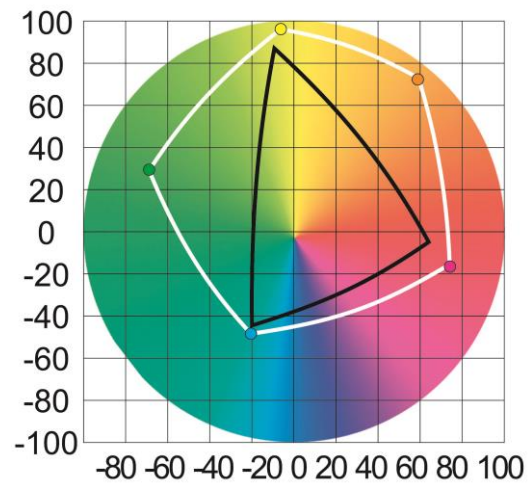


Figure 2: Experimental Screen Printing Hexachrome™ colour gamut vs common CMYK reproduction

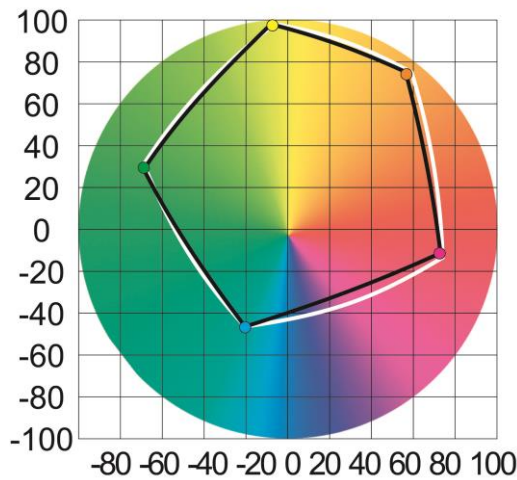


Figure 3: Experimental Hexachrome™ screen printing colour gamut (white line) vs reference offset one (black line)

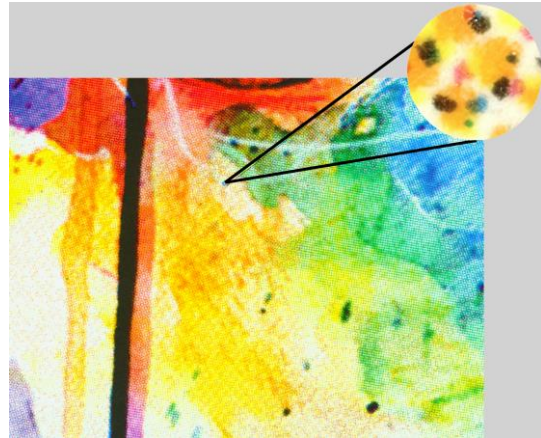


Figure 4: Hexachrome™ screen printing reproduction with detailed magnification which images 6 basic colours arranged in a rosette

7. CONCLUSIONS

Hexachrome™ screening methodology was modified and transferred in the screen printing technique with very good results giving the opportunity to reproduce both Artworks and commercial prints by just following the typical methodology for ink formulation and colour standardization that is developed during this study. The expansion of the colour gamut that can be used with screen printing is impressive. In combination with the purity of the screen printing inks and their vivid colours a great comparative advantage is suggested over the other imaging (printing) techniques.

In this study, an experimental methodology was developed in order to transfer expertise from the area of Hexachrome™ offset screening to the Hexachrome™ screen printing screening. Many

screening techniques were investigated, some of them used in the past and abandoned for many and different reasons. As we figured, since technologies are upgrading and market demands change, we have to reconsider the usability of older techniques that remained on the sidelines for many years until nowadays that could be used much more efficiently than in the past. Single-angle screening was abandoned from the Graphic Arts Industry mainly cause of the lack of knowledge combined with the wrong choose of application field. Hexachrome™ system did not became a great commercial success perhaps because Pantone addressed in the wide world of offset printing and not the most niche market of screen printing, packaging and branding applications that are looking for better quality and colour accuracy. Artwork reproduction was a convenient field for the progress of the technique development that took place in this study. We recognize that a very important expected field of the developed application beyond Artwork reproduction is packaging and branding applications.

8. REFERENCES

- [1] Abbott, S: "How to be a great screen printer", 1st Edition, (MacDermid Autotype Ltd, Oxford, UK, 2008), pages 93-122.
- [2] Dennings, D.: "Understanding Mesh Geometry, Stencil Resolution and Measuring Systems for Quality Control", SGIA Journal, (1998).
- [3] Fry, S.: "Six degrees of separation: A look at the hexachrome™ high fidelity color reproduction system", Visual Communications Journal, pages 49-53., (1999).
- [4] Jeffrey, N.: "Premium Colors", American Printer, volume 214 (2), pages 46-48., (1995).
- [5] Johansson, K., Lundberg, P., Ryberg, R.: "A Guide to Graphic Print Production", 2nd Edition, (John Wiley & Sons, Inc. Hoboken, New Jersey, 2007), page 148
- [6] Kang, H. R.: "*Digital Color Halftoning*", 1st Edition, (SPIE/IEEE Press, USA, 1999).
- [7] Latanision, I. M.: "A Comparison between the staggered position one-angle screening method and the multi-angle screening method in terms of misregistration when printing process color on newsprint", Master thesis, Rochester Institute of Technology, pages. 3-5., (1992).
- [8] Murakami Screen USA, "The Power of S Threads", URL <http://murakamiscreeen.com/the-power-of-s-mesh> (last request: 29-09-2014).
- [9] Tsigonias M.: "Raster frequency and imaging quality for Offset and Flexography Printing", GA Magazine, volume 39, page 46-48., (2002).
- [10] Tsigonias M.: "Heptachrome instead of seven colour printing", GA Magazine, volume 27, pages 18-19. (2001).
- [11] Pantone, "How we see color", URL <https://www.pantone.com/pages/pantone/pantone.aspx?pg=20133&ca=10>, (last request: 29-09-2014).

THE POSSIBILITY OF USING INKJET FOR PRINTING ON METAL PACKAGING

Igor Majnarić¹, Ana Slugić¹, Mateja Puhalo¹, Ivana Bolanča Mirković¹, Slaven Miloš²,¹University of Zagreb Faculty of Graphic Arts, Zagreb, Croatia²MGK-Pack, Rijeka, Croatia

Abstract: Printed packaging surely is the most perspective field of graphic technology. Packaging is the crucial part of the good placement of products on the market, while constant competition increment makes it even more important. Even though paper is the uppermost material used for packaging production, there are some products (meat products, beverages, fluids...) that demand materials of greater resistance and firmness, like metals. Traditionally, metal packaging is printed in offset printing technique, but digital Inkjet techniques that use UV curing systems also have the possibility to print on any material, accordingly also metals. This enables personalization of metal packaging, short runs and more relevant proof sheet printing. The possibility of Inkjet printing on the steel tin plates (that are normally used for offset printing) will be analyzed in this paper. The aim of the experiment is to determine the successfulness of color printing in Inkjet printing technique onto metals and the possible usage of it for the proof sheets printing. The efficacy of the reproduction of UV LED Inkjet inks on the metal substrate will also be determined. To define every relevant printing parameter (gamut, CIE $L^*a^*b^*$ values, ΔE , ΔL , ΔC , ΔH) and quality of reproduction of the smallest screen dots, colorimetric and imaging analysis were applied. For the printing of samples on the metal and paper substrate, Roland VersaUV LEC-300 machine was used, applying ECO-UV CMYK colors and UV curing system. Measurements were done by spectrophotometer and colorimeter X-Rite DTP20 Pulse. Results have shown there is a possibility of printing on metal substrates using Inkjet. Average color differences of CMYK patches, between metal and paper substrate, suggest that cyan ($\Delta E_{C,metal-paper,avg}=4,50$) and black ($\Delta E_{K,metal-paper,avg}=4,63$) give the best reproductions. Magenta and yellow show somewhat higher color differences between metal and paper substrate, which is caused by the lower lightness of the metal substrate itself ($\Delta E_{M,metal-paper,avg}=6,57$; $\Delta E_{Y,metal-paper,avg}=5,61$). Reproductions of dark hues and solid colors are especially good. Light hues and low halftone values should be avoided or corresponding corrections should be made before printing.

Key words: metal packaging, UV Inkjet printing, proof sheet printing

1. INTRODUCTION

The quality of the printing technique is measured by the quality of the image and hue reproduction. The aim of this paper is to determine both successfulness of reproduction of basic process colors on the metal substrate and their deviations in regard to the reference paper substrate. Accordingly, intention is to appoint the possibility of metal packaging printing with the usage of Inkjet printing technique.

When developing new metal packaging, proof sheets are often printed on inadequate substrates like paper or cardboard. Therefore, obtained prints and results cannot be relevant. It would be suitable to use Inkjet printers instead and print on the metal substrate itself, since they are affordable, compact and intended for short runs and in the same time can print on almost all types of media. Hence, the possibility of Inkjet usage for the needs of metal packaging proof sheets printing will also be researched in this paper.

The main characteristic of Inkjet printing techniques is the formation of the liquid ink droplets on the nozzles, which are then being ejected onto the substrate, generating desired content (Cameron, 2005). There are two basic principles of Inkjet technology: continuous and drop on demand (DOD) Inkjet. In this experiment, DOD-principle based technique is going to be used, specifically, piezo Inkjet. In DOD printing systems, a single drop of liquid ink is being formed only when it is needed. This way there is no need to dispose waste ink, because there is no any of it. All DOD Inkjet systems use digital image impulse in order to initiate ink droplet generation (Cameron, 2005). Piezo Inkjet systems use deformation of nozzle micro chamber (therefore, the variation of its volume) in order to generate and eject ink droplet. The piezo-ceramic element that is located in the micro chamber makes this possible, because it changes its shape when affected by electrical charge (Kipphan, 2001). The reduction of the micro chamber volume causes ink meniscus formulation at the opening of the nozzle, which is being ejected onto the substrate when the

micro chamber returns to its primary shape. Due to fully impermeable substrate, printing on metals is one of the most complex printing processes. To bypass the impermeability of the substrate, special inks that dry instantly are used. Last few years UV-curing inks, that dry immediately when being exposed to UV electromagnetic radiation, are being used. The aim is to replace standard UV mercury vapor lamps, due to their great energy consumption, with more economic LED light sources. In the experiment of this paper, UV-curing inks adapted for piezo Inkjet technique were used (Magdassi, 2010; Page, 2006). The thickness of the printed ink layer in Inkjet can amount up to 15 μm (in multicolor print even 20 μm), meaning UV curing must be conducted at high radiation energies, in order to successfully dry such thick ink layer. The reason of thick ink layer lays in the minimal amount of photoinitiators needed to start the drying process. When drying UV-curing inks, the combination of all three UV spectrum fields (UVA, UVB and UVC) are usually used (first dryer is made of lamps that emit longwave UV radiation, that provides good adhesion of the ink onto the substrate; lamps of the second dryer emit shortwave UV radiation, that dries the surface area of the ink layer). The speed of the print depends on the frequency of ink droplets ejection. Whereas ejection frequency amounts mostly between 5 and 40 KHz, the speed of the print itself also cannot be high and wears up to 0,5 m/s (Kokot, 2007).

2. METHODS

For the needs of the experiment, two types of substrate were used – metal substrate (coated white tin, 0,27 μm thick) and paper substrate (EMBLEM Solvent Perfect Poster 150, white coated 150 g/m² paper). The samples were printed with piezo Inkjet printer Roland VersaUV LEC-300. Printer uses ECO-UV inks and, in accordance with our experiment, four process inks (CMYK) were printed. Inks are UV-curable, for which purpose printer has two UV LED lamps. Before printing, linearization of the tone reproduction curve was made, using the spectrophotometer X-Rite DTP20 Pulse and RIP software VersoWorks. Settings of the RIP software used for the print of the samples were identical for both substrates: *Print quality: high; CMYK; Halftone: dither; Direction: uni-direction*. On both substrates the same plate (with MonacoProfile pre-defined 378 color patches) was printed. Colorimetric values of the 378 color patches on the samples were measured with spectrophotometer X-Rite DTP20 Pulse. Measured data were represented as L*a*b* values showed in software ColorShopX and saved as text file (.txt). Text files were imported to the MonacoProfiler software, whereby ICC profiles for each substrate were generated and converted to the visual gamut space with Monaco Gamut Works software.

Text file with the results of the colorimetric measurement was also imported to Microsoft Office Excel, where L*a*b* values of cyan, magenta, yellow (25, 50, 70 i 100% HV) and black (33, 66 i 100% HV) were extracted. They were used for the calculation of differences in color (ΔE), lightness (ΔL) and chroma (ΔC) between two substrates. Thereat mathematical formula ΔE_{2000} was used, defined as:

$$\Delta E_{00} = \sqrt{\left(\frac{\Delta L'}{k_L S_L}\right)^2 + \left(\frac{\Delta C'_{ab}}{k_C S_C}\right)^2 + \left(\frac{\Delta H'_{ab}}{k_H S_H}\right)^2 + R_T \left(\frac{\Delta C'_{ab}}{k_C S_C}\right) \left(\frac{\Delta H'_{ab}}{k_H S_H}\right)} \quad (1)$$

For the needs of image analysis, samples were captured with DinoLite camera, while magnified by Leica DM2500 microscope (magnification of 50x). Personal IAS device was used to measure the areas of singular dot elements (whereby areas of 5% HV of CMYK patches were measured).

3. RESULTS AND DISCUSSION

3.1 Gamut

The color gamut of the tone reproduction is defined as volume of the three-dimensional CIE L*a*b* space that displays the range of reproduced colors. Figure 1 shows color gamut of measured samples, whereat two different substrates printed with same printing settings (same printer, same UV-curing ink, same content printed, same RIP-settings) are being compared. Thereby the analysis of the substrate impact to the color range reproduction was made possible.

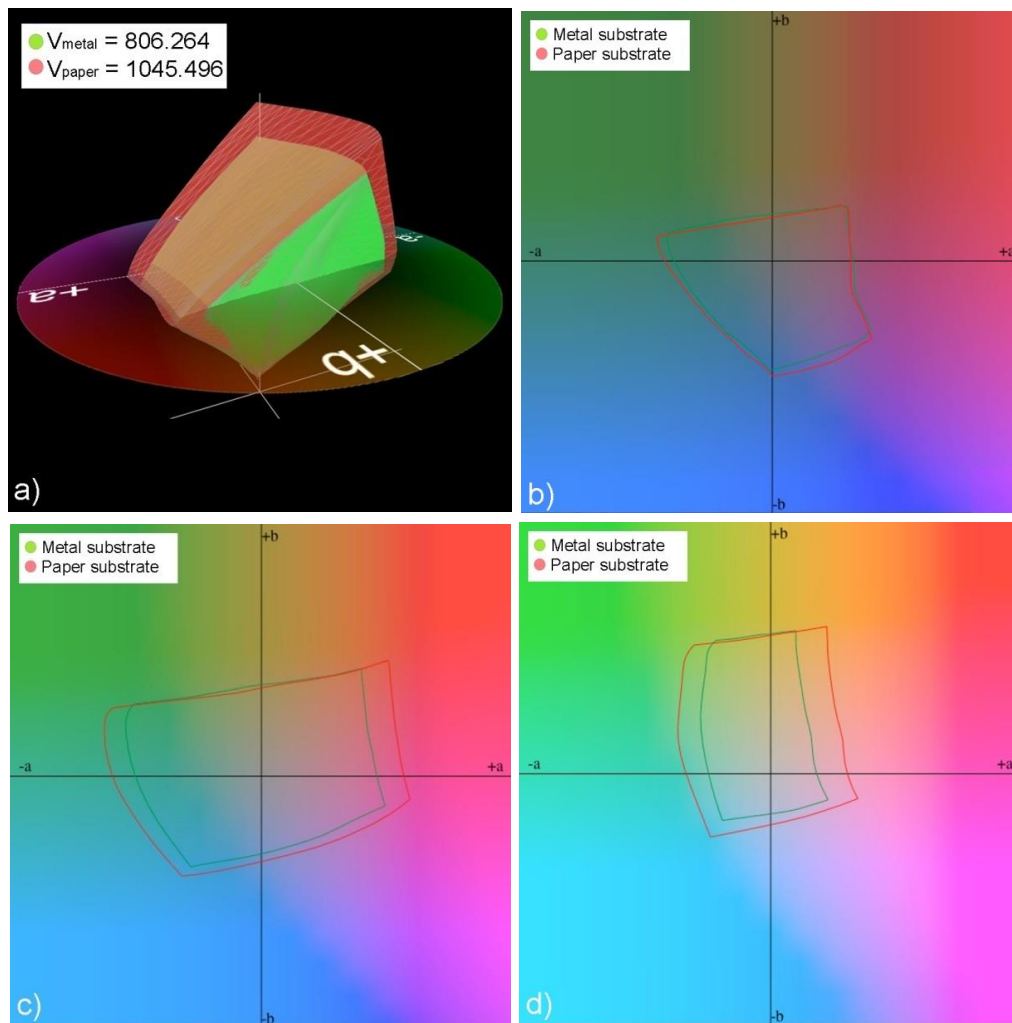


Figure 1: Comparison of the color gamut for two substrates – metal and paper
a) 3D view b) section L=30 c) section L=50 d) section L=70.

The relation of the gamuts in the CIE $L^*a^*b^*$ space and their volumes can be seen on the Figure 1a. Difference between gamut volumes is $\Delta V_{\text{metal-paper}}=239,232$ volume units. Metal has obviously smaller gamut volume than paper, mostly as a consequence of light tones not being reproduced (what is also proved on gamut intersections at L=30, L=50 and L=70). On the other hand, darker tones are well reproduced (Figure 1b, intersection L=30) and in that area metal does not deviate significantly in relation to paper. In middle tone areas (Figure 1c, intersection L=50), in relation to paper, metal shows notable gamut decrease in both directions of a^* axis (green and red tone areas). Metal substrate gamut in light tones area (Figure 1d, intersection L=70) is considerably smaller than paper gamut. Deviation is especially remarkable in red and green tones and, to a lesser extent, in blue tones. The cause of such poor light hues reproduction can be explained by the $L^*a^*b^*$ values of the substrates itself (Table 1).

Table 1: $L^*a^*b^*$ values of used substrates

	L^*	a^*	b^*
Paper	94,49	0,72	-2,36
Metal	85,46	-0,38	-4,08

It is notable that metal substrate has significantly lower lightness values than paper ($\Delta L^*_{\text{metal-paper}}=9,03$). Consequently, all colors printed on metal are darker, what lead to good reproduction of dark tones and light tones loss.

3.2 Colorimetric analysis

3.2.1 Color differences ΔE_{00}

In favor of better understanding of the color difference analysis, it is important to recognize optimal values and ΔE tolerances prescribed by the graphic process standards. The most recent standard for digital print is *PSD – ProcessStandard Digital*, which is the base of the ISO 15311 (currently in the adoption procedure). According to it, three print quality categories (A, B and C) have been introduced. Depending on the quality category, color differences should not exceed given values:

- Quality type A: $\Delta E^*_{ab} \leq 2,5$ for substrate, $\Delta E^*_{ab} \leq 3,5$ for 100% CMYKRGB and 50% CMYK
- Quality type B: $\Delta E^*_{ab} \leq 3,5$ for substrate, $\Delta E^*_{ab} \leq 5,5$ for 100% CMYKRGB and 50% CMYK
- Quality type C: $\Delta E^*_{ab} \leq 4,5$ for substrate, $\Delta E^*_{ab} \leq 7,5$ for 100% CMYKRGB and 50% CMYK (Kraushaar, 2012)

Color differences (ΔE_{00}) of CMYK colors between two substrates can be viewed at Figure 2. Figure contains four chart groups, of which every single group represents specific halftone value of CMYK patches (100%, 75%, 50% and 25% HV for CMY and 100%, 66% and 33% HV for K).

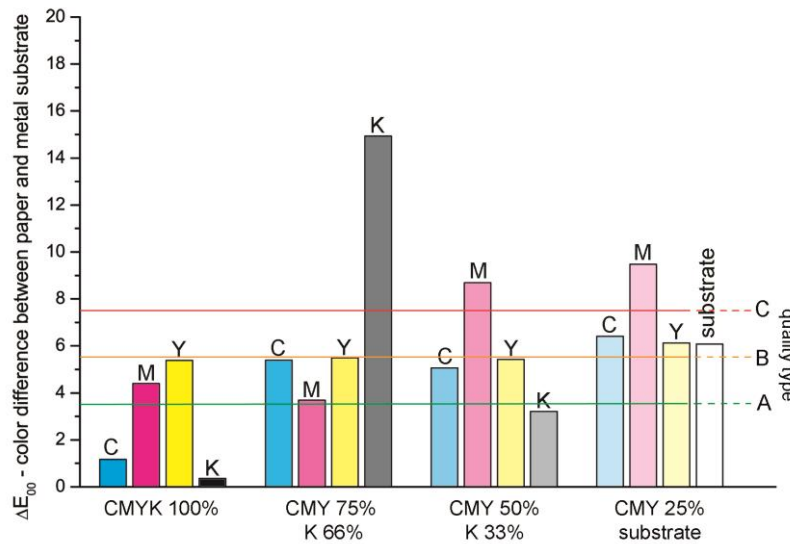


Figure 2: Color differences, ΔE_{00} , between metal and paper substrate

Color difference between metal and paper substrate is the least notable in solid tone patches. As the halftone value decreases, color difference between substrates increases, which is an evidence of substrate impact on the printed color itself. It is also a point of interest that different colors tend to show different ΔE deviations for particular halftone values.

Considering solid tone patches, yellow color manifests the greatest ΔE deviation ($\Delta E_{Y100\%,metal-paper}=5,38$) and that difference in color stays pretty permanent, regardless to halftone value decrease ($\Delta E_{Y25\%,metal-paper}=6,13$). Cyan shows very small ΔE deviation in solid tone patches ($\Delta E_{C100\%,metal-paper}=1,17$), but the color difference increases significantly in middle tone patches and culminates in light tones ($\Delta E_{C25\%,metal-paper}=6,40$). Magenta acts differently. Its color difference between paper and metal in solid tone patches is notable ($\Delta E_{M100\%,metal-paper}=4,40$), then decreases on 75% HV and increases enormously in light tone patches ($\Delta E_{M25\%,metal-paper}=9,48$). Magenta's color difference in light tones is too high and exceeds all quality category tolerance values. Black color also shows a specific change. While its color difference in dark and light tones is low and meets the highest quality type ($\Delta E_{K100\%,metal-paper}=0,36$), ΔE in middle tone patch (66% HV) is tremendous ($\Delta E_{K66\%,metal-paper}=14,94$). In the last chart group color difference between substrates themselves can be seen ($\Delta E_{metal-paper}=6,08$).

3.2.2 CIE $L^*a^*b^*$ values showed in three-dimensional spaces

To figure out the source of color differences, it is needed to generate CIE $L^*a^*b^*$ 3D color diagrams. Figure 3 shows four diagrams, each of them showing diagram from one of the CMYK colors. For easier comparison, diagrams are showed in correspondingly uniformed scales.

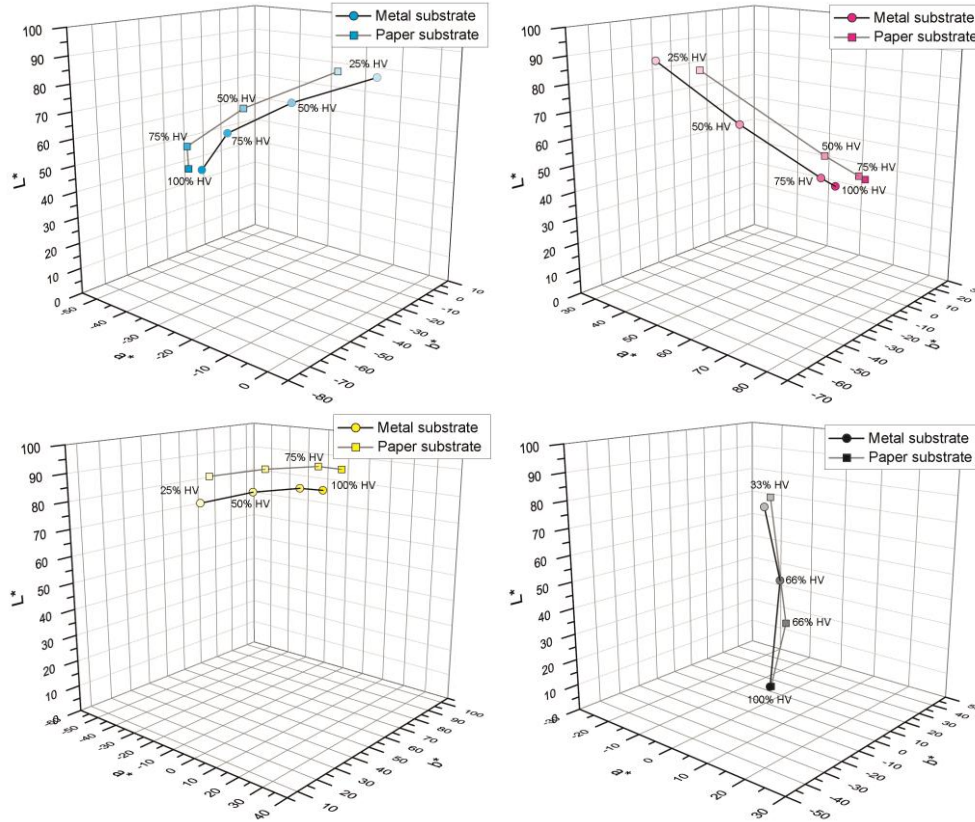


Figure 3: CIE $L^*a^*b^*$ values of CMYK patches

The common characteristic for all four colors is uniformed difference with regard to used substrate. Every color has a characteristic color difference curve, whose shape remains consistent no matter of the substrate used. For all colors, compared to paper substrate curve, curve that represents metal substrate is slightly shifted to the negative lightness direction ($-L^*$) and that alteration is the greatest in yellow patches. The cause of the shift can be found in lesser lightness of the metal substrate itself (Table 1).

Comparison of the diagrams shows the tendency of different direction of the colorimetric change, depending on the color. As expected, black does not show any chromatic change (its alteration is pointed in lightness direction (L^*)). Yellow color slightly changes in lightness and the main of its change lies in chromatic difference. Cyan and magenta have more or less equal change direction and they change both in chroma and lightness. All three chromatic colors (CMY) reveal colorimetric changes towards achromatic centre of CIE $L^*a^*b^*$ space (lesser saturation).

When looked closely at each of the four diagrams, it can be noticed that cyan patches with greater half-tone value printed on paper substrate change in $-a^*$ and $-b^*$ direction (away from the achromatic centre). That change suggests its greater saturation and can be explained by permeability of the paper substrate that could lead to greater pigment saturation. Diagram that shows magenta patches reveals unevenness of the saturation change, depending on the half-tone value change. Unevenness is more significant on the paper substrate curve, where light tones deviate the most and decreases half-tone value increases ($\Delta a^*_{M50-25\%, \text{paper}}=38,75$; $\Delta a^*_{M75-50\%, \text{paper}}=7,38$; $\Delta a^*_{M100-75\%, \text{paper}}=1,16$). Such change suggest the greater dot gain on dark tone patches, while its source probably lies in permeability of paper substrate, causing greater pigment saturation and joined screen elements. The greatest impact on color reproduction, metal substrate shows in yellow patches ($L^*_{Y100\%, \text{paper}}=86,95$; $L^*_{Y25\%, \text{paper}}=93,21$). That also explains very small changes of

yellow tones in lightness direction – in lighter tone patches dark metal substrate has higher impact and makes them darker, so they don't differ in lightness from more saturated, solid patches. Change of yellow patches in chroma is even and takes place on b^* axis, in achromatic center of CIE $L^*a^*b^*$ space.

Black color shows the most even tone reproduction curves, regarding substrates used, and its change straightly occurs on L^* axis. Unlike all the other colors, where darker metal substrate lowered the lightness of printed patches, black color is not impacted by it.

3.2.3 Lightness and chromatic differences (ΔL_{00} and ΔC_{00})

Figure 4 shows the lightness (ΔL_{00}) and chromatic differences (ΔC_{00}) of CMYK colors in regard to two different substrates. Differences in color originate from differences in lightness and chroma. By observing the separate change diagrams for both of them, it can be determined where the changes occurred.

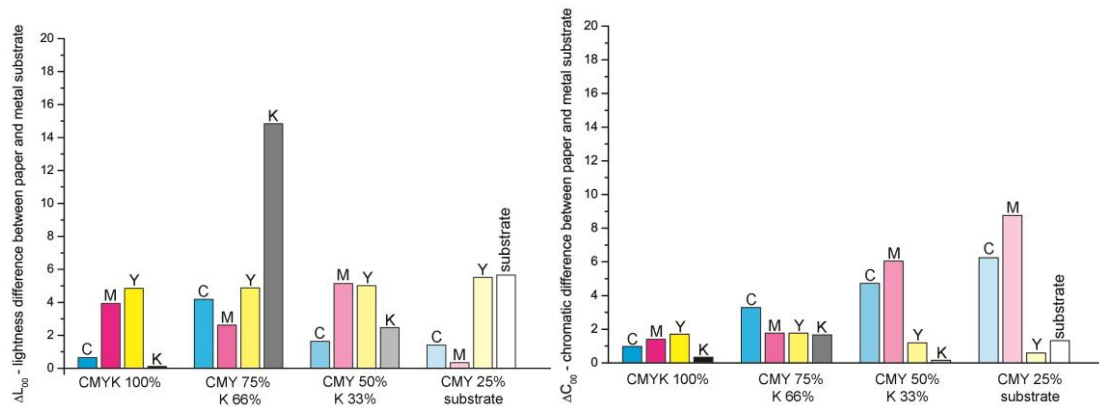


Figure 4: a) Lightness differences, ΔL_{00} , between metal and paper substrate
b) Chromatic differences, ΔC_{00} , between metal and paper substrate

By comparing those two diagrams, it can be concluded that color difference in solid tone patches, that majorly occurred only in magenta and yellow color patches, originated mostly from lightness difference ($\Delta L_{M100\%}=3,94$; $\Delta L_{Y100\%}=4,85$). There was also a minor difference in chroma ($\Delta C_{M100\%}=1,40$; $\Delta C_{Y100\%}=1,70$).

The similar thing also occurred in middle tone patches. Difference in lightness is significantly higher than chromatic difference in patches of all four colors (especially in black color patch, as it would be expected, since no chromatic pigments are used in black color). In middle tone patches cyan has the greatest chromatic difference of all colors ($\Delta C_{C75\%}=3,29$).

Interesting shift in differences happens in middle tone patches. Difference in chroma starts to be higher than lightness difference, especially in cyan and magenta patches. In the lightest tone patches (25% HV) magenta ($\Delta L_{M25\%}=0,34$; $\Delta C_{M25\%}=8,76$) and cyan ($\Delta L_{C25\%}=1,41$; $\Delta C_{C25\%}=6,25$) show almost only change in chroma, while yellow shows only lightness difference ($\Delta L_{Y25\%}=5,52$; $\Delta C_{Y25\%}=0,59$).

3.3 Image analysis

In order to determine the cause of greater color deviations in light tone patches, it is needed to analyze the reproductions of screen elements in the lightest tone patch (due to good visibility and recognition of each screen element, 5% halftone value patch was used). Observed patch was magnified by 50 times using Leica DM 2500 microscope.

By the visual evaluation of the microscopic images, obvious difference between substrate surface structures was spotted. Metal substrate shows the cleanest image of the screen elements. Uniformed formulation of the screen elements (with regard to the fact that FM screening was used on these samples, so geometrically regular arrangement of the screen elements can't be expected) can also be seen on metal substrate.

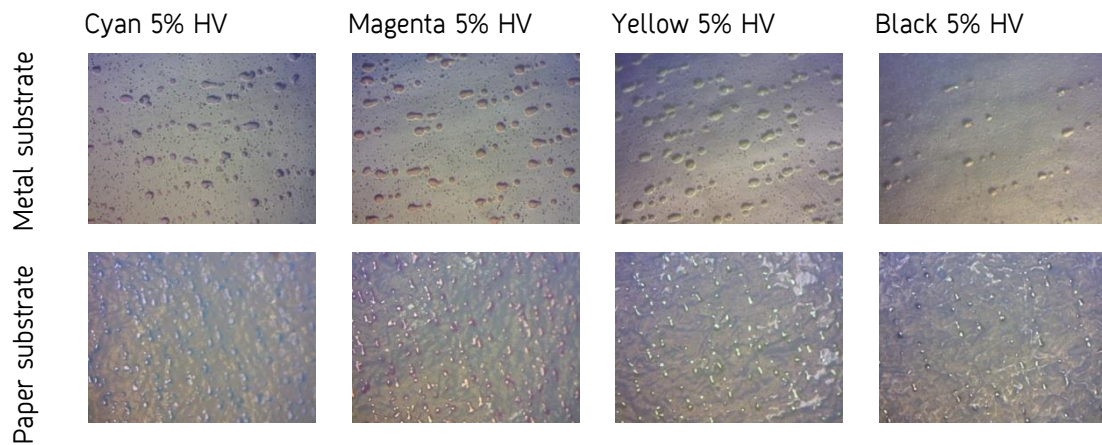


Figure 5: Microscopic images of CMYK color patches (5% HV patches) printed on metal and paper substrate (magnified 50x)

Deviation is notable only in black color patch and its distribution should be increased (so that it would meet corresponding halftone value of the patch). In comparison to the paper substrate, screen elements on the metal substrate have somewhat bigger area (due to impermeability and smoothness of the metal substrate), but their number is higher.

3.4 Screen elements area

Area of the each screen element was measured with Personal IAS device (patches of 5% halftone value and 2.54x2.54 cm selection area were measured). On the selected area, device detects single screen element and measures its area. Given valuables were statistically processed and visualized by the box diagrams. Figure 6 shows the distribution of area valuables for each screen element, for cyan, magenta, yellow and black color, printed on two substrates.

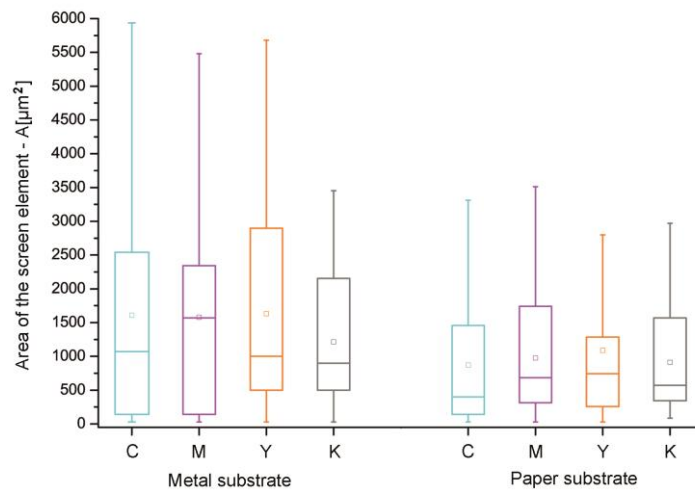


Figure 6: Area of the screen element of CMYK colors printed on paper and metal substrate

In Inkjet printing technique, the size and position of screen elements is depending on the size of formulated ink drops, respectively the surface tension of the liquid ink. Diagrams showed on Figure 6 display the mean of the screen elements area valuables and their distribution. Scattering of screen element area valuables (A) printed on metal substrate is evidently higher in all color patches (apart from black), than the ones printed on paper substrate.

By the calculations of average valuables of screen element areas, all colors show tinier screen element reproduction on paper substrate ($\Delta A_{C,metal-paper}=734,15 \mu m^2$). This can be explained by the impermeability and smoothness of metal substrate surface that caused spillage of the ink and therefore the increasement of the area of the screen element itself.

4. CONCLUSIONS

Paper substrate generates better reproduction of the tones, whereas it has greater gamut volume ($\Delta V_{\text{metal-paper}}=239,232$ volume units). Metal substrate shows good reproduction of dark tones, while light tones reproduction is poor. The range of tone reproduction is decreasing from dark toward light tones, together with tones on the edge of the gamut (saturated light colors). That can be explained by the low lightness of the metal substrate itself (its difference to paper substrate it amounts $\Delta L^*=9.03$). For the better reproduction of light tones, the usage of whiter base ink is suggested.

For the metal substrate, the tone reproduction curve, for all four colors, deviate towards darker tones (that deviation is, as expected, the highest in yellow color). In the solid tone patches differences in color (ΔE_{00}) for cyan and black color between paper and metal substrate are very low ($\Delta E_{C100\%,\text{metal-paper}}=1,17$; $\Delta E_{K100\%,\text{metal-paper}}=0,36$) and therefore belong to quality category A. For magenta and yellow those differences are higher ($\Delta E_{Y100\%,\text{metal-paper}}=5,3$; $\Delta E_{M100\%,\text{metal-paper}}=4,40$) and belong to quality category B.

In dark tone patches, the reproduction of black color (66% HV) is the most problematic ($\Delta E_{K66\%,\text{metal-paper}}=14,49$) and doesn't meet values of any quality category. The cause for that can be found in lightness differences ($\Delta L_{K66\%,\text{metal-paper}}=14,84$) that didn't occurred due to colorimetric differences of substrates but impermeability of the metal substrate (it lead to connection of screen elements). Notable deviations in middle darker tones (75% HV) are spotted in yellow color ($\Delta E_{Y75\%,\text{metal-paper}}=5,49$) and cyan ($\Delta E_{C75\%,\text{metal-paper}}=5,39$), but those differences meet criteria of quality category B.

Lighter middle tones (CMY 50% HV) reveal notable color differences between substrates for all three colors. The color difference keeps increasing in 25% halftone value patches where it amounts: $\Delta E_{M25\%,\text{metal-paper}}=9,48$; $\Delta E_{C25\%,\text{metal-paper}}=6,40$; $\Delta E_{Y25\%,\text{metal-paper}}=6,13$. Black is getting stabilized at low halftone values and its color difference lies almost in quality category A tolerance borders ($\Delta E_{K33\%,\text{metal-paper}}=3,21$). Light tone patches (25% HV) for cyan and yellow belong to quality category C, while light tone patches (25% HV) of magenta show too high color differences to meet any of the quality categories.

The average values of color differences of CMYK colors between metal and paper substrate suggest that cyan ($\Delta E_{C,\text{metal-paper,avg}}=4,50$) and black ($\Delta E_{K,\text{metal-paper,avg}}=4,63$) color have the best reproduction that belongs to quality category B. Magenta and yellow have poorer reproduction and belong to quality category C ($\Delta E_{M,\text{metal-paper,avg}}=6,57$; $\Delta E_{Y,\text{metal-paper,avg}}=5,61$).

The uniformed formulation of screen elements on the metal substrate was determined by image analysis. Compared to paper substrate, the number of screen elements on metal substrate is lower, but their area is higher ($\Delta A_{C,\text{metal-paper}}=734,15 \mu\text{m}^2$). The cause to that can be found in the smoothness and impermeability of metal substrate.

The usage of Inkjet technology for metal packaging printing is possible with color corrections in dark tones and solid areas. The printing of lighter tones is more problematic, whereas focus to better print of base white color is suggested.

5. REFERENCES

- [1] CameronN. Luft, "Ink-Jet Printing," in *Coatings Technology Handbook*, 3rd ed., no. 25, A. A. Tracton, Ed. CRC Press, 2005, p. 25; 1–4.
- [2] KipphanH., *Handbook of print media*. Berlin: Springer-Verlag, 2001.
- [3] KokotJ., Ed., *UV technology - A Practical Guide for all Printing Processes*. Berufsgenossenschaft Druck und Papierverarbeitung, 2007.
- [4] KraushaarA., "ProcessStandard Digital - Handbook 2012." Fogra Graphic Technology Research Association, 2012.
- [5] Magdassi, The Hebrew University of Jerusalem, *The Chemistry of Inkjet inks*. Singapore: World Scientific Publishing Co. Pte. Ltd., 2010.
- [6] Page A., "Developments in Radiation Curing Inks." Pira International Ltd., Great Britain, 2006.
- [7] PuukkoP., IlmonenA., LamminmäkiT., SundqvistS. „UV-inkjet Ink Penetration and Its Effect on Print Quality Formation and Drying“, *Proceedings NIP25 and Digital Fabrication (2009.)*, pp. 566–569.

COLOUR DIFFERENCES RESULTING FROM DRYING PROCESS OF CONVENTIONAL PRINTED AND IN-LINE UV-VARNISHED CARDBOARD SAMPLES

Gorazd Golob¹, Igor Gerl², Mitja Bobnar², Matej Pivar¹

¹ University of Ljubljana, Faculty of Natural Sciences and Engineering, Ljubljana, Slovenia

² EGP, Škofja Loka, Slovenia

Abstract: Colour differences were measured during drying process of Avanta Prima and Excellent Top cardboard samples, printed using four conventional lithographic inks taken from Pantone catalogue, in-line coated with water-based primer and varnished using UV-varnish on the top. We measured colour spectra, CIELAB values and colour differences immediately after printing and in different time intervals with final measurements after 24 h. Colour constancy varied between different colours and substrates. The highest $\Delta E^*_{ab} = >10$ colour difference in relation to standard value was achieved at Pantone 072C (blue) colour printed on Excellent Top substrate after 24 h, however even at the first approved print, made by using originally delivered ink, we only achieve $\Delta E^*_{ab} = >5$.

Uneven changes of reflection spectra during drying process at Pantone 2592C (violet) and Pantone 432C (dark grey) represent a challenge for further research based on lab-simulation of used printing and varnishing process and measurement and analysis of IR spectra obtained on FTIR-ATR spectrophotometer. Spectral changes confirmed changes in chemical composition of printed samples coated with a primer after drying.

Key words: Pantone, in-line UV-varnishing, color difference, reflection spectra, IR spectra analysis

1. INTRODUCTION

The main goal of our investigation was measurement and analysis of colour differences of typical packaging products for pharmaceutical industry. On this market there are very high demands and expectations on achieved colour values, defined in CIELAB system with acceptable colour differences and the constancy of printed cardboard boxes is a common part of contracts and good business practice. Some of the colours, taken from Pantone catalogue, printed using conventional lithographic oxidative drying inks, in-line coated with water-based varnish, dried with IR and hot-air dryer and finally in-line varnished using UV-varnish, cured with mercury lamps has been reported in the past as not stable enough during final drying process in the hours or even days after their processing. The final result can also be different using different print substrates, so we decided to use two different cardboards. Our challenge was not only a measurement of colour values and differences according to the standard. We tried to find the reason for colour changes during the drying process to get an opportunity for future improvements.

2. METHODS

Our investigation has been performed in two steps. First we printed a test-form with four different Pantone colours in-line varnished on Man Roland R706 printing press with two varnishing units and drying/curing systems. After measurements and first analysis of results we repeated a part of the experiment in lab-conditions to perform analysis of IR spectra.

2.1 Printing on Man Roland R706 printing press

Printing conditions:

- Standard set-up of the press.
- Room temperature 20 °C.
- Dampening solution with DS Acedin, 8.2 % IPA, temperature 7.3 °C.
- Conventional inks Pantone 072C (blue), Pantone 2592C (violet), Pantone 432C (dark grey) and Pantone 1505C (orange).
- Water-based primer, dried using hot air and IR drying systems.
- UV varnish, cured using mercury lamps.
- Print substrates: Avanta Prima and Excellent Top coated cardboards.

Measurement of reflection spectra and colour values was performed using SpectroEye spectrophotometer (D65, 2°, pol filter on). The measuring head was positioned in the middle of the test-field, on random sheets taken from the ream of >200 sheets during drying process. Measurements have been performed immediately after printing (< 1 min), after 5, 15, 30 min and after 1, 2, 4, 8 and 24 h.

2.2 Lab-printing and varnishing

Printing and varnishing conditions:

- IGT-A2 lab printer with 8 µm ink layer thickness.
- Conventional printing inks Pantone 2592C and Pantone 432C.
- Water-based primer, applied using screen-printing technique, mesh 120 threads/cm, drying with hot air (50 °C, 1 min).
- UV-varnish, applied using screen printing technique, mesh 120 threads/cm, curing using UV dryer (658 mJ/cm², 5 m/min).
- Print substrate Avanta Prima.
- Final drying using oven (50 °C, 6h).

IR spectra measurement and analysis (Sućetaka and Yates, 1995):

- Measurements immediately after printing and varnishing (ink only, primer only, ink+primer, UV-varnish only, ink+primer+UV-varnish, other combinations of layers).
- FTIR-ATR measurements on Perkin Elmer Spectrum GX, diamond crystal, range 5000-500 cm⁻¹, 32 scans/sample.
- Analysis of IR spectra using BioRad, KnowItAll, module AnalyzeIt software with IR spectra database.

3. RESULTS

Only most interesting results for two colours are shown in this report, more results are available in published version of diploma work (Gerl, 2014).

3.1 Results of measured reflection spectra and colour values

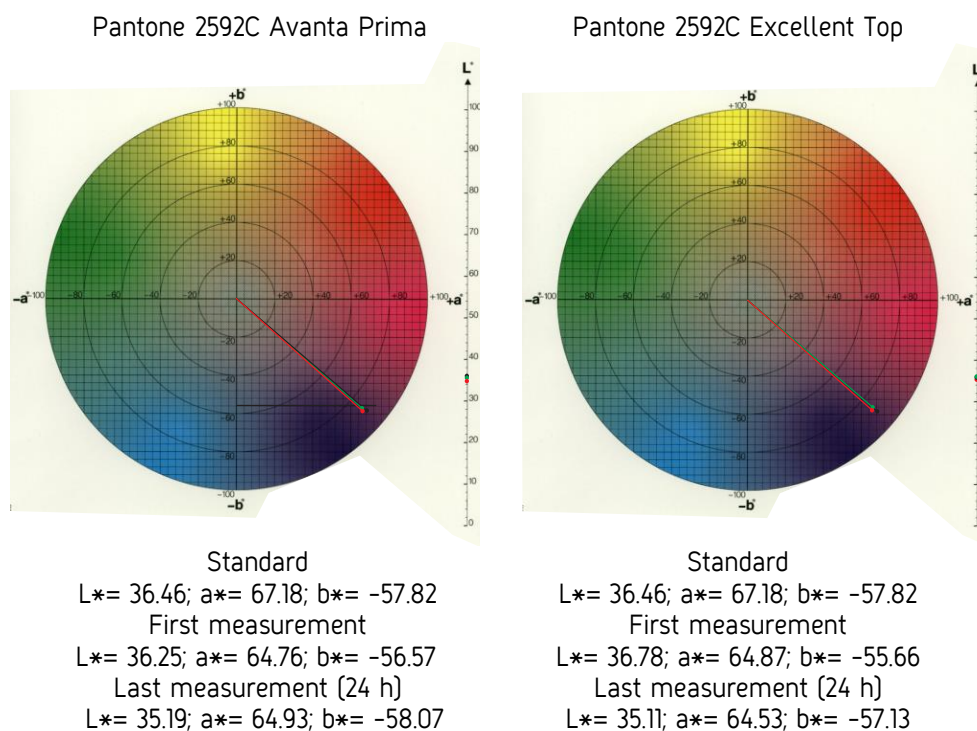


Figure 1: CIELAB values of Pantone 2592C colour printed on two substrates.

CIELAB colour values for Pantone 2592C on two substrates are presented in Figure 1, ref-lection spectra of the same colour printed on Avanta Prima substrate are presented in Figure 2. CIELAB colour values for Pantone 432C on two substrates are presented in Figure 3, reflection spectra of the same colour printed on Avanta Prima substrate are presented in Figure 4.

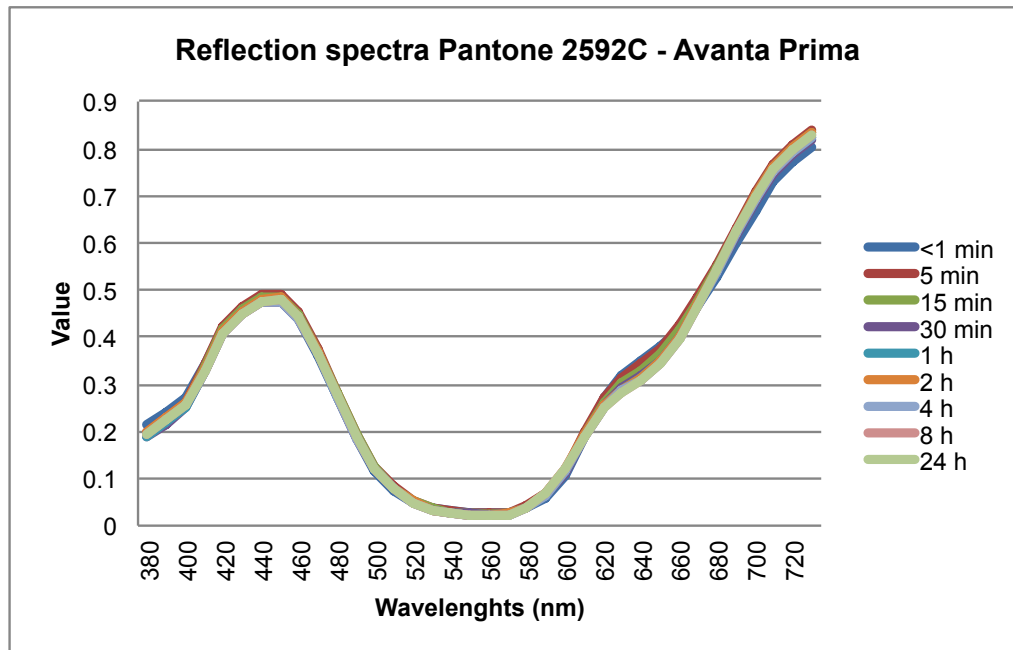


Figure 2: Variations of reflection spectra of Pantone 2592C printed on Avanta Prima substrate during drying process.

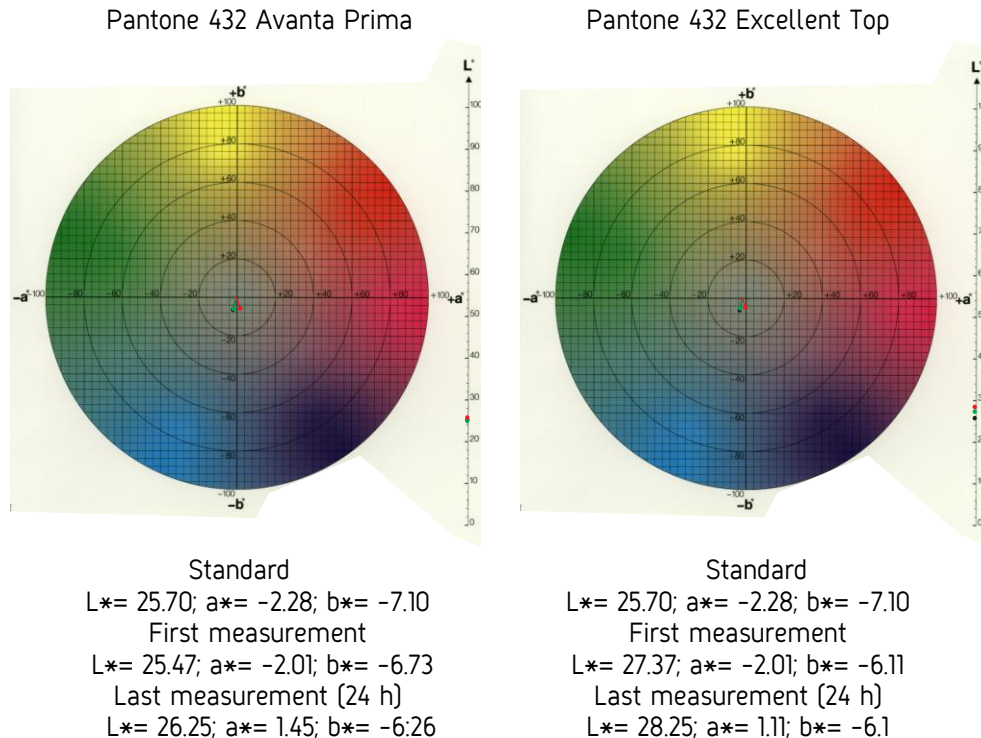


Figure 3: CIELAB values of Pantone 432C colour printed on two substrates.

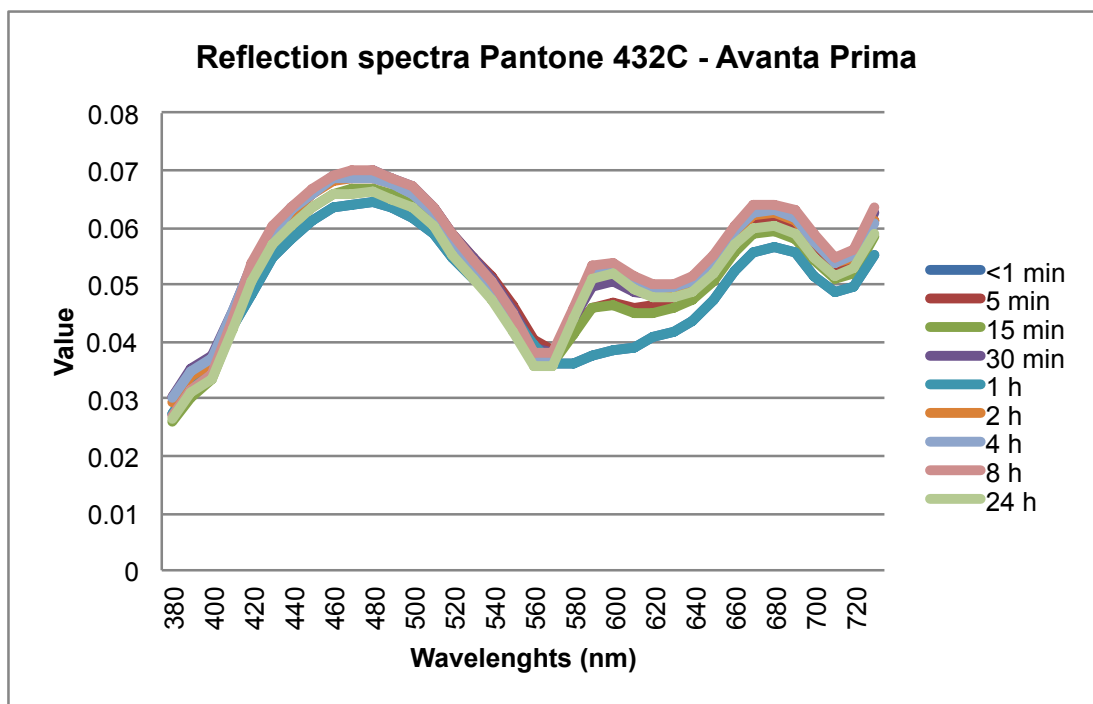


Figure 4: Variations of reflection spectra of Pantone 432C printed on Avanta Prima substrate during drying process.

3.2 IR spectra measurement results

The most interesting results of IR spectra measured using FTIR-ATR method were obtained with the samples of printed and primer coated cardboard, where changes of peaks are clearly visible (Figure 5 and 6).

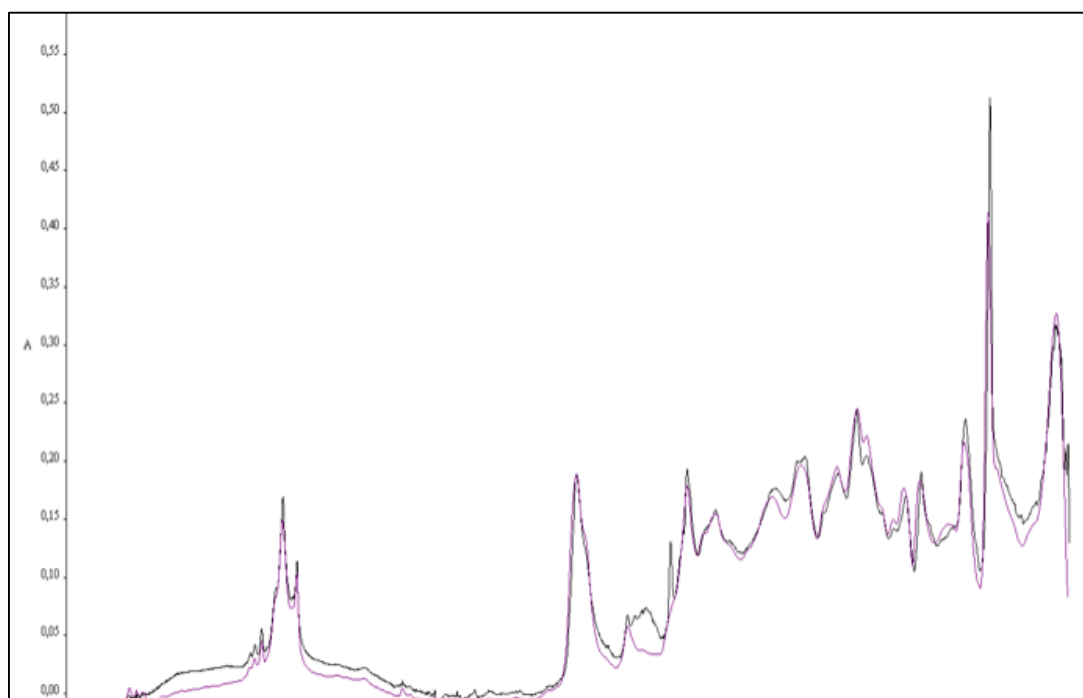


Figure 5: IR absorption spectra of Pantone 2592C coated with primer, measured immediately after printing and coating (bp_2592_9_00.sp) and after 6 hours drying time at 50 °C (bp_2592_15_00.sp).

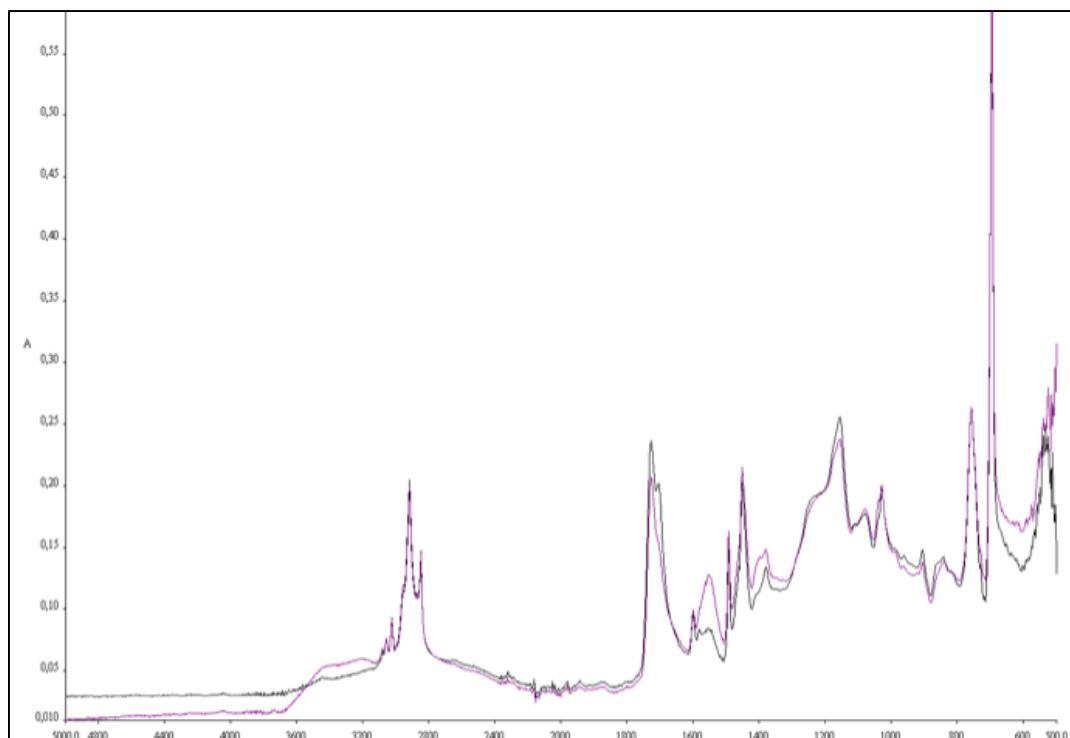


Figure 6: IR absorption spectra of Pantone 432C coated with primer, measured immediately after printing and coating [432 siva B_P_suh.sp] and after 6 hours drying time at 50 °C [432 siva B_P_suh_6h.sp].

4. COMMENTS AND CONCLUSIONS

Visual assessment and measurements of colour changes during drying process of the samples, printed and varnished using printing press confirmed our predictions and former experience. Noticeable changes in colour Pantone 2592C were observed mostly at the beginning of the drying process, however after 24 h we achieve acceptable colour difference $\Delta E^*_{ab} = <3$ on both substrates.

Highest colour differences with visible red colour cast were achieved on samples printed with Pantone 432C colour. Measured colour difference $\Delta E^*_{ab} = <4$ on Avanta Prima and $\Delta E^*_{ab} = <5$ on Excellent Top substrates were still within the acceptable tolerance limits.

Colour values of all samples were acceptable, with $\Delta E^*_{ab} = <5$, after 24 h drying time, however relatively big changes in lightness, chroma and hue have been observed and measured, mostly at the beginning of the drying process.

By using FTIR-ATR (Fourier transform infrared-attenuated total reflectance) IR spectroscopy method we obtain information on chemical bonds and functional groups of the samples. In both cases, for Pantone 2592C and Pantone 432C samples, coated with a primer, the reduction of some spectra peaks after drying was present in the range of 1400 to 1600 cm^{-1} . Analysis of the IR absorption spectra (Figure 7) gave us information on the changes in chemical composition of the samples after drying process.

For both samples the reduction of the proportion of the ketones (R-CO-R), azo groups ($\text{RN}=\text{NR}$), nitrile group ($-\text{C}=\text{N}$), nitro compounds ($-\text{NO}_2$) and other chemical functional groups or compounds containing nitrogen (N) has been found. These compounds and functional groups include chromophores that may change the color of the sample. Design of the experiment and the precision of the analytical method used does not allow for a definitive confirmation of those assumptions, but it is a good starting point for any subsequent in-depth analysis of the color changes of printed and varnished samples.

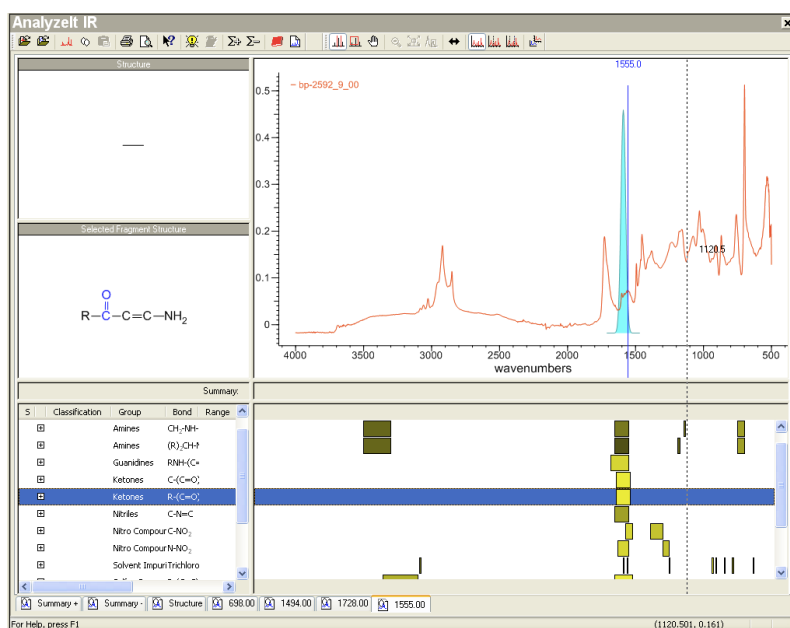


Figure 7: Overview of the determination of the chemical composition of the Pantone 2592C sample with appropriate software and database (BioRad, KnowItAll, Analyzelt IR module).

5. REFERENCES

- [1] Gerl, I.: „Problem barvne reprodukcije na kartonski embalaži“, diplomsko delo, Univerza v Ljubljani, NTF, (2014).
- [2] Knowitall, URL www.knowitall.com/academic/ (last request 10-10-2014).
- [3] Perkinelmer, URL www.perkinelmer.com/ (last request 08-10-2014).
- [4] Sućetaka, W.; Yates, J. T. Jr.: “Surface Infrared and Raman Spectroscopy: Methods and Applications”, (Plenum Press, New York, 1995).

INFLUENCE OF SILICA NANOPARTICLES IN PCL OVERPRINT COATING ON THE COLOR CHANGE OF OFFSET PRINT

Josip Bota¹, Maja Brozović¹, Zlata Hrnjak-Murčić²

¹ University of Zagreb, Faculty of Graphic Arts,

² University of Zagreb, Faculty of Chemical Engineering and Technology,

Abstract: This paper presents research on the influence of polycaprolactone (PCL) nanocomposite overprint coating on the color change of offset printed paperboard. To investigate this issue color test card was developed via spectrophotometric software and offset printed on paperboard. The color values of the printed sample were measured before and after the coating application to facilitate the measurement and comparison of the results. The coatings applied on the printed sample were three different concentrations (1%, 2% and 3%) of silica nanoparticles in PCL biopolymer. The research found a color change in all investigated samples. It is observed that adding silica nanoparticles to PCL coatings improve the color stability of the coated samples. Detailed analysis of hue (ΔH), chroma (ΔC) and lightness (ΔL) of the tested samples show that PCL coating with 2% silica nanoparticles result in the least amount of color change.

Key words: Polycaprolactone; silica; nanocomposite; color change; packaging;

1. INTRODUCTION

Today, in graphic technology biopolymers in combination with nanoparticles are used for improvement of cellulose packaging properties. They are mostly applied to improve the mechanical properties of paperboards that are commonly used in the packaging industry. The targeted area of research is the improvement of two major barrier properties; water and oil paper resistance. There is also a need to increase lipid oxidation resistance for cellulosic packages that contain fatty foodstuffs [Arora & Padua, 2009; Recalde et al., 2012]. Introduction of silica (SiO_2) nanoparticles in the coating can change the wetting properties of the paperboard surface [Stepien et al., 2011; Chen 2012], so other changes should be observed as well.

The great advantage of using biopolymers for coating instead of synthetic polymers is because of their biodegradability and lower environment impact of packaging materials. Nanotechnology combined with biopolymer is a broad area of interdisciplinary research. It combines development and industrial activity, manufacture, processing and application of polymer materials filled with particles and/or devices that have one or more dimensions of the order of 100 nanometers (nm) or less [Utracki, 2004; Paul & Robeson, 2008; Sinha & Bousmina, 2008; Sinha & Okamoto, 2003]. The extraordinary potential of this technology to provide enabling routes for development of high-performance materials has attracted the attention of researchers, from physics, chemistry, and biology to engineering [Silvestre et al., 2011].

Color change is common in the printing industry. Quality control and colorimetry are used to improve the uniformity of print. Adding varnishes on printed materials usually change the color properties so a color profile must be made to preserve the color relations. CIELAB system compares a sample to a standard and makes a numerical determination based on the perceived color difference [Luo, 2001]. It is a color space with dimension L for lightness and a and b for the color-opponent dimensions, based on nonlinearly compressed CIE XYZ color space coordinates, and is used to determine a numerical description of a color change.

Biopolymer and nanocomposite coatings are mostly used in the production process of cellulose materials. The result is a prepress product with defined specifications ready for print. As a result a paperboard must not be oleophobic due to the transfer of ink. This is mostly important for offset print. The focus of this paper was to study the influence of overprint biopolymer nanocomposite coating on the color change of offset print. This investigation has been made in order to see do nanoparticles in polycaprolactone (PCL) coating keep or change the color values of print on paperboard. The objective of this work was to examine the induced changes in color properties in coatings with different percentages of added dispersed nanoparticle.

2. METHODS

2.1 Materials

Paperboard of 230 g/m², GD2 grade (Umka color®) is commonly used material in the packaging industry and was cut into 30cm x 35cm sheets samples. The coating has been made from polycaprolactone (PCL) biopolymer, (molecular mass: Mw ~14,000, Mn ~10,000) Aldrich®. As the nanofiller hydrophobic fumed silica (AEROSIL® R 8200), SiO₂ content > 99.8, specific surface area (BET) 220 ± 25 m²/g, EVONIK Industries was used. The ethyl-acetate solvent (C₄H₈O₂) [99%], Kemika® was used for the coating preparation.

2.2 Print sample preparation

The examined colors were basic colors of subtractive color synthesis and key black (CMYK) with a tonal value increase (TV) scale from 10–100% with a step every 10%. Color test card were prepared via X-rite Color Port® software and exported as a TIFF file. Prepress was sent to be printed with implemented Process Standard Offset printing developed by Fogra® (ISO 12647-2) to ensure good print quality. The color test card was 20cm x 25cm in size.

2.3 Coating preparation

The coating was prepared by dissolving 10g of PCL polymer granulates in 90g of etil-acetate solvent, solution was heated at 40 °C, stirred about 30 min to get a homogenic 10% solution, using a magnetic stirrer. The coatings on the printed color test card samples were prepared from PCL polymer solution by varying the concentrations of silica nanoparticles. Four different coatings were prepared without silica (K/P/Si/0) and by adding 1 mass% (K/P/Si/1), 2 mass% (K/P/Si/2), 3 mass% (K/P/Si/3) of silica dispersing them with a homogenizer for 8 min at 15000 rpm.

2.4 Coating application

The coating was applied using the K202 Control Coater in controlled condition defined by the ISO 187:1990 standard. The wet coating thickness was defined with the standard coating bars to 40 µm. All coatings were applied on the printed side of the paperboard.

2.5 Measurement procedure

The Color test on the printed color test card samples was carried out by spectrophotometric software, X-Rite il Pro® spectrophotometer. The exact CIE LAB colorimetric values for forty colors were measured before and after the application of the tested coatings. The results were obtained as an average of five measurements for each sample.

3. RESULTS

Obtained CIE XYZ spectrophotometer results for the studied samples (K/P/Si/0, K/P/Si/1, K/P/Si/2 and K/P/Si/3) were converted into CIE Lab color space. The CIE XYZ color values of printed paperboard test card were measured before and after coating to calculate and presented the induced color change (ΔE). The results are calculated according to formula for the color difference (ΔE) defined in 2000. In the year 2000, CIE reviewed and upgraded the 1994 color difference formula to ΔE_{00} . By this redefinition the perceptual uniformity issue has been resolved. After the ΔE redefinition several authors reviewed this formula and confirmed that when selecting a conventional color difference formula for predicting color difference involving different magnitudes, ΔE_{00} should be used (Wang et al., 2012).

3.1 Color difference

The results of color difference (ΔE_{00}) of the printed paperboard card coated by PCL nanocomposites are presented in Figures 1–4. The colors of print were influenced by different PCL coatings due to various fractions of silica nanoparticles. The results show the color difference in relation to the tonal value increase (TV) for offset printed paperboard samples (K/P/Si/0, K/P/Si/1,

K/P/Si/2 and K/P/Si/3]. From the results a substantial color difference is observed comparing samples with and without silica nanoparticles in PLC coatings.

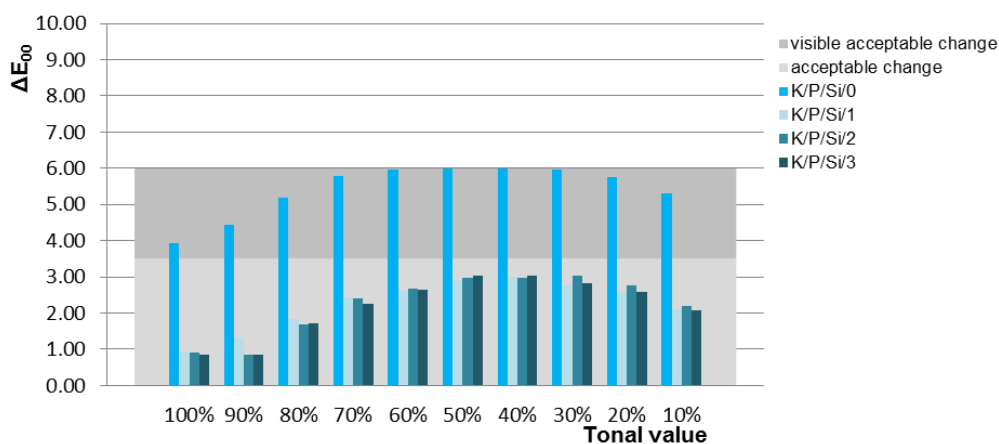


Figure 1: Dependence of the color difference (ΔE_{00}) of cyan color on the tonal values increase (TV) for the printed paperboard card coated by PCL nanocomposites

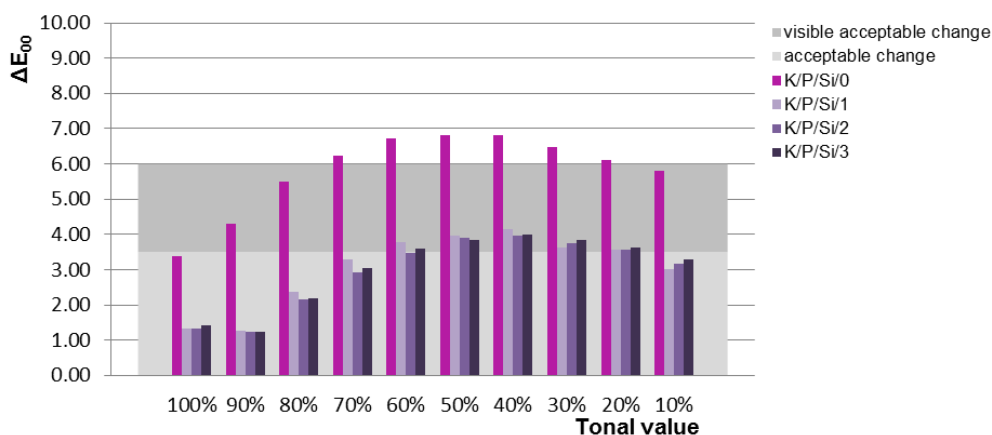


Figure 2: Dependence of the color difference (ΔE_{00}) of magenta color on the tonal values increase (TV) for the printed paperboard card coated by PCL nanocomposites

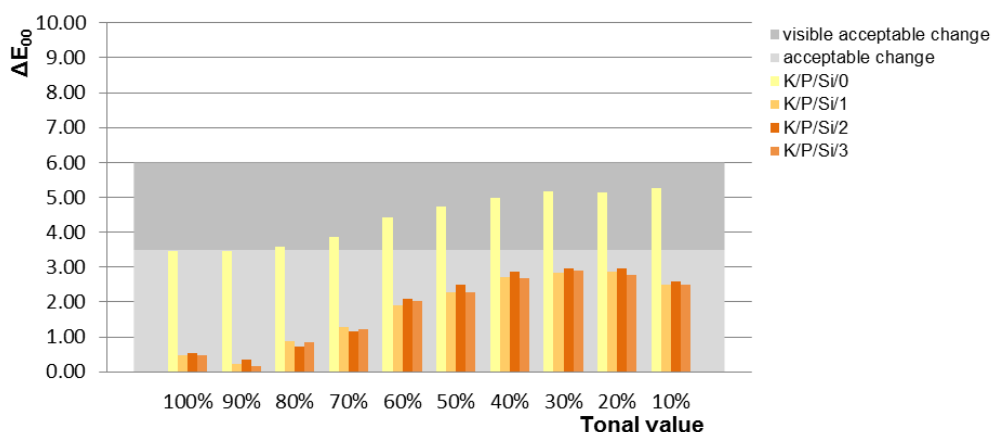


Figure 3: Dependence of the color difference (ΔE_{00}) of yellow color on the tonal values increase (TV) for the printed paperboard card coated by PCL nanocomposites

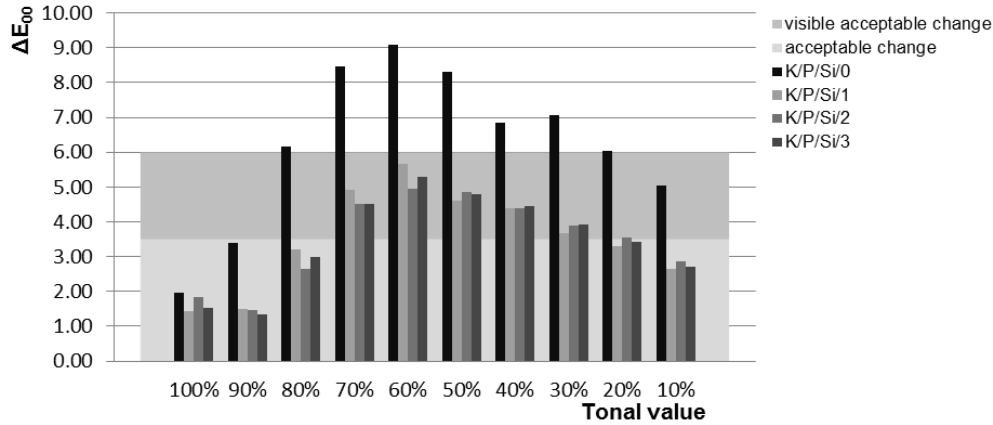


Figure 4: Dependence of the color difference (ΔE_{00}) of black color on the tonal values increase (TV) for the printed paperboard card coated by PCL nanocomposites

3.2 Analysis of the color difference

The color difference can be divided and analyzed by three main parameters: hue (ΔH), chroma (ΔC) and lightness (ΔL), as the description of the color changes. Hue difference describes a Euclidean difference between two color samples. The current ISO 12647-7 norm includes the allowed hue difference for primary colors and grayscales. Figure 5 from a to d shows the dependence of hue difference for cyan, magenta, yellow and black colors (CMYK) on the tonal values increase of the printed paperboard card coated by PCL nanocomposite coatings.

From the presented results it can be seen that cyan color (Figure 5 a) displays both positive and negative ΔH in different tonal values. On the other hand, magenta (Figure 5 b) display positive while yellow and black (Figure 5 c and d) show negative ΔH through the whole tonal value increase.

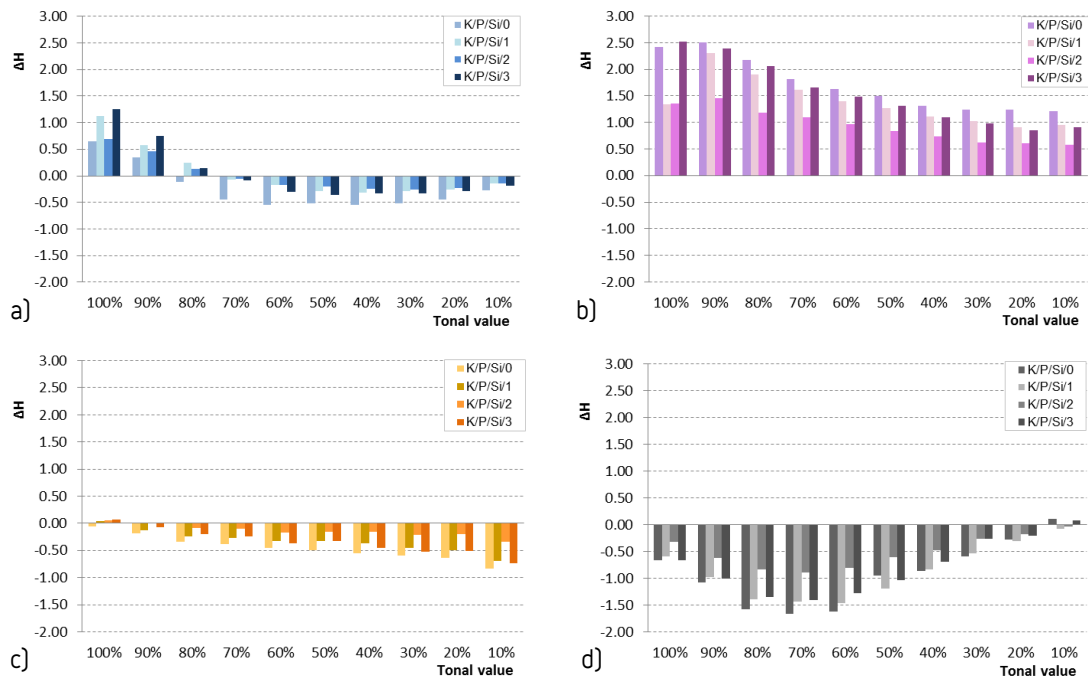


Figure 5: Dependence of the hue difference (ΔH) on the tonal values increase (TV) of: a) cyan; b) magenta; c) yellow; d) black for the printed paperboard card coated by PCL nanocomposites

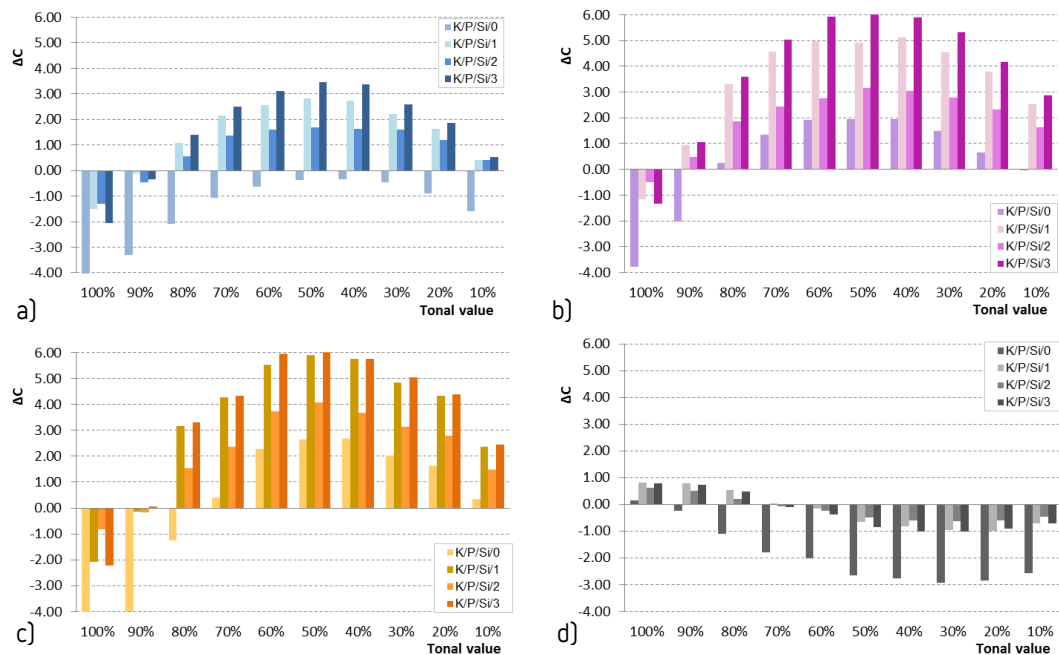


Figure 6: Dependence of the chroma difference (ΔC) on the tonal values increase (TV of): a) cyan; b) magenta; c) yellow; d) black for the printed paperboard card coated by PCL nanocomposites

For the studied samples (K/P/Si/0, K/P/Si/1, K/P/Si/2 and K/P/Si/3) a difference in chroma (ΔC) was also analyzed, as chroma indicates the change of color saturation. The results are presented in Figure 6 a to d and describe the chroma change in relation to CMYK tonal value increase and different PCL nanocomposite coatings. From the obtained results it can be seen that CMY colors (Figure 6 a to c) have a negative chroma in the full tonal values range, while in the same range black shows a positive ΔC . The other tonal values for CMY colors show a positive chroma with peaks in the 50% TV; and a negative ΔC for the black especially in 30% of the tonal value field.

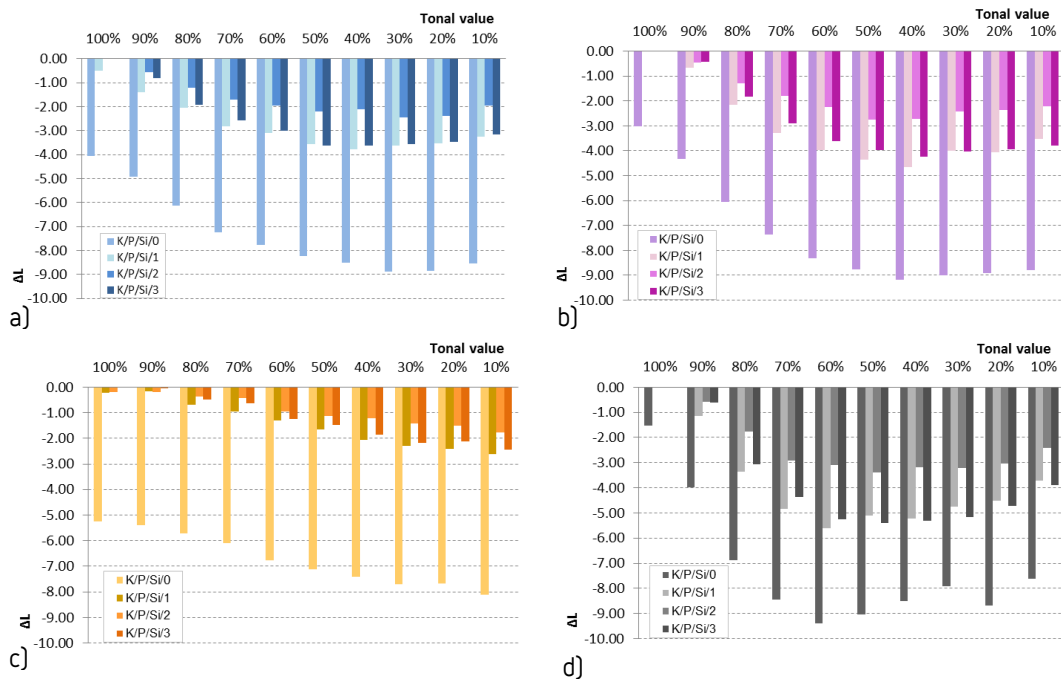


Figure 7: Dependence of the lightness difference (ΔL) on the tonal values increase (TV of): a) cyan; b) magenta; c) yellow; d) black for the printed paperboard card coated by PCL nanocomposites

For the printed paperboard card coated by PCL nanocomposites a change in lightness is also studied and results are presented in Figure 7 a to d. They show a decrease in lightness (ΔL) for all studied samples. It is important to point out that the decrease in lightness is significantly lower for the samples of printed paperboard samples coated by PLC with silica with regards to the samples without silica nanoparticles.

4. DISCUSSION

The color difference of CMYK colors for the printed paperboard card coated by only PCL (without silica) show significant changes in comparison to the samples with PLC nanocomposite coatings (Figure 1 to 4). It can be seen that the color difference of CMYK colors for the samples of pure PCL coatings and PCL with silica approximately the same through the whole tonal value increase range. For example, cyan color change coated with pure PCL is about 3 values higher than the coating with nanocomposites. For all colors (CMYK) the ΔE_{00} is considerably higher in the 30%–80% tonal value increase. The color difference (ΔE_{00}) for magenta and black in the 30% to 70% tonal value range of the samples with PCL coatings without silica even exceed the visible acceptable change ($\Delta E_{00} > 6$). The literature [12] instructs ΔE values to 3.5 are not visible to an untrained eye, while values up to 6 are acceptable but there is an obvious color change and values beyond 6 are visible and unacceptable. For samples with PCL nanocoatings, with different silica concentrations, most of the values are below the 3.5 target mark and yellow color show the lowest ΔE_{00} (under 3) for all tonal values. This is because yellow ink is the lightest in CMYK print and always has the least visible color change. As seen in the results it was expected that full tones would have a smaller color difference than mid and light tones due to the intensity of the ink.

Considering hue difference (ΔH), (Figure 5) it can be seen that the highest changes are found in magenta and black colors. For magenta the 90% and 100% tonal values (Figure 5 b) show the highest ΔH and for black it is in the 60% – 80% range. The hue difference for cyan and yellow are considerably lower. Positive ΔH values for cyan (in the 80% to 100% tonal value range) and the negative values of yellow indicate the hue change towards the green area. The remaining part of the cyan tonal values range (10% to 70%) show a change towards the blue colors. Magenta tonal values point to the hue change in the red color area. To satisfy the proofing norm for hue difference, a maximum tolerance of 1.5 is permitted in gray areas and 2.5 in the primary colors. All results coincide with this values (Figure 5) accept the 60% to 80% tonal values of pure PCL coating for black color (Figure 5 d).

Chroma difference (ΔC) is analyzed from the results in Figure 6 where it can be seen that the highest chroma change is for magenta and yellow colors. Samples with pure PCL coatings show a substantially lower and negative ΔC in comparison to samples with PCL nanocomposites. Further on it is observed that the highest positive chroma change is seen for the sample with 1% and 3% of silica (K/P/Si/1 and K/P/Si/3) for yellow and magenta especially in the 30% to 60% TV. The smaller chroma values are observed in cyan, while black colors mostly have negative ΔC results. Chroma values of full tones are negative for CMY colors due to the difficulty of improving the saturation adding matte coating to print.

Figure 7 shows that the negative ΔL values of PLC coated samples are significantly larger compared to PCL nanocomposite coated samples. Analyzing by color of PCL nanocomposite samples indicate that yellow color (Figure 7 c) has the lowest ΔL values, then follow cyan (Figure 7 a), magenta (Figure 7 b) and black (Figure 7 d). Comparing PCL nanocomposite samples a notable difference in lightness can be found due to the different concentrations of silica nanoparticles. As in the hue and chroma difference, PCL nanocomposite coating with 2% SiO₂, shows the best ΔL . Adding varnish type coatings to print have the biggest influence on chroma and lightness (Simonot&Elias,2004). These are also the main causes for the ΔE_{00} values in the observed coatings (figures 6 and 7). The matte finish of the coatings disperses the light, so a decrease in lightness was expected.

An increase of refractive index of the polymer composite with added inorganic oxides is observed (Salamone, 1996). Such composite materials have attracted considerable attention due to their potential in creating new high performance materials for optical, electrical and other application. As the organic and inorganic substances usually have very different diffraction index, when combined in inorganic-organic composite they can be optically transparent due to the nanoscale size of present particles. This advantage is used to obtain optical coatings with high refractive index. From the literature (Andradi&Helmman,1975; McMaster, 1975) is known that the concentration

of the components in the polymer composite substantially affect homogeneous dispersion of the particles in the polymer matrix. When one of the components is present in low fraction, completely miscible polymer composite can be obtained. If the (nano)particles are homogeneously, uniformly dispersed in a polymer matrix, this means that regular structures were created. Furthermore, it is also known (Fox et al., 1987) that homogeneity of a multi-component material is dependent on the miscibility of the starting components, such as the PCL polymer and silica nanoparticles. When starting components are miscible they establish interactions at the molecular level, which results in formation of a homogeneous, regular structure of the composite. Thus, it was developed the methods to evaluate the miscibility of polymers by measuring the transparency of the polymer blends/composite. If the polymer blend is transparent polymers are miscible at the molecular level and, conversely, immiscible polymers form opaque (foggy) blends. This is explained by the structure that occurs during mixing, that is, whether regular or irregular structure is obtained.

5. CONCLUSIONS

In this study the influence of PCL coating and nanoparticles of silica in PCL coating on offset print was observed. The results show that the biggest influence on color change has the pure PCL coated on offset printed paperboard card. It is also shown that adding silica nanoparticles improve the visual properties of the PCL coating, as well as mechanical. Comparing the PCL coated samples with different concentrations of silica nanoparticles it can be concluded that 2% concentration of silica in PCL shows the best result in hue, chroma and lightness. This is probably the result of the regular structure achieved due to the optimal concentration of silica nanoparticles. Quality control allows the color changes influence by this coating, but for best results a color profile should be made. Some indicated difference in hue, chroma and lightness can be compensated with certain limitations during prepress. Color profiling and color compensations are common when combining print with varnish or plasticization due to the surface change (Simonot&Elias, 2004). For a better understanding of the influence of the coating on the color change, and for color profiling of the coating, an analysis of a larger color patch should be made. The color patch should include various combinations of CMYK values. This coating thickness was selected because pure PCL coated samples showed a borderline color change acceptance, so further investigations should be made on the influence of PCL coating and silica nanoparticles on offset print with different thickness, as well as a comparison of their mechanical properties. It is also important to investigate the biopolymer nanocomposite interactions with different print inks and paperboards.

6. REFERENCES

- [1] Andradi L. N, Helmann G. P.: "The percolation limits for two-phase blends of PMMA and copolymers of styrene and MMA" *Polymer*, Volume 34, Issue 5, 0032-3861(93)90209-S, 1993.
- [2] Arora A., Padua G.W.: "Review: Nanocomposites in Food Packaging", *Journal of Food Science*, Volume 75, Issue 1, 1750-3841, 2009
- [3] Chen, W., Wang, X., Tao, Q., Wang, J., Zhenga, Z., Wang, X.: "Lotus-like paper/paperboard packaging prepared with nano-modified overprint varnish", *Applied Surface Science*, Volume 266, 2012.12.018
- [4] Fox, D. W., Allen, R. B., Mark H. F., Bikales N. M., Overberger C. G., Menges G., "Encyclopedia of Polymer Science and Engineering", Vol. 3 (Eds, Wiley, New York, 1987.) page 758
- [5] Kurt Schläpfer : "Farbmetrik in der Reproduktionstechnik und im Mehrfarbendruck", (UGRA c/o EMPA St. Gallen, 1993) page 68
- [6] Luo, M. R., Cui, G., Rigg, B.: "The Development of the CIE 2000 Colour-Difference Formula: CIEDE2000" *Color Research & Application*, Volume 26, Issue 5, 10.1002/col.1049, 2001
- [7] McMaster, L. P., *Advanced Chemistry Series* 142 (1975) page 43.
- [8] Paul, D. R., Robeson, L. M., "Polymer nanotechnology: nanocomposites" *Polymer*, Volume 49, Issue 15, 2008;49:3187-204.
- [9] Recalde, I., Devis, A., Prats, L., Aucejo, S.: "Improvement of barrier properties and wettability of biodegradable coated paper and cardboard", 16th International Coating Science and Technology Symposium 2012 proceedings (ISCST: California CA, USA, 2012),

- [10] Stepien, M., Saarinen J. J., Teisala, H., Tuominen, M., Aromaa, M., Kuusipalo, J., Mäkelä, J. M., Toivakka, M.: "Surface chemical characterization of nanoparticle coated paperboard" *Applied Surface Science*, Volume 258, Issue 7, 2011.11.048
- [11] Sinha Ray, S., Bousmina, M. "Polymer nanocomposites and their applications".(Valencia, CA (USA): American Scientific Publishers; 2008.) page 154
- [12] Sinha Ray, S., Okamoto, M.: "Polymer/layered silicate nanocomposites:a review from preparation to processing", *Progress in Polymer Science*, Volume 28, Issue 11, 2003;28:1539–642.
- [13] Silvestre, C., Duraccio, D., Cimmino, S.: "Food packaging based on polymer nanomaterials", *Progress in Polymer Science*, Volume 36, Issue 12, 2011.02.003
- [14] Simonot, L., Elias, M.: "Color Change Due to a Varnish Layer" *Color Research & Application*, Volume 29, Issue 3, 10.1002/col.20008, 2004
- [15] Salamone J. C.: "Polymeric materials encyclopedia", Vol. 12,(CRC Press, Boca Raton, 1996.) page 758.
- [16] Simonot, L., Elias, M.: "Color Change Due to Surface State Modification" *Color Research & Application*, Volume 28, Issue 1, 10.1002/col.20008, 2004
- [17] Utracki, L.A.: "Clay-containing polymeric nanocomposites" , vols. 1 and 2. (Shawbury (UK): RAPRA Technology Ltd.; 2004.) page 238
- [18] Wang, H., Cui, G., Luo, M., Ronnier, Xu, H.: "Evaluation of Colour-difference Formulae for Different Color-difference Magnitudes", *Color Research & Application*, Volume 37, Issue 5, 10.1002/col.20693, 2012

ANALYSIS OF PRINTED DOT FIDELITY ON PAPER SUBSTRATES MADE OF TRITICALE STRAW FIBRES

*Ivana Plazonić, Irena Bates, Željka Barbarić-Mikočević,
University of Zagreb, Faculty of Graphic Arts, Zagreb, Croatia*

Abstract: Texts and images in graphic industry are made of small dots, thus the printed dot fidelity greatly affects image reproduction quality as one of its most important elements. However, reproduction quality does not only depend on printing techniques and inks used in the printing process but also on paper substrates. As paper industry is faced with a global deficiency of wood raw materials, alternative sources of virgin cellulose fibres play an important role in the paper production. For that purpose, this research was performed on paper substrates produced by mixing fibres isolated from triticale straw and recycled wood fibres in different weight rations. In order to isolate cellulose fibres, the triticale straw was exposed to alkaline treatment using two methods. The printability of handsheets, laboratory paper substrates made of fibres isolated from triticale straw, was analysed by way of classifying dot fidelity. The handsheets were printed using UV-curable inkjet printer. Dot fidelity was observed by analysing images comparing seven different dot dimensions in relation to their dot area and dot shape descriptors (roundness, aspect ratio and solidity). Determined dot characteristics on six different paper substrates with triticale fibres were compared against a control paper substrate made only of recycled fibres.

Key words: dot area, dot fidelity, dot shape descriptors, image analysis, paper substrate, triticale straw fibres

1. INTRODUCTION

Small dot is the most important element in a multi-colour reproduction of the text and images in graphic industry. The shape and characteristic of each dot play an essential role in the perception of reproduction quality. Dot quality is impacted by the printing technique, the characteristics of the ink or toner and the properties of paper. Nowadays the demand for papers made of recycled fibres is still growing. Still, even with the maximum use of recycled fibres, there will always be a need for virgin fibres to replenish the inevitable fibre attrition from repeated recycling [Hubbe et al, 2007]; [Minor et al, 1992]; [Nazhad, 2005]. Virgin fibres sourced from forests could be replaced by agricultural residues such as triticale straw left over after the harvest for food crops.

For that purpose, this research of printed dot fidelity was made on paper substrates produced by mixing fibres isolated from triticale straw and recycled wood fibres in different weight rations. The printability of paper substrate depends on the ability to reproduce dots of the desirable size and shape.

The print quality of text or image depends on the resolution of imaging systems, on the quality of the shape of individual image elements, on the ability to transfer different amounts of ink per image element and on the screening. One of the most important factors which affect the print result is the ink's property to spread away along the fibres of the paper substrate. Since the appearance of printed dots is different than the appearance of defined dots in the digital form, the printed dots became the subject of studies in many researches. In order to provide a more detailed description of a dot, researchers mostly use dot area and dot shape descriptors [Fleming et al, 2002]; [Doyle, 2000]; [Stančić et al, 2012].

This research presents the analysis of printed dot fidelity on paper substrates made of triticale straw fibres based on dot area, roundness, aspect ratio and solidity.

2. METHODS AND MATERIALS

Equipment, materials and methods used in virgin fibres isolation are published in previous papers [Plazonić et al, 2014]; [Bates et al, 2014]. Fibres for preparing paper substrate were isolated from triticale straw by two types of alkaline treatments meeting the conditions presented in Table 1.

Table 1: Pulping conditions

		Method 1.	Method 2.
Used straw		360 g	
Pre-treatment	Chemical NaOH, %	-	16
	Bath ratio	-	1:10
	At 25°C	-	24 h
Decantation		-	+
Treatment	Chemical NaOH, %	16	-
	Tap water	-	10 l
	Bath ratio	1:10	1:5
	At 120°C, 170 kPa	60 min	60 min
Decantation and rinsing		2 × 10 l	
Defibration	Tap water	23 l	
	At 24°C	40 min	
	pH	8,5 – 9,0	

Paper substrates, the printability of which was researched, were laboratory sheets made of recycled wood fibres and virgin fibres isolated from triticale straw according to a Table 2.

Table 2: Paper substrates

Paper substrate	%		
	Recycled wood fibres	Virgin fibres isolated from triticale straw	
		Alkaline treatment with pre-treatment	Alkaline treatment without pre-treatment
N	100	0	0
N1TR1	90	10	0
N2TR1	80	20	0
N3TR1	70	30	0
N1TR2	90	0	10
N2TR2	80	0	20
N3TR2	70	0	30

Altogether, seven different paper substrates (42.5 g/m², 20 cm diameter) were produced using Rapid Köthen Sheet Machine. Every paper substrate had two sides: wire side (bottom side) and felt side (top side), each with different characteristics. Smoothness of the felt side is a very important paper property for print quality. The smoothness of the surface in the felt side of all paper substrates, which was later printed for the purposes of further analysis, was determined by Bekk Smoothness tester (Figure 1).

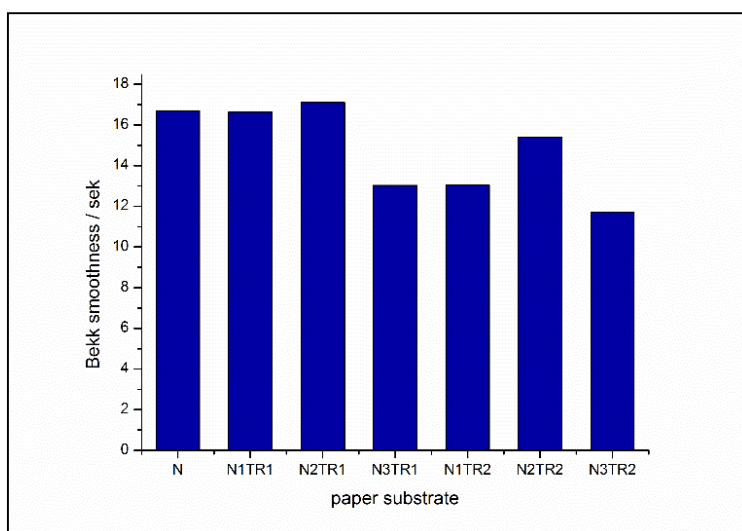






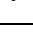









Figure 1: Bekk smoothness of paper substrates

All paper substrates were printed by AGFA, Anapurna M1600, UV-curable inkjet printer. The inkjet process is a computer to print technology, where the ink is transferred directly to the substrate by means of a jet system. Reproduction is controlled directly by a raster image processor on the basis of the print job described entirely in a digital form. In this technology, ink is sprayed from nozzles, which means that no image carrier (printing plate) is needed. The aforementioned UV-curable inkjet printer (AGFA, Anapurna M1600) has the print-heads of 1024 nozzles with a droplet volume of 12 pl for colours, which produce high quality solids and tonal rendering at up to 720 x 1440 dpi. The printability of used paper substrates was analysed by way of classifying dot fidelity. The shapes of ideal dots and printed dots are presented in Table 3. In images of printed dots the image background noise can be observed. . This appearance is caused by the presence of a uniform distribution of very small satellite ink droplets in the non-image area [Oliver et al., 2002].

Table 3: Dot shapes

Ideal dots						
Radius of dots (mm)						
0.350	0.250	0.150	0.125	0.100	0.075	0.050
						
Printed dots						
						

The equipment used to measure reproduction quality of printed dots was DinoLite and ImageJ software. DinoLite is a digital microscope with magnification of 200x. ImageJ is a public software which was used to measure and calculate the dot area and dot shape descriptors (roundness, aspect ratio and solidity) of digital images. An ideal reproduced dot is envisaged as a perfect sharp circle without any mechanical gain and of consistent density [Fleming et al, 2003]. Dot area is defined as number of pixels located within the boundary of a segmented printed dot and is calculated according to equation 1.

$$Area = \pi \times radius^2 \quad (1)$$

Major axis of an ellipse is its longest diameter which goes through the centre and its ends are widest points of the shape. In addition, minor axis crosses the major axis at the centre and its ends are the narrowest points of the ellipse. Based on these parameters, two additional features, roundness and aspect ratio, i.e. elongation, could define the shape modifications of an ideal dot (equations 2 and 3) [Fleming et al, 2003]; [Doyle, 2000].

$$Roundness = \frac{4 \times Area}{\pi \times Major Axis^2} \quad (2)$$

$$Aspect Ratio = \frac{Major Axis}{Minor Axis} \quad (3)$$

Solidity (convexity) indicates whether an object has an irregular border or not. It is determined by using the gift wrapping algorithm as an algorithm for calculating the convex area (equation 4) [Rodriguez et al, 2012].

$$Solidity = \frac{Area}{Convex area} \quad (4)$$

All measurements were repeated 10 times on each paper substrate made of straw fibres as well as on control substrates. Statistical analysis was performed in Origin Lab 8.0.

3. RESULTS AND DISCUSSION

Dot fidelity was observed for the purpose of establishing the most suitable weight ratio of triticale straw fibres in paper substrate for achieving good reproduction quality. Dot area, roundness, aspect ratio and solidity were measured on six different paper substrates with triticale fibres and compared against a control paper substrate (N) made only of recycled fibres.

Dot area increment measured on different paper substrate is presented in Figure 2.

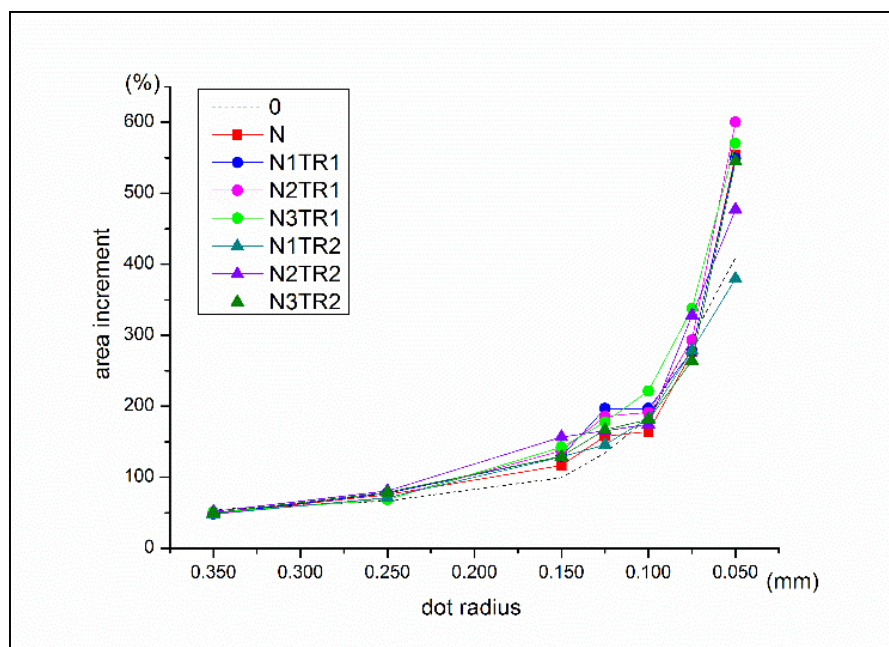


Figure 2: Dot area increment measured on different paper substrates in relation to the dot radius

Prints, which were obtained on market newspaper (named as 0) and prints obtained on laboratory paper substrate (named according Table 2) have similar trends in relation to the printed dot radius. Namely, dot area increment on all paper substrates was equal or very similar in dot sizes with radius of 0.350 mm (50.195 ± 2.184) and 0.250 mm (73.706 ± 5.207). In smaller dot sizes, the variations in dot area increments were bigger and the dot area increments alone were very high, especially in dots with radius of 0.050 mm which can achieve an increment of up to 600.28%.

The influence of paper substrate on dot shape descriptors was observed on seven different radius of dots as presented in Figures 3a–g. Analysis of dot shape descriptors included analysis of roundness, solidity and aspect ratio. Parameters roundness and aspect ratio describe the shape modification of an ideal dot. Namely, there values in an ideal, printed, dot are 1. Parameter solidity describes the regularity of a dot border and also has a value 1 in an ideal printed dot.

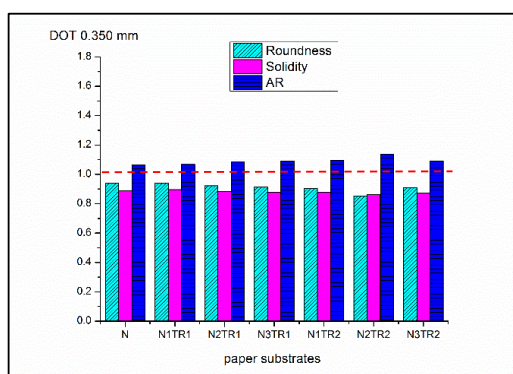


Figure 3a: The dot shape descriptors of 0.350mm dot radius

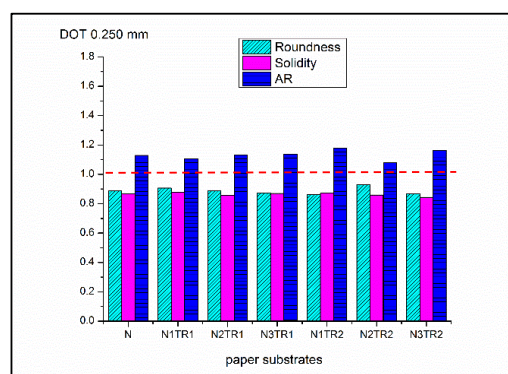


Figure 3b: The dot shape descriptors of 0.250mm dot radius

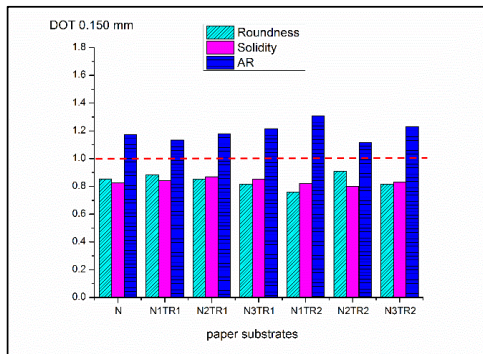


Figure 3c: The dot shape descriptors of 0.150mm dot radius

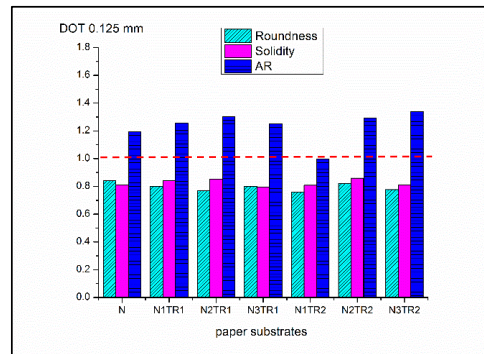


Figure 3d: The dot shape descriptors of 0.125mm dot radius

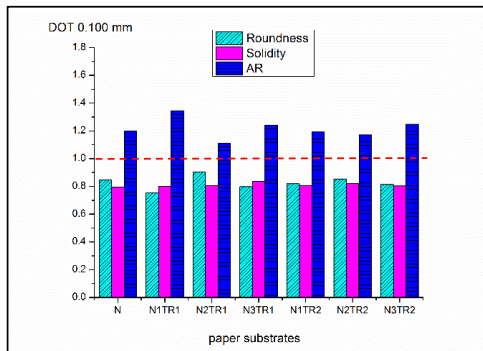


Figure 3e: The dot shape descriptors of 0.100mm dot radius

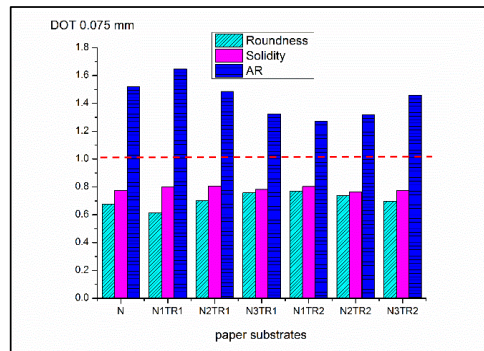


Figure 3f: The dot shape descriptors of 0.075mm dot radius

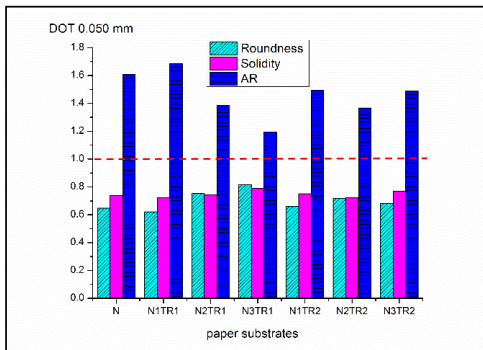


Figure 3g: The dot shape descriptors of 0.050mm dot radius

Results presented in Figures 3a-g show that dots with higher radius had aspect ratio (AR) close to value 1. The values of aspect ratio were increasing with the decreasing of dot radius (values varying from 1 to 1.7). The aspect ratio values measured in dots with higher radius were not affected by the composition of paper substrate (Figure a-d). That was not the case in dots with smaller radius (Figure 3e-g), where the AR values were different when compared against a control paper substrate made only of recycled fibres (N). The highest AR value was observed in N1TR1 sample in relation to all small printed dots that were analysed. Laboratory paper substrates made of raw materials containing 30% of triticale fibres (N3TR1) had the smallest AR values, if compared to a control paper (N) (Figure 3e-g).

The roundness and solidity of dots were equal to the ones for a circle and less resembling the ones of any other closed shape. Having observed each dot size, it could be concluded that values for roundness and solidity were similar in all analysed paper substrates. These values decreased as the dot radius was smaller. The least round and the most elliptical dots were the ones with 0.050mm dot radius (Figure 3g).

4. CONCLUSIONS

The size of dots printed on a paper substrate typically increases from its original defined size in a digital form. This phenomenon is usual for printers, especially for ink jet technology where the ink is sprayed from the nozzles. Reproductions made on laboratory paper substrates produced of fibres isolated from triticale straw compared against the ones made on market newspaper have equal and similar trends of dot growth for all dot sizes. The size and shape, in particularly small printed dots, depend significantly on the features of the paper substrate. The surface of a paper substrate (smoothness), which is defined by its composition, strongly affects dot gain, especially the smallest printed dots. From the results obtained in a relation to aspect ratio, it can be concluded that the aforementioned shape descriptors had the highest deviations for all analysed dot radiuses. This parameter is used to describe a shape modification, thus the highest elongation, which was observed in the smallest printed dots, provided most elliptical shape. It was confirmed that the roundness and solidity values decrease with the decrease of the dot size.

The research presented in this paper proved that the ratio of fibres isolated from triticale straw in laboratory sheets made of recycled wood fibres has a positive impact on dot reproduction quality. Higher dot fidelity offers a more uniform and sharper image reproduction as well as clearer boundaries and more legible text.

5. ACKNOWLEDGMENTS

This research has been performed within the project "Straw triticale as a source of fibre in the production of newspaper" supported by the University of Zagreb.

6. REFERENCES

- [1] Bates, I., Plazonić, I., Koren, T.: "The reproduction quality of the lines on paper substrates with straw fibers", Proceedings of joint conference Wood Pulp & Paper Polygrafia academica 2014, (FCHPT STU: Bratislava, Slovakia, 2014), pages 276–281.
- [2] Doyle, M.: "Measuring the imperfect dot", Proc. IS&T's NIP16: 2000 International Conference on Digital Printing Technologies, (IS&T: Vancouver, B.C., Canada, 2000/16), pages 640–642.
- [3] Fleming, P. D., Cawthorne, J. E., Mehta, F., Halwawala, S., Joyce, M. K.: "Interpretation of Dot Area and Dot Shape based on Image Analysis", Proceedings of the IS&T NIP18: International Conference on Digital Printing Technologies, (IS&T: San Diego, USA, 2002), pages 218–222.
- [4] Fleming, P. D., Cawthorne, J. E., Mehta, F., Halwawala, S., Joyce, M. K.: "Interpretation of Dot Fidelity of Ink Jet Dots Based on Image Analysis", Journal of Imaging Science and Technology 47 (5), 394–399, 2003.
- [5] Hubbe, M. A., Venditti, R. A., Rojas O. J.: "What happens to cellulosic fibers during papermaking and recycling? A review", Bioresources 2 (4), 739–788, 2007.
- [6] Minor, J. L., Atalla, R.H.: "Strength loss in recycled fibers and methods of restoration", Proceedings of Materials Research Society symposium, (Materials Research Society: San Francisco, USA, 1992/266), pages 215–228.
- [7] Nazhad, M. M.: "Recycled fibre quality – A review", Journal of industrial and engineering chemistry 11 (3), 314–329, 2005.
- [8] Oliver, J., Chen, J.: "Use of Signature Analysis to Discriminate Digital Printing Technologies", Proc. IS&T's NIP18: 2002 International Conference on Digital Printing Technologies, (IS&T: San Diego, USA, 2002), pages 218–222.
- [9] Plazonić, I., Barbarić-Mikočević, Ž., Džimbeg-Malčić, V.: "Chemical composition of triticale straw as a paper fiber source", Proceedings of joint conference Wood Pulp & Paper Polygrafia academica 2014, (FCHPT STU: Bratislava, Slovakia, 2014), pages 292–297.
- [10] Rodriguez, J. M., Johansson, J.M.A., Edeskär, T.: "Particle Shape Determination by Two-Dimensional Image Analysis in Geotechnical Engineering", Proceedings of Nordic Conference on Soil Mechanics and Geotechnical NGM, (Danish Geotechnical Society: Copenhagen, Denmark, 2012/27), pages 207–218.
- [11] Stančić, M., Novaković, D., Tomić, I., Karlović, I.: "Influence of substrate and Screen thread count on reproduction of image elements in screen printing", Acta Graphica: Journal for Printing Science and Graphic Communications 23 (1–2), 1–12, 2012.

INFLUENCE OF SUBSTRATE THICKNESS ON THE REPRODUCTION QUALITY OF SCREEN PRINTED POLYMER MATERIALS

Branka Ružičić¹, Mladen Stančić¹, Rastko Milošević², Milana Sadžakov²

¹University of Banja Luka, Faculty of technology,

Department of Graphic engineering, , Banja Luka, Bosnia and Herzegovina

²University of Novi Sad, Faculty of technical science,

Department of Graphic engineering and design, Novi Sad, Serbia

Abstract: Print quality includes the desired color reproduction and adequate reproduction of image elements. In this paper were analyzed transparent polymer materials printed by screen printing technique. Research has primarily consisted of an analysis of macro non-uniformities, and as additional quality parameters, the results of reproduction of text and MTF on obverse and reverse side of print. Considering the results, it can be concluded that the thickness of the substrate affect the macro non-uniformity, and the reflection from the substrate also increases the macro non-uniformity measured from the reverse side of printing. Results of the analysis of text reproduction and modulation transfer function analysis indicate certain changes of these parameters measured on the reverse side of the print and compared to the obverse side. So it was determined that printing surface, with its characteristics, significantly affects the print quality.

Key words: polyethylene films, obverse and reverse print measuring, macro non-uniformity, text reproduction, MTF

1. INTRODUCTION

Polyethylene as a printing substrate is the mostly widely used plastic on earth with an annual production of approximately 80 million tons. [Szentgyörgyvölgyi et al., 2010] The primary markets for this plastic include films, carrying bags, and sacks. Roughly 67% of global polyethylene demand falls into these categories. Some examples of these applications include agricultural, multi-layer, and shrink films, as well as reinforcements for levees. Polyethylene, which is soft, ductile, and flexible, is additionally utilized for strong, elastic goods, such as screw caps, lids, and coatings. [Ceresana Research, 2010] Polymer substrates are mostly printed by flexographic technology, with low viscosity-inks, but it can be printed beside flexographic, by screen printing and, with technology advances, by ink jet printing technique. Disadvantage of flexographic technique is high cost to implement. [Kipphan, 2001] Screen printing has a great advantage in the area of cost and low-circulation production. Requirements for its use are very modest and it can in essence be carried out anywhere in the world with little prerequisites. Also it is simple, fast, reproducible, flexible and adaptable. [Lee et al., 2008; Krebs et al., 2009] PE-LD is low density polyethylene ($0.910 - 0.925 \text{ g cm}^{-3}$), it's highly branched and contains relatively high amorphous content which results in outstanding clarity in film for food packaging. [Malpass, 2010] Polyethylene as a material has some characteristics that greatly affect the final result of the product. Beside transparency that shows the distortion of an object observed through examined film, also a huge impact has the haze. Haze represents scattering of light by a film that result in a cloudy appearance or poorer clarity of objects when viewed through the film. More technically, haze is the percentage of light transmitted through a film that is deflected more than 2.5° from the direction of the incoming beam. This property is used to describe transparent and translucent films, not opaque films. Haze is greatly influenced by material selections and product design. Additives and coatings usually contribute to increased haze. Also, thicker films will be hazier than thinner films. Additional variables, like process temperatures in the different stages of film-making, can further affect haze, so they are tightly controlled. [Vujković, 2007] In case of reverse printing, i.e. printing on the underside of a transparent film, substrate characteristics can affect image quality in a variety of ways. [Kipman, 1998] Quantitative assessment of colour reproduction is not enough for defining overall print quality. It is proven that print quality doesn't represent monotonous function of hue, saturation and value. [Fedorovskaya et al., 1997; Pedersen et al., 2009] Quality attributes as contrast, sharpness, macro-uniformity are not connected with colour reproduction but certainly have affect on print quality. They are directly connected with line and

dot quality, that represent component of any image. (Dhopade, 2009) As important print quality attributes it can be appoint: contrast, sharpness, noise/graininess, edge raggedness, effective resolution, text quality, micro uniformity, macro non-uniformity, gloss uniformity etc. (Pedersen et al., 2009). Non-uniformity of solid-tone print density, known as print mottle, is one of the basic irregularities affecting print quality. Causes of print mottle are various, for example: printing pressure, printing speed, rubber blanket, paper surface roughness, ink and fountain solution transfer and absorption, etc. (Kawasaki et al., 2009). Print mottle parameters of interest in this research are: contrast, correlation, entropy, energy and homogeneity. It was found that low contrast, low correlation, low entropy, high energy and high homogeneity correspond to uniform grey level distribution, i.e. low print mottle (Hladnik et al., 2011; Chen, 1998). It was also discovered that entropy parameter correlates the best with human texture perception (Gebeješ et al., 2012). Many researchers have questioned and acknowledged the importance of quality attributes, however, they did not reach the conclusion which of them are the most important. Engeldrum in his work states that observers most likely will not be able to perceive more than five quality attributes simultaneously. (Engeldrum et al., 2004) Common way to assess print sharpness is by measuring modulation transfer function (MTF). MTF represents the contrast at a certain spatial frequency compared with low frequency. Spatial frequency is usually measured by cycles or pairs per length unit (mm or inch), although most common unit are cycles per pixel or line width per picture height of the observed image (LW/PH). High spatial frequency corresponds to fine details (Rilovski, 2011.) The ability of a system to reproduce details is captured in its modulation transfer function. MTF is commonly measured by slanted edge method. The slanted edge method is often used to measure the MTF of a scanner or any capture device and can be adapted to measure the MTF of a printing system (Bonnier et al., 2010). Some of quality components are line width and its variations, raggedness and sharpness. Line raggedness indicates deviation of printed lines from ideal geometric shape, and is the undesired line property that leads to a reduction in print quality. Line raggedness can be characterized measuring area and perimeter of lines and comparing this values with ideal. Overexpressed line raggedness causes low sharpness of printing, and can cause text to become unclear or bold. (Stančić et al., 2013) Ink bleeding tends to make lines wider hence estimating the line width changes could determine the bleeding degree. The evaluation of bleeding on small letters can give information about text readability. In cases when ideal letter area and perimeter deviates significantly from measured values, it will indicate poor text readability. (Stančić et al., 2012)

It should be pointed out that the aim of this study was to investigate the influence of transparent polyethylene film thickness on printing quality. Analysis primarily included macro non-uniformity, but also important quality attributes as text quality and MTF, were also examined. For these print quality parameters evaluation was used the method of digitally analysed scanned imprint pictures in specified softwares.

2. METHODS AND MATERIALS

This research included four different thicknesses of polymer material of the same composition. The material that is used is PE-LD low density polyethylene ($0.910 - 0.925 \text{ g cm}^{-3}$). Used thicknesses are 30, 35, 38 and 110 μm . The samples were printed with screen printing technique. Test image, used in research, was created using Adobe Illustrator CS5.5 software. Test image dimensions was 210 x 297 mm and contains different elements used for print quality control. Elements used for obtaining the results were 2.54 x 2.54 mm solid tone patches, ISO 12233 test chart with slanted edge and 8 pt text. Screen with thread count of 120 threads per cm was used for printing plates. Printing plates were made conventionally using linearized positive films. As a photo sensitive coating was used Sericol Dirasol 22 emulsion. Exposure was performed 90 seconds with RUVA lamp (40 W), where the distance from lamp to screen measured 20 cm. Printing speed amounted to 15 cm per second, squeegee hardness - 85 Shore Type A, while snap-off distance measured 4 mm. Ink used for printing was Sericol Polyscreen yellow colour PS-043/1 (Mid Chrome). Fixation of printed samples was carried out on room temperature in duration of 4 hours. After fixation the printed sheets were digitalized by Mustek 1200 ub plus flat scanner for further analysis. Scanning resolution was set as 1200 spi and all auto functions were turned off. Print mottle assessment of the prints was conducted via GLCM image processing method (Grey Level Co-occurrence Matrix), using MATLAB software, after which five solid-tone surface uniformity parameters were extracted. It uses a matrix that keeps track of how often different combinations - pairs - of pixel intensity (grey level) values in a specific spatial relationship and

distance occur in an image, which makes it possible to compute various first and second order statistical parameters or texture measures (Rilovski et al., 2011). There were 3 quadratic samples [2.54 cm x 2.54 cm] for each material thickness, a total of 12 samples. After printing, the samples were scanned. Then, scanned images were scaled to dimensions of 500 x 500 pixels, in order to prepare the samples for subsequent GLCM image processing and extraction of five solid-tone surface uniformity parameters (contrast, correlation, entropy, energy and homogeneity).

MTF was measured by slanted edge method. During the analysis, one edge of digitalized test image is selected as the region of interest (ROI). The analysis is visualized in Figure 1. In each line of the ROI is a transition from black to white – a step function (Figure 1a). The position of the transition of each step function is estimated and the lines are shifted, so that the transitions are all vertically aligned. Then the average of all the shifted step functions is calculated along this vertical line to reduce the influence of noise (Figure 1b). The derivative of this mean step function is ideally a Dirac delta function, but in reality it is a peak of a certain width (Figure 1c). The absolute value of the Fourier transform of this peak is the MTF (Figure 1d) (Bonnier et al., 2010). In this work we used MTF50 parameter. MTF50 parameter was determined by Imatest SFR software. MTF50 is spatial frequency where MTF is 50% of the low frequency MTF. Print quality of observed image could be established based on MTF50 parameter. It is necessary to divide MTF50 value (in LW/PH unit) with image height (inch as unit). In this work image height was 11.7 inch. To determine print quality obtained values are compared with reference values. Table 1 is guide to quality requirements.

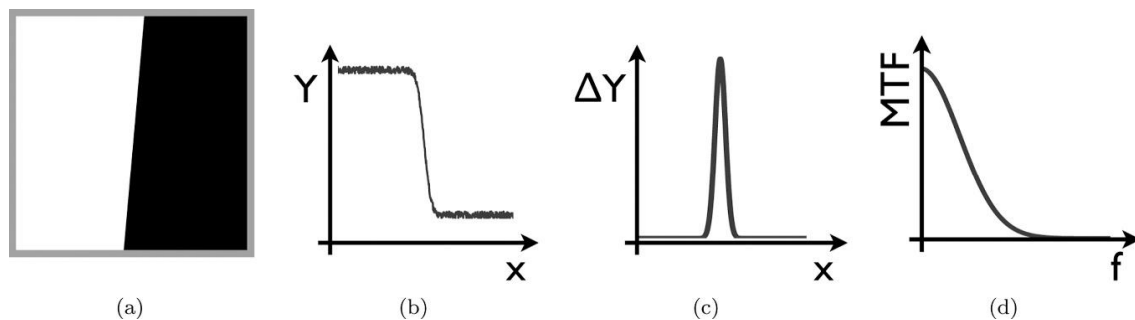


Figure 1: Basic principle for the MTF measurement with the slanted edge method: (a) region of interest, (b) average of Y values from shifted lines, (c) derivative with noise suppression, and (d) Fourier transform and normalization resulting in an estimation of the MTF (Bonnier et al., 2010)

Table 1.: Print Quality level according MTF50 parameter and image height

	Quality level
150	Excellent – Extremely sharp at any viewing distance
110	Very good – Large look excellent, though they won't look perfect under a magnifier. Small prints still look very good.
80	Good – Large prints look OK when viewed from normal distances, but somewhat soft when examined closely. Small prints look soft (adequate, perhaps, for the “average” consumer).

In order to evaluate text readability, we measured the area and perimeter of letter “s” size of 8 pt and comparing these values with area and perimeter values of ideal image created using a computer in resolution of 1200 ppi. These values were calculated using ImageJ software, implemented in Java for the creation, visualization, editing, processing, and image analysis (Rasband, 2000).

3. RESULTS AND DISCUSSION

3.1 Macro non-uniformity analysis

In Figure 2 are presented different solid-tone surface uniformity parameters (contrast, correlation, entropy, energy and homogeneity), recorded with in the prints made on two sides of polyethylene using four different thicknesses. For all films, it can be noticed low values of contrast and entropy and high values of energy and homogeneity on all thicknesses which represent good, uniform reproduction of solid-tone surface. Correlation parameter has lower values also, which supports the low print mottle. Recorded print mottle parameters values on polyethylene films show good behaviour for all five considered parameters. One thing interesting for this paper is comparison of obverse and reverse printed side, and the difference can be noticed. Low values of contrast and entropy from the obverse side are lower on the reverse side, and high values of energy and homogeneity are higher on the reverse side. Correlation parameter has lower values also, which supports the low print mottle, but on the reverse side, these values are higher than on the obverse side.

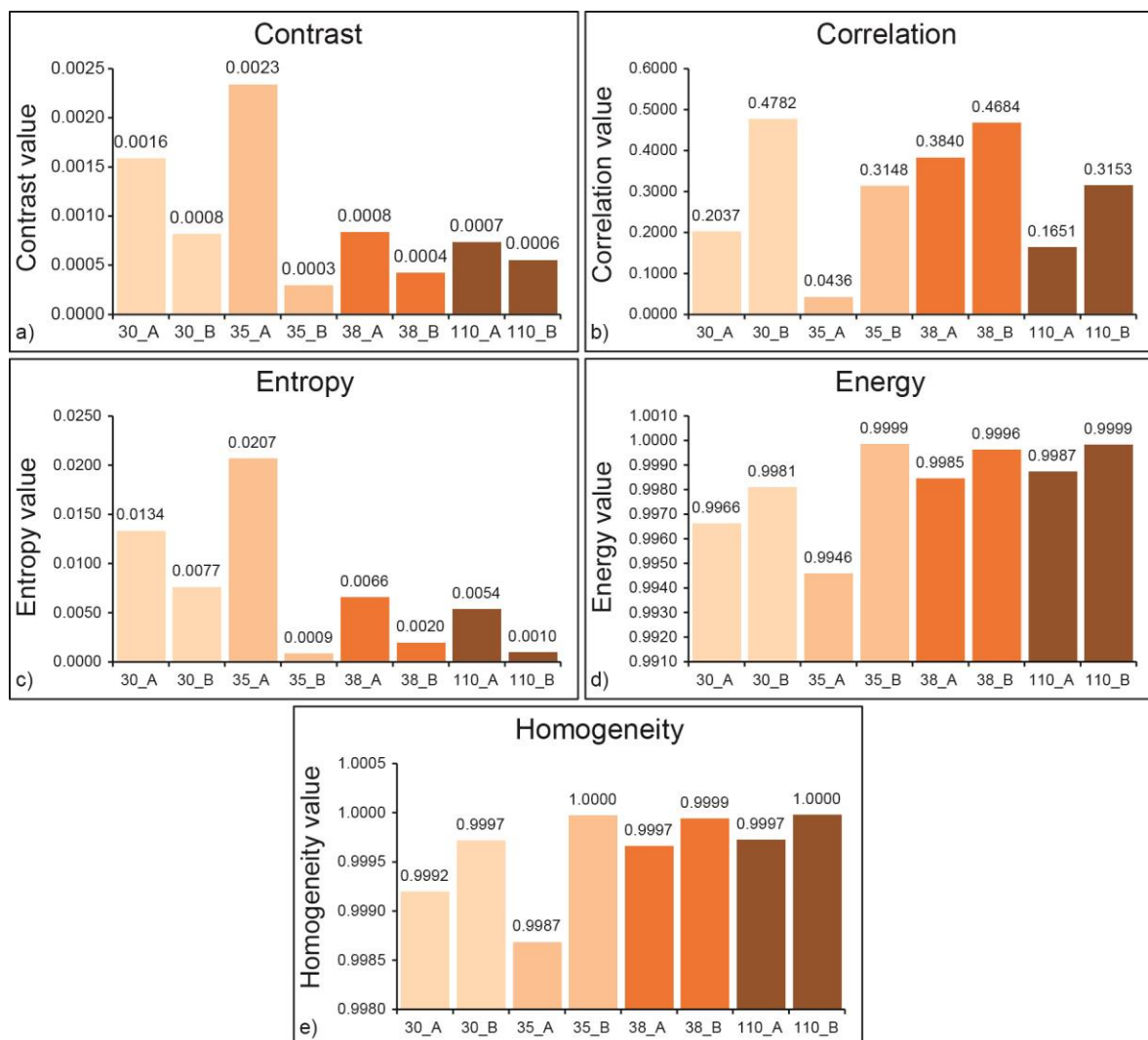


Figure 2: Values of different print mottle parameters: (a) Contrast; (b) Correlation; (c) Entropy; (d) Energy; (e) Homogeneity (Note: Numbers 30, 35, 38 and 110 denote a film thickness in μm , A stands for obverse side of print, and B stands for reverse side of print)

3.2 Modulation transfer function analysis

The print sharpness was assessed by measuring modulation transfer function (MTF). Results obtained from the polyethylene substrates, where the MTF was measured on the ISO 12233 test chart by slanted edge method, are given in Table 2.

Table 2: MTF parameter value

Sample	MTF 50 (LW/PH)		Sample	MTF 50 (LW/PH)		Sample	MTF 50 (LW/PH)		Sample	MTF 50 (LW/PH)
30_A	1608		35_A	1507		38_A	1407		110_A	989.6
30_B	1251		35_B	1246		38_B	1350		110_B	772.6

Observing the obtained results, it can be noticed that the polyethylene thickness have an impact on MTF 50 value. Film with a lowest thickness has the highest values and the highest thickness film has the lowest value of MTF parameter. Hence, the increase of film thickness leads to a decrease of print sharpness, i.e. thinner films have higher quality level on the same distance. Also on Figure 3 it is noticeable that film impact on reverse side print, and every value obtained with measuring on the reverse side has lower values then values obtained with measuring on the obverse side of print.

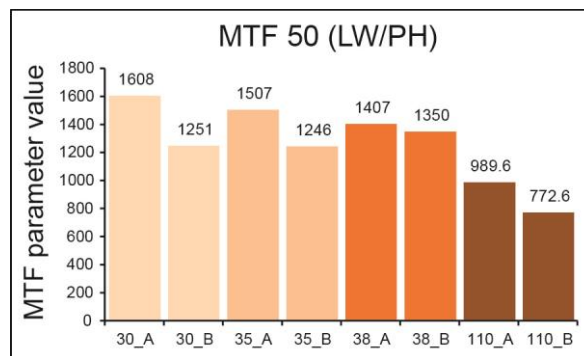


Figure 3: Graphic representation of MTF parameter values

Print quality of observed images was established by dividing MTF50 value with image height 11.7 inch. The results are shown in Table 3.

Table 3: Quality level obtained by the MTF 50 parameter and observed image height

Sample	Quality level		Sample	Quality level		Sample	Quality level		Sample	Quality level
30_A	137.44		35_A	128.80		38_A	120.26		110_A	84.58
30_B	106.92		35_B	106.50		38_B	115.38		110_B	66.03

The resulting quality level indicates that the prints printed on thinner films (30, 35 and 38 μm) possess very good quality level, while prints printed on film with much higher thickness (110 μm) possess a good quality level.

3.3 Text readability analysis

In order to evaluate text readability, we measured the area and perimeter of letter "s" (size 8 pt) and compared it to an ideal letter "s" created using a computer in resolution of 1200 ppi. Results of area and perimeter movements are shown on Figure 4.

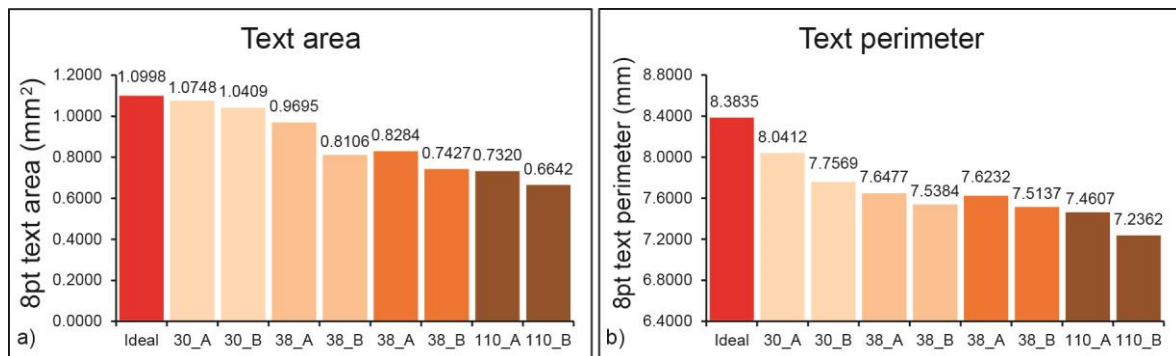


Figure 4: Graphic representation of movements of 8 pt letter "s": a) Area values; b) Perimeter values

Text area and perimeter results indicate that films of all thicknesses show a difference in a relation to an ideal text area and perimeter. The smallest difference is with the thinnest film, and a difference increase with increasing of film thickness, so the biggest difference is with the thickest film of 110 μm . Also on this graphics it can be noticed that there is a difference between obverse and reverse side of print. So, text area and perimeter have a drop of values on reverse side in relation to obverse side of print and reduction of the letter area results in poor text readability.

4. CONCLUSION

The aim of this paper is to point out the influence of the substrate during the reverse print on the transparent polymeric materials. Low-density polyethylene films were printed with screen printing technique and the print was examined through the transparent substrate. In the aim of determining the influence of the substrate, the basic attributes of print quality were analyzed: macro non-uniformity, modulation transfer function and text readability.

Macro non-uniformity parameter obtained using GLCM image analysis method showed that film thickness don't have much influence on print mottle, but same parameters show that the reverse side of print have more uniform solid-tone surface ink coverage and lower print mottle effect. The print sharpness was assessed by measuring modulation transfer function (MTF). It showed that the increase of film thickness leads to a decrease of print sharpness, i.e. thinner films have higher quality level on the same distance. Text readability assessment showed that letter areas and perimeters clearly deviated from the ideal for both sides of every substrate thickness used. This results in poor readability.

Considering all the results, we can conclude that the substrate with its thickness affects the quality of print. In the aim of further knowledge the influence of transparent film thickness on some other important quality attributes or influence of other material properties such as: surface tension, surface roughness, dampening and contact angle on the print quality.

5. REFERENCES

- [1] Bonnier, N., Lindner, A., J., "Measurement and compensation of printer modulation transfer function", *Journal of Electronic Imaging*, 19 (1), 1 – 22. [2010].
- [2] Ceresana Research, 2010, Market Study: Polyethylene – LDPE, URL <http://www.ceresana.com/en/market-studies/plastics/polyethylene-ldpe/> [last request: 2014-09-11]
- [3] Chen, Y.: „Image analysis methods for paper formation evaluation“, M.A.Sc. thesis, University of Toronto, Canada, 33, [1998].
- [4] Dhopade, A.: "Image quality assessemnet according to ISO 13660 and ISO 19751", Test Targets 9.0, 43 – 50, [2010].
- [5] Engeldrum, P. G.: "A Theory of Image Quality: The Image Quality Circle", *Journal of Imaging Science and Technology*, 446 – 456, [2004].
- [6] Fedorovskaya, E., A., De Ridder, H., Blommaert, F.: "Chroma variations and perceived quality of colour images of natural scenes", *Color research and application* 22, 2, 96 – 110, [1997].

- [7] Gebeješ, A., Tomić, I., Huertas, R., Stepanić, M.: „A preliminary perceptual scale for texture feature parameters“, *Proceedings of the 6th International Symposium on Graphic Engineering and Design, Novi Sad, Serbia*, ISBN 978-86-7892-294-7, pp. 195-202, Faculty of Technical Science, Novi Sad, (2012).
- [8] Hladnik, A., Lazar, M.: „Paper and board surface roughness characterization using laser profilometry and gray level cooccurrence matrix“, *Nordic Pulp and Paper Research Journal*, Vol 26, No. 1/2011, ISSN: 0283-2631, 99-105, (2011).
- [9] Kawasaki, M., Ishisaki, M.: (2009). „Investigation into the Cause of Print Mottle in Halftone Dots of Coated Paper: Effect of Optical Dot Gain Non-uniformity“, (URL: <http://www.tappi.org/content/06IPGA/5-4%20Kawasaki%20M%20Ishisaki.pdf> last request: 2014-09-14)
- [10] Kipman, Y.: „Image Quality Metrics for Printers and Media“, IS&T's Conference - Image Processing, Image Quality, Image Capture, Systems Conference, Portland, 183-187, (1998).
- [11] Kipphan, H., „Handbook of print media: Technologies and Production Methods“, Springer, Berlin, 137-140, (2001).
- [12] Krebs, F., Jørgensen, M., Norrman, K., Hagemann, O., Alstrup, J., Nielsen, T., Fyenbo, J., Larsen, K., Kristensen, J.: „A complete process for production of flexible large area polymer solar cells entirely using screen printing - First public demonstration“, *Solar Energy Materials and Solar Cells*, 93, 422-441, (2009).
- [13] Lee, T. M., Choi, Y. J., Nam, S. Y., You, C. W., Na, D. Y., Choi, H. C., Shin, D. Y., Kim, K. Y., Jung, K. I.: „Color filter patterned by screen printing“, *Thin Solid Films*, 516, 7875-7880, (2008).
- [14] Malpass, D., B.: „Introduction to Industrial Polyethylene: Properties, Catalysts, and Processes“, John Wiley & Sons, Inc., New Jersey, 8, (2010).
- [15] Novaković, D., Stančić, M., Karović, I., Kašiković, N., Vukmirović, V., Milošević, R.: „Influence of surface roughness on print quality on digitally printed self adhesive foils“, *Journal of Print and Media Technology Research*, Vol. 2, No 2, 67-76, (2013).
- [16] Pedersen, M., Bonnie, N., Hardeberg, J., Albregtsen, F.: „Attributes of a new image quality model for color prints“, *Proceedings of Color Imaging Conference*, Albuquerque, New Mexico, USA, 204 – 209, (2009).
- [17] Rasband, W. S., ImageJ, U. S. National Institutes of Health, Maryland, USA, <http://rsb.info.nih.gov/ij/>, 1997-2006.
- [18] Rilovski, I., Karlović, I.: „Digital print sharpness as a quantitative tool for print quality assessment“, *Proceedings of Printing Future Days Conference*, Chemnitz University of Technology, Germany, ISBN: 978-3-86135-623-3, pp. 31-36, VWB, Berlin, Germany, (2011).
- [19] Rilovski, I.: „Quality control of sharpness of reproduction of digital prints“, Master thesis, Department of Graphic engineering and design, Faculty of technical science, Novi Sad, p. 32, (2011).
- [20] Stančić, M., Novaković, D., Kašiković, N., Vukmirović, V., Ružičić, B.: „Influence of material composition on print quality digitally printed textile substrates“, *Tekstilna industrija*, 1, 37-43, (2013).
- [21] Stančić, M., Novaković, D., Tomić, I., Karlović, I.: „Influence of Substrate and Screen Thread Count on Reproduction of Image Elements in Screenprinting“, *Acta Graphica*, 23, 1-12, (2012).
- [22] Szentgyörgyvölgyi, R., Novotny, E.: „Investigation of flexographic printing on PE and BOPP foils“, *Proceedings of GRID '10*, Novakovic, D. (Ed.), Novi Sad, Serbia, 2010, FTN, GRID, NOVI SAD (2010), pp. 337-342.
- [23] Vujković, I., Galić, K., Vereš, M., „Ambalaža za pakiranje namirnica“, Tectus, Zagreb, (2007).

PARAMETERS OF REPRODUCTION AND THEIR INFLUENCE TO APPEARANCE OF MOIRÉ PATTERN IN LITHOGRAPHIC OFFSET PRINTING

Zoran Gazibarić¹, Predrag Živković²,

¹Banjaluka College, Graphic design and visual communication department,
Bosnia and Herzegovina

²University of Belgrade, Faculty of Technology and Metallurgy, Belgrade, Serbia

Abstract: The appearance of Moiré pattern can significantly affect the quality of offset reproduction. It is formed by superimposing of fine details of two or more structures. It appears in printing when: screen structures are misaligned because of misregistration (it is very difficult to predict it, because it is not visible on the proof), inappropriate combination of screen frequency and screen angles is used, an original halftone that contains patterned objects is scanned and exposed or when fine details of continuous tone original are superimposed with input frequency of scanner or with CCD element structure of digital camera. The aim of this work is to investigate the influence of reproduction parameters, such as screen frequency, imaging resolution, register accuracy or input bit-map resolution to appearance of Moiré pattern. Tests will be done on a limited number of combinations of screen frequencies and input resolutions. The test result will be recommendations, which parameters combination should be avoided and which to use so that Moiré pattern could be minimized on the final printing product.

Key words: Moiré, quality, reproduction, screening

1. INTRODUCTION

Moiré effect is the appearance of an interference pattern generated by overlapping of two regular fine structure placed in a particular position (Xiangdong, 1996; Amidror and Hersch, 1994). These structures may be parallel lines, or a network of evenly distributed dots or other fine elements.

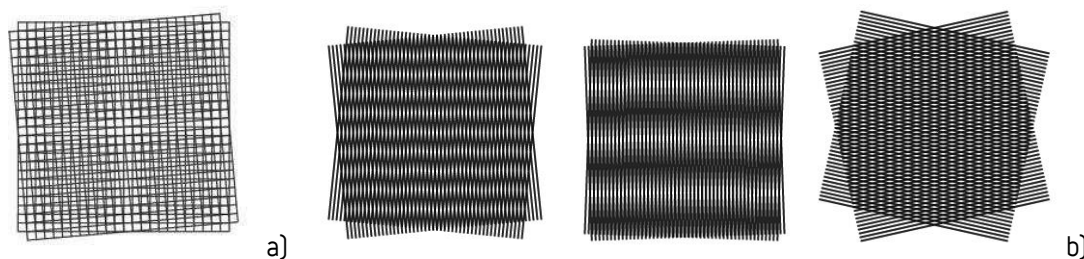


Figure 1: Moiré effect caused by overlapping of: a) two grids; b) two linear structures under different angles

Moiré effect can occur during processing of digital information, for instance:

- taking pictures of textured objects, when texture overlaps with the grid of CCD cells for image acquisition (Figure 2);



Figure 2: Typical Moiré effect during taking pictures of texturized materials

- scanning of already printed samples with screen dot structure;
- because of misregistration in printing;
- because of inadequate screen angles for certain separation in printing;
- because of inadequate ratio between input resolution of bit-map and screen-ruling of AM raster.

When selecting the reproduction parameters one must take into account dependence between screen ruling and imaging resolution in order to obtain a satisfactory number of gray levels [Linotype-Hell, n.d.; Expert Guide, 2002]. The dependence is shown in Figure 3a. For instance, in order to obtain 256 gray levels with 150 lpi AM raster, it is necessary to expose with resolution of approximately 2500 dpi. By increasing the imaging resolution the number of pixels that form screen dot also increases, while their size decreases, so it is possible to create larger number of dots with different size, i.e. larger number of different tone values. (Figure 3 b).

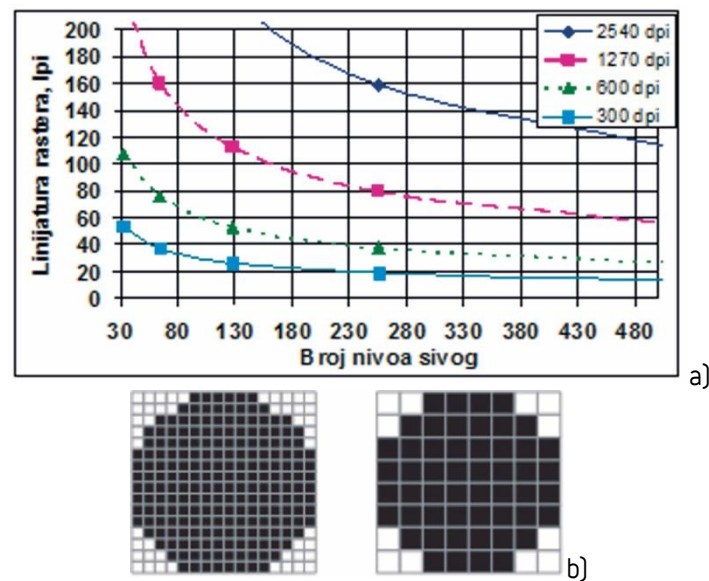


Figure 3: a) Dependence between screen ruling, imaging resolution and number of gray levels on the printed illustration; b) dots of the same screen ruling and tone value, exposed with larger (left) and smaller (right) resolution

Screen angles are chosen to provide as big as possible angle distance between separations. However, instead of separating the quadrant into four equal pieces for four separations (c, m, y, k), the strong separations (c, m, k) are shifted for 30° and yellow separation is shifted for only 15° from neighboring colors. Since it is low contrast color, Moiré effect that is less visible. Standard set of angles is: c 15° (or 75), m 75° (or 15), y 90° and k 45° (Figure 4) (ISO 12647-2:2004). In the case that there would be another interference between screen structure and some technological structure (anilox in flexo printing, silk in screen printing), all angles are additionally shifted for another 7,5°.

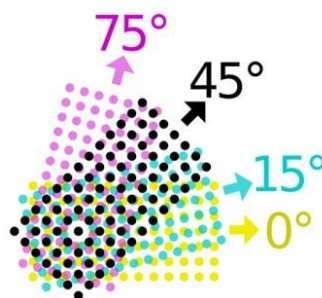


Figure 4: Typical screen angles

Mutual position of screen structures of individual separations can be disrupted because of misregistration in printing, and, in some cases Moiré effect can occur. It is recommended that resolution of bit-map of final size should be approximately two times bigger than screen ruling (Kipphan, 2000; LaserSoft Imaging, n.d.). However, this should be considered as a guideline only, since sometimes it is possible to obtain more than satisfactory reproduction even if bit-map resolution is smaller than recommended, and, in other cases, increasing the bit-map resolution can help to obtain better reproduction.

In this paper the effect of the dependence of bit-map resolution on screen ruling at a constant imaging resolution on the appearance of printed multi-color illustrations and Moiré effect is examined. In addition, it is examined whether a minor misregistration of individual colors in the printing has any influence on the occurrence of Moiré effect (Gordon, Pritchard, 2001).

2. EXPERIMENTAL

A test form is created from bit-maps of different resolution, which are printed with AM raster of different screen rulings. The bit-maps with totally different type of motif are selected. The first bit-map is created by photographing the colorful natural scene, and the second by photographing the uniformly painted object in professional studio. Photography of uniformly painted object is rather sensitive to occurrence of Moiré effect because it is easy to notice even minimal deviation from average background color. On the other hand, average photography with lot of differently colored parts which dynamically interchange is much less sensitive to occurrence of Moiré effect. The test form (Figure 5) consists of four groups of fields:

- uniformly colored bit-maps with different input resolutions, printed with different AM screen ruling;
- color photographs with different input resolutions, printed with different AM screen ruling;
- control color bars and
- auxiliary bars.



Figure 5: Test form

Uniformly colored bit-map is created by photographing of the professionally illuminated flat surface by Canon 7D camera. Bit-map was converted from RAW format into JPG of different resolutions by Adobe Photoshop. The bit-map of the girl is created using the same procedure. The color control bar was included into test form to provide means for pre-setting and regulation of the printing press. The auxiliary bars were included in the test form in order to increase color consumption and make all adjustment of the printing press easier.

All elements of the test form are put together by CorelDRAW, and PDF was created, which then was ripped several times, each time with Euclidian dot shape and different screen ruling (100, 116, 133, 142, 150, 158, 175, 187 and 200 lpi). One-bit bit-maps created from RIP are again combined using Adobe Photoshop, in order to get four final separations with bit-maps of different input resolution as well as different screen ruling, positioned as follows:

Screen ruling, lpi	Input resolution, dpi								
100	72	400	300	225	200	175	150	116	100
116	100	72	400	300	225	200	175	150	116
133	116	100	72	400	300	225	200	175	150
142	150	116	100	72	400	300	225	200	175
150	175	150	116	100	72	400	300	225	200
158	200	175	150	116	100	72	400	300	225
175	225	200	175	150	116	100	72	400	300
187	300	225	200	175	150	116	100	72	400
200	400	300	225	200	175	150	116	100	72

Those one-bit final separations are again processed in the RIP and exposed to offset plates using CtP Lüscher X-pose 130 with imaging resolution of 2400dpi. The prints are made by printing press Heidelberg Speedmaster CD 102LX, which was equipped with pre-setting and regulating mechanism Printflow and scanning densitometer X-RITE EasyTrax. In order to examine an influence of small misregistration to occurrence of Moiré pattern in prints, after printing the correctly registered sheets, some separations are deliberately shifted for small distance. In the first step the cyan printing plate was shifted for 0,07 mm in lateral, circumferentiala diagonal direction. In the second step cyan plate was shifted together with magenta plate, both in the same direction. This is in most cases considered as acceptable deviation in production print. Prints are visually examined in order to determine the reproduction quality of fine details on color photography and occurrence of Moiré pattern. Furthermore, it was examined whether small misregistration could influence the occurrence of Moiré patterns.

3. RESULTS AND DISCUSSION

Analysing the reproduced illustration it was observed that, at lower screen rulings, increasing the input resolution of bit-map above the recommended value improves the quality of reproduction (sharpness, fine details). For instance, for 100 lpi it was possible to see improvement up to input resolution of 400 dpi, which is two times higher than recommended. (Figure 6).

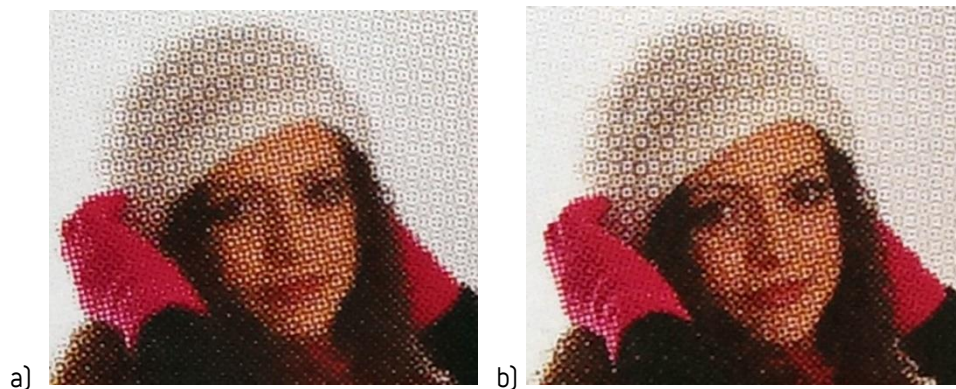


Figure 6: Details on the reproduction a) 100 lpi - 100 dpi, b) 100 lpi - 400 dpi

At finer screen ruling, eg 200 lpi , an average observer with bare eye can not see a significant difference in the quality of reproduction after input resolution of 225, although the input resolution is almost two times lower than recommended (Figure 7).



Figure 7. Details on reproduction: a) 200 lpi - 225dpi, b) 200 lpi - 400 dpi

Table 1 shows maximal input resolution of photographs printed in this experiment with different screen ruling, after which an average observer cannot notice significant improvement of the reproduction quality.

Table 1: Maximal input resolution of photographs printed in this experiment with different screen ruling, after which an average observer cannot notice significant improvement of the reproduction quality

Screen ruling, lpi	100	116	133	142	150	158	175	187	200
Input resolution, dpi	400	400	300	300	300	225	225	225	225

Analyzing the uniformly colored bit-maps, it was observed that input resolution does not influence on occurrence of Moiré pattern, for constant screen ruling. Moiré patterns in bit-maps printed with certain screen ruling look the same for all input resolution, from 72 to 400 dpi. If there is no Moiré pattern for some screen ruling, it is the case for all input resolution.

Moiré pattern was observed in this experiment on uniformly colored bit-maps for following screen rulings: 116, 133, 142, 175, 187 and 200 lpi. The very coarse Moiré pattern was obtained for screen ruling 133 and 175 lpi, the less coarse for 116 and 142 lpi, and the finest for 187 and 200 lpi. At screen ruling of 100, 150 and 158 lpi there were no visible Moiré pattern.

It was impossible to find Moiré pattern on all reproduced color photographs. Analyzing the slightly misregistered prints it was determined that slight misregistration (for 0,07 mm for c and c and m together in the same direction) does not influence on occurrence of Moiré effect - it was the same as on prints with good registration.

4. CONCLUSION

Analyzing the prints made in this work it could be concluded that it is possible to increase the reproduction quality at lower screen ruling by increasing the input resolution of bit-maps over the recommended value. For screen ruling of 100 lpi an increasing of the reproduction quality of the print was observed until the maximum resolution of 400 dpi that is used in this experiment was achieved.

At higher screen rulings it is possible to obtain satisfactory reproduction quality with input resolution that is lower than recommended value. The input bit-map resolution does not influence occurrence of Moiré pattern.

Moiré pattern was observed on all printed uniformly colored bit-maps, except for screen rulings of 100, 150 and 158 lpi. Moiré pattern was not observed on any color illustration with small areas of dynamically interchanged colors.

5. REFERENCES

- [1] Amidror, I., Hersch, R.D.: Victor Ostromoukhov, Spectral Analysis and Minimization of Moiré Patterns in Colour Separation, *Journal of Electronic Imaging*, 3(3), p. 295–317, 1994.
- [2] Expert Guide; An Introduction to Screening Technology, Heidelberg, 2002, URL http://home.zcu.cz/~jezekjan/screening_technology_eng.pdf
- [3] Gordon Pritchard, Misregistration on press, *The print guide*. URL <http://the-print-guide.blogspot.com/2011/08/misregistration-on-press.html>, 2011
- [4] ISO 12647-2:2004(E): Graphic technology — Process control for the production of half-tone colour separations, proof and production prints — Part 2: Offset lithographic processes
- [5] Kipphan, H.: *Handbuch der Printmedien Technologien und Produktionsverfahren*, Springer Verlag, 2000, p. 524
- [6] LaserSoft Imaging, Calculating the scan resolution, URL <http://www.silverfast.com/show/calc-resolution/en.html>
- [7] Linotype-Hell, Technical Information, Resolution and Screen Ruling, URL <http://www.greenharbor.com/LHTIfolder/lhti9241.pdf>
- [8] Xiangdong L.: *Analysis and Reduction of Moiré Patterns in Scanned Halftone Pictures*; Ph.D.thesis, Faculty of Virginia Polytechnic Institute and State University, Blacksburg, 1996

UV LIGHT EXPOSURE EFFECTS ON PRINT MOTTLE OF INK-JET PRINTED TEXTILE MATERIAL

Rastko Milošević¹, Nemanja Kašiković¹, Mladen Stančić², Branka Ružičić²

¹University of Novi Sad, Faculty of Technical Sciences,

Department of Graphic Engineering and Design, Novi Sad, Serbia

²University of Banja Luka, Faculty of Technology, Graphic Engineering,

Banja Luka, Bosnia and Herzegovina

Abstract: Print mottle is a common print defect, so its evaluation is vital in print quality assessment. The aim of this research is print mottle, i.e. solid-tone print uniformity estimation of polyester textile material printed using ink-jet technology. GLCM image processing method was chosen for solid-tone print uniformity assessment, as it proved to be good surface roughness and print mottle estimator. An attempt was made to determine influence of several factors on solid-tone print uniformity: different ink deposits (1 and 5 ink layers), accelerated weathering process (UV light exposure), different color spaces for image processing and different scanning resolutions for printed samples digitalization. Samples were also visually compared in order to get qualitative information about its solid-tone print uniformity and check the reliability of GLCM image processing method types.

Key words: print mottle, solid-tone ink uniformity, GLCM, ink-jet

1. INTRODUCTION

Ink-jet printing is one of the fastest growing imaging technologies, which compared to conventional printing methods among other advantages has other benefits as well, such as: lower amounts of energy, water and ink consumption, and lower waste material generation (Malik, Savita and Sushil, 2005); (Karanikas, Nikolaidis and Tsatsaroni, 2013). During exploitation of printed textile products, they are usually exposed to various influences like washing treatment and exposure to daylight (UV light), which cause textile fibers modification and change in color reproduction, so inks designed for ink-jet printing on textile materials need to satisfy various fastness criteria, especially wash and light (Stančić et al, 2014); (Karanikas, Nikolaidis and Tsatsaroni, 2013). Besides its wide range of qualities and advantages comparing to screen printing process, ink-jet technology has its own limitations like low productivity, poorer color reproducibility, complicated machine maintenances, occasional clogging of nozzles, jaggies (digital artifacts in edges), banding (lines of missing color), satellites (extra drops of ink), lower color depth (Malik, Savita and Sushil, 2005); (Yang and Naarani, 2007); (Tse et al, 1998). These print quality issues in digital printing of textiles can be categorized as: 1) appearance-related issues (line definition, text quality, resolution, image noise, optical density, tone reproduction and gloss) 2) color-related issues (color gamut, color matching and color registration); 3) permanence issues (light fastness and water fastness); and 4) usability issues (presence of defects), where print quality parameter which is in the focus of this research, solid-tone print uniformity falls into the first category group, the appearance-related issues (Tse et al, 1998). All mentioned print quality parameters are affected in greater or lesser extent by different fabric characteristics such as: 1) fabric structure (plain weave, twill, sateen and knit), 2) yarn size and thread count, 3) yarn type (combed vs. carded), 4) fabric treatment (bleached vs. mercerized) (Tse et al, 1998). Concerning UV light impact on the ink-jet printed polyester samples, it is proven that UV light colourfastness can be improved with thicker ink deposits (higher number of ink layers) as well as that UV light exposure increases printed surface reflectivity, i.e. prints become lighter (Kašiković et al, 2012). Print mottle or solid-tone print uniformity usually occurs in the manner of systematically structured patterns which the human vision system notices very easily due to its perfect responsiveness for pattern detection (Petersson, 2005). The reflectance inhomogeneities creating print mottle are caused by different reasons: uneven amount of ink that is transferred onto the substrate material during printing process, inhomogeneous ink penetration into substrate material, variations in surface porosity and substrate material formation, clogging of nozzles in ink jet heads which may lead to striped prints etc. (Elton & Preston, 2007); (Fahlcrantz, 2005). Solid-tone print uniformity assessment in this investigation was conducted with the aid of GLCM (Grey Level

Co-occurrence Matrix) image processing method, because it proved to be good surface roughness as well as print mottle estimator. GLCM, also known as the gray level spatial dependence matrix, is a table that keeps track of how often different combinations, pairs of pixel intensities (gray level values), occur in a specific spatial relationship and distance in an analysed image (Hladnik and Lazar, 2011). GLCM image processing method was applied on previously scanned ink-jet printed samples, in order to test this method's reliability in solid-tone print uniformity estimation. GLCM is an old feature extraction method for texture classification that was proposed back in 1973 (Haralick, Shanmugam and Dinstein, 1973). It enables extraction of second order parameters, which provides information about spatial relationships of image pixels, and shows in what extent printed solid-tone surface is uniform by calculating certain parameters from the generated GLCMs, e.g. contrast, correlation, entropy, energy and homogeneity (Petrou & Sevilla, 2006). Print mottle characterization was conducted using MATLAB software, and a plugin proposed by Uppuluri (2008), which provides information about 22 parameters, out of which the most relevant and used in literature, as well in this investigation are: 1) Contrast, which measures the intensity contrast between a pixel and its neighbor over the whole image, 2) Correlation, which is a measure of how correlated a pixel is to its neighbor over the whole image, 3) Entropy, which is a measure of any system's disorder, and is used to assess how regular the pixel values are within an image, 4) Energy, also known as uniformity, which is a measure of local homogeneity, enabling the information of how uniform the texture is, 5) Homogeneity, which defines the closeness of the distribution of elements in the GLCM to its diagonal (Hladnik & Lazar, 2011); (Chen, 1998). It was found that contrast, correlation, entropy, energy and homogeneity parameters can be used for print mottle assessment (Hladnik & Lazar, 2011); (Fahlcrantz, 2005). Low contrast, low correlation, low entropy, high energy and high homogeneity correspond to uniform gray level distribution, i.e., indicate a uniform, smooth surface (Hladnik & Lazar, 2011); (Chen, 1998). Energy and entropy parameters correlate very well with the visual ranking of the cyan and black printed samples so they, according to these findings, have a good potential to be used as predictors of solid-tone print uniformity (Hladnik & Lazar, 2011).

It is predicted that thicker ink deposit (higher number of ink layers) will diminish both color and yarn characteristics effects (structure and surface roughness) of the white textile material, and will contribute to a more uniform solid-tone surface. UV light exposure will definitively lead to the fading of the prints, but it may also lead to uneven fading of the whole printed areas due to initial inability to always print precisely the same ink amount on each subsequent sample over its whole surface. So it is predicted as well that UV light exposure will lead to poorer solid-tone print uniformity of the samples. It was also investigated what influence have color space and scanning resolution on GLCM image processing results of solid-tone print uniformity.

2. METHODS

For the experimental part of the research, two sample sets (5 cm x 5 cm) were prepared, made of 100% polyester textile material (fabric weight: 141,3 g/m² and thread count of (p/10 cm): warp 260 x weft 120). All the samples were printed with ink-jet printing machine Mimaki JV22 - 160 using two process J-ECO print NANO NP-60 inks (cyan and black) and two ink deposits (1 and 5 ink layers). After printing, all samples were dried in drying tunnel cabinet (Tunnel 160) on 130 °C for 180 seconds. One sample set was subjected to accelerated weathering process (UV light exposure) using Xenotest® Alpha simulator, before which samples were cut, so that the available printed areas of each sample for further GLCM analysis became 1 cm x 1 cm. After UV light exposure treatment, both sample sets were digitalized (using flatbed Canon CanoScan 5600F scanner) at three different resolutions (1200 dpi, 600 dpi and 300 dpi) and subjected to GLCM analysis for obtaining quantitative solid-tone print uniformity results. Different scanning resolutions were used to determine impact of this factor on solid-tone print uniformity results, and to check possible appearance of excessive image noise at higher scanning resolutions.

Applied MATLAB function proposed by Uppuluri, (2008) provides information about 22 GLCM parameters, out of which the most relevant and used in literature, as well as in this investigation are: contrast, correlation, entropy, energy and homogeneity as suggested in references (Hladnik and Lazar, 2011); (Hladnik et al, 2010); (Chen, 1998). Those five parameters should be interpreted as follows: low values of contrast, correlation and entropy parameters, while high values of energy and homogeneity parameters correspond to a uniform grey level distribution, indicating a uniform solid-tone print surface (Hladnik and Lazar, 2011); (Chen, 1998). Besides this MATLAB function, which calculates GLCM parameters based on L channel of L*a*b* color space, two modifications

were made on it, the first in which GLCM parameters were calculated based on all three channels of HSL color space, and the second one, where the parameters were calculated on greyscaled images. When calculating the GLCM, certain factors should be taken into account, such as: number of grey levels (256 grey level images), distance between two pixels of the GLCM ($d=1$ pixel) and an orientation (θ , four angles: 0° , 90° , -45° and 45°). Scanned sample images were also presented and visually compared as well, receiving that way qualitative information about their solid-tone print uniformity, in order to verify previously obtained quantitative results and conclusions.

3. RESULTS AND DISCUSSIONS

In this section of the paper will be presented obtained values of GLCM parameters (contrast, correlation, entropy, energy and homogeneity) for different solid-tone patches printed with cyan and black ink using two ink deposits (1 and 5 ink layers) on polyester textile material. Samples were scanned with three different scanning resolutions (1200 dpi, 600 dpi and 300 dpi), and three different image processing types were used: 1. extracting and processing L channel of $L^*a^*b^*$ color space, 2. processing all three channels of HSL color space and 3. greyscaled image processing. Also, visual comparisons of the samples will be presented in order to verify results obtained via GLCM image processing method.

3.1 Cyan ink solid-tone print uniformity analysis

If we look at the samples scanned at 1200 dpi resolution in Figure 1a (cyan ink L channel), it can be noticed that almost all GLCM parameters indicate better solid-tone print uniformity results for the samples which were subjected to UV light exposure after printing process (light green bars – 1 ink layer, yellow bars – 5 ink layers) comparing to untreated samples (dark green bars – 1 ink layer, ocher bars – 5 ink layers). Only correlation parameter in both cases (samples printed with 1 and 5 ink layers) shows the opposite. Scanning samples at 600 dpi and subsequent image processing gave similar results. Exposed samples to UV light, printed with 1 ink layer (light blue bars) show better results for all five GLCM parameters, i.e. better solid-tone print uniformity than unexposed ones (dark blue bars). In case of the samples printed using 5 ink layers, differences between GLCM parameters of UV light exposed (red bars) and unexposed samples (dark red bars) are in lesser extent pronounced than in case of samples printed with 1 ink layer. This is especially noticeable for contrast and homogeneity parameters. According to GLCM data, UV light treated samples (red bars) showed better solid-tone print uniformity for three out five parameters (correlation, entropy and energy). The last results set in Figure 1a refers to calculated GLCM parameters using 300 dpi scans, where is the same trend present, concerning both sample groups (samples printed with 1 and 5 ink layers). Better solid-tone print uniformity is again on the side of the UV light exposed samples (light purple bars), while samples printed with 5 ink layers have less pronounced solid-tone print uniformity distinction (grey and black bars), where only three out five GLCM parameters show better results in favour of the UV light exposed samples (contrast, energy and homogeneity).

Concerning solid-tone print uniformity comparison between the samples printed using different number of printed ink layers, general trend shows that samples printed with 1 ink layer contributes to better solid-tone print uniformity for both UV light exposed and unexposed samples, and for all GLCM parameters. An exception is correlation parameter of 600 dpi and 300 dpi scans, where 5 ink layer prints showed better results.

Obtained GLCM parameters results shown in Figure 1b (HSL) indicate almost identical trend as previously analysed results from Figure 1a. UV light exposed samples scanned at 1200 dpi, printed both with 1 and 5 ink layers show better solid-tone print uniformity results for all GLCM parameters except for correlation. Other two data sets extracted from 600 dpi and 300 dpi image scans, indicate better solid-tone print uniformity results for UV light exposed samples as well.

Solid-tone print uniformity between the samples printed using different ink layer number show identical trend as in previous analysis. Generally better solid-tone print uniformity possess samples printed with 1 ink layer, but as well as in previous case (L channel), correlation parameter indicates better GLCM parameters results of the 5 ink layer prints for samples scanned at 600 dpi and 300 dpi.

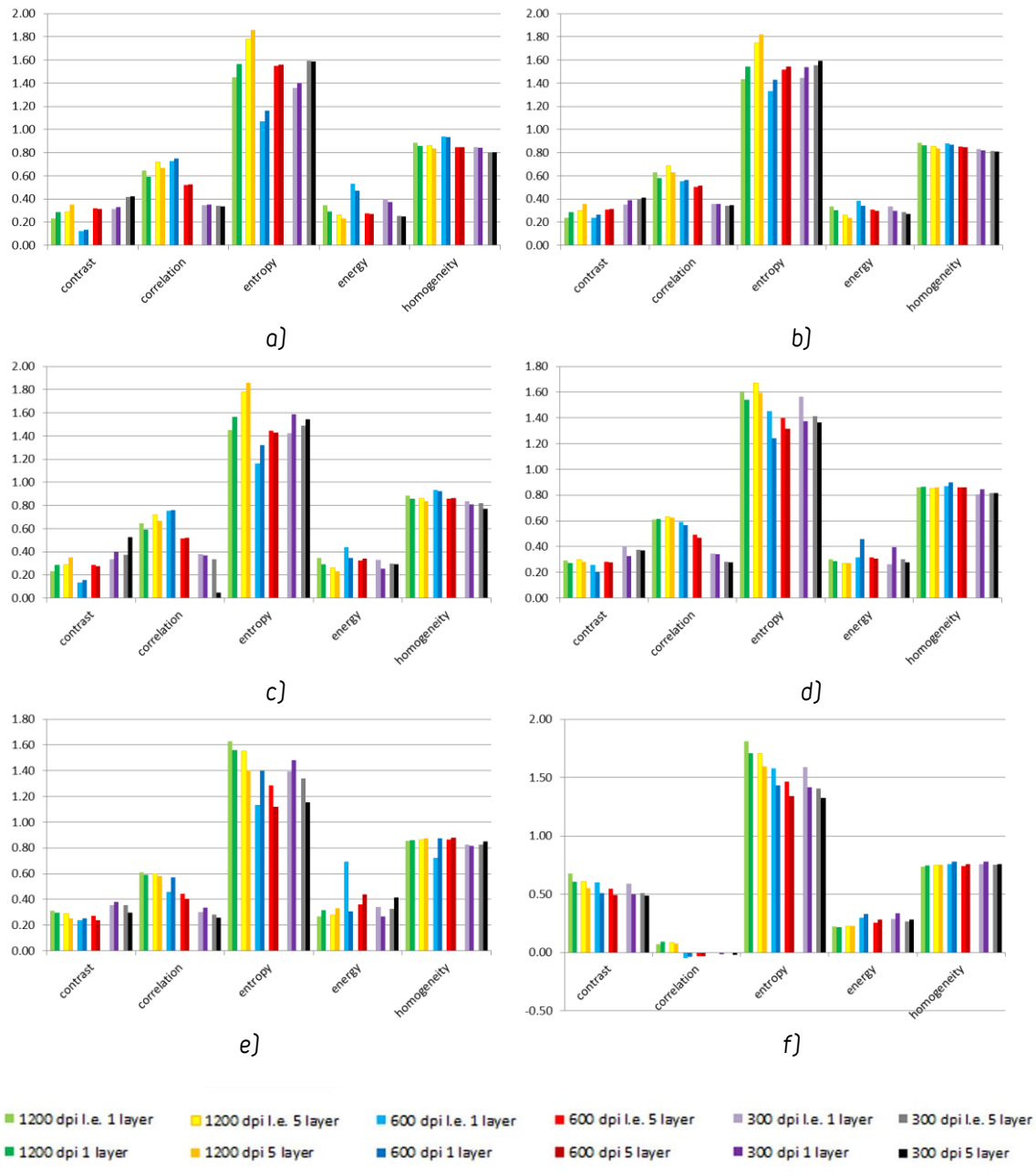


Figure 1: GLCM parameters comparison for samples scanned with three different resolutions, using three different processing types: a) cyan ink - L channel, b) cyan ink - HSL, c) cyan ink - Greyscale, d) black ink - L channel, e) black ink - HSL and f) black ink - Greyscale

In Figure 1c are presented GLCM parameters results obtained from the greyscaled images. For samples scanned at 1200 dpi, obtained GLCM results trends are pretty the same as in previous two analyses (L channel processing and all three channels processing of HSL color space). In case of 600 dpi scans, identical trend show samples printed with 1 ink layer, while samples printed with 5 ink layers show that unexposed samples (dark red bars) possess better solid-tone print uniformity than UV light exposed (red bars). In case of the samples scanned at 300 dpi, again generally better solid-tone print uniformity showed UV light exposed samples printed with 1 (light purple bars) and 5 print layers (grey bars) than unexposed samples printed using the same ink deposit (dark purple and black bars), except the correlation parameter. Again generally better solid-tone print uniformity showed samples printed with 1 ink layer, except in cases of correlation parameter for 600 dpi and 300 dpi scans and in case of entropy and energy parameters of UV light untreated samples scanned at 300 dpi.

3.2 Black ink solid-tone print uniformity analysis

In Figure 1d, if we look at the data of 1200 dpi scanned samples, it can be noticed that samples printed with 1 ink layer and were not subsequently subjected to UV light exposure (dark green bars) show better results for three out of five GLCM parameters (contrast, entropy and homogeneity) comparing to the samples which were after printing exposed to UV light (light green bars). Unexposed samples printed with 5 ink layers (ocher bars) show better solid-tone print uniformity results for all GLCM parameters. Concerning samples scanned at 600 dpi both UV light unexposed samples, printed with 1 and 5 ink layers (dark blue and dark red bars) show better results for all GLCM parameters comparing to samples which were treated with UV light except in case of energy parameter for sample printed with 5 ink layers. Now in consideration come samples that were scanned at 300 dpi. Unexposed samples printed using 1 ink layer show superior results (dark purple) for all solid-tone print uniformity parameters comparing to UV light treated samples. In case of the samples printed with 5 ink layers, untreated ones (black bars) possess better characteristics for three out of five parameters (contrast, correlation and entropy) comparing to UV light exposed ones printed with the same ink amount (grey bars).

Regarding solid-tone print uniformity between the samples printed using different ink deposits (ink layers) in case of 1200 dpi scanned samples better uniformity show samples printed using 1 ink layer for all GLCM parameters. In case of the samples scanned at 600 dpi, and UV light exposed, better solid-tone print uniformity was established for 5 ink layer prints (red bars) for three GLCM parameters (correlation, entropy and energy), while regarding untreated samples, better result showed samples printed with 1 ink layer (dark blue bars) for all parameters except correlation. In case of 300 dpi scans, better GLCM results were obtained for unexposed 1 ink layer printed samples (for contrast, energy and homogeneity parameters), and for UV light exposed ones better solid-tone print uniformity was obtained for 5 ink printed samples for all GLCM parameters.

Using processed images in HSL color space, Figure 1e, following results were obtained: samples scanned at 1200 dpi, that were not subjected to UV light exposure, printed both with 1 (dark green bars) and 5 ink layers (ocher bars) show better results for all considered GLCM parameters in comparison to UV light exposed ones; samples printed with 5 ink layers without UV light exposure, that were scanned at both 600 dpi and 300 dpi (dark red and black bars) indicate better solid tone print uniformity for all GLCM parameters comparing to the samples which were UV light treated (red and grey bars); UV light exposed samples, scanned at 600 dpi and 300 dpi, printed with 1 ink layer (light blue and light purple bars) show better results than untreated samples printed using the same ink amount and scanning resolution (dark blue and dark purple bars). Concerning solid-tone print uniformity between the samples printed using different ink layers number, better solid-tone uniformity show both UV light treated and untreated samples printed with 5 ink layers than samples printed with 1 ink layer, which were scanned at 1200 dpi. UV light untreated samples scanned at 600 dpi and printed with 5 ink layers showed better results for all GLCM parameters comparing to the untreated ones printed with 1 ink layer, while UV light treated samples printed with 1 ink layer show generally better solid-tone print uniformity results (for contrast, entropy and energy parameters). Both UV treated and untreated samples printed with 5 ink layers showed better solid-tone print uniformity, exception is only energy parameter for UV light exposed samples where sample printed with 1 ink layer possesses better result than sample printed with 5 ink layers.

In Figure 1f are presented GLCM parameters results obtained from greyscaled images. For samples scanned at 1200 dpi, better solid-tone print uniformity showed unexposed samples printed with 5 ink layers (ocher bars) for all GLCM parameters, and unexposed samples printed with 1 ink layer for contrast, entropy and homogeneity parameters. 600 dpi and 300 dpi scans provided similar results, where untreated samples printed both with 1 and 5 ink layers showed better GLCM results. An anomaly occurred in those two data sets which is that negative results of correlation parameter were obtained, so whether if we include or exclude data of this GLCM parameter it would not affect previous statement about solid-tone print uniformity of the UV light treated and untreated samples.

GLCM parameters results obtained from the samples scanned at 1200 dpi, indicate better solid-tone print uniformity on both UV light treated and untreated samples printed with 5 ink layers (dark green and ocher bars) comparing to samples printed with 1 ink layer (light green and yellow bars). Considering 600 dpi and 300 dpi prints, very similar GLCM results were obtained for both UV light treated and untreated samples printed with different ink deposits (1 and 5 ink layers).

In order to visually compare the samples, in Figure 2. are presented UV light exposed (right columns) and unexposed samples (left columns) printed using cyan and black ink with 1 (upper rows) and 5 ink layers (lower rows) scanned at three different resolutions (1200 dpi, 600 dpi and 300 dpi). It can be noticed that cyan ink prints have very similar and hardly distinctive solid-tone print uniformity regardless of UV light application as well as ink deposit used. The samples that were subjected to UV light exposition are slightly lighter in color, but this effect on solid-tone print uniformity is not or is very hard to percept. These similarities between the samples are the main reason for the presence of difficulties to find relations between obtained GLCM parameters results and visual comparison of the samples. As well different scanning resolution did not influence in greater extent perception of solid-tone print uniformity between the samples.

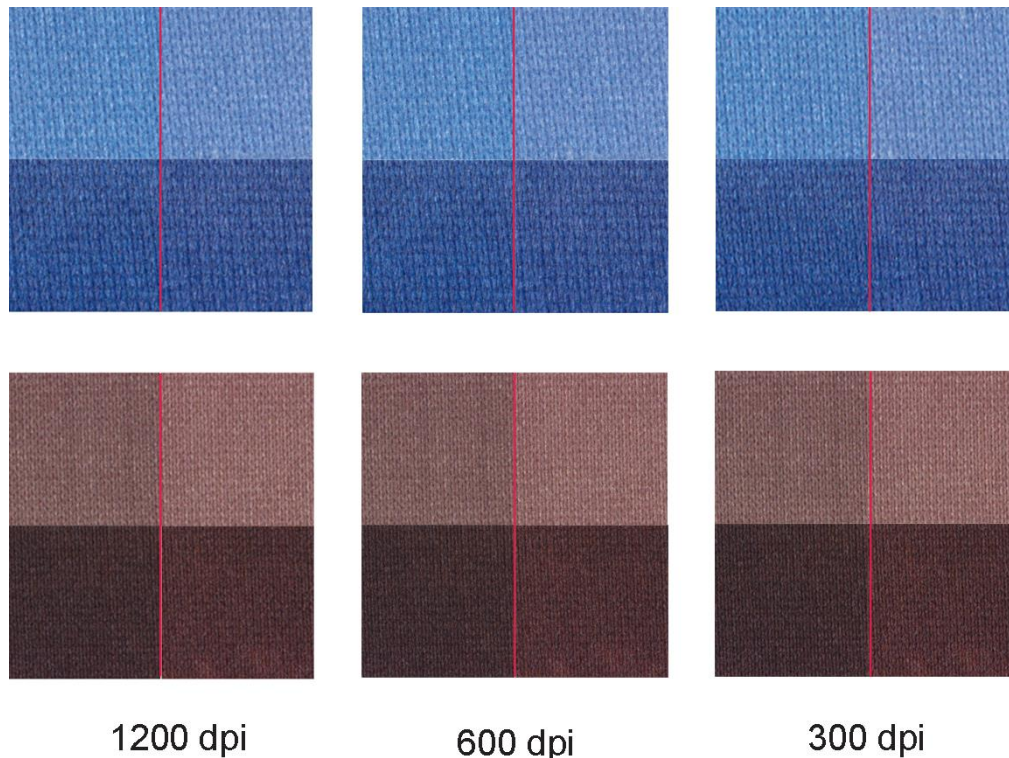


Figure 2: Cyan and black ink prints comparison: 1 ink layer (upper rows) and 5 ink layers (lower rows), before (left columnes) and after UV light exposure treatment (right columnes), scanned using three different resolutions, 1200 dpi, 600 dpi and 300 dpi

In case of black ink prints, ink fading is more pronounced between the UV light exposed and unexposed samples than between cyan ink prints. It can be easily spotted that this contributed to the poorer solid-tone print uniformity especially between the samples printed with 5 ink layers, where lighter areas can be observed at the bottom as well as in the middle of the samples. In respect of the samples printed with 1 ink layer, similarly to the cyan ink prints, solid-tone uniformity differences are very difficult to distinct. As well as in case of cyan ink prints, different scanning resolution did not affected much the perception of solid-tone print uniformity of the samples. Visual comparison confirmed its accordance with the previously conducted GLCM image processing analysis of the samples printed with 5 black ink layers, according to which samples printed with 5 black ink layers that were not subsequently UV light exposed possess better solid-tone print uniformity.

4. CONCLUSIONS

In this research we tried to determine impact of several different factors on solid-tone print uniformity calculation using GLCM method. Those factors were: UV light exposure of the samples, two different ink deposits application (1 and 5 ink layers), three scanning resolutions (1200 dpi, 600 dpi and 300 dpi) and three image processing types within GLCM image processing method in MATLAB software (processing of L channel of $L^*a^*b^*$ color space, processing of all three

channels of HSL color space and greyscaled images processing). From the obtained and presented results of GLCM analysis, we can conclude that mentioned factors affect solid-tone print uniformity results generated by GLCM image processing method.

The best performance in case of black ink prints, i.e. in accordance with visual observations (Figure 2), showed image processing in HSL color space and scanning resolution of 1200 dpi, where UV light untreated samples printed with both 1 and 5 ink layers showed better results for all five considered GLCM parameters. As well, this set up produced better solid-tone print uniformity for samples printed with 5 ink layers irrespective of UV light exposure treatment. These findings confirmed our hypothesis that thicker ink deposit will contribute to a more uniform solid-tone surface, as well as that UV light exposure may lead to uneven fading of the printed areas, generating that way more pronounced solid-tone print nonuniformity of the samples.

In case of cyan ink prints, it is very difficult to relate obtained solid-tone print uniformity results to the visual representation of the samples in Figure 2, because both UV light exposed and unexposed sample sets are very similar. Exposed ones are a bit lighter as a consequence of UV light treatment, but in regard to solid-tone print uniformity they do not possess noticeable distinctions.

5. ACKNOWLEDGEMENT

This work was supported by the Serbian Ministry of Science and Technological Development, Grant No.: 35027 "The development of knowledge and production in graphic arts industry".

6. REFERENCES

- [1] Chen, Y.: "Image analysis methods for paper formation evaluation", M.A.Sc. thesis, University of Toronto, Canada, page 33, [1998]
- [2] Elton, N. J., Preston, J. S.: „Application of Imaging Reflectometer Mapping to Students of Print Mottle in Commercially Printed Halftone Prints", URL <<http://www.surfoptic.com/AN5%20Print%20mottle%20studied%20with%20RI%20mapping.pdf>> [last request 05.10.2014.]
- [3] Fahlcrantz, C.: "On the Evaluation of Print Mottle", Doctoral Thesis, School of Computer Science and Communication, [2005]
- [4] Haralick, R.M., Shanmugam, K., Dinstein, L.: "Textural Features for Image Classification", IEEE TSMC, volume 3 (6), pages 610–621, [1973]
- [5] Hladnik, A., Lazar, M.: "Paper and board surface roughness characterization using laser profilometry and gray level cooccurrence matrix", Nordic Pulp and Paper Research Journal, volume 26 (1), pages 99–105, [2011]
- [6] Hladnik, A., Krumpak, G., Debeljak, M., Gregor Svetec, D.: "Assessment of paper surface topography and print mottling by texture analysis", Proceedings of ImageJ User & Developer Conference, 2010, Luxembourg 2010
- [7] Karanikas, V., Nikolaidis, N., Tsatsaroni, E.: "Disperse ink-jet inks with active agents: properties and application to polyester and polyamide fibers", Textile Research Journal, volume 83 (5), pages 450–461, [2013]
- [8] Kašiković, N., Novaković, D., Karlović, I., Vladić, G.: "Influence of Ink Layers on The Quality of Ink Jet Printed Textile Materials", Tekstil ve Konfeksiyon, volume 22 (2), pages 115–124, [2012]
- [9] Malik, S. K., Savita, K., Sushil, K.: "Advances in ink-jet printing technology of textiles", Indian Journal of Fibre & Textile Research, volume 30 (1), pages 99–113, [2005]
- [10] Petersson, J.: "A Review of Perceptual Image Quality", Department of Science and Technology, Linköping University Electronic Press, [2005]
- [11] Petrou, M., Sevilla, P.G.: "Image Processing Dealing with Texture", First edition, (John Wiley & Sons, West Sussex, England, 2006), Chapter 1
- [12] Stančić, M., Kašiković, N., Novaković, D., Dojčinović, I., Vladić, G., Dragić, M.: "The Influence of Washing Treatment on Screen Printed Textile Substrates", Tekstil ve Konfeksiyon, volume 24 (1), pages 96–104, [2014]
- [13] Tse, M., Briggs, J., C., Kim, Y., K., Lewis, A., F.: "Measuring Print Quality of Digitally Printed Textiles", Proceedings of IS&T NIP14 International Conference on Digital Printing Technologies, [1998], (Toronto, Ontario, Canada) URL <http://www.researchgate.net/publication/242216607_Measuring_Print_Quality_of_Digitally_Printed_Textiles/links/00b7d52a5f26a294d8000000> [last request 05.10.2014.]

- [14] Uppuluri, A.: „GLCM texture features“, URL
<<http://www.mathworks.com/matlabcentral/fileexchange/22187-glcmm-texture-features>>,
(last request 21.01.2014)
- [15] Yang, Y., Naarani, V.: "Improvement of the lightfastness of reactive inkjet printed cotton",
Dyes and Pigments, volume 74 (1), pages 154-160, (2007)

DETERMINATION OF SUBSTRATE AND HALFTONE DOT SHAPE INFLUENCE ON IMAGE REPRODUCTION WITH IMAGE DIFFERENCE METRIC

Igor Karlović¹, Ivana Tomić¹, Ivana Jurić¹, Danijela Randelović²

¹ *University of Novi Sad, Faculty of Technical Sciences,*

Department of graphic engineering and design, Novi Sad, Serbia

² *University of Belgrade, Institute of Chemistry, Technology and Metallurgy (ICTM) –
Centre of Microelectronic Technologies (CMT), Belgrade, Serbia*

Abstract: Differences in halftoned images are influenced by halftoning technique, halftone dot shapes, line count, printing process and substrate properties. The measurement of colour patches on control bars via densitometric and colourimetric measurement of colour patches does not guarantee good results in final image appearance of differently halftoned samples. By using image difference metrics – based on human visual system (HVS) we can evaluate more precisely the differences in final image appearance. S-CIELAB is an extension of the CIE L*a*b* Delta E colour difference formula. It includes a spatial processing step, prior to the CIELAB ΔE calculation, so that the results correspond better to colour difference perception by the human eye. As different paper substrates have different absorption and surface properties, the ink spreading is also different on these surfaces. Since the ink spreading changes the spatial distance between separate halftone dots there is a possibility that paper substrates will influence the image difference measured through S-CIELAB values. We had printed three types of images on 5 different paper substrates using ink jet – Epson Stylus A3 printer. As ink jet inherently uses frequency modulated halftoning we used GMG Dot Proof software for AM halftone dot shape generation. The images which were halftoned with elliptical and square halftone dot shapes were printed on paper substrates and were scanned and evaluated using S-CIELab module in Matlab software. On the bases of the results we can indicate that the substrate influence the difference magnitude of the reproduced images calculated with S-CIELab image difference metric.

Key words: S-CIELab, halftoning, ink jet paper

1. INTRODUCTION

The quality control of the reproduction in the graphic arts is dynamic field of investigation with imminent enhancement of quality control methods and procedures. Many printing technologies already have a full scoped ISO standardized procedure for the quality control workflow from digital data to the final print inspection. This is true mainly for the conventional printing technologies like offset and flexography while the digital printing due to its large variability in technologies, inks and substrates is still waiting for the corresponding standard. The newly announced ISO standard (ISO/DTS 15311-1 Graphic technology -- Requirements for printed matter for commercial and industrial production -- Part 1: Measurement methods and reporting schema) which is expected in the future will most probably broaden the colour quality control. Standard colour difference formulas like the CIELAB ΔE , ΔE_{94} and ΔE_{00} are widely used in the graphic industry as a quick quality control parameter. These formulas perform excellently for large uniform colour patches (test targets and control strip measurement), but are not suitable for image quality metrics. With the advent of digital image processing technologies new image quality metrics can be used with the aim of constructing the total image appearance quality control model. This model will encompass the classic colorimetry procedures already used in printing, digital image processing and data obtained from the visual appearance testing on human observers.

2. STATEMENT OF THE PROBLEM

Subjective assessment of print quality is rather straightforward, where a group of observers can be asked about the quality of the printed image. However, assessment of printed images by IQ (image quality) metrics is not straightforward. The original image is of a digital format and the printed image is of an analog format, because of this the printed image must be digitalized before we can carry out IQ assessment with IQ metrics (Pedersen, 2010). Image quality modelling

has been the focus of research over the course of many years. An extensive overview of the different techniques in the design and evaluation of various modeling techniques is presented by Engledrum (Engledrum, 2004 and 1999) and Pedersen (Pedersen et al., 2011). The same author gives a general definition of image quality modeling which states that it is the creation of a mathematical formula that is capable of predicting human perceptions of quality. In a report by Pedersen and Hardeberg more than 100 image quality metrics have been reviewed (Pedersen&Hardeberg, 2009). Some of the image quality metrics are based on the Human Visual System and some are not, and also some of the image quality metrics are suitable just for digital images. Johnson (Johnson, 2003) in his PhD extensively describes the possibilities of using different image quality modules for building a Image Difference Framework where S-CIELab is one of the modules in a more complex framework set. One of the main goals in setting up a device-independent modelling of image appearance is the creation of a model capable of predicting magnitudes, and not just thresholds of differences (Johnson, 2003). The S-CIELAB extension includes a spatial processing step, prior to the CIELAB ΔE calculation, so that the results correspond better to colour difference perception by the human eye. The image data are transformed into an opponent-colours space. Each opponent-colors image is convolved with a kernel whose shape is determined by the visual spatial sensitivity to that colour dimension; the area under each of these kernels integrates to one. The calculation is pattern-colour separable because the color transformation does not depend on the image's spatial pattern, and the spatial convolution does not depend on the image's colour. Finally, the filtered representation is transformed to a CIE-XYZ representation, and this representation is transformed using the CIELAB formulae. The resulting S-CIELAB representation includes both the spatial filtering and the CIELAB processing (Zhang&Wandell, 1997). While some authors tested S-CIELab on digital images with good results over similar image quality metrics (He et al., 2011), other have tested it also on printed images (Johnson, 2003; Phillips, 1999 and Zhang et al. 1997). Their results imply that the S-CIELAB calculation extends CIELAB by incorporating factors related to the pattern-colour sensitivities of the human eye and that it can be used to measure colour differences in digital images. S-CIELAB can be used to improve predictions concerning the visibility of halftone textures with some short fallings in predicting perceptibility for the patches that contained low frequency vertical banding or significant moiré-like patterns (Phillips, 1999). Some recent work on image difference measures (Lissner, Preiss, Urban, 2011) also uses S-CIELab as module in deriving linear, polynomial and factorial blended image quality metrics.

We have adopted the S-CIELAB method as it resembles to the colour difference metric with which are the graphic professionals in the printing industry most familiar and based on current work concerning the development of the ISO standard for digital printing. While in our previous work (Karlovic et al., 2013) we focused on halftoning parameters of digital images in this work we wanted to test the influence of printed materials and the suitability of S-CIELab on evaluating these kind of ink jet printed samples. Previously we had tested the influence of different halftone shapes on digital images appearance and found very small(not significant) differences. In this paper we have extended the study of dot shapes (two types) on different substrates. In earlier studies it was determined that the rule of thumb for halftone dot shape is to keep the edge/area ratio small because the dot periphery is mostly the source of the noise (Hains, 1996). The halftone dot shape influences the sudden tone jump in the mid tone areas because the dots join (dot edges start to touch each other) at the same time. The checkerboard pattern found in mid tones is sometimes distorted by using elliptical dots when the tone jump at the midpoint is too noticeable. Unlike square dots that join all four corners at once in the checkerboard pattern, elliptical dots join two corners at 50% area coverage thus giving less tone jump (Kodak, 1986). However, elliptical dots produce a chaining effect that can be more visually noticeable (Kang,1999).

3. METHODS AND MATERIALS

For the experimental part ink jet printing on proof quality papers was chosen due to small variability of the printing process and good control of the ink drops deposition. We had used Epson Stylus Pro - piezo ink jet printer. Test target used in the experiment contained three images for evaluation from the ECI 2002 visual test form (containing specific image colours – skin and metallic colour, pastel colours and saturated colours) which were halftoned and ripped to TIFF files using Harlequin RIP. AM halftoning with fixed line count of 150 lpi and elliptical and square dot shape was used. The printing was performed through GMG Dot Proof which guaranteed the quality of the AM dot formation. We have used 5 different substrates which were mainly proof

type papers (GMG Proof Paper glossy 250 g/m², GMG Proof matte 250 g/m², OmniJet glossy 200 g/m², OmniJet semmi gloss 200 g/m² and Kunstdruck glossy coated paper 130 g/m²). After printing and drying the samples had to be re-digitalized for the S-CIELAB evaluation. For the digitalization we have used CanonScan 5600F using 1200 spi sampling rate and Adobe RGB to retain the maximum colour gamut of the scanned samples. The samples were cropped to 4600x4600 ppi to match the original non-halftoned continuous tone digital data. The scanned images were compared with the digital originals in Matlab in order to obtain the S-CIELab difference. The obtained data was gathered and processed and are presented in the results.

4. RESULTS

From Figure 1. we can observe the differences within paper substrates and image types for the elliptical halftone dot shape. The highest overall differences from the substrates had the Kunstdruck 130 g/m² (26.78 for the saturated colour image type, 17.85 for the skin and metallic colour image type and 17.01 for the pastel colours image type). OmniJet semmigloss 200 g/m² had in average the lowest S-CIELab values for all image types (9.97;14.63 and 11.41) while in average lower grammage proof grade ink jet papers had slightly smaller S-CIELab values than the 250g/m² grammage proof papers.

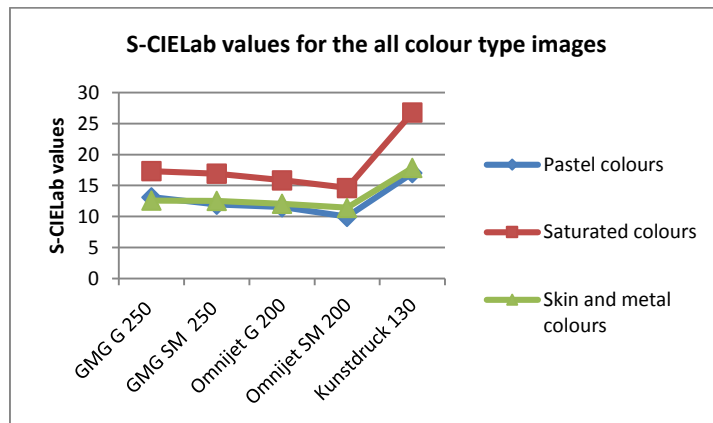


Figure 1: S-CIELab values for different substrates and image types (elliptical dot)

The differences in halftone dot structure is presented in Figure 2 which shows 42 x times magnification. Different surface and printability properties of paper substrates influences the dot spreading on the surface.

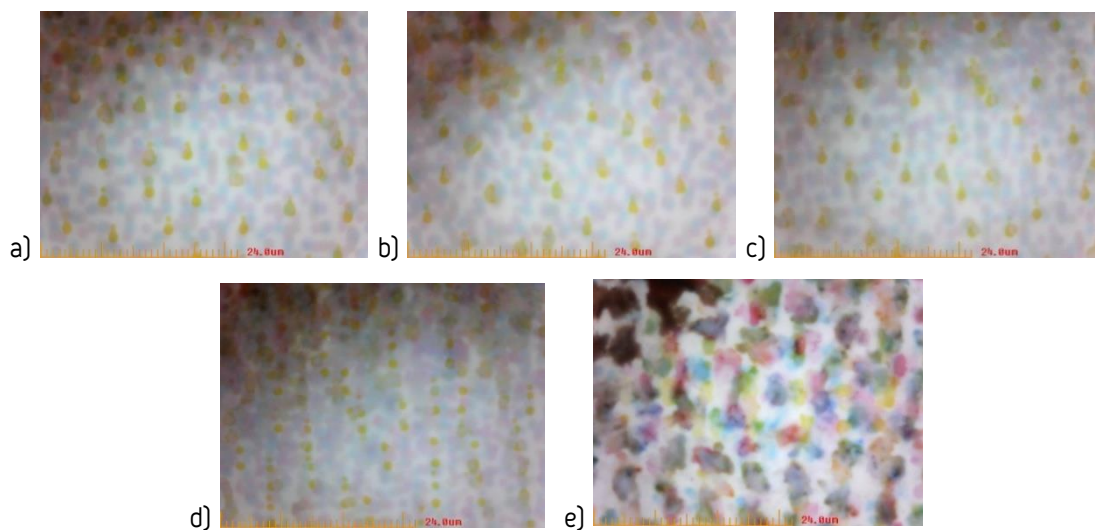


Figure 2: Images of dot structures (42x magnification) on a) GMG gloss b) GMG semmigloss c) OmniJet gloss d) OmniJet semmigloss e) Kunstdruck paper

From Figure 2. we can see the ink spreading on Kunstrdruck type paper which is not suitable for ink jet printing due to large amount of ink bleeding. On other substrates on this scale of magnification certain smaller differences in dot structure is observable where the semmigloss substrates tend to hold better the dot structure than gloss type proof papers. In Figure 3. are presented the results for the square dot shape. Previously we have found that on halftoned digital images this type on halftone shape gives the smallest S-CIELab difference value.

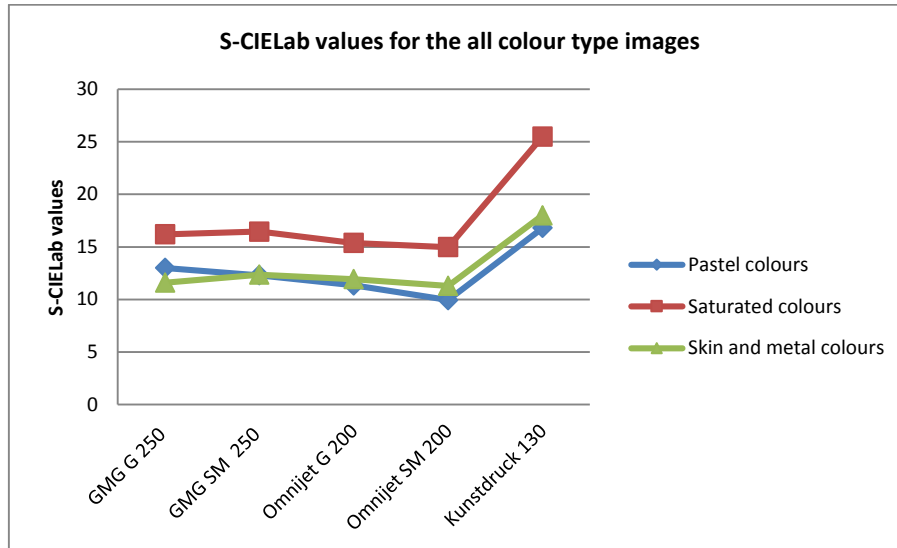


Figure 3: S-CIELab values for different substrates and image types (square dot)

From Figure 3. it can be observed that again the image with saturated colours had the the largest S-CIELab difference in average with the highest value for the Kunstrdruck type substrate (25.5). The smallest differences were measured for the Pastel type colour image Omnijet semmigloss paper with the value of 9.93, while for the skin and metal colours image had the smallest S-CIELab value for the GMG glossy paper with the value of 11.29 for the Omnijet semigloss paper. In average with some smaller deviations like for the Omnijet papers for the saturated colours (15.85;14.63) all other values printed with square halftone dot had lower values than the elliptical dot samples. This result indicate that halftone dot shape produce some small variations on different paper stocks and S-CIELab can notice. The differences in spreading of square halftone dot structure is presented in Figure 4.

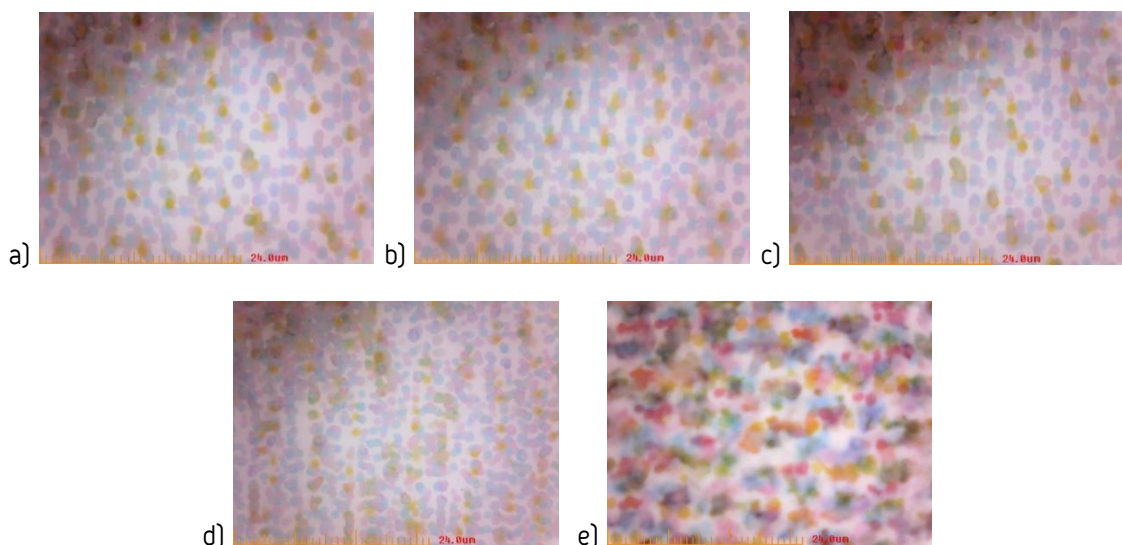


Figure 4: Images of dot structures (42x magnification) on a) GMG gloss b) GMG semmigloss c) Omnijet gloss d) Omnijet semmigloss e)Kunstrdruck paper

5. CONCLUSIONS

The differences in image type variation are most probably due to colour conversion of printed digital data back to digital form where the more saturated colours are more desaturated during printing. The scanned version are then more susceptible to large differences with fully digital saturated colours on the original image. Another phenomena that could be also accounted is that saturated colours have more ink on the substrate and thus more possibility of change due to the surface properties. These effects will be investigated more thoroughly in the future experiments. In overall semmgloss substrates had in average smaller S-CIELab values for all image types and the images indicate different ink spreading on different substrates. The next step in the research would include the determination of ink absorptivity of substrates and other surface properties as well image analysis methods. Human observers should also be included in some future research involving printed halftoned samples with different halftone dot shapes and substrates. S-CIELab remains a good methodology for image quality metrics as a starting point which can be further improved with advanced colour appearance technology (iCAM for example) but for the printing industry simple methods remain a necessity for easier implementation in the quality checking process.

6. ACKNOWLEDGMENTS

This work was supported by the Serbian Ministry of Science and Technological Development, Grant No.:35027 "The development of software model for improvement of knowledge and production in graphic arts industry".

7. REFERENCES

- [1] Eastman Kodak Company, Halftone Methods for the Graphic Arts, 1986
- [2] Engeldrum P.G., A Theory of Image Quality: The Image Quality Circle, Journal of imaging science and technology, 48 (5), 251-255, 2004
- [3] Engeldrum P. G., Image quality modeling: Where are we? In *Image Processing, Image Quality, Image Capture, Systems Conference* (IS&T, Savannah,USA, 1999), 251-255
- [4] Johnson G.M., Measuring images: differences, quality and appearance, PhD thesis, Rochester Institute of Technology, 2003
- [5] Hains C.M., Digital Halftoning, Tutorial notes, IS&T/SID 4th Color Imaging Conference, November 19, 1996
- [6] He L., Gao X., Lu W., Li X., Tao D., Image quality assessment based on S-CIELAB model, Signal, Image and Video Processing, 5(3), 283-290
- [7] Kang R. H., Digital Color Halftoning, (SPIE-IEEE Press, Washington, 1999), 190
- [8] Karlović I., Tomić I., Jurić I., The influence of halftone dot shapes on S-cielab values Proceedings of 4th International Joint Conference on Environmental and Light Industry Technologies, Obuda University, 20-22 November, Budapest, 2013
- [9] Lissner I., Preiss J., Urban P., Predicting Image Differences Based on Image-Difference Features, Proceedings of 19th Color and Imaging Conference, (IS&T:San Jose ,USA, 2011)
- [10] Pedersen M., Hardeberg J.: Survey of full-reference image quality metrics, Høgskolen iGjøviksrapportserie, 2009 nr. 5, URL: http://brage.bibsys.no/xmlui/bitstream/handle/11250/144194/rapport052009_elektroniskversjon.pdf?sequence=1 (last request: 2014-08-27).
- [11] Pedersen M., Bonnier N., Hardeberg Y. J., Albrechtsen F., "Image quality metrics for the evaluation of print quality", Proceedings of SPIE 7867, Image Quality and System Performance VIII 2011 (SPIE:San Francisco, USA, 2011), 786702-1-19
- [12] Phillips J., Evaluation of S-CIELAB Using Halftone Color Patches, M.S. Project, Rochester Institute of Technology, 1999
URL: <http://www.cis.rit.edu/~jbp3319/pdf/JBPhillipsMSProject.pdf> (last request: 2014-08-11)
- [13] Zhang X., Silverstein D.A., Farrell J., Wandell B.A., Color Image Quality Metric S-CIELAB and Its Application on Halftone Texture Visibility, Compcon97 : Book of proceedings, (IEEE, San Jose, USA, 1997), 44-48
- [14] Zhang X., Wandell B.A. A spatial extension of CIELAB for digital color image reproduction, Journal of the Society for Information Display, 5(1), 61-63, 1997

VISUAL EXPERIENCE OF GRAININESS

Ivana Jurić¹, Igor Karlović¹, Ivana Tomić¹, Sunčica Zdravković²¹ University of Novi Sad, Faculty of Technical Sciences,

Department of Graphic Engineering and Design, Novi Sad, Serbia

² University of Novi Sad, Faculty of Philosophy, Department of Psychology,
Novi Sad, Serbia

Abstract: Graininess is one of the 14 attributes for controlling the digital prints defined by the ISO standard 13660:2001. ISO 13660:2001 metric of graininess is the standard deviation of density of print's small areas. This attribute can help to detect small variations in terms of lightness. The aim of this study was to investigate whether there is a relationship between the measured values of graininess and its visual salience. Samples were printed on coated paper (130g/m²) using Xerox DocuColor 252 (a digital printing machine). The graininess of six samples (each sample contained different black tone value, ranging from 30-80%, with an increment of 10%) was quantified with measurement device Personal IAS that is based on image analysis method. The participants' task in the experiment was to place the six samples in order of increasing value of graininess. Statistical analysis of the results did not reveal any direct relation between the values measured by the device and the human visual evaluation. That is, participants were not able to distinguish graininess at different tonal values.

Key words: digital printing, graininess

1. INTRODUCTION

The term graininess, also known as micro-uniformity, has been borrowed from photography where it is defined as the character of a photographic image when it appears to be made up of distinguishable particles, or grains. Today this term is used more broadly to refer to small-scale (micro) non-uniformity. In electronic imaging systems, graininess is "the term used to describe the perceived noisy fluctuation related to granularity" (Lee, 2005, pp.574). The perception of image noise depends on the image details, the illumination, and the colour of the target. Graininess is defined as "the subjective perception of a random pattern of brightness or colour fluctuation" (Lee, 2005, pp.574). For us, another related term is also important, that is granularity defined as "the objective measurement of the local density variation, such as the standard deviation or the Root Mean Square (RMS) granularity" (Lee, 2005, pp.574). Measure of image noise is the standard deviation of the measured signal when the image is a flat field of a uniform exposure. In electronic imaging, this measure is called the RMS noise and in photography, the RMS granularity (Lee, 2005). The RMS granularity measures the noise of film. It is a measure of the variability for an area of the uniform film density (usually 1.0D), obtained by a densitometer with 48µm aperture. It is calculated as a standard deviation of the mean of a series of density measurements. It does not measure film grain size, but rather the variability of image density in an area with "theoretically" uniform density (Vitale, 2009).

Kodak developed the Print Grain Index method for graininess quantification (Kodak, 2000). The Print Grain Index method replaced the RMS granularity and offered a different scale, which cannot be compared to RMS granularity. Currently, the Kodak's method applies only to color negative films.

A number of different methods have been proposed to quantify image graininess (Dooley and Shaw, 1979; Engeldrum, 1998; Mishra and Rasmussen, 2000; Hino, 1995; Kodak, 2000; ISO 13360, 2001; Tse and Forrest, 2009). Some methods have been developed to control graininess of digital electronic system, film or photography.

ISO metric and Composite Noise Index CNI (Tse and Forrest, 2009) are used for quantification of graininess of digital prints. Tse and Forest (2009) have developed objective metric, CNI index, which includes both micro- and macro- uniformity (graininess and mottle). The CNI index is still under development and has not been implemented anywhere, although the authors claim that CNI index correlates with subjective perception of image uniformity better than ISO metric. In this paper we used ISO metric to quantify micro-uniformity (graininess), because this metric is explained and implemented in measurement devices.

1.1 ISO metric for graininess quantification

When it comes to printed samples alone, ISO 13660:2001 standard defines graininess as: “aperiodic fluctuations of density at a spatial frequency greater than 0.4 cycles per millimeter in all directions” [ISO 13660, 2001, pp.10]. Figure 1 depicts samples with different graininess level.

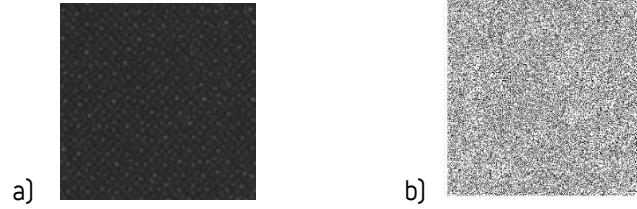


Figure 1: Graininess; a) lower level and b) higher level

For graininess quantification it is necessary to define a region of interest (ROI), as shown in Figure 2. The ROI is a region of 161mm^2 with smallest dimensions of at least 12.7 mm. The ROI is further divided into at least 100 uniform, non-overlapping square tiles. Within each tile, there are 900 measurements of density of 900 evenly-spaced non overlapping areas. For each tile (i) m_i is the average of these measurements [ISO 13660:2001]. Graininess is calculated according to the equation (1):

$$GI = \frac{\sqrt{\sum_{i=1}^n \sigma_i^2}}{n} \quad (1)$$

where σ_i is the standard deviation of optical density measurements within tile i and n is the total number of tiles.

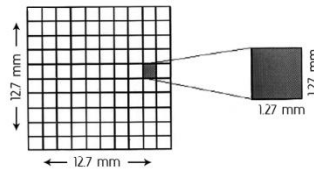


Figure 2: ROI divided into tiles and tile with dimensions

Although standardize procedure for obtaining graininess in printing is well developed and precisely described, it is still unclear whether a human observer can perceive such differences. Using ISO 13660:2001 we can quantify graininess, but it does not provide us the relation with visual experience. That is, not only we do not know the optimal range of graininess for human visual experience, but we do not even know the threshold sensitivity.

The aims of this study were to establish the relationship between the graininess, one of the major attributes for controlling the digital prints and human experience of graininess. More precisely we were hoping to establish the range in which humans can detect changes in graininess, i.e. absolute and discrimination thresholds [Kingdom and Prins, 2010]. The absolute thresholds will specify the range below and above which human observers cannot detect any change. The discrimination threshold will inform us about the minimal change in graininess that can be perceived, allowing us to establish an optimal range of changes that should be used in printing. Briggs (2002) claims that human vision is the most sensitive to non-uniformity in luminance rather than in colour or chroma. Hence, in this initial study we only used patches with different gray scale values, while colour or chroma were excluded.

2. MATERIALS AND METHOD

The experiment was conducted in two phases. In the first phase we produced the samples using previously described formulas and in the second phase human observers classified those samples. The first phase included the graininess' quantification of the printed samples in order to compare it with the visual experience in the second phase.

Phase 1. We used one paper type, the coated paper (130g/m²). Digital printing machine based on electrophotography, Xerox DocuColour 252, was chosen for printing. We produced six samples containing different tone value of black (30–80% TV, in the steps of 10%). These particular tone values were chosen because they've ensured a linear increase of graininess. Figure 3 shows scanned samples used in the experiment.

Graininess was measured using portable measurement device Personal IAS. This device quantifies comprehensive print quality attributes according to ISO 13660:2001. It has an integrated high resolution CCD camera.

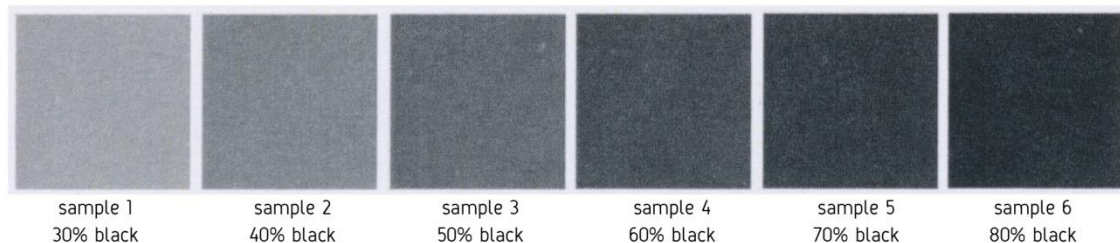


Figure 3: Scanned samples used in experiment

Phase 2. The six samples were used in a psychophysical experiment, both as the basis for measurement and in a subsequent correlation with the visual rank.

2.1 Participants

Ten participants (5 male and 5 female) estimated graininess of printed samples. All of them had normal or corrected to normal visual acuity and normal color vision. In order to control influence of prior knowledge and experience, only half of the participants were experts (students of graphic engineering), while the other half were random students from other faculties.

2.2 Apparatus and stimuli for visual evaluation

Six grey samples (16x16cm), were presented on the table opposite the observer. Observers were positioned 40 cm from the samples, as in Rasmussen et al. (2006). At those positions the samples subtended a visual angle of 21,8°. Samples were evaluated in such a manner that only diffusely (non-specularly) scattered light was taken into account.

2.3 Procedure

The illumination and the samples were set before the participant's arrival. The samples were placed in a different random order for each participant.

The participants were asked to place their head on a chin rest, in order to maintain a constant distance from the samples during the experiment. Then the task was described to them allowing also for a couple of minutes to adapt to viewing conditions in the room. The participants' task was to line up the samples in order of increasing value of graininess. For visual assessment, grade 1 stands for the most visible graininess and grade 6 stands for the least visible graininess.

3. RESULTS AND DISCUSSIONS

To obtain the visual significance of graininess, first we wanted to establish how humans perceive and respond to the simplest scale. Table 1 summarizes results derived in both phases of the experiment. According to the results obtained when measuring samples by the device, we can notice that graininess increases for samples with smaller tone value. Mid-tones are grainier than shadows and highlights, as might be expected because mid-tones are composed of smaller size of dots (AM raster).

Participants did not rate the samples in the same manner. A good example of the discrepancy between the results from the two phases is the sample with 30% TV. It has a highest graininess value in the first phase and the least visible graininess in the second phase. Additionally, standard

deviation was high for the measured sample of participants revealing notable disagreements in the human responses.

Table 1: Graininess – physical measures and visual grades

Samples	1	2	3	4	5	6
Graininess	12,87	11,20	8,50	5,67	4,10	2,17
Visual grade (average)	1,925	3,850	3,275	3,450	4,375	4,125
Std.Err. (visual grade)	0,20996	0,31531	0,22642	0,20239	0,19509	0,27778
coefficient of determination R^2 :	0,559					

Table 2: Statistical analysis of the results (visual evaluation), ANOVA: Single Factor

Samples	Sum	Average	Variance
1	77	1,925	1,76
2	154	3,850	3,98
3	131	3,275	2,05
4	138	3,450	1,64
5	175	4,375	1,52
6	165	4,125	3,09

Source of Variation	SS	df	MS	F	P-value
Between Groups	152,5	5	30,5	10,863	0,00000
Within Groups	547,5	195	2,808		
Total	700	200			

In Figure 4, results are presented graphically. We can notice that physical measures (red curve) and subjective grades (blue curve) do not have the same shape of the curve, nor they have the same trend. From this and according to coefficient of determination ($R^2=0.559$) we can conclude that there is no direct relation between the physical values and visual grades.

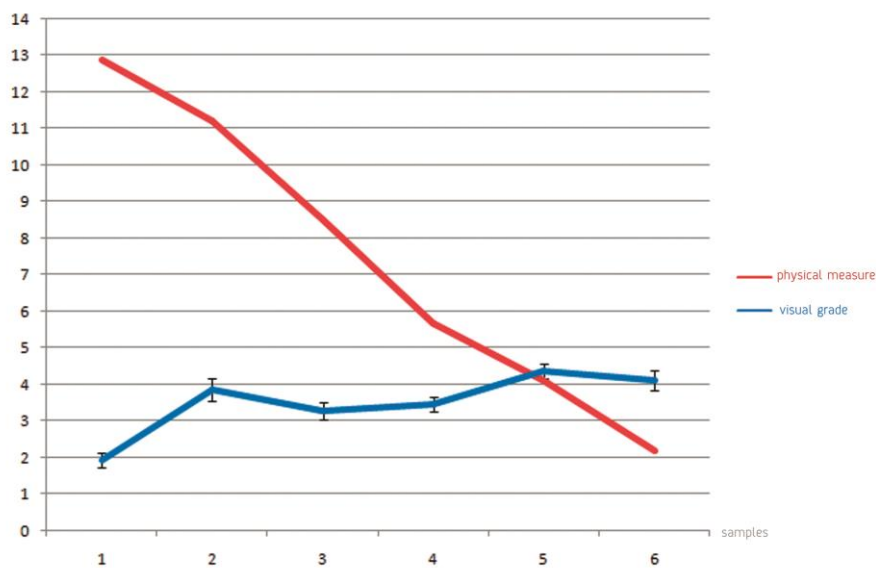


Figure 4: The relation of physical values and visual grades of graininess

4. CONCLUSIONS

The goal of this study was to examine a relation between the ISO defined parameter graininess and visual experience of graininess. Standard ISO 13660:2001 prescribe procedures and methods for measuring 14 attributes, but does not provide any reference to perception, in order to know whether a sample is poor, satisfactory, good, very good or perfect. There are no defined quality categories.

In order to define quality categories for graininess, we started with this initial study. First we wanted to see if human visual system could distinguish samples with different graininess. Therefore, we chose six samples with different tonal values, printed on the coated paper. According to our results we can conclude that there is no strong positive linear correlation between the physical measures and visual grades. This result is in sharp contradiction with regular printing practice that relays on the attribute of graininess. However, we tend to believe that long-standing printing practice could not survive had it not been enhancing print quality attributes. Hence, it might be useful to rethink the methodology used in this initial study.

We can think of two methodological reasons that lead to our result. One reason might be the instruction for visual assessment, which even our expert-participants did not understand. The other might be the production of samples. It is very possible that variability of tone value on samples suppressed graininess, being more salient visual quality. Maybe this is the reason the participants did not understand the instruction. In order to eliminate the influence of the different tonal values, it is required to generate samples in some other way. It is necessary to choose a field with a constant tone value and vary only the value of graininess. At this moment we are uncertain how such samples can be produced.

5. ACKNOWLEDGMENTS

This work was supported by the Serbian Ministry of Science and Technological Development, Grant No.: 35027 "The development of software model for improvement of knowledge and production in graphic arts industry".

6. REFERENCES

- [1] Briggs, J.C.: "Application note: Graininess Measurements on Halftones", Quality Engineering Associates, Inc, 2002
- [2] Dooley, R. P. and Shaw, R. "Noise Perception in Electrophotography", Journal of Applied Photography. Eng. 5, pp. 190-196, 1979
- [3] Engeldrum, P. G.: "Absolute Graininess Thresholds and Linear Probability Models", Proc. IS&T 1998 PICS Conf., IS&T, Springfield, VA, p. 231, 1998
- [4] Hino, M.: "A New Method for the Graininess Evaluation", Proc. IS&T NIP11 Conf. IS&T, Springfield, VA, p. 489, 1995
- [5] ISO /IEC 13660, Information Technology – Office Equipment – Measurement of image quality attributes – Binary Monochrome text and graphic images. First edition, Reference number ISO/IEC 13660:2001[E]. Geneva, Switzerland: International Organization for Standardization and International Electrotechnical Commission, 2001
- [6] Kingdom, F.A.A. and Prins, N.: "Psychophysics. A Practical Introduction". 1st edition. Academic Press, ISBN : 978-0-12-373656-7, 2010
- [7] Kodak: "Print Grain Index", Technical Data, Color Negative Film, 2000
- [8] Lee, H.C.: "Introduction to Color Imaging Science", United States of America by Cambridge University Press, New York, ISBN: 978-0521843881, pp. 564-572, 2005
- [9] Mishra, B. and Rasmussen, R.: "Micro Uniformity: An Image Quality Metric for Measuring Noise", Proc. IS&T 2000 PICS, pp.75-78, 2000
- [10] Rasmussen, D.R., Donohue, K.D., Ng, Y.S., Kress, W.C., Gaykema, F., Zoltner, S.: "ISO 19751 macro-uniformity", Proc. SPIE 6059, Image Quality and System Performance III, 60590K, 2006
- [11] Tse, M.K. and Forrest, D.: "Towards Instrumental Analysis of Perceptual Image and Print Quality," IS&T: The 25th International Congress on Digital Printing Technologies and Digital Fabrication, Sept. 20-25, Louisville, Kentucky, 2009
- [12] Vitale, T.: "Film Grain, Resolution and Fundamental Film Particles", [Online], Available at: http://vitaleartconservation.com/PDF/film_grain_resolution_and_perception_v24.pdf, 2009, (Last visited: 24.09.2014.)

THE SURFACE COVERAGE ANALYSIS OF METAL SUBSTRATE PRINTED WITH UV INKJET INK

Milana Sadžakov¹, Bojan Banjanin¹, Branka Ružičić², Boris Adamović³

¹ University of Novi Sad, Faculty of Technical Sciences,

Department of Graphic Engineering and Design, Novi Sad, Serbia

² University of Banja Luka, Faculty of Technology, Banja Luka, Bosnia and Herzegovina

³ Company NS Plakat, Novi Sad, Serbia

Abstract: The main aim of this research was to analyze if UV ink surface coverage is dependent on roughness when printed on metal substrate by Inkjet technology. Inkjet technology is contactless technology which covers the surface with ink by spreading the droplets directly from print head. This can make the surface unevenly covered. This paper presents the analysis of four metal substrates with different surface roughness covered with one and two ink layers printed with UV inkjet piezoelectric technology. The printed surface was analyzed for two types of unevenness: visual and physical. The visual assumes analysis of print mottle by using GLCM method, while the physical represents measuring of surface area that stayed uncovered by ink. The results showed that the print mottle decreases by increasing the surface roughness, while the surface ink coverage increases by decreasing the surface roughness. Surfaces covered with two layers have better results of ink area coverage and print mottle than surface covered with one layer.

Key words: UV Inkjet, surface coverage, metal substrate, roughness

1. INTRODUCTION

Nonporous, rigid substrates like metal have been usually printed by flexography, offset printing, screen printing and nowadays by ink jet printing. Inkjet printing is contactless, already familiar method for placing electronic data on many different substrates like paper, PVC, etc. and nowadays is present in almost every office and household. However, recently much effort is invested in turning inkjet printing into multifunctional tool able to be used many industrial manufacturing processes.

The inkjet process is the process where the ink is transferred directly onto the substrate, without the printing plate. The print quality of ink jet printing depends on several parameters such as inks, substrate, printing machine and software [Saeideh, 2013]. More specifically the quality of the print is highly dependent on droplet spreading, which is controlled by both ink properties (surface tension and viscosity) and greatly by substrate absorption properties (surface tension, roughness, and porosity) [Lee et al., 2002; Jurič et al. 2013]. There are two drop formation techniques widely used in high speed inkjet printing: continuous inkjet (CIJ) and a drop-on-demand (DOD). In drop-on-demand (DOD) inkjet printing, the ink drops are ejected from the printing head only when get electric pulse. The drop ejecting can be induced by piezo current, heat, or electrostatic forces. Print heads of DOD are low-cost, simple, and compact. They can make the drop size very small leading to high resolution. However, disadvantage is the low drop frequency, and requirement of maintaining the nozzle during operation. Inks for DOD systems may be classified to aqueous, non-aqueous, phase change and UV-curable inks according to their base or to dye-based and pigment-based inks according to the type of the colourant. Important parameters for ink formulations are flow properties and stability of the ink, jet stability, surface tension, conductivity, and purity [Alan, 2003]. UV-curable inks are present in the graphic printing and PE industries for many years. They have a completely different structure than conventional printing inks. They are mainly used in the printing of non-absorbent materials such as plastics and metal sheets, but also for high-grade card products and labels. There are UV inks for all conventional printing technologies as well as for the ink jet technology. The main structure of UV inks is consisted of oligomers, monomers, fillers, photoinitiators, photosensitizer and additives. Oligomers have a high molecular weight and serve for the same function as a resin used in conventional inks. They are the mainstay of a UV cured ink film and responsible for the flexibility, chemical resistance and elasticity of the ink film. Monomers serve as low molecular diluents. They are helping in the viscosity reduction and help out the ink to flow. After curing, oligomers create a tough and

durable ink film while the monomers become part of the polymer matrix. The photoinitiators and photosensitizer components of a UV ink serve as catalysts and are usually of a free radical [Sughosh, 2013; Kipphan, 2001].

The advantages and disadvantages of radiation-curing (UV) inks [Eubert, 2009]:

Advantages:

- Immediate curing (1–100 ms)
- Low temperature cure
- Solvent free
- No VOC emissions
- Flexibility
- No drying in ink unit
- Solvent and chemical resistance
- High mechanical stability

Disadvantages

- Difficult to clean
- Require strong solvents during cleanup
- Dryer design is at a high technical level
- Increased ink handling demands for reasons of health and safety.

Substrate surface topography has a strong influence on its optical and physical properties as well as on the print quality [Lepoutre, 1989; Oyvind et al., 2007]. Print quality based on surface unevenness can be divided in two categories to physical print quality and visual print quality. Physical quality represents even ink coverage of surface, without absence of ink in total area coverage, while visual print quality represents –uniform reflection from a printed surface or transmission of light through a translucent specimen known as mottle.

When the human eye look over a mottled surface it recognizes changes in the luminance over the area. These changes can differ across a wide range of spatial frequencies. Perception occurs when the human mind determines which mottle pattern forms specific images of interest. Every levels of magnification, the degree of mottle is determined by the spatial distribution of the changes of luminance levels [Roy, 2001].

In this paper will be analyzed how surface roughness of metal substrate and number of ink layers affects surface coverage of UV ink. Samples will be observed and evaluated in two different ways. Visual unevenness called print mottle will be measured by GLCM calculation and physical unevenness that assume analysis of parts of surface area that stayed uncovered by ink will be measured using ImageJ software and Threshold Colour plug-in.

2. MATERIALS AND METHODS

The investigation was performed on aluminum (electrochemically grained and anodized– 99,5% Al) substrates with four different surface roughness. Surface roughness was evaluated by contact stylus roughness meter Roughness Tester TR 200. To characterize surface roughness, parameters R_a , R_z and R_p were obtained [Pavlović et al., 2012]. For all samples cut-off length was adjusted at 0.8 mm and evaluation length was set up at 5, range was $\pm 40\mu\text{m}$ and it was used R-C filter. Samples are ordered alphabetically from the least rough surface to the roughest surface (A, B, C, D), as can be seen on Figure 1.

Printed test form was made from two solid squares of cyan colour. One is printed with one layer of ink (A1, B1, C1, D1) and the other with two layers (A2, B2, C2, D2), dimensions 10 x 10 cm. Substrates were printed with Hewlett Packard UV ink jet piezoelectric printing machine FB7600 with DOD drop formation technique. Ink drop was 42pl, resolution 508x500 dpi and it was printed in 3 passes. After printing, samples were scanned by scanner Canon CanoScan5600F at resolution 1200spi that is recommended by standard ISO24790:2012.

Analyses of area coverage were performed in ImageJ software by using Threshold Colour v1.12a plug-in proposed by G. Landini in 2010 [Landini, 2010]. To separate areas of interest there were

used saturation channel from HSL separations. Dimensions of tested samples were 40x30 μm . Images were taken with Vicinity camera at magnification of x42. Calculations for GLCM were performed in MATLAB software. Used code is proposed by Uppuluri in 2008 (Uppuluri, 2008). The distance (d) between two pixels whose repetition is examined, was 1 pixel. The orientation (θ) was the average of the possible four (0° , 90° , -45° and 45°). Parameters of importance taken into account for print mottle analysis were contrast, correlation, entropy, energy and homogeneity (Jurič, 2013).

3. RESULTS AND DISCUSSION

Roughness profiles for every substrate are presented in Figure 1 for longitudinal and transverse direction and in Table 1 are presented measured values.

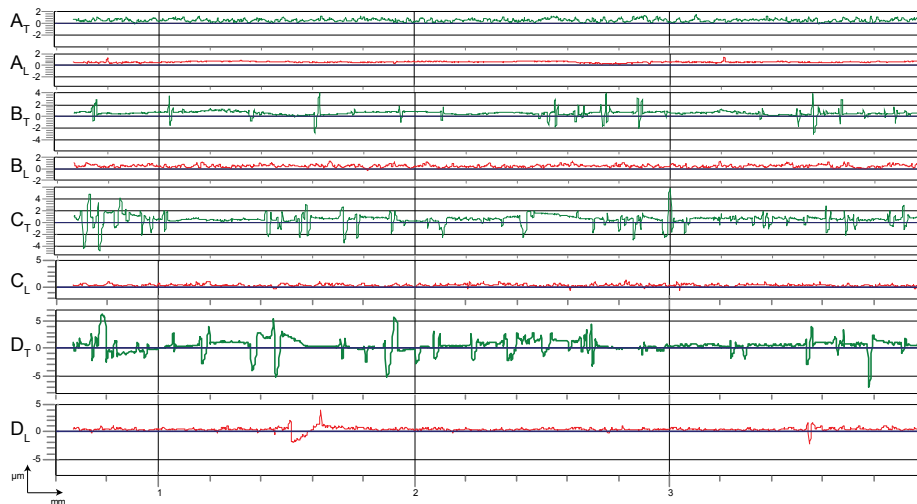


Figure 1: Transversal (A_T , B_T , C_T , D_T – green) and longitudinal (A_L , B_L , C_L , D_L – red) profiles of substrates roughness

Table 1: Results of measured parameters of roughness

	A		B		C		D	
	long.	trans.	long.	trans.	long.	trans.	long.	trans.
Ra	0.10157	0.19129	0.17633	0.23833	0.186167	0.5984	0.2726	0.78786
Rz	0.76286	1.46571	1.34567	4.63533	1.381167	9.71	1.9232	12.29
Rp	0.35957	0.80629	0.6865	2.528	0.719333	4.7168	0.9754	6.72186

Roughness in longitudinal direction does not show significant increase when parameters Ra and Rp are observed. However increase of Rz parameter is more significant which means that average distance between the highest peak and lowest valley are increasing. In transversal direction appears remarkable growth of roughness, as expected.

How for this investigation was important to observe unevenness of surface coverage there were analyzed parts of surface without ink. Results taken into account for analysis of uncovered area were average size, percentage of surface and perimeter. Based on results presented on Figure 2 it is obvious that there is a trend between number of layers and uncovered surface, regarding to lower values of unevenness measured on all samples with two layers. Samples with two layers also present a linear trend with surface (Figure 3) roughness unlike samples with one layer (Figure 4). Sample C1 have less uneven ink surface coverage than sample B1 which can be seen in results of average size and percentage of area.

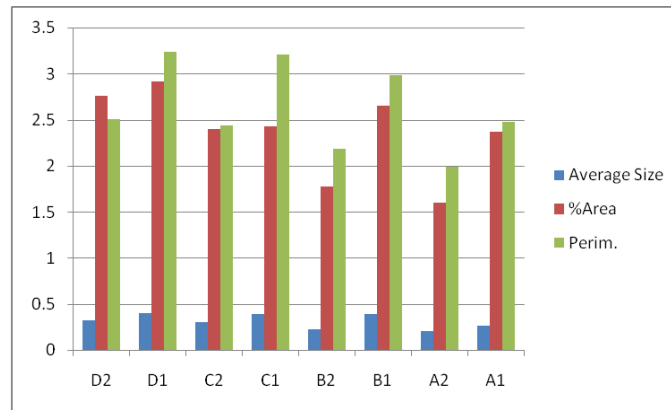


Figure 2: Surface unevenness parameters for samples with one and two ink layers

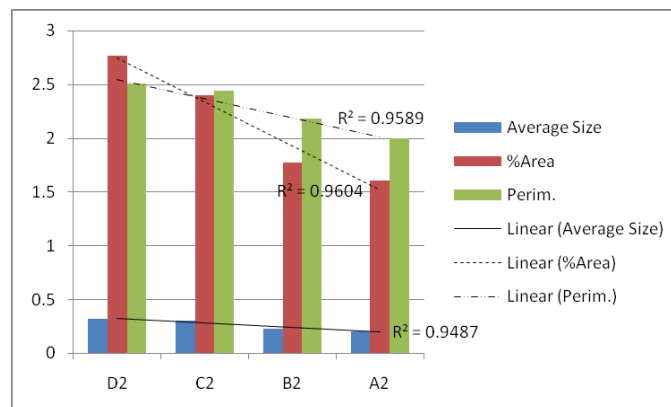


Figure 3: Surface unevenness parameters for samples with two ink layer

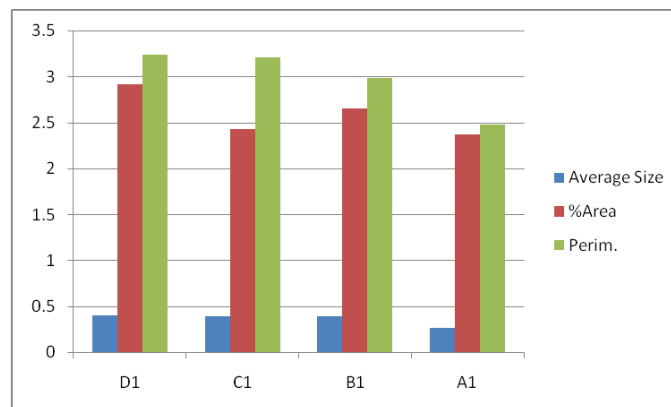


Figure 4: Surface unevenness parameters for samples with one ink layer

To determine print nonuniformity known as print mottle, five GLCM parameters were analyzed: contrast, correlation, entropy, energy and homogeneity (Figure 5-6). Other studies came out with conclusion that low contrast, low correlation, high energy and high homogeneity correlate with a uniform, smooth surface (Hladnik, 2011), that lower value of entropy corresponded to the low print mottle (Chen, 1998) and that print mottle is not in direct correlation with surface roughness.

Based on results in this study, print uniformity depends on surface roughness which is more noticeable on samples with two layers of ink (Figure 6). With increase of surface roughness contrast and entropy decreases, however energy and homogeneity increases. Samples with one ink layer also have a similar influence of surface roughness, but results of samples C1 and D1 have same deviations. Sample C1 shows higher energy and sample D1 shows higher contrast and entropy, but lower homogeneity.

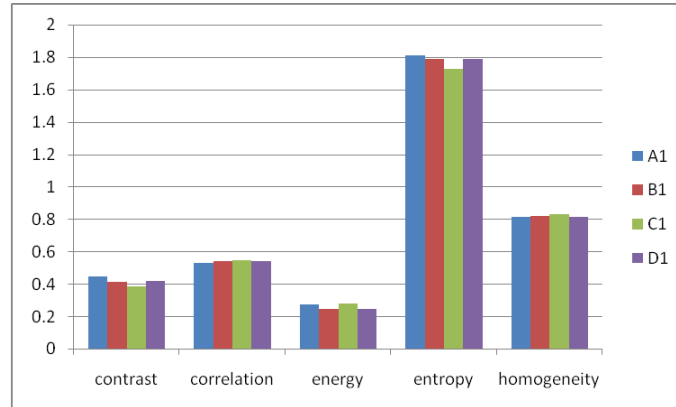


Figure 5: GLCM parameters for samples with one ink layer

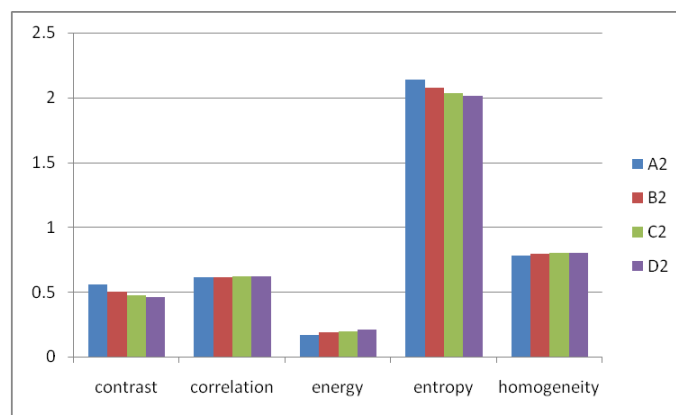


Figure 6: GLCM parameters for samples with two ink layers

4. CONCLUSION

Ink coverage is very important factor for both the visual and the physical quality evaluations of the printed sample. Physical characteristics are important in printed circuit boards and other electronics that are printed with metal inks, while visual quality is in correlation with visual impression of printed pictures. In this investigation results show that physical and optical results are in reverse correlation. Unevenness of ink surface coverage increase with surface roughness growth, despite that print mottle is less manifested on surfaces with higher roughness. If assume that higher energy means better uniformity, sample C1 shows correlation between print mottle and ink surface coverage.

In future investigations is planned to repeat production of samples C1 and D1 and discover why it came to irregularities in results.

5. ACKNOWLEDGEMENTS

This work was supported by the Serbian Ministry of Science and Technological Development, Grant No.: 35027 "The development of software model for improvement of knowledge and production in graphic arts industry".

6. REFERENCES

- [1] Alan, H., Mike, W., Hall, K., Theory of inkjet technology, Seminar material of Ink Jet Academy, Information Management Institute, Lisbon, 2003.
- [2] Chen, Y.: "Image analysis methods for paper formation evaluation", M.A.Sc. thesis, University of Toronto, Canada, page 33, 1998.

- [3] Eubert C.-G.: "Effects of Oligomer-to-Monomer on Ink Film Properties of White UV Curable Gravure Ink for Printing on Biaxially Oriented Polypropylene", Rochester Institute of Technology, page 99, 2009.
- [4] Hladnik, A., Mihael, L.: "Paper and board surface roughness characterization using laser profilometry and gray level cooccurrence matrix.", *Nordic pulp & paper research journal* 26 (1), 99-105, 2011.
- [5] Jurič, I., Novaković, D., Karlović, I., Tomić, I.: "Influence of Gloss and Surface Roughness of Coated Ink Jet Papers on Print Uniformity." *Acta Graphica* 24, 2013.
- [6] Kipphan, H.: ed. "Handbook of print media: technologies and production methods", (Springer, 2001.), pages 133. and 687.
- [7] Landini, G. (2010.): "Threshold Colour v1.12a", URL <http://www.mecourse.com/landinig/software/software.html>, (last request: 5.9.2014.)
- [8] Lee, H.-K., Joyce, M.K., Fleming, P.D., Cameron, J.H.: "Production of a Single Coated Glossy Inkjet Paper Using Conventional Coating and Calendering Methods", *Proceedings from TAPPI Coating and Graphic Arts Conference and Trade Fair, Orlando, FL, USA*, pp. 24, 2002.
- [9] Lepoutre, P.: "The structure of paper coatings: An update", *Progress in Organic Coatings*. 17(2), 89-106, 1989.
- [10] Oyvind, E., Erik, J., Oyvind, W.-G.: "The influence of paper surface roughness on ink pigment distribution." *Appita Journal* 60 (5), page 384, 2007.
- [11] Pavlović, Ž.: "Karakterizacija površinske strukture neštampajućih elemenata CtP termalne štamparske forme za ofset štampu.", PhD thesis, University of Novi Sad, Serbia, page 74, 2012.
- [12] Roy, R., Daniel, C.: "Predicting Half-Tone Print Mottle Using Digital Imaging & Stochastic Frequency Distribution Analysis.", In *annual meeting-pulp and paper technical association of Canada* (Pulp and Paper Technical Association of Canada; 1999.), vol. 87 (B), B155-B158, 2001.
- [13] Saeideh, G.-K.: "The effect of paper appearance on printed color of inkjet printer.", *Color Research & Application* 38, (4), 284-291, 2013.
- [14] Sughosh, S.-B.: "Formulation and Evaluation of Resistive Inks for Applications in Printed Electronics.", 2013.
- [15] Uppuluri, A. (2008): "GLCM texture features.", URL <http://www.mathworks.com/matlabcentral/fileexchange/22187-glcm-texture-features>, (last request: 27.6.2013.)

Colour research and application

WHERE ARE THE STANDARDS OF DIGITAL PROJECTION?

Iva Molek¹, Tadeja Muck², Dejana Javoršek²

¹Multimedia and Graphic Technology Secondary School, Ljubljana, Slovenia

²Faculty of Natural Sciences and Engineering, Ljubljana, Slovenia

Abstract: Although digital projection has been an established method of presentation for some time now and continues to gain on popularity, the field of accurate colour display is relatively unexplored. Experience has shown that colours are displayed inaccurately or imprecisely, yet the sources that would determine how precisely, in fact, they are displayed, cannot be found not even in established institutions, such as UGRA. Projectors have had a very long history and over the last few years, they have become a component part of every serious presentation. In our research, digital projection of projector NEC NP210 was examined and measurements were performed according to the instructions and recommendations of the ISO standards. Screen illumination (Ev) of digital projection was performed and evaluated according to the ISO 11315-1:2003 standard, the screen luminance (Lv) test was performed according to the ISO 11315-2:2011 standard, while measurements of the projected images were evaluated according to the ISO 12646:2010 standard. Calibration and profiling were performed using the application *basICColor display 4.1.22* in combination with the *iPro spectrophotometer*, whereas the photometric and colorimetric accuracy of digital projection were evaluated using the digitalized colour chart *Color Checker Classic*. It was established that the projection evaluation based on chromaticity, graduation, channel, grey balance, and colour gamut according to the ISO 12646:2010 standard is relatively complicated and time-consuming. The results have shown that colorimetric accuracy evaluation by using a digitalized *Color Checker Classic* test chart is the only that produces useful results, especially if the chromatic colours display with a focus on skin tones and achromatic colours with a focus on grey balance and chromaticity respectively are separately examined.

Key words: digital projector, standards, projected colour, profiling.

1. INTRODUCTION

Projectors have had a very long history and over the last few years, they have become a component part of every serious presentation. Nowadays digital projectors are used to project static and dynamic contents, and function with the help of a wide array of various projection technologies and modules respectively. With the aid of the digital projection modules we can choose from different pre-set options; some projectors can be geometrically calibrated (manual setting of contrast, brightness, correlated colour temperature) and characterized.

Digital projection was conducted and evaluated in accordance with the standards ISO 11315-1:2003, ISO 11315-2:2011, and ISO 12646:2010.

Standard ISO 11315-1:2003 (Photography - Projection in indoor rooms - Part 1: Screen illumination test for still projectors) [ISO 11315-1:2003] specifies the (laboratory) method for determining the utilised luminous flux of the projector and uniform distribution of illumination in dark spaces for all types of still projections. The comparison of screen illumination with different projection systems for practical use is enabled by the standardized system of uniformity measurement.

Standard ISO 11315-2:2011 (Photography - Projection in indoor rooms - Part 2: Screen luminance test for still and video projection) [ISO 11315-2:2003] specifies the screen illumination and screen luminance measurement (Lv), as seen by the (seated) viewer in all types of optical projection of still and moving pictures in dark spaces. As optical characteristics of screen surface have a direct influence on luminance (Lv), the screen should be treated as an integral part of the projection system in the context of this standard. Comparison of screen luminance (Lv) in different projection systems for practical use is enabled by the standardized system of illumination measurement. Standard ISO 12646:2010 (Graphic technology - Displays for colour proofing - Characteristics and viewing conditions) [ISO 12646:2010] includes provisions for observing conditions in screen preview of printed material and soft proofing respectively. Some are useful in digital projection, especially if we want to display colours as precisely as possible. In order to examine digital projection we need only a few provisions, since it cannot be expected that the

projected images would display better than the ones displayed on high-quality computer screens. The display of colour on screen does not depend on observing conditions in the room alone, but on many other factors: uniformity, size, resolution, observing distance, projector calibration, and programme settings of its driver. Even in the best projectors, precise colour display is limited by precise colour transformations between the colour space, enabled by the digital projection in given circumstances. Digital projection is not as demanding, as printing material need not be simulated. However, it is in the user's interest that in such cases as exact display as possible is reached.

2. METHODS

In order to perform the experimental part as part of this research we had various types of equipment at our disposal. The projector we used for the experimental part is a low-priced NEC NP210 classroom digital projector, based on the DLP technology, EyeOne Pro (X-Rite) spectrophotometer, characterization software, and other necessary equipment (studio lighting, plumb line, level, tape measure, air-conditioning appliance and thermometer, etc.) that enabled performance under controlled and repeatable conditions.

2.1 Determining Screen Illumination (Ev) According to the ISO 11315-1:2003 Standard

Digital projector was placed in a room eight hours before performing a test on it according to the manufacturer's instructions, so that the projection surface is 1–2 m². DPT-W315 colour chart was projected to the screen and thus the projector was heated for at least 30 minutes. We began measuring the light conditions; we dimmed the room and measured illumination (lx) in the central field. DPT-W315 (R = G = B = 255) colour chart was used for establishing screen illumination (Ev). During measuring the instrument was placed maximum 20 mm from screen. Screen illumination was measured in the centre of all nine fields of the chart. Measurements were performed using different digital projector modules, in this case sRGB and High Bright in Presentation. Sample measurements average \bar{E} ($\bar{E} = E_{v1-9}$) was calculated and projection surface A was measured in m². Utilised luminous flux Φ ($\Phi = E_{v1-9} \times A$) was calculated in lumens, as well as uniformity of screen luminance g2-6 ($g2-6 = E_{min(1, 3, 7, 9)} / E_5 \times 100$). The calculated uniform screen illumination (Ev) should be higher than 50.

2.2 Determining Screen Luminance (Lv) According to ISO 11315-2:2011 Standard

The same DPT-W315 colour chart was used for determining screen luminance (Lv) of the projection screen as for determining illumination according to this standard. Digital projector was placed so that the projection surface was 1–2 m². The measuring instrument set on the tripod was placed in the projection axis on two thirds of the distance between the screen and the last row of the viewers. The instrument was sighted in the centre of the colour chart's central field and the measurement of screen luminance (Lv) in the centre of the L2 screen was performed. The tripod was moved back to the position B, that is, half of screen's width to the left, sighted to point 1, and measurement L1B was performed. From the same position and using the same procedure, point 3 was sighted to and L3B measurement was performed. Tripod with the instrument was moved to position C and by adequate sighting, measurement of L1C and L3C was performed (measuring can be seen on Figure 1). Screen luminance (Lv) in the centre of the projection screen L2 should not be lower than 50 cd/m². The uniformity of screen luminance (Lv) g2 is the quotient of minimum and maximum value measured in % and must not be lower than 50%.

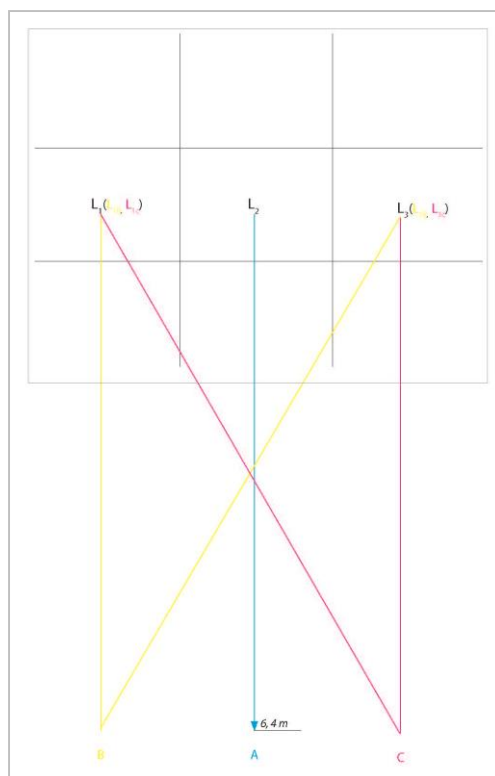


Figure 1: Measuring Screen Luminance (L_v) of the projection screen.

2.3 Measurement of Projected Images According to SIST ISO 12646:2010 Standard

Because of the extensiveness of the standard, merely the measurements of gradation, colour range and colorimetric accuracy are focused on and performed a test of light conditions prior to measurements and profiling.

After 45 minutes of heating the projector measurements of the unprofiled projection were performed in adequate modules sRGB and Movie. Calibration and profiling of the digital projector were performed using well-established applications iMatch 3.6 and basIColor display 4.1.22 in combination with spectrophotometer EyeOne Pro (i1Pro). In all cases the desired values that fit the reproduction of the standardized colour space sRGB were set, whereas the white point luminance was defined by 100 cd/m^2 instead of the standard 80 cd/m^2 . Higher value of luminance was chosen because the projected reproductions are observed from much greater distance than computer screens, which sRGB colour space is adapted to. We started with gradation measurements, that is, colour charts of the centred grey fields were projected to the projection screen one after another. Tristimulus values X, Y, Z were measured; gamma, which should be in the area 1,8–2,4, was calculated. Colour charts DPT-SPC were projected one after another in order to measure the colour range of the digital projector. Chromatic coordinates x, y and u' , v' were calculated, so that the brightness of white colour is defined by $L^* = 100$. The colorimetric accuracy of the digital projection was evaluated by using the 24 fields of the *Color Checker Classic* colour chart. One after another, colour charts were projected to the screen and tristimulus values X, Y, Z of the central field were measured on each of them. Colour differences ΔE^*_{ab} between the displayed and reference values were calculated.

3. RESULTS

3.1 Determining Screen Illumination (E_v) and Screen Luminance (L_v) According to the ISO 11315-1:2003 and ISO 11315-2:2011 Standards

Table 1 and Table 2 clearly show that the projection fulfils the requirements of the standards in every aspect and module. Correlated colour temperature reached is lower than 6500 K in all cases. In sRGB module, where it should reach 6500 K, is actually the lowest, namely, 6107 K.

Screen illumination falls from top to bottom diagonally from left to right. Field 1 (Ev1) is always the least illuminated and the field 9 (Ev9) is always the most illuminated, yet screen luminance in all modules is approximately the same, most likely within the repeatability of the measuring method (spectrophotometer adjustment). As expected, screen illumination is the lowest in sRGB module and the highest in High Bright module. Screen luminance (Lv) is also the lowest in the sRGB module and the highest in High Bright module, while its uniformity on screen practically does not change.

Table 1: Screen illumination (Ev) of the digital projector NEC NP210.

Measuring fields - charts DPT-W315	sRGB Module		High Bright Module		Presentation Module	
	Ev (lx)	CCT (K)	Ev (lx)	CCT (K)	Ev (lx)	CCT (K)
Ev1	320	6268	918	6556	792	6568
Ev2	367	6100	1045	6366	906	6377
Ev3	346	6014	1000	6282	845	6265
Ev4	389	6212	1127	6524	962	6526
Ev5	367	6100	1115	6401	933	6396
Ev6	420	6017	1263	6297	1082	6296
Ev7	423	6174	1206	6434	1058	6466
Ev8	446	6073	1322	6383	1127	6378
Ev9	518	6009	1489	6244	1294	6241
Ev	400	6107	1165	6387	1000	6390
Uniformity g ₂₋₆	87,19 %		82,33 %		84,88 %	
Φ (lm) ³	684		1992		1710	

Table 2: Screen luminance (Lv) uniformity of the digital projector NEC NP210.

Measuring fields - charts DPT-W315		Lv (cd/m²)		
		sRGB Module	High Bright Module	Presentation Module
Position A	Central field L2	97,561	282,11	241,51
Position B	Left field L1B	88,23	252,20	216,23
	Right field L3B	85,02	244,04	210,38
Position C	Left field L1C	87,53	251,22	213,80
	Right field L3C	88,32	254,79	218,67
	Uniformity g ₂	87,14 %	86,63 %	87,11 %

3.2 Measurement Procedure of Projected Images According to SIST ISO 12646:2010 Standard

3.2.1 Gradation

It has been established that all graduations in the dark tone area deviate too much from the desired values, yet as expected, in the absolute average gradation in the default Movie module deviates the most, and the least in sRGB module. By profiling Movie module, better results than in default sRGB module could not be reached. We approached it the most by using the iPro+basICC display 4.1.22 profile, Lv = 100, which is followed by the profiled projection using the profile iPro/iBeamer. There is no improvement even if we increase the desired luminance of the white point Lv = 150 in the iPro+basICC display 4.1.22 profile, Lv = 150 (which can be seen in Figure 2).

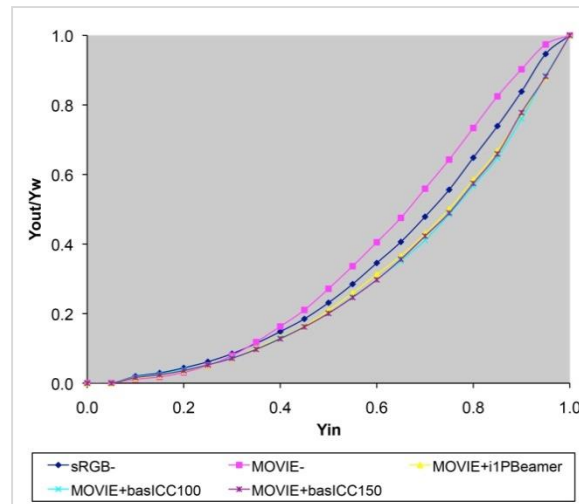


Figure 2: Gradation of the digital projector NEC NP210.

3.2.2 Colour gamut

Colour gamut of the modules (sRGB in Movie) and the profiled module (Movie) of the digital projector does not display any fundamental differences neither in the chromatic diagram u',v' , nor in the chromatic diagram x,y , which can be seen in Figure 3. Colour differences can be noticed only on the triangles in the $L^*(C^*uv)$ diagrams, which demonstrate the colour space. By profiling the Movie module, colour space cannot reach such size as by using the default module sRGB, which is marked by green colour in the $L^*(C^*uv)$ diagram shown in Figure 4a. A slight increase of the colour space has been reached in colours magenta and cyan, which can be seen in the $L^*(C^*uv)$ diagram shown in the picture 4b, using the basICC display 4.1.22+i1Pro (Movie+baICC label) profile for magenta. The results have shown that by using the Movie profile one cannot reach such colour gamut as by using the default sRGB module.

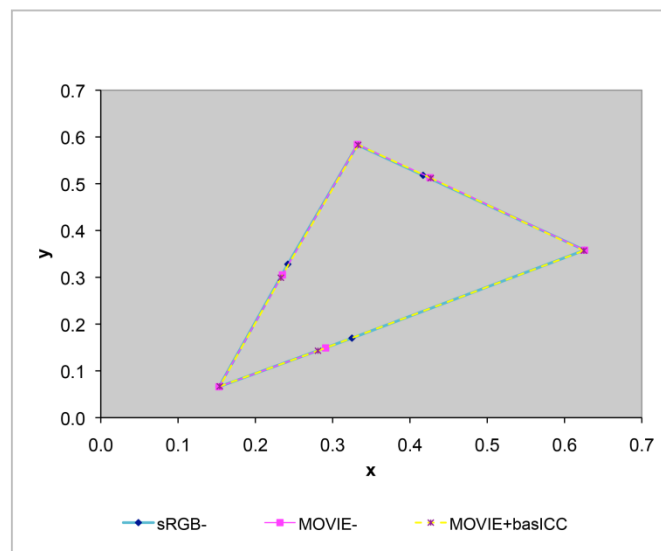


Figure 3: Colour gamut of the digital projector NEC NP210.

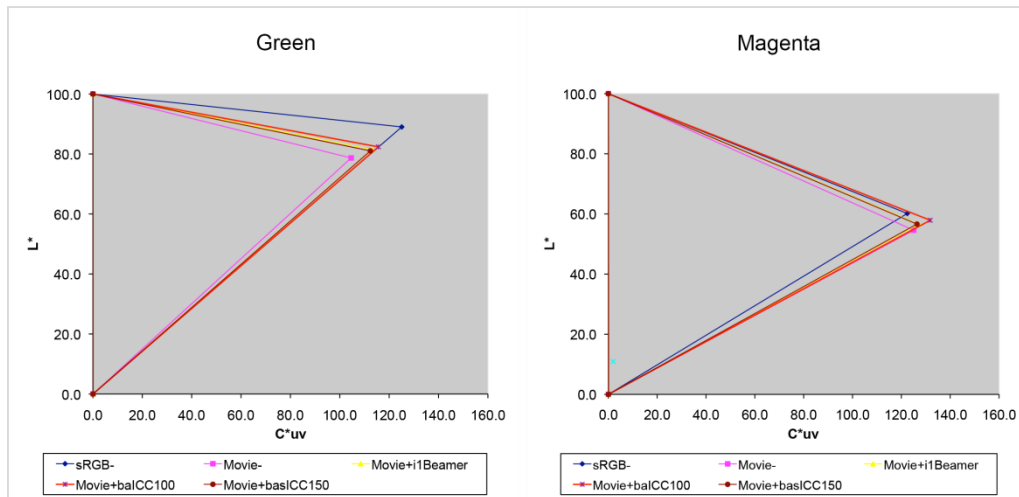


Figure 4: Lightness in the relation to chroma for Green and Magenta colour of the digital projector NEC NP210 projection modules.

3.3 Colorimetric Accuracy According to the ISO 12646:2010 Standard

The measurement results of the *Color Checker Classic* colour chart, displayed in profiled modules *Movie* and *sRGB* in studio conditions, are shown in Table 3. The desired values of ΔE^*ab according to the standard ($Mx \Delta E^*ab < 5,0$ in $max \Delta E^*ab < 10$) with these measurements cannot be reached regardless of which module or profile is used. Profiled projections reproduce colours worse than the default *sRGB* module, even if the depiction of colours is improved compared to the default *Movie* module. The display in the default *Movie* module is the worst with the average discrepancy of dE^*ab 11,4 and maximum dE^*ab 17,82. The test that was performed with the *i1Beamer* and *basICColor* display 4.1.22 applications, improved the unprofiled projection in the default *Movie* module – by using the *i1Beamer* application with the average dE^*ab 6,57 and maximum dE^*ab 16,28, and the application *basICColor* display 4.1.22 (Lv 150) with the average dE^*ab 6,64 and maximum dE^*ab 16,53. However, dE^*ab 17,28 was still too high in colour cyan, which cannot be displayed well by the standardized *sRGB* colour space already by definition. By profiling the *sRGB* module we do not reach an improvement, the result is even worse.

Table 3: Colorimetric Accuracy of the profiled *Movie* Module and *sRGB* Module, evaluated by *Color Checker Classic* colour chart

	sRGB	Movie	Movie i1Beamer	Movie basICC sRGB (Lv 100)	Movie basICC sRGB (Lv 150)	sRGB basICC sRGB (Lv 100)
All colours						
Mx dE^*ab ($<5,0$)	5,71	11,14	6,57	10,21	6,64	11,58
Max dE^*ab ($<10,0$)	11,87	17,82	16,28	18,80	16,53	17,66
Tones only						
Mx dE^*ab ($<5,0$)	3,43	9,14	3,56	7,60	4,45	8,29
Max dE^*ab ($<10,0$)	5,59	11,82	6,03	12,40	10,08	14,85

4. DISCUSSION

The control and evaluation of the projection on the basis of chromaticity, gradation, channel and grey balance, and colour gamut according to the ISO 12646:2010 standard is quite complicated and time-consuming.

Spectrophotometer iIPro was used for colorimetric evaluation of the projected colours. The instrument has certain imperfections and does not enable a totally irreproachable evaluation, since inconsistent results are given in measuring the emission of the projected colours, which reflects the most in establishing gradations and colour gamut. Inconsistency of the measurements intensifies according to the measuring and projection distance or size and screen luminance (Lv) of the projection surface respectively. The cause for this lies in the more difficult sighting of this instrument, although geodetic level was used in performing measurements. Spectrophotometer iIPro measurements are best performed when the measuring distance equals the projection distance. For colorimetric evaluation (and profiling) a more precise laboratory instrument with non-problematic sighting would be required, such as the latest instrument, the basICColor DISCUS.

The very choice of the appropriate default module, whether for the direct projection or for the colour management, presents the main issue. Testing of gradation and colour gamut do not enable the differentiation of quality of neither projection modules nor colour profiles. Evaluation of colorimetric accuracy by using digitalized colour chart Color Checker Classic provides usable results, especially if we examine the display of chromatic colours with emphasis on skin tones, and achromatic colours with emphasis on grey balance or chromaticity respectively.

Considering the fact that semi-professional and professional projectors are very expensive, colour management by using machine calibration and profiling shows perspective, e.g. in better screens, where there are a number of (inadequate) projection modules and/or settings which we can experiment with, without reaching useful results.

On the other hand, any kind of colour management of digital projection is efficient and sensible only if it assures similar quality or colour differences than the colour display on screens certified according to the ISO 12646:2010 standard. Following the example of UDACT, it is a necessary and reliable tool for digital projection certification.

It is not sensible to profile (colour manage) digital projections for home, office or average school use, it is better to choose the most appealing projection module and correct it regarding on projector's competences and based on the visual evaluation of the Color Checker Classic colour chart and other test images.

We should realise that it is a long-lasting process, as the same projector displays colours differently in different circumstances and the results cannot be transferred.

At the current state of digital projection and colour management the latter does not offer any significant advantages. To this purpose software and measuring instruments will have to be strongly improved. With the existent equipment only colorimetric analysis and studio projectors profiling in the chosen projection module and colour space make sense.

5. CONCLUSION

Digital projection with the analysed projector (and probably all others) meets all the provisions of the ISO 11315-1:2003 and ISO 11315-2:2011 standards in all modules, and is equal or better than analogic projection.

Digital projection according to the ISO 12646:2010 standard is not comparable to the display by using high-quality CRT or LCD computer screens. Colour management of digital projection is still in its infancy. At the current state of digital projection and colour management the latter does not offer any significant advantages. To this purpose software and measuring instruments will have to be strongly improved.

In order for the digital projection to be equal to the display of colours on certified computer screens, an adequate standard (ISO) is required, which will deal with digital projection exclusively, a reliable instrument with an appropriate software support for credible measuring and profiling, an application for a fast, irreproachable choice of the projection module and reliable digital projection certification, professional digital projectors without the possibility of choosing a number of projection modules and settings, yet with an efficient machine calibration chosen according to the desired display.

6. REFERENCES

- [1] About projectors, URL < <http://www.aboutprojectors.com/NEC-NP210-projector-reviews.html>>. (last request: 2013-05-16.).
- [2] Graphic technology – Displays for colour proofing – Characteristic and viewing conditions. ISO 12646:2008.
- [3] Graphics technology and photography – Viewing conditions. ISO 3664:2009, page 34.
- [4] How DLP technology works, URL <<http://www.dlp.com/technology/how-dlp-works/>>. (last request: 1. 11. 2011).
- [5] Kunihiro, S. in Akira, K. Desktop color handbook 07. Eizo Nanao Corporation, 2007, pages 23–68.
- [6] Matt, S. Gut getroffen. Kalibrierung mit Eye-One Beamer, Page 08. 2003, pages 86 – 88.
- [7] NEC portable projector NP216/NP215/NP210/NP115/NP110. User's Manual, URL <http://www.nec-display.com/dl/en/pj_manual/np215.html> (last request: 2013-12-26).
- [8] Park, S. in Park, G. G. Active calibration of camera-projector systems based on planar homography. Korea : School of Computer Science and Engineering, Kyungpook National University, Daegu, 2010, pages 320-322.
- [9] Photography – Projection in indoor rooms – Part 1: Screen illumination test for still projection. ISO 11315-1:2003.
- [10] Photography – Projection in indoor rooms – Part 2: Screen illumination test for still and video projection. ISO 11315-2:2011.

THEORY OF TWIN COLORANTS RESPONSE IN VISUAL AND INFRARED SPECTRUM

Vujić Žiljak -Jana ¹, Agić Ana ², Stanimirović - Žiljak Ivana ², Nassirzadeh M. ³¹Polytechnicum Zagabiense²Faculty of Graphic Arts, Zagreb, Croatia³Graphic Arts Technology, Athens TEI, Greece

Abstract: Till appearance of Infraredgraphic® we were occupied only with the visual part of the spectrum, meaning the part people can see. Managing with colors and dyes we widen to first part of near infrared, and the whole range of interest we separate to three parts: visual (400-700 nm, V), spectrum part of transient divarication (700-850 nm) and Z spectrum domain (850-1000 nm). We manage absorption and reflection of light from colorants in the whole region from 400 to 1000 nm with aim of creating new securing graphic system. Visual and infrared spectrum are carrying individual (separate) graphics, where the second one is observed through appropriate "infrared glasses". We are introducing new cognitions about colors, investigations and printing praxis with two assortments of dyes that achieve the same response in visual, but different spectral values in infrared spectrum. A new theory in graphic arts science is being established, entitled "dyes and color twins". Discovery of twins dyes and colors managing, creating twin color twins, is based on CMYKIR separation that has purpose to merge two different, independent images in unique printing form for conventional printing reproduction processes. The document contains multiple information, that each belongs to its own color twin. In the article is presented four color print of a postal stamp in INFRAREDGRAPHIC® technique, twins spectrograms from the same postal stamp, scanning results in several blockage points of V and Z spectrum.

Key words: postage stamps, twin colorants, CMYKIR separation, double image, dye color management

1. INTRODUCTION

Visual spectral part, meaning part used in most reproductions is well and quality elaborated. Related color managing system, CMM module, CMY separation and various reproduction matching are adjusted for present image processing and manipulating, are incorporated in most standard applications. Existing viewing, comparing, evaluating and measuring color systems are limited to visual part of spectrum, designated as 'V' (approximately 400 to 700 nm) with corresponding spectrophotometric curves, illuminants, standard observer functions and other items defined to specification. Infraredgraphic (IRG) opened new area in scientific world: educating and study of security graphics, new methods of image hiding and marking goods and products for instrumental observing with equipment in neighborhood (Žiljak et al, 2013). Each color hue can be observed at two physical states according to set-up of C,M,Y,K compositions, two different material ingredients. Accent is on the same color hue, meaning that all colorants in visual (V) have the same spectrum, that can be demonstrated as a absorption vs light frequency graph. That is the reason that such composing, creating and colorants are designated a new term 'dye twins' (Vujić et al, 2014) (Vujić et al, 2014) (Agić et al, 2013). Dyes from the 'twins' group have different spectral values in infrared spectrum, 'Z' spectrum part (1000 nm), people do not 'see' it, but it can be detected with infrared cameras. Each color has a specific spectral curve, what is its 'fingerprint', including related color evaluating system. Observed twin pairs must have defined and identical spectrograms in visual, (Agić et al, 2013) (Žiljak et al, 2012). Colorants from 'twins' area have different spectral values in infrared spectrum, 'Z' spectrum part (1000 nm), that human can not observe, but it can be instrumentally detected with IR camera. Values in visual should be the same (Agić et al, 2013) (Žiljak et al, 2012).

Each color has its specific spectral curve, its 'fingerprint', followed by corresponding colorimetric data (visual). According to L*a*b* model, 3D space coordinate system annotating and calculating difference between two points in that space, after printing. Colorimetric ΔE criterion is defined:

$\Delta E = \sqrt{[(L_1 - L_2)^2 + (a_1 - a_2)^2 + (b_1 - b_2)^2]}$. According to specification, ΔE value lower or equal 3 is acceptable, values larger than 6 are not.

This criterion was not sufficient for experimental equalizing two dyes in V spectrum. New theory in graphic science is established, named 'dyes and color twins'. Discovery of managing twins

colors and dyes, twin pairs creating is based on CMYKIR separation, that has goal to merge two independent images in unique form, for conventional printing reproduction techniques. Document contains multiple information, belonging to each twin separately (Žiljak, 2013). Presented example is four color post stamp print in INFRAREDGRAPHIC-IRG technique.

Special significance IRG procedure achieved when IRG adopted the information of absorption of light in infrared Z-value, where spectral difference in near IR at 1000 nm is measured. (Žiljak et al, 2012). There came out, that determining of spectral curve was a salvation. These dye curves show places in parts of process dyes curves where increasing or decreasing of dye amount is needable. Spectral curves appliance decreased number of iterations while tuning IRG requests in equality in V, and diversity of dyes in Z. This established new twin color theory of colors and dyes, beginning with CMYKIR separation works, (Žiljak et al, 2009) (Agić et al, 2013), till publishing in Polytechnic and Design publication and Blaz Baronic Conference.

2. COLORS, DYES AND CORRESPONDING SPECTRA

Broadening reproduction system from visual to NIR domain, appliance of CMYKIR separation and study of infraredgraphic (IRG) brought variety of new elements in color-system management. It occurred specially when in INFRAREDESIGN® theory (Pap et al, 2010) drag in absorption spectral difference in near IR, where spectral curve determination was very beneficial. (Žiljak Vujić et al, 2014). NIR domain investigation, Z-camera implementation and Z-parameter definition indicated that NIR domain should be treated in three parts. For twin pairs adjustments in V, regression analysis for under-color transition (UCT) exchange is used (Agić, et al 2014). Infrared graphic opened a new scientific field: examination of security graphics, new image hiding and marking of products methods, and detecting that with instrumental equipment that is in neighborhood.

Table 1: $L^*a^*b^*$ and ΔE for twin pairs combinations

Twinpairs	L	a	b	ΔE
D3 V	83,033	-2,991	-6,148	2,960
D3 Z	84,099	-0,717	-7,715	
B5 V	72,971	-6,094	-26,031	2,445
B5 Z	73,935	-6,085	-23,784	
G10 V	73,921	24,211	-16,284	3,995
G10 Z	73,097	20,778	-18,153	

When printed, we got spectrograms for various twin pairs, eg dyes D3, B5 and G10, $L^*a^*b^*$ and control ΔE . Colors and dyes are $L^*a^*b^*$ determined, but for each item we have V and Z dye, as for D3V and D3Z with common ΔE value. Each new printing is immediate correction in Z(K40). The aim is to get better data in role of parameter correction in regression equation (Vujić, 2014). Figure 1–4 express twin pairs differentiation area on two Z values, in domain above 800 nm.

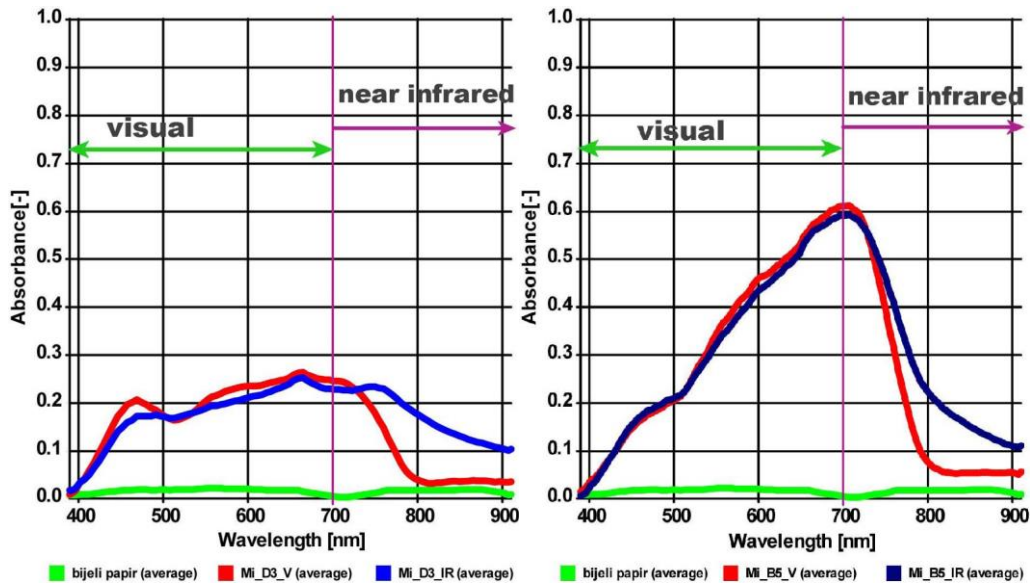


Figure 1: Broadened D3 dye spectrogram

Figure 2: Broadened B5 dye spectrogram

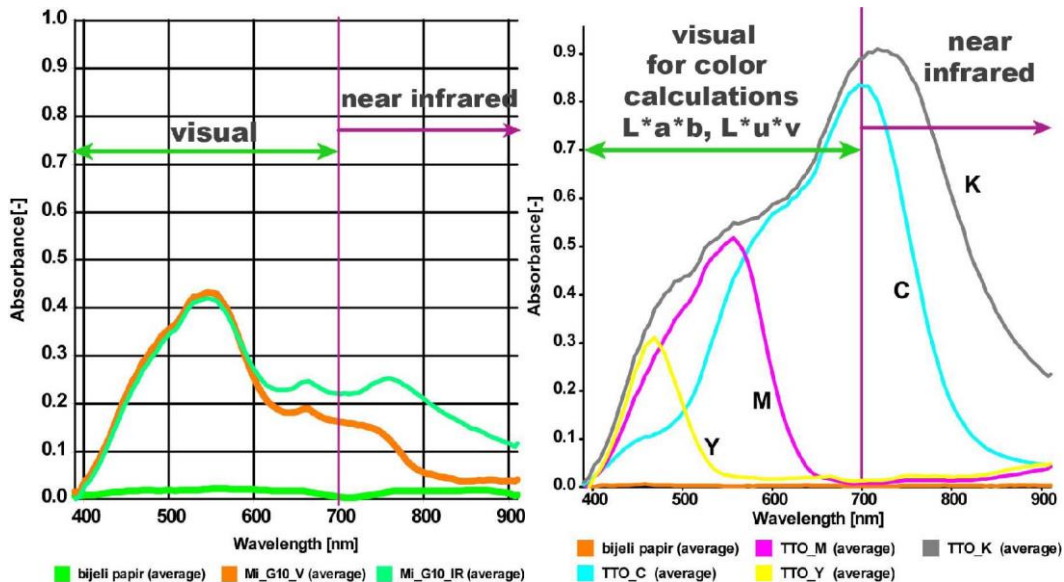


Figure 3: Broadened G10 dye spectrogram

Figure 4: Brodened spectrogram of system dyes (Bernasek et al, 2014)

3. VISUAL, TRANSIENT AND Z DOMAIN

'Color management' is a great item in computer aided reprography. It implies only visual domain from 400-700 nm, bare eye human vision domain, or human color perception. In this spectral part the claim is that color twins have identical, or quite simmilar spectrograms.

InfraredGraphics broadens to near infrared domain starting at 700 nm. First: the begin of this part is examined, named transient part where twins disjoin. One of the twins has 'zero' value above 800 nm. Here starts the second part of twins spectrum part, annotated as Z spectrum. (Žiljak et al, 2013) In that part the second twin is positive: at least 0.1 light apsorption value. Difference ΔZ is measured with Z-camera, calibrated at 1000 nm. To that continued part Z-image is associated, that should be invisible in V spectrum. That the way Z-image hiding from RGB camera. (Agić et al, 2013). ZRGB camera contains two lens systems, two different filters, for V and Z domain. IRGraphics is subjected to that principle of broadened color management, entitled 'color dye management'. That broadened system colors are managed in a way to mark graphic

product with two images that manifest in two spectral domains. Z-value is distanced for 300 nm from the area where human color recognition ends.

That 300 nm is enough distanced from transient part (700–800 nm), where absorption properties of twin pairs diverse, according to INFRASREDESIGN theory.

If dye 3D is observed, there is a significant deviation of twins in 600–700 nm area. From spectrogram can be concluded that amount of cyan dye has to be readjusted. This information would not be obtained only from ΔE calculation. Twin pairs theory enabled new guidances, sense and usefulness of dye spectrum calculations. (Žiljak et al, 2008.) Calculated numerical values are obtained on basis of formulations (Vujić, 2014) published on Blaz Baronic Symposium (Vujić, 2014), Examination results are:

ΔE criterion is not finally compiled. Variety of dyes and calculating data for calculation and adjusting regression curves. For now model that is achieved for first visual-infrared stamp is acceptable. Somewhere unwanted, hidden image can be perceived. Print values are values from published equation. (Vujić, 2014) Input values for spectrum are values from the print. Achieved Lab values differ a little from planned input ones, the reason are specific paper and dye properties. ZRGB camera at the same time is a video camera. Floral, fauna, recognition in people and vehicle circulation is observed in dual spectra. Video camera produces large amount of pictures, that are analysed with purpose of searching for extraordinary specificity. In that way new applications for recognition and integrating V and Z image are being developed (Vujic et al, 2014).

4. EXPERIMENTS WITH COLOR AND DYE TWINS

We showed that step spectrum shift that transformes from visual to IR spectrum, and stepwise loss of chromaticity, till only hidden image detectavle only in NIR stays. Example is realised by 'cut off' filter system on Preojektina 4500 Model. Figure 5 and Figure 7 show difference between graphics: first in visual, and second in infrered spectrum. Two completely differnt graphic



Figure 5: Post stamp-visual.



Figure 6: Scanning with 570 nm blocking



Figure 7: Post stamp scanned at 715 nm

Figure 8: Barrier scanning at 850 nm

solutions are contentally bounded. Van Gogh's sunflower are in visual, on the same place where Van Gogh's portrait in Z spectrum is. Or, Mona Lisa' portrait is in visual, and Leonardo's portrait in Z stage. Barrier scanning shows 'transition area', annotated as spectrum part from 700–800 nm., fig 6. Mixture of two images is displayed, and that is the reason why Z-value(1000 nm) is set at 300 nm further from visual part. Figure 7 displays enough clear Z image already at 850 nm, and V image fully vanished.

First post-stamps are realised, and they got it's purpose. There is a lot of publications about them, and the last one with declared spectral analysis, was made by author of the post-stamp itself (Vujić, 2014). Already second post stamp is brought out containing V and Z transformation, treating minerals. It was a mentioned thematics, and will be presented at GRID conference 2014 in visual and infrared stage.

It must be pointed out that some color certain V spectrum doesnt mean important in reproduction sense. Except in forensic, in defining some dye composition. Twin dyes spectra show twins matching quality in V domain, and projected diversity in Z domain, the fact that describes IRG system. Double spectrograms are new item in forensics. Spectral analysis has a new importance.

5. CONCLUSION

Broadening visual spectrum to near infrared and creating common domain, with no respect that that broadening is instrumentally visualised, opens variety printing options and applications. Safe and unfailling double image creating, dual graphics opens unforeseen reproduction features in very wide applications and possibilities options with standard reproduction systems. Differentiation 'double colors' for reproduction purposes and defining 'transient' domain from 700 to 800 nm, and a domain of 1000 nm ensures its definition and stability. Z-parameter as a defining factor inside NIR domain assigns differentiation stage that are visually or instrumentally displayed, but they present unity. There is a situation, where not standard dyes stage is estimated, already new dyes can be created from independent ones, with programmed characteristics. This additional develops printing system, allows supplemental protection, designers and simmlar effects, various materials and media usage, but points out further investigations, working new models out and forming new systems.

6. REFERENCES

- [1] Agić, D., Stanimirović Žiljak, I., Agić, A., Stanić Loknar: "DEGRADATION OF DUAL IMAGE FOR VISUAL AND NEAR INFRARED SPECTRUM AT REPEATED CMYK/RGB RENDERING", Journal of Graphic Engineering and Design, volume 4 (1), pages 13-16., (2013).
- [2] Agić, A., Bernasek, A.: "BLIZANCI BOJILA ZA PROŠIRENJE INFRA INFORMACIJSKE TEHNOLOGIJE", Polytechnic and Design, volume 1 (1), Tehnicko veleučilište Zagreb, pages 27-33, (2013).
- [3] Agić, D., Žiljak Stanimirović, I., Agić, A.: "APPLIANCE OF TWINS AS A WAY FOR ACHIEVING SECURE HIDDEN IMAGE IN INFRARED TECHNOLOGY, Polytechnic and Design, volume 2 (2), pages 143-152., (2014).
- [4] Bernasek, A., Žiljak Vujic, J., Ugljesic, V.: "BLIZANCI BOJILA ZA PROŠIRENJE INFRA INFORMACIJSKE TEHNOLOGIJE", Polytechnic and Design, volume 2 (2), pages 163 - 169., (2013).
- [5] INFRAREDESIGN® Trademark No: 11977964, Listing of European Mark, Clasification: 16, 25, 35, 40, 42
- [6] Pap, K., Žiljak, I., Žiljak-Vujić, J.: "IMAGE REPRODUCTION FOR NEAR INFRARED SPECTRUM AND THE INFRAREDESIGN THEORY", Journal of Imaging Science and Technology, volume 54 (1), pages 10502 -1-10502-9., (2010).
- [7] Žiljak Stanimirović, I., Agić, D., Žiljak Vujić, J.: "HIDDEN INFRARED IMAGE IN A UNIFORM CMYK SEPARATION HUE", Journal of Graphic Engineering and Design, volume 3 (2), pages 8-11., (2012).
- [8] Žiljak Vujić, J.: "SPECTRUM OF TWINS DYES ON A POSTAGE STAMP IN IRD TECHNOLOGY", Međunarodna konferencija tiskarstva, dizajna i grafičkih komunikacija Blaž Baromić, (Senj, 2014).
- [9] Žiljak, V.: "COLLECTIVENESS OF VISUAL AND Z-INFRARED SPECTRUM IN THE SECURITY PRINTING" Annual 2013 of the Croatian Academy of Engineering (Zagreb, 2013), pages 373- 396.
- [10] Žiljak Vujić, J., Bernašek, A., Žiljak Stanimirović, I.: "THE TWINS SPECTRUM OF THE BLUE COLOUR Z14 FOR OFFSET PRINTING ACCORDING TO INFRAREDESIGN THEORY", Međunarodna konferencija tiskarstva, dizajna i grafičkih komunikacija Blaž Baromić, (Senj, 2014).
- [11] Žiljak Vujić, J., Morić, B., Rudolf, M., Friščić, M.: "POSTAGE STAMPS WITH HIDDEN ID INFORMATION IN SECURITY Z VALUES,TEM," Technics Technologies Education Management, volume 8 (4), pages 1466-1473., (2013).
- [12] Žiljak, V., Pap, K., Stanimirović, I., Vujić, J.: "MANAGING DUAL COLOR PROPERTIES WITH THE Z- PARAMETER IN THE VISUAL AND NIR SPECTRUM, Infrared Physics & Technology, volume 55 (4), (2012).
- [13] Žiljak, V., Pap, K., Žiljak, I.: "CMYKIR SECURITY GRAPHICS SEPARATION IN THE INFRARED AREA", Infrared Physics and Technology, volume 52 (2-3), pages 62-69., (2009).
- [14] Žiljak, I., Pap, K., Žiljak-Vujić, J.: "INFRAREDESIGN", Zagreb: Fotosoft, 2008 (monografija),. ISBN 978-953-7064-09-9, Zagreb, (2008).
- [15] Vujic Z J., Rajković, I., Žiljak Stanimirović, I.: "SIMULTANO VIDEO SNIMANJE U VIZUALNOM I INFRACRVENOM SPEKTRU PROŠIRENE V/R STVARNOSTI", Polytechnic and Design, volume 2 (1), pages 73-78., (2014).

LIGHTFASTNESS EVALUATION OF PRINTS USING GAMUT VOLUME AND VOLGA SOFTWARE

*Hana Smejkalová, Petr Dzik, Michal Veselý,
University of Brno, Faculty of Chemistry, Brno, Czech Republic*

Abstract: This article addresses recent approaches to the evaluation of lightfastness in both classically- and digitally-printed photographs. It presents an experimental method used to measure colour changes. As a consequence, a proprietary software VolGa for the gamut volume calculation was created. The primary goal is to investigate the influence of additional protection in the enhancement of lightfastness. The lightfastness of digitally-printed images was investigated by means of accelerated ageing. Samples were created by printer on different print media. The surface of the final prints was left untreated or modified by varnishing or lamination. In this way, the sample set monitored print behaviour under the influence of light. The colour changes in the samples were evaluated in terms of measured reflective spectra, from which colorimetric evaluations were made. The results were processed using VolGa software. Actual print-life was calculated from dependence of loss of normalized gamut volume upon exposure. Finally, the effects of the receiving layer employed, whether ink alone or with additional surface treatment, are discussed.

Key words: VolGa, gamut volume, lightfastness

1. INTRODUCTION

The traditional silver-halide colour photographs are produced in the dark room by optical exposure of photosensitive paper. Image forming is based on changes of crystal structure of silver halide upon irradiation. In the course of time a new digital printing techniques have replaced this obsolete method. The main cause is an increasing number of digitally recorded images. At present, a problem of fading of inkjet prints brings a complication which has arisen with the breakout of digital printing techniques. Properties and image permanence of the traditional photographs are well known in a consumer community. However, a general awareness of storing and handling the digital images is missing. Therefore, it is advisable to provide the consumers an overview of this topic.

2. DIFFERENT APPROACHES TO COLOR PERMANENCE EVALUATION

The image permanence of traditional silver-halide materials is evaluated according to regulations that are set by the ISO 18909 standard [ISO 18909:2006; Kipphan, 2001]. It is logical to test digital images by analogy to silver-halide photography. However, the application of ISO 18909 standard brings many problems as these techniques are different in their nature. Colour dyes of traditional photograph are incorporated in emulsion forming layers adhered to a paper which was sealed by a plastic coating, whereas printed dyes or pigments are digitally deposited in the form of very small droplets onto paper creating one unsealed layer. The thus obtained surface is susceptible to absorption of ambient ozone which has a strong oxidative effect. The permanence determination is made more difficult by photo-catalytic fading of mutual compounded dyes which results in uneven fading across a density scale. As modern inkjet printers utilize more than the four primary CMYK colours, more test patches and extended test charts are needed. From the general methodological point of view, the use of densitometric statusA filter set [ISO 18909] for monitoring print fading is not suited for wide variety of inkjet inks since absorption maxima of the dyes and pigments used in digital printing do not match entirely the spectral characteristics of the filter set. Therefore, the ISO 18909 standard cannot be used for testing images produced by the digital printing techniques [Wilhelm et al, 2004]. This implies that there is no measuring technique specified by ISO suited for inkjet printing so far.

3. EVALUATION BY COLOUR GAMUTE VOLUME CHANGES

The presented article deals with a new general method proposed for monitoring of colour print fading, suitable for all presently used techniques. It is based on the determination and comparing of gamut volume of a test chart obtained by the appropriate technique (Veselý, 2010). The colour gamut volume is defined as a subset of a 3D colour space (usually CIE Lab) encompassing all the colours accurately reproduced by the device (see Figure 1). It is a measure on how large the colour range of a device is achievable.

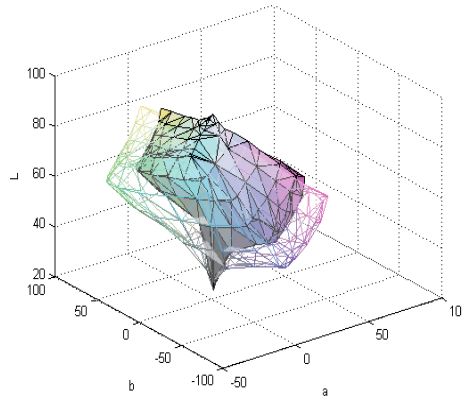


Figure 1: Colour gamut in 3D CIE Lab colour space

Datasets of colour coordinates are usually obtained by reflection colorimetric measurements of particular patches. Printer profiling testcharts can be conveniently used for determining gamut volume (Tastl, 2006). The method for estimating colour gamut works as follows.

- Identification of gamut vertices
- Approximation gamut by a polyhedron
- Calculation the volume of the polyhedron

Thus we obtain a convex hull of the set that resembles the gamut. The convex hull is the smallest convex set that contains all the points (Barber, 1996). Vertices are identified by the combination of a non-linear convexing transformation with a convex hull algorithm (Balasubramanian, 1997). First, the center of gravity CG is assumed to lie inside the gamut. The distance of each of the point from the CG is normalized in order to set all the values between 0 and 1. Then, a non-linear transformation is performed for some parameter γ (Dzik, 2012).

4. VOLGA APPLICATION AND PARAMETER GAMMA

The role of parameter gamma is very important for controlling the polyhedron approximation. The value of parameter reaches from 0 to 1. The higher γ is, the more gamut volume is gained. On the contrary, lower γ values result in lower gamut volume. Figure 2 well illustrates the influence of parameter on the degree of the convexing transformation on real samples. The graph is accompanied by images showing 2D cross-section plots for L level 50. The optimal degree of convexing was determined empirically from Figure 2 and γ value of 0.1 was chosen.

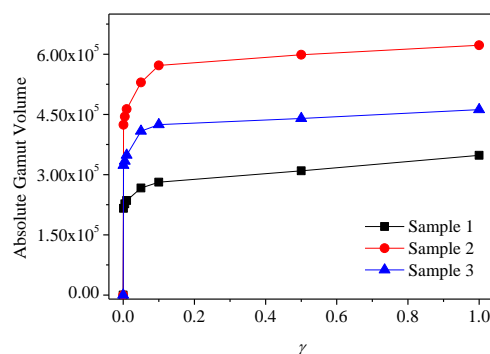


Figure 2: Color gamut in 3D CIE Lab color space

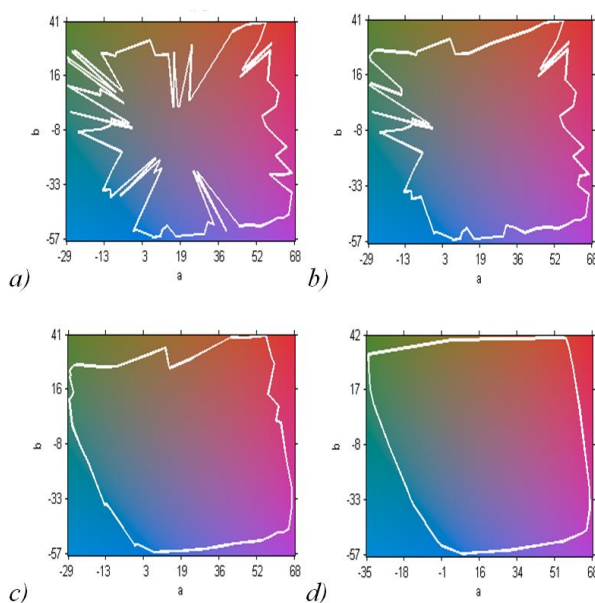


Figure 3: 2D cross-section plots for γ values a) 0.001, b) 0.01, c) 0.1 and d) 1.0

Gamut volumes are calculated by the VolGa application. This proprietary software utilizes MatLab and was designed to visualize gamut in 3D in $L^*a^*b^*$ space or in 2D as a cross section, where L^* is selectable. In addition, the utility encompasses colour difference heat map and plot of gamut volume evolution with trend fitting and fading rate calculation. The application is offered for free on a VolGa web site to make it available for other users [Dzik, 2012].

The VolGa enables batch processing of multiple samples. A switching in the dataset is performed in the main control panel. The menu offers the choice of setting the spacing between the successive measurements, such as hours, days or years. It is possible to compare the two concrete files in the respective dataset. Then the menu enables to choose the type of graphic output. Results are written as a text file.

5. ENHANCEMENT OF PRINT LIGHTFASTNESS

Factors that affect the longevity of images are light, dark keeping, temperature, humidity, and gaseous pollutants. Equally the paper used will affect the rate of fade and different grades of dyes will yield significantly different results. Additional layers, such as lamination or varnish, protect images from moisture, abrasion, and light exposure. It is proved that the treated samples exhibit better lightfastness and a resistance to smudging. Therefore, surface treatment with varnishing or lamination can be conveniently used for protection of printed surfaces [Kipphan, 2001].

6. EXPERIMENTAL

A detailed study of samples was conducted. The samples were produced by printer utilizing an early-generation dye based ink set with a low lightfastness and printed different types of papers. The standard X-Rite il calibration target RGB 1.5 was printed without colour management. The image surface was left untreated or modified by varnishing or lamination.

Accelerated aging tests of samples were performed in a Q-sun Xenon test chamber Model Xe-1-B without window filter to simulate outdoor display of images. The irradiation intensity was set on $0.68 \text{ W m}^{-2} \text{ nm}^{-1}$ at 340 nm and corresponds to an illumination intensity of 93.6 klx. The value was measured using an optometer. The temperature of black panel was kept at 63 °C by air circulation.

An X-rite Eye One reflection spectrophotometer was used to measure reflectance spectra of images. The printed samples were measured before experiment and after each exposure in a test chamber. An incremental exposure dose was estimated at 12 hours which corresponds to 1.12 Mlx h. The test was terminated after 120 hours of exposition. Recorded spectra for each exposure step were converted into $L^*a^*b^*$ coordinates for 2° observer and D50 illuminant.

The comparative print permanence evaluation was processed using stand-alone application VolGa utilizing MatLab libraries. The best-fit value of $\gamma \cong 0.1$ was applied generally for all samples (see the chapter 4). An actual print-life was calculated according to equation (1) derived from dependence of loss of normalized gamut volume upon exposure dose. The end-point criterion was adopted to be 30% gamut volume drop as in the ISO standard 18909. The parameter α is a measure of the gamut shrinkage rate. All points of the dataset follow exponential trend and the plot satisfies the equation for first-order equations. This parameter can be seen as the rate constant only if the calculation is preformed from the equivalent age increments. Otherwise, if it is calculated from exposure dose, the parameter has a meaning of fading coefficient.

$$y = \exp(-ax) \quad (1)$$

One standard day exposure dose was accepted to be 5 400 lx h (Wilhelm, 2004). Therefore, the equivalent sample age A can be expressed as follows.

$$A[\text{days}] = \frac{H[\text{lx h}]}{5\,400[\text{lx h day}^{-1}]} \quad (2)$$

7. RESULTS AND DISCUSSION

The following graph depicts influence of surface treatment on lightfastness of samples. According to expectation, the normalized gamut volume decreases exponentially with increasing exposure dose. The smallest colour differences were observed with laminated sample. Varnish treated sample and untreated sample showed significantly higher gamut volume loss. Although it can be stated that in case of untreated surface the loss was greater.

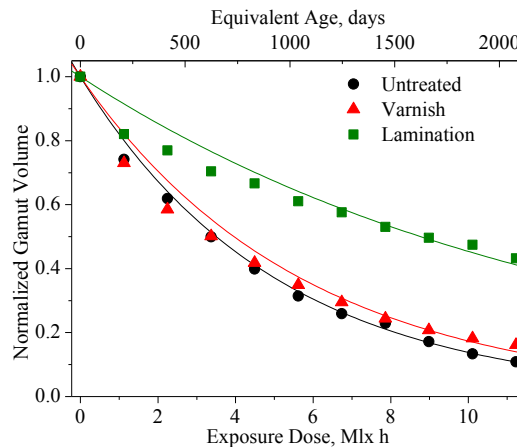


Figure 4: Gamut volume shrinkage rate

The 2D cross-section plots contain black and white border which depicts a colour gamut of the print right before and after exposition. Equally, cross-sections show a significant enhancement of print lightfastness by lamination. An increase in protection by varnish is almost negligible.

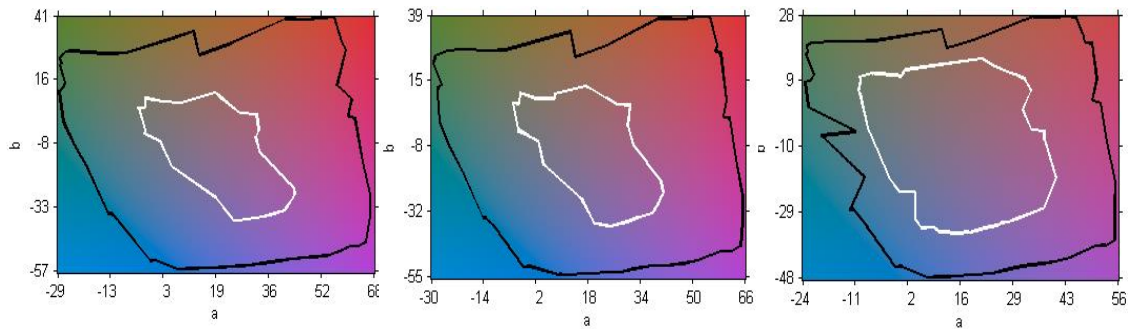


Figure 5: 2D cross-section plots for samples after 60 hours of exposure which equals 1040 days (untreated on the left, with varnish in the middle, with lamination on the right)

Table 1: Lifetime prediction expressed in years

Surface treatment	Untreated	Varnish	Lamination
Lifetime	0.9	1.0	2.3

8. CONCLUSION

The presented paper deals with one of methods used for stability experiments. Gamut volume seems to be a suitable global measure of colour changes of the studied sample. Relative gamut volume changes plotted as a function of exposure dose can be used to determine fading rate parameters, which can be further used to compare the lightfastness of different media or predict their lifetime, if the end-point criteria are known.

From the general methodological point of view, our approach introduces a universal tool for monitoring and evaluation of print fading kinetics, regardless of the technology of their production. It addresses all the problems inherently associated with modern digital printing techniques. This method is equally suited for gas fading studies as well. Gamut volume is easy to imagine and interpret which makes the method accessible even for the non-professional audience. The authors therefore believe that gamut volume can be accepted as the preferred measure. The VolGa application was compiled into a standalone application recently and is offered to other users for free non-commercial use [VolGa microsite, 2012].

9. REFERENCES

- [1] Balasubramanian, R., Dalal, E.: "A method for quantifying the color gamut of an output device", Color Imaging: Device-Independent Color, Color Hard Copy, and Graphic Arts II, [SPIE Proceeding, San Jose, CA, 1997].
- [2] Barber, C.B., Dobkin, D.P., Huhdanpaa, H.: "The Quickhull Algorithm for Convex Hulls", ACM Transactions on Mathematical Software, vol. 22, issue 4, (New York, USA, 1996), pages 469-483.
- [3] Dzik, P., Fürst, T.: "Image Permanence Evaluation by Color Gamut Volume Changes", Journal of Imaging Science and Technology (Springfield, VA 22151, USA, 2012), pages 060506-1-060506-9.
- [4] Dzik, P.: VolGa microsite, URL <http://www.fch.vutbr.cz/cs/laboratore/volga/volga-download.html> 10. 10. 2014.
- [5] ISO 18909:2006 Photography: Processed photographic colour films and paper prints - Method for measuring image stability, (Geneva, 2006).
- [6] Kipphan, H., "Handbook of print media", (Springer, New York, 2001).

- [7] Tastl, I., Koh, K.-W., Rossing, D., Berfanger, D.M., Moroney, N.: "ICC Profile Based Defect Simulation", 14th Color Imaging Conference: Color Science and Engineering Systems, Technologies, Applications, (Scottsdale, Arizona, 2006), pages 230-233.
- [8] Veselý, M., Dzik, P., Káčerová, S.: "Optical densities vs. gamut volumes for image lightfastness evaluation. An experimental study", 14th International Conference on Printing, Design and Graphic Communications, (University of Zagreb, Zagreb, HR, 2010), pages 27-35.
- [9] Wilhelm H.: "A review of accelerated test methods for predicting the image life of digitally-printed photographs", Annual Conference of the Imaging Society of Japan, (Tokyo, Japan, 2004), pages 81-84.
- [10] Wilhelm, H., McCormick-Goodhart, M.: "Progress towards a new test method based on CIELAB colorimetry for evaluating the image stability of photographs", IS&T's 13th Int. Symposium on Photofinishing Technologies, The Society for Image Science and Technology, (Las Vegas, Nevada USA., 2004), pages 27-30.

CLASSIFICATION AND CLUSTERING: TWO MACHINE LEARNING TOOLS FOR COLOR IMAGE SEGMENTATION

Aleš Hladnik, Tadeja Muck, Ivana Palančuk

University of Ljubljana, Faculty of Natural Sciences and Engineering, Ljubljana, Slovenia

Abstract: Image segmentation is a crucial digital image processing step that decisively affects the outcome of any higher-level operation such as pattern recognition and image understanding. It can be defined as a procedure that subdivides (partitions) an image into its constituent regions or objects. All the pixels in the same region are similar with respect to some characteristic or computed property, such as color, intensity, or texture. Adjacent regions are significantly different with respect to the same characteristic(s).

Color in a digital image often contains valuable information about the scene or object being imaged, which can be lost during the routine color-to-grayscale image conversion. This fact together with a rapid increase in the power of personal computers caused color image segmentation algorithms to be readily available on modern PCs. Numerous approaches have been developed during the last decades that enable efficient segmentation of images based on color. Sometimes conversion from RGB into a suitable color space, such as Lab, YIQ, YCbCr is necessary before the segmentation step can be accomplished.

The presentation will after a brief overview of color image segmentation schemes focus on two typical algorithms that will be explained through a machine learning viewpoint. K-nearest neighbor classification is an example of a supervised learning algorithm where the aim is to learn a mapping from the input to an output whose correct values are provided by a supervisor. In unsupervised learning, on the other hand, there is no such supervisor and we only have input data and the aim is to find the regularities in the input. K-means clustering algorithm belongs to this class of machine learning methods.

Efficiency of the two algorithms will be discussed using several synthetic, computer generated color images as well as photographs.

Key words: color image segmentation, K-means clustering, nearest neighbor classification, image processing, machine learning

1. INTRODUCTION

From the machine vision workflow viewpoint, image segmentation can be seen as a bridge between the low-level image processing operations, e.g. noise reduction or edge extraction that enhance the input image, and the high-level operations, which are aimed at object recognition and scene interpretation. Compared to the monochrome – grayscale – image approaches, segmentation of color images must take into account the fact that the latter ones consist of three (or more in case of multispectral images) channels, i.e. R, G, B or their linear or non-linear transformations. Since manipulation of digital color images is widespread in modern graphic arts industry, possessing at least a basic knowledge of the most frequently implemented algorithms for their segmentation is highly recommended. In the paper we focus on two classical techniques: K-means clustering and nearest neighbor classification. Their performance was assessed on images containing objects or regions with a low number of clearly distinguishable colors: red, green, blue, yellow and background.

1.1 Color image segmentation approaches

Digital image segmentation can be defined as a procedure that subdivides (partitions) an image into its constituent regions or objects [Gonzalez et al., 2004]. All the pixels in the same region are similar with respect to some characteristic or computed property, such as color, intensity, or texture. Adjacent regions are significantly different with respect to the same characteristic(s) [Shapiro and Stockman, 2001].

Color in a digital image often contains valuable information about the scene or object being imaged, which can be lost during the routine color-to-grayscale image conversion (e.g. hue or

saturation). Numerous approaches have been developed during the last decades that enable efficient segmentation of images based on color. Sometimes conversion from RGB into a suitable color space, such as Lab, YIQ or HSI is required before the segmentation step can be accomplished. A comprehensive overview (Figure 1) of color image segmentation schemes is given in [Cheng et al., 2001].

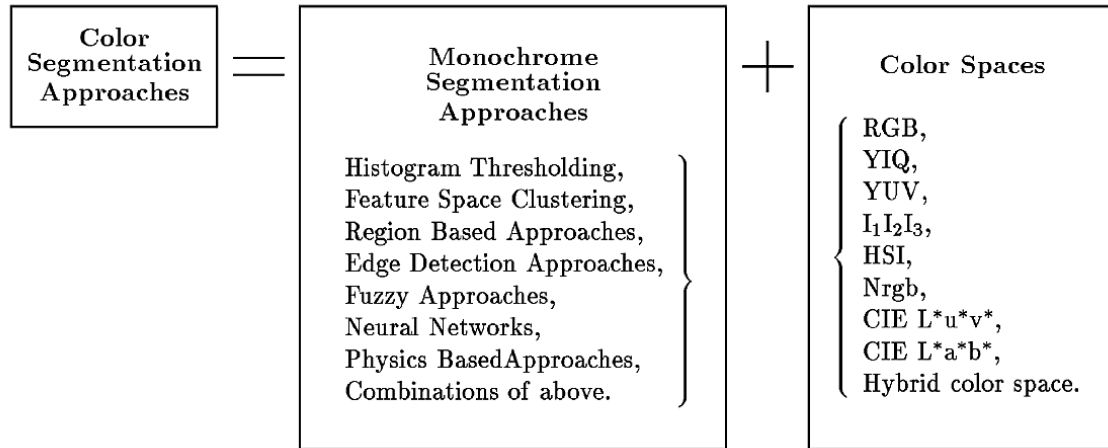


Figure 1: Commonly used color image segmentation methods [Cheng et al., 2001]

Region based approaches assume that a region is a subset of connected pixels which share similar color properties, such as hue or chromaticity (= color without the luminance component). These techniques look for subsets of connected pixels whose colors are homogeneous. They can be categorized into two main classes, depending on whether the distribution of the pixel colors is analyzed either in A) the image plane (region growing or region merging techniques) or B) in the color space. While both region growing and region merging techniques privilege the spatial interactions between pixels and analyze the colors of the pixels only to grow or merge regions, their drawback is that they require an a priori knowledge of the images in order to adjust the used parameters.

Analysis in the color space – class B) – takes advantage of the characterization of each pixel P of an image I by its color point $I(P)$ in this space. Since the pixels are represented by points in a three-dimensional color space, this approach assumes that homogeneous regions in the image plane give rise to clusters of color points in the color space. Each cluster corresponds to a class of pixels which share similar color properties. These clusters are generally identified by means of an analysis of the color histogram or a cluster analysis procedure and are mapped back to the original image plane to produce the segmentation.

Edge detection approaches assume that adjacent regions representing different objects present local discontinuities of colors at their boundaries (edges, borders) and edge detection methods try to detect these discontinuities. The result is a binary image composed of edge and non-edge pixels. Generally, these methods are based on applying a first order derivative filter – gradient – in order to detect edges. Locations of gradient maxima which are higher than a threshold generate edge pixels. Although these segmentation methods are applicable in practice, they have been much less frequently used compared to the region construction-based techniques due to various drawbacks such as the non-connectedness of detected edge pixels.

1.2 Supervised and unsupervised learning

Color image segmentation can also be approached through the machine learning perspective. Machine learning algorithms can be subdivided into two major groups: supervised and unsupervised. In supervised learning, the aim is to learn a mapping from the input to an output whose correct values are provided by a supervisor. In unsupervised learning, there is no such supervisor and we only have input data. The aim is to find the regularities in the input [Alpaydin, 2010].

1.3 K-means clustering

K-means clustering (KMC) is one of the most widely used clustering algorithms. KMC works by breaking the dataset of objects (observations) into K different clusters (Figure 2). K has to be specified by the user before running the algorithm. Note that this is an unsupervised learning method, since the user does not label individual categories/clusters.

First, the algorithm randomly creates K initial cluster centers, also referred to as seeds. Next, it assigns all the other objects to one of these seeds based on the object-seed proximity. First demarcation lines between the K clusters are made by drawing perpendicular bisectors between the seeds. Then the centroids for each of the newly created K clusters are calculated and they become new cluster centers. The procedure of assigning objects to these new cluster centers repeats and the K cluster centers are recalculated. This whole procedure iterates several times and stops as soon as the distances between the new and the previous K centroids fall below a certain threshold.

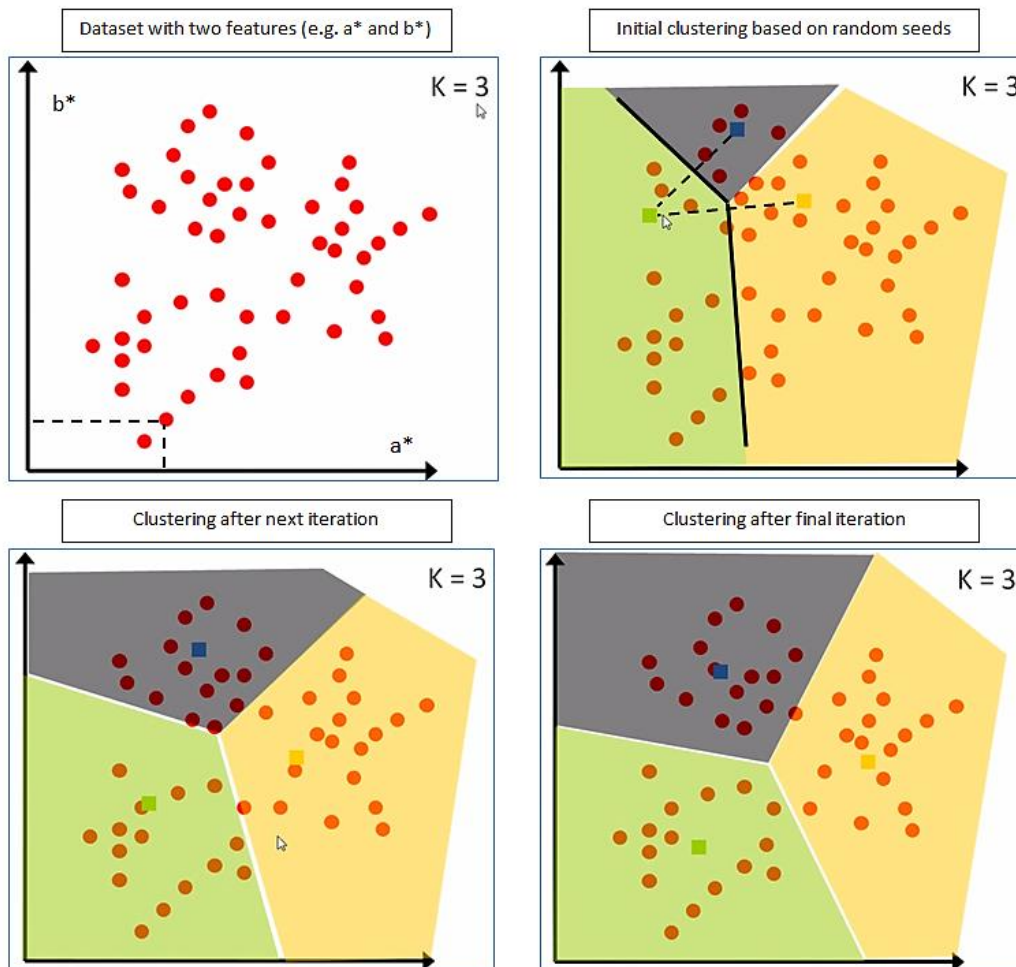


Figure 2: Mechanics of K-means clustering (KMC) algorithm

1.4 Nearest neighbor classification

Nearest neighbor classification (NNC) is a classical representative of a supervised learning algorithm. The training samples – objects or observations – are vectors in a multidimensional feature space, each with a class label. The training phase of the algorithm consists only of storing the feature vectors and class labels of the training samples.

In the classification phase, k is a user-defined constant, and an unlabeled vector – test point – is classified by assigning the label that is most frequent among the k training samples nearest to that query point. In our study, k was equal to 1.

2. MATERIALS AND METHODS

Before implementing KMC and NNC procedures, color images of interest were converted from RGB to CIE $L^*a^*b^*$ color space and the corresponding luminosity component (L^*) was discarded. Consequently, only the two chromaticity components (a^* and b^*) that contain color information – hue and saturation – about each image pixel were retained. The resulting data were then subject to the two algorithms. Apart from specifying the number of seeds, i.e. the number of distinct colors, no other user input was necessary in case of the unsupervised-based KMC. On the other hand, being a supervised learning algorithm, NNC required the user to interactively select a small triangle sample region for each color so that each sample region's average color in a^*b^* space was computed. These color markers were then used to classify each image pixel.

Several synthetic, computer generated images as well as photographs were tested. The goal was to estimate the efficiency and appropriateness of the two algorithms to perform color-based segmentation using images varying in the distribution and number of distinct colors comprising the image. All calculations were performed in Octave.

3. RESULTS AND DISCUSSION

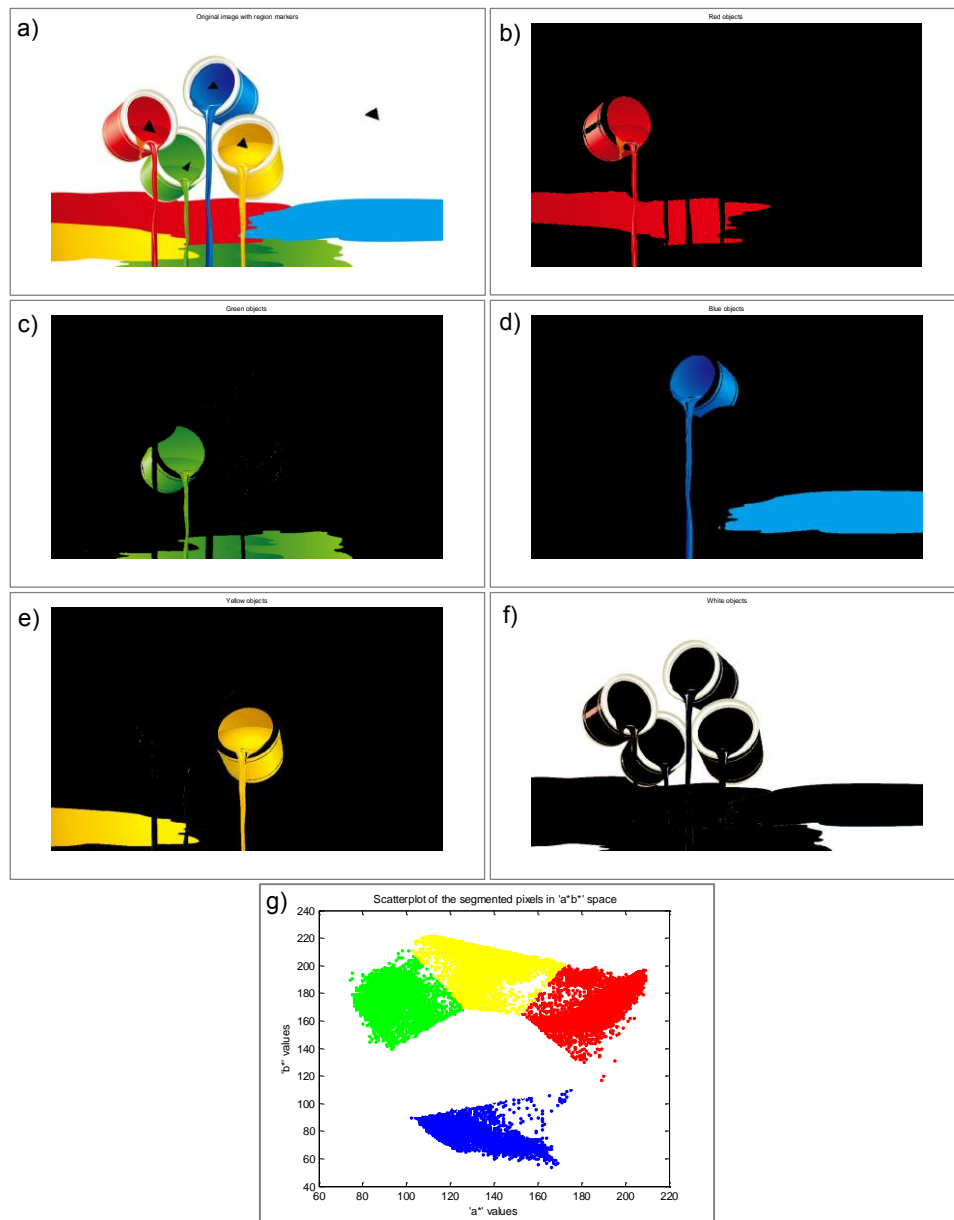


Figure 3: Color segmentation of a synthetic image using nearest neighbor classification (NNC) algorithm

High color segmentation accuracy was achieved with computer generated images that contain large regions of uniform colors (usually as a result of a vector drawing) using either of the two algorithms. Result of implementing NNC on an illustrative synthetic image is presented in Figure 3. After a user had specified five color markers interactively using triangles (Figure 3a), the algorithm successfully separated the original picture into five regions/images containing strictly red, green, blue, yellow objects and white background, respectively. Note that the algorithm was robust enough to be insensitive to the variations in colors' brightness. Scatter plot of the segmented pixels in $a*b*$ space (Figure 3g) shows a^* and b^* coordinates of the individual colors. Results of applying unsupervised clustering algorithm (KMC) (Figure 4) are almost identical to those obtained by NNC.

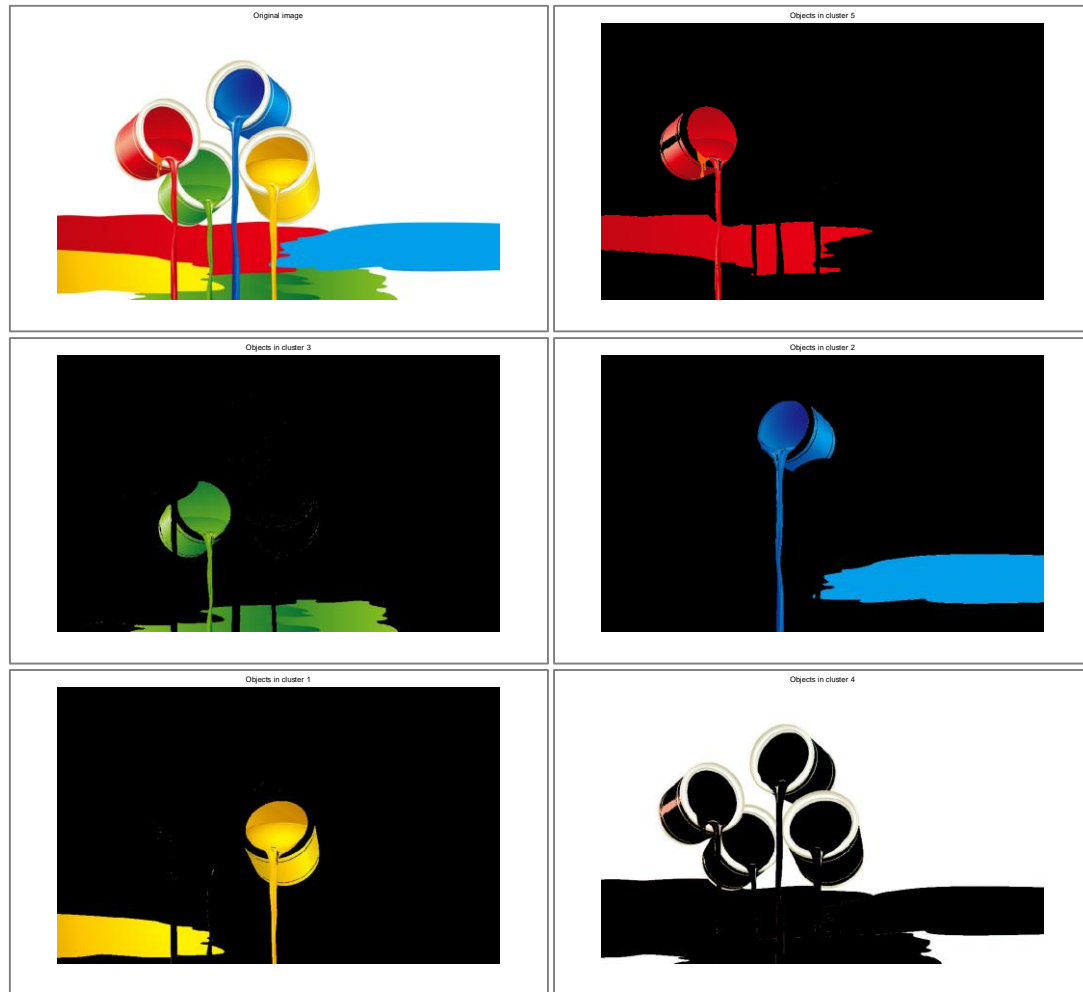


Figure 4: Color segmentation of a synthetic image using K-means clustering (KMC) algorithm

Color segmentation of photographs, on the other hand, proved a much more challenging task. Results using NNC and KMC algorithms on a typical photo are presented in Figures 5 and 6, respectively.

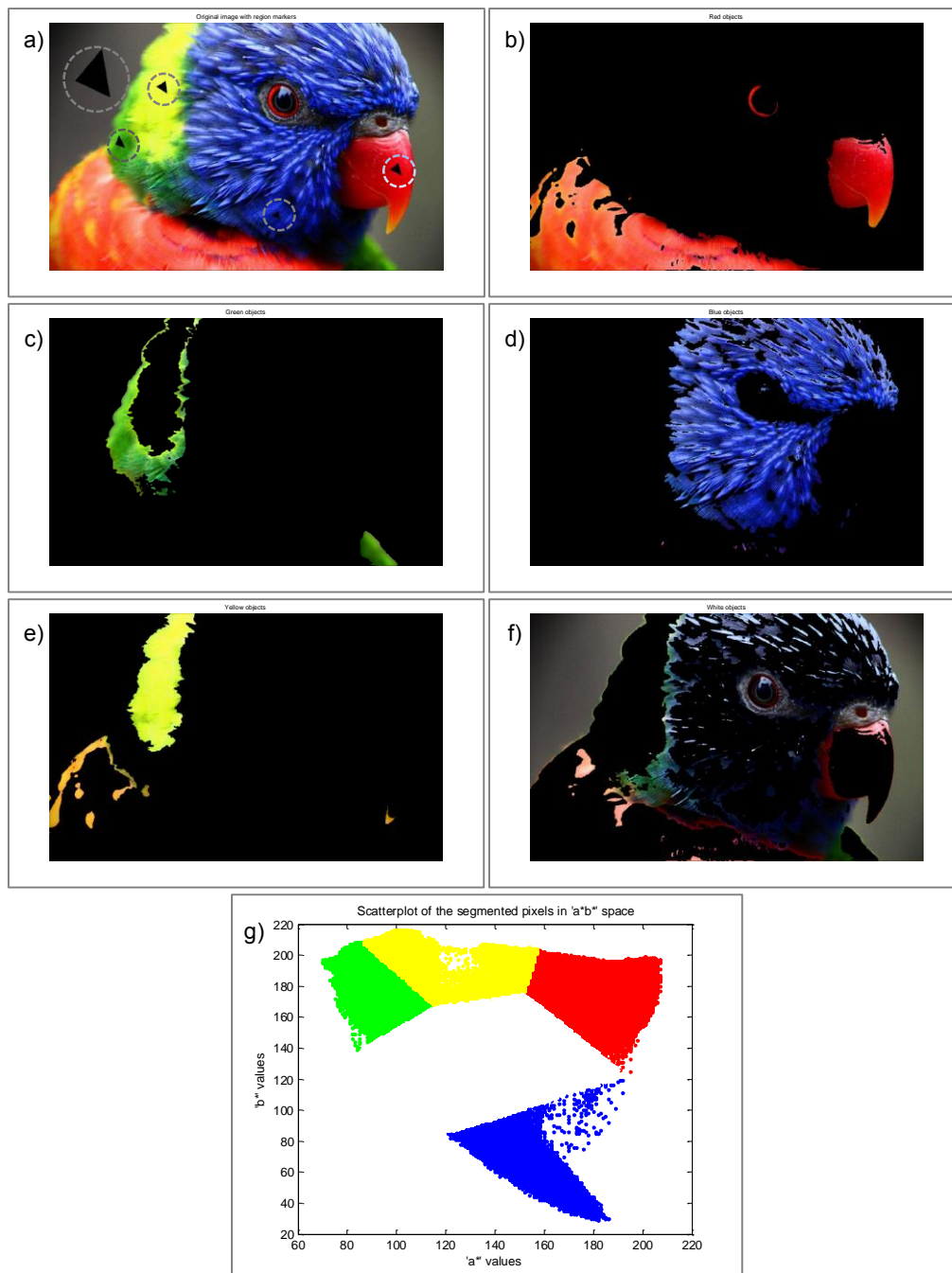


Figure 5: Color segmentation of a photograph using nearest neighbor classification (NNC) algorithm

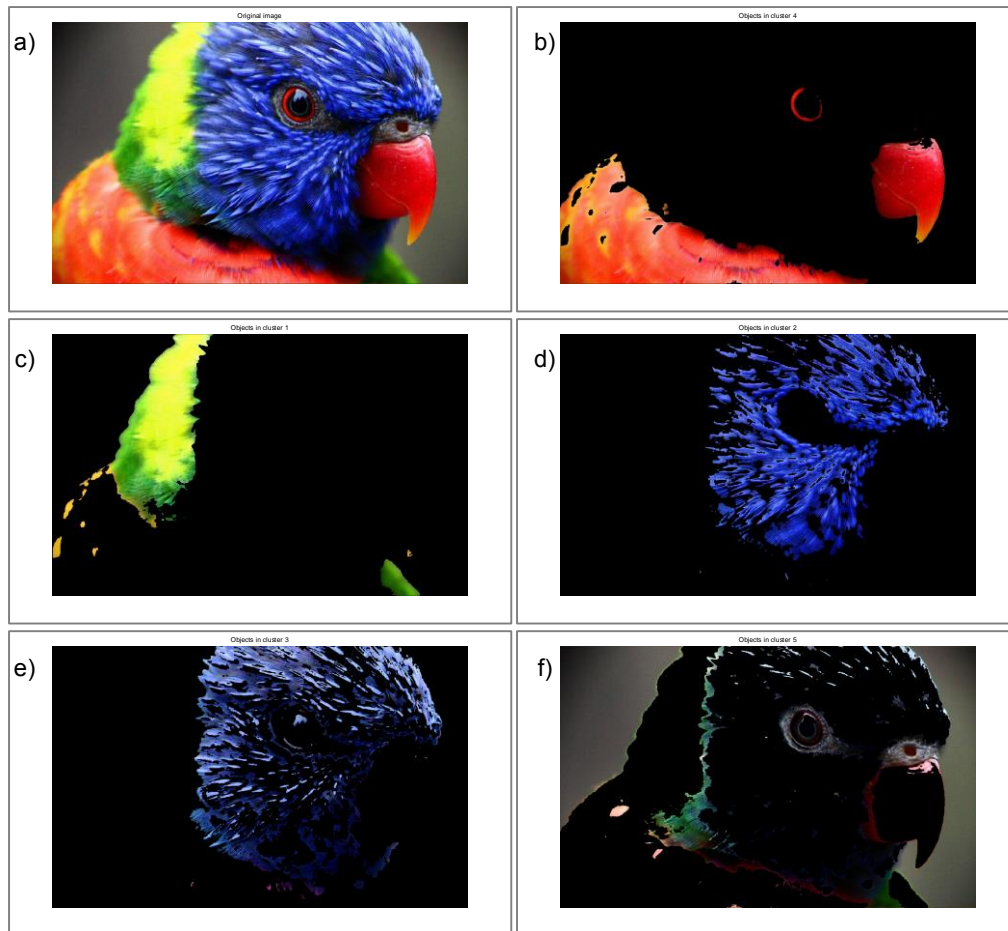


Figure 6: Color segmentation of a photograph using K-means clustering (KMC) algorithm

In the case of NNC (Figure 5), the algorithm relatively successfully segmented and separated red, green, blue and yellow colored regions of the parrot's head, although some yellow pixels were erroneously classified into the red class (Figure 5b). Human observers would also argue that the green class (Figure 5c) contains too many pixels with a yellow hue and the yellow class (Figure 5e) too many green pixels. Such "mistakes" can easily be explained by the fact that in RGB additive color scheme yellow color is obtained by mixing red and green components. It also has to be kept in mind that the location and size – which are both user defined – of the triangle color markers (Figure 5a) exclusively determine the average color (i.e. values of a^* and b^* components) that is characteristic for each individual class. The background class (Figure 5f) obviously contains pixels with less saturated as well as achromatic color shades that were not attributed to any other class.

Unlike with NNC, when running KMC algorithm (Figure 6) a user is not in a position to indicate a typical – a "correct" – member for each cluster and without this human assistance the automatic color segmentation performance is much poorer. In particular, pixels with either green or yellow hue are now assigned to a single cluster (Figure 6c) while blue pixels were attributed to one of the two clusters (Figures 6d and 6e) apparently depending on their saturation. Only the red (Figure 6b) and background (Figure 6f) clusters can be regarded as acceptable to a human observer.

4. CONCLUSIONS

In the presented preliminary study we limited ourselves to the images characterized by a low number of clearly distinct colors. The obtained results show that when an image contains homogeneous – in terms of hue and saturation – regions that are clearly separated from one another, both color segmentation algorithms perform very well. With natural scene photos, with often extremely high local fluctuations in values of individual pixels' color components, however,

accuracy of color segmentation using the unsupervised algorithm (KMC) is less than satisfactory. In future work we intend to examine other parameters that affect segmentation of color images as well as to test more recent algorithms that have been used successfully even on complex images containing numerous objects with a poor contrast to the background, such as active contours (Reddy et al., 2012).

5. REFERENCES

- [1] Alpaydin, E. (2010): "Introduction to Machine Learning", (Cambridge MA, USA: MIT Press), page 11.
- [2] Cheng, H. D., Jiang, X.H., Sun, Y., Wang, J.: "Color image segmentation: advances and prospects", Pattern Recognition 34, 2259-2281, 2001.
- [3] Gonzalez, R. C., Woods, R. E., Eddins, S. L. (2004): "Digital Image Processing using MATLAB", (New Jersey, Prentice Hall, 2004), page 378.
- [4] Reddy, G. R., Chandra, M. M., Ramudu, K., Rao, R. R.: "Active contour based color image segmentation". Communications in Computer and Information Science. In: Global Trends in Information Systems and Software Applications, 2012, Vol. 270, pages 173-185.
- [5] Shapiro, L. G., Stockman, G. C.: "Computer Vision", (New Jersey, Prentice-Hall, 2001), pages 279-325.

COLOUR TO TEXTURE FUSION IN HSI COLOUR SPACE

Ivana Tomić¹, Rafael Huertas², Ivana Jurić¹¹University of Novi Sad, Faculty of Technical Sciences,
Department of Graphic Engineering and Design, Novi Sad, Serbia²Facultad de Ciencias, Departamento de Óptica, Granada, Spain

Abstract: Colour mapping is a well-known problem with many approaches in the bibliography. The term itself refers to the function that transforms colours of a source image to the colours of a target image with an intention to visually match the target scenery. Simplified case implies having only one target colour which is applied (i.e. fused) to the source image. This approach is often referred to as 'colour to texture fusion' and is used in textile and apparel industry to predict the appearance of a textured sample if dyed in another colour. Over the years many methods for colour to texture mapping/fusion have been developed. They are divided mainly according to the type of the source image (grey-scale or coloured) and/or the information used to quantify the texture. In addition, different colour spaces have been employed, with the distinctions in the computation of the final image colour coordinates. In this paper we present three methods for colour to texture fusion which can be used when the target image is not available or known. As a source for the mapping process we used colour image of a texture, while the target colour values were taken from the pre-defined colour centres set. Fusion itself was performed in HSI colour space. It was shown that the intensity channel can be seen as the main carrier of the texture information, but in some cases the contribution of the other two channels should not be neglected as well. Hence, we tested and compared three different methods, modifying and adjusting the ideas from different previous works. In the first case hue and saturation channels from the source image were discarded and only the intensity component, as it is the main texture descriptor, was taken for the fusion. The second method relied on discarding only the hue component from the source image, since for our sample set in most of the cases hue channel exhibited the smallest variation. Third method implied using the information from all the channels of the source image, since hue channel was not completely uniform. Efficiency of each of the proposed approaches had been evaluated both visually and by obtaining the similarity ratio, where the source image was taken as the reference. The results indicate that the best similarity with the source image is obtained if the second method was used for the fusion, showing that for colour to texture fusion in general saturation component from the source image should not be neglected.

Key words: texture, colour mapping, HSI colour space.

1. INTRODUCTION

In the colour mapping process colour coordinates of the final image are usually computed pixel-wise by taking into account both the coordinates of the source and the target image. The image that serves as a base for mapping is referred to as *the source image*, while the reference image, which represents the goal of the mapping process, is denoted as *the target image*. Accordingly, colour values used to alter the source image can be designated as *the target colour values*. The biggest challenge of the colour mapping process is to reproduce the texture colour image accurately, so that it perceptually matches the target image (Xin & Shen, 2003). In the case of colour to texture fusion, target image is often the digitized physical sample dyed into desired colour. Since the different surface properties of the materials and their inner structure determine how they will react when dyes or colorants are applied, many of the models for mapping the colour onto the texture are built upon the knowledge of the target and/or source image. According to the information used to quantify the texture, there are 3 main groups of models for colour and texture fusion as explained in (Shen & Xin, 2005). These are often abbreviated as GCM (grey-to-colour mapping), CCM (colour-to-colour mapping) and DICH (dichromatic based mapping). First group of models deals with mapping the colour to grayscale images. In this case source image contains only one channel and the goal is to deduct the 3-D (RGB) information from it which is, in essence, an ill-posed problem. However, it is possible due to the high correlation of RGB colour channels as presented in (Xin & Shen, 2003). Some other approaches

can also be found among the algorithms for colorizing grayscale images with or without user intervention (Welsh et al, 2002; Levin et al, 2004; Nie et al, 2007). In CCM models spatial distribution of a source image is already available through all of the 3 channels. Since this is the 3-D to 3-D transformation CCM models can be applied in different spaces (RGB, LCH, $\alpha\beta$ etc.) (Montag & Berns, 2010; Ruderman et al, 1998; Reinhard et al, 2001). Third group contains only one type of the mapping, based on the model of dichromatic reflection developed by Shafer (Shafer, 1985). It can be used both if the source image is coloured (these groups of algorithms are usually abbreviated as DICH-CC) and when it is greyscale (i.e. DICH-GC methods).

In textile and apparel industry, source image is usually coloured. Hence, CCM or DICH-CC models can be applied to visualize the appearance of a textured sample in distinctive colours before it is actually produced (Shen & Xin, 2005). Comparing different approaches it was shown that DICH-CC models together with the CCM methods based on LCH and RGB colour spaces provide the results that resemble the target image the most (Shen & Xin, 2005). In this work authors relied on assessing the efficiency of a simulation by calculating the similarity ratio between simulated and target image (physical sample died into the target colour).






The motivation for this work was to define a CCM mapping model which can be applied for colour to texture fusion for simulating the appearance of different texture patterns in cases when target image is not available. Observing the interaction of a colour channels in different colour spaces, it was decided to perform the mapping in HSI colour space. It is one of the most commonly used in computer vision applications and it provides almost independent channels for lightness, saturation and hue, which is essential when dealing with the textures (as it was that the lightness component is the most important for the texture description) (Haralick et al., 1973). Three approaches for this fusion are derived, which differ in the amount of information taken from the colour channels of source image and target colour. The goal of this paper was to define which one of these approaches provides the most relevant results, by taking into account only the source image and the desired colour. These approaches, together with the evaluation method are presented within the next section.

2. METHOD

2.1 Selection of the texture samples and colour centres

In order to perform and to evaluate the efficiency of colour to texture fusion model, the first step was to define the source images and target colours, i.e. the samples and colours to be applied. The goal was to define a set with a reasonably high number of sample-colour combinations, in which enough of the variance regarding both texture strength and colour parameters existed. Textured samples were chosen from the KTH-TIPS and KTH-TIPS2 database (Mallikarjuna et al, 2006; Fritz et al, 2004) by taking into account the results presented in (Gebejes et al, 2013; Gebejes et al, 2012). In these dataset all images have a resolution of 200x200 px (72 dpi). In both formed mentioned papers GLCM method was applied for the characterization of textured samples, where it was shown that both entropy and homogeneity values calculated from the GLCM provide very good correlation with visual perception (Gebejes et al, 2012). Thus, samples used in this paper were textured colour images with homogeneity values closest to 0, 0.25, 0.5, 0.75 and 1. In this manner good spacing regarding the texture strength was obtained. In the rest of the paper they will be denoted as "Sample 1", "Sample 2" ... "Sample 5". Visual differences were also taken into account when selecting the samples, as seen in Table 1.

Table 1: Source images used for the colour fusion

Sample no.	1	2	3	4	5
Homogeneity value	1	0.75	0.48	0.25	0
Sample appearance					

Colour centers were chosen so that they ensure good gamut coverage of sRGB colour space as plotted in CIELAB. sRGB reference viewing environment corresponds to conditions typical of monitor display viewing conditions and they were taken into account as a starting point for all the further calculations. Thirty chromatic and three achromatic colour centres were chosen. Describing the colours in term of lightness, hue and chroma (CIELCH), the chromatic samples had L^* of 20, 50 and 80, h_{ob} of 18° , 90° , 162° , 234° and 306° , while C_{ob}^* was chosen to be the maximum and half the maximum value of the chroma in sRGB colour space. For the hue centres we decided to use defined angles in order to achieve better representation of the unique hues (Kuehni, 1999). On the other hand, the achromatic samples were defined with L^* of 20, 50 and 80. The distribution of the chosen centres in CIELAB colour space is shown in Figure 1.

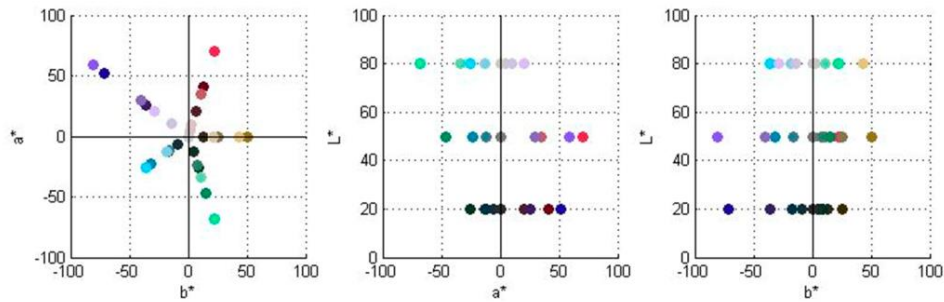


Figure 1: Distribution of the selected colour set in CIELAB colour space

2.2 Defining the fusion model

In order to define the fusion model we decided to adapt some of the ideas from previous studies (Lucassen, 2011; Shen & Xin, 2004) and to perform the mapping with both source image and target colour given in a HSI colour space. By transforming our image set to HSI colour space, normalizing each colour channel to the range of 0-1 and assessing the channels uniformity it was noticed that the hue channel is the most uniform for the samples 1-3 (those with the highest homogeneity), while in the case of samples 4 and 5 the saturation channel exhibited the highest uniformity (Table 2). The results show that the samples are ordered by uniformity, with sample 1 the most uniform and sample 5 the least. Overall, there are two groups, samples 1-3 more uniform, and samples 4-5 less. The appearance of the sample 3 channels in HSI colour space is given in Figure 2.

Table 2: Standard deviation for the HSI channels for all the samples (lowest values of coordinates for samples are marked bold)

	St. dev. H	St. dev. S	St. dev. I
Sample 1	0.0080	0.0541	0.0220
Sample 2	0.0087	0.0701	0.0618
Sample 3	0.0138	0.0895	0.0959
Sample 4	0.1772	0.0983	0.1541
Sample 5	0.3063	0.2634	0.3414

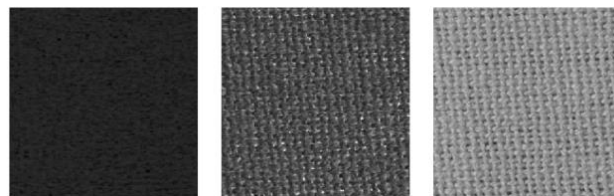


Figure 2: (a) H , (b) S and (c) I channels of sample 3 from our set

Taking this variability into account three approaches were considered for mapping target colour to the source image:

1. Method. Discarding the hue and saturation component from the source image and taking only intensity component, as it is the main texture descriptor.
2. Method. Discarding only the hue component from the source image, since the hue channel exhibits the smallest variation.
3. Method. Taking into account all the channels from the source image, since hue channel is not completely uniform.

First approach was chosen because it was used in many of the previous studies. Even though hue channel exhibits some variations, it was regarded as mostly uniform and all the variations were neglected simplifying the computation. Same stands for the saturation channel. Here, colour to texture fusion is performed in a way that only intensity channel were taken from the source image and was merged with the hue and saturation channels that correspond to the selected target colour. Intensity channel was normalized with the mean intensity value of the source image as:

$$I_t^i = \frac{I^i}{I_{(mean)}} I_t \quad (1)$$

Where I_t^i is the target intensity of a pixel i ,
 I^i is the source intensity of a pixel i ,
 $I_{(mean)}$ is the mean value of the intensity of a source image,
 I_t is the intensity of the target colour.

Second approach followed the basic idea by discarding the information from the hue channel of the source image. However, in this case, saturation component from the source image was included since it was shown that it had almost as much variations as the intensity. Saturation channel was normalized in the same manner as intensity in Eq. (2):

$$S_t^i = \frac{S^i}{S_{(mean)}} I_t \quad (2)$$

Where S_t^i is the target saturation of a pixel i ,
 S^i is the source saturation of a pixel i ,
 $S_{(mean)}$ is the mean value of the saturation of a source image,
 S_t is the saturation of the target colour.

Third approach was proposed because, in fact, hue channel was not completely uniform. Hence, hue component from the source image was not disregarded but instead used in a combination with the rest two channels. Since in HSI colour model hue is measured in degrees, hue channel was normalized as follows:

$$H_t^i = H^i - H_{(mean)} + H_t \quad (3)$$

Where H_t^i is the target hue of a pixel i ,
 H^i is the source hue of a pixel i ,
 $H_{(mean)}$ is the mean value of the hue of a source image,
 H_t is the hue of the target colour.

2.3 Evaluation: visual evaluation and similarity ratio

Evaluation of each of the fusion methods was first conducted visually, checking for the non-expected changes in colours and the presence of the artefacts. Furthermore, computed images for every sample were then compared with the corresponding source image by obtaining the

similarity ratio as described in (Shen & Xin, 2005). This metrics is based on calculating the ΔE^*_{ob} differences between each pixel of a source image and its mean CIELAB colour value, plotting the histogram of those differences with the defined scale and intersecting it with the equally obtained histogram of the target image. Similarity ratio falls in a range of 0-1, where higher values denote more similar images. Since histogram of each image contains the amount of the ΔE^*_{ob} differences, we believe that this metrics can be used to predict whether some significant change in texture structure or undesired colour shifts had been introduced with the fusion method used. Hence, we calculated similarity ratio for each of our samples and methods used by comparing the source image with the results of colour fusion.

3. RESULTS AND DISCUSSION

Observing the computed images visually, it was concluded that the third method (where the hue of the source image is somewhat considered) performs the worse, leading to the images with a lots of artefacts and errors in general. This is more emphasized for the images obtained from samples number 4 and 5, for which the change in hue was higher (Table 2). Figure 3 shows the results of the fusion for sample 4 with all of the target colours with the hue of 234° . Re-coloured versions of the samples 1-3 showed the noticeable errors, in a visual analysis, in the case of achromatic and the red colours (h_{ob} of 18°). For a colour representation of the figures please refer to the digital version of this paper.

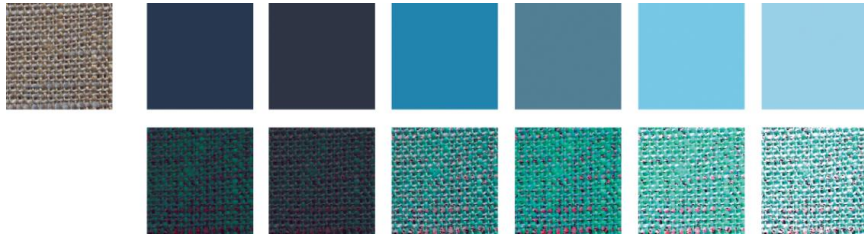


Figure 3: In the first row from left to right: the source image, and the appearance of the target colours with the hue of 234° (each two with the lightness of 20, 50 and 80, the maximum and half-maximum saturation); in the second row, results of the fusion performed by the third method (resulting images are placed below the corresponding target colours).

Images where fusion methods 1 and 2 were used were, in general, visually very well reproduced. The exception was sample 4 when method 2 was employed. Both methods lead to visually similar results for the samples 1-3, but for samples 4 and 5 and the blue hue different results were obtained, as shown in Figure 4. In this figure the results of a colour-to-texture fusion for the 5 source images are presented in case where target colour had CIELCH coordinates of $L^* 50$, $C^*_{ob} 39$ and $h_{ob} 234^\circ$. Visually similar results were obtained for all the rest of the target colours. It is worth noting that samples 4 and 5 have the highest variation among intensity, saturation and hue (Table 2).



Figure 4: Results of fusion process when the methods 1 and 2 were used. In the first row, source images 1-5 and the appearance of the target colour; in second row, results of the first fusion method; in the third row, results of the second fusion method.

Since it was clear that the third fusion method did not ensure visually satisfying results, it was decided to exclude it from the further assessments. For both methods 1 and 2, similarity ratios between each of the source images (samples 1-5) and the fusion-resultant images (re-coloured versions) were obtained, thus 33 values for each sample and each method. Mean values and standard deviations for the 5 source images and for both methods are presented in the Figure 5.

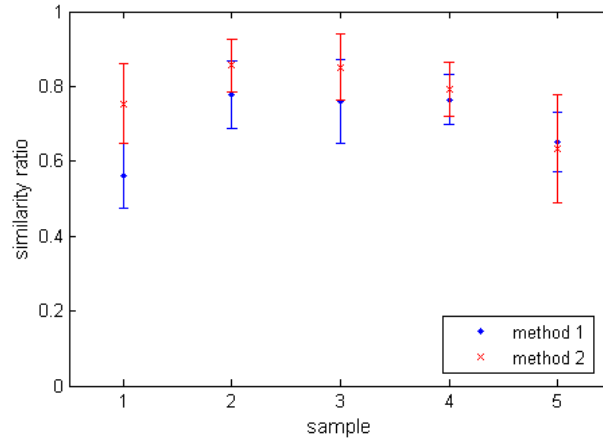


Figure 5: Similarity ratios for each of the 5 source images (i.e. samples) used (Mean and StDev)

From the Figure 5 it can be seen that the second method, which takes into account both intensity and saturation components of the source image, leads to the better results for almost all the samples. In case of the source sample 4 the difference between the methods is very small (lower than the standard deviation) while for the sample 5 the first method provided slightly better results. The later difference can easily be neglected since it is not significant (mean value for the first method was 0.652, while for the second it was 0.633).

Among the 5 source images, number 2 was shown to be the easiest to re-colour, since in this case the highest similarity with the original image is obtained. First method showed the worst performance in the case of the most uniform image (sample 1), while the least uniform image (sample 5) was problematic for both of the methods used.

4. CONCLUSIONS

In this paper we presented three easy methods for colour to texture fusion with the purpose of re-colouring textured samples when target image is not available. Fusion itself was performed in HSI colour space, and the proposed methods differed by the amount of the information taken from the source image channels. Method which took into account hue of the source image did not performed well, leading to the images with a lot of artefacts and colour shifts. The other two methods, from which the first took only intensity channel information from the source image and the second both intensity and saturation, visually produced similar results in most cases. After computing the similarity ratios for both of these methods, it was concluded that, in the case of chosen sample set, better results were obtained if saturation of the source image is not neglected, especially in the case of source images with small variation over the colour coordinates. In order to confirm these findings future work would include psychophysical experiment with perceptual tests to define which method produce images that look more natural to human observers.

5. ACKNOWLEDGMENTS

This work was supported by the Serbian Ministry of Science and Technological Development, Grant No.:35027 "The development of software model for improvement of knowledge and production in graphic arts industry" and the research project FIS2013-45952-P (Ministerio de Ciencia e Innovación, Spain).

6. REFERENCES

- [1] Fritz, M., Hayman, E., Caputo, B., Eklundh, J. O.: "THE KTH-TIPS database", Computational Vision and Active Perception Laboratory (CVAP), Stockholm, Sweden, 2004. Url <http://www.nada.kth.se/cvap/databases/kth-tips/> (last request: 10.09.2014.)
- [2] Gebejes, A., Huertas, R., Tomić, I., Stepanić, M.: "Selection of optimal features for texture characterization and perception", Proceedings of The Colour and Visual Computing Symposium 2013, (The Norwegian Colour and Visual Computing Laboratory: Gjøvik, Norway, 2013), pages 1–5.
- [3] Gebejes, A., Tomić, I., Huertas, R., Stepanić, M.: "A preliminary perceptual scale for texture feature parameters", Proceedings of 6 International Symposium on Graphic Engineering and Design, GRID12, (Fakultettehničkih nauka, Grafičkoinženjerstvo i dizajn: Novi Sad, Serbia, 2012), pages 195–201.
- [4] Haralick R.M., Shanmugam K., Dinstein, I.: "Textural Features of Image Classification", IEEE, 3(6), 1973.
- [5] Kuehni, R.G., Marcus, R.T.: "An Experiment in Visual Scaling of Small Color Differences", Color Research & Application 4, 83–91, 1979.
- [6] Levin, A., Lischinski, D., Weiss, Y.: "Colorization using optimization". In: SIGGRAPH 2004 Conference Proceedings (ACMSIGGRAPH: Los Angeles, USA, 2004), 689–694, 2004.
- [7] Mallikarjuna P., Targhi A.T., Fritz M., Hayman E., Caputo B., Eklundh JO.: "THE KTH-TIPS2 database", Computational Vision and Active Perception Laboratory (CVAP), Stockholm, Sweden, 2006. Url <http://www.nada.kth.se/cvap/databases/kth-tips/> (last request: 10.09.2014.)
- [8] Montag, E.D., Berns, R.S.: "Lightness dependencies and the effect of texture on suprathreshold lightness tolerances", Color Res. Appl. 25, 241–249, 2000.
- [9] Nie, D., Ma, Q., Ma, L., Xiao, S.: "Optimization based grayscale image colorization", Pattern Recognition Letters 28, 1445–1451, 2007.
- [10] Reinhard, E., Ashikhmin, M., Gooch, B., Shirley, P.: "Color Transfer Between Images", IEEE Comput. Graph. Appl. 21, 34–41, 2001.
- [11] Ruderman, D.L., Cronin, T.W., Chiao, C.-C.: "Statistics of Cone Responses to Natural Images: Implications for Visual Coding", Journal of the Optical Society of America A 15, 2036–2045, 1998.
- [12] Shafer, S.A.: "Using color to separate reflection components", Color Res. Appl. 10, 210–218, 1985.
- [13] Shen, H.-L. Xin, J.: "Computational models for fusion of texture and color: a comparative study", Journal of Electronic Imaging 14 (3), 033003, 2005.
- [14] Welsh, T., Ashikhmin, M., Mueller, K.: "Transferring Color to Greyscale Images", In: Proceedings of the 29th Annual Conference on Computer Graphics and Interactive Techniques, SIGGRAPH '02, (ACM: New York, USA, 2002), pages 277–280.
- [15] Xin, J.H., Shen, H.-L.: "Computational model for color mapping on texture images", J. Electron. Imaging 12, 697–704, 2003.

THE INFLUENCE OF VIEWING CONDITIONS ON COLOUR GAMUT OF RED-GREEN VISION DEFICIENCIES

*Neda Milić, Nemanja Kašiković, Dragoljub Novaković
University of Novi Sad, Faculty of Technical Sciences,
Department of Graphic Engineering and Design, Novi Sad, Serbia*

Abstract: Colour vision deficiency represents an inability to perceive differences between some of the colours that can be distinguished in the case of normal colour vision and affects in different forms approximately 8% of the male and 0.4% of the female population. Red-green vision deficiencies, characterized by dysfunction or absence of L or M cone types, comprise majority of all colour vision deficiencies. These deficiencies entail a loss of hue discrimination and result in a reduced colour gamut which is defined and experimentally confirmed with comprehensive researches over past decades. Despite the relevance of viewing environment in which object is observed, little has been published on how it affects people with common colour vision deficiencies. The aim of paper is to simulate the influence of viewing conditions on colour gamut of anomalous colour vision by including CIECAM02 transformations. The conclusions deduced from the analysis of simulated images are that decreasing in colour temperature of illuminant leads to even more reduced colour gamut and, thus, to enhanced number of hardly distinguishable colour combinations; while changing viewing surround from average to dark leads to better image contrast. The results of study can be used for defining compensating colour adaptation for certain viewing environment.

Keywords: colour vision deficiencies, viewing conditions, CIECAM02, colour gamut, illuminant

1. INTRODUCTION

Colour deficient observers have difficulties on daily basis when retrieving information encoded with colour in digital and printed content associated with abnormalities in colour recognition and colour discrimination. Their inability to discriminate differences between some colours combinations that can be distinguished in the case of normal colour vision often hampers comprehension of the content. Therefore, the colour information accessibility for anomalous vision population should be important issue, especially in cases like public traffic maps, geographic maps, safety and technical manuals etc.

In addition to taking into account the irreparable limitation of their visual system, designers should also consider the viewing conditions in which the content is observed.

The normal colour vision is trichromatic due to the existence of three types of cones (photoreceptors) within retina, commonly called L, M and S cones because of their highest sensitivity to long-wave, middle-wave and short-wave bands of the spectrum, respectively (Sharma, 2003). Figure 1a presents spectral sensitivity functions of L, M and S cones.

Based on the number of functional cone types, we can distinguish three main categories of CVDs (Sharpe, 1999):

- Monochromacy is the most severe case of CVD with only one or none of cone types functional. This condition is also known as total colour blindness since vision is reduced to one dimension (greyscale vision).
- Dichromacy is a severe form of CVD with vision reduced to two dimensions which occurs when one cone type is absent: the L type in the case of protanopia, the M type in deuteranopia, and the S type in tritanopia.
- Anomalous trichromacy is a category that includes those CVD cases with colour discrimination range from slightly (close to normal vision) to severely reduced (close to dichromatic vision). This condition happens when all photoreceptors are present, but one cone type has altered sensitivity: the sensitivity function of L type is shifted closer to the M type's function in the case of protanomaly (Figure 1b), the sensitivity of M type is shifted toward longer wavelengths in deuteranomaly (Figure 1c), and the S type is closer to normal M type in tritanomaly (Figure 1d).

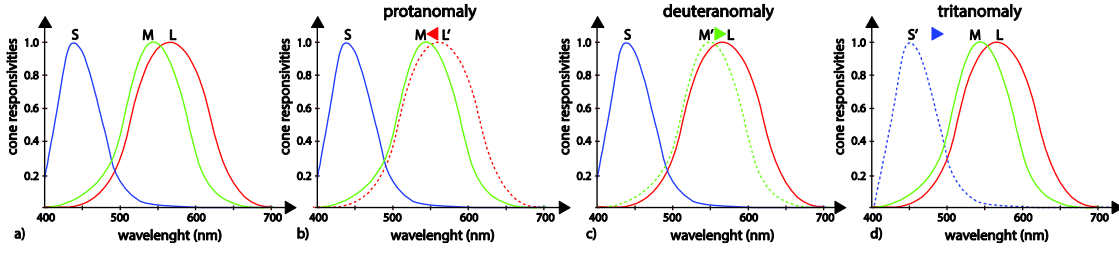


Figure 1: The sensitivity functions: a) normal trichromacy, b) protanomaly (the anomalous L type), c) deuteranomaly (the anomalous M type), d) tritanomaly (the anomalous S type)

The prevalence of colour vision deficiencies that include dysfunctional or missing L and M cones is over 99% of all CVD cases with 1:3 ratio between dichromatic (protanopia and deuteranopia) and anomalous trichromatic types (protanomaly and deuteranomaly) (Machado, 2009). These CVD types have common name red–green blindness.

From the aspect of the colour matching experiments, protanope and deuteranope observers can match any colour with a certain mixture of two spectral stimuli, while protanomalous and deuteranomalous observers require three primaries for colour matching with matching combination of primaries largely or slightly different from the normal vision combination.

1.1 Simulation of anomalous colour vision

The normal colour vision depends on three cone types differently sensitivity to different wavelengths, although their sensitivity functions are overlapping in large band of spectrum (see Figure 1). According to the Young–Helmholtz trichromatic vision theory, the combination of three cone responses, noted as L, M and S, is interpreted as a specific colour sensations in the vision centre (Wyszecki and Stiles, 2000):

$$[L, M, S] = \int [l(\lambda), m(\lambda), s(\lambda)] E(\lambda) d\lambda, \quad (1)$$

where $l(\lambda)$, $m(\lambda)$, $s(\lambda)$ represent the spectral sensitivity functions and $E(\lambda)$ is the spectral power distribution of colour stimuli which is lost after entering the eye. Stimuli with different spectral compositions that evoke the same combination of cone responses will appear alike (Mollon and Regan, 2000). Although the trichromatic theory is based on additive colour matching experiments, it cannot give satisfactory explanation for certain colour appearance phenomena (e.g., the opponent nature of afterimages or simultaneous contrast) (Fairchild, 2005). These phenomena are explained with adjacent colour vision theory– Hering's opponent-colour theory that specifies colour appearance based on three opponent channels: one achromatic, white-black (WS), and two chromatic, red-green (RG) and yellow-blue (YB) (Fairchild, 2005). The most accurate approximation of colour vision system is given in the stage-theory which combines the trichromatic theory as the first retinal stage and an opponent-colour theory as the second stage (Wyszecki and Stiles, 2000). Figure 2 illustrates signal encoding in the stage-theory.

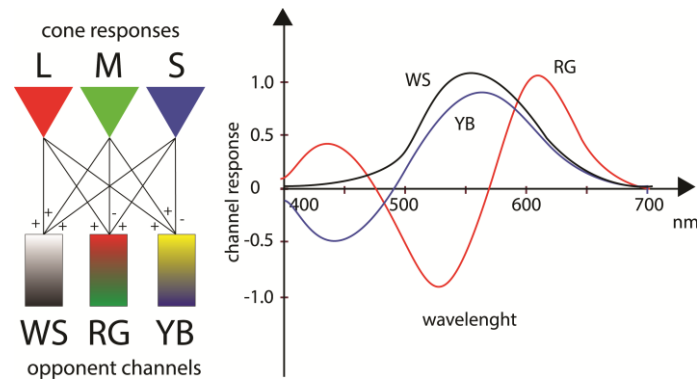


Figure 2: Schema of the encoding of cone response into opponent channels and spectral response functions of opponent channels in the case of an average trichromat– one achromatic channel, white-black (WS), and two chromatic channels, red-green (RG) and yellow-blue (YB)

Compared with trichromatic vision, red- green CVDs have a loss of discrimination of stimuli that differ only in the intensity of the red-green channel.

There are many proposed methods for simulating red-green dichromatic deficiencies based on experimentally defined hues that appear the same to dichromats and to normal observers (Brettel, et al., 1997). Those are achromatic colours and the stimuli of 475nm (a blue hue) and 575nm (a yellow hue).

The method defined by Brettel et al. (1997) and Vienot et al. (1999) explains mapping trichromatic into dichromatic colour gamut using LMS space in which the orthogonal axes represent cone responses. Figure 3 demonstrates mapping of colour stimulus to the red-green dichromatic gamut in direction parallel to the missing cone response (L or M) (Brettel et al., 1997).

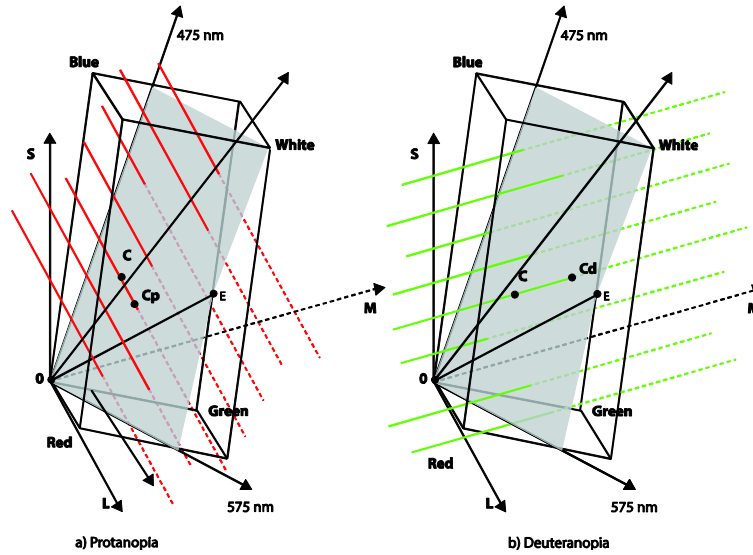


Figure 3: Projection of colour stimulus to dichromatic colour gamut (grey half-planes divided by the achromatic axis and anchored on points specifying the invariant stimuli 475 nm and 575 nm). The dichromatic version for a given colour stimulus C is found with projection to a particular half-plane in direction parallel to the missing cone response:

a Protanopia (CCP \parallel L axis), **b** Deuteranopia (CCd \parallel M axis)

Directions parallel to missing cone response are called confusion lines since the points that lie on them are perceived as the same colour by the particular type of dichromats. The simplified model of dichromacy simulation calculates the missing cone response with linear transformations (Vienot et al., 1999):

$$L_p = 2.02344 M - 2.52581 S, M_D = 0.494207 L + 1.24827 S, \quad (2)$$

while the other two cone responses are unchanged.

Unlike well-established simulation methods for dichromatic vision, there is no universal mapping from normal to anomalous trichromatic colour gamut, since it covers a large variety from almost normal to weak colour discrimination such in the case of dichromacy.

The recent method defined by Machado et al. (2009) simulates anomalous trichromacy by shifting the spectral sensitivity function of the anomalous cone type:

$$L_p(\lambda) = l(\lambda + \Delta\lambda_L); M_d(\lambda) = m(\lambda + \Delta\lambda_M); S_T(\lambda) = s(\lambda + \Delta\lambda_S), \quad (3)$$

where $l(\lambda)$, $m(\lambda)$, and $s(\lambda)$ are the cone sensitivity functions for normal colour vision and $\Delta\lambda_L$, $\Delta\lambda_M$, and $\Delta\lambda_S$ represent the amount of shift applied to the L, M, and S anomalous cones, respectively.

The simplified version of Machado's method, based on the stage theory of colour vision, approximates anomalous trichromatic RGB values by a single matrix multiplication Φ_{CVD} :

$$\begin{bmatrix} R_{CVD} \\ G_{CVD} \\ B_{CVD} \end{bmatrix} = \Phi_{CVD} \begin{bmatrix} R \\ G \\ B \end{bmatrix} = \Gamma_{normal}^{-1} \Gamma_{CVD} \begin{bmatrix} R \\ G \\ B \end{bmatrix}, \quad (4)$$

where Γ presents class of transformation matrices that map the RGB values to the opponent channels:

$$\begin{bmatrix} WS \\ YB \\ RG \end{bmatrix} = \Gamma \begin{bmatrix} R \\ G \\ B \end{bmatrix} = \begin{bmatrix} WS_R & WS_G & WS_B \\ YB_R & YB_G & YB_B \\ RG_R & RG_G & RG_B \end{bmatrix} \begin{bmatrix} R \\ G \\ B \end{bmatrix}, \quad (5)$$

According to Machado's simulation, protanomaly with a spectral shift of approximately 20 nm is very similar to protanopia by Brettel et al.'s method. The sensitivity function of the anomalous L type is, in that case, almost entirely overlapping with the function of normal M cone type (Machado 2009). This also applies for deuteranomaly.

1.2 Viewing conditions

The CIECAM02 colour appearance model is defined as a tool for predicting accurate colour appearance under various viewing conditions after the adaptation of the human visual system to changes (Fairchild, 2005). This mathematical model transforms initial colour values the perceptual colour attributes: the absolute attributes of brightness (Q), colourfulness (M) and hue (h) and the relative attributes of lightness (J), chroma (C), saturation (s), and, again, hue (h). These perceptual attributes, which are both device-independent and independent of the viewing conditions, are then calculated back to original colour space using the inverse transformation from XYZ values are computed and taking into account the final viewing conditions (Fairchild, 2005). Despite the relevance of viewing environment in which colour sample is observed, little has been published on how it affects people with common colour vision deficiencies. Baraas et al. (2010) tested the colour constancy of people with dichromatic red-green CVDS and came to conclusion that protanopes and deuteranopes perform more poorly than normal trichromats in a task requiring the discrimination of illuminant changes from surface-reflectance changes. The problem with colour constancy is more emphasized for the artificial scenes than in the case of natural ones. The same authors conducted one more study (Barras et al., 2006) with individuals with protanomaly and deuteranomaly as subjects and normal trichromats as a control group in which colour-constancy of natural scenes was analysed under various illuminants. Protanomals performed more poorly than deuteranomals, while both test groups had worse scores than control normal vision group. This paper analyses influence of illuminant and viewing surround as main viewing conditions on colour gamut of red-green vision deficiencies.

2. METHOD

The procedure includes 3 steps:

1. Predicting the influence of illuminant changes (from the initial CIE D65 illuminant to F11 and A illuminants) and viewing surround (from average to dark) on colour appearance applying CIECAM02 transformations; then
2. Mapping the initial colour gamut adapted to changed viewing conditions into the gamut of individuals with different types and severities of red-green vision deficiencies and
3. Analysis of the obtained colour gamuts.

The image processing was done using a software module in Photoshop CS3, while image colour gamuts are compared visually in software Chromix ColorThink and quantitatively using Matlab custom functions. As a test chart for creating profiles (gamuts) was used the ECI chart.

Accounting initial viewing conditions settings selected by the user, the software module converts digital RGB pixel values of the input image into device-independent X, Y, Z tristimulus values, and then into the perceptual colour attributes. After that, the module performs the inverse transformation back to RGB values, using the final viewing conditions settings and generates the final image preview. The initial viewing conditions are:

- white point or CIE standard illumination: D65;
- degree of adaptation: auto adaptation,
- background luminance Yb: 20%,
- adapting field luminance La: 20 cd/m².

Simulations of red-green CVDs were obtained using Machado's method for different types: protanomaly and deuteranomaly and severities of 0.2, 0.4, 0.6, 0.8 and 1 which correspond, respectively, to spectral sensitivity shifts of anomalous cone type of approximately 4, 8, 12, 16 and 20 nm. The sensitivity shift of 20 nm is very close to dichromatic vision (severity 1).

3. RESULTS AND DISCUSSIONS

Figure 4 presents protanomalous and deuteranomalous versions of original hue circle with white point set to D65, and of the same image after auto adaptation to illuminants F11 and A.

When the white point (illuminant) in forward transformation is different from the white point in inverse transformation, the colour appearance model performs a chromatic adaptation. Unrelated to colour vision deficiencies, the increase in illuminant temperature causes the colour appearance to be shifted towards the blue chromaticities and the decrease will shift the colours to yellow chromaticities along the yellow-blue opponent channel. Since individuals with red-green CVDs have a loss of colour information in the red-green opponent channel to certain extent correlated to the type and the level of deficiency, the illuminant changes should more severely affect this population compared to normal trichromats and enhance the number of hardly distinguishable colours for them.

The simulated images show that decreasing in colour temperature of illuminant leads to reduction in blue-part part of hue range. The reduction of yellow hue range is expected with a colour temperature increase, but it is not considered in this study due to the fact that illuminants with high colour temperatures are rarely used in real-life scenarios.

The same phenomenon can be observed in Figure 5 that shows the influence of increased colour temperature on the reduction of chromaticity diversity in a^*-b^* chromaticity plane (CIE $L^*a^*b^*$ colour space).

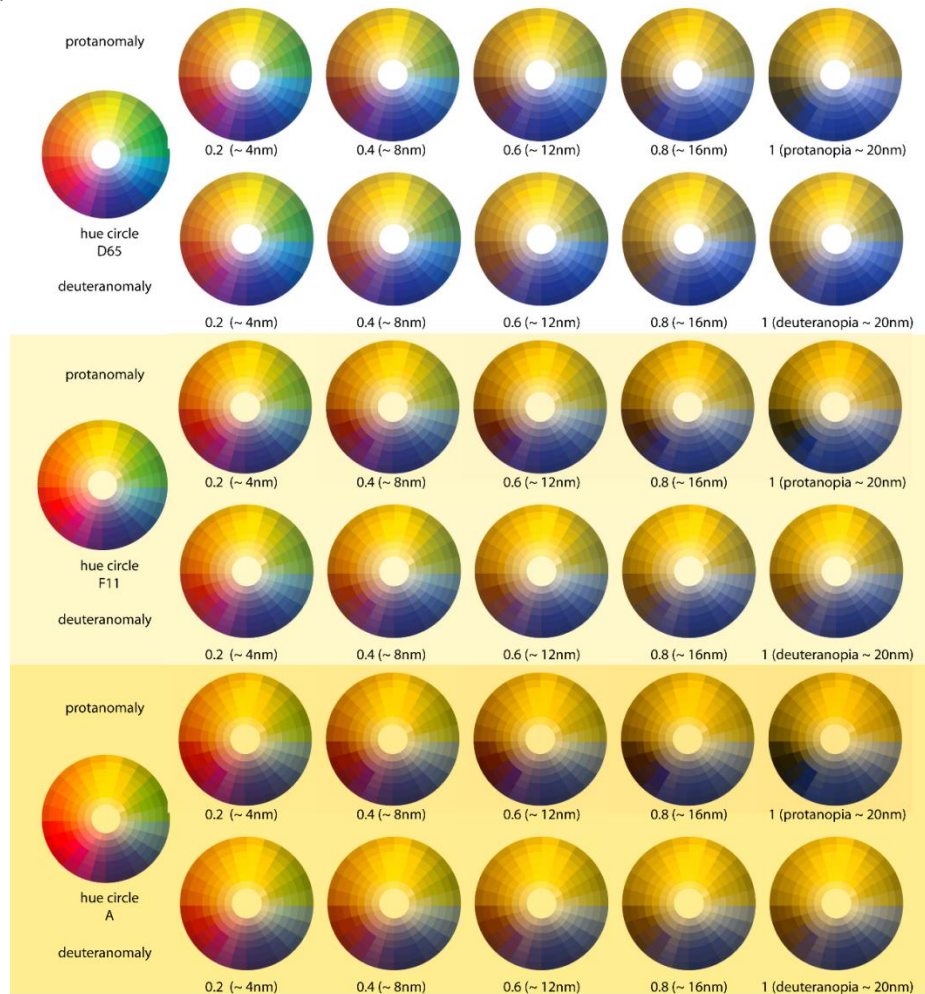


Figure 4: Simulation of protanomalous and deuteranomalous perception (Machado et al.'s approach) of original hue circle with white point D65, and after auto adaptation to illuminants F11 and A

The computation analysis of profiles obtained from simulated ECI charts show that illuminant temperature decreases affect similarly protanomals and deuteranomals, although the deuteranomalous gamut is slightly larger than the protanomalous gamut after the change from D65 illuminant to F11 and A. These results are consistent with conclusions from the study of Baraas et al. [2006, 2010] and can be noticed also in Figure 5.

Figures 6a and 6b demonstrate that during the changes of illuminant under which the image is observed (but with constant absolute luminance of illuminant), there are no changes in L (lightness) colour coordinate.

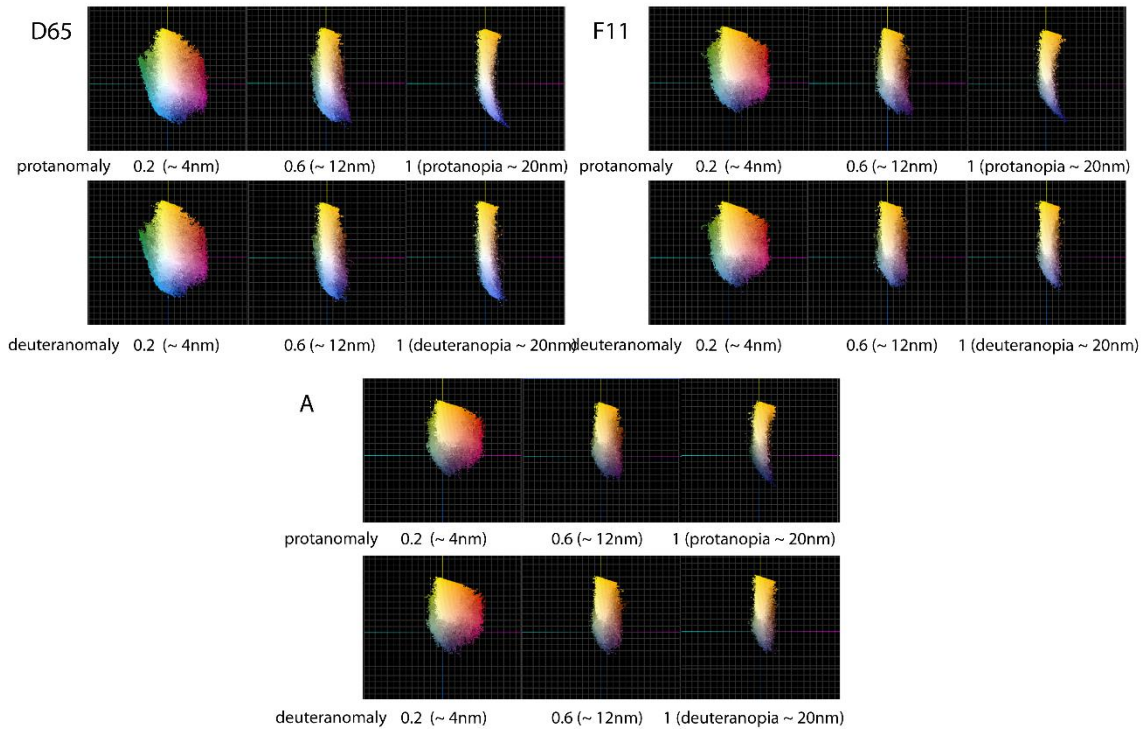


Figure 5: Change in colour gamut caused by illuminant change from illuminant D65 to F11 and A of protanomalous and deuteranomalous vision with different severities presented in a^*-b^* chromaticity plane (the chromaticity diversity)

Figures 6c and 6d demonstrate that changing viewing surround from average to dark leads to better colour contrast. This conclusion is consistent with previous research and applies both for anomalous and normal colour vision.

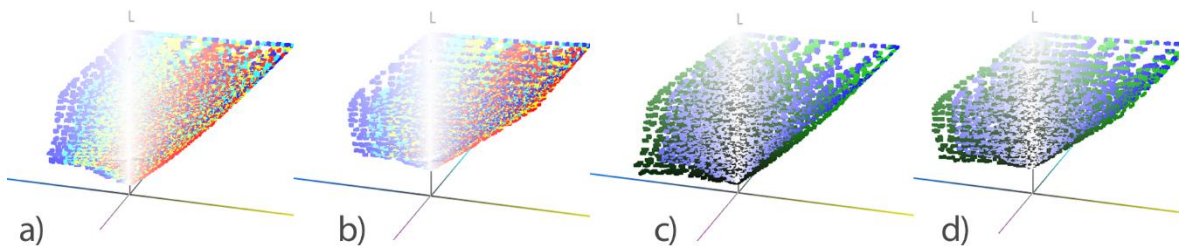


Figure 6: Change in colour gamut caused by illuminant change (red: A, yellow: F11, blue: D65) for: a) Protanopia and b) Deuteranopia simulation; Change in colour gamut caused by viewing surround change (blue: D65, average; green: D65, dark) for: c) Protanopia and d) Deuteranopia

4. CONCLUSIONS

Well established simulation tools show that red-green colour vision deficiencies affect the entire colour spectrum and they are much more complex than the stereotypical inability to tell red from green. Despite the relevance of viewing conditions to everyday visual tasks, little has been published on how they affect observers with the common red-green colour-vision deficiencies.

The aim of the present work was to test the extent to which illuminant and viewing surround can hamper already limited vision of this population.

The study conclusions can be used for defining compensating adaptation for certain viewing environment in the cases of protanopia/maly and deuteranopia/maly. That compensation would include enhancing the colour temperature of the light source or the display's white point and reducing the luminance in viewing surround.

5. ACKNOWLEDGEMENT

This work was supported by the Serbian Ministry of Science and Technological Development, Grant No.:35027 "The development of software model for improvement of knowledge and production in graphic arts industry"

6. REFERENCES

- [1] Baraas, R., Foster, D., Amano, K., Nascimento S.: "Anomalous trichromats' judgments of surface colour in natural scenes under different daylight", *S.Vis Neurosci.* 23(3-4), 629-635, 2006.
- [2] Baraas, R., Foster, D., Amano, K., Nascimento S.: "Colour Constancy of Red-Green Dichromats and Anomalous Trichromats", *Investigative Ophthalmology & Visual Science* 51(4), 2286-2293, 2009.
- [3] Brettel, H., Vienot, F., Mollon, J.: "Computerized simulation of colour appearance for dichromats", *J Op Soc. Am* 14, 2647- 2655, 1997.
- [4] Fairchild, M.: "Colour Appearance Models", (Chichester, John Wiley & Sons, 2005.)
- [5] Machado, G.M., Oliveira, M.M., Fernandes, L.A.F.: "A Physiologically- based Model for Simulation of Colour Vision Deficiency", *IEEE Transactions on Visualization and Computer Graphics* 15, 1291-1298, 2009.
- [6] Mollon, J., Regan, B.C.: "Cambridge colour test", (Cambridge, UK, Cambridge Research Systems, 2005)
- [7] Sharma, G.: "Digital Colour Imaging", (London, UK, CRC Press, 2003.)
- [8] Sharpe, T.L.: "Colour Vision: from genes to perception", (Cambridge, UK, Cambridge University Press, 1999.)
- [9] Vienot, F., Brettel, H., Mollon, J.: "Digital video colourmaps for checking the legibility of displays by dichromats", *Colour Research and Application* 24, 243-252, 1999.
- [10] Vienot, F., Brettel, H., Ott, L., Ben M'Barek A., Mollon, J.: "What do colour-blind people see?", *Nature* 376, 127-128, 1995.
- [11] Wyszecki, G., Stiles, W.S.: "Color Science: concepts and methods, quantitative data and formula", (Chichester, John Wiley & Sons, 2000.)

Print management and simulation

PRINCIPAL QUESTIONS OF THE FUTURE'S PRINTING SALES

László Koltai, Csaba Horváth

*Óbuda University, Rejtő Sándor, Faculty of Light Industry and Environmental Engineering,
Institute of Media Technology and Light Industry Engineering, Budapest, Hungary*

Abstract: How many times have you heard someone say that print is dead? It may be a tough time for printing industry, but we all know the world of print is much bigger than the average person understands ... and it is certainly not dead. The paper seeks to dispel that myth and to help our industry find its meaning and purpose once again through the development of innovative printed products. From author's perspective, we need to think about new ways to use the equipment we have on our pressroom floors, new markets to serve, and new ways to get the attention and talk to prospective customers. This paper is not a business theory or "insider intelligence" for sales people – instead it showcases unique, creative, and innovative products that make print practical. It shares concrete examples of how real world business looked to markets outside of their normal customer base, harnessed change, and come out on top. The paper describes how you can conceive, design, research, test, market and launch new products from within your organization. With these steps it is possible to learn how to enhance sales and productivity by breaking into and existing markets through the development of product that reinvent the purpose and uses of printing and get the salespeople into offices where they can share ideas instead of waiting to "get the order".

Key words: Keywords: marketing, print sales, graphic communication business, innovation

1. INTRODUCTION

Since the invention of movable type the printed word has been the foundation of the Western society. Print communications accelerated the exchanges of ideas and enabled the modern organization of human society. In this "Age of Information" we speak Print as an Original Information Technology, yet printers' profit margins are trending downward.

2. CHANGING PERCEPTIONS, CHANGING FOCUS

If all that we know – high-volume print runs, mass-produced printed media, big money marketing collateral print production – has moved to the Internet, how do feed our presses? How do we regain that significant portion of business that provided us with our daily bread?

In retrospect, perhaps this change in consumer demand was induced by the colour of the very collars worn within our industry. Printing has always been portrayed as a blue collar, craft based manufacturing sector united by a doctrine that encourages extended turnaround times, costly rush fees, and disdain for designers, marketers, and print buyers.

In fact, the predictions being cast by the pundits at the centre of the industry sometimes seem to suggest that just using the word "print" implies negativity within the community that purchase printed products. Apparently, the word that provides a more calming effect upon the masses – and better defines what it is that we actually do—is "communications", which suggests that we are "communication providers".

It raises the fundamental need to define what is the printer actually does. Is he or she a printer, marketing solutions provider or a communications provider?

3. TRENDS FOR SUCCESS

Underlying specific analysis of where print competes well and where it doesn't are four megatrends which have been enabled and are propelled by electronic media and technology. That is, electronic technology makes these megatrends possible for print publishers by accelerating creative process. New media and new non print distribution channels make these megatrends imperative for print publishers if they are to successfully compete.

These megatrends have been in place for nearly fifty years. They are pervasive. They will continue to force change, and we ignore them only at our peril. If we can push them faster, we will profit from them. The four megatrends are:

- More colour
- More targeting
- Faster distribution
- Interconnectivity

3.1 More colour – the first megatrend

The explosion of web offset and high-end colour systems in the 1970s enabled an explosion of magazines and catalogs colour. By the late 1990s low-cost desktop colour systems made the colours universally available both print and online. Today, everyone can afford colour and everyone knows it communicates better than black and white.

Some may argue that this trend has run its course. In slower economic times there are pauses as people watch what they must to preserve their budgets. But economic cycles inevitably end and with next uptick colour will become more pervasive.

3.2 More targeting is the second megatrend

Direct marketing, including consumer catalogs has been the fastest-growing segment of print industry for twenty years – and for good reason.

Most forecast of print growth are consistent with two basic conclusions. First, on-to-one colour printed will grow explosively from a fraction of a percent of the total print market to perhaps a few percent over next decade. Second, more than all of the net growth in printing in the next decades across all segments of print media will be in colour for counts under five thousand identical copies. That conclusion speaks volumes about the need to focus on changeover costs and order transaction costs. In this arena, communications and electronic imaging technology are not threat but rather a strength for print media and for the printer.

3.3 Faster distribution is the third megatrend

How fast is fast? – Mission: „Document solutions – Done right, Anytime, Anywhere.

What is the value in quick turnarounds?

We should reduce the time in every aspect of communication. What was acceptable today will not be in the future. There is always value in shorter schedules. It can be found in better inventory control, later merchandising decisions, more rapid response to customer needs, faster time to market for new product or offering, or more time for the creative process.

If we focus on uninterrupted flow and the cost of work in process, „faster“ and „smoother“ are frequently also more efficient and less costly.

3.4 Interconnectivity

Today the conversation goes an additional step. Files are received electronically and logged in the production system and the customer has immediate confirmation. Proofs sent electronically to the customer, to be printed on printers that have been calibrated to match the prepress system. The customer can know the press schedule at glance and verify that all elements have been transmitted and that all elements and all proofs have been received. The customer can access job schedule progress information through every step from receipt of images and list of postal transmittals.

If this is your mode of operation, your customers feel well informed: they have confidence that you can and will deliver. You now know better about your customers think and what they expect. Your customers know better about how you plan and perform for them. Once customers have had this experience, they will not want to lose the information and control you have given them.

4. MEGATRENDS AND STRATEGY

The four megatrends are descriptors of sea change in the entire range of communication media. In looking at any graphic arts or publishing business the first measure of the health of the business should be to ask:

„How well are we equipped to lead in a world where competitive products and services will continuously have greater graphic and colour value, will be produced faster from inception delivery, and will be targeted with messages individualized to smaller audience segments?“

If the answer is not a resoundingly positive one, the first task is to reposition your strategy to win in this environment.

5. RECREATING AND REINVENTING PRINT

Five hundred years is a long time to exist as an industry. Printing, after all, was the fundamental keystone for so many important movements throughout history. Adaptation and the ability to gain the necessary skills and expertise within the craft are the primary takeaways to filter through hundreds of years of rich and diversified history known as the printing industry.

Then how – with this deeply set hold on tradition – do we change our mindsets into thinking we can actually change an industry?

Printing is a lagging industry. We have tendencies to lurk outside companies waiting for them to tell us what they need to have printed or what next big campaign they are going to launch. Rarely do we get an opportunity to research, observe, and/or learn from them. To many, this may be a foreign concept, as printers are not trained to be progressive and additive, rather they are conditioned to be order takers and solutions providers – all after the fact.

To begin, companies must break existing paradigms associated with current business strategy. And, as we learned, the printing industry has a long and respected tradition of being secondary or extending set prominently at the periphery of corporate existence.

Competition is fierce and set with very visible boundaries. However, printing firms must now look beyond the boundaries, work their way in from the periphery and look across alternative industries, across strategic groups, across buyer groups, across complementary product and service offering, across the functional-emotional orientation of industry, and even across time.

It's time to think differently and break tradition. It is time to supplement production through the development of products that challenge the role of the printer within business world as we know it. to any one

Instead of waiting to “get the order”, printers must infiltrate markets with products that enhance buyers – a classification that is quite existential, that it is pertinent to anyone functioning in any role within an employee institution – and surpass needs with wants.

Companies that succeed in product development are called demand creators. Demand creators spend incalculable hours on research learning to understand the people.

These demand creators have very distinguishing characteristics that contribute to their success.

- They emphatically listen to their customer.
- They are engaged in continuous experimentation and perpetual improvement.
- They are always finding ways in which to preserve their individuality and/or brand.

Webb and Romano posited as follow: “The future of the printing communications industry is in offering a service, not a product. On the basis, the business needs to shift from task-based. you need to be on call to offer service on an ongoing basis, not just at discrete points when they need something printed.”

6. CONCLUSION

It is time to begin searching our genealogical past, to rediscover the entrepreneurial roots that founded our industry and contributed to the greatest knowledge for change. But we are also a resilient industry comprised of bright, educated, and innovative people.

We can emerge an industry that changes the way it does business, no longer a lagging industry but a forward-thinking and progressive manufacturing industry. But to do so will require strong leadership-leadership that can leap the hurdles navigate the obstacles, manage the emotional barriers, and communicate the vision.

7. REFERENCES

- [1] Macro, K.: The Future of Print Sales, Printing Industries Press, ISBN: 978-0-88362-770-9, Sewickley, PA, 2013
- [2] Moffitt, M. D.: To be a Profitable Printer, GATFPress, ISBN: 978-0-88362-442-7, Sewickley, PA / Printing Industry of America, Alexandria, 2003
- [3] Webb, J. – Romano, R.: Disrupting the Future: Uncommon Wisdom for Navigating Prints' Challenging Marketplace, Strategies for Management Inc., Harrisville, RI, 2010

MIS TOOLS TO INCREASE SUSTAINABILITY

António de Sousa Ribeiro¹, Paulo do Souto², Branko Mihorko³

¹CEO of SISTRADE Software Consulting, S.A., Porto, Portugal

²Director of SISTRADE Software Consulting, S.A., Porto, Portugal

³Country Manager of SISTRADE Software Consulting, S.A., Ljubljana, Slovenia

Abstract: The current economic situation and the signs of recovery appear to influence every sector of the industry with no exception. Forward-looking companies invest in quality relative projections and sustainable development. These days, printing and packaging producers not only have to forecast the price-sensitive consumers' behaviour and impress them with the products but also search for the smart solutions which reduce costs and time while keeping the high quality standards. From producer's point of view, these solutions imply more investment in terms of equipment, raw materials as well as human resources.

Effectiveness is no longer enough to stay ahead of the competitors; efficiency is the new goal of the companies. After a clear understanding of the dynamics of the market as well as sustainability trends and best practices, many companies seek for the most efficient solution to keep up with all the requirements. The answer for many is the innovation and MIS solution, which nowadays without doubt qualifies to be on the top of innovations in the company and a way to more sustainable business.

MIS solution is more than just an ERP, it leads to sustainable development. The company not only knows the detailed information about the production processes, including the consumption and waste but it also allows analysing company's profitability. The industries are able to monitor the pillars of sustainability, such as environment, for instance, manage energy consumption within the company or monitor eco-efficiency. Another solution contributing to the increase of efficiency is maintenance management, which results in the improvement of the planning as well as the raise of equipment life-cycle.

To conclude, MIS helps increasing profit by lowering operating costs, saving time, facilitating access to the data and optimising the use of resources. The companies have the critical information about the operations and procedures which allows the managers to make better decisions.

Key words: MIS, ERP, sustainability, efficiency, eco-efficiency, energy management, SCADA, Shop Floor Control, MES, Manufacturing Execution System, maintenance management, Overall Equipment Effectiveness, OEE, Analysis of Mass and Energy Flow, AMEF, Environmental Performance Evaluation, EPE, Life Cycle Assessment, LCA.

1. CHALLENGES OF PRINTING INDUSTRY COMPANIES

The incentive to technological advancement, as well as the continued development of different forms of engagement enables a better overview of the challenges that the companies of various printing industry sectors are facing in the already challenging global scenario. It is essential to emphasize that monitoring of consumer preferences assume important positions in the establishment of vertical relationships between the hierarchies. At the organizational level, the constant dissemination of information positively affects the correct prediction of the development guidelines for the future. Increasingly, companies reach the conclusion that the perception of difficulties leads to the improvement of strategic knowledge to achieve excellence. Many of them decide to branch out from the orthodox solutions and seek for innovations and the means to increase the efficiency that ensures sustainable growth.

Our industry and market knowledge leads us to define that MIS tools not only allow the efficient work within the company, they lead to sustainability. This paper will give a brief idea of the four main tools contributing to innovation and efficient company growth.

2. MANUFACTURING EXECUTION SYSTEM (MES) - THE RIGHT INFORMATION AT THE RIGHT TIME

Manufacturing Execution System is a critical part of modern manufacturing environment that collects and analyses production data, supervises quality control and monitors scheduling. The technology solutions of data acquisition, industrial supervision, planning and production control allow the users to monitor and supervise the data acquisition devices of various participants in the manufacturing process and may act in the field by controlling remote inputs/outputs or programmable logic controllers - PLCs. It also allows one to plan job orders on time, monitor real-time production process according to the pre-set routing, to control the movement of materials and hence make a production control more efficient. The tool turns out to be a complement to the management systems and production control.

This system involves the placement of collection points, with the installation of industrial consoles (e.g. for groups of machines or for each machine), registered by barcode or by touch, the number of job orders, operations, incorporated materials, machine identifications, operator identifications (and other) and also the elements for quality control. To complement the data collection via console, there is also a possibility of a collection solution based on direct data acquisition through machines or PLCs. Whenever the machine or production line provides a communication port with known protocol, it is possible to obtain and process the data that the machine delivers. It is completely customizable to suit each plant layout, multi factory, supports various sections and any type of resource, either a machine, a production line or a manual resource with human support. Example of such presents Figure 1:

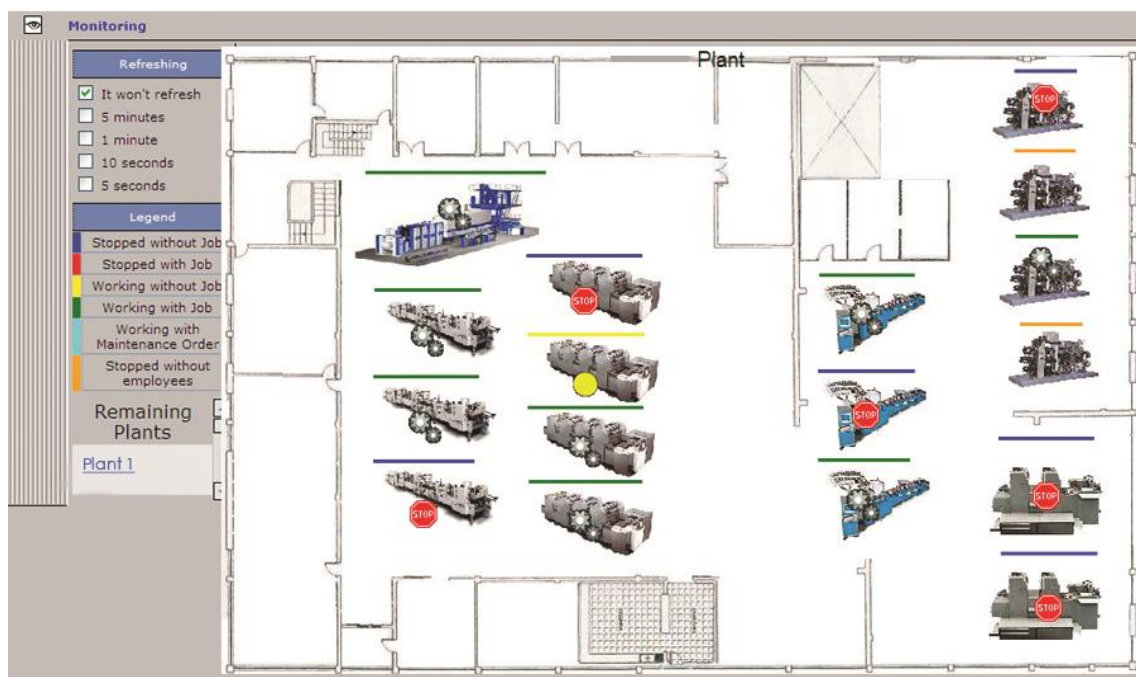


Figure 1: Plant monitoring

Its main objective is graphical monitoring of the production status as well as the operating status of each resource. Through synoptic panels, each of the processes can be monitored.

As part of the monitoring and production steering system, comes the management of raw materials with the definition of product trees, formulation, manual and automatic consumption conform factors for incorporation.

In order to maximise the use of the equipment and to know the process performance improvement it allows evaluating Overall Equipment Effectiveness (OEE) by work centre or plant. It is counted using three main separate components – Availability, Performance and Quality. Each of these components provides data that serve for the future process improvement. Overall Equipment Effectiveness helps to minimising or eliminating the losses to get the closest results to the ideal performance.

The system has interfaces that allow the "shop floor" to define the formulation of a given production process. Through the selection of raw materials, lots and incorporation factors, it is possible to change in the collection interface, the standard formulation that is defined in the job order. The output of stock or raw materials or semi manufactured, may be made by manual registration, reading the bar code of the lot and introducing quantity or by automatic output to the quantities produced. Whenever there is a production record, the system may terminate the stock of raw materials in the amount proportional to the factor of incorporation. Manufacturing Execution System is ideal to improve the manufacturing processes. It also provides a real-time feedback which results in more accurate information on costs as well as reduction of waste.

3. ENERGY MANAGEMENT – TAKING INTO ACCOUNT ECONOMIC AND ENVIRONMENTAL OBJECTIVES

Once, power was considered abundant, nowadays companies consider it a resource that must be carefully managed. In a company the implementation of an energy management system may result in a 10% improvement in energy consumption. It ends up serving as an implementation of a new energy source. An energy management system can inform the user when, where and how the energy resources of a company are spent.

The system provides real-time information of a set of parameters related to the power monitoring by equipment or by machine and the possibility to monitor the energy analyser placed in each machine. One of the important tools resumes in real-time information about energy consumption and alerting in specific points of the process if the differences between the actual and optimized consumption exceed certain value.

By knowing how much, when and how the resources are being consumed, the company can take corrective actions in order to reduce energy consumption.

Energy optimization solutions of production process have various benefits, namely, the autonomy to undertake a program of energy management capable of producing cost savings that persist over time or real-time data, which is available to facilitate decision making. The companies can reduce energy costs and improve process and activity performance. Energy optimization solutions can also increase the overall level of awareness within the organization and in the entire value chain, the benefits of systematic energy management.

Given these and much more benefits companies can reduce environmental impacts resulting from the activity, protect themselves from unstable energy markets as well as gain competitive advantage over companies that tend to neglect energy and environment related social responsibilities. Energy efficiency can be understood as the ability to run the same job with less consumption and in an increasingly demanding market, lower energy costs mean a more competitive company.

4. MAINTENANCE MANAGEMENT – KEEP THE EQUIPMENT RUNNING AT HIGH CAPACITY

Applying maintenance management becomes essential as companies are increasingly using technology and modern equipment to increase the production, carrying a huge investment at this level. Using maintenance management tools help controlling the equipment maintenance of the company, either machines or components, starting with the setting of maintenance plans, records of preventive maintenance and corrective action up to the release of the maintenance orders. In any production process, the use of resources such as machines, materials subsidiaries, etc. is a constant. These resources have a cost. Business managers should take into account all these variables in the final products. Situations such as the maintenance of machines and their times (which affect the planning of the MRP and production, and also the time of delivery to final customer), malfunctions, human error, etc. should be predicted, planned, recorded and integrated. Maintenance management increases efficiency, the life cycle of equipment and improves planning.

5. ECO-EFFICIENCY – TRANSFORM UNSUSTAINABLE DEVELOPMENT TO SUSTAINABLE

Eco-efficiency unites two "eco" dimensions - economy and ecology, to relate the product or service value to environmental influence. The primary goal of eco-efficiency is to increase the net value of the company/process/product "Do More With Less".

Eco-efficiency can be performance metrics of sustainable companies and organisations, in order to show the economic and ecological progress, translated by contribution (value) for the welfare and corresponding more or less efficient use of environmental, economic and human resources. The quantification of eco-efficiency stimulates business valorisation, either by revenues of the effective cost reduction (of materials, energy and environmental damages), or by transparency in the communication of product/processes features.

Eco-efficiency tools help to support decision that combine environmental performance with economic performance. The aim is to quantify the eco-efficiency of a company or process/service, and the assessment of its progress compared to objectives and targets set. The decision support tool is also an improvement scenario simulator allowing iterative convergence of the decision with the objectives and targets and the management of alternative hypotheses.

In order to lead company to sustainable development is it necessary to understand the difficulties in quantifying the environmental aspects, especially when it is not implemented a solid structure of information on the use of resources, namely materials, water and energy, for this reason Analysis of Mass and Energy Flow (AMEF), is crucial for the planning of environmental management activities.

The aim of AMEF is to propose the basic guidelines for determining critical resource flows, as well as their potential in terms of economic savings and environmental improvements. It is also necessary to draw attention to the need for data communication and monitoring of selected environmental aspects which registration is essential for continuous improvement in pollution prevention, this evolution will be quantified by eco-efficiency ratios.

In this context, the determination of eco-efficiency depends on the effort that is intended to develop in AMEF and installed monitoring infrastructures.

Another crucial part is Environmental Performance Evaluation. The methodology of Environmental Performance Evaluation provides the characterization of environmental performance in terms of the intensity of environmental aspects.

The result will be an environmental performance of the study unit, characterized by significant environmental aspects, not the environmental impacts, but the environmental risk they pose and the contribution to the aims of eco-efficiency.

Eco-Efficiency calculation implies the quantification of environmental influence's value of the process or product/service under analysis. In order to achieve this calculation, it is necessary to use an approach based on Life Cycle Assessment (LCA).

LCA is an internationally standardized methodology, through ISO standards, which allows obtaining detailed information related to the environmental influence's value of a product, process or service. Through this methodology, it is possible to set the key aspects and/or potential environmental impacts associated to each one of the stages of a life cycle from the acquisition or extraction of raw materials till their production, use and end of life.

Eco-efficiency helps companies develop and implement sustainability oriented strategy, focusing on transparency, technological innovations and social cooperation in order to achieve the objectives. Eco-efficiency is no longer a synonym of resource and environment saving but also a force leading towards innovation and competitiveness and consequently better financial performance.

6. COMPETITIVE ADVANTAGE IN COMPETITIVE ECONOMY

It is important to question how much competitiveness in commercial transactions presents tendencies in order to approve directions towards progress. The commercial success is achieved offering creation of added value and innovative solutions and providing flexible responses to the changing requests.

For modern companies to improve the quality of products is just as important as it is to be more sustainable and MIS solution meets both objectives without the increase of the use of resources and without negative impacts on the environment. The key is to make the most of the available solutions which is to transform continued innovation into sustainable growth through new technologies.

Effective planning and monitoring, data collection and well as analysis facilitate decision making, help improving environmental, social and economic development and are the basis for the sustainable growth of the company.

THE DEVELOPMENT OF KNOWLEDGE BASE SYSTEM FOR THE IDENTIFICATION OF THE PARAMETERS OF THE PRINTING PROCESS

Željko Zeljković, Dragoljub Novaković, Darko Avramović, Stefan Đurđević
University of Novi Sad, Faculty of Technical Sciences,
Department of Graphic Engineering and Design, Novi Sad, Serbia

Abstract: Modern computer and software systems offer a new approach in the development of a knowledge base about the processes, process parameters and graphic systems as complex structures that combine a wide variety of knowledge. Modern acquisition of knowledge in today's level of development of computer and programming systems enables a new concept of distance learning. If the knowledge base contains good and important data, it can be used for making quick decisions regarding the process for the implementation of the system. Modern knowledge base can be defined as the base of expert knowledge about the processes and parameters of complex systems from which you can get with a lot of conclusions that reliability can identify certain procedural problems. This paper suggests an approach to the concept of the development of modern knowledge base in order to identify the parameters of the printing process.

Key words: parameters of the printing process, knowledge base, modern computer and software systems

1. INTRODUCTION

Printing process is a complex process with a number of important parameters. A variety of these parameters is a variable character and they are usually functionally dependent. They are specific for printing techniques in which they are implemented so that they differ in the techniques of conventional and digital printing. Conventional printing has specific features which are related to the most important phase of the process and the elements through which the process is implemented and the implementation of elements of the process. Some of the essential elements of the implementation process are related to the entrance where the most important materials are. The materials are processed in a printing machines out of which the products of the press and all of the associated parameter come out. Knowledge base can be related to all process parameters. Knowledge base is the basis of modern decision making by using expert approach to problem identification. The most common approaches encountered in the literature are control systems that take fewer parameters in the process of decision making, whereas less common are the systems of concept which take into account a larger number of parameters. Modern systems need the ability to input new parameters by the user of software solution, which can extend the range of parameters.

Programming systems of the modern approach are related to artificial intelligence and expert systems. Research in the field of artificial intelligence is developing a program that will allow computers to behave in a way that could be characterized as intelligent. The first study is related to the early days of computing. The idea of creating a machine that will be able to perform a variety of tasks intelligently, was a central preoccupation of computer scientists who are committed to research of artificial intelligence during the second half of the 20th century. Modern research in artificial intelligence is oriented to expert systems in a limited scope, and constantly directing towards the creation of intelligent autonomous functional units.

Artificial intelligence as a concept in a broad sense refers to the capacity of an artificial construct for implementing functions that characterize human thought. Research in the field of artificial intelligence is developed through technological development of increasingly complex computer systems, through programs that seek to train the computer to understand the written and verbal information, create summaries, give answers to specific questions or redistribute the data to users who are interested in specific parts of the information. In the field of artificial intelligence, there are a number of different approaches, of which the most dominant are the development of expert systems, the development of neural networks and fuzzy logic. The development of these systems in the printing process requires a systematic approach and analysis [Zeljko et al, 2008].

Expert systems are intelligent computer programs that emulate the type of problem the way it is made by experts and are one of the most important areas in the study of artificial intelligence.

Systems solve real problems in various fields that would otherwise require human expertise. The aim is that computer program always gives correct answers in a given area, not worse than the experts, but it is difficult to reach. This raises a less ambitious goal, i.e. asks the system to assist in decision making. The basis of decision-making are knowledge bases with developed programming systems of decision making. For the area of the printing process it is the knowledge base on the parameters of the realization process.

2. PARAMETERS FOR PROCESS REALIZATION

Reliable and efficient operation of the offset printing process is dependent on a number of parameters, including its surface for printing, printing form, color printing, wetting agent, and the elements of the machine.

Printing forms are posted on the printing form cylinder holder. They are usually metal or rarely multimetal, printing sheets of artificial material or paper. Surface tension and effect of cohesion and adhesion have a direct impact on the printing form. Surface tension manifests itself as a force that tends to minimize the boundary surface, and is the consequence of the existence of intermolecular forces. Cohesion is the physical properties of the substance, caused by intermolecular attraction between similar molecules within a body or substance that seeks to unite them, while adhesion is a phenomenon when two dissimilar materials are linked to each other, having been brought into contact with each other. Cohesion is always greater than the adhesion. Substrate is usually printed on the paper, then semi-cardboard and cardboard. The most important characteristics influenced by material, i.e. its foundation, are the printing characteristics of the materials such as smoothness, permeability, moisture ... In addition to printing characteristics, the pH of the material is very important for printing and mechanical resistance of the material. The choice of colors is based on the substrate to be printed, and it plays an important role. The choice of colour depends on the characteristics of the printing substrate.

Basic characteristics and properties of color are consistency, adhesion, tack, thixotropy, strength, cohesion, viscosity, and a number of other factors.

Printing machine has many elements, so that different parameters of influence can bind to a lot of these elements.

All this points to the complexity of the allocation of a number of factors determining the knowledge base of process impacts that should be integrated in a modern software system. Nowadays learning systems that will enable the user to quickly understanding processes in it can join these systems.

3. THE RESULTS OF MODEL DEVELOPMENT

The concept of modern programming systems is based on the most significant parameters that have the largest impact on the printing quality. It is developed in a way that has the ability to input new parameters from the user, so that the range of parameters can be expanded. Figure 1 shows a model developed on the basis of contemporary knowledge in the implementation of printing process. The model is defined as ES GRID and develops as a system according to the principles of building expert systems.

The model is designed in such a way that data can be entered, modified or deleted, then you can perform searches of the desired data, educate - to teach users some information and to be extensible and to bring new knowledge from the user.

At the input the system receives data on the printing material, printing machines, products and parameters, and they all make for an extensible knowledge base. At the output of the system one can be obtain the listing of the entered data, the user correction parameters if the print quality deviates from the desired, as well as information on the impact of individual parameters to train users. In addition to data, which are input, the user can make the diagnosis or to his system offer solutions to any arising problem that occurred. Knowledge base is extensible so that users himself can bring some new information to the existing knowledge base.

The concept of the knowledge base is based on data on materials for print, printing machines, products and parameters.

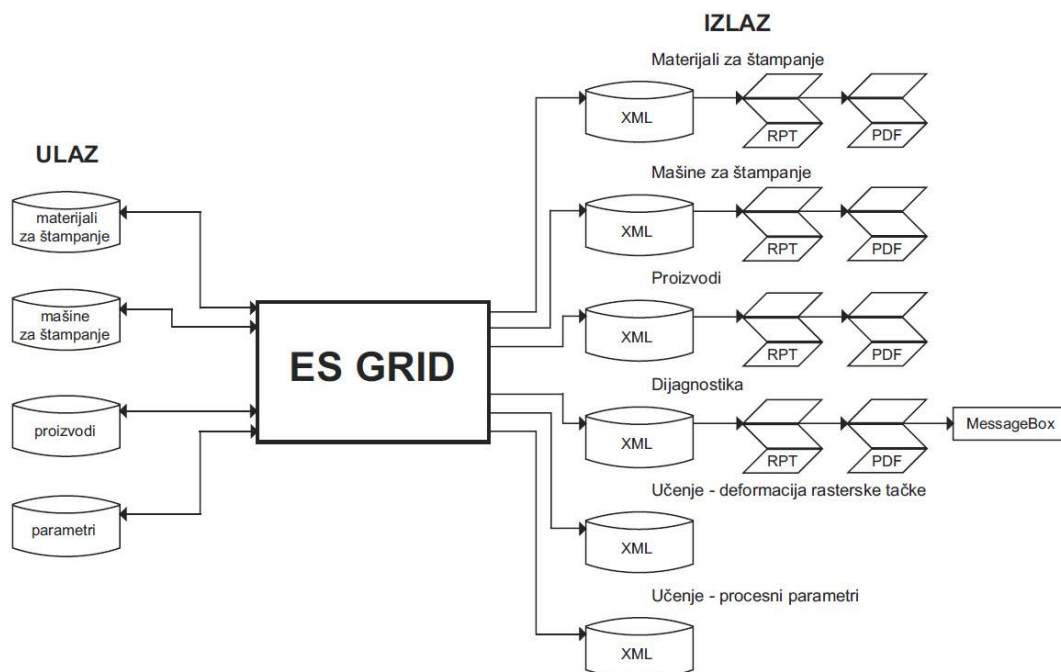


Figure 1. Model of the database system ES GRID

The data are stored in a database that contains special tables for details. Figure 2 shows a table. For example, for materials for print, there is a table called `tbl_Papir` for printing machines table `tbl_Masine` etc..

All Tables	<<
tbl_Papir	⤴
tbl_Papir : Table	
tbl_Proizvodi	⤴
tbl_Proizvodi : Table	
tbl_Masine	⤴
tbl_Masine : Table	
tbl_Parametri_Vrednosti	⤴
tbl_Parametri_Vrednosti : Table	

Figure 2: Tables inside the base

An example of a complex table with relevant information about the parameters. The parameters are divided into categories. Figure 3 shows the structure of this table.

The parameters are structured in such a way that the user can recognize that it is precisely defined parameter. The parameters are defined through their ID fields with their specifics. For all the parameters algorithms are defined. The algorithm can be defined as an effective procedure for solving a problem in a finite number of steps. Effective means that the steps defined by procedures feasible and clearly defined. It is very important that the number of these final steps, i.e. the procedure to be performed in a finite time.


	Field Name	Data Type	
	ParametarVrednostID	AutoNumber	req
	ImeParametra	Text	req
	Kategorija	Text	req
	PapirID	Number	def. value 0
	MasinalID	Number	def. value 0
	ProizvodID	Number	def. value 0
	VaziUvek	Text	
	VaziPapir	Text	req
	VaziMasina	Text	req
	VaziProizvod	Text	req
	MinVrednost	Number	Single req
	MaxVrednost	Number	Single req
	OpisManje	Memo	req
	OpisVece	Memo	req
	AkcijaManje	Memo	req
	AkcijaVece	Memo	req
	Opis	Memo	

Figure 3: Table of data on parameters

Figure 4 presents one of many algorithms which are used to manipulate parameters of the database. In parameters, as well as products, besides the possibility of manipulating the database, there is an overview of the particular parameter. In addition to these properties, there is a possibility of the web display of selected parameters in the xml option, as well as information about them sorted by categories. When you select the option to view information about them, there is the option of modification of the XML document where the user cannot enter or change the new knowledge in the field that is being analyzed. To be able to edit the xml, it is necessary that a user has installed a program for editing XML documents. The review of algorithm for the parameters is given in Figure 4. The future development is presented by dashed lines.

The developed system has a main menu, a database of all the parameters, navigation, Web presentation of all materials, presentation of reports, working with databases, working with parameters, input parameters, modification of parameters, deleting parameters, view of parameters, working with products and diagnostics. For illustration Figure 5 shows the menu layout of diagnosis.

Diagnosis is a kind of problem solving the operator has come upon on a certain machine. Diagnosis is directly linked to the data stored in the knowledge base, which indicate that it is also associated with a form of expert interviews. Since the system is not directly connected with the printing machine, a system based on the entered values of parameters measured compares the measured value parameters with the recommended limits in terms of press given by the user. If the parameter is not within the prescribed limits, the system will easily determine where the error occurred, and warn the user of the error, giving the error description, and suggesting steps to give the parameter limits of allowable values. The importance of diagnosis is reflected in the high speed inference and decision-making, the reduction of maculation, i.e. wrongly printed sheets through timely identification of deviations of a parameter of the allowable limit.

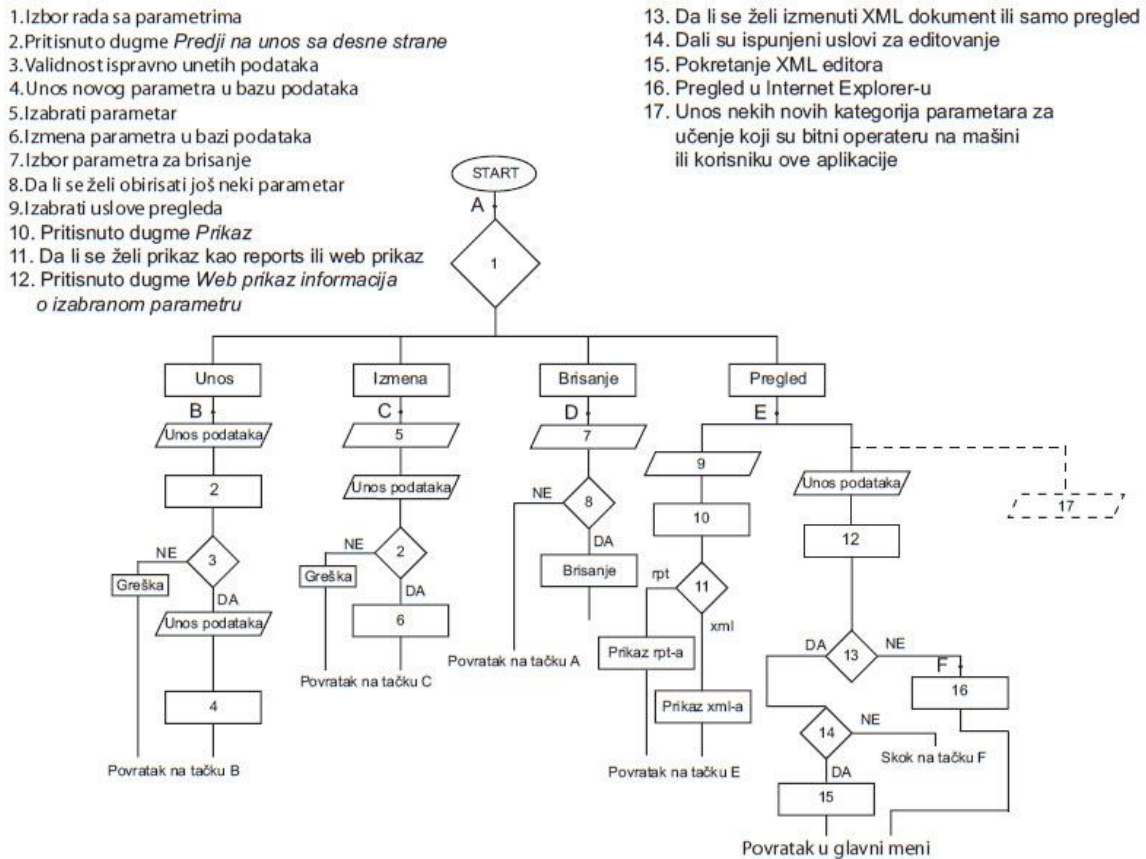


Figure 4: The algorithm for the parameters

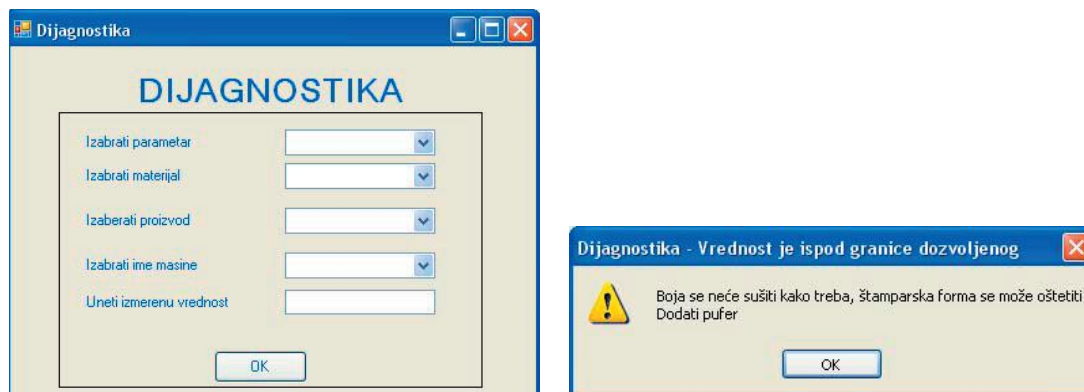


Figure 5: Layout of a large number of menu – menu diagnosis

The system is developed so that the user has the possibility of education based on knowledge about the effects of certain parameters on the quality. Since the knowledge base is extensible, one can enter any new information in order for the user to be able to have the possibility of further education. The addition of new knowledge about the influence of certain parameters on the quality of the print, which are related to the education of users is done by modifying the existing xml document. To view these documents, it is necessary that the user has installed a web browser, and to amend the documents you need to have an xml editor.

4. CONCLUSION

This paper presents the research from which was developed a system that will allow monitoring of parameters that influence the quality of printing. The developed system ensures that data can be entered, modified or deleted, searching for the desired information, learning about the impact of individual parameters. Knowledge base is extensible, allowing the incorporation of new knowledge by the users. The paper presents a conceptual set and certain segments that will be developed to make the system directly receive parameter values and compare with the prescribed limits. The developed system allows the user to have fast access to the relevant parameters and the system has extensible knowledge base to which you can add new knowledge to make the system more functional and efficient. The system allows for easy diagnostics and fault-finding with deviations of parameters and gives advice to eliminate those errors. Developed solution allows for multi-user operation.

5. ACKNOWLEDGEMENTS

This work was supported by the Serbian Ministry of Science and Technological Development, Grant No.: 35027 "The development of software model for improvement of knowledge and production in graphic arts industry".

6. REFERENCES

- [1] Anon. .NET Framework, URL:http://sr.wikipedia.org/wiki/.NET_Framework (last request: 2010-11-15)
- [2] Anon. Veštačka inteligencija, URL:http://sr.wikipedia.org/sr-el/Вештачка_интелигенција (last request: 2010-11-15)
- [3] Anon. Ekspertski sistemi, URL:http://sr.wikipedia.org/sr-el/Експертски_систем (last request: 2010-11-15)
- [4] Anon. Neuronske mreža, URL:http://sr.wikipedia.org/sr-el/Неуронске_мреже (last request: 2010-11-15)
- [5] Konjović Z., Obradović Đ.: "Fuzzy logika - radni materijal", Fakultet tehničkih nauka, Novi Sad, 2004
- [6] Microsoft, MS Office 2007, URL: <http://office.microsoft.com/sr-latn-cs/access-help/novine-u-u-programu-microsoftoffice-access-2007-HA010024185.aspx> (last request: 2010-11-15)
- [7] Novaković D.: "Grafički procesi", Fakultet tehničkih nauka, Novi Sad, 2013
- [8] Zeljković Ž., Novaković D., Karlović I.: "Savremeni prilaz identifikaciji procesnih parametara ofset štampe", Zbornik radova Četvrtog naučno - stručnog simpozijuma GRID 2008, Fakultet tehničkih nauka, Novi Sad, 2008, str.
- [9] Zjakić, I.: "Upravljanje kvalitetom ofsetnog tiska", Hrvatska sveučilišna naklada, Zagreb, 2007.

Environmental protection in graphic arts

CELLULOSE BASED CARTONBOARD ESTER RETENTION

Rozália Szentgyörgyvölgyi ¹, Eliza Angeli ²¹Obuda University, Rejtő Sándor Faculty of Light Industry and Environmental Engineering, Budapest, Hungary²Obuda University, Doctoral School on Materials Sciences and Technologies, Budapest, Hungary

Abstract: Gravure printed cellulose based packaging materials always contain small amount of retained solvents after printing. Residual solvents migrated to the packed product might change its taste and flavour, that potentially cause a loss of brand confidence and market share of the end-user, in consequence it became a need to measure retained solvents amount in the gravure printed packaging materials. In order to avoid off-flavour and off-taste effect, the solvent retention values must be kept under the maximum tolerance specified by the Food Industry. The major end-user companies have their own specified limits on acceptable total and individual solvent retention levels. Isopropyl acetate and ethyl acetate are considered as critical solvents due to their highest retained amount in the printed packaging out of all the solvents detected. In this study cellulose based, FBB type, 225 gsm and 230 gsm unprinted cartonboards with multiple coating on top side, coated and uncoated on reverse side had been studied in order to determine their retained isopropyl acetate and ethyl acetate content. The interaction between board pieces and esters vapour was analysed with the help of desiccator. The amount of absorbed solvents was measured by gas chromatography. It was concluded that coating has a significant influence on the retained solvent results of cellulose based, FBB type cartonboards.

Key words: gravure, evaporation, solvent retention, coating, gas chromatography

1. INTRODUCTION

Packaging materials having food contact required to be manufactured to meet strict food industrial standards, thus unhealthful printing inks and solvents should not be used in printing and strictly prohibited the cartonboard substrate to contain any ingredients harmful for health. The residual solvent content of gravure printed cartonboard packaging shall not exceed the limits specified by the industry, mainly due to health reasons, but solvent retention of printed packaging might also have a significant influence on packed product sensory properties like odour, taint and flavour. The specified maximum solvent retention of printed packaging materials has been more and more difficult to keep in tolerance due to challenging graphics and high production speed on modern gravure printing machines; and due to high solvent ratio of gravure printing inks applied (Argent, 2008) (Huber et al, 2002). Cellulose based cartonboard parameters having influence on solvent resistance have to be analysed to find the main reasons for high solvent retention characteristics. In a series of investigations we aim to study the main characteristics like moisture content, coating and other structural parameters of fiber based, FBB type cartonboard that might have an influence on solvent retention.

2. METHODS

Almost all packaging materials contain printing. Gravure printing is considered the best printing method to achieve high quality printed results if designs with especially metallic colours requested to be printed. In gravure printing method, the liquid ink is transferred from a metal based cylinder to the surface of the substrate. Metal based image cylinder is rotating in the ink tank; consequently the full surface of the cylinder is covered by ink that is removed by a doctor blade from the non-image areas. Ink from the image cells are transferred to the substrate surface by high pressure generated by the impression roller. Each colour is printed by one printing unit, after each printing unit the ink layer is dried and solvents are evaporated in the drying unit by heating the substrate with hot air. After drying a part of the solvents remains in the ink and absorbed into the cardboard from the ink layer. This is the retained solvent in the substrate that is called solvent retention. Liquid gravure printing ink consists of pigments, resins and solvents; manufactured and used with low viscosity and with conventional or metal pigments.

Drying method of gravure ink is pure evaporation – as shown on Figure 1 – and done on high temperature, speed and ventilation. Volatile solvents are particularly important in gravure technology, used in order to settle low viscosity and to change pigment concentration and ink density.

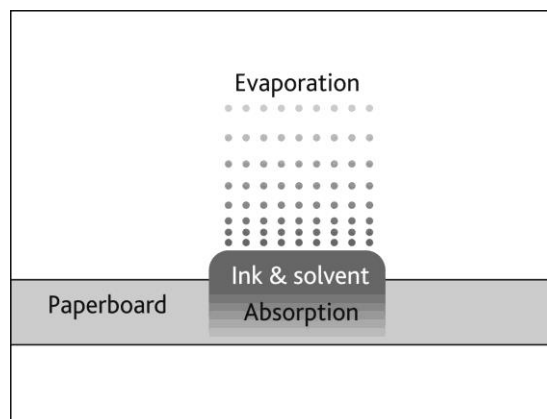


Figure 1: Ink absorption and evaporation drying principle

Main solvents used in the industry: alcohols, esters, aliphatic and aromatic compounds, glycols, ketones. Solvent-based gravure inks always retain certain amount of solvents in the ready-made printed package but the use of metallic inks could affect higher solvent retention as thicker ink film layers are required, and the metallic ink components behave like a physical barrier on solvent evaporation [E Todd, 1994] [Gawkill et al, 1988] [Kipphan, 2001] [Argent, 2008].

Paperboards are classified into 3 categories: cartonboards, containerboards and specialty boards. Paperboard basis weight is usually higher than 150 g/m². Cartonboard is a common name for paper products used for packaging cartons and it is a multilayer material constructed from more than one fiber layer – in general consist of three or more pulp layers – simultaneously manufactured on a multilayer paperboard machine. Cartonboard packaging materials are mainly used for food, cigarettes, milk and pharmaceutical products. Cartonboards are divided into several subgrades, Table 1 shows the typical classification – made based mainly on the used raw materials – with abbreviation of grades used in the paper and board industry. Most of the cartonboard grades are pigment coated for the good printed results and properties; top side is often double coated, sometimes triple coated; backside can be either coated or uncoated according to the printability and design requirements [Paulapuro, 2000] [Niskanen, 2012] [Lehtinen, 2000].

Table 1: Cartonboard grades and abbreviations

Grade	Abbreviation
Folding boxboard	FBB
White lined chipboard	WLC
Solid bleached (sulphate) board	SBS
Solid unbleached (sulphate) board	SUS
Liquid packaging board	LPB

Folding boxboard type cartonboard is widely used in the packaging industry but typically in cosmetics, tobacco, pharmaceutical, confectionery and food industrial segments in the grammage range of 160-450 gsm. FBB multiply cartonboard general structure from top to backside: coating layer (2 or 3 coating layers); top ply: chemical pulp (bleached soft wood or bleached hard wood); middle ply: mechanical pulp (groundwood, pressure groundwood, thermo-mechanical pulp) or CTMP (Chemi-Thermo-Mechanical Pulp) and machine broke added; back ply: chemical pulp (bleached soft wood or bleached hard wood). Depending on the end-use requirements top side of FBB can be double or triple coated, back side can be single coated or uncoated [Paulapuro, 2000]. The typical FBB structure can be seen on Figure 2.

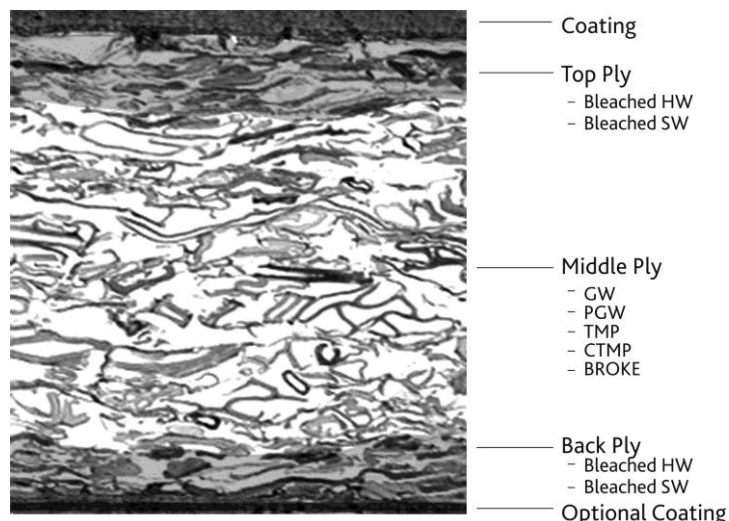


Figure 2: Typical folding boxboard structure

Coating improves the cartonboard printing properties, fills the cavities and covers the base board surface, consequently increases the smoothness significantly. Coating has notable effects on the board properties: ink absorption decreases, surface strength increases and dusting decreases, gloss and opacity – maybe also brightness – increases, mechanical strength decreases when coated and uncoated boards at the same basis weight compared. Coating colour is an aqueous suspension applied to one or both sides of cartonboard that contains pigments (kaolin clay, calcium carbonate, talc), binders (SB-latex, starch, acrylate latex), co-binder (carboxy methyl cellulose) and usually various additives (lubricant, insolubilizer) (Lehtinen, 2000) (Niskanen, 2008). Paper and board brightness requirement increased significantly during the last few years; consequently there was a need to use a coating additive called optical brightening agent (OBA). Fluorescence is a phenomenon where the fluorescent substance molecules become electronically excited by absorbing light energy that energy is then emitted at a higher wavelength. On the market the most of OBAs are derivatives of bis(triazinylamino)stilbene (Lehtinen, 2000).

3. EXPERIMENTAL

In this study we analyse the ethyl acetate and isopropyl acetate retention results of three cellulose based, 225-230 gsm, FBB type cartonboards (Table 2) and determine the role and importance of coating on the substrate solvent retention and release.

Table 2: Tested cartonboard grades and their characteristics

Grade	Grammage, gsm	Coating, top / back	Brightness, top / back	OBA, top / back	Construction
Board A	225	yes / yes	90 / 85	yes / yes	
Board B	230	yes / no	82 / 72	no / no	
Board C	225	yes / no	87 / 72	yes / no	

Major international food manufacturing companies have specified the limits of acceptable solvent retention level in their specification sheets over the years that includes ethyl acetate, a very important odorous solvent used in the gravure printing technology (Huber et al, 2002). Retained

solvent amounts are detected by gas chromatography (GC) that is a chemical analysing process in order to separate chemicals in a complex sample whereas sample is vaporised and inserted onto the head of chromatographic column for the investigation of volatile compounds. The interaction between the cartonboard test pieces and solvent vapour was studied with the help of desiccator. Cartonboard pieces were placed in the desiccator (Figure 3), 100 ml solvent had been poured into it beforehand than lid close thus cartonboard pieces absorbed the solvent vapour. Each desiccator contained only one solvent: isopropyl acetate or ethyl acetate. Testing made in an air-conditioned laboratory where temperature was 23 °C and RH 50%, samples were also conditioned in the same room for 24 hours before pieces were cut for the desiccator test. The moisture content of board samples was determined and samples were weighed so that the amount of pulp in each specimen was 0.3 g (abs. dry weight). Four sample pieces and four reference pieces were placed into the desiccator. The pieces were left in the desiccator for one hour, after that the sample holder with the samples and references was removed. One sample and one reference piece were enclosed immediately in headspace vials with 1 ml triacetin, the other pieces were left under constant conditions to allow the absorbed solvents to evaporate freely. Pieces of sample and reference were bottled in the same way after 5 min, 15 min and 90 min, the amount of absorbed solvent was measured by Clarus 580 Perkin Elmer gas chromatography equipment.

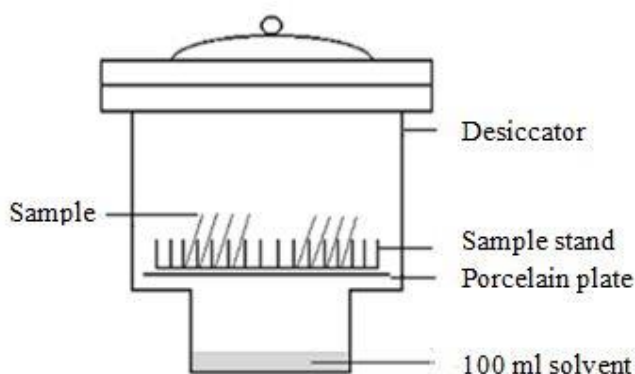


Figure 3: Experimental arrangement of the desiccator test

Headspace-gas chromatography (HS-GC) process consists of two steps. First, the sample is placed in a vial having a gas volume above it and the vial that is closed, then thermostatted at a constant temperature in HS oven until equilibrium is reached between the two phases. An aliquot of the vial's gas phase (HS) is then introduced into the carrier gas stream which carries it into the column, where it is analysed. The two steps of HS-GC can be seen on Figure 4 (Kolb and Ettre, 2006) (Stenius, 2000).

Cartonboard sample is transferred into a headspace vial which is closed tightly and heated to 70°C for one hour. Subsequently, gas phase solvent concentrations are determined by HS-GC and reported in mg/m².

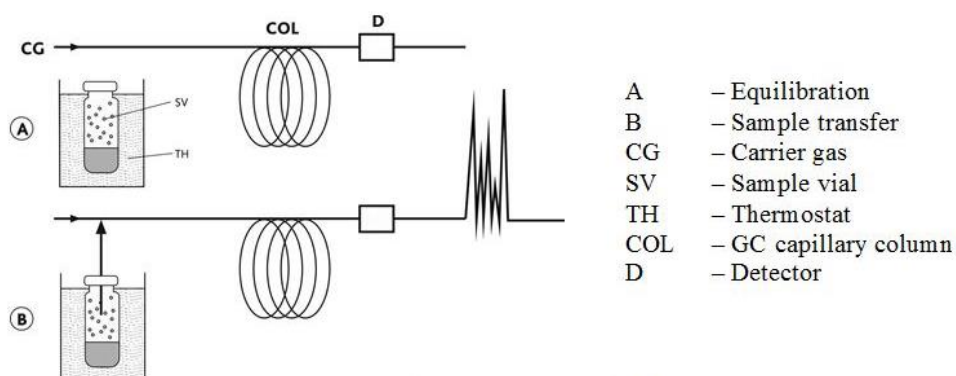


Figure 4: HS-GC principle

4. RESULTS AND DISCUSSION

Cellulose based FBB type substrate samples with and without backside coating and OBA were taken and retained solvents were measured by GC in 4 time periods: immediately after 60 minutes sample conditioning in desiccator, than after 5 minutes, 15 minutes and 90 minutes airing. Comparative investigation made on isopropyl acetate and ethyl acetate retention results of Board A, B and C.

4.1 Isopropyl acetate retention analyses

Retained isopropyl acetate of 3 cartonboards (Board A, B and C) has been measured by GC in 4 time periods; isopropyl acetate retention results of all the 3 boards were nearly on the same level right after 1 hour desiccator conditioning (Figure 5), than isopropyl acetate content of the board samples decreased dynamically, however it turned out, that Board B without backside coating and without OBA had the highest retained isopropyl acetate at any time period after airing when solvent retention measured and Board A – with coating and OBA on both sides of the board – had the lowest isopropyl acetate level measured the same time. It was established, that absorbed isopropyl acetate evaporated the slowest in case of Board B, consequently the solvent stagnated in the board structure compared to Board A and Board C – both has OBA in the top coating – where isopropyl acetate evaporated more freely from the board structure.

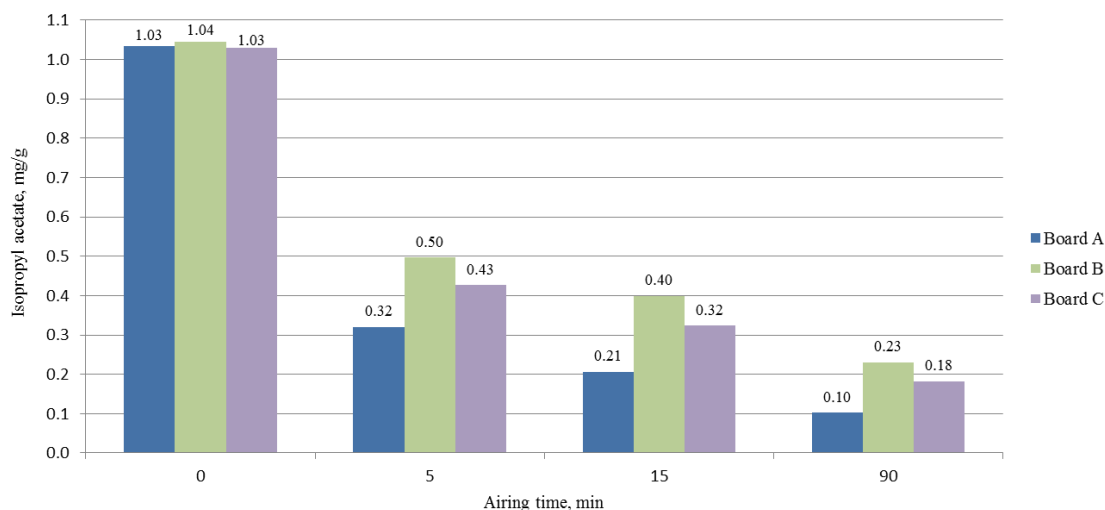


Figure 5: Isopropyl acetate retention results of 3 cartonboards (Board A, B and C) measured in 4 time periods

4.2 Ethyl acetate retention analyses

Clearly visible on Figure 6, that ethyl acetate is a more critical solvent due to high solvent retention volumes and low evaporation speed compared to isopropyl acetate. As experienced in practice during test prints, it could take even up to 2 weeks for high ethyl acetate retention of printed blanks to be decreased to the specified level.

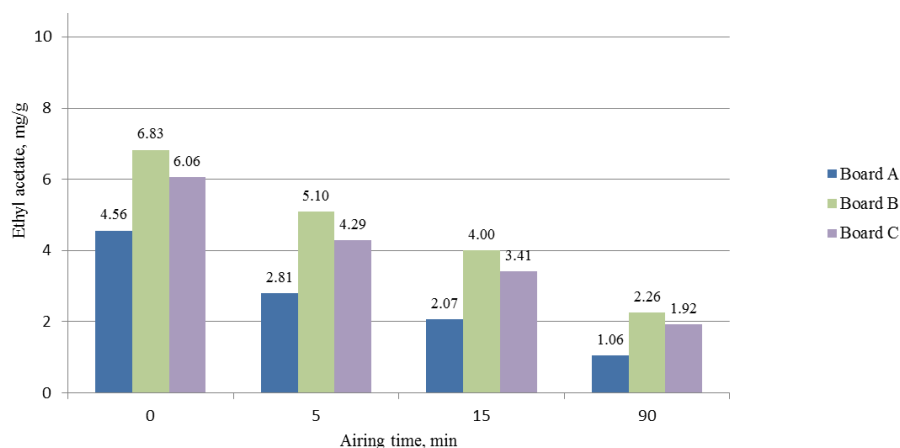


Figure 6: Ethyl acetate retention results of 3 cartonboards (Board A, B and C) measured in 4 time periods

It was established that Board B without backside coating and OBA had the highest ethyl acetate retention out of all the 3 boards analysed in the whole testing period and Board A – with coating and OBA on both sides – had all along the lowest ethyl acetate level. Right after the 1 hour desiccator conditioning the absorbed ethyl acetate amount was the lowest in Board A (with coating and OBA on top and back sides of the board), 33,2% lower than in Board B, consequently it was concluded that coating and OBA has a positive effect on the solvent retention, they might behave as a physical barrier.

Board C – with coating and OBA on the top side, but uncoated reverse side – behaved similarly as Board B, slightly lower ethyl acetate retention detected.

After 90 min airing the ethyl acetate content of Board A, B and C decreased appreciably compared to the results measured right after the 1 hour desiccator conditioning: 76,8% lower ethyl acetate retention of Board A, 66,9% lower of Board B and 68,3% lower of Board C; that is a minor difference between the Board B and C.

4.3 SEM analyses

Based on the investigation done by desiccator with esters, GC measurements indicate that the retained isopropyl acetate and ethyl acetate content of Board B (without backside coating and OBA) was the highest and the lowest results received in case of Board A that has coating and OBA on top and back sides of the substrate during the whole investigation period.

Structure of Board A – with the lowest ester retention – and Board B – with the highest ester retention – was investigated by Scanning Electron Microscope (SEM) where an electron microscope produced images of a sample by scanning it with a focused beam of electrons. Structural difference of Board A and B can easily be recognised on Figure 7, not only the both sides closed surface of Board A is visible but a slightly more open inner structure of Board B that might partly resulted the high ester retention.

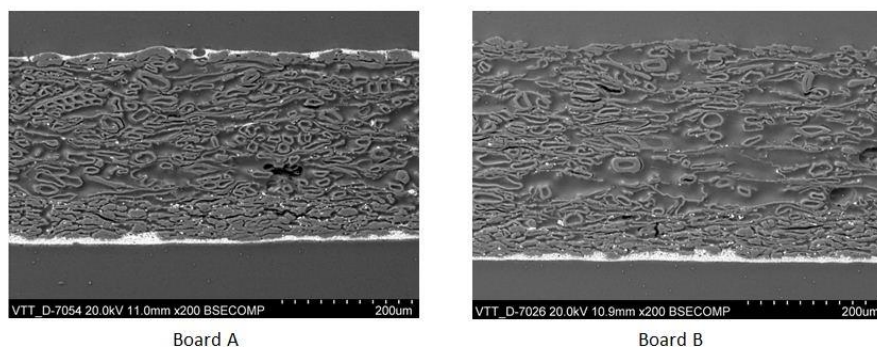


Figure 7: SEM image of Board A and B

5. CONCLUSIONS

In this study we aimed to determine the role and importance of coating and OBA in the fiber based, FBB type board on ester – isopropyl acetate and ethyl acetate – retention and release. We have analysed the residual solvent content of three different boards – Board A, B and C – in 4 time periods: immediately after 1 hour sample conditioning in desiccator, than after 5 minutes, 15 minutes and 90 minutes airing. Comparative investigation made on isopropyl acetate and ethyl acetate retention results of Board A, B and C.

This work shows that absorbed isopropyl acetate and ethyl acetate evaporated the slowest in case of Board B, consequently the solvent stalled in the board structure compared to Board A and Board C – both has OBA in the top coating – where isopropyl acetate evaporated more freely from the board structure.

It has been concluded, that the absorbed isopropyl acetate and ethyl acetate amount was the lowest in Board A with coating and OBA on top and back sides, the highest figures in Board B without backside coating and OBA, consequently it has been declared that coating and OBA has a notable effect on the solvent retention. This might lead to the conclusion that coating and OBA behave as a physical barrier, namely the ink and solvent absorption might decrease.

In our further studies we aim to analyse additional cellulose based FBB type cartonboard characteristics might have an influence on solvent retention and resistance.

6. REFERENCES

- [1] Angeli, E., Klebert, Sz., Szentgyorgyvolgyi, R.: "Influence of Gravure Printed Cellulose Based Cartonboard Moisture Content on Solvent Retention", Proceedings of 4th International Joint Conference on Environmental and Light Industry Technologies 2013 (Budapest, Hungary, 2013), pages 427-435.
- [2] Argent, D.: "Solvent Retention in Packaging", Paper, Film and Foil, volume 82 (10), page 14, (2008).
- [3] Todd, E. R. : "Prining Inks: Formulation Principles, Manufacture and Quality Control Testing Procedures", 1st Edition, (Pira International, 1994), page 96-101
- [4] Gawkill, E., Ellison, B.: "Gravure Inks" in Leach, R.H.: "The Printing Ink Manual", 4th Edition, (Blueprint, London, 1988), pages 368 - 434
- [5] Huber, M., Ruiz, J., Chastellain, F.: "Off-Flavour Release From Packaging Materials and its Prevention: A Food Company's Approach", Food Additives and Contaminants, volume 19 (1), pages 221-228, (2002).
- [6] Kipphan, H.: "Handbook of Print Media: Technologies and Production Methods", 1st Edition, (Springer, Berlin, 2001), pages 137-138, 171-171
- [7] Kolb, B., Ettre, L.: "Static Headspace-Gas Chromatography: Theory and Practice", 2nd Edition, (John Wiley & Sons, Inc., Hoboken, NJ, 2006), chapter 1
- [8] Lehtinen, E.: "Pigment Coating and Surface Sizing of Paper", 11th Edition, (Fapet Oy, 2000), pages 14-27, 298-299.
- [9] Niskanen, K.: "Mechanics of Paper Products", 1st Edition, (Walter De Gruyter GmbH & Co. KG., Berlin, 2012), pages 34-35.
- [10] Niskanen, K.: "Paper Physics", 2nd Edition, (Papermaking Science and Technology, 2008), pages 132-135.
- [11] Paulapuro, H.: "Papermaking Science and Technology", (Tappi Fapet Oy, 2000), pages 56-58.
- [12] Stenius, P.: "Forest Products Chemistry (Papermaking Science and Technology)", (Tappi Fapet Oy, 2000), pages 111-112.

EFFLUENT CHARACTERISTICS FROM NEWSPAPER CHEMICAL FLOTATION DEINKING

*Marina Vukoje, Ivana Plazonić, Željka Barbarić-Mikočević
University of Zagreb, Faculty of Graphic Arts, Zagreb, Croatia*

Abstract: In paper recycling industry flotation deinking is one of the most applied technique in which great amount of water and chemicals have been used. According to that, effluents from paper recycling industry can be huge environmental problem. It is of great importance to find a process that will give a good quality of recycled pulp but also effluents with minor inorganic and organic pollution. In this study effluent characteristics from deinking flotation of naturally aged daily newspaper were examined. The influence of chemicals used in three recycling process were compared. In the first recycling process defined deinking chemicals according to INGEDE Method 11 were used. In the second recycling process oleic acid as surfactant and naturally gained alkali, Eco-alkali, were used while the third one was done using the same chemicals as in the first process where sodium hydroxide was replaced with Eco-alkali. The effluents obtained after all chemical flotation deinking processes were analysed by standard analytical methods, in terms of the concentration of the sulphate and nitrate, total organic compound, chemical oxygen demand, pH and electrical conductivity. According to the results it could be conclude is it possible to discharged effluents into the environment without treatment or they need to be pre-treated before discharging into the environment.

Key words: effluent characteristics, deinking chemicals, deinking flotation, newspaper

1. INTRODUCTION

Pulp and paper industry is considered as one of the major polluters of the environment due to discharging great amounts of highly coloured and toxic effluents. This industry which consumes a significant amount of resources, raw materials and energy is constantly growing. In paper industry, water is a vital component for many industrial operations and is utilized for a wide range of purposes. Therefore, the most important problem which pulp and paper industry is facing today is disposal of tremendous volumes of waste water. Discharging insufficiently treated effluents into the environment results in serious problems for aquatic life. The majority of pollutants originate from raw materials, applied processes and chemistry, internal recirculation of the effluents for recovery and the amount of water being used in a particular process. The effluents often contains high amounts of various organic and inorganic materials (Ali et al, 2001; Giri et al, 2014; Kesalkar et al, 2012; Maheshwari et al, 2012).

Recycling and sustainability are nowadays the main trends in paper recycling industries. The flotation process is recognized as one of the most important sub-systems in a wastepaper recycling mill because it provides a low cost and effectively removes ink particles from recycled pulp (Finch et al, 1999). For offset prints, alkaline deinking appears the best solution (Dumea et al, 2009). INGEDE Method 11 (INGEDE, 2009) based on alkaline conditions become standard practice all over the world. According to the method, 81% of the offset prints (mainly newspapers and magazines) achieved a positive assessment of their deinkability (Faul, 2010). This widely used traditional chemical deinking process requires the usage of large quantities of chemical agents. All approaches commercially applied to date have not been environmentally friendly and at the same time successful in producing fibre qualities necessary for printing and writing grades. Researching efficiency of newspaper flotation deinking, the idea of naturally gained and easily prepared alkali chemical instead sodium hydroxide was born. For preparing this novel alkali, called Eco-alkali, wood fly ash collected after hardwood ignition has been used. Gained results in previous researches (brightness of the deinked pulp and the number of visible ink specks per unit surface area) have point out that Eco-alkali could be successfully used in newspaper flotation process (Plazonić et al, 2012a; 2012b).

In this research the influence of Eco-alkali on wastewater organic pollution was analysed. The effluent characteristics from newspaper chemical flotation deinking according to INGEDE Method 11 was compared with those gained using Eco-alkali.

2. EXPERIMENTAL

2.1 Materials

Raw material used in the chemical flotation deinking process was daily Croatian newspaper which was kept in a room away from sunlight and high moisture for a year. Newspapers are coldset offset prints, printed by offset news inks applied on paper substrate made from recycled fibre. In deinking process conventional chemicals and Eco-alkali were used. Eco-alkali is prepared as described in earlier published studies (Plazonić et al, 2012a; 2012b). Chemical composition obtained by ion chromatography (IC) and inductively coupled plasma mass spectrometer (ICP-MS) of Eco-alkali, presented in Table 1, was published in those studies as well (Plazonić et al, 2012a; 2012b).

Table 1: Chemical composition of Eco-alkali obtained by IC and ICP-MS methods; pH=12.08, conductivity = 20.0 mS/cm, $\gamma = 1,010 \text{ g/cm}^3$

IC method		ICP-MS method	
Anion	Concentration, mg/L	Element	Concentration, mg/L
SO ₄ ²⁻	675.9	K	5781
NO ₃ ⁻	46.1	Na	162.6
Cl ⁻	27.2	Ca	10.65
F ⁻	3.78	P	7.1
		B	5.73
		Mg	4.45
		Fe	2.30
		Al	0.35
		Cu	0.105
		Ag	0.10
		Mn	0.03
		Zn	0.06
		Pb	0.01
		As	0.01

2.2 Methods

2.2.1 Flotation deinking

For efficient removing ink particles from recycled newspaper via flotation deinking mildly alkali media is necessary. In Trial 1 (T1) alkali media was achieved by sodium hydroxide, while in Trial 2 (T2) and 3 (T3) for that purpose Eco-alkali was used. Utilized chemicals in all-made trials, which were carried out under the same experimental conditions, are presented in Table 2. All deinking trials were made according schematic view presented in Figure 1.

Table 2: Chemicals utilized in all chemical flotation deinking processes

Chemical	Chemical dosage related to dosage of oven-dry newspaper		
	Trial 1 (T1) (INGEDE Method 1)	Trial 2 (T2)	Trial 3 (T3)
Alkali	0.6% sodium hydroxide	33.5% Eco-alkali	33.5% Eco-alkali
Sodium silicate	1.8%	-	1.8%
Hydrogen peroxide	0.7%	-	0.7%
Surfactant	0.8% oleic acid	0.8% oleic acid	0.8% oleic acid

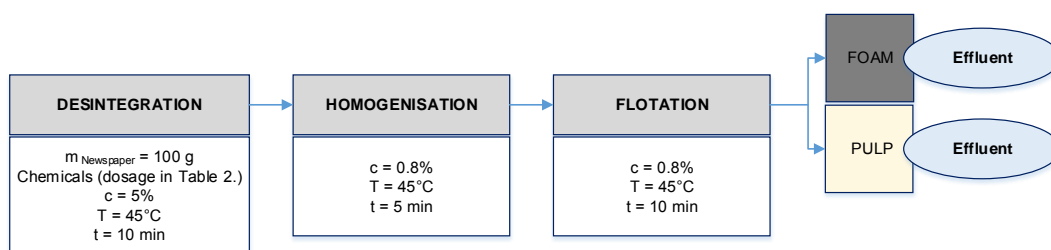


Figure 1: Schematic view of chemical flotation deinking

Flotation deinking generates deinked pulp and wastewater effluents (from pulp and foam). The aim of this work was only determination of effluents characteristics. For that purpose effluents were collected after flotation process.

2.2.2 Collection of effluent samples and analysis

The effluents obtained from all deinking trials were filtrated through Büchner funnel in order to remove residual pulp before provided analysis. The effluent samples were collected from foam and pulp after flotation deinking step (Fig 1.) and analysed in terms of the pH, electrical conductivity (EC), sulphate, nitrate, Total Organic Compound (TOC) and Chemical Oxygen Demand (COD) values. Measurements were carried out according to the standard methods (Table 3). pH and EC values were determinate by a WTW Multi 9310 (InoLab_IDS) while HACH DR/890 Colorimeter was used for Sulphate, Nitrate, TOC and COD concentration measurements.

Table 3: Standard methods used for effluent characteristics determination

Physico-chemical characteristics	Method Applied for laboratory analysis
pH	pH Meter
Electrical conductivity (EC), $\mu\text{S}/\text{cm}$	Potentiometry
Sulphate, mg/L	Colorimetry - SulfaVer4 Method (with Powder Pillows)
Nitrate, mg/L	Colorimetry - Cadmium Reduction Method High Range
Total Organic Compound (TOC), mg O_2/L	Colorimetry - Direct method High Range, Test' N Tube
Chemical Oxygen Demand (COD), mg C/L	Colorimetry - Reactor Digestion Method High Range

Effluents samples collected after each trial were analysed for the required parameters (presented in Table 3) in order to serve as a pollution indicator.

3. RESULTS AND DISCUSSION

Influence of different chemical agents, added in a disintegration stage of deinking process, on effluent characteristics is presented at Figures 2a-f.

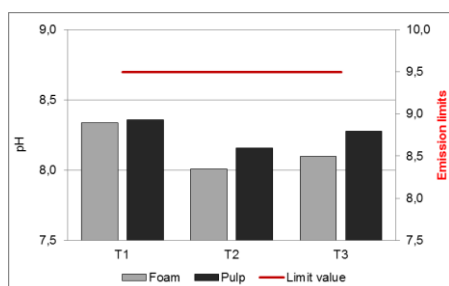


Figure 2a: Effluents pH values

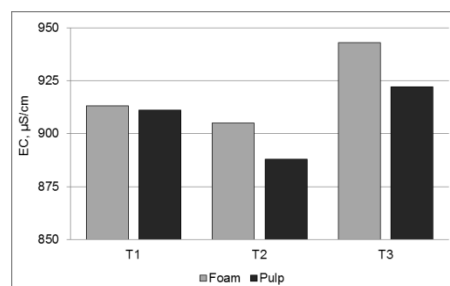
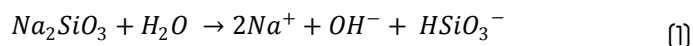


Figure 2b: Effluents electrical conductivity (EC) values

The hydrogen-ion concentration is an important quality parameter of effluent. The results of effluents pH value (Figure 2a) showed that an alkaline medium which is necessary for deinking process was achieved in all-made trials (from 8.007 to 8.357). The effluents derived after flotation deinking by Trial 1 (T1) have higher pH value compared to effluents obtained from trials where

Eco-alkali was used (T2 and T3). It can be explained due to strong alkali NaOH which was used in INGEDE method (T1) and chemical composition of Eco-alkali used in T2 and T3 (Table 1). The effluent obtained after provided T2 trial showed lower pH value than effluent collected after trial T3 in which Eco-alkali was mixed with sodium silicate and hydrogen peroxide in disintegration stage of deinking process. It is known that soluble silicates also contribute alkalinity of pulp suspension during deinking process and allow the process to be carried out at a lower pH value than possible when using caustic soda alone. Namely, the sodium silicate solution is a source of alkalinity, derived from free hydroxyl groups according to Equation 1. (Ferguson, 1992).



Electrical conductivity results for all collected effluents are presented at Figure 2b. The results are in the range of 888 up to 943 $\mu\text{S}/\text{cm}$.

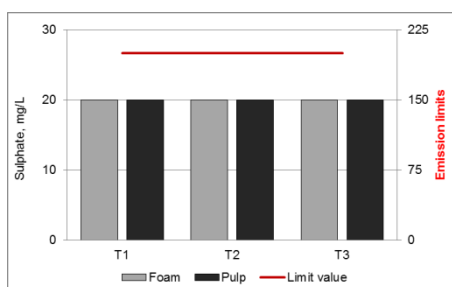


Figure 2c: Effluents sulphate values

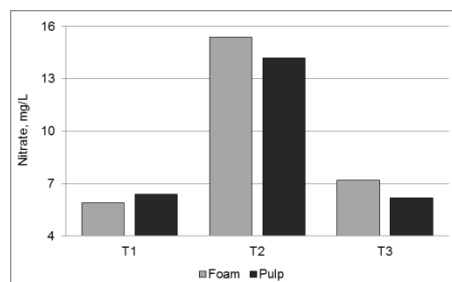


Figure 2d: Effluents nitrate values

Sulphate and nitrate are common contaminants in effluents. The results of sulphates concentration (Figure 2c) showed that they are not strongly influenced by chemical composition of used chemicals in deinking flotation. In all-made trials measured sulphate concentration is the same (20 mg/L) in foam effluent as well as in pulp effluent.

Used chemicals in flotation deinking have much higher influence on nitrate concentration in derivate effluents. Figure 2d clearly shows that the highest nitrate concentration is measured in effluent collected after Trial 2. (15.4 mg/L in foam and 14.2 in pulp). Nitrate concentration is drastically reduced in effluent if in disintegration stage sodium silicate and hydrogen peroxide are added to Eco-alkali (to 7.2 mg/L in foam and 6.2 in pulp). The minimum nitrate concentration is achieved in effluents collected after flotation deinking via INGEDE Method (T1).

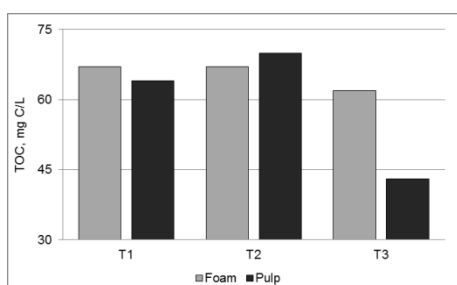


Figure 2e: Effluents TOC values

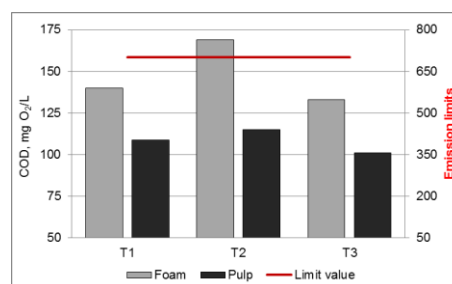
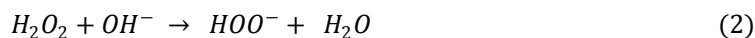


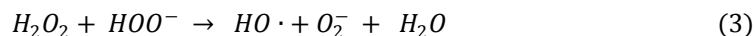
Figure 2f: Effluents COD values

Total Organic Carbon (TOC) and Chemical Oxygen Demand (COD) are terms used to describe the measurement of organic contaminants in a water system. TOC and COD values in flotation deinking effluents are strongly influenced by chemical composition of used raw material and chemicals. Old newspapers contains cellulose fibres, lignin, hemicelluloses and high fines content, which may be extracted out during the deinking process into the wastewater effluent and in thus contributing to higher TOC and COD values (Lee et al, 2011). Influence of chemicals used in deinking process can be positive or negative on organic matter in effluent. At Figure 2e-f it is clearly showed that effluents derivate from trial T2 have highest measured TOC and COD values. This appearance could be explained of using Eco-alkali without other chemicals. Addition of

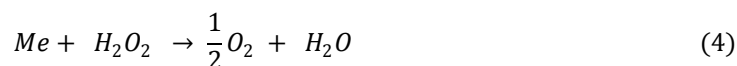
sodium silicate and hydrogen peroxide in disintegration stage of deinking process (trials T1 and T3) decrease TOC and COD values. Namely, hydrogen peroxide is a source of perhydroxyl anion (HOO^-) in reaction with strong alkali. The peroxide reaction with alkali is shown in Equation 2. (Ferguson, 1992).



As the pH value of pulp suspension is higher production of this anion is higher as well. The presence of sodium silicate in disintegration stage contributes to alkalinity of suspension (Equation 1.) and consequently on higher perhydroxyl anion concentration. The perhydroxyl ion in reaction with hydrogen peroxide gives hydroxyl radicals (Equation 3.), which are acting as a high oxidation agents in pulp suspension (Ferguson, 1992).



Hydroxyl radicals strongly influence on TOC and COD values because they can oxidise present organic matter in effluent. Therefore, effluents collected after trials T1 and T3 have much lower TOC and COD values from those collected after T2 deinking process. The effluent collected after T3 trial showed the lowest TOC and COD values what is in correlation with Eco-alkali chemical composition. Namely, Eco-alkali has abundant metals which can positively influence on TOC and COD values. It is well known how heavy metals like manganese, copper, and iron can influence on hydrogen peroxide stability in alkaline solution. The decomposition reaction of hydrogen peroxide is shown in Equation 4. (Ferguson, 1992).



The pH value, COD and sulphate concentrations of the effluent from all-made deinking trials are within the limits of Croatian legislative (NN 80/13, 2013) and can be safely discharged into the environment without any treatment. At Figures 2.a, c, f. their emission limits in paper industrial waste waters effluents are presented. TOC values and nitrate concentrations for paper industrial effluents are not defined by this legislative; they are only defined for surface water (TOC 30 mg C/L, Nitrate 2,0 mg/L). The summary of effluent characteristics determinate in this research is presented in Table 4.

Table 4: Summary of effluent characteristics from newspaper chemical flotation deinking

Physico-chemical characteristics	T1		T2		T3	
	Foam	Pulp	Foam	Pulp	Foam	Pulp
pH	8.337	8.357	8.007	8.158	8.097	8.277
Electrical conductivity (EC), $\mu\text{S}/\text{cm}$	913	911	905	888	943	922
Sulphate, mg/L	20	20	40	20	20	20
Nitrate, mg/L	5.9	6.4	15.4	14.2	7.2	6.2
Total Organic Compound (TOC), mg/L	67	64	67	70	62	43
Chemical Oxygen Demand (COD), mg/L	140	109	169	115	133	101

4. CONCLUSIONS

Pulp and paper industry is disturbing the ecological balance of the environment by discharging a wide variety of raw wastewater (effluent). Depending upon the nature of raw material and used chemical agents, effluents from the paper industry are characterized by colour, extreme quantities of Chemical Oxygen Demand, Total Organic Compound, Biochemical Oxygen Demand, pH, chlorinated compounds, suspended solids (mainly fibres), fatty acids, tannins, resin acids, sulphur and sulphur compounds, etc. Thus, aquatic toxicity due to effluents derivate from this industry is an acute problem on a worldwide scale that needs to be resolved. This type of pollution caused by effluents is a complex environmental problem. So far, there are plenty treatment processes which are used to minimise these effects (reduction via aerobic, anaerobic and abiotic routes). But other strategy for resolving this problem is the use of alternate, cleaner technologies which could

give the same quality of the pulp. In this research it is confirmed that chemical agents significantly influence on wastewater effluent generated during chemical flotation deinking. The best physico-chemical characteristics of effluent from flotation deinking are achieved in trial 3, where Eco-alkali together with sodium silicate and hydrogen peroxide was used. The wastewater effluent produced from the Trial 3 was lower in pH, TOC and COD values than the chemical deinking process via INGEDE Method (T1). Measured electrical conductivity, sulphate and nitrate concentration of effluents from T1 and T3 are nearly the same or the same values. Therefore, Eco-alkali was found to have high potential as an alternative to the sodium hydroxide in flotation deinking process. According to obtained results this type of naturally gained alkali made from hardwood fly ash can definitely find use in the paper recycling industry.

5. ACKNOWLEDGMENTS

This research has been performed within the project "Straw triticale as a source of fibre in the production of newspaper" supported by the University of Zagreb.

6. REFERENCES

- [1] Ali, M., Sreekrishnan, T.R.: "Aquatic toxicity from pulp and paper mill effluents: a review", *Advances in Environmental Research*, 5, 175-196, 2001.
- [2] Dumea, N., Lado, Z., Poppel, E.: "Differences in the recycling Behaviour of paper printed by various techniques", *Cellulose chemistry and technology*, 43 (1-3), 57-64, 2009.
- [3] Faul, A. M.: "Quality requirements in graphic paper recycling", *Cellulose chemistry and technology*, 44 (10), 451-460, 2010.
- [4] Ferguson, L.D.: "Deinking Chemistry", *Tappi Journal*, Deinking Seminar Notes, TAPPI PRESS, Atlanta, 75-83, 1992.
- [5] Finch, J.A., Hardie, C.A.: "An example of innovation from the waste management industry: Deinking flotation cells", *Minerals Engineering*, 12 (5), 467-475, 1999.
- [6] Giri, J., Srivastava, A., Pachauri, S.P., Srivastava, P.C.: "Effluents from Paper and Pulp Industries and their impact on soil properties and chemical composition of plants in Uttarakhand, India", *Journal of Environment and Waste Management*, 1 (1), 026-032, 2014.
- [7] INGEDE, International Association of the Deinking Industry 2009, URL: <http://ingede.com/ingindx/methods/ingedemethod-11p-2009.pdf>. (last request 12-8-2014)
- [8] Kesalkar, V.P., Khedikar, I.P., Sudame, A.M.: "Physico-chemical characteristics of wastewater from Paper Industry", *International Journal of Engineering Research and Applications (IJERA)*, 2 (4), 137-143, 2012.
- [9] Lee, C.K., Ibrahim, D., Ibrahim, C.O., Rosli, W.D.W.: "Enzymatic and chemical deinking of mixed office wastepaper and old newspaper: paper quality and effluent characteristics" *BioResources* 6(4), 3859-3875, 2011.
- [10] Maheshwari, R., Rani, B., Saxena, A., Prasad, M., Singh, U.: "Analysis of effluents released from recycled paper industry", *Journal of Advanced Scientific Research*, 3 (1), 82-85, 2012.
- [11] Papić, S., Grčić, I., Koprivanac, N., Meixner J.: "Obrada industrijske otpadne vode iz proizvodnje vinil-klorida primjenom koagulacije, flokulacije i Fentonova procesa", *Polimeri*, 31 (3-4), 100-106, 2010.
- [12] Plazonić, I., Barbarić-Mikočević, Ž., Džimbeg-Malčić, V., Ignjatić Zokić, T., Milčić D.: "The New Environmental Friendly Newspaper Deinking Approach", *ANQUE's International Congress of Chemical Engineering 2012*, (ANQUE ICCE 2012: Sevilla, Spain, 2012), 70-71, 2012.
- [13] Plazonić, I., Džimbeg-Malčić, V., Barbarić-Mikočević, Ž.: "A Novel Eco-Alkali Chemistry in Newspaper Flotation Deinking", *Acta graphica*, 23, 91-98, 2012.
- [14] Pravilnik o graničnim vrijednostima emisija otpadnih voda, *Narodne novine* br. 80/13, 2013.

APPLICATION OF BENTONITE BASED FENTON CATALYST IN THE PROCESS OF REACTIVE DYE DEGRADATION

Milena Bečelić-Tomin¹, Đurđa Kerkez¹, Miljana Prica², Božo Dalmacija¹,
Dragana Tomašević¹, Gordana Pucar¹,

¹University of Novi Sad, Faculty of Sciences, Department of Chemistry,
Biochemistry and Environmental Protection, Novi Sad, Serbia

²University of Novi Sad, Faculty of Technical Sciences,
Department of Graphic Engineering and Design, Novi Sad, Serbia

Abstract: In the present study, cobalt oxide precursor was prepared and used for fabricating metal-bentonite composit. Composit was impregnated with Fe-salt and tested as catalyst in the Fenton process of Reactive Blue 4 degradation. Under the following experimental conditions: 50 mg/L Reactive Blue 4 solution; pH 3; 22° C; 20 mM H₂O₂ and 0.5 g/L catalyst dosage, 95.5% decolourization and 69.9 % COD removal could be achieved with 180 min of reaction. Hence, taking into account the favorable catalytic properties and low leaching of iron ions (<2 mg/L), impregnated bentonite catalyst is a promising catalyst for anthraquinone reactive dye degradation.

Key words: impregnated bentonite, Fenton process, reactive dye

1. INTRODUCTION

Textile manufacturing is one of the largest industrial producers of wastewaters, which are characterized by strong colour, highly fluctuating pH, high chemical oxygen demand (COD), and biotoxicity. Reactive dyes are frequently used for dyeing cotton, wool, and polyamide fibres. Traditional processes for treatment of these effluents prove to be insufficient to clean up the important quantity of wastewaters after different operations of textile dyeing and washing [Lahkimi et al., 2007]. In recent years, promising results have been achieved in the treatment of textile wastewaters using Advanced Oxidation Processes (AOPs) [Hammami et al., 2007; Sadik, 2007; Arslan-Alaton et al., 2008; Gözmen et al., 2009; Lei et al., 2010]. These processes involve the generation of HO° radicals which are considered the most powerful oxidizing agents in aqueous phase [Deng et al., 2010]. One of the methods of degradation of organic compounds in wastewater is Fenton process which involves of hydrogen peroxide and Fe ion to generate hydroxyl radicals in the solution [Wang, 2008]. Heterogeneous catalytic oxidation usually have some advantages such as easily operating at room temperature and normal pressure. Heterogeneous catalysts can be synthesised using cheap material supports such as activated carbon, clays, silica, etc. Clays have several advantages as a catalyst, due to their particular properties and structures as well as their abundance and low cost [Gil, 2000 et al.; Jiang, 2009]. Certainly, in the development of clay minerals as catalysts, their chemical functions generally need to be intensified to improve efficiency or effectiveness [Zhou et al., 2011]. A current trend is to use clay minerals to host nanoparticles. This strategy is a useful way to construct a stable platform for active nanocatalysts [Zhou and Keeling, 2013].

The aim of this work was examination of possibilities of use of the clay composites containing nanoparticles of cobalt oxide as catalyst in Fenton process of Reactive Blue 4 (RB4) decolourization.

2. METHODS

Commercial RB4 (CAS No. 13324-20-4, EC No. 236-363-6, pH 4.78), H₂O₂ (30 wt. %), H₂SO₄, NaOH, Na₂CO₃, Fe(NO₃)₃·9H₂O were obtained from Sigma-Aldrich and CoSO₄·xH₂O from MERCK. All chemicals used were analytical grade and used without further purification. All solutions were prepared with deionised water. All experiments were conducted at room temperature (25 ± 0.5°C). Figure 1 presents the structure of the dye investigated.

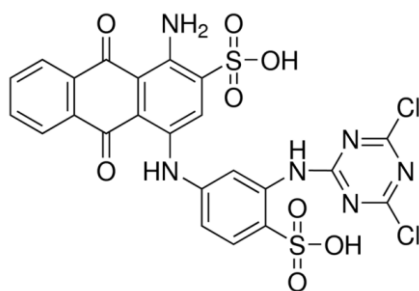


Figure 1: Structure of RB4 dye

Bentonite (Claris-p70) which was used in experiments is product of company Bentoproduct Ltd. from Šipovo. The bentonite had the following characteristics: montmorillonite (88–92 %), C.E.C. (90–120 meq/100 g), moisture (8–10%), pH (8–10 (5 g/100 ml)), As (<2 ppm), Pb (<2 ppm), Fe (<0,015 %), Na (<0,8 %), Ca (<0,8 %).

To prepare the cobalt precursor, has been used modified method according to the procedure of (Li et al., 2008). Cobalt hydroxide is prepared by stirring 100 ml of a 0.05 M $\text{CoSO}_4 \cdot 7\text{H}_2\text{O}$ and 33 ml of NaOH. After 30 min of ageing, hydroxide solution was added to 50 ml of acetic acid, thus forming the metal precursors. Then, these precursors are easy added to the prepared suspension of clay and stirred vigorously. After continuous stirring for 1 h, prepared samples were impregnated with 0.2 mol/L solution of $\text{Fe}(\text{NO}_3)_3 \cdot 9\text{H}_2\text{O}$. Prepared suspension was vigorously stirred 15 min and left at room temperature 24h. After ageing time, all the suspensions were centrifuged and the resulting solids were washed three times with deionized water, re-dried for 24 h at 100 °C and calcinated at 500°C (4 h).

The prepared samples were labelled as: B_R —raw bentonit, B_{Co} —bentonite pillared with Co^{2+} and $\text{B}_{\text{Co/Fe}}$ —bentonite pillared with Co^{2+} and impregnated with Fe^{3+} .

The experiments of Fenton process were conducted on a jar test apparatus (FC6S Velp scientific, Italy), where reactive mixtures with 0.1L volumes were continually mixed in 0.5 L laboratory cups, at 150 rpm. The experiments were performed in the following manner: firstly, the appropriate PA dosage (0.5–1.5 g L^{-1}) was added to the model dye solution (RB4 concentration from 50 to 200 mg L^{-1}), which was followed by pH adjustment to the desired value (2.5–5.2), and the addition of the required amount of H_2O_2 (5–25 mM). Each experiment lasted 180 min. Samples were centrifuged at 12000 rpm for 15 min to remove solid particles. The aliquots were subsequently filtered through a 0.45 μm pore size membrane filter and immediately analyzed thereafter.

Structural analysis of prepared materials (B_R , B_{Co} and $\text{B}_{\text{Co/Fe}}$) was performed by using 77 K N_2 adsorption–desorption isotherms by Autosorb iQ Surface Area Analyzer (Quantochrome Instruments, USA). Samples were outgassed at 120 °C for 2 h before running isotherms. Multi-point BET (Brunauer–Emmett–Teller) method was used to determine specific surface area. Mesopore volumes were derived from desorption isotherms using BJH (Barrett–Joyner–Halenda) model and micropore volumes were calculated using t-test method.

Decolourization of the synthetic dye solution was monitored by absorbency (A) at $\lambda_{\text{max}}=594.78$ nm (UV/VIS spectrophotometer, Shimadzu, Japan). Chemical oxygen demand (COD) concentrations were determined by Termoreactor ECO6, Velp Scientifica, Italy. The pH was measured by pH-meter inoLap pH/ION 735 (WtW GmbH, Germany).

3. RESULTS

3.1 Structural characteristics of bentonite

Structural characteristics of raw and modified bentonite derived from N_2 adsorption–desorption isotherms, are presented in Table 1. B_{Co} has a similar structural characteristics as well as the B_R while sample $\text{B}_{\text{Co/Fe}}$ has lower values of the parameters that characterize the structure of the material.

Table 1: Structural characteristics of raw and modified bentonite

Sample	Parameter				
	BET (m ² /g)	Micropore t-test (cm ³ /g)	BJH method mezopore (cm ³ /g)	Total pore volume (cm ³ /g)	Average pore diameter (Å)
B _R	97.162	0.028	0.076	0.1026	21.2
B _{Co}	99.780	0.031	0.074	0.0956	19.17
B _{Co,Fe}	88.337	0.025	0.075	0.0914	20.7

3.2 Catalytic activity of the modified bentonite

Decolourization efficiencies obtain applying raw and modified bentonite (B_R, B_{Co} and B_{Co,Fe}) and different process (Fenton process with H₂O₂ or adsorption process without H₂O₂) are shown on Figure 2. Decolourization efficiencies achieved by applying B_{Co,Fe}+H₂O₂ was 95.5%. Other processes have not proved to be effective (decolourization of approximately 10%).

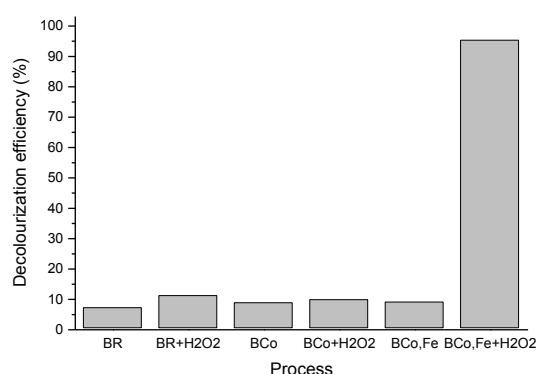


Figure 2: Decolourization efficiency of RB4 dye using raw and modified bentonite

The effects of various experimental parameters (solution pH, initial concentration of H₂O₂, catalyst (B_{Co,Fe}) and dye RB4 concentration) on process efficiency and iron leaching are presented in Figure 3.

The effect of initial pH on the RB4 removal was investigated in the range of 2.5 to 5.2 (Figure 3a). There is general agreement in the literature that is optimal pH for Fenton process pH 3 because the solution is not acidic enough to cause significant leaching of iron, on the other hand, such environments do not cause the conditions for precipitation [Iurascu et al., 2009; Herney-Ramirez and Madeira, 2010]. In this study, the maximum dye (95.5%) removals was obtained at pH 3. High efficiency is achieved at pH 2.5 (95.6%) also, but at this pH values was detected the greatest leaching of iron, 1,28 mg L⁻¹.

Figure 3b shows the dependency of RB4 degradation efficiency on the initial concentration of H₂O₂. The high efficiency of approximately 95% was obtained at an initial hydrogen peroxide concentration of 5-20 mM H₂O₂. The optimal concentration is 20 mM H₂O₂, because at this concentration is achieved the high efficiency of decolourization and a minimum value of leached iron (0.2 mg L⁻¹).

The effect of B_{Co,Fe} concentration on the efficiency of the process was analyzed within the 0.5-1.5 g L⁻¹ range (Figure 3c). Increasing the amount of catalyst B_{Co,Fe} leads to a decrease of Fenton process efficiency. On the other hand, there is an increase in the iron content in the solution with increasing amounts of catalyst.

The effect of the initial concentration of RB4 on the decolourization was investigated at 50, 100 and 200 mg L⁻¹ RB4 (Figure 3d). In the case of samples with a concentration of 100 and 150 mg L⁻¹ RB4 degradation efficiency are high also, but there is a significant increase in the leaching of iron, 1,887 mg L⁻¹ and 2,104 mg L⁻¹ respectively.

The efficiency of the applied treatment in mineralization of the RB4 solution was measured under optimal conditions (50 mg/L Reactive Blue 4 solution; pH 3; 22 °C; 20 mM H₂O₂ and 0.5 g/L catalyst dosage) determined in optimization of decolourization process in the prescribed contact time. Maximum reduction of COD reached after 180 min from the start of the reaction was 69.9 %.

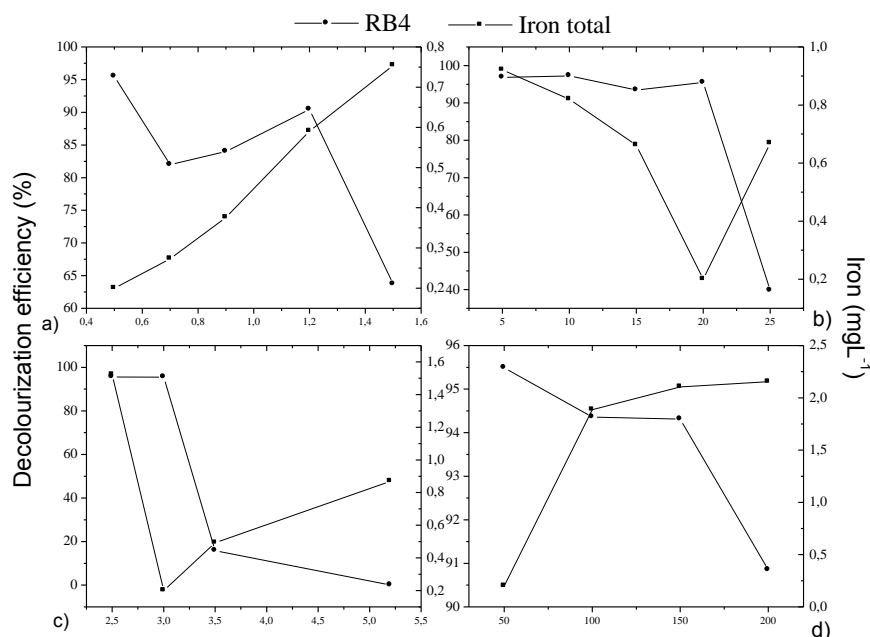


Figure 3: Effects of operational parameters on process efficiency and iron leaching: a) pH; b) H₂O₂ concentration; c) catalyst concentration; d) RB4 concentration

4. DISCUSSION

According [Fabrizzi et al., 2002], the common characteristics after incorporation of the cationic precursor into modified and non-modified support are the reduction of the specific surface area and pore volume as a result of the partial blocking of the pores by catalytic precursors. In this case, higher surface area of raw bentonite in comparison to B_{Co} suggests that the latter sample is subjected to compact packing in the interlamellar layer resulting in more serious pore blocking that inhibits the passage of nitrogen molecules [Caglar et al., 2009]. These results are in the contrast to the results obtained by [Li et al., 2008] which indicate an increase in the surface of laponite after modification. It is assumed that is the reason for this disagreement in the first place kind of clay which is used in the process of modification. Namely, the surfaces in delaminated structure of laponite are more accessible for nitrogen molecules during the gas sorption experiments. The delamination of clays could enhance significantly their surface areas as well as pore volumes. In addition, because the laponite platelets are very small, the edge areas in this type of clay can contribute significantly to the total surface areas. Thus the increased edge surfaces generated from the part breakdown of the clay platelets are also partially responsible for the enhancement of the specific surface areas [Li et al., 2008]. In contrast, the edge area for montmorillonite is typically very small (<1%) of the total surface area for the particles. The edge surface area for montmorillonite is therefore expected to be less important for the enhancement of the specific surface areas [Saunders et al., 1999]. Certainly, results for the average pore diameter are approximate values (~ 20 Å), so we can assume that (1) metal particles entering the smaller pores, thereby increasing the pore size and (2) metal particles enter the larger pores reducing the mean pore size. Therefore, these two reverse trend does not lead to significant changes in average pore size [Su et al., 1999].

The share of the dye adsorption on the surface of raw and modified bentonite in the overall efficiency of decolourization is low (processes without H₂O₂ in Figure 2). It can be concluded that application of modified bentonite in Fenton processes (B_{Co,Fe}+H₂O₂) plays an important role in the RB4 removal.

The results indicate that the Fenton process with the use of B_{Co,Fe} as well as the conventional Fenton process [Walling, 1975; Kang et al., 2002], shows highest efficiency for pH ≤ 3 and decreasing trend of decolourization efficiency with increasing pH of solution.

RB4 removal is enhanced with increasing H₂O₂ dosage until reaching the optimum dosage, since it is the source of •OH radicals produced in the Fenton process. Leaching of iron is not only a consequence of the acidic conditions of the reaction, but also consequence of extremely important

relationship of the catalyst and concentration of H_2O_2 (Sotelo et al., 2004; Martínez et al., 2005). According (Herney-Ramirez and Madeira, 2010; Nidheesh et al., 2013; Hassan and Hameed, 2014), fall of the efficiency is due to production of HO_2^\bullet caused by abstraction of HO^\bullet by the present excess of hydrogen peroxide in solution.

Harmful effect of increased amounts of catalyst, in this case, 1.5 mg L^{-1} , where the efficiency is low (63.71%), and leaching of the highest (0.754 mg L^{-1}), can be explained by the great increase in the Fe (III) ions due to the increase of the total content dissolved solids catalyst which had a negative impact on efficiency (Babuponnusami and Muthukumar, 2014).

Generally, increasing the dye concentration to values above 100 mg L^{-1} decreased the dye degradation effect. Namely, the increase of the dye concentration leads to an increase in the dye molecules in the solution, with the same number of $\bullet\text{OH}$, which has such an effect as a consequence. In heterogeneous Fenton process, the reaction occurs at the catalytic surface between $\bullet\text{OH}$ radicals generated at the active sites and RB4 molecules adsorbed on the surface. Thus, when the RB4 concentration is too high, the number of active sites available is decreased by the RB4 molecules due to their competitive adsorption on the catalytic surface. In addition, the intermediates product of RB4 oxidation might also compete for the limited adsorption sites with RB4 molecules, which blocked their interactions with Fe(II)/Fe(III) active sites (Lahkimi et al, 2007, Chen et al., 2008).

5. CONCLUSIONS

Bentonite pillared with Co^{2+} and impregnated with Fe^{3+} has been proved to be a superior catalyst for decolourization of RB4 in a modified Fenton process. The best operation parameters for the modified Fenton oxidation are 0.5 g L^{-1} of catalyst ($\text{B}_{\text{Co,Fe}}$), and 20 mM of H_2O_2 for an initial RB4 concentration of 50 mg L^{-1} at pH 3. Under these conditions, 95.5% decolourization and 69.9% mineralization of RB4 in aqueous solution was achieved within a 180 min reaction time. Values of leached iron are in the range which is below the permitted limits determined in the EU Directives.

6. ACKNOWLEDGMENTS

This research was financed by the Ministry of Science and Technological Development of Republic of Serbia (Project III43005 and TR37004).

7. REFERENCES

- [1] Arslan-Alaton, I., Gursoy, BH, Schmidt, JE: "Advanced oxidation of acid and reactive dyes: effect of Fenton treatment on aerobic, anoxic and anaerobic processes", *Dyes and Pigments*, 78, 117–130 2008.
- [2] Babuponnusami, A., Muthukumar, K.: „A review on Fenton and improvements to the Fenton process for wastewater treatment" *Journal of Environmental Chemical Engineering*, 2, 557–572, 2014.
- [3] Caglar, B., Afsin, B., Tabak, A., Eren, E.: „Characterization of the cation-exchanged bentonites by XRPD, ATR, DTA/TG analyses and BET measurement" *Chemical Engineering Journal*, 149, 242–248, 2009.
- [4] Chen, A., Ma, X., Sun, H.: "Decolorization of KN-R catalyzed by Fe-containing Y and ZSM-5 zeolites" *Journal of Hazardous Materials*, 156, 568–575, 2008.
- [5] Deng, Y., Rosario-Muniz, E., Ma, X.: "Effects of inorganic anions on Fenton oxidation of organic species in landfill leachate" *Waste Management and Research*, 30(1), 12–19, 2010.
- [6] Fabrizio, P., Burgi, T., Burgener, M., Doorslaer, S., Baiker, A.: "Synthesis, structural and chemical properties of iron oxide-silica aerogels" *Journal of Materials Chemistry*, 12, 619–630, 2002.
- [7] Gil, A., Gandía, L.M., Vicente, M.A.: "Recent advances in the synthesis and catalytic applications of pillared clays" *Catalysis Reviews-Science and Engineering*, 42, 145–212, 2000.
- [8] Gözmen, B., Kayan, B., Gizir, MA, Hesenov, A.: „Oxidative degradations of reactive blue 4 dye by different advanced oxidation methods" *Journal of Hazardous Materials* 168,129–136, 2009.
- [9] Hammami, S., Oturan, N., Bellekhal, N., Bellekhal M., Oturan, MA: "Oxidative degradation of direct orange 61 by electro-Fenton process using a carbon felt electrode: application of the experimental design methodology", *Journal of Electroanalytical Chemistry* 610, 75–84, 2007.

- [10] Hassan, H., Hameed, B.H.: „Fe-clay as effective heterogeneous Fenton catalyst for the decolorization of Reactive blue 4“ *Chemical Engineering Journal*, 171, 912–918, 2011.
- [11] Herney-Ramirez, J., Madeira, L.M.: „Use of pillared clay-based catalysts for wastewater treatment through Fenton –like processes“ in „Pillared clays and related catalysts“ (ed. Gil, A., Korili, S.A., Trujillano, R., Vicente, M.A.) [Springer science, New York, ISBN 978-1-4419-6669-8, 2010], 129.
- [12] Iurascu, B., Siminiceanu, I., Vione, D., Vicente, M.A., Gil, A.: „Phenol degradation in water through a heterogeneous photo-Fenton process catalyzed by Fe-treated laponite“ *Water Research*, 43, 1313–1322, 2009.
- [13] Jiang, J., Ma, K., Zheng, Y., Cai, S., Li, R., Ma, J.: „Cobalt salophen complex immobilized into montmorillonite as catalyst for the epoxidation of cyclohexene by air“, *Applied Clay Science*, 45, 117–122, 2009.
- [14] Kang, N., Lee, D.S., Yoon, J.: „Kinetic modeling of Fenton oxidation of phenol and monochlorophenol“ *Chemosphere*, 47, 915–924, 2002.
- [15] Lahkimi, A., Oturan, M.A., Oturan, N., Chaouch, M.: „Removal of textile dyes from water by the electro-Fenton process“ *Environmental Chemistry Letters* 5, 35–39, 2007.
- [16] Lahkimi, A., Oturan, M.A., Oturan, N., Chaouch, M.: „Removal of textile dyes from water by the electro-Fenton process“ *Environmental Chemistry Letters*, 5, 35–39, 2007.
- [17] Lei, F., Shi-Jie, Y., Guo-quan, Z., Feng-Lin, Y., Xiao-Hong, F.: „Degradation of azo dyes using in-situ Fenton reaction incorporated into H₂O₂-producing microbial fuel cell“ *Chemical Engineering Journal* 160, 164–169, 2010.
- [18] Li, J.J., Mu, Z., Xu, X.Y., Tian, H., Duan, M.H., Li, L.D., Hao, Z.P., Qiao, S.Z., Lu, S.Q.: „A new and generic preparation method of mesoporous clay composites containing dispersed metal oxide nanoparticles“ *Microporous and Mesoporous Materials*, 114, 214–221, 2008.
- [19] Martínez, F., Calleja, G., Melero, J.A., Molina, R.: „Heterogeneous photo-Fenton degradation of phenolic aqueous solutions over iron-containing SBA-15 catalyst“ *Applied Catalysis B: Environmental*, 60, 181–190, 2005.
- [20] Nidheesh, P., Gandhimathi, R., Ramesh, S.T.: „Degradation of dyes from aqueous solution by Fenton processes: a review“ *Environmental Science and Pollution Research*, 20, 2099–2132, 2013.
- [21] Sadik, W.A.: „Effect of inorganic oxidant in photodecolourization of azo dye“, *Journal of Photochemistry and Photobiology A: Chemistry* 191, 132–137, 2007.
- [22] Saunders, J.M., Goodwin, J.W., Richardson, R.M., Vincent, B.: „A small-angle X-ray scattering study of the structure of aqueous laponite dispersions“ *Journal of Physical Chemistry: B*, 103, 9211–9218, 2009.
- [23] Sotelo, J.L., Ovejero, G., Martínez, F., Melero, J.A., Milien, A.: „Catalytic wet peroxide oxidation of phenolic solutions over a LaTi_{1-x}Cu_xO₃ perovskite catalyst“ *Applied Catalysis B: Environmental*, 47, 281–294, 2004.
- [24] Su, H., Zeng, S., Doing, H., Zhang, Y., Hu, R.: „Pillared montmorillonite supported cobalt catalysts for the Fisher-Tropsch“ *Applied Clay Science*, 46, 325–329, 1999.
- [25] Walling, C.: „Fenton’s reagent revisited“ *Accounts of Chemical Research*, 8, 125–131, 1975.
- [26] Wang, S.: „A comparative study of Fenton and Fenton-like reaction kinetics in decolourisation of wastewater“ *Dyes and Pigments*, 76, 714–720, 2008.
- [27] Zhou, C.H., Keeling, J.: „Fundamental and applied research on clay minerals: From climate and environmental to nanotechnology“ *Applied Clay Sciences*, 74, 3–9, 2013.
- [28] Zhou, C.H.: „An overview on strategies towards clay-based designer catalysts for green and sustainable catalysis“ *Applied Clay Science*, 53, 87–96, 2011.

THE AMOUNTS AND PROPERTIES OF DUST RELEASED FROM LASER PRINTERS

Borislav Simendić¹, Vesna Marinković¹, Vesna Teofilović², Nevena Vukić²¹ Higher Education Technical School of Professional Studies, Novi Sad, Serbia² University of Novi Sad, Faculty of Technology, Novi Sad, Serbia

Abstract: In the last decade, sales of laser printers have increased. Nowadays every office and more and more homes own one or even more. But like any other technology, this should be used with precautions due to health concerns that have been pointed out. Some studies have found increased levels of ultra-fine particles in offices with laser printers. It is known that inhalation of ultra-fine particles can cause respiratory problems. To understand how to use laser printer safely, without any risk, it is necessary to study this problem more thoroughly. In this study Casella Microdust Pro device was used for the determination of the particles concentration in the air during operation of laser printer. This device can measure the concentration of particles between 0.01 and 2500 mg/m³ using the techniques of light scattering angle. Two identical printers were chosen and tested with different operation speeds and print quality. Obtained results showed that during operation, laser printers release ultra-fine particles, but the particle concentration number did not exceed the maximal allowed limit of 4 mg/m³. For comparison of toner particles and particles emitted from laser printer was used Apex pump with filter to collect particles emitted from laser printer during operation. Toner particles were obtained directly from toner. All samples were recorded at Motic microscope and results were compared. Differences in size and shape were observed. It was shown that particles emitted from laser printer are not the plain toner particles. When toxicity of toners is being studied, it is important to study not only toners, but also particles that are collected directly from the laser printer during its operation.

Key words: laser printer, toner particles, dust concentration, occupational health.

1. INTRODUCTION

In almost every industry, there is dust, whether it is used as a raw material, utility product, or created as intermediate product, waste material or finished product (Simendić et al, 2012). Dust, char and various gases mixed with moisture help carbon dioxide to create a cloud (buffer) above the ground, which causes the greenhouse phenomenon (Simendić et al, 2012). For occupational health purposes, the dust is classified by size into three categories (Milanko et al, 2010):

- Respiratory dust, diameter smaller than or equal to 5 µm, small enough to penetrate deep into the lungs (alveoli) in the neck, throat and upper respiratory tract.
- Inhalable dust, diameter size of 10 µm, which is usually trapped in the nose, throat and upper airways.
- The total dust, all airborne particles regardless of their size and composition.

Dust is present in printing and media technology, as well. In the process of laser printing, toner particles when activated through external influences, mixed with dust that is already in the printer, and the cellulose particles of dust that are created from friction between the paper and printer rollers under the influence of heat, form tiny dust particles that can remain in the air some time (Tang et al, 2012). In such a floating state it is highly likely that these particles penetrate the respiratory system and leave the consequences to human health. Extensive tests conducted by McGarry et al. showed that workers in the office are constantly exposed to certain concentrations of particles. Most of them are in the ultrafine range, but majority of these particles is not emitted from the printer.

Morawska et al. have been studying and comparing the high- and low-emitting printers in order to determine what the crucial difference between them is. They found out that main difference is the temperature instability of the heater during the short break between printing two pages. If the printer does not reduce the energy that causes the heating before the next paper is fed, the temperature rapidly rises until it loads a new sheet to absorb excess heat.

Vensing et al. investigated the characteristics and the number of ultra-fine particles (UFP) emitted by laser printers and multifunction devices during operation. Results from test chamber confirmed that laser printers emit fine particles with aerodynamic diameters up to 100 nm. They showed that the test chamber is useful tool for physicochemical characterization, as well as for comparison of different printers under controlled and standard conditions. They also concluded that a direct link between the results of the test chamber and offices with printers is very weak, due to the different behavior of particles in them, as well as a long residence time in the indoor air of aerosols, especially in the case of poor air mixing or ventilation. In addition, they showed efficacy of commercially available filters on the reduction of the UFP concentration. They concluded that the installation of external filter does not automatically lead to a reduction in the concentration of UFP. Significantly decreasing of total emission of UFP by using an efficient filter is possible only if the air flow through the printer is designed on the way that most of the UFP is released out of the printer through a defined opening.

Koivisto et al. have found a relationship between the measurements in the test chamber and the motion of particles in the room considering the ventilation system and based on that relationship, created a model of motion of printer emissions in the room. This model can be used in studies of internal sources of emissions, or as a tool for development and design of ventilation systems.

For these reasons it is important to determine the concentration of dust particles that is released during printing process. In this paper, we tried to determine the impact of printer resolution, date of production of printer and the size of the room to the average concentration of dust particles in the air, in order to determine the safest way of handling the printer.

2. EXPERIMENTAL

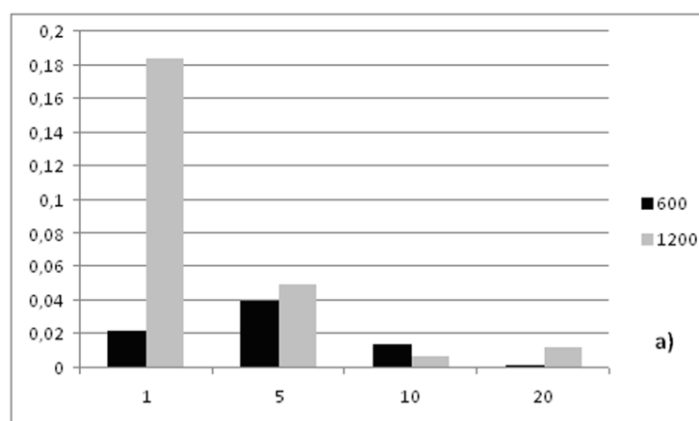
The average concentrations of particles in the air during printing were measured using a device Microdust Pro, Casella (UK). This device can measure concentrations of particles in the following range from 0.1 to 2500 mg/m³.

The results of dust concentration measuring in real time are shown as TWA, average value of the mass concentration of total dust. First measuring was performed at the distance of 5 cm from the printer. The data was obtained for quantity of 1, 5, 10 and 20 sheets. For newer and older printer printing was done at 600 and 1200 dpi. For newer printer measuring was done in econo mode (mode for toner saving), as well. For newest printer, measuring was done in the best, normal and draft mode. Second measuring was performed at a distance of 1 m from printer.

The dust from the laser printer was analyzed by microscope, Motic (PRC) with magnification 20 x, daylight. Particles size was measured approximating the three points.

3. RESULTS

Figure 1 presents results of measured concentrations of dust particles during printing of 1, 5, 10, and 20 sheets at a different printing resolutions (Figure 1a: The influence of resolutions during printing on older printer (600 and 1200 dpi); Figure 1b: Printing is done in the normal and econo mode with resolutions of 600 dpi and 1200 dpi, where higher resolution means that higher amounts of toner particles are applied to the printing surface; Figure 1c: Printing is done on the newest printer in the best, normal and draft mode).



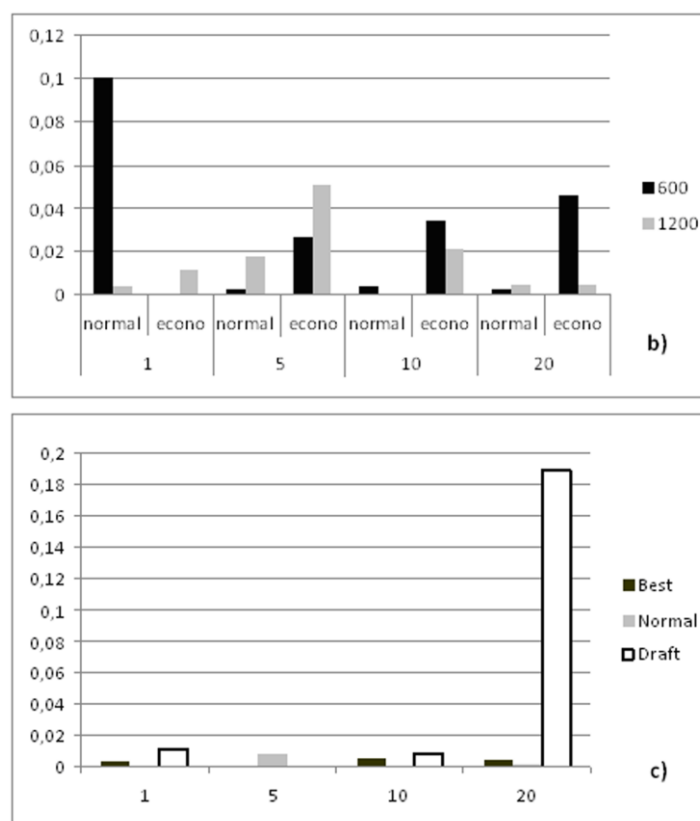


Figure 1: The influence of volume on the concentration of dust particles at different resolutions in a) older, b) newer and c) the newest printer

Figure 2 shows measured concentrations of dust in real time during printing volume of one sheet with a resolution of 1200 dpi.

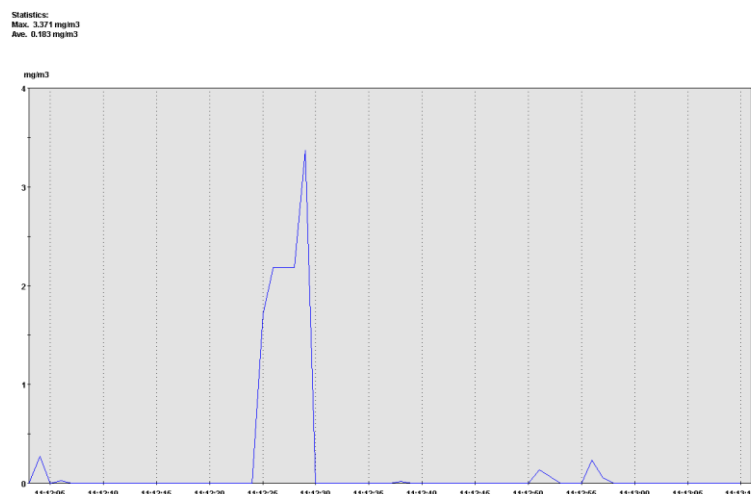


Figure 2: The concentrations of dust in real time during printing volume of one sheet

From the Figure 2 it can be seen that the maximal concentration reaches a value of 3.37 mg/m³ after 30 s and immediately after, value drops to less than 0.5 mg/m³. The average value of this measure amounted to 0.103 mg/m³, which is significantly lower value than the maximal allowed value, which is 4 mg/m³. Figure 3 shows measured concentration of dust in real time during printing volume of 20 sheets with a resolution of 1200 dpi.

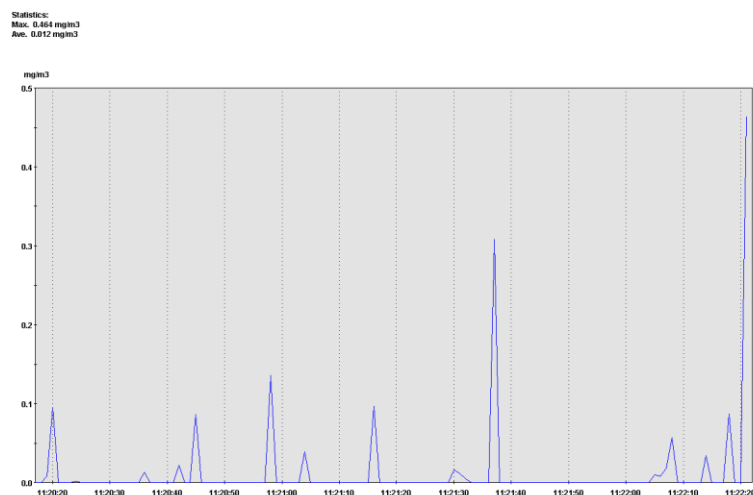


Figure 3: The concentrations of dust in real time during printing volume of 20 sheets

From the Figure 3 it can be seen that the maximal concentration is significantly lower than in the previous case and reaches a value of 0.464 mg/m^3 after 120 s. The average value of this measure is 0.013 mg/m^3 , which is significantly lower value than the maximal allowed value [4 mg/m^3]. By measuring dust concentration of particles at the distance of 1 m from the printer, concentration of dust was 0 mg/m^3 .

The results of microscopic analysis are shown in Figure 4.

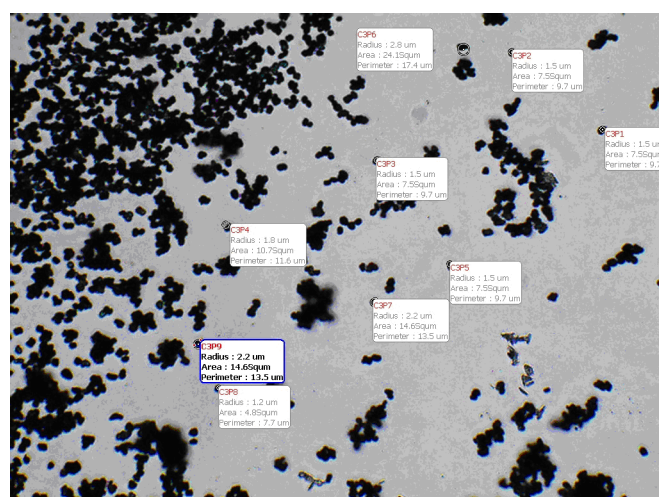


Figure 4: The appearance of dust from the printer with magnification 20 X

The results which determine the share of individual fractions of particles based on microscopic analysis are shown in Table 1.

Table 1: Weight content of the particle size of the toner dust

Particles	The content of the particles [%]
The diameter less than $2.5 \mu\text{m}$	38.2
The diameter of $2.5 \mu\text{m}$ to $10 \mu\text{m}$	45.3
The diameter larger than $10 \mu\text{m}$	14.5

4. DISCUSSION

At the beginning of the printing process, the average concentration of the particles was higher, in some cases, more than 1 mg/m^3 probably due to accumulated dust, which is activated when the printing is started and lifted into the atmosphere. During printing of five sheets, average

concentration decreases to less than 0.1 mg/m^3 . The average particle concentration and maximal particle concentration were greater at a resolution of 1200 dpi, probably as a result of greater activity of printer at 1200 dpi. Achieved concentrations are within tolerable limits of 4 mg/m^3 . However, during long-term printing in a closed room it is possible that concentration of dust particles increases and crosses the limit. For this reason, as a preventive measure, a room containing a laser printer should be periodically ventilated.

Comparing the econo and normal mode, it can be seen that the average and maximal concentrations of dust during printing in econo mode are lower than the initial concentrations of dust when using the normal mode. After printing of five sheets in econo mode, dust concentration becomes higher than in normal mode, which indicates that the fixation of toner particles to the surface is weaker in the econo mode than in normal mode. The absence of particles in the range of 1 m is probably due to scattered movement of particles in all directions from the printer. That is why in the range of 1 m from printer, concentration of particles in the air is diluted to less than 0.1 mg/m^3 . Based on the microscope analysis results, it can be noticed that the content of particles smaller than $10 \text{ }\mu\text{m}$ is more than 85% (totally suspended dust), wherein the inhalation dust content is 45.3%, and respiratory dust content is 38.2%. The inhalation dust that comes from the toner (45.3%) will remain in the front parts of the respiratory tract, and 38.2% of respiratory dust will come in the alveoli, and then into the bloodstream.

5. CONCLUSION

In the industrial toxicology, where is necessary to adjust production and occupational safety measures, is important to know maximal allowed concentrations (MAC), i.e. concentrations of a gas, vapor or dust to which employee can be exposed eight hours/five days a week for several years without any consequences to health. In this paper is shown that during the operation of a laser printer, a certain amount of dust is released in environment, which can have a negative impact on human health. Measured average dust concentrations are within acceptable limits. Results of analysis in econo and normal printer mode showed that the econo mode releases greater amounts of dust compared to the normal mode. Measurement of particles concentration during printer operation in real time showed that the dust concentration is higher at the start of printing and decreases during printing process.

From the results of the dust concentration at a distance of 1 m from the printer, it was concluded that 1 m is optimal distance in which operator will be safe from inhaling potentially harmful amount of dust particles. The microscope analysis of dust samples showed that printer dust content which can penetrate into the alveoli was 38.2%. Since in this paper is shown the impact of the laser printing process on the emission of dust, further investigations had to take into account the influence of the printing substrate on this problem. It is necessary to create a standard for measuring the concentration of dust particles in the air, and to determine maximal allowed concentrations of these particles for the working environments with printers and copier machines.

6. REFERENCES

- [1] Koivisto, A.J. et al.: "Impact of particle emissions of new laser printers on modeled office room", *Atmos. Environ.* 44 (17), 2140–2146, 2010
- [2] McGarry, P. et al.: "Exposure to Particles from Laser Printers Operating within Office Workplaces", *Environ. Sci. Technol.*, 45 (15), 6444–6452, 2011.
- [3] Morawska, L. et al.: "An Investigation into the Characteristics and Formation Mechanisms of Particles Originating from the Operation of Laser Printers", *Environ. Sci. Technol.*, 43 (4), 1015–1022, 2009.
- [4] Simendić, B. et al.: "Značaj određivanja prašine mineralnog porekla u keramičkoj indutriji", *Zbornik radova "Bezbednosni inženjering"*. Novi Sad, Serbia, 2012.
- [5] Tang, T. et al.: "Investigations on cytotoxic and genotoxic effects of laser printer emissions in human epithelial A549 lung cells using an air/liquid exposure system", *Environ. Mol. Mutagen.*, 53 (2), 125–135, 2012.
- [6] V. Milanko et al.: "Neophodnost određivanja opasnih količina prašine u indutriji", *Zbornik radova "Bezbednosni inženjering"*. Kopaonik, Serbia, 2010, 447–454.
- [7] Wensing, M. et al.: "Ultra-fine particles release from hardcopy devices: Sources, real-room measurements and efficiency of filter accessories", *Sci. Total Environ.*, 407 (1), 418–427, 2008.

DECOLOURIZATION OF REACTIVE RED 120 BY AN ADVANCED FENTON PROCESS IN CONJUNCTION WITH ULTRASOUND

Đurđa Kerkez¹, Milena Bečelić-Tomin¹, Miljana Prica², Dragana Tomašević¹,
Gordana Pucar¹, Božo Dalmacija¹, Srđan Rončević¹;

¹ University of Novi Sad, Faculty of Sciences, Department of Chemistry, Biochemistry and Environmental Protection, Novi Sad, Serbia

² University of Novi Sad, Faculty of Technical Sciences, Novi Sad, Serbia

Abstract: In this study, nano zero valent iron stabilized with carboxymethyl cellulose [CMC-nZVI] was used as catalyst in the Fenton process of Reactive Red 120 (RR120) decolourization. Under the following experimental conditions: 50 mg/L RR120 solution; pH 3; 25°C; 4mM H₂O₂ and 11.2 mg/L CMC-nZVI dosage, 87% decolourization could be achieved with 60 min of reaction. Coupling the Fenton system with the ultrasound has further contributed to increasing the efficiency of decolourization of the tested dye, reaching 97%. Also, the maximum decolourization was achieved in a relatively short period of time, which contributes to energy savings due to the shortening of the whole process. Overall increase in acoustic power and period of active pulsation had positive effect on the efficiency of decolourization of this azo reactive dye.

Key words: Fenton process, ultrasound, azo dye, nano zero valent iron

1. INTRODUCTION

Dyes are important sources of water pollution and their degradation products may be carcinogens and toxic to mammals. It is estimated that about 15% of the total production of dyes are lost and discharged in the effluent during dye production and dying process. Azo dyes make up the majority (60–70%) of the dyes applied in textile processing and are considered to be recalcitrant, non-biodegradable and persistent (Al-Amrani et al., 2013; Fu et al., 2010). Various treatment methods, such as coagulation and flocculation, adsorption and ultrafiltration have been investigated to remove azo dyes from the wastewater. These high cost processes do not destroy dye molecules but only transfer them from one phase to another (Arslan-Alaton et al., 2008).

Fenton process is particularly attractive and effective to degrade a wide range of azo dyes. It is also relatively cheap and easy to perform compared to other AOPs processes. More recently nZVI is widely applied for wastewater treatment and organic compounds degradation in Fenton system (Choi and Lee, 2012). nZVI has the advantage that the small particle size results in a large specific surface area and great intrinsic reactivity of surface sites. However, nZVI nanoparticles tend to either react with surrounding media or agglomerate, resulting in significant loss of reactivity. To prevent particle aggregation, a wide variety of stabilizers have been proposed to modify nZVI particle surface characteristics (Wang et al., 2013; He and Zhao, 2005; Ponder et al., 2000). Also, recently, there is developing research about coupling the Fenton system with the ultrasound due to the synergistic effect, which accelerates the oxidation process (Weng et al., 2013).

This research is concerned with the optimizing the parameters of the heterogeneous Fenton process using nano zero-valent iron stabilized with carboxymethyl cellulose [CMC-nZVI] for the decolourization of azo dye solution of Reactive Red 120 (RR120). Also, further research has included testing and optimization of ultrasound usage in order to further improve the efficiency of decolourization process.

2. METHODS

All chemicals were purchased commercially and were used without further purification. CMC-nZVI was prepared using conventional liquid-phase method by the reduction of ferric iron by borohydride. Two initial sets of experiments were conducted to determine the optimum conditions for RZ B-NG degradation.

By conducting batch experiments, various parameters affecting the degradation of RR120 using CMC-nZVI in Fenton system were investigated, such as nanomaterial dosage, H₂O₂ concentration, solution pH, initial dye concentration and reaction kinetics. Reaction mixtures were stirred at 150

rpm at room temperature ($25 \pm 2^\circ\text{C}$) to desired time intervals. Following this, the solutions were centrifuged and the residual dye concentration was measured.

Decolourization of synthetic dye solution was monitored by absorbance measurement, A , at the wavelength of maximum absorbance, λ_{max} (512 nm), using a UV Vis spectrophotometer PG Instruments UV 1800 (Shimadzu, Japan). Ultrasound experiments were conducted on the unit BANDELIN electronic SONOPULS, typ: UW 2200, Berlin, 2013. The efficiency of dye decolourization was obtained by the application of the following formula (1):

$$(A_0 - A_t)/A_0 \times 100 = \text{Decolourization efficiency (\%)} \quad (1)$$

All experiments were performed in triplicate and results are presented as average values of the triplicate data. For dye degradation kinetic analysis mathematical model according to Behnajady, 2007 (Behnajady et al., 2007) was used.

3. RESULTS

The study included determination of optimal conditions for decolorization of RR120, while varying the CMC-nZVI dosage, hydrogen peroxide concentration, pH, initial dye concentration and determination of the reaction kinetics. The obtained results are shown in Figure 1.

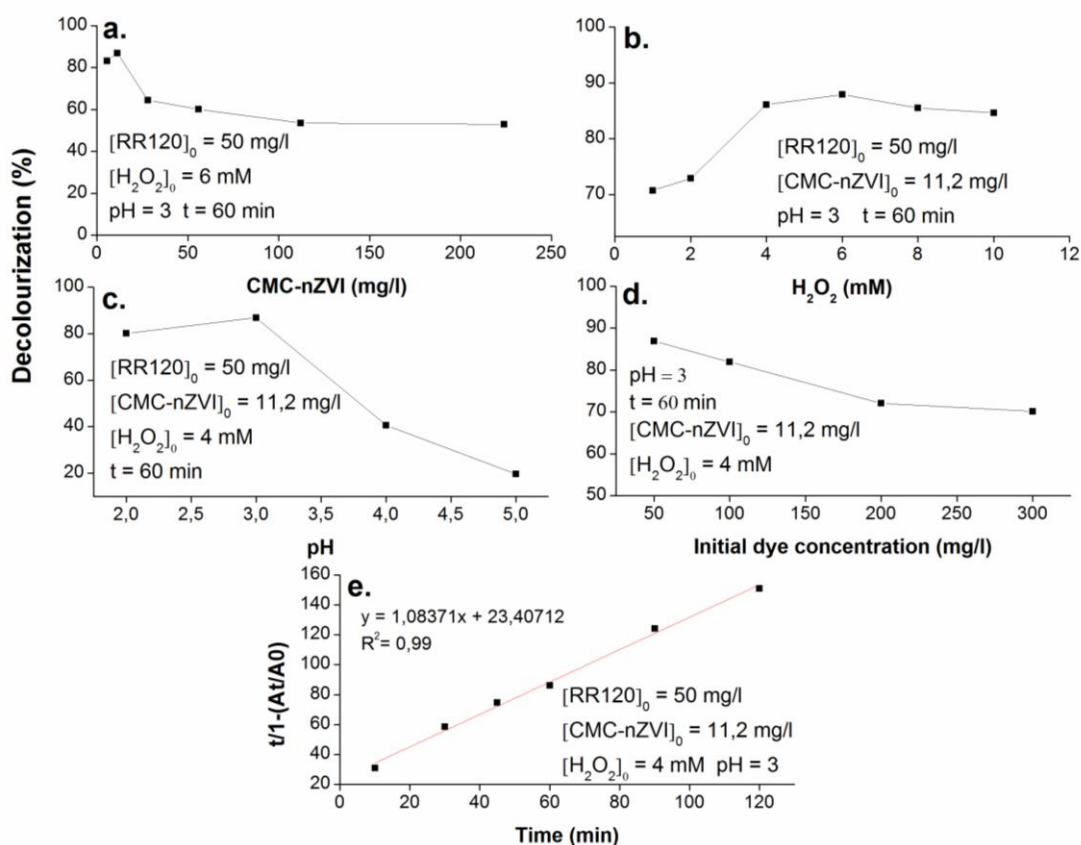


Figure 1: Optimization of RR120 solution decolourization, a. Effect of CMC-nZVI dosage; b. Effect of H_2O_2 concentration; c. Effect of initial solution pH; d. Effect of initial dye concentration; e. Kinetics

Figure 1a shows the dependence of the efficiency of RR120 solution decolourization regarding the concentration of CMC-nZVI. Increasing the concentration of CMC-nZVI led to the increased decolourization efficiency due to higher concentration of active sites on the surface of nanomaterials which accelerated the initial Fenton reaction. The optimum concentration of CMC-nZVI was 11.2 mg/l wherein the decolourization efficiency was 87%. Further increase in the concentration of nanomaterials did not contribute to decolourization increase (Ghaneian et al., 2008). This may be explained by the fact that higher concentrations of iron ions could lead to

scavenging of $\text{HO}\cdot$ radicals (Hassan and Hameed, 2011), and induce the decrease in dye decolorization. Also the high iron loading can lead to nZVI particles agglomeration resulting, again, in decreased decolorization efficiency. Figure 1b shows the dependence of the efficiency RR120 solution decolourization regarding the applied hydrogen-peroxide concentration. H_2O_2 concentration was varied within the range of 1 to 10 mM. The highest decolourization efficiency of 86% was achieved at an initial H_2O_2 concentration of 6 mM. However, due to cost effectiveness the concentration of 4mM was used in further experiments because the results do not significantly differ from those with 6mM. When the hydrogen peroxide concentration was greater than 6mM the decolourization efficiency of RR120 was almost unchanged or even decreased. Namely, in the presence of excess H_2O_2 , its scavenging effect towards $\cdot\text{OH}$ radicals is significant, resulting in the formation of less reactive species such as $\text{HO}_2\cdot$. Figure 1c shows the influence of solution pH on the RR120 decolourization, as one of the most important parameters which influences the Fenton process. The effect of pH was monitored at the values of 2, 3, 4 and 5 (which is the pH value of dye solution without additional adjustment). It can be seen that the most effective decolorization was achieved at pH 3, stating 87% (Hassan and Hameed, 2011). The effect of the initial dye concentration is shown in Figure 1d. The highest decolourization efficiency was achieved at a concentration of 50 mg/L. It can be seen that with dye concentration increase, the decolourization efficiency decreases. The presumed reason is that when the initial concentration of RR120 is increased, the $\text{HO}\cdot$ concentration is not increased correspondingly (Rache et al., 2014).

R^2 value of 0.99, derived from a linear regression of the kinetic experiment confirms the use of the chosen model for the analysis of the kinetics, and the resulting value of the coefficient indicates that the nZVI stabilized with carboxymethyl cellulose is an excellent heterogeneous source of catalytic iron in the Fenton system, as can be seen in the Figure 1e (Behnajady et al., 2007).

3.1 Establishing the effect of ultrasound on the decolorization of the RR120 solution

Once the optimum conditions of the Fenton oxidation, CMC-nZVI/ H_2O_2 , for RR120 solution decolourization, the ultrasound, CMC-nZVI/ H_2O_2 /US was applied in the selected time interval (5 min). In Figure 2a the results of the decolourization efficiency of Fenton process with or without the use of ultrasound are shown. It can be seen clearly, that the use of ultrasound contributed to the acceleration of Fenton reaction, particular in the initial stage of the process. Also in Figure 2b, comparison of Fenton process with ultrasound, and the use of the sole hydrogen-peroxide and the CMC-nZVI in combination with ultrasound are presented.

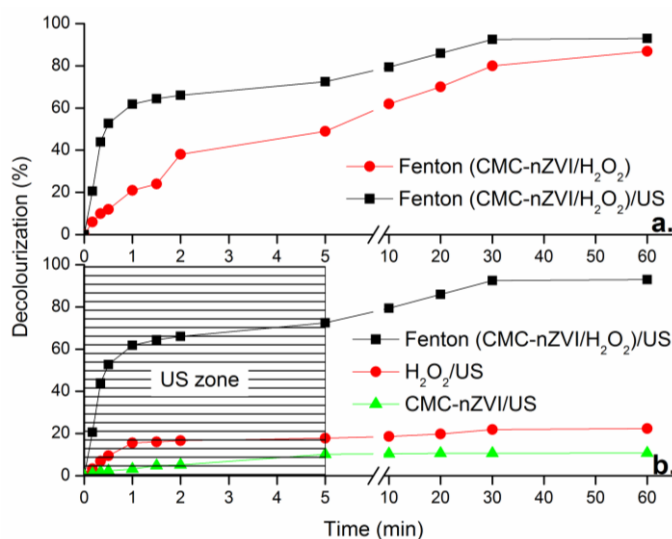


Figure 2: a. Comparison of CMC-nZVI/ H_2O_2 and CMC-nZVI/ H_2O_2 /US process;
b. Comparison of CMC-nZVI/ H_2O_2 /US, H_2O_2 /US and CMC-nZVI/US process on the efficacy of RR120 solution decolourization

It can be seen that when using CMC-nZVI/H₂O₂/US system achieved decolourization efficiency was 93%, while at the same time in the system H₂O₂/US and CMC-nZVI/US achieved decolourization efficiencies were 22 and 11%, respectively (Ghaneian et al., 2008). Ultrasound power is then varied by the power amplitude 10%, 25% and 50%. The obtained results are shown in Figure 3. The ultrasound power is an important factor influencing the rapid formation of Fe²⁺ as a result of a cavitation increase. With a stronger force higher efficacy of decolourization, in shorter time, was achieved. The study also involved varying the active pulsation of ultrasound at power of 50% with the used cycle pulsing of 1, 5 and 9. The results are shown in Fig 4. The efficiency of decolourization of RR120 solution increases with the increase of the active interval of ultrasound pulsation, as there is a longer time period of solution exposure to the ultrasound.

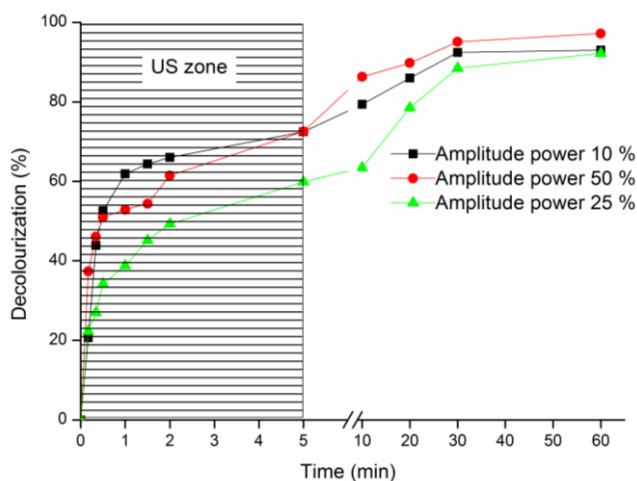


Figure 3: Decolourization efficiency of RR120 solution at different ultrasound amplitude power

Nevertheless, differences in the results obtained, when the active interval is 0.5 to 0.9 seconds are negligible and it is energy-efficient to use a shorter active interval in which the decolourization efficiency achieved is 97%.

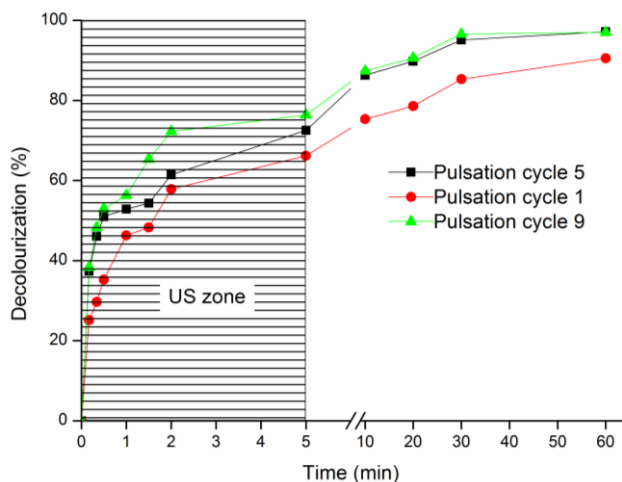


Figure 4: Decolourization efficiency of RR120 solution at different active pulsation cycles of ultrasound

4. CONCLUSIONS

This paper focused on examining the possibility of using nano zero valent iron coated with carboxymethyl cellulose [CMC-nZVI] for decolourization of RR120 solution. The study involved comparison of different operating conditions: CMC-nZVI dose, H₂O₂ concentration, pH value of the solution, initial dye concentration as well as monitoring the reaction kinetics.

Based on the obtained results it can be concluded that the nano zero-valent iron in combination with carboxymethyl cellulose shows high reactivity, and achieves high decolourization efficiencies. Also, mentioned parameters of Fenton systems have a great impact on the efficiency of the process. The most effective decolourization of the dye solution of RR120 was achieved at a CMC-nZVI dosage of 11.2 mg/l, dye concentration of 50 mg/l, H₂O₂ concentration of 4 mM, and the pH 3. When these conditions were applied the achieved decolourization efficacy was 87%. The use of ultrasound has further contributed to increasing of the decolourization efficiency. Also, the highest decolourization efficiency was achieved in a relatively short period of time, which contributes to energy savings due to the shortening of the entire process. Overall increase in power amplitude and period of active pulsation contributed to increasing of the decolourization efficiency. When using ultrasound for 5 minutes, with amplitude power of 50% and active pulsation period of 0.5 seconds, the decolourization efficiency increased, as the Fenton reaction was accelerated. Maximum decolourization efficacy achieved was 97%.

5. ACKNOWLEDGMENTS

The project is co-financed by kind support of Provincial Secretariat for Science and Technological Development of the Autonomous Province of Vojvodina (Grant no. 114-451-1158). Additionally, the authors acknowledge the financial support of the Ministry of Education and Science of the Republic of Serbia (project No. III43005).

6. REFERENCES

- [1] Al-Amrani, WA., Lim, PE., Seng, CE., Ngah, WSW.: "Factors affecting bio-decolorization of azo dyes and COD removal in anoxic– aerobic REACT operated sequencing batch reactor", J Taiwan Inst Chem E., <http://dx.doi.org/10.1016/j.jtice.2013.06.032>. 2013.
- [2] Arslan-Alaton, I., Gursoy, BH., Schmidt, JE.: "Advanced oxidation of acid and reactive dyes: Effect of Fenton treatment on aerobic, anoxic and anaerobic processes", Dye Pigments. 78, 117–30, 2008;
- [3] Behnajady, MA., Ghanbary, F., Modirshahla, N.: "A kinetic model for the decolorization of C.I Acid Yellow 23 by Fenton process", J Hazard Mater., 148, 98–102, 2007.
- [4] Choi, K., Lee, W.: "Enhanced degradation of trichloroethylene in nano-scale zero-valent iron Fenton system with Cu(II)", J Hazard Mater. 211– 212, 146– 53, 2012.
- [5] Fu, F., Wang, Q., Tang, B.: "Effective degradation of C.I. Acid Red 73 by advanced Fenton process", J Hazard Mater. 174, 17–22, 2010.
- [6] Ghaneian, SJ., Ghanizadeh, G., Hashemian, M.T., Moussavi, G., Khavanin, A., Rezaee, A.: "Decolorization of Reactive Blue 19 from Textile Wastewater by UV/H₂O₂ Process", J. Appl. Sci. 8, 1108–1112, 2008.
- [7] Hassan, H., Hameed, BH.: "Fe–clay as effective heterogeneous Fenton catalyst for the decolorization of Reactive Blue 4", Chem Eng J. 171, 912–8, 2011.
- [8] He, P., Zhao, D.: "Preparation and characterization of a new class of starch stabilized bimetallic nanoparticles for degradation of chlorinated hydrocarbons in water", Environ Sci Technol 39, 3314–20, 2005.
- [9] Ponder, S., Darab, J., Mallouk, T.: "Remediation of Cr(VI) and Pb(II) aqueous solutions using supported, nanoscale zerovalent iron", Environ Sci Technol. 34, 2564–69, 2000.
- [10] Rache, ML., García, AR., Zea, HR., Silva, AMT., Madeira, LM., Ramírez, JH.: "Azo-dye orange II degradation by the heterogeneous Fenton-like process using a zeolite Y-Fe catalyst—Kinetics with a model based on the Fermi's equation", Appl Catal B-Environ. 146, 192– 200, 2014.
- [11] Wang, X., Yang, J., Zhu, M.: "Effects of PMMA/anisole hybrid coatings on discoloration performance of nano zerovalent iron toward organic dyes", J Taiwan Inst Chem E. <http://dx.doi.org/10.1016/j.jtice.2013.08.019>. 2013.
- [12] Weng CH., Lin, YT., Chang, CK., Liu, N.: "Decolourization of direct blue 15 by Fenton/ultrasonic process using a zero-valent iron aggregate catalyst", Ultrasonics Sonochemistry 20, 970–977, 2013.

THE LEACHING OF ZINC FROM PRINTED GRAPHIC PRODUCT WASTE

Savka Adamović¹, Miljana Prica¹, Jelena Radonić¹, Maja Turk Sekulić¹,
Dragan Adamović¹, Snežana Maletić²

¹ University of Novi Sad, Faculty of Technical Sciences, Novi Sad, Serbia

² University of Novi Sad, Faculty of Sciences, Novi Sad, Serbia

Abstract: When considering different types of pollutants in landfill leachate, metals are especially interesting because of their persistence and toxicity. Laboratory leaching tests are common tools in aiding the assessment of long-term impact of contaminated materials on the soil-groundwater pathway, as they determine the source term as an expression of release potential of water soluble contaminants during the disposal of waste materials. The discharge of metals into a landfill is not limited to a short period. For a long period after the dumping at a landfill, and also after the closure of a landfill, the leaching of heavy metals will continue. Obviously, the waste graphic products, as part of municipal waste solid components, may have different environmental risks based on the metals leached. This paper is aimed at determining the metal leaching potential of soil deposited printed graphic product waste and identifying the factors that affect their metal emission based on the results of the leaching tests.

Key words: printed graphic product waste, zinc, leaching, soil, landfill

1. INTRODUCTION

Waste legislative in Republic of Serbia gives opportunity for establishment of arranged system for waste management but its implementation is not at a satisfying level at the moment, especially in the area of recycling of all kinds of graphic products (Monte et al., 2008). Strategic approach is needed for resolving this problem, with clearly defined action plan in whose making all relevant governmental institutions should take part in. Significant contribution to environmental protection could be achieved by implementation adequate steps with used and wasted graphic products.

Lack of recycling of graphic products waste, causes another problem – potential of its component leaching to different environmental mediums. Generally, many kinds of printed graphic products are part of municipal solid waste (MSW). As the final MSW disposal method, landfill is a widely accepted technology, especially in developing countries. However, treatment of MSW by landfill has been, and still is, connected with a risk of pollution (Long et al., 2011). The large number of cases of groundwater pollution at landfills and substantial resources spent in remediation suggest that landfill leachate is a significant source of pollutants (Kassasi et al, 2008; Prechtai et al., 2008).

When considering different types of contaminants in landfill leachate, heavy metals are especially dangerous because of their persistence and toxicity. Heavy metals can be transferred to the ecosystem components such as underground water and crops, and can thus affecting human health through the water supply and food web. The printed graphic products waste may contain metals that are potentially dangerous for the environment. Those potentially hazardous pollutants, after printed graphic products waste disposition and degradation can migrate to different mediums and have a negative impact on the environment, initially in the soil of sewage and municipal landfills. Accordingly, it is necessary to monitor their impact through migration (leaching) from printed graphic products waste in defined environmental medium (firstly to sewage and municipal landfills soil). More over, changes in environmental conditions, such as acidification (acid rain), changes in the redox potential conditions or increases in organic ligand concentrations can cause metals mobilisation from the solid to the liquid phase and favour the contamination of surrounding groundwaters.

It is very important to design laboratory scale experiments that can mimic acidic and high organic load conditions in landfills. Essentially, degree of leaching from printed graphic products waste is defined by leach resistance. Leaching is known to be a complex phenomenon because many factors may influence the release of specific constituents from a waste over a period of time. These factors include major element chemistry, such as pH value, redox potential, complexation, liquid-to-solid ratio, contact time, etc. Since not enough is known about the chemical species present in printed graphic products waste and their behaviour over time, the long-term performance of this waste forms is difficult to predict. Overall, the leaching of

pollutants from printed graphic products waste after their disposal into land may have certain implications on the environmental management activities especially in Serbia since highest percentage of these products is still deposited in landfills.

This paper presents the leaching potential of zinc from printed graphic product waste into the water and soil based on the use of laboratory scale leaching (migration) tests.

2. MATERIALS AND METHODS

Leaching (migration) test was performed to investigate the possibility of zinc removal from waste color printed poster in simulated environmental mediums. Waste printed poster samples for test migrations, were fragmented in pieces of the same size 7.0 cm x 8.0 cm (total area: 56.0 cm²) and mass of samples were 10±0.01 g. All samples were immersed into 50 ml of following neutral leaching solution (pH 7.0) only and with the leaching solutions (pH 7) above soil layer. Soil was sampled from municipal landfill with the initial zinc concentration of 62.1±0.9 mg kg⁻¹. Distilled water was used for all the solutions with the zinc concentration below detection limit. BLANK poster was printed with the primary (CMYK, TOYO INK CO., LTD., Japan) inks by sheetfed offset printing technique. The test was performed on duplicate only with the leaching solution and the same amount of printed graphic product waste and relative standard deviation was less than 3%. This is the 60 day test and the analyzes were carried out in 1, 2, 3, 4, 5, 10, 20, 30, 40 and 60 day at room temperature. The concentrations of zinc in the solution and soil were determined using an atomic absorption spectrophotometer (Thermo Scientific - Solaar S Series AA spectrometer), flame technique in accordance with USEPA method 7000B after addition of HNO₃ (65%, p.a., Merck, Germany). For the calibration curve, stock solution containing 1000 mg of zinc/ml (AccuStandard, Inc. USA) was used. To compare experimental data and theoretical predictions of zinc impact from printed graphic product waste on soil we also used the partition coefficient, K_{sw} (K_s/K_w) from literature data [Đukić, 2003], by using concentration of zinc leached in neutral solution.

3. RESULTS AND DISCUSSION

Figure 1 presents zinc concentrations during the 60 day experiment of migration from investigated printed graphic product waste when neutral solution was used as leaching solution.

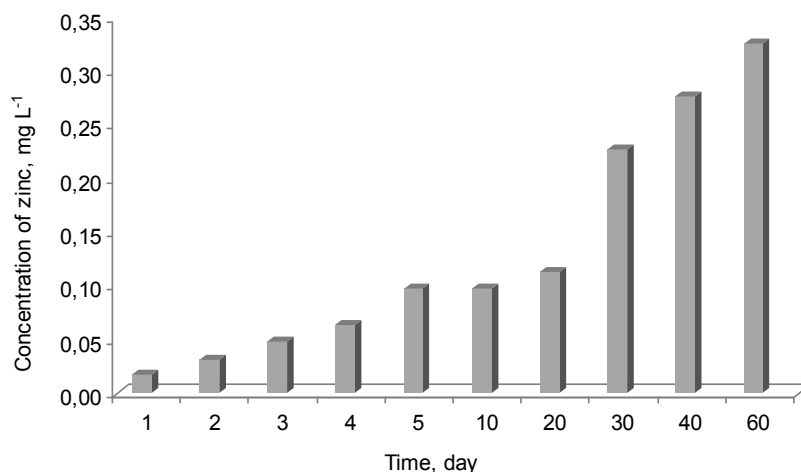


Figure 1: Zinc concentration (mg L⁻¹) in neutral (pH 7) leaching solution

From following product zinc showed migration: concentrations of zinc when neutral solution was used as a leaching solution were in range from 0.016 to 0.326 mg L⁻¹. Zinc concentration showed exponential growth with the increasing of contact time between printed product waste and the neutral solution.

Figure 2 presents zinc concentration during the 60 day experiment in the soil. Based on the results shown in Figure 2, we can conclude that the concentration of zinc is below the value set by the official regulations for soil (RS 23/94, RS 88/2010). The increase in zinc concentration varied over a range from 0.81 to 2.72 mg kg⁻¹ and increased with an increase of contact time between of

printed graphic product waste and the soil. Further ex-situ and in-situ testing are needed for a more realistic and detailed assessment of the impact of zinc from printed graphic product waste on environmental mediums, especially over a longer period of time as in real conditions this is a long term deposition.

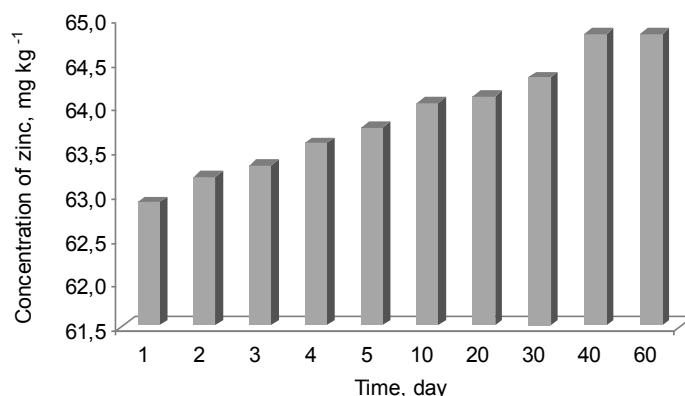


Figure 2: Zinc soil concentration (mg kg⁻¹) during the leaching experiment

Assessment of the impact of the migration of zinc from the investigated printed graphic product (poster) waste was made on the basis of mean values of the distribution coefficients K_{sw} for zinc, taken from literature data (Đukić, 2003):

$$K_{sw} = \frac{c_s}{c_w} \quad (1)$$

where are: K_{sw} - distribution coefficient (L kg⁻¹), c_s - zinc concentration in the soil (mg kg⁻¹) and c_w - zinc concentration in the water (mg L⁻¹).

Zinc soil concentrations were calculated and presented in Table 1. They represent the concentration that could originate from printed graphic product waste which was used in the experiment.

Table 1: Evaluation of zinc soil concentration (mg kg⁻¹) based on the distribution coefficients K_{sw}

Time (day)	1	2	3	4	5	10	20	30	40	60
c_s	1.2	1.4	1.6	1.7	1.8	2.0	2.1	4.3	5.2	6.2

Based on the results shown in Table 1, we can conclude that the concentrations of zinc in real experiment were lower than the predicted values. This could be due to the site specific soil properties that certainly need to be investigated and included in the further studies. Heavy metals, once introduced into the soil, remain for many years and, depending on their behaviour, are a potential threat to the ecosystem and human health. The speciation of heavy metals considerably influences their behaviour in the environment. Although no generally accepted definition of the term exists, speciation can broadly be defined as the identification and quantification of the different defined species, forms or phases in which an element occurs. The physico-chemical speciation of an element in environmental media controls its mobility and, ultimately and its bioavailability. Metals arising from different pollution sources enter the soil and may be partly retained by soil components. The processes of metal retention by solid phases of the soil are controlled by different mechanisms, such as adsorption to surface active mineral and organic constituents, diffusion in the primary and secondary mineral structures and precipitation as secondary phase. The organic matter, clay minerals, as well as Fe and Mn oxides are the most important components determining the sorption and desorption of heavy metals in soils (Vega et al., 2006). The organic components form stable metal-organic complexes with a variety of metals, while clay minerals and oxides concentrate heavy metal ions through surface ion exchange and metal-complex surface adsorption. Metal behaviour relies on various reactions, such as complexation reactions, ion exchange, sorption and desorption, precipitation and dissolution reactions, which are a function of both the properties of soil constituents and the chemical

speciation of trace metal (Bang and Hesterberg, 2004). Complexation reactions with organic ligands are known to influence the mobility of metal by either increasing or decreasing its sorption on mineral surfaces. Among the organic ligands, humic substances are the most important compounds naturally occurring in soils, sediments and waters. Among the various functional groups on humic substances, carboxyl and phenolic OH groups, the acidic functional groups, have high complexation capacities with metal ions enabling humic and fulvic acid to bind and/or remove heavy metals from soil. Based on all this, further ex-situ and in-situ testing are needed for a more realistic and detailed assessment of the impact of zinc and other heavy metals from printed graphic products waste on environmental mediums.

4. CONCLUSION

As the final MSW disposal method, landfill is a widely accepted technology, especially in developing countries. In Vojvodina, most part of the municipal solid waste is landfilled, but this kind of might be connected with a risk of pollution. Concentrations of zinc when neutral solution was used as a leaching solution were in range from 0.016 to 0.326 mg L⁻¹, while in soil it was in the range from 62.9 to 64.8 mg kg⁻¹. Zinc concentration showed exponential growth with the extension of contact time between waste product, solution and soil. From the results, we can see that there is some influence on quality of environmental mediums but concentrations of metals in soil are still below maximum allowable limits. This is an initial study and experiment should be spread to wider sorts of printed graphic products and in a longer time scale.

5. ACKNOWLEDGMENT

The authors acknowledge the financial support of the provincial secretariat for science and technological development, Autonomous Province of Vojvodina, in the frame of projects applied under the No. 114-451-4133/2013-03.

6. REFERENCES

- [1] Bang, J., Hesterberg, D.: "Dissolution of trace element contamination from two coastal plain soils as affected by pH", *Journal of Environmental Quality* 33 (3), 891-901, 2004.
- [2] Đukić, M.: "Distribution of some dangerous substances in the sediment-water systems at the Ratno Ostrvo Location in Novi Sad", Master thesis, Faculty of Sciences, University of Novi Sad, 2003 (in Serbian).
- [3] Kasassi, A., Rakimbei, P., Karagiannidis, A., Zabaniotou, A., Tsiouvaras, K., Nastis, A., Tzafeiropoulou, K.: "Soil contamination by heavy metals: measurements from a closed unlined landfill", *Bioresource Technology* 99 (18), 8578-8584, 2008.
- [4] Long, Y.Y., Shen, D.S., Wang, H.T., Lub, W.J., Zhao, Y.: "Heavy metal source analysis in municipal solid waste: Case study on Cu and Zn", *Journal of Hazardous Materials* 186 (2-3), 1082-1087, 2011.
- [5] Monte, M.C., Fuente, E., Blanco, A., Negro, C.: "Waste management from pulp and paper production in the European Union", *Waste Management* 29 (1), 293-308, 2008.
- [6] Official Gazzete RS 88/2010 (in Serbian).
- [7] Official Gazzete RS 23/94 (in Serbian).
- [8] Prechthai, T., Parkpian, P., Visvanathan, C.: "Assessment of heavy metal contamination and its mobilization from municipal solid waste open dumping site", *Journal of Hazardous Materials* 156 (1-3), 86-94, 2008.
- [9] Vega, F.A., Covelo, E.F., Andrade, M.L.: "A versatile parameter for comparing the capacities of soils for sorption and retention of heavy metals dumped individually or together: results for cadmium, copper and lead in twenty soil horizons", *Journal Colloid and Interface Science* 327 (2), 275-286, 2008.
- [10] USEPA 7000B, Flame Atomic Absorption Spectrophotometry.

Digital and web media

COMPARISON OF IMAGE PROCESSING OPERATIONS FOR ADJUSTMENT AND EVALUATION OF RENDERINGS GENERATED WITH DIFFERENT RENDERING ENGINES

*Helena Gabrijelčič Tomc, Nika Bratuž, Dejana Javoršek, Andrej Javoršek,
University of Ljubljana, Faculty of Natural Sciences and Engineering, Ljubljana, Slovenia*

Abstract: The field of 3D computer generated graphics is at its highest point being more popular every day and with demands of users getting even higher. The process of generating 3D computer graphics is complex and depends on great number of factors and their interplay and final result is anything but simply predictable. One of the factors influencing rendered image are certainly rendering engines whose working is combination of sophisticated algorithms. Not many research was done towards of understanding their influence on rendered image. Other downside is lack of standardised evaluation method in the field of 3D computer generated graphics. In this research, image processing operations were used to evaluate and to adjust 3D computer generated images. It was concluded that all applied methods can be used to adjust or improve image and that some methods can provide useful insight into differences between images. Furthermore, operations were applied on different colour and intensity channels and sometimes better results can be achieved when operating on intensity channel.

Key words: CIECAM02 colour appearance model, 3D computer generated graphics, 3D rendering

1. INTRODUCTION

Describing optical occurrences in physical world is a complex task and can be fulfilled only to some extent, but things tend to get even more complicated in 3D virtual space where all interactions between light and matter are generated by algorithms. 3D rendering is a complex process of converting 3D virtual space to 2D computer generated images and can be described in several steps. Generally, the process of generating 2D image consist of modeling, where basic geometry is set up and texturing, where optical characteristics of material are defined. Next to afore mentioned factors, camera and light source are also essential components and required to generate an image (Chopine, 2011). All this information about scene is taken into account by rendering engines, which in technical terms perform calculations that translate the scene from mathematical approximations of natural and optical occurrences to 2D image. Conversions are performed by calculations of different rendering algorithms built in rendering engines and can result in non-photorealistic or photorealistic effects (Erzetič, 2010). Rendering engines range from basic ray tracing algorithms to advanced algorithms that may include (bidirectional) path tracing, photon mapping and unbiased rendering. From users point of view, final visualization is a sum of (too) many factors and cannot be easily predicted. Trial and error approach can be time consuming, especially when rendering complex photorealistic images, so post production is certainly one of the solutions. Besides, each rendering method has some advantages or limitations when applied to 3D objects (Pharr, 2010). Performance assessment of rendering engines in 3D computer graphics is difficult, since it lacks proper testing methods and testing scenes that would provide reliable results and repeatability. Visual evaluation is one of the options, but cannot always provide measurable results and depends on many factors. One of the options not only for assessment but also for improvement of computer generated images is application of image processing operations, which include, but are not limited to histogram adjustments, spatial filtering and edge detection (Hladnik, 2010). Image processing operations can be performed on colour channels (e.g. red, green and blue) or on intensity channel, such as lightness or intensity. Typical representative of former type is RGB colour model and its derived colour spaces, used widely in the field of computer graphics and in software applications. Less represented are colour spaces based on intensity or lightness channel, despite the fact that human eye perceives differences on intensity level more easily then between colours (Burge, 2009). Colour pickers in computer graphics software usually offer intensity or lightness based options seeming that they are more intuitive for users than colour based pickers. Which method provides better results depend on a task performed (Gonzalez, 2009).

In this research, image processing operations were used as a tool for post-production and as a mean of image evaluation. The aim of this research was to determine which way of application of image processing operation is most suitable for certain situation and whether these operations can serve as general evaluation mechanism.

2. MATERIALS AND METHODS

In our research, images with simple background and single object (either draped dynamic cloth object or basic geometric object) were used. Also present on the scene, but not visible in rendered image were camera and light source. All setup parameters are listed in Table 1. Selected images were setup in either 3ds Max or Blender. Images containing dynamic cloth objects were set up identically for both rendering engines in 3ds Max. Images were rendered with Scanline renderer, which is based on visible surface determination and with mental ray, based on ray tracing and photon mapping algorithms. Scanline Renderer is a default versatile rendering engine that renders a scene as a series of from top to bottom generated horizontal scanlines. In mental ray, a production-quality rendering application, indirect illumination is produced by global illumination (in general terms photon mapping), final gather, caustics, ambient occlusion and the combination of irradiance particles and importons (visual particles) (3ds Max, 2014). 15 different images for each rendering engine were processed. Images containing basic geometric objects were rendered in Blender with Cycles rendering engine using path tracing algorithm and again 15 images with differently coloured objects were processed.

Table 1: Rendering parameters.

	3ds Max		Blender
Rendering engine	Scanline	mental ray	Cycles
Object	dynamic cloth object		basic geometric object
Lightning and intensity	standard light (omni): I=0.8,		spotlight, I=4000
Camera and focal length	target, 50 mm		automatic, 35 mm
format and size	tiff, 1920 × 1920		png, 800 × 800 pixels
Image processing	histogram adjustment, edge detection		spatial filtering

All image processing operations were carried out in Matlab with built-in functions (Image Processing Toolbox, 2014) with addition of Colour space Transformations (Getreuer, 2011). The course of image processing is shown in Figure 1.

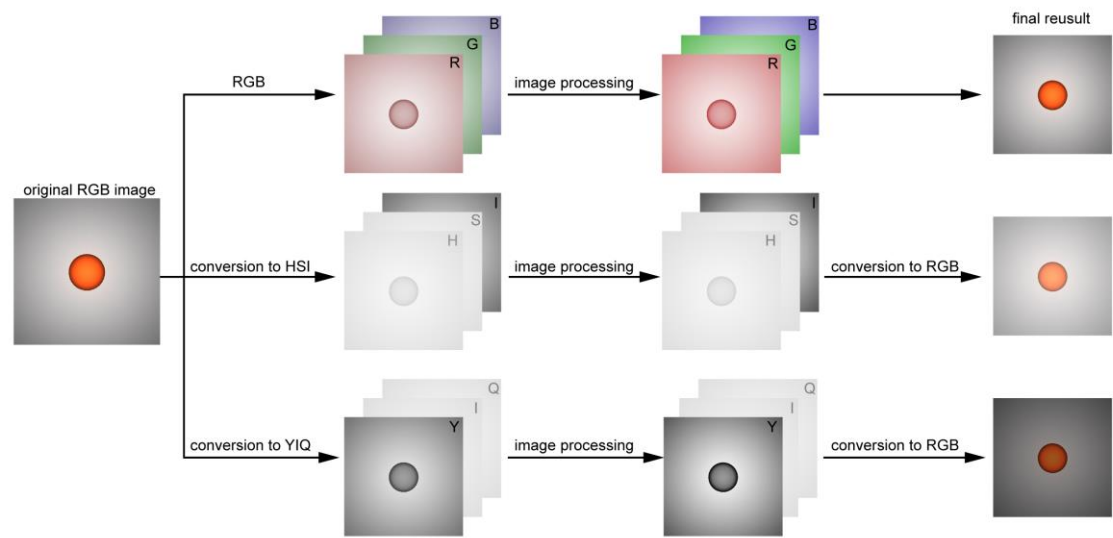


Figure 1: The course of image processing.

Original RGB image was converted to HSI and YIQ colour space. HSI colour space is intensity based colour space, composed of hue H, saturation S and intensity component I. YIQ colour space is used for encoding TV signals and is composed of luminance Y and two chromatic components I and Q (Burge, 2009). Image processing was performed on R, G and B channels simultaneously and on intensity channel I from HSI colour space and lightness channel Y from YIQ colour space separately to seek out most suitable method for given task.

First histogram adjustment was performed on images rendered with 3ds Max to improve image contrast and to evaluate differences between rendering engines. Histograms were stretched to its limits with *imadjust* and *stretchlimit* functions in Matlab (Image Processing Toolbox, 2014). Next, edge detection with Canny operator was performed on the same images to further demonstrate difference between rendered images with *edge* function in Matlab (Image Processing Toolbox, 2014). Finally spatial filtering was applied to images rendered with Blender's Cycles rendering engine. Due to its path tracing algorithm, Cycles produces noise on images, rendered with low number of ray passes. It can be avoided by running larger number of passes, which is time consuming or in post-production. Noise was reduced with average filter with *imfilter* and *fspecial* function (Image Processing Toolbox, 2014). Median filter was also applied as *medfilt2* function in Matlab (Image Processing Toolbox, 2014). Three representative samples for each operation were selected to be evaluated and are presented in the following section.

3. RESULTS AND DISCUSSION

To begin with, histogram stretching on RGB, I and Y channel was performed on samples rendered with Scanline rendering engine. Results are shown in Figure 2.

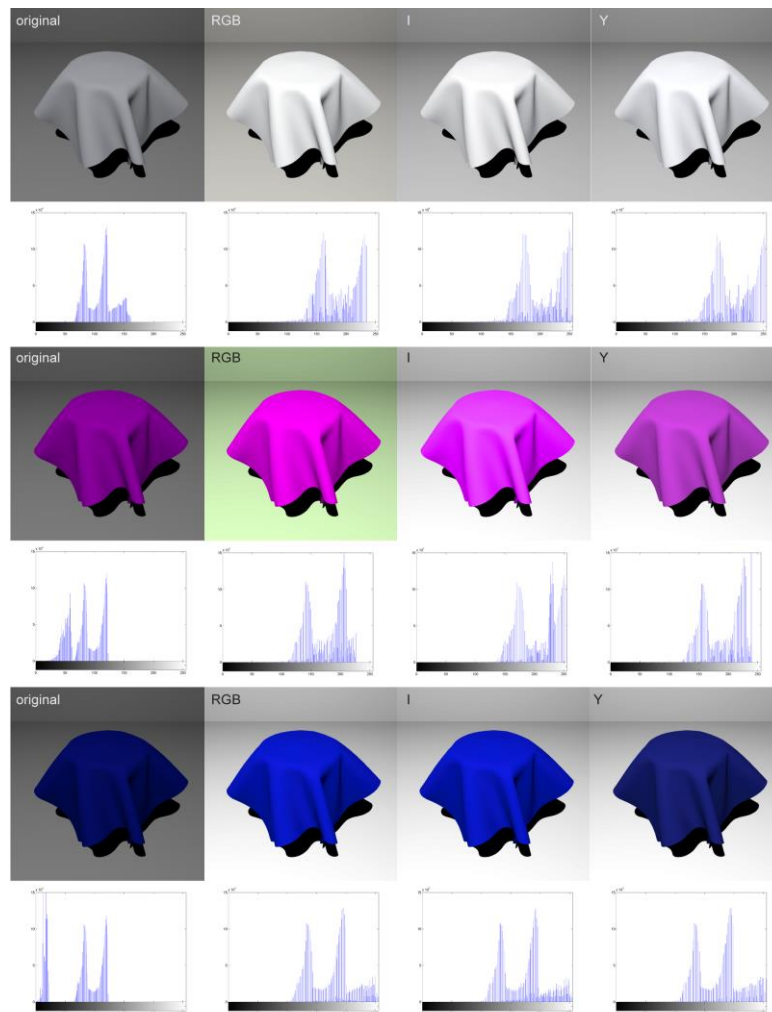


Figure 2: Histogram adjustment for original image rendered with Scanline rendering engine and images, adjusted on RGB, I and Y channel with corresponding histograms.

Contrast is visibly improved and adjusted images seem lighter which is most notable in the background. Lightness and saturation of dynamic cloth object depend on adjustment method. Histograms of original images are leaning to the left with very narrow distribution, high peaks and small coverage due to nature of original image with few colours and intensities. As a result, adjusted histograms cannot cover full range, but form comb distribution and peaks that lean toward lighter intensities. Shape of adjusted histogram depends on adjustment method and so does adjusted image. Firstly, unwelcome complementary tint on the background can be noticed when operating on RGB channels of dynamic cloth object, meanwhile object's colour is not affected. Tinting of the background is not present when adjusting on I or Y channel since both channels are intensity channels and do not contain any information about colour. Both methods present satisfactory results, though some highlights can become white when operating on I channel and saturated colours become less saturated in comparison with other methods when operating on Y channel. This occurrence is visible in Figure 2 for magenta and blue image.

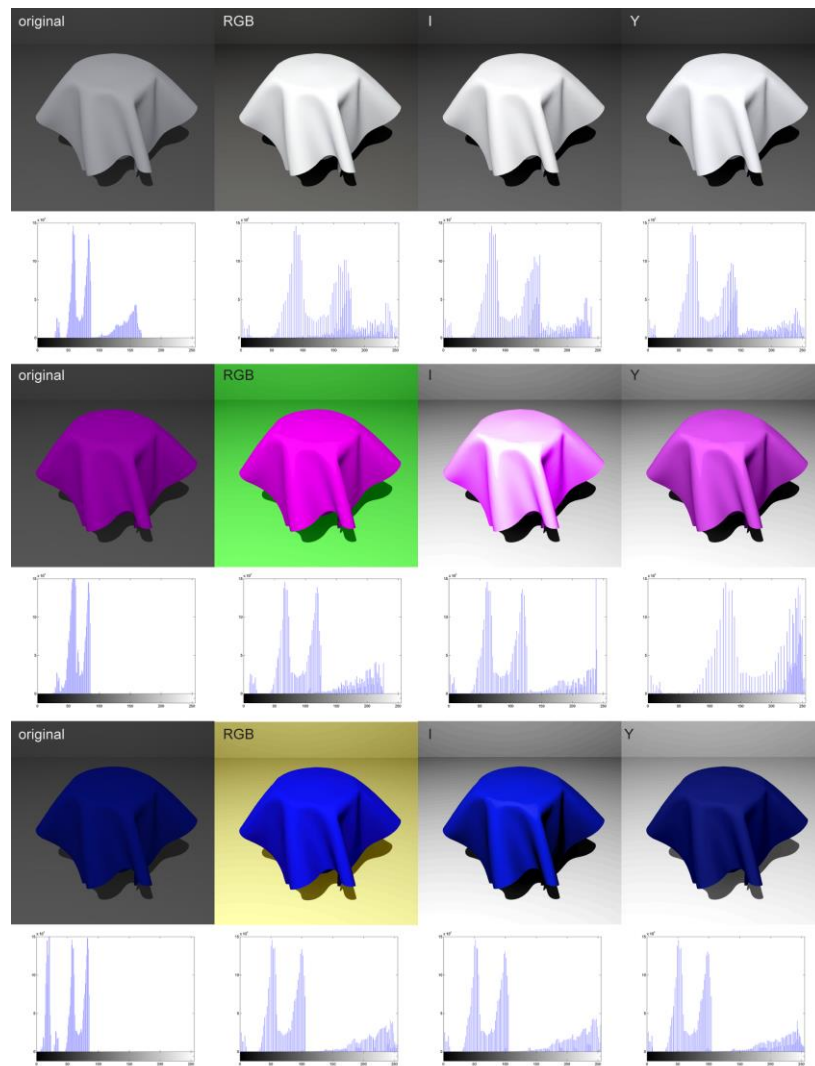


Figure 3: Histogram adjustment for original image rendered with mental ray rendering engine and images, adjusted on RGB, I and Y channel with corresponding histograms.

In Figure 3 the results of histogram adjustment for images generated with mental ray are shown. Again, contrast is ameliorated, resulting in lighter background and more saturated colours of dynamic cloth objects. Histogram of original image is narrow and differs from histogram of original image generated with Scanline rendering engine. Adjusted histograms do not cover whole intensity range and their peaks lean toward left, but still cover more intensities than adjusted histograms for Scanline rendered images. Tint of the background is again present when operating

on RGB channels. Despite that fact, colour of dynamic cloth object keeps its hue and becomes more saturated and lighter. There is no tint present when stretching histograms on I and Y channels. Results obtained by operating on I channel are not pleasing, since in most cases posterization is present and is clearly visible for magenta sample. Operating on Y channel provides reasonably good results though less saturated than with other two methods. Even in that case, some posterization is visible.

In this section, histograms were used to adjust contrast on rendered image and to evaluate renderings. Despite the same setup and general appearance images rendered with Scanline and mental ray differ. This difference is notable when comparing histograms of original image. Histograms differ in shape and intensity coverage and moreover, the results of adjustment diverge too. Most pleasing results when adjusting original image rendered with Scanline were obtained when operating on I channel, meanwhile none of the applied methods performed well on images render with mental ray. In that case, applied method should be altered to obtain satisfactory results.

Correspondingly, edge detection with Canny operator was also used to indicate differences between renderings. In Figure 4 results of edge detection for three images rendered with Scanline are presented. Largest number of details is obtained when operating on RGB channels, since all three channels are taken into account. Only one intensity channel is considered when operating on I and Y channels so the number of details is reduced. In all three cases most details occur where dynamic cloth object is and with very little information about background. Shadow is also represented with edge detection.

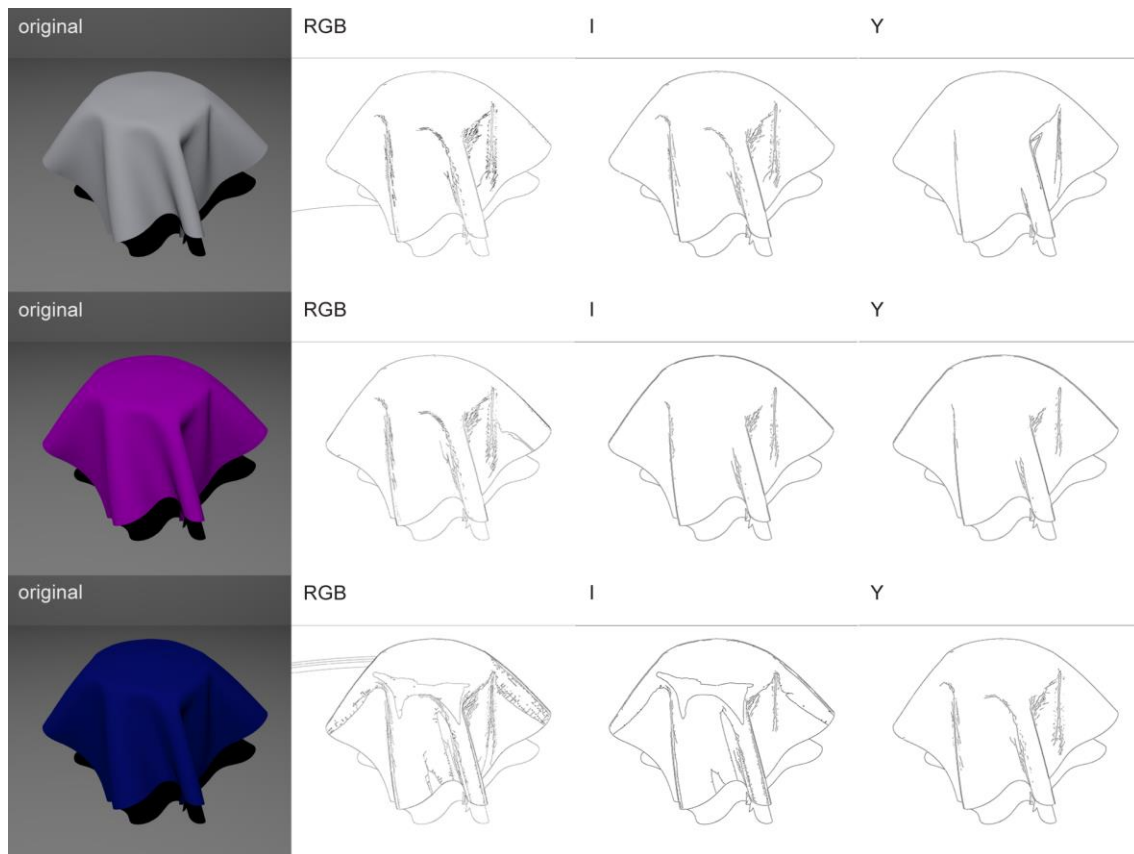


Figure 4: From left to right: original image rendered with Scanline rendering engine and result of edge detection on RGB, I and Y channel.

In Figure 5 results of edge detection for three images rendered with mental ray are presented. In comparison with images rendered with Scanline, greater number of details is present. Most details can be obtained when operating on RGB channels and little less detail when operating on intensity channels I and Y. It seems like that the number of details shown depends on colours' hue. It is interesting that there is no continuous pattern concerning the number of details in the background.

With the use of edge detection it can be confirmed that despite similar appearance of original images, Scanline and mental ray rendering engine render images differently.

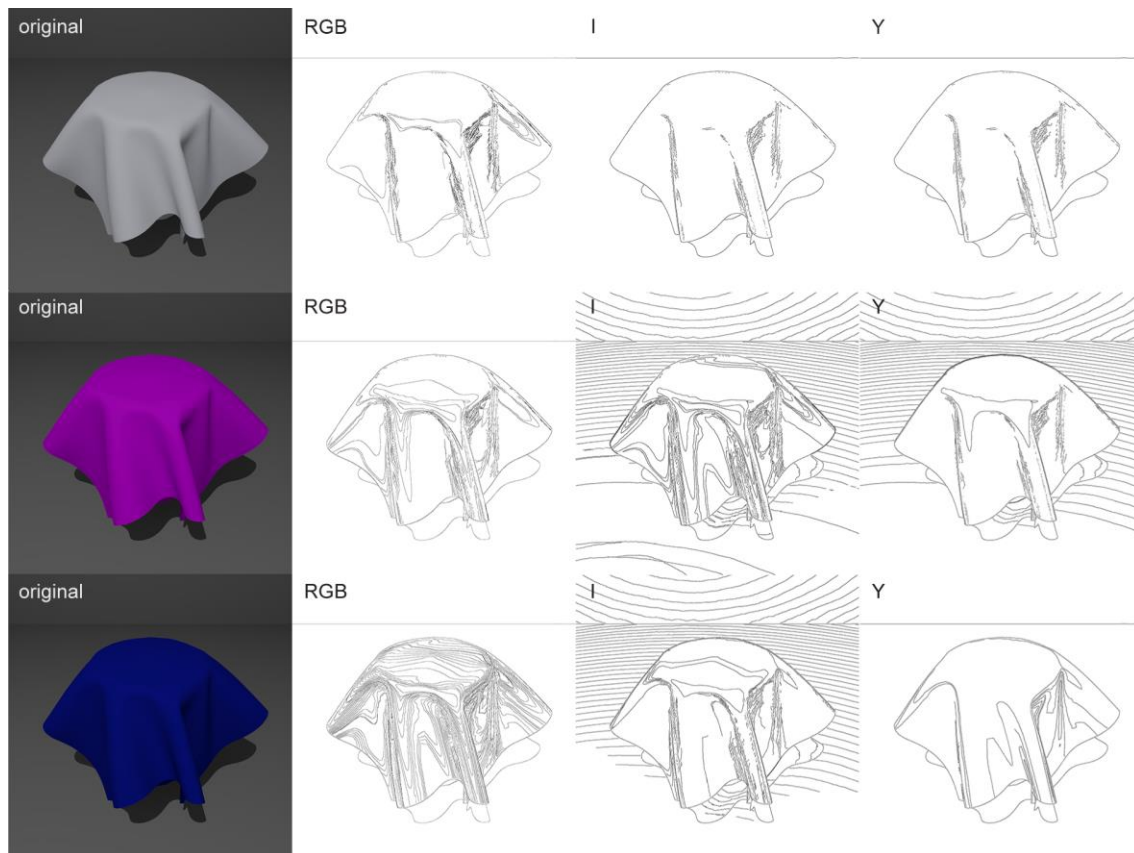


Figure 5: From left to right: original image rendered with mental ray rendering engine and result of edge detection on RGB, I and Y channel.

Finally, images rendered with Cycles in Blender were processed. In Figures 6 and 7 cropped images are presented since noise appears mostly along the edges of basic object. In Figure 6 it is clearly visible that original images contain noise both on the object and in the background and that edges of basic object are serrated, all due to working of rendering algorithm. It was also noticed that quantity of noise increases with lightness of affected object. Firstly noise was removed with average filter the size 3×3 matrix on RGB, I and Y channel. Noise reduction on RGB channel was most successful, since noise was removed on all three channels composing image. Geometric objects also retained their original hue when using this method. Noise removal on I channel failed and even though noise was reduced adjusted image lost all information about colour, except for white object. It was assumed that this was consequence of applied algorithm in connection with selected image. Reducing noise on Y channel provided good results though in some cases hue of geometric object shifted, especially for darker colours. In addition, it has to be noted that success of each method depends on amount of noise present in each image. In our case, noise removal was least successful for image with white geometric object because there was far more noise in the original image.

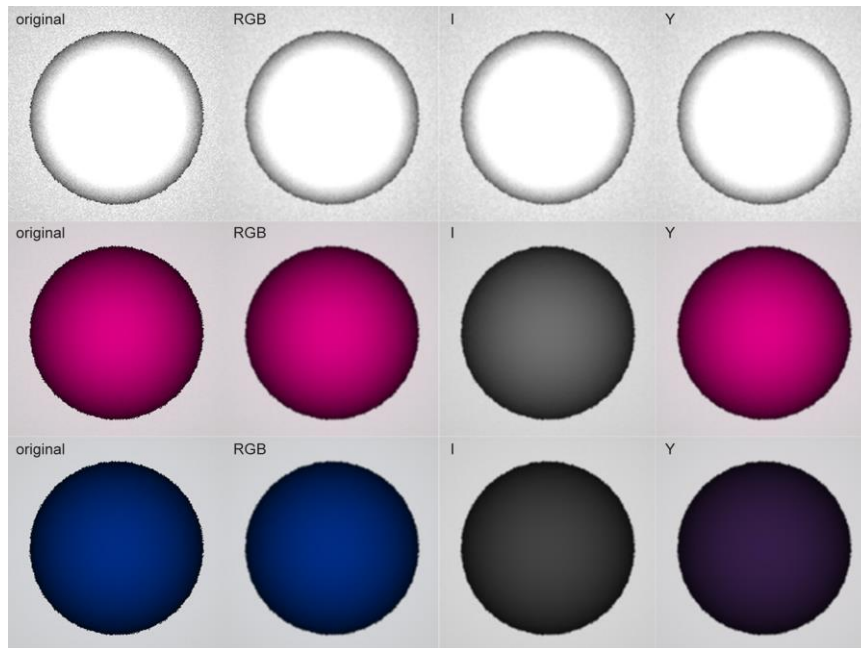
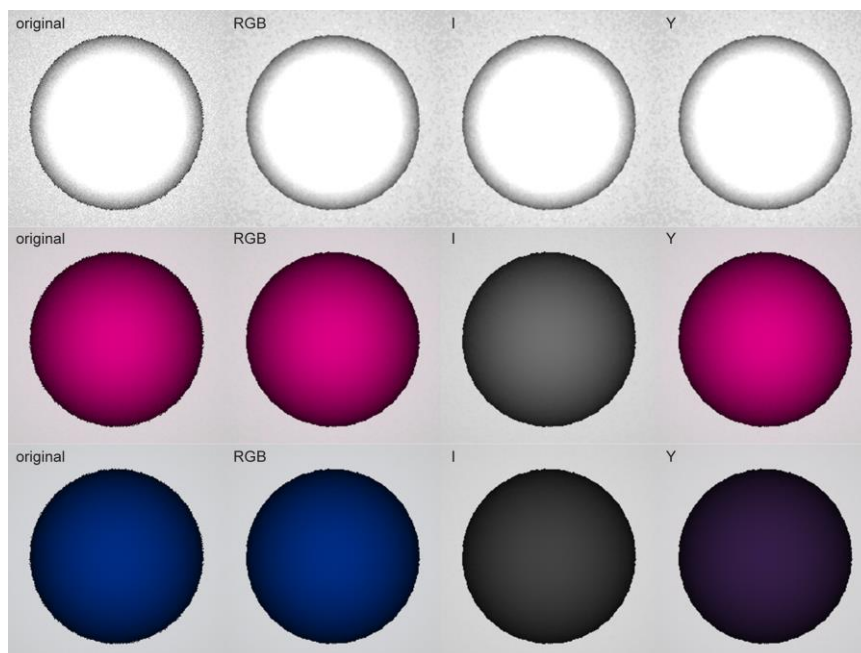


Figure 6: Noise removal with average filter. From left to right: original image rendered with Cycles rendering engine and results of noise removal on RGB, I and Y channel.

Second noise removal method applied was filtering with median filter, again the size of 3×3 matrix. Results are presented in Figure 7. It can be noticed that these results are differ from noise removal with average filter. Again, best results were obtained when operating on all three RGB channels. Noise removal on I channel provided satisfactory results only for white coloured object without hue and failed on coloured geometric objects. Additionally, colour shift is visible when operating on Y channel. Difference between filtering methods is visible in the manner noise was removed, especially for white geometric object. Edges after applying average filter were softer and background seems blurred, meanwhile edges retain their sharpness after application of median filter. Depending on task, image softening can me undesirable effect. Anyway, both used methods provide best results for noise removal in comparison with other methods (Hladnik, 2010).



4. CONCLUSIONS

In this research, image processing operations were applied on generated images rendered with Scanline and mental ray rendering engine in 3ds Max and with Cycles rendering engine in Blender. It was found out that all applied operations, except spatial filtering, Results of image adjustment depended not only on used method but also on image that was adjusted. It was concluded that desired results heavily depend on task performed and in some cases results undesired for one task can be desired for the other. Furthermore, it was also established that not only already widely used histograms are useful tool for image analysis, but also that their manipulation can provide practical insight into differences between images. To conclude with, image processing and its operations can be successfully used in the field of 3D computer generated graphics and can prove tools for both image adjustment and image analysis.

5. ACKNOWLEDGMENTS

This paper was part financed by the European Union and European Social Fund. Authors would also like to thank Mr. Roman Habicht from HSH d.o.o.

6. REFERENCES

- [1] "3ds Max", URL <http://www.autodesk.com/products/3ds-max/overview> (last request 2014-09-10).
- [2] Burger, W., Burge, M. J.: "Principles of Image Processing : Fundamental Techniques" , (Spinger-Verlag, London, 2009), 273 pages.
- [3] Chopine, A.: "3D Art Essentials : The Fundamentals of 3D Modeling, Texturing, and Animation", (Focal Press, Burlington, 2011), 228 pages.
- [4] Erzetič, B, Gabrijelčič, H.: "3D od točke do upodobitve", second edition, (Pasadena, Ljubljana, 2010), 275 pages.
- [5] Getrauser, P.: "Colorspace transformations", URL <http://www.mathworks.com/matlabcentral/fileexchange/28790-colorspace-transformations> (last request 2014-09-09).
- [6] Gonzalez R., C., Woods, R., E., Eddins, S., L.: "Digital Image Processing Using MATLAB", (Gatesmark, 2009) 844 str.
- [7] Hladnik, A., Muck, T.: "Obdelava digitalnih slik v grafiki", (Univerza v Ljubljani, Naravoslovnotehniška fakultata, Oddelek za tekstilstvo, Ljubljana, 2010), 100 pages.
- [8] "Image Processing Toolbox", URL <http://www.mathworks.com/products/image/> (last request 2014-09-09).
- [9] Pharr, M., Humphreys, G.: »Physically Based Rendering : From Theory to Implementation«, second edition, (Elsevier, Burlington), 2010, 1167 pages.

GRAPHICAL SYSTEM VISUALIZATION IN A VIRTUAL SPATIAL ENVIRONMENT AS A LEARNING METHOD

Ivan Pinčjer, Slobodan Nedeljković, Irma Puškarević, Željko Zeljković
University of Novi Sad, Faculty of Technical Sciences,
Department of Graphic Engineering and Design, Novi Sad

Abstract: Finding the most efficient way of learning has always presented a challenge, both for those that teach and those that learn. Different theories and schools have done their best in the past to bring the process of learning closer to man and man closer to process of learning. The way in which the human brain takes the information and transforms it into knowledge is still one of the important scientific questions today. Using new technologies in the process of learning has most often involved the impossibility of the traditional and usual way of learning for various reasons. It can be said that every technological innovation had its application in the development of learning. To use the advantage provided by the technology in order to obtain more permanent knowledge is an obligation of those that are supposed to transfer the knowledge. This paper presents a modern method of learning the working processes of graphical systems by using the advantages offered by virtual environment, as well as spatial system representation. The way of producing one such system is also presented, through the elements such as real system functioning analysis, task to be performed by the virtual system, the way of interacting between the student and the system, as well as the problems that can appear in the process of learning in the virtual environment.

Key words: visualization, virtual environment, learning

1. INTRODUCTION

Many of the institutions in the higher education have come to realize that, next to the theoretical knowledge, their students need to be, as much as possible, brought up to speed with the practical application while they are still in the course of their studies. Use of virtual space enables the creation of the necessary elements in order to transfer the knowledge and experience gained by practice to the students. Use of virtual environment for the purpose of introducing students to the devices and machines used in the graphic industry, has enabled access to virtual graphic devices and machines to an unlimited number of students, without the time or spatial limit. Students rarely have the opportunity to see a specific graphical system up close, and even more rarely the opportunity to operate it. In a virtual environment, these opportunities can be exploited without any limitations. Furthermore, they can see the internal structure of a system, device or a machine without fear that they will in any way endanger the proper performance of the system, cause system failure or endanger their own safety.

2. VISUALIZATION IN VIRTUAL ENVIRONMENT AS A CONSTRUCTIVIST LEARNING METHOD

Design of virtual environment learning is based on the constructivist learning theory. It postulates that there is no unique form of knowledge, instead every person forms their own knowledge (Von Glasersfeld, 1984.) A person is in the process of learning when they, during a conscious browsing of the knowledge base, discover holes in their knowledge or discover inconsistencies between their current representation of knowledge and their experience (Slavin, 1994). Also, learning can be observed from a social standpoint as a result of interpersonal communication between the students (Vygotsky, 1978).

In order to optimize the learning time, all three concepts of learning should be implemented in modern virtual learning environments. The first concept should be implemented through the possibility of non-linear access to and manipulation of some of the key components of a device or a graphic machine. It is also important to mention here the possibility of repetition of any of the processes being learned. In such a manner the students absorb the knowledge in a way that is most suitable and easier for them to understand unlike the linear principle which is often hard for students to understand, because of the inability to influence its speed. The second principle is defined by visualization through the virtual environment of applied theory that is fully explained

by the theoretical part. In such a way the difference between the empirical and theoretical knowledge is maximally negated, and the absorption of knowledge is encouraged. It should be emphasized that the working experience obtained in such a manner is artificial, however, that is why it is given special attention, both in the areas of correct system performance and realism of presentation. Further research is needed to determine the difference between the reality and virtual experience, which is how the real experience in virtual space could be called. The social aspects and communication depend upon whether the virtual experience is available over the internet or only in the computer classroom, which is why this problem will not be dealt with in this paper.

Since the student has been given a very wide freedom of movement inside the virtual space, attention should be paid to a few key parameters in order for the learning to be efficient. The research findings, points that learning can be jeopardized without appropriate instructions, i.e. guidance through the virtual space (Ge et al. 2000). The Introduction and explanation manual needed before the beginning of learning in the virtual environment enable the students to understand what results they need to achieve and what events they can expect to happen inside the virtual space. This kind of introductory lesson can also be achieved by a demonstration in the instructor's own 3D virtual space. Furthermore, the instructor is expected to know his students. This implies defining such tasks that the students can understand, i.e. during the process will not lead to cognitive overload, which can lead to drop out (Nonis 2005). It should be mentioned that doing business today cannot be imagined without the constant education and improvement of employee knowledge. For companies this creates the problem of sending the employees to training or courses. Aside from the employees being absent, further expenses are incurred by the need for accommodation and food for those that are in training. It is clear that sending the employees to courses is a privilege of the biggest companies, which can afford it and in such a way increase their market advantages, against the developing companies. Furthermore, the environment in which the courses take place is often not controlled, i.e. various distracting factors can appear which will influence the quality of obtained knowledge. Very often that environment is unfamiliar and creates a feeling of discomfort in the course takers, both from the fact that they are separated from their working environment and the fear that they will not perform well in the sense of understanding of the presented material and, because of that, be perceived as the ones that don't have previous knowledge in a certain area.

3. 3D ENVIRONMENT

In order for the student to get acquainted with the systems presented in virtual environment as best as possible, one option has surfaced as a solution which will enable the students to get more complete picture about the system from various aspects, as well as influence their ability to store information into knowledge. It has been shown that 3D representation influences the activation of spatial memory which can be a part of long-term memory (Cockburn 2004). Realism of representation contributes to lesser abstractness of theory and, by association, improves the process of memorizing with the subjects. The reason which lead to the decision to introduce the subject to the virtual space is the desire to provide the opportunity to immerse oneself without distraction, and with the least possible amount of outside influence, into a friendly, not alien, virtual environment which has the task of capturing the subject's attention and toning down the distracting outside influences. Such an environment creates the feeling of familiarity and the presence in the virtual world, which acts as a positive influence on the subject's participation in the learning process and his engagement in the exploration of the virtual space, through which every step becomes the part of learning process. The same as playing video games on the computer, user enters a world in which he can move within the given parameters and the larger the world the longer it will keep him occupied. The possibility of a virtual tour of a laboratory equipped with different graphic systems provides the opportunity to view them from all sides, dismantle them to basic parts, put them to work and get to know the theory that enables the system to function, which creates an expanded reality and improves the knowledge, which is not withheld by any criteria. Such knowledge without the unknown parameters is longer lasting and enables better learning since it creates a single logical unit, rounds out the complete process of learning in such a way that theoretical parts are explained by visually active representations, whereas the visual representations are defined by theoretical text. Knowledge obtained so completely is more permanently stored and harder to forget. In this manner fast feedback information is obtained which is essential for the efficiency of learning (Byrne 1996).

4. MODELING

The ways of visualization and their comparison was one of the scopes of this research, both in the 2D and 3D visualization variants. Visualization enables the representation and simulation of various complex systems both for industrial and scientific purposes. It is often the case that visualization is used to represent the principles of functioning, as well as the parts that are not visible, and is a part of some closed unit. Visualization plays an important role in the creation of the principles of improvement in learning and production through learning with the help of modern technology. One of the very important aspects of visualization is that it takes place in real time. This means that there are no video sequences, where the observer has to follow a single linear action. Instead the observer can interact in the real time by influencing, manipulating and exploring the visualized object and advance his knowledge. When it is necessary to show the principle on which the machine works, or to show specific components and sub-systems, it is necessary to dissemble the machine all the way to single units in order to show the system that needs to be visualized. For a successful realization of this kind of research it is necessary to have knowledge of modeling techniques in 3D applications, principles and shadowing techniques that are very important for a realistic representation. It is necessary to define the role of textures, ways of simulation and animation techniques, as well as types of light sources and illumination. The rendering process plays a significant role since it is the key element in securing high quality visualization. Every interactive system uses a programming language in order to facilitate communication between the elements and the system. Programming language Action Script is used for this purpose.

This programming language supports a very wide spectrum of possibilities in creating the most diverse forms of interactivity. The Development of concept is based on interaction and learning. Figure 1 shows a segment of a developed solution for spatial visualization with theoretical elements of knowledge database of the machine, applied technology and elements.

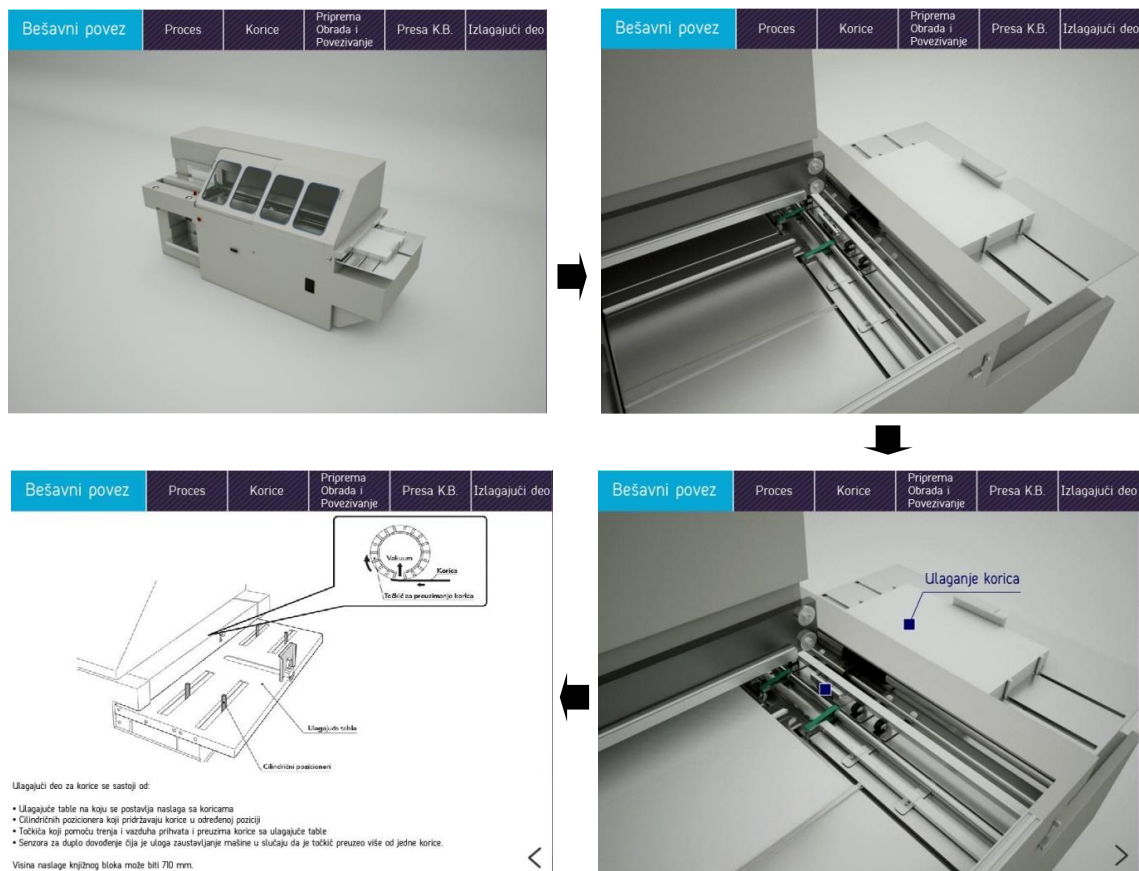


Figure 1: Spatial visualization with theoretical elements of knowledge database

The making of models in the virtual space consisted of gathering a large number of referential photographs of a real model that was to be visualized. The Technical documentation of the graphical system was consulted and in such a manner precise data on dimensions, schematics and projections was obtained. During the process of material collection special attention was given to those elements that would be processed in the theoretical part of the application also. In this way a connection is created between the practical application and theory with minimal departure between those two areas (Dalgarno 2002). As the virtual system needs to mimic the behavior of the real system it is necessary to show the way in which the real system works, adequately present the key parts and their mutual relationships during the production process that is being simulated.

The Production process that the machine or system performs during their operation is shown in the form of an animation. The Advantage of animation over a static picture has been experimentally proven (Novakovic et al. 2013). Further improvement is to include the animation as a part of the virtual space. The Animation is placed in the virtual space in such a way as to be shown in the same manner as the machine would operate in front of the operator, in a real system. The same as in a real system interaction between the operator and system is expected, in such a way that operator inputs the command, and the system performs it in a certain time interval, without the influence of the operator. Each of these segments can be further analyzed by accessing the active elements and their theoretical explanation (Figure 1). This interaction between the application and the student enables the student to develop much higher level of understanding concerning the complete system (Dalgarno & Hedberg 2001).

Non-linearity of learning is represented here through the possibility of activation of any segment of machine operation and its analysis without concern for the phase in which the process is currently in. For example, output device of the system can be analyzed, even though no material entered the system and was processed previous to the output phase. This kind of activity is impossible in the real system, but in the virtual system it enables a fast access to elements of interest.

5. DISCUSSION

Concerning the learning process depends on the number and distribution of reviews, special attention is given to the intensity of learning. The Learning intensity in the ordinary system of courses and training is quite high, and most often reduced to the least possible amount of time due to expenses. During that period there often appears a fatigue in logical and cognitive learning and further student's participation in that course becomes futile. By way of electronic learning the student can distribute the intensity of learning according to his own preferences and to pursue it for days, months, or years, as opposite to being exposed to it for just a short period of time. It can be concluded that short-term high intensity learning is suitable for simple skills, while shorter learning intervals, with the possibility of a higher number of reviews, are suitable for more complex skills and acquisition of knowledge. By analyzing deficiencies of learning in school, direct influence was achieved on the factors that have shown themselves to be negative in the ordinary way of giving courses and training, even school activities. The School environment is often perceived as painstaking and hard, which in itself singled out the principle of learning in virtual environment as an ideal solution. Learning in schools is often connected to abstract tasks which are far apart from concrete activities. By the use of proposed solution learning is tied to concrete activities, whose result can be seen momentarily and in any moment during the process of learning. The School learning is often characterized to be devoid of context, directed at mechanical and routine acquisition of knowledge without the possibility of deeper understanding and application in the end. Each of these negative reflections on school learning has been addressed and specifically corrected in the proposed manner of learning.

The complete application is discretely permeated by sequences that facilitate unintentional, spontaneous and intuitive learning, which engages the student to participate in the training with interest. The result is cognitive learning by which experience and practice, obtained in the virtual environment, consequently cause changes in the abilities of performing the wanted activity, as is already the case in training pilots with a flight simulator.

Barracough and Guymer (1998) suggest that people will accept more information if that information was to be received by more senses. For this reason additional media is integrated into application. Accessibility of different media depends upon the system being shown, and what is available is photograph, video, speech that will provide added help to acquisition of knowledge.

6. CONCLUSION

With the development of IT technology and ever more and more accessible internet connection, there is an expansion of different remote learning applications, as well as virtual environments for learning, that exploit these new technologies in their entirety. The graphic industry too has noticed the possibility of applying these new technologies in educational purposes. Considering the scarce availability of machines, their price, space limitations inside the printing companies, as well as the need to stop the production in order to demonstrate the operation of a certain machine to the students, the advantage of getting to know the operation of graphical systems in virtual environment is obvious. In this way, students can, next to getting to know the operation of the system, interact with it, i.e. input commands that the system will perform, all without fear that the system will fail due to unprofessional handling. Every student can have the system on the monitor in front of them and operate it, repeat the actions of the system in an unlimited number of tries and have an insight into specifically chosen theoretical segments concerning exactly the part of the system they are viewing, which makes stopping the simulation to consult theoretical texts on system operation unnecessary. That is certainly an obvious advantage in view of realistic system presentation where the student is merely a passive observer in uncontrolled and most often non-stimulating learning conditions (large number of students, inadequate noisy environment, and inability to influence the observed system).

Without excluding any other learning activity, integration of this kind of a system into the learning process with the goal of improving knowledge acquisition is recommendable. Diversity of systems that can be represented in this manner is considerable and limited only by the financing of their virtualization.

Application of such system in knowledge acquisition can be simple if it functions as support to the traditional type of learning. As such, this way of learning is applicable immediately and its benefits cannot be disputed. Situation can get very complicated if this way of learning is required to be the only way, in which case many questions arise, like motivation, degree of giving up, cognitive overload related to inadequacy of the material or the listener, and finally, objective evaluation of the results of knowledge acquisition.

7. ACKNOWLEDGEMENTS

This work was supported by the Serbian Ministry of Science and Technological Development, Grant No.: 35027 „The development of software model for improvement of knowledge and production in graphic arts industry“.

8. REFERENCES

- [1] Barraclough, A., & Guymer, I. (1998). Virtual reality – A role in environmental engineering education? *Water Science & Technology*, 38(11), 303–310.
- [2] Byrne, C., 1996. *Water on Tap The Use of Virtual Reality as an Educational Tool*. Cambridge: Cambridge University Press. Available at: <http://ebooks.cambridge.org/ref/id/CBO9780511974823>.
- [3] Cockburn, A., 2004. Revisiting 2D vs 3D implications on spatial memory. *Proceedings of the fifth conference on Australasian ...*, 28, pp.25–31. Available at: <http://dl.acm.org/citation.cfm?id=976314> [Accessed August 6, 2014].
- [4] Dalgarno, B., 2002. The potential of 3D virtual learning environments: A constructivist analysis. *Electronic Journal of Instructional Science and ...*, pp.1–19. Available at: http://ascilite.org.au/ajet/e-jist/docs/Vol5_No2/dalgarno.html [Accessed August 6, 2014].
- [5] Dalgarno, B. & Hedberg, J., 2001. 3D learning environments in tertiary education. *Ascilite'01: Meeting at the crossroads*, pp.33–36. Available at: http://www.researchgate.net/publication/228697077_3D_learning_environments_in_tertiary_education/file/9fcfd50ac4d45350cb.pdf [Accessed August 6, 2014].
- [6] Ge, X., Yamashiro, K. & Lee, J., 2000. Pre-class planning to scaffold students for online collaborative learning activities. *Educational Technology & Society*, 3(3), pp.1–16. Available at: http://www.ifets.info/journals/3_3/b02.html [Accessed August 6, 2014].
- [7] Nonis, D., 2005. Virtual Environments [3D VLE]. *IT Literature Review, Educational Technology Divison, Ministry of Education, Singapore*, pp.1–6.

- [8] Novaković, D., Milić, N. & Milosavljević, B., 2013. Animated vs. Illustrated Software Tutorials. *The International Journal of Engineering Education* 2, 29(4), pp.1013–1023.
- [9] Tavanti, M. & Lind, M., 2001. 2D vs 3D, implications on spatial memory. *IEEE Symposium on Information Visualization, 2001. INFOVIS 2001.*, 2001, pp.139–145. Available at: <http://ieeexplore.ieee.org/lpdocs/epic03/wrapper.htm?arnumber=963291>.
- [10] Von Glasserfeld E (1984) An Introduction to Radical Constructivism In P W Watzlawick (ed) *The Invented Reality* (pp 17-40) New York: W Norton and Company.
- [11] Vygotsky L S (1978) *Mind in Society The Development of Higher Psychological Processes* Cambridge Massachusetts: Harvard University Press.

INFLUENCE OF RENDERING ENGINES ON COLOUR REPRODUCTION

Nika Bratuž¹, Tim Jerman², Helena Gabrijelčič Tomc¹, Dejana Javoršek¹

¹University of Ljubljana, Faculty of Natural Sciences and Engineering, Ljubljana, Slovenia

²University of Ljubljana, Faculty of Electrical Engineering, Ljubljana, Slovenia

Abstract: Despite vast technological progress in last decades colour presentation and reproductions issues on different media still have not been solved to full extent. One of the available solutions to maintain constant colour appearance are colour appearance models and though being around for more than forty years are still barely used in practical applications, especially not in connection with 3D computer generated graphics. Process of generating 3D graphics is complex and several factors can influence colour on generated image. In this research, three different rendering engines were used in combination with CIECAM02 colour appearance model to generate 3D computer graphics. It was concluded that CIECAM02 colour appearance model can be successfully used in 3D computer generated graphics and provides better visual matching. It was also found out that rendering engines treat colours differently.

Key words: CIECAM02 colour appearance model, 3D computer generated graphics, 3D rendering

1. INTRODUCTION

Accurate presentation of colour plays important role in nowadays technology dependent world. Some common and standardised methods can be used to maintain and predict constant colour appearance in cross-media reproduction, including colour appearance models (Fairchild, 2005). Basis for numerical evaluation of colours was set in the beginning of 20th century and is still in use, however, research has shown that next to observer, light source and stimulus many other factor influence the appearance of colours. Some of this factors are incorporated in colour appearance models, which were firstly developed in the seventies and have yet to gain their place in practical application (Javoršek et al, 2013). Current CIE approved colour appearance model that was developed in 2002 is called CIECAM02. It is a simple and efficient model that performs well in practical application, such as colour management, colour gamut mapping or for calculation of colour differences. Exploration of its functionalities and limitations has again became popular in last few year, henceforth some suggestions for corrections and improvements have been proposed recently (Luo et al, 2013). Despite that, no research of application of CIECAM02 on 3D computer generated graphics was conducted.

At the same time as first colour appearance models were developed first 3D computer graphics were generated. Use of 3D computer generated graphics in everyday life has become prevalent with disposability of suitable software, increasing processor power of computers and other developments in computer graphics in last years and decades. With growing popularity and usage of 3D computer generated graphics also some problems and demands have arisen and one of them is certainly quality and standardised realistic reproduction of colour, mostly in fields of architecture, anthropology, archaeology, fine arts, industrial design, automotive industry and even medicine (Chopine, 2011). Making of 3D computer generated graphics is complex process dependent on multiple factors and its mutual interaction and can be divided in several stages. First is 3D modeling, followed by application of material or texture properties that also carry information about colour. To render an image, a camera and light source need to be set up, the model geometry should be correct, while interaction of light with matter is generated by rendering engine. Final results and rendered colour can not only be affected by factors associated with 3D modeling and rendering, but also by some colour appearance phenomena. The final result is hardly predictable without detailed knowledge of applied algorithms and functions, that influence colour. In addition, colour management is rarely inbuilt in 3D modeling and rendering software and despite its complexity the process of rendering must be time and power efficient (Erzetič et al, 2010). Only few researches on the subject of interaction of materials and lightning in 3D computer generated graphics with colour were conducted with collective conclusions that colour attributes of computer generated models are perceived differently than rendering algorithms predict (Koch, 2010, Fleming, 2003, Doerschner, 2004, Motoyoshi, 2007). The aim of this research was to investigate influence of different rendering engines on colour reproduction by applying

CIECAM02 colour appearance model to an object in different viewing conditions in 3D scene in computer graphics software Blender.

2. METHODS

Blender is free open source software with user-friendly interface and abilities of high-priced commercial software. A simple scene was set up in Blender, consisting of background, object (sphere), light source and camera. Background and object were made of diffuse material without specular reflection. Three different rendering engines were used: Blender Render and Cycles that are built-in and plugin rendering engine Yafaray. Blender Render and Yafaray render images on principle of ray tracing, meanwhile Cycles works as a path tracer. Diffuse shader for object and background was set to Lambert for Blender Render and Yafaray and to BDSF (combination Lambert and Oren-Nayar) for Cycles. Camera was set to automatic and behind the camera was a spotlight with white light and spot in shape of cone with constant falloff. Intensity of light changed with rendering engine and was controlled by grey test chart. Image size was set to 800×800 pixels in sRGB colour space. Even though Blender supports colour management it was turned off. Despite being called colour management, Blender does not manage colours as we are used to from other application, but only provides gamma linearization. 1331 RGB colour samples were generated and applied as input colours on lighter background. Output colours on darker background were defined as non adapted and adapted colours. Non adapted colours remained the same as input and adapted colours were calculated with CIECAM02 colour appearance model. All three images are shown in Figure 1.

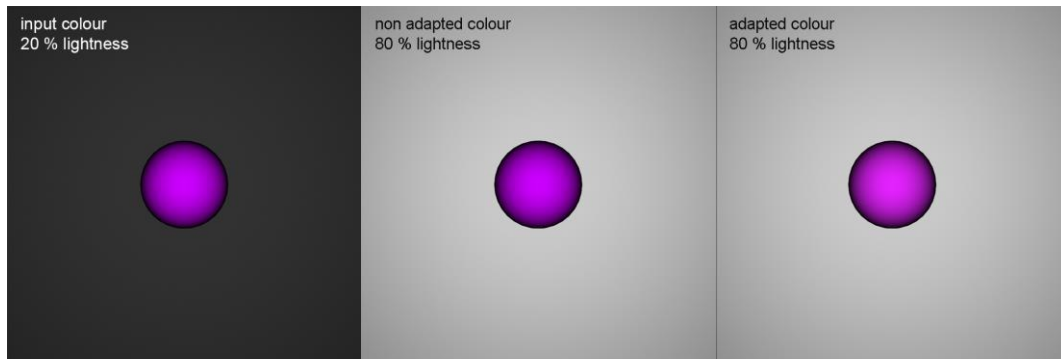


Figure 1: Input colour on darker background, non adapted colour on lighter background and adapted colour on lighter background.

From input RGB values input XYZ values were calculated and adapted to CIECAM02 lightness J , chroma C and hue h . Reverse model was used to calculate adapted XYZ and RGB values. All parameters are shown in Figure 2. Furthermore, CIEDE2000 was calculated between corresponding pairs of images and average and lightest colours were obtained for each rendered colour. Colours were also presented graphically in CIELAB colour space for better visual observation.

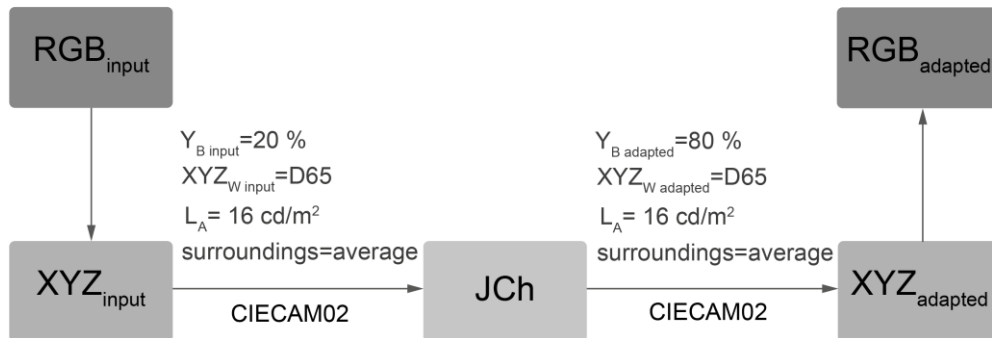


Figure 2: Course of colour adaptation with CIECAM02 colour appearance model and its parameters.

3. RESULTS AND DISCUSSION

Firstly, mean colour difference CIEDE2000 was calculated between CIELAB values of input and non adapted and input and adapted colours (Table 1). Zero colour difference was expected between input and non adapted colours, since same values were input, but it can be observed colour difference grater than zero for Cycles rendering engine. This suggests that colours rendered with Cycles are affected by background, meanwhile Blender Render and Yafaray disregard background when rendering colours. Mean colour difference were grater than zero between input and adapted colours, which was expected due to manner in which colours are treated by CIECAM02 colour appearance model. Lowest mean colour difference between input and adapted colours was obtained for Blender Render, followed by Yafaray and largest colour difference was obtained with Cycles, which was expected after brief visual evaluation.

Table 1: Mean CIEDE2000 (ΔE_{00}) colour difference calculated between input and non adapted and input and adapted colour for Blender Render, Cycles and Yafaray.

Rendering engine	mean ΔE_{00}	
	input - non adapted	input - adapted
Blender Render (BR)	0	3.28
Cycles (CY)	1.67	6.29
Yafaray (YF)	0	4.42

Next, CIELAB values were calculated for each average colour of each given sample to show how colours are affected by rendering engine. First the lightness L^* of average colour is presented for each rendering engine. Firstly it can be observed that points are grouped due to selection of input colours and that average lightness is quite lower for Blender Render and Yafaray then for Cycles (Figure 3). Input and non adapted colours for Blender Render seem the same and lightness of adapted colours increased due to adaptation to lighter background. Similar situation can be observed for Yafaray, though colours are lighter then Blender Render. As mentioned before, average colours rendered with Cycles are lighter and their distribution differs from Blender Render, especially for colour with lower lightness. Colours, rendered with all rendering engines, shifted in the adapted image as a consequence of adaptation to lighter background. This shift is especially visible for darker colours in lower left corners.

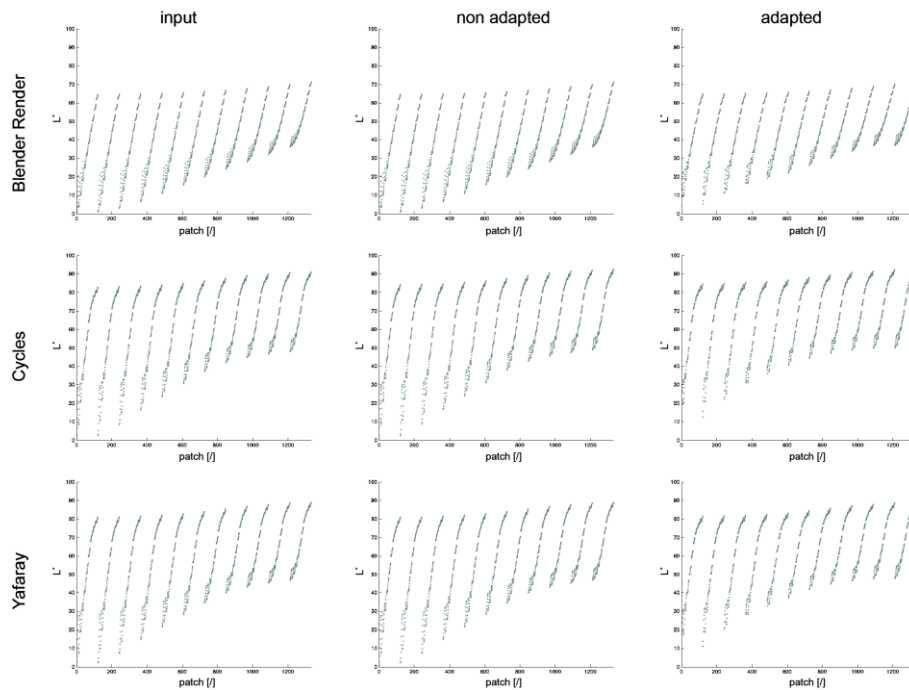


Figure 3: Lightness L^* of each colour patch for input, non adapted and adapted colours rendered with Blender Render, Cycles and Yafaray.

In Figure 4 a^* and b^* coordinates are shown for each rendering engine for average colours. It can be noticed that gamut corresponds that of sRGB colour space. In charts that show adapted colours shifting and grouping along lines emerging from the centre is visible, especially for Blender Render. For Cycles and Yafaray the layout of colours is different from Blender, which was already observed when analysing average lightness L^* for each colour. Grouping for adapted points can be seen but is not as obvious as for Blender Render.

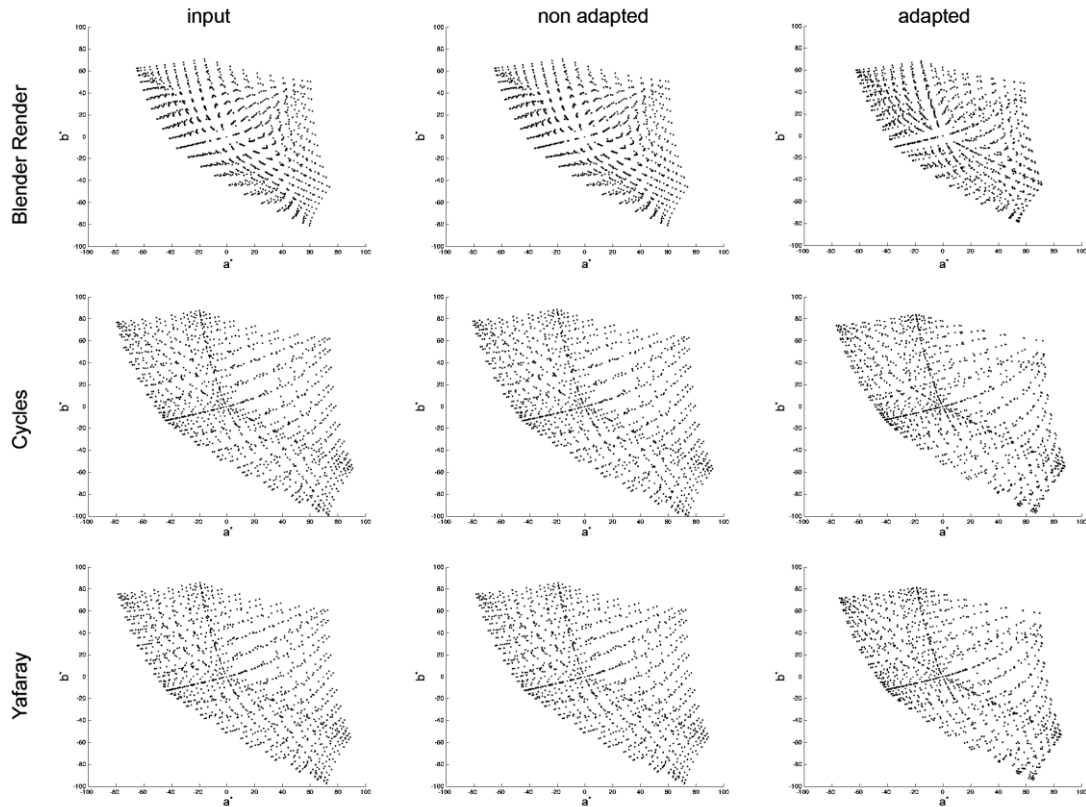


Figure 4: a^* and b^* coordinates of each colour patch for input, non adapted and adapted colours rendered with Blender Render, Cycles and Yafaray.

In Figure 5 the relationship between lightness L^* of lightest colours labelled as L^*_s and lightness of average colours labelled as L^*_p is shown for each rendering engine for input, non adapted and adapted colours. This relationship is linear for Blender Render with some exception in darker regions. Shift towards lightest colours is visible after adaptation due to adaptation to lighter background. The relationship between L^*_s and L^*_p is not linear for Cycles and Yafaray. Darker colours are grouped into sever groups and lighter colours are spread out and depending on this occurrence there can be defined four ways in which colours are treated by Cycles and Blender Render from darkest to lightest colours. It seems that colours are shaded based on their lightness. An interesting shift can also be seen for adapted colours for Blender Render and Cycles. All colours shift due to application of CIECAM02 colour appearance model, but for some colours shift is larger than for others, mostly for colours with larger average lightness L^*_p . It can also be observed that darker colours shift toward lighter colours and lighter colours shift slightly towards darker.

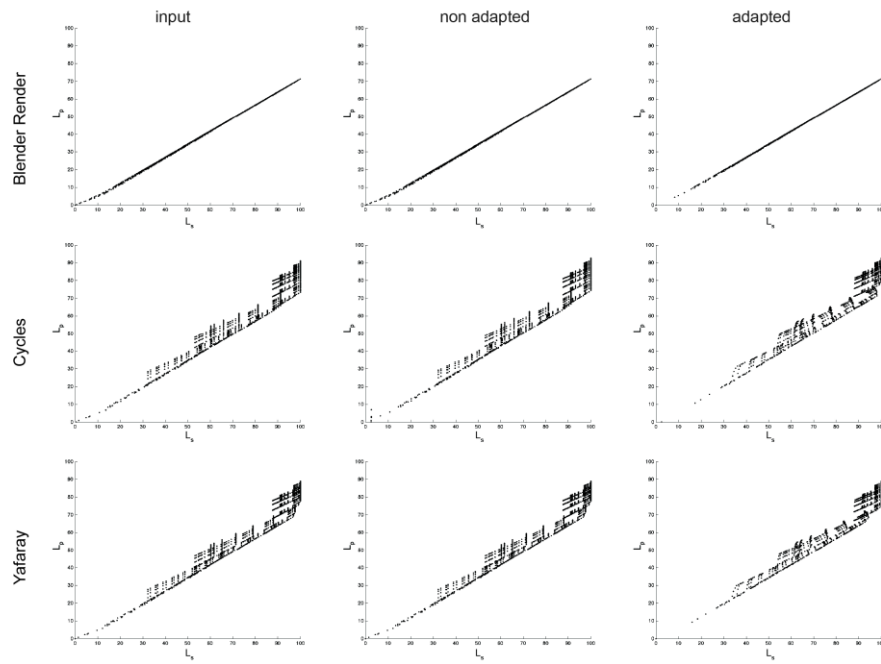


Figure 5: Relationship between lightness L^* of lightest colours L^*_s and lightness of average colours L^*_p for input, non adapted and adapted colours rendered with Blender Render, Cycles and Yafaray.

In Figure 6 the relationship between chroma C^* of lightest colours labelled as C^*_s and chroma of average colours labelled as C^*_p is shown for each rendering engine for input, non adapted and adapted colours. It is again obvious that Blender Render treats colours differently than Cycles or Yafaray. Relationship between C^*_s and C^*_p for Blender Render seems linear without many deviations, meanwhile colour rendered with Cycles and Yafaray are more scattered. There is also visible difference between Cycles and Yafaray, namely in parts with lower chroma in lower left corner of each diagram. Relationship between chroma of adapted colours for Blender Render remains linear but it changes for Cycles and Yafaray. Again, it can be mostly visible in regions with lowest and highest chroma where the change depends on chroma of original image.

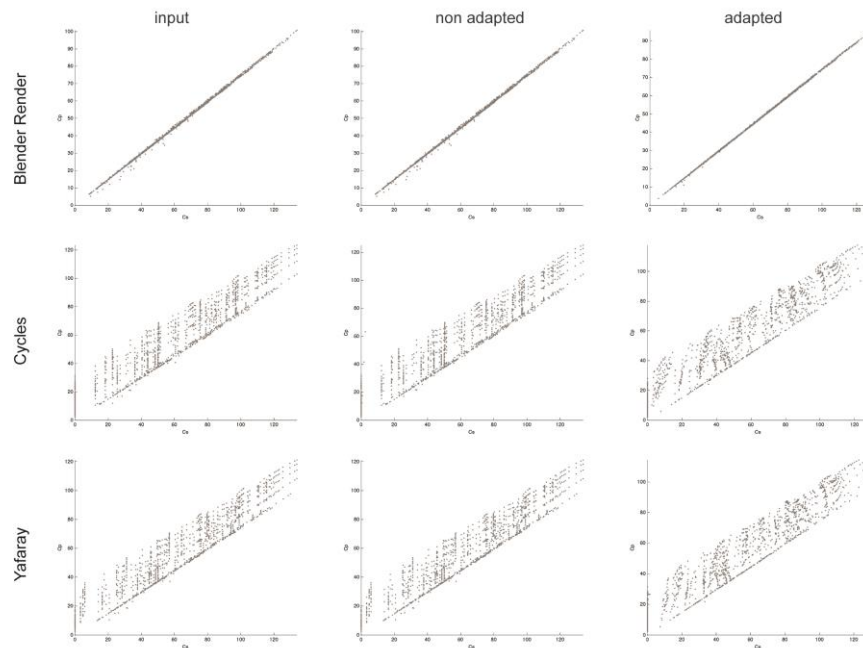


Figure 6: Relationship between chroma C^* of lightest colours C^*_s and chroma of average colours C^*_p for input, non adapted and adapted colours rendered with Blender Render, Cycles and Yafaray.

4. CONCLUSIONS

It can be concluded, that render engines do not render colours equally and that even one render engine does not affect all colour equally. This conclusion is firstly supported by comparison of mean CIEDE2000 values between input and non adapted and input and adapted colours where Cycles was most conspicuous. Next, with comparison of L^* , a^* and b^* values it was confirmed that there are notable differences between render engines. Finally, the relationship of lightness L^* and chroma C^* between lightest and average colours revealed that colours are treated differently based on lightness and chroma when colours were rendered with Cycles or Yafaray. Meanwhile, for achieving preservation of colour perception, colour appearance model CIECAM02 was successfully applied to 3D computer generated image.

All things considered, the field of colour reproduction in 3D computer generated graphics is quite unexplored and more research including visual testing need to be done to fully understand the way colours are generated.

5. ACKNOWLEDGMENTS

This paper was part financed by the European Union and European Social Fund. Authors would also like to thank Mr. Roman Habicht from HSH d.o.o.

6. REFERENCES

- [1] Chopine, A.: "3D Art Essentials: The Fundamentals of 3D Modeling, Texturing, and Animation", (Focal Press, Burlington, 2011), 228 pages.
- [2] Doerschner, K., Boyaci, H., Maloney, L.T.: "Human observers compensate for secondary illumination originating in nearby chromatic surfaces", *Journal of Vision*, 4 (2), 92-105, 2004.
- [3] Erzetič, B., Gabrijelčič, H.: "3D od točke do upodobitve", second edition, (Pasadena, Ljubljana, 2010), 275 pages.
- [4] Fairchild, M.: "Color appearance models", (John Wiley & Sons, Chicester, 2005), 385 pages.
- [5] Fleming, R.W., Dror, R.O., Adelson, E.H.: "Real-world illumination and the perception of surface reflectance properties", *Journal of Vision*, 3 (5), 347-368, 2003.
- [6] Javoršek, D., Karlovič, I., Muck, T.: "Reproduciranje barv in barvno upravljanje", (Univerza v Ljubljani, Naravoslovnotehniška fakulteta, Ljubljana, 2013), 275 pages.
- [7] Koch, J., Henrich, N., Mueller, S.: "Spatial color confidence for physically based rendering settings on LC displays", *Proceedings of the International Conference on Computer Graphics Theory and Applications (GRAPP, Angers, France, 2010)*, pages 173-180.
- [8] Luo, M. R., Li, C.: "Advanced Color Image Processing and Analysis", (Springer Science+Business Media, New York, 2013), pages 19-58.
- [9] Motoyoshi, I., Nishida, S., Sharan, L., Adelson, E.H.: "Image statistics and the perception of surface qualities", *Nature*, 447, (7141), 206-209, 2007.

THE INTEGRATION OF TTI SENSOR OF SMART PACKAGING AND MODERN PERSONAL PORTABLE DEVICES

Stefan Đurđević, Željko Zeljković

University of Novi Sad, Faculty of Technical Sciences,
Department of Graphic Engineering and Design, Novi Sad, Serbia

Abstract: The packaging development industry shows significant steps forward in terms of the application of what makes the latest technology. Nowadays, the area of modern manufacturing technology is particularly applicable to food packaging. The application of polymer nanotechnology can produce new packaging materials with improved mechanical, barrier and antimicrobial properties, together with nanosensors to detect and monitor the conditions of food during transport and storage.

Packaging that monitors the conditions of packaged food in order to give information about the quality of food during storage and transport is called intelligent packaging. What is important to ensure is the follow-up over a period of what makes harmful changes to the packaging and its packed contents. Temperature variations of packaging for food over the time can lead to significant changes in the safety and quality of food, and usually lead to food spoilage. Time-temperature indicators (TTI) that are present on the market operate with mechanisms based on different principles. They are usually based on the systems of the polymerization reaction, enzyme systems, system components of photosensitive organic pigments, or a change in the pH value or the basis of the reaction of diffusion. In order for the results to be valid and to be quick to come to full knowledge (information) by monitoring today's modern technology can make a connection between what exists and what is just being created. Based on that it may lead to rapid information specifically to devices such as smart phones, tablet devices, smart watches and "Google glasses". This paper presents one of the possible solutions that can find its wider application.

Key words: packaging materials, intelligent packaging, time-temperature indicators, sensors, food quality

1. INTRODUCTION

1.1 Modern packaging materials

The main function of food packaging is to maintain the quality and safety of packaged food during storage and transport, but also to extend the shelf life by preventing unfavorable factors or conditions such as harmful microorganisms, chemical contaminants, oxygen, moisture, light, external forces, etc. Food containers should prevent the creation or release of moisture, to protect from contamination by microorganisms and is a barrier when there is leakage of water vapor, oxygen, carbon dioxide and other volatile compounds, but also to meet the basic properties of packaging materials such as mechanical, optical and thermal properties (Rhim et al, 2013). In the packaging industry for food the main interests have always been the proper use of packaging materials and methods to reduce the food losses and provide safe and healthy food products. Because of the improved performance characteristics of the nanocomposite in packaging materials such as oxygen barrier properties to carbon dioxide and water vapor, strong mechanical strength, thermal and chemical stability, recycling, biodegradability, dimensional stability, heat resistance, good optical properties, the production of antimicrobial active and antimycotic surface, track and signaling microbiological and biochemical changes, food packaging has become one of the most important areas of technological development of nanocomposites (Rhim et al, 2013). Table 1 shows that nanocomposites have already led to several innovations with potential applications in the food packaging sector.

Table 1: Innovations and the application of nanocomposites in food packaging

• Improved packaging properties: mechanical, thermal, barrier properties
• Biodegradability: enhanced biodegradation

• Active packaging: shelf life extension, oxygen scavenger, antimicrobial
• Intelligent packaging: interaction with the environment, self-cleaning, self-healing, indication of deterioration
• Delivery and controlled release: nutraceuticals, bioactive compounds
• Monitoring product conditions: time temperature indicator (TTI), freshness indicator, leakage indicator, gas detector
• Nanosensor: indication of food quality, growth of microorganisms
• Nanocoating
• Antimicrobial
• Information on product: RFID, nano-barcode, product authenticity

Intelligent or smart packaging is intended to monitor and provide information about the quality of the packaged food or its surrounded environment to predict or decide the safe shelf life. The intelligent/smart packaging may respond to environmental conditions, alert a consumer to contamination of pathogens, detect harmful chemicals or degradation products caused by food deterioration, indicate food quality, and initiate self-healing. The control and manipulation of nanosized clay platelets made it possible for the creation of smart materials, by combining the wide type of properties provided by the clay with the functionality of organic components. The intelligent packaging application of nanocomposite is mainly based on the function of package to provide information about keeping the product quality such as package integrity (leak indicator), time-temperature history of the product, time-temperature indicators (TTI), and tracing the origin of the packaged food products, nano barcodes or radio frequency identification (RFID).

2. TIME-TEMPERATURE INDICATORS (TTI)

To control the quality of a refrigerated products it is of particular importance to permanently determine the temperature of storage, and a finding that the cooling was not interrupted during storage or transport. For continuous temperature monitoring of a packaged product for the desired period using the so-called time-temperature indicators (TTI). A TTY is a small measuring instrument that records the temperature change with time. Indicators respond to changes in temperature, for example by changing the color. The indicator shows, for example, that in a certain time period maintaining the desired temperature cooling is not the same all the time. One should bear in mind that the time-temperature indicators do not always determine the actual temperature of the packaged product, but the surface temperature of the packaging. There are a number of different patented indicator systems, and some of them are already in use. There are simple temperature indicators - TI, which are also placed on the surface of the packaging. They only give information about whether the product in the packaging in storage compatibility was exposed to a higher or lower temperature than the set, but not how long the product has been exposed to this temperature. These indicators suggest only that the cold chain is interrupted during storage. The control of the elapsed time is very important for the storage of food products and pharmaceutical products. A large number of time-temperature indicators (TTI) based on the different chemical and physical characteristics have been developed. Most of the products show color change over a certain period of time. This type of time monitoring is very simple and acceptable for most users.

Variations in the temperature of food can lead to a change in the safety and quality of the product. Time-temperature indicator (TTI) can be described as a simple, inexpensive device for easy measurement of changes in the temporal temperature dependence that reflects the whole or part of the history of the temperature at which food is placed [Taoukis et al, 1989]. Time-temperature indicators recently available in the market operate on mechanisms based on different principles. Principles of operation of time-temperature indicators are mechanical, chemical, enzymatic or microbiological irreversible change, usually expressed as a visible indication in the form of mechanical deformation, color shift or color change [Taoukis et al, 2008]. For chemical or physical response, it is based on chemical reaction or physical change towards time and temperature, such as acid-base reaction, melting, polymerization, etc. While for biological response, it is based on the change in biological activity, such as microorganism, spores or enzymes towards time or temperature [Ottles et al, 2008] [Kuswandiet et al, 2011]. The rate of change is temperature dependent, increasing at higher temperatures similarly to the deteriorative reactions responsible for product quality deterioration. The visible response of the TTI thus cumulatively reflects the time-temperature history of the product it accompanies [Taoukis et al,

2008). TTIs must be easily activated and then exhibit a reproducible time-temperature dependent change that is easily measured. This change must be irreversible and ideally mimic or be easily correlated to the food's extent of deterioration and residual shelf life. TTIs may be classified as either partial history or full history indicators, depending on their response mechanism (Selman et al, 1995). TTIs may be classified into three categories (Taoukis et al, 2003):

- **Critical temperature indicators (CTI)** show exposure above (or below) a reference temperature. Denaturation of an important protein above the critical temperature or growth of a pathogenic microorganism is other important cases where a CTI would be useful.
- **Critical temperature/time integrators (CTTI)** are useful in indicating breakdowns in the distribution chain and for products in which reactions, important to quality or safety, are initiated or occur at measurable rates above a critical temperature. Examples of such reactions are microbial growth or enzymatic activity that is inhibited below the critical temperature.
- **Time temperature integrators or indicators (TTI)** give a continuous, temperature dependent response throughout the product's history. Commercially available TTIs are given in Table 2.

Table 2: The manufacturers and models of commercially available time-temperature indicators

Product	Company
MonitorMark	3M
Timestrip®	TimestripPlc
Fresh-Check®	LifeLines
Checkpoint®	Vitsab
OnVu TTI	OnVu
[eO]®	Cryolog
TT Sensor TTI	Avery Dennison

The 3M MonitorMark® (3M Co., St Paul, Minnesota) is diffusion-based indicator label and is on the color change of an oxidable chemical system controlled by temperature-dependent permeation through a film (Figure 1). The action is activated by a blue-dyed fatty acid ester diffusing along a wick. A viscoelastic material migrates into a diffusely light reflective porous matrix at a temperature dependent rate. The response rate and temperature dependence is controlled by the tag configuration, the diffusing polymer's concentration and its glass transition temperature and can be set at the desirable range (Ahvenainen et al, 1997) (Taoukis et al, 2008). MonitorMark™ has two versions, one intended for monitoring distribution, the threshold indicator for industry, and other intended for consumer information, the smart label (Kuswandiet et al, 2011). Response of the indicator is measured by the progression of the blue dye along the track, and this is complete when all five windows are blue.



Figure 1: 3M MonitorMark®

The Timestrips® (Timestrip UK Limited, UK) are smart labels for monitor how long a product has been open or how long it has been in use (Figure 2). Temperature monitoring at home is also very important for food safety. Timestrip® is a single-use consumer activated smart-label for monitoring elapsed time on perishable products. It was designed to enable consumers to record time elapsed since activation of the label. This functionality is particularly suitable for packaging or labeling perishable products or products requiring regular maintenance or replacement (refrigerated and frozen products). It automatically monitors lapsed time, from 10 minutes to 12 months. The label is automatically activated when the consumer opens the packaging or it can be

supplied as an external label that consumers can manually activate when they first use a product [Selman et al, 1995] [Kuswandi et al, 2011].

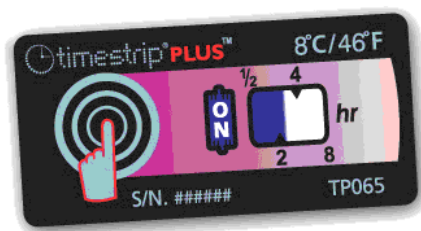


Figure 2: Timestrips@

The Fresh-Check®TTI (Temptime Corp., Morris Plains, NJ, USA) is based on a solid state polymerization reaction, resulting in a highly coloured polymer (Figure 3). The response of the TTI is the colour change measurable as a decrease in reflectance [Taoukis, 2008]. The indicator consists of a small circle of a polymer surrounded by a printed reference ring. The inside polymer circle darkens if the package has experienced unfavorable temperature exposures (Summers, 1992), and the intensity of the color is measured and compared to the reference color scale on the label [Kruijff et al, 2002]. The faster the temperature increases, the faster the color changes occur in the polymer. Consumers are advised not to consume or purchase the product, regardless of the “use-by” date [Han et al., 2005]. This indicator may be applied to packages of perishable products to ensure consumers at point-of-purchase and at home that the product is still fresh. These indicators have been used on fruitcake, lettuce, milk, and frozen food.

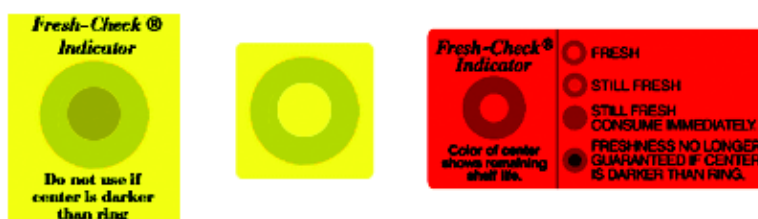


Figure 3: Fresh-Check®TTI

The CheckPoint®TTI (VITSAB A. B., Malmö, Sweden) is a simple adhesive label based on enzymatic system (Figure 4). These labels react to time and temperature in the same way that food product reacts, and thus gives a signal about the state of freshness and remaining shelf life. The TTI is based on a colour change caused by a pH decrease that is the result of a controlled enzymatic hydrolysis of a lipid substrate. Hydrolysis of the substrate causes acid release and the pH drop is translated into a colour change of a pH indicator from deep green to bright yellow to orange red.



Figure 4: CheckPoint®TTI

The OnVu™ TTI (Ciba Specialty Chemicals&Freshpoint, SW) is a newly introduced solid state reaction TTI (Figure 5). It is based on photosensitive compounds, organic pigments e.g. benzylpyridines, that change colour with time at rates determined by temperature. The TTI labels consist of a heart shaped ‘apple’ motif containing an inner heart shape. The image is stable until activated by UV light from an LED lamp, when the inner heart changes to a deep blue colour. A filter is then added over the label to prevent it being recharged. The blue inner heart changes to white as a function of time and temperature. The system can be applied as a label or printed directly onto the package [Taoukis et al, 2008] [Tsironiet et al, 2008].

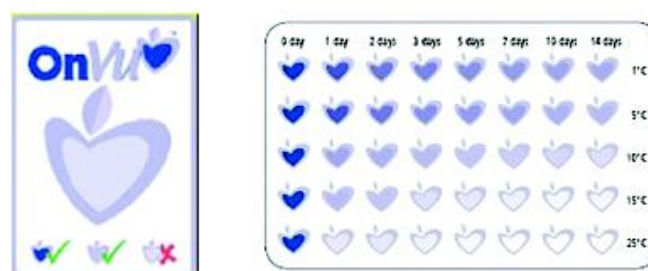


Figure 5: OnVu TTI

The (eO)[®] TTI (CRYOLOG, Gentilly, France) is based on a time-temperature depended pH change caused by controlled microbial growth selected strains of lactic acid bacteria that is expressed to colour change through suitable pH indicators (Figure 6). Prior to utilization, these TTIs are stored in a frozen state (-18 °C) to prevent the bacterial growth in the TTI medium. As they are very thin, their activation is obtained simply by defrosting them for a few minutes at the room temperature. Once they are put on the food, and in case of temperature abuse, or when the product reaches its use by date, the temperature-dependent growth of the TTI microorganisms causes a pH drop in the tags leading to an irreversible color change of the medium chromatic indicator, which becomes red (Ellouze et al., 2008) (Taoukis, 2008).



Figure 6: (eO)[®] TTI

The TT Sensor - TTI (Avery Dennison Corp., USA) is based on diffusion-reaction concept (Figure 7). A polar compound diffuses between two polymer layers and the change of its concentration causes the colour change of a fluorescent indicator from yellow to bright pink (Taoukis, 2008). Many new types of TTIs have recently been developed. For example, Rani and Abraham (2006) developed new enzyme reactions for a low-cost TTI and Wanihsuksombat et al (2008) developed prototype of a lacticacid-basedtime-temperatureindicator for monitoring food quality. Galagan and Su (2008) developed a novel colorimetric TTI based on fadable ink. Vaikousi et al (2009) developed a new TTI system based on the growth and metabolic activity of a *Lactobacillus sakei* strain for monitoring food quality throughout the chilled foodchain. Yan et al (2008) developed a new amylase-type TTI based on the reaction between amylase and starch.



Figure 7: TT Sensor TTI

As it can be seen from the previous examples of sensors, most are based on the irreversible reactions associated with the colorimetric changes that occur over time, and can be detected visually (Figure 8).

The main advantage of TTI is that it can be placed on the surface of the packaging and has the effect that there is no need for approval if the chemical composition of the sensor is hazardous for food in packaging because they are not in contact.

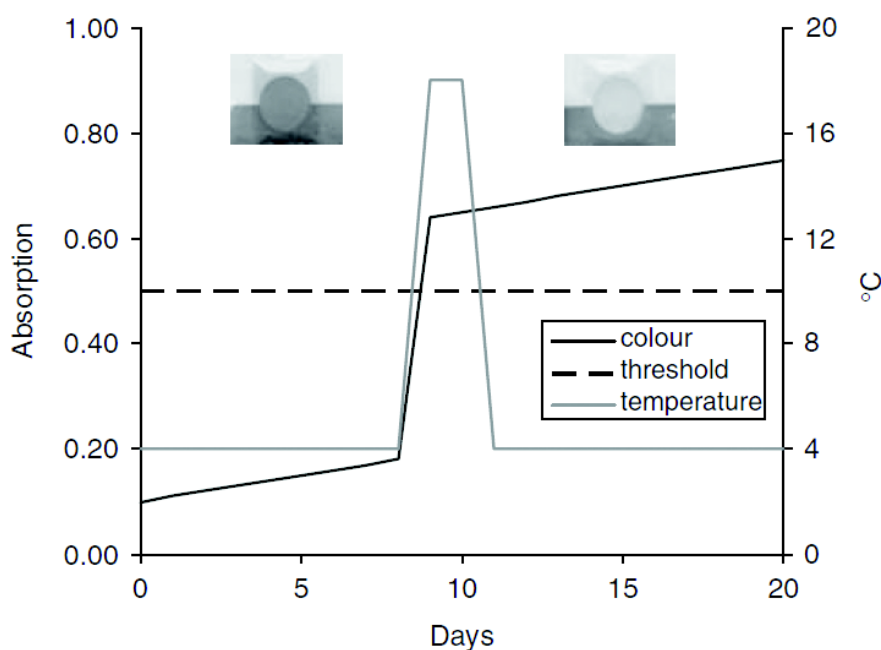


Figure 8: Schematic representation of the color change indicator based on changes in time and temperature

3. RFID TEMPERATURE MONITORING OF FOOD PACKAGING

Nowadays the introduction of RFID has raised the question, can these electronic devices be used for monitoring the temperature history as well? Indeed, this is possible with so-called active RFIDs (RFID with internal power supply in the label) that are coupled to a temperature sensor. In contrast to the visual TTIs, they can tell us not only if the food product has been exposed to a high temperature, but also when this has happened because these devices log the temperature in time (at the moment with only a limited time resolution). A major drawback of these electronic devices, in particular active RFIDs, is that their cost price is still far too high to be applied in single food packaging.

Today there are solutions of electronic recorders with built-in memory, but not in commercial use. Workers in the 3M company invented THID (device for indication of temperature history). Yet another product that communicates with the computer when reading the "Tattletale thermograph." This thermograph records temperature changes in memory and can be programmed to record in intervals of 5,5-6h during the 32 months. Functional temperature range is -41 to 85 °C [Yam, 2009].

4. RESULTS

4.1 Knowledge base of active and intelligent packaging

Due to the high cost of RFID chips when it comes to primary (retail) packaging, as well as the adjustment process of signals of personal mobile devices, it is necessary to link information between sensors and mobile devices on the basis of the already present solutions. Overview of the present solution is in the knowledge base of active and intelligent packaging (Figure 9).

Knowledge base has been formed to gather concrete solutions for the application of sensors and indicators on active and intelligent packaging. The software tools Adobe Photoshop, Adobe Flash, Autodesk 3Ds Max and Deep Exploration have been used for developing application. The final form of the application is the html page as the base educational and html extension allows readability in almost all modern computing platforms that have a web browser [Đurđević, 2013]. Figure 9 shows the interface section of the application that shows an example of intelligent packaging systems, time-temperature indicators.

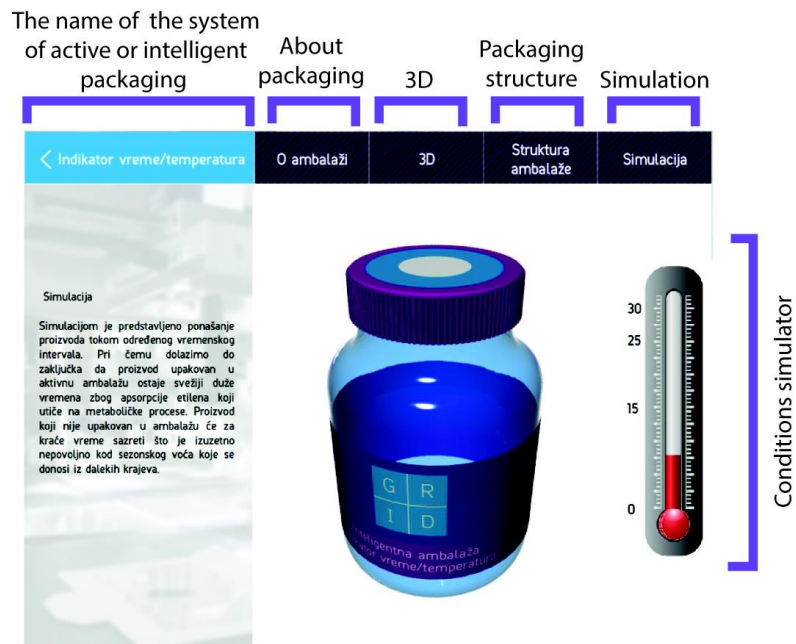


Figure 9: The application interface of knowledge base of active and intelligent packaging

The application has the following interface elements (Figure 9):

- The name of the system of active or intelligent packaging - a concrete example of the "Time-temperature indicator";
- Navigation (buttons):
 - About packaging (theoretical basis)
 - 3D (display with the ability to control and separate additional explanatory segments of packaging)
 - Packaging structure (basic elements of the cross-sectional packaging and animation interaction with the product)
 - Simulation (animation behavior of products under certain conditions)
- Conditions simulator (animation calendar or thermometer) depending on whether the time and/or temperature affect the content packaging (Đurđević, 2013).

4.2 Schematic integration of TTI sensors with modern portable personal devices

After analyzing the existing solutions of indicators on intelligent packaging and smart label solutions from different manufacturers one comes up with the concept solutions.

As it can be seen in Figure 8, colorimetric change of the sensor is directly related to time and temperature. It is also the only parameter whose analysis we come to hear about the freshness. The sense of sight is operational tool for obtaining information about the freshness, but how eyesight is not perfect for all users should be given information converted into a signal that can be useful for providing various types of control freshness (visual, sound, touch).

Today's modern mobile devices and mobile devices future thinking on mobile phones, tablet devices, smart watches, "Google glasses" have a built-in camera. Camera sensors on the devices have different quality, and the need for analyzing signals have reference values of the initial and final color of the indicator. In this way, it would be necessary to establish a system of three points, two references and an indication of freshness. And then a simple approach of the device to a variety of platforms and hardware specifications could be recorded, which could be analyzed in the background device. When analyzing the color of the indicator by comparing with the reference points in order to avoid the possibility of affecting the quality of the camera device, the current brightness of the room where the package is located. With the information that formed the basis of three key points you need to get the device identification of the allotted time period duration, expressed in days, months or years. This information could be placed on the label in the form of codes or tags that are analyzed together with benchmarks. A schematic overview is given in Figure 10.

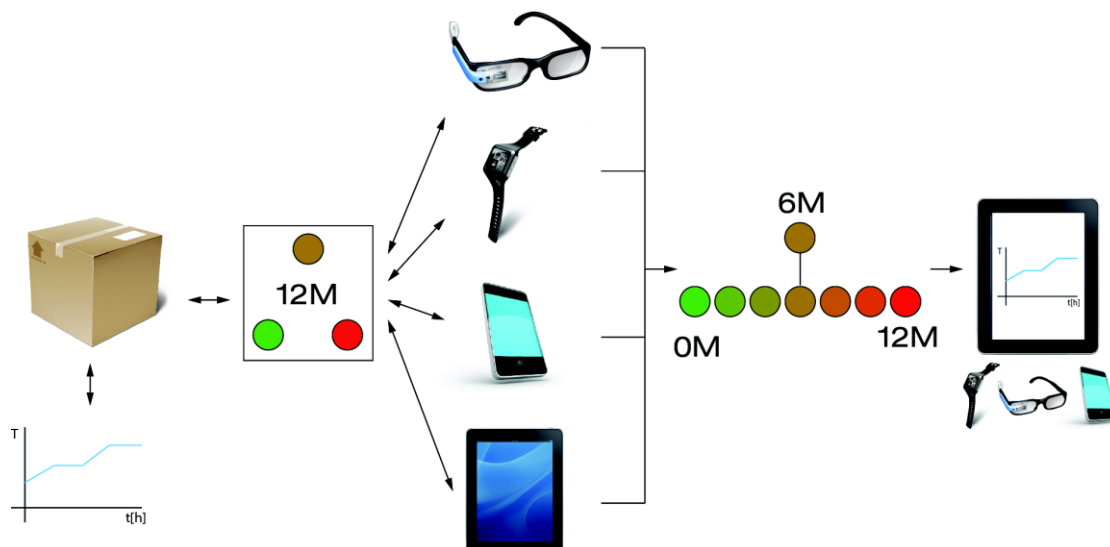


Figure 10: Schematic representation of the modern flow of information on changing the time and temperature of the product

Because of the need for speed of getting information, in accordance with the capabilities of software tools for other purposes, there would be the possibility of graphical analysis at the time of observation, within the background of the process unit.

The system indicator based on visual analysis of the current solutions is acceptable, but the problems we face are:

- Limitation of the number of users who can use these indicators (people who do not see the entire color spectrum: protanopia, tritanopia, deuteranopia),
- Information about the freshness in the form of color is not fast enough and informative requirements analysis, subjective and entails the possibility of mistake,
- Uniformity of information about the freshness of the existing solutions of indicators based on color changes.

Through integration of personal devices one could reduce the possibility of errors, provide information more quickly, and turn it into a signal which we could manipulate and adapt it to the users' desires. Different indicator principles turn colorimetric change into different spectra. The color indicator manufacturers CheckPoint@TTI changed from dark green to orange-red color of the indicator OnVu TTI changing shades of blue, (eO) @ TTI changes color from red to green, and TT Sensor TTI changes color from yellow to light pink, etc. All of these systems can be developed within the software, deployed on a device that will create uniformity and provide objective information to the user.

5. DISCUSSION

Schema of integration of TTI sensors with modern portable personal devices shows an idea that is the basis for further development. Limitations of mobile devices in terms of recognition of color are overcome by the concept of sampling the reference values when processing the image. Today's mobile devices with a camera understand color in RGB system, which is satisfactory for the purpose of comparing the two color value. Conceptual solution is adjustable irrespective of the colorimetric change of the indicator in the change in the freshness of the product. Provision of subjective value about the freshness of products and provision of information about the freshness of users who do not see the whole spectrum of colors is the main advantage and reason for development of the system. Popularity of the use of mobile devices and applications within the same would surely brought advantage to producers from the point of advertising their products.

6. CONCLUSIONS

Contemporary packaging materials are subject to daily development. The future of packaging for food is the integration of sensors and indicators to the level of primary packaging that interacts with the end user. The paper gives a detailed overview of the solutions by the time-temperature indicator (TTI), and review of solutions RFID system for monitoring the freshness of the product. With the development of technology opens up greater opportunities applying indicators on food packaging because of the reduction of the cost of the same. Current acceptable solutions are based on the concept of smart labels (smart labels) to a different way of providing information on the freshness of the product. Schema integration TTI sensor with modern portable personal devices in the concept for the development of these solutions to uniformity of the final information about the freshness of the product. In this way, interactive packaging instead of subjective information sends objective information about the freshness of the product to user, overcoming the problem of limited number of users, and providing information faster uniforming it in order for it to be more understandable to user.

7. REFERENCES

- [1] Ahvenainen, R., Hurme, E.: "Active and Smart Packaging for Meeting Consumer Demands for Quality and Safety", *Food Additives & Contaminants*, 14, page 753–763. (1997).
- [2] Đurđević, S., Novaković, D.: "Razvoj baze znanja aktivne i inteligentne ambalaže", *Zbornik radova Fakulteta tehničkih nauka*, 28(10), page 1769–1772, (2013).
- [3] Ellouze, M., Pichaud, M., Bonaiti, C., Coroller, L., Couvert, O., Thuault, D., Vaillant, R.: "Modelling pH evolution and lactic acid production in the growth medium of a lactic acid bacterium: application to set a biological TTI", *International Journal of Food Microbiology*, 128, page 101–107, (2008).
- [4] Galagan, Y., Su, W.: "Fadable ink for time-temperature control of food freshness: Novel new time -temperature indicator", *Food Research International*, 41, page 653–657, (2008).
- [5] Han, J, Ho, C., Rodrigue, E.: "Innovation in food packaging", (Elsevier Academic Press, London, 2005), page 138–155.
- [6] Kruijff, N., Beest, M., Rijk, R., Sipilainen, T.: "Active and intelligent 250 Adriana Pavelková packaging: applications and regulatory aspects", *Food Additives & Contaminants*, 19, page 144– 162, (2002).
- [7] Kuswandi, B., Wicaksono, Y., Abdullah, A., Lee Y.- H., Ahmad, M.: "Smart packaging: sensors for monitoring of food quality and safety", *Sensorry and Instrumentation for Food Quality*, 5, page 137–146, (2011).
- [8] Otles, S., Yalcin, B.: "Intelligent food packaging", *Log Forum*, URL: http://www.logforum.net/pdf/4_3_4_08.pdf (last request: 2014-08-20).
- [9] Rani, D., Abraham, T.: "Kinetic study of a purified an ionic peroxidase isolated from *Eupatorium odoratum* and its novel application as time temperature indicator for food materials", *Journal of Food Engineering*, 77, page 594–600 (2006).
- [10] Rhim, J., Park, H., Ha, C.: "Bio-nanocomposites for food packaging applications", *Progress in Polymer Science*, 38 (10-11), page 1629–1652, (2013).
- [11] Selman, J., Rooney, M.: "Active food packaging", 1st edition, (Blackie Academic & Professional, London, 1995), page 215–237.
- [12] Summers, L.: "Intelligent packaging for quality", *Soft Drinks Management International*, 36, page 32–33, (1992).
- [13] Taoukis, P., Labuza, T.: "Applicability of time-temperature indicators as shelf life monitors of food products", *Journal of Food Sciences*, 54, page 783–788, (1989).
- [14] Taoukis, P., Labuza, T.: "Time- temperatur e indicators (TTIs)", *Novel food packaging techniques*, page 590, (2003).
- [15] Taoukis, P., Kerry, J., Butler, P.: "Smart Packaging Technologies for Fast Moving Consumer Goods", (John Wiley&Sons, 2008), page 61-74.
- [16] Tsironi, T., Gogou, E., Velliou, E., Taoukis, P.: "Application and validation of the TTI based chain management system SMAS (Safety Monitoring and Assurance Sytem) on shelflife optimalization of vacuum packed chilled tuna", *International Journal of Food Microbiology*, 128, page 108–115, (2008).

- [17] Vaikousi, H., Biliaderis, C., Koutsoumanis, K.: "Applicability of a microbial Time Temperature Indicator (TTI) for monitoring spoilage of modified atmosphere packed minced meat" *International Journal of Food Microbiology*, 133, page 272–278, (2009).
- [18] Wanihsuksombat, C., Hongtrakul, V., Suppakul, P.: "Development and characterization of a prototype of a lactic acid– based time–temperature indicators for monitoring food product quality", *Journal of Food Engineering*, 100, page 427–434, (2010).
- [19] Yam, K. -L., Takhistov, P., Miltz, J.: "Intelligent packaging: concepts and applications", *Journal of Food Sciences*, 70, (2005).
- [20] Yam, K. -L.: "Wiley encyclopedia of packaging technology", (A John Wiley & Sons, Hoboken, 2009), page 360–582.
- [21] Yan, S., Huawei, C., Limin, Z., Fazheng, R., Luda, Z., Hengtao, Z.: "Development and characterization of a new amylase type time– temperature indicator", *Food Control*, 19, page 315–319, (2008).

ANALYSIS OF THE MESSAGE TRANSPORT SYSTEMS IN AJAX APPLICATIONS USING IMAGES

Darko Avramović, Gojko Vladić, Vladimir Zorić

Faculty of Technical Sciences, Graphic Engineering and Design, Novi Sad, Serbia

Abstract: AJAX applications are now one of the most common types of web applications. They allow the implementation of very complex tasks. They are usually composed of components. These components communicate with each other through a variety of systems and message formats. Among the most common are JSON and XML formats. Besides transport of textual data these types of transport can transfer binary data as well. The purpose of this study was to investigate the characteristics of communication within AJAX applications using various image formats. Images are compressed to different degrees and methods of compression. Images are transported between components and thus the optimal level and compression method is determined by measuring time intervals during pictures transport through the system. Another factor for the selection of optimal compression is the visual factor – acceptable or as few traces of JPEG compression. The ultimate goal is to determine the optimal method and compression in applications dealing with any vision processing or working with images (for example Web2Print systems).

Key words: AJAX, performance, images, transport

1. INTRODUCTION

During the past several years many things have changed in sphere of web design and applications/programming. Unlike web sites which were made like 10 years ago, today's web sites and web applications heavily rely on AJAX (Asynchronous Javascript And Xml) [Draganova, 2010, Mesbah and Deursen, 2009]. AJAX presents a set of technologies and a new way of creating and designing applications. These technologies work together to provide functionality of different parts of an application. Each of these technologies provide unique functionality to the application [Dahlan and Nishimura, 2008; Eernisse, 2006]. One of the primary goals of Ajax implementation on Web applications is to improve the user's experience of response time. The response time is defined as the time between sending a request and receiving the response. By reducing response time, Ajax can provide a significantly better user experience. Ajax can improve response time by communicating with the server without full-page requests. With this new change comes a whole set of new challenges, mainly due to the fact that AJAX shatters the metaphor of a web 'page' upon which many classic web technologies are based. One of these challenges is testing such applications [Bozdog et.al., 2009; Marchetto et.al. 2008; Mesbah et.al., 2008].

AJAX application testing can be performed using any conventional method. The testing can be performed on both client and server side. Some sorts of client-side testing tools include Selenium, WebKing, and Sahi which allow many kinds of capture and trigger methods triggered by application users. Also, the testing can be performed using any type of data (textual, binary, etc...). Beside the testing applications mentioned, custom testing applications can be made for testing purposes.

2. METHOD

Research method involves usage of images for AJAX application data transport system performance tests. There were two sizes of images:

large – resolution 2560x1600 screen pixels, 72ppi, RGB

small – resolution 454x340 screen pixels, 72ppi, RGB

Also, there were two types of images:

images with text and no gradients, called "text images"

images with shapes with gradients, called "shape images"

Figures 1 and 2 present the images used during the experiment.

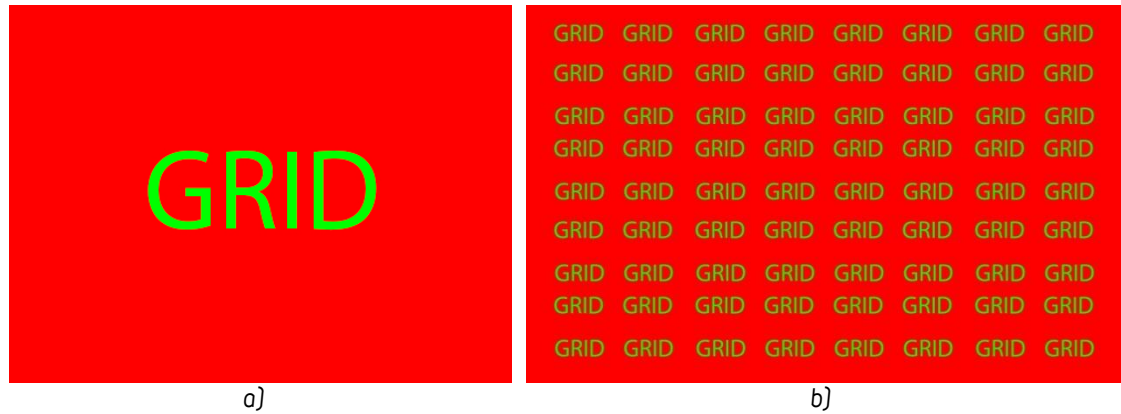


Figure 1: "Text images", a) small (hereinafter Image 1), b) large (hereinafter Image 2)

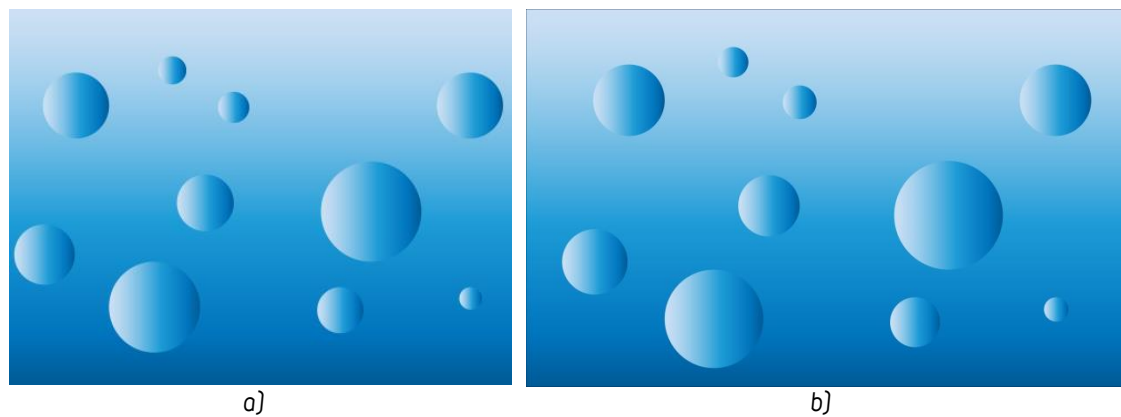


Figure 2: "Shape images", a) small (hereinafter Image 3), b) large (hereinafter Image 4)

Why these two types? The selection has been made based on contents. The contents of these images were supposed to be somewhat opposing. On one side there is text with sharp edges and only one color on top of single color background. On the other side there are multiple shapes colored using gradients on top of gradient background.

There were 36 samples of each image from Figures 1 and 2. Each compressed using different compression ratio and compression method. Compression methods used for experiment were: Baseline (Standard), Baseline Optimized and Progressive (3 scans). So, there were 36 samples of image from Figure 1a, 36 samples of image from Figure 1b, 36 samples of image from Figure 2a and at the end 36 samples of image from Figure 2b. Out of each of 36 samples 12 were compressed using Baseline (Standard) compression method, 12 were compressed using Baseline Optimized compression method and 12 were compressed using Progressive (3 scans) compression method. Photoshop version CS6 was used for compression purposes.

The images were processed using specially designed application (activity diagram presented on Figure 3). The application consisted of two main components (Figure 4):

- *Sender component* – the component which processes the images and sends them to responder component.
- *Responder component* – the component which receives the image and returns a response to sender component.

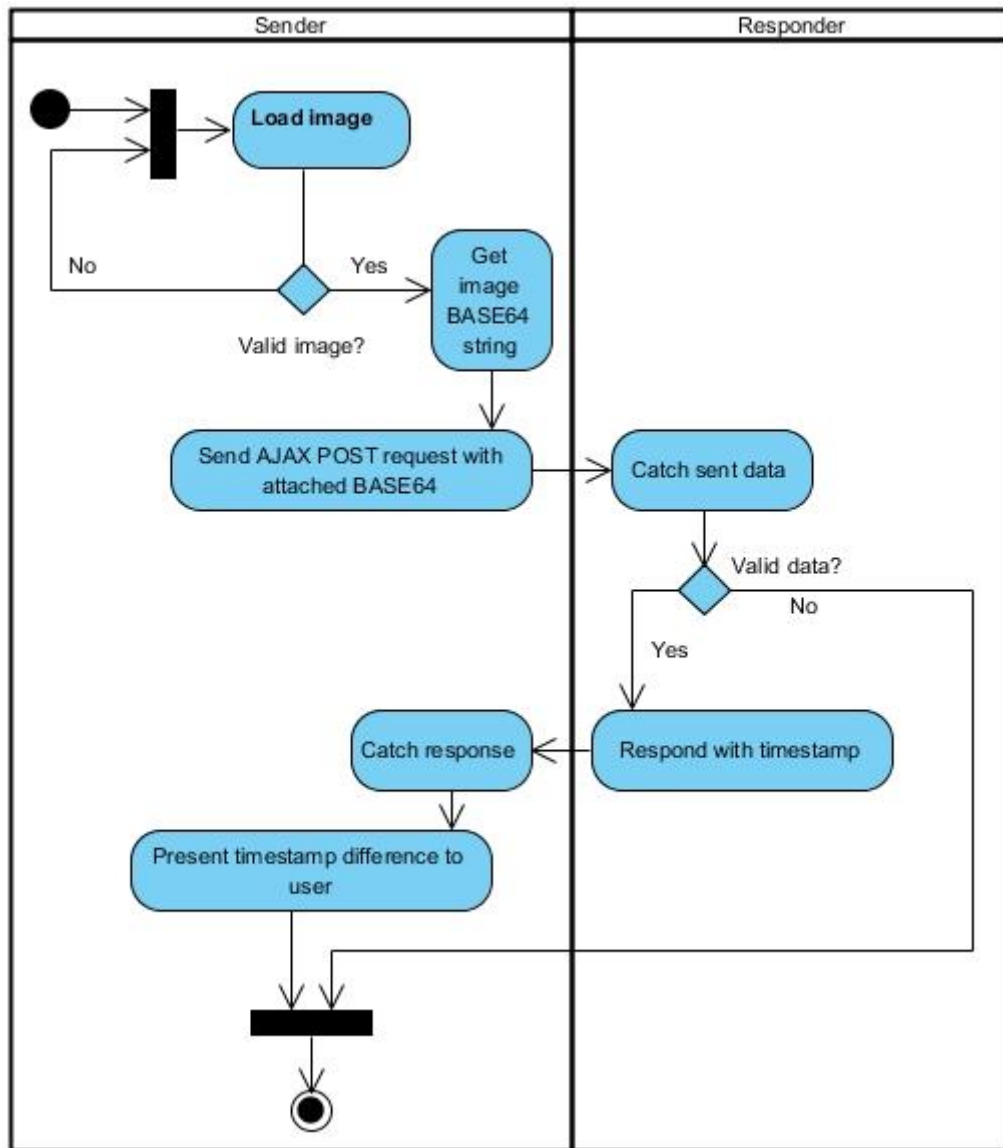


Figure 3: Testing application activity diagram

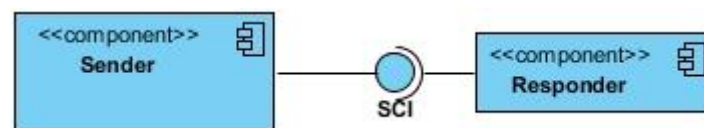


Figure 4: Testing application component diagram

Based on everything said till this point, the aim of this study was to determine optimal compression type and image quality for both quality satisfaction and satisfactory transfer speed inside an AJAX based application. Image quality was subjectively perceived based on JPEG compression footprints.

Testing environment:

- Intel Core2Duo processor
- 8GB RAM
- Microsoft Windows
- Apache 2.2.4 with PHP 5.5.x

3. RESULTS AND DISCUSSION

Figures 5 to 8 present file sizes depending on compression method. The x-axis presents file [1 through 12] and the y-axis presents the file size in kilobytes. In case of Image 1, file sizes are not too high, just under 40KB. There is no noticeable pattern depending on image quality (compression level) and compression method. Sometimes the file size is greater in case of Baseline Optimized compression method versus Baseline Standard compression method although it is known that Baseline Optimized compression method has slightly better compression ratio (About.com, 2014).

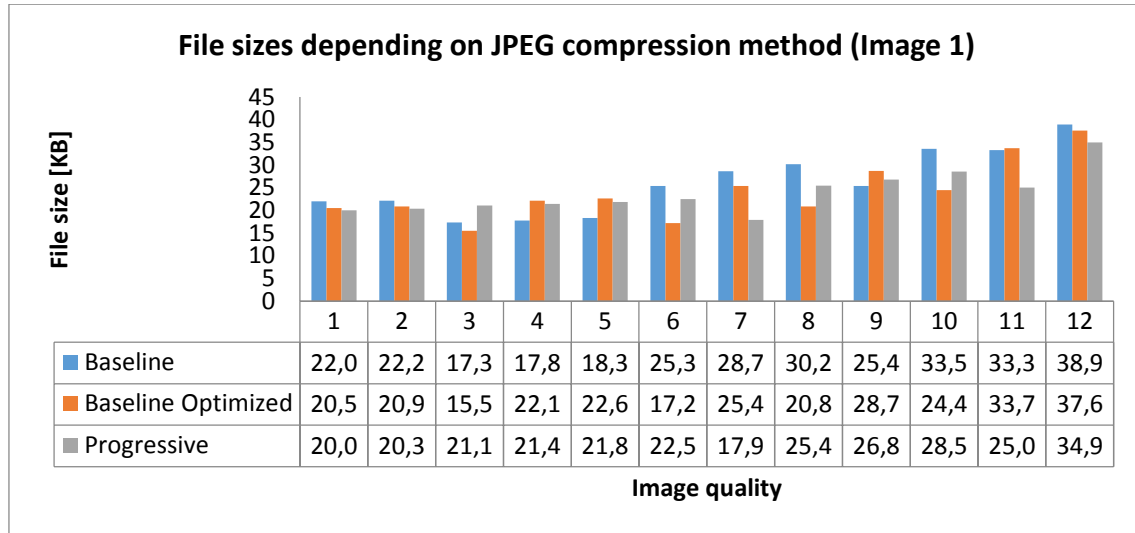


Figure 5: File sizes depending on JPEG compression method (Image 1)

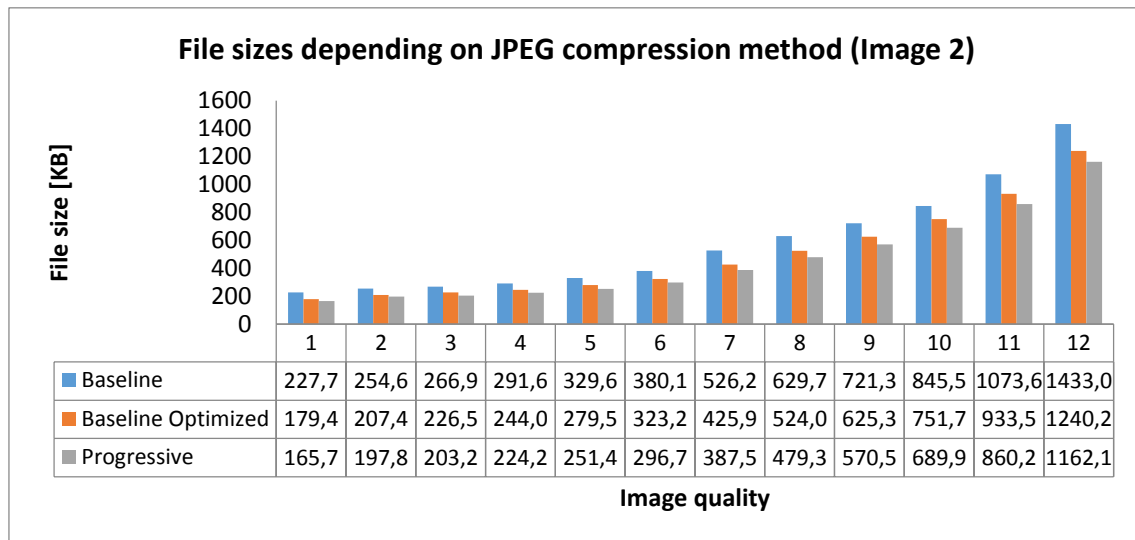


Figure 6: File sizes depending on JPEG compression method (Image 2)

In case of Image 2, the situation is different. There is obvious file size-compression method dependency pattern. Baseline Standard compressed image files are the largest. Figures 7 and 8 present similar pattern.

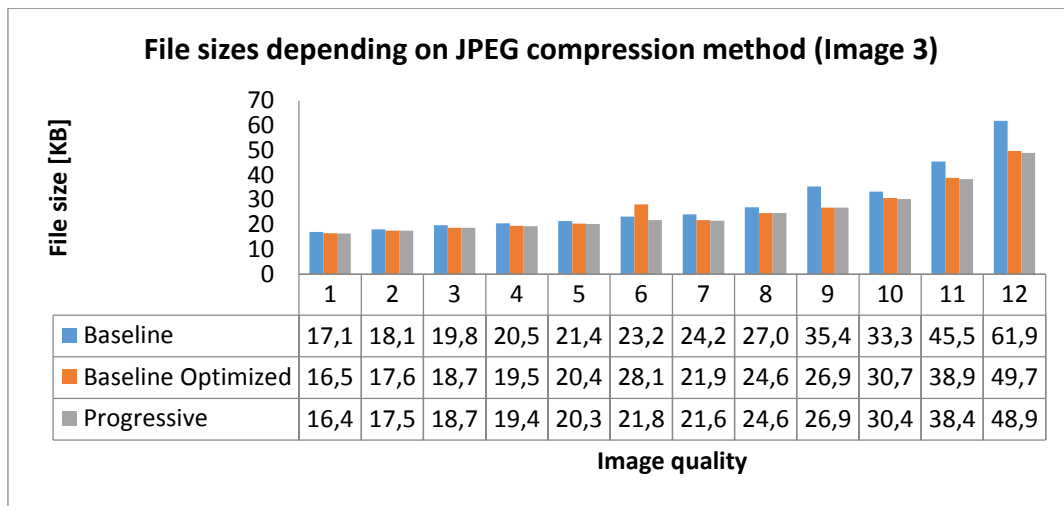


Figure 7: File sizes depending on JPEG compression method (Image 3)

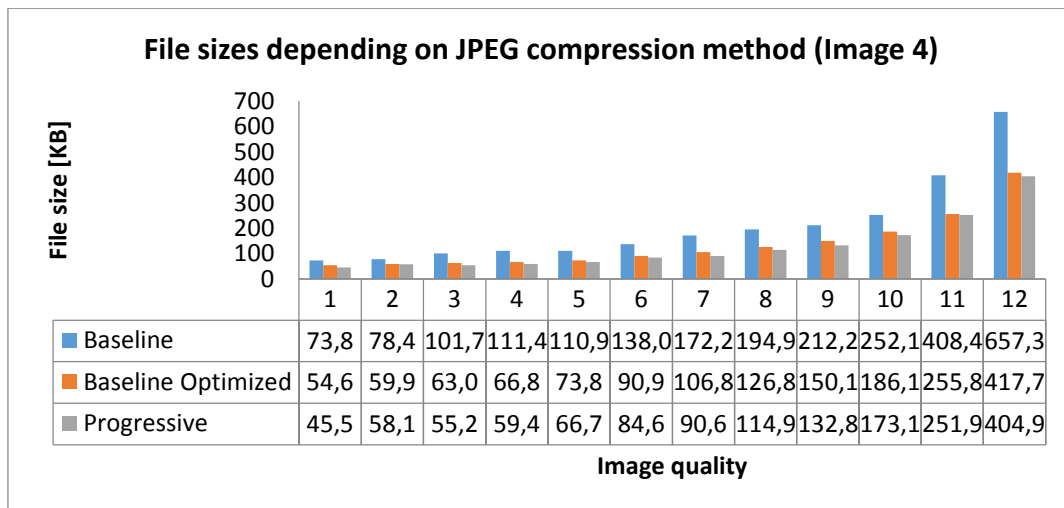


Figure 8: File sizes depending on JPEG compression method (Image 4)

Figures 9 to 12 present file size growth rate depending on image quality (compression ratio) for all three compression methods. All four figures show the highest file size growth ratio in case of Baseline Standard compression method. The lowest growth rate is characteristic for Progressive compression method. The conclusion was made based on linear function slope.



Figure 9: File size growth against image quality (Image 1)

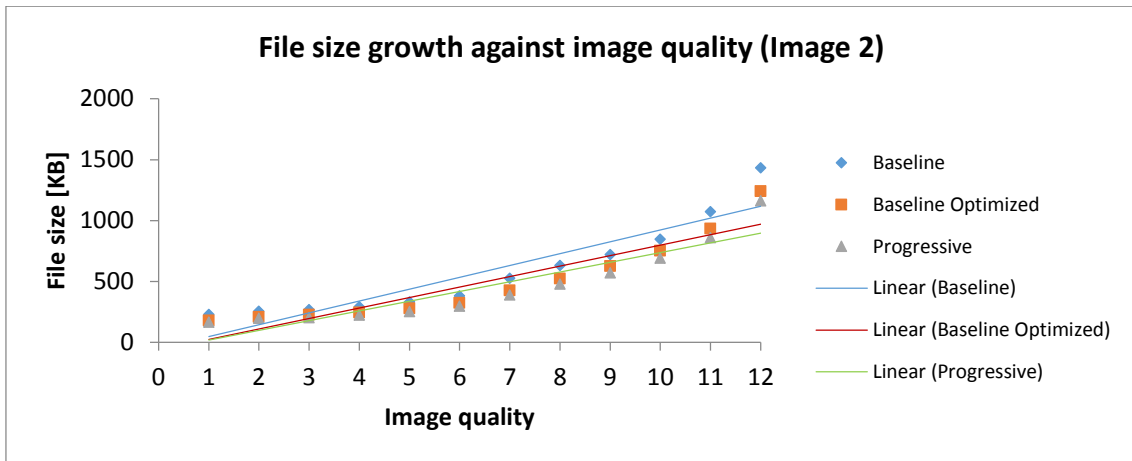


Figure 10: File size growth against image quality (Image 2)

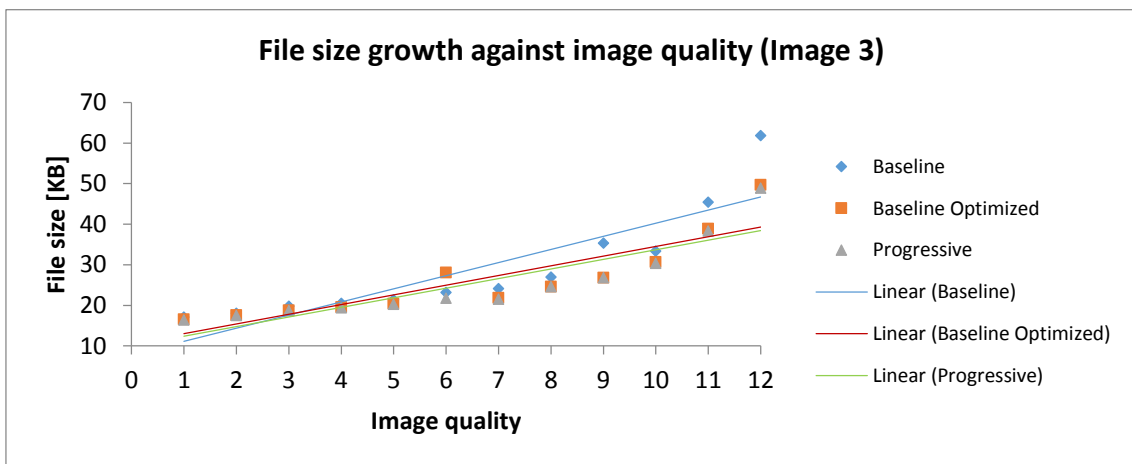


Figure 11: File size growth against image quality (Image 1)

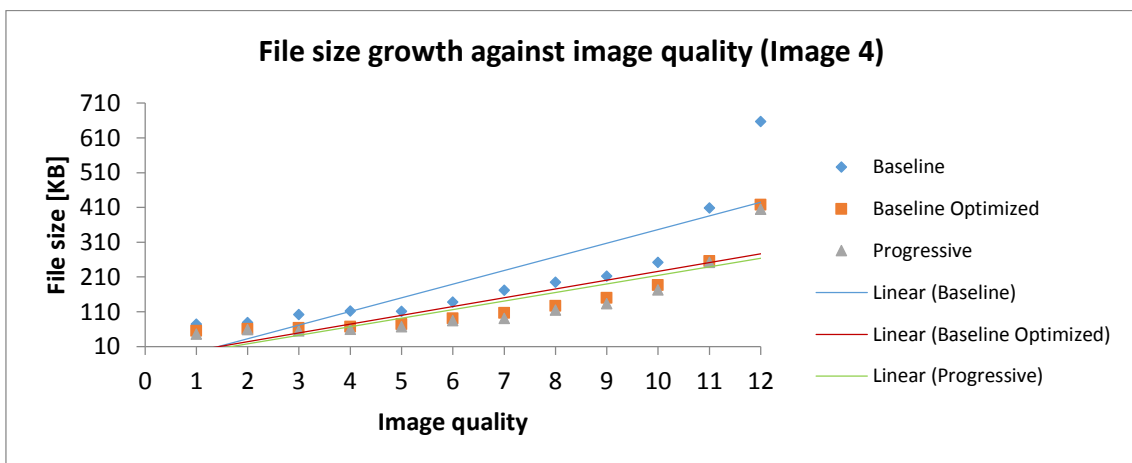


Figure 12: File size growth against image quality (Image 1)

Average response time is presented on figures 13 through 16. It is noticeable that the linear functions are in fact declining opposite to expectations. Common sense tells that the larger file is the longer it takes to transfer it. In this case it is conversely. Average response time actually drops with image quality (file size) increase. The same situation is noticeable in case of all four images. Figure 13 shows quite uniform response time values (reason: very quick response time under 14ms) but the decline is present towards higher image quality. Figure 14 presents a huge response time

drop in case of Image 2. A huge drop in response time is present between image quality level 6 and image quality level 7 and between level 11 and level 12. Lowest response time is actually in case of highest quality images. Figure 15 presents similar results to Figure 13. Gentle function decline is present. Figure 16 presents the lowest linear function decline.

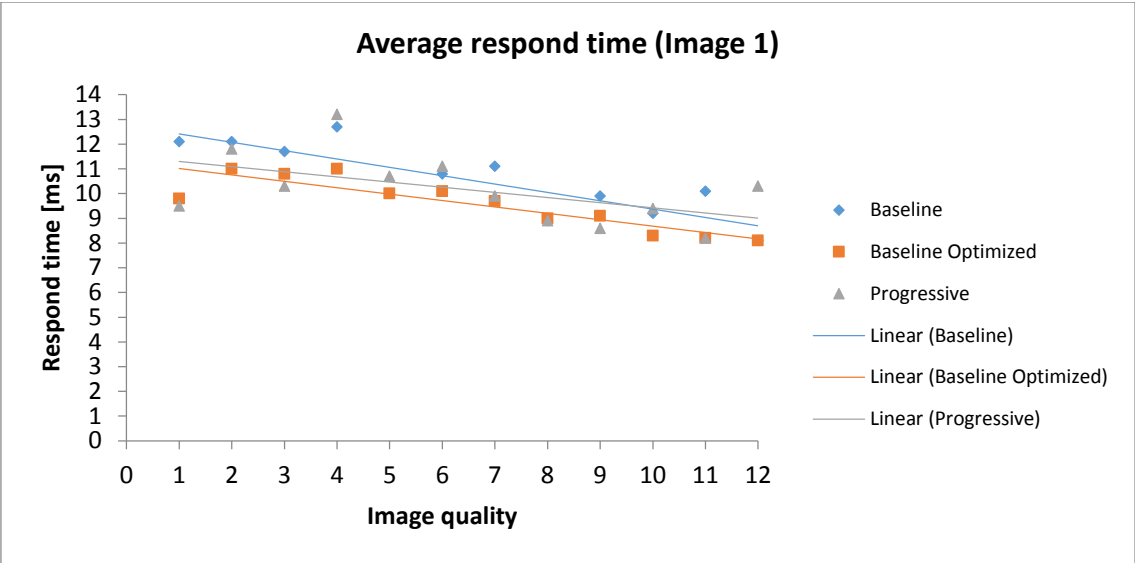


Figure 13: Average response time (Image 1)

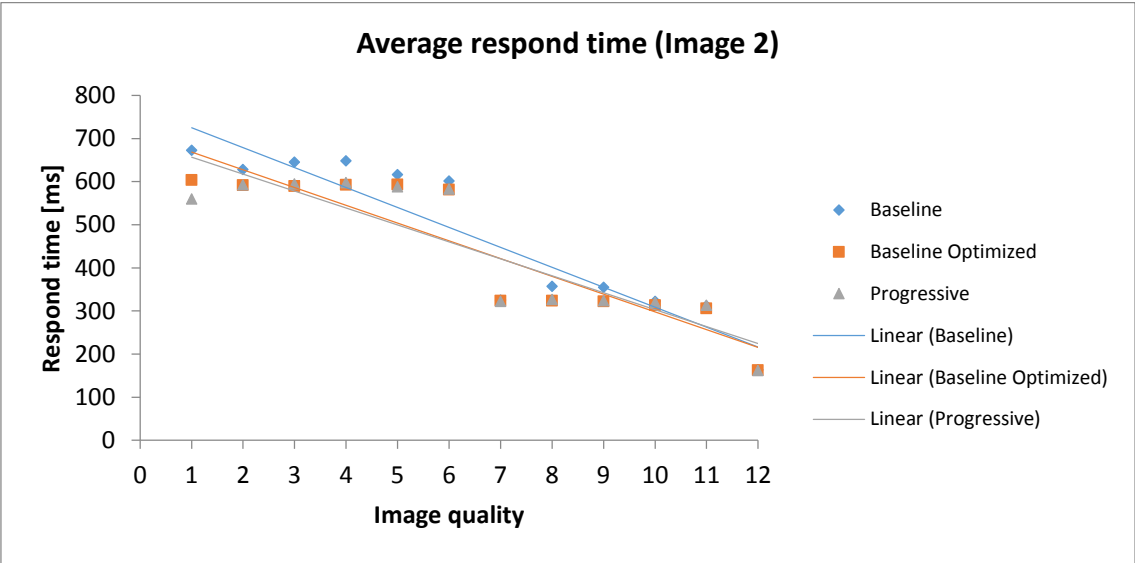


Figure 14: Average response time (Image 2)

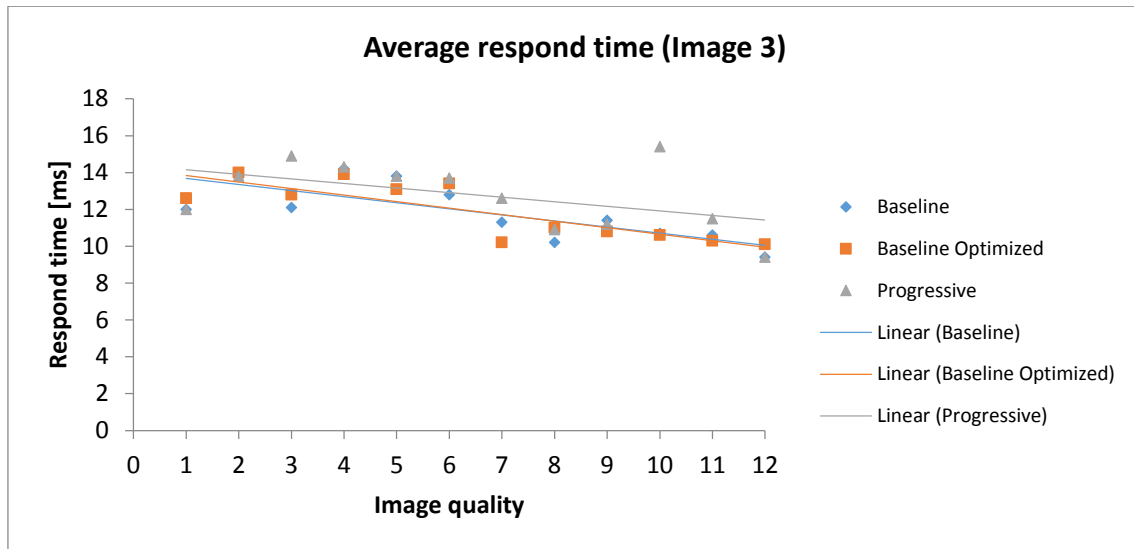


Figure 15: Average response time (Image 3)

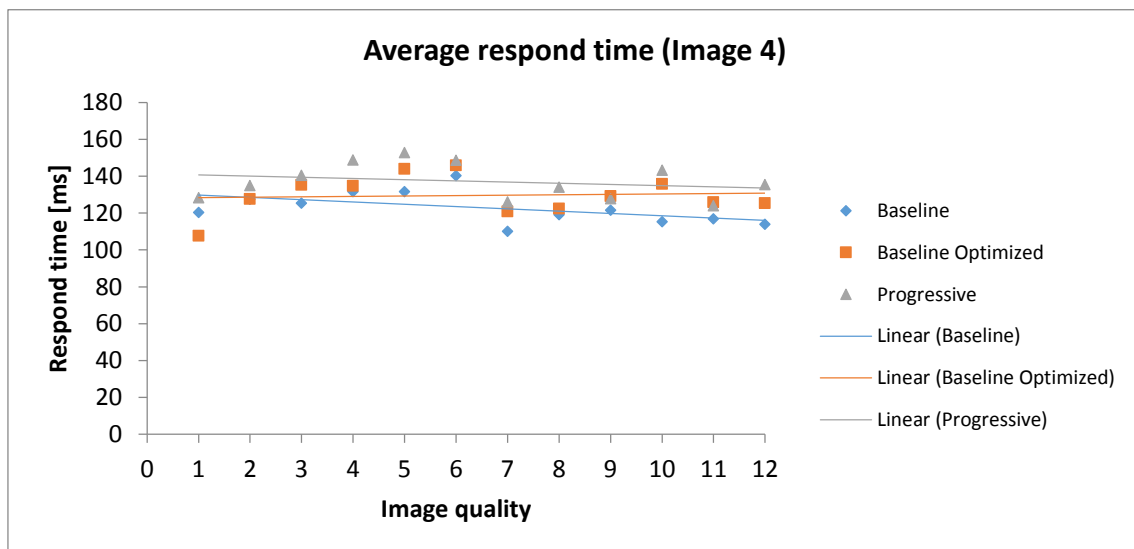


Figure 16: Average response time (Image 4)

At the end the question is: which compression method and compression level is best for optimal AJAX application internal data transfers (in case of images). According to research results, for small images with single color text on single color background optimal compression method is Baseline Optimized with lowest compression level. All response times for the image are fairly low but the mentioned situation is the best solution. For large images with single color text and single color background situation is similar. All three compression methods gave fairly similar results. The only question is which compression level to choose. Answer can be found on figure 14 – lowest compression level/highest image quality using any compression method. In case of small images with shapes and gradient fills/backgrounds, situation is similar to other type of small images. Slight function decline is present but Progressive compression method in cooperation with image quality level 12 performed the best. In case of large images with shapes and gradient fills/backgrounds, the situation is slightly different from same sized images of other type. Namely, smaller linear function decline is present but all three compression methods performed equally. The best solution in this case is Baseline Standard method with image quality 7, but results for images compressed using lowest compression level aren't far away. In fact, lowest response time in this case is achieved using Baseline Optimized-compressed images with highest compression level, but that cannot be the optimal solution because of poor image quality (SSIM 0,977671) (Figure 17a). Image quality 7 offers fairly good image quality with acceptable amount of JPEG footprint (SSIM 0,989943) (Figure

17b). Thus, it can be concluded that (in case of Image 4) Baseline Standard compression method with image quality 7 or more is good solution.

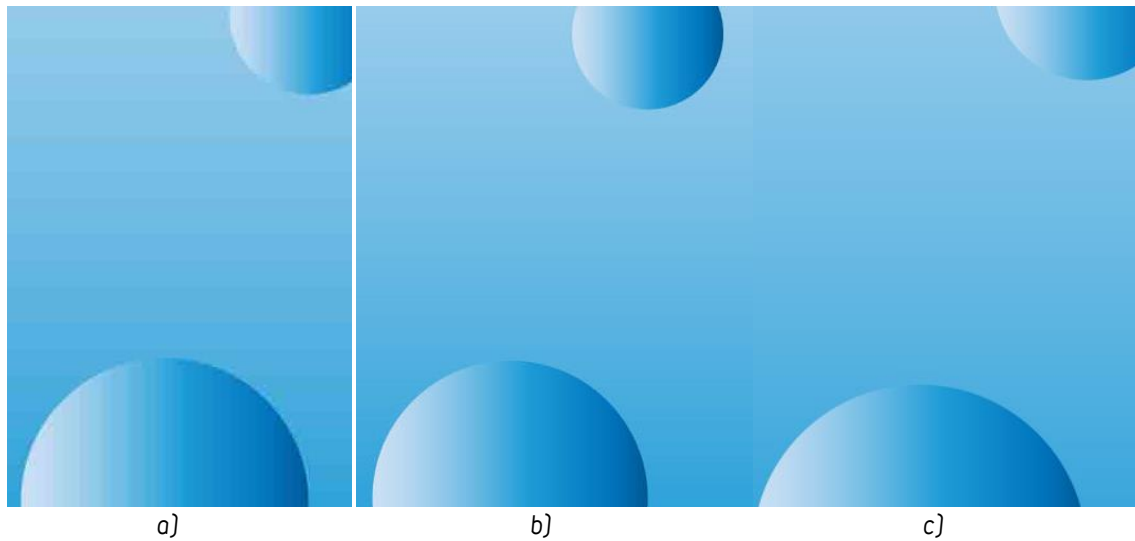


Figure 17: Image 4; a) image quality 1, b) image quality 7, c) image quality 12

Figure 18 presents SSIM maps for images from Figure 17a and 17b.

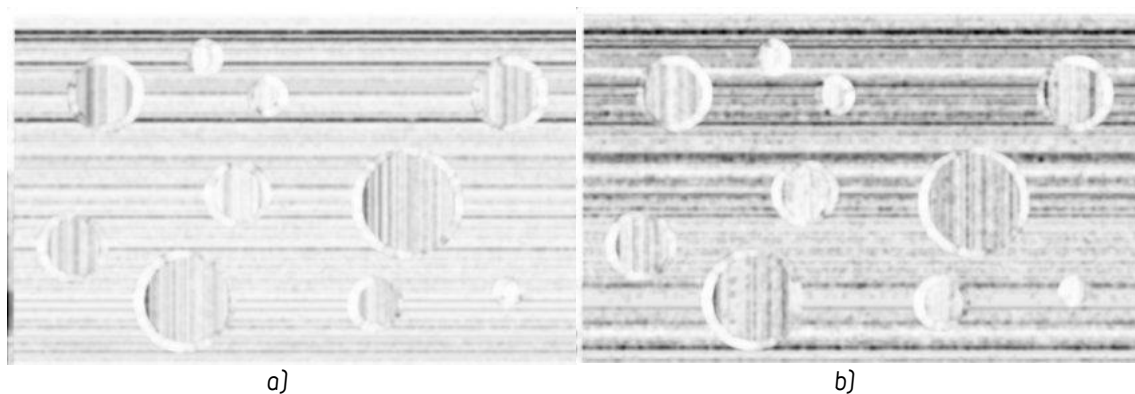


Figure 18: SSIM Maps; Image 4 Baseline Optimized Image quality 1, Image 4 Baseline Optimized Image quality 7

4. CONCLUSIONS

The research was conducted using carefully selected images. The images were chosen to be opposite in terms of content. Images were processed using reliable image processing software. The tests were conducted using specially created application used under specially prepared environment. The application recorded results presented within the paper. From the research it can be concluded that image transfer speed inside AJAX application depends on image contents, image compression method and image quality (compression level). Image contents as a factor impacts the transfer by reducing the speed in case of images with shapes and gradient fills/backgrounds. Images with text single color elements and single color backgrounds performed slower. The best compression method for large shape images turned out to be Baseline Standard. On the other hand, for images with text elements Baseline Optimized compression method took the lead. In case of image quality, the research shows that (contrary to common sense) transfer speeds for highest quality images were in fact the smallest.

5. ACKNOWLEDGMENTS

This paper was supported by the Serbian Ministry of Science and Technological Development, Grant No.: 35027 "The development of knowledge and production in graphic arts industry"

6. REFERENCES

- [1] About.com: "Which Graphics File Format Is Best To Use When?", URL <http://graphicssoft.about.com/od/graphicformats/f/summary.htm> (last request: 2014-09-30).
- [2] Bozdag, E., Mesbah, A., van Deursen, A.: "Performance testing of data delivery techniques for Ajax applications", *Journal of Web Engineering*, 8(4), pp 287-315 2009.
- [3] Dahlam, A. A., Nishimura, T.: "Implementation of Asynchronous Predictive Fetch to Improve the Performance of Ajax-Enabled Web Applications", *iiWAS '08 Proceedings of the 10th International Conference on Information Integration and Web-based Application & Services*, pp 345-350, ACM New York, ISBN: 978-1-60558-349-5
- [4] Draganova, C. (2007), "Asynchronous JavaScript Technology and XML", in *JICC 11, 11th Annual Conference of Java in the Computing Curriculum*, London.
- [5] Eernisse, M.: "Build Your Own AJAX Web Applications", SitePoint Pty. Ltd., USA, 2006.
- [6] Marchetto, A., Tonella, P., Ricca, F.: "State-based testing of Ajax web applications", In *Proc. 1st IEEE Int. Conference on Sw. Testing Verification and Validation (ICST'08)*, pp121-130. IEEE Computer Society, 2008.
- [7] Mesbah, A., Deursen, A.: "Invariant-Based Automatic Testing of AJAX User Interfaces", *ICSE '09 Proceedings of the 31st International Conference on Software Engineering*, pp210-220, IEEE Computer Society Washington, ISBN: 978-1-4244-3453-4
- [8] Mesbah, A., Bozdag, E., van Deursen, A.: "Crawling Ajax by inferring user interface state changes", In *Proc. 8th Int. Conference on Web Engineering (ICWE'08)*, p122-134. IEEE Computer Society, 2008.

Design, typography and
user experience

THE USE OF COLOR IN VISUAL PRODUCT MESSAGE REDESIGN

Lidija Mandić, Ante Poljićak, Maja Strgar Kurečić
University of Zagreb, Faculty of Graphic Arts, Zagreb, Croatia

Abstract: Colors are an integral part of non-verbal communication. We often use them in order to show our feelings. People react differently to certain colors. They cause different moods and behavior. In this research a label of a traditional product is redesigned in such a manner as to appeal to different age groups. The subjective consumers' feelings of color in relation to the surface have been analyzed in this work. To determine the influence of the media, a survey has been conducted to determine the effect of colors displayed on screen or printed on the label. The colors on the label are observed in relation to the packaging (to be specific, with the shape and look of the bottle). The aim of this research is to highlight the importance of colors that communicate through product design to a particular customer. Result showed that the unusual design of this product was selected from the most of people. This was certainly contributed to its packaging appearance, but most color that emphasized the essential characteristics of the labels, and its color.

Key words: color, design, marketing

1. INTRODUCTION

Graphic design is a form of applied art dealing with the organization of visual elements. It includes typography, illustration and photography, for visual communication of ideas and messages, in order to inform, convince and educate (Cass). Good design also incorporates the functionality, efficiency and expediency. Specifically, it should be noted that there is a big difference between design and art. A work of art we could or could not understand, we observe it and enjoy its forms. However, the design has a purpose or goal that is trying to accomplish. For example, in industrial design when creating chairs, strive is that the design meets the aesthetic but primarily functional way of creating. The design aims to serve man, and applies in everyday life. However, among all the visual elements we use to make the design look better, the color is still the strongest. Visual excitation can strongly affect humans. Color is an absolute marketing tool. It includes special philosophy that communicates with users, thus affecting the psychology of people with the aim of selling a particular product. It causes a certain consumers reaction, thought thought-provoking and produces feelings. We are surrounded by colors like it or not. Because there are welcome designers speaking of his visions are creating a certain ambiance. It helps potential customers to discover a preference for a certain color, to feel comfortable and positive in this environment (McClurg). Liking or not liking the color depends on many parameters. One of them is the geographical location: so the Germans and Austrians prefer forest green, Mountain Scots prefer muted green, while in Japan moisture and vagueness sets of soft and pure color. One of the parameters is a learned behavior and therefore imposed a subtle sense of color during adulthood (Lupton, Phillips, 2008). Former research pointed that people generally prefer lighter than the darker colors. Blue is the most popular color, followed by red, green, purple, orange and yellow. The background significantly affects the experience of color. Studies have confirmed that when the colors viewed on a neutral gray color, there is a difference of opinion between men and women to a sense of individual colors. So women prefer more saturated and stronger colors like red, and orange and yellow, while men prefer darker colors. The impact of color is extremely pronounced in food. It has been observed that people do not want to consume food if the color is different from color they expected. There is a link between certain types of food and different flavors with color packaging products.

There are any many psychological tricks for marketing purposes. One of them is Luscher's effect. According to the research, it was found that certain colors of product cause the effect that represents its complementary color. So for example the products advertised shaving products are often packaged in blue. The complementary colors are yellow and orange, symbolizing the muscles and strength, and thus transmit the hidden message. The same technique is served and Coca-Cola. Their products are packed in red, that is complementary to green, and achieves the required "cold" hidden from.

2. GRAPHIC DESIGN

The tools that are required to create graphic designs are images, text and colors. Of course there are additional elements depends from designer to designer, to enhance the communication of certain ideas to the audience. Good design involves graphical elements in balance with the aim for proper transfer of messages. Typography is the tool by which written idea gets a visual form. Studies have shown that the grayscale background is the best choice while observing certain typography, because the gray color exudes neutrality, tranquility and equanimity, and thus combines elements. The choice of visual forms can have a significant impact on the readability of written ideas and feelings to the reader. Care must be taken in spacing, and line spacing. Poor spacing can cause a good font looks bad and vice versa. The rule is that smaller amounts of text should be smaller spacing and larger should have a greater spacing.

Typography can cause a neutral effect or stir the passions, may symbolize artistic, political, or philosophical movement, and yet on the other hand express some characteristics of a person or organization (Wheeler, 2013). The letters vary from pure characters forms a pleasant eye to those dramatic, dynamic, yearning for attention, for example those used in the newspaper for ads and headlines. Typography is anything but static, which continues further development.

The image is a graphic element in the design world is brought to life. Whether the emphasis is absolutely on the image or is it just extra element on the label or in another form, does not change the fact that it has a major role in achieving the visual identity of the product. Images are effective because they generate instant communication with the audience. These are good guidelines to follow when determining target groups and the aesthetics of a project. But bad means used to achieve the image may diminish or suppress certain message. Figure 23 shows a photograph art installation made of raw materials for future produces that we use every day. The image is a graphical element that is necessary.

3. EXPERIMENT

The aim of this work is a project of redesigning the visual message of the product. The redesign is the process of shaping based on relevant interdisciplinary design premises, but as the content of the work takes existing, old product (Evans, 2001). Changing its structure, but its function is mainly determined. The design is based on the definition of the problem, then continues with a program of direct the research and development, leading to project development and prototyping. The process ends with the distribution of the product and in this way meets the needs of where it started. High quality product design can provide a temporary advantage over the competition. The strategy of quality and exceptional design requires continuous innovation. It is recommended, even if the present design is satisfactory and functional, to look forward ideas to redesign the product to get the necessary refreshments, and kept the already acquired customers and attract new ones. To begin our story about the redesign of the visual message, we need a set of old products and labels. Figure 1 shows the old design of the product (old label with the accompanying packaging). The label was more focused classic layout. The message was clear, and immediately knew about the product in question. This visual solution in use is a little more than a year. Initially, the design has met the functional and aesthetic criteria. But after a while, manufacturer started to think about redesigning labels.



Figure 1: Old design

The appearance of the product is advisable to renew for a period of five years or less, mainly because of the perceived shortcomings, improvements and training, as well as survival. This is especially true for large organizations that have sufficient funds to invest in the redesign, to be able to quickly change and adapt to market their products. Due to the redesign of the product is more cost. Figure 2 shows graphics solutions of labels.



Figure 2: The proposals for new labels

The guidelines which are addressed when thinking about redesigning products were simplicity, visibility and functionality. Although the bulk of the work was focused on the design of labels, of great importance was the packaging, which raise the value of the product.

The ability to choose the visual message requires at least two solutions. But to make the choice for a new label with two different designs was very narrowed and truncated, visual solutions were few. Since the target group included a wide population, regardless of gender and age, the design of the labels should include the tastes of all the groups to which the study was conducted. Therefore, the visual effects are significantly different from the minimalist, to the traditional ones. The first of the five solutions represents one variant of which is the sheer extra virgin olive oil. Color is the first element that subconsciously tells and hints about which product might work. The second element, ballots, is set to make the crown of the tree. The green line that divides the label on two surfaces gives the feeling of elegance. With a combination of the name of the oil that is set vertically, the label gets a modernistic look. We could say that this design could attract an audience, who are not conventional oriented.

The second proposal design is a simple and recognizable solution, which interacts with the audience at a glance. Placed on a black background, white or cream color was the first choice, and to highlight and to avoid uniformity, one leaf is painted, and thus breaks the monotony. The image and text are associated with leaf and thus make a whole.

The excitement of third design lies in the fingerprint. His first meaning refers to the element that reveals the shape of tree. The second meaning reveals to the origin. The term Ma'tera created by a combination of the Latin language with Croatian dialect. In the first case means my country. Finger print going through names, seals and confirms this. In another case, when we read Ma'tera without apostrophes get the word Matera used in Dalmatia for the mother. Since here fingerprint reveals identity. The impression has been placed in strategic locations. When taking a bottle, thumb falls into the contours of print, so the customer can easily identify with the product.

The fourth label at first glance looks sting, curved connected with typography. However, there is a story behind it. When creating this design, the idea was to do something unexpected, and even a bit contradictory. During the research, the majority of candidates who filled in the survey, had their vision of this design. It represented facing olive, with the top at the point where the line connects with an apostrophe of oil's name. However, hypothetical story was that figure shows pregnant belly. The controversy is obtained when reading the following text on the label, the extra virgin olive oil. Maybe the label will not find its target group, but perhaps the simplicity manages to win the audience.

The fifth solution is an example of traditional and classic looking labels for olive oil. The tree that dominates easily communicates with an audience. Since these visual solutions are often used in such products, there is a high probability that most appeal to precisely this label.

In addition to packaging has a functional role and protects the content contained within it from external influences, it also has an aesthetic function. In this case the object of study was the

aesthetic side of the packaging. The choice boiled down to two bottles. At first glance they might look similar, but in combination with the label gives a completely different look and feel. In Figure 3 is shown two types of bottles. Black bottle is not typical or normal appearance for storing olive oil on store shelves, but it is very elegant and opens the door for the use of all products. Because of its black color is achieved by a sense of luxury. This product allows better placement on the market and of course successful sale.



Figure 3: Black and green bottle

4. RESULTS

First labels were presented without accompanying packaging to focus only on them. This was followed by a presentation of package, also alone without a label, and finally a combination of both. The task for participants was to select the best label, and ultimately the best overall impression of a product. Proposal 5 was chosen because of its design and good communication between design, colors and messages 69%. Clarity is in second place with 29% and typography as the last 2%. The winning packaging is a black bottle with 54% of votes. Light green bottle had 46%. Selected packaging was chosen because of the elegance of the product 51%, followed by association with a product 31%, respectively followed unconventionality 8%, 6% convenience and tradition 4%. To demonstrate the success or failure of the product redesign, the task of the last and the penultimate issue was to evaluate the redesigned product line and the old look of the product. The average score of the new design was 5, while the old product received three.

5. CONCLUSIONS

According to the results of the survey, the label that presents tradition was selected. This shows that it is easier to choose a common solution for certain products. In addition to labels, the participants were asked to choose the packaging. A black bottle, which represents a new look of traditional product, was selected. For overall impression, the black bottle in combination with pregnant belly is won. The packaging adds new value to product, but also the color that emphasized the essential characteristics of the labels. The redesign was needed since the first graphical solution was rated an average score of a new design with a maximum grade

6. REFERENCES

- [1] Cass, J.: "What is graphic design", URL <http://justcreative.com/2007/11/28/what-is-graphic-design> (last request: 2013-06.24).
- [2] Evans, P.: "Graphic Design Makeovers: How to Redesign for Maximum Impact", (North Light Books, 2001).
- [3] Lupton, E., Phillips, J.C.: "Graphic Design: The New Basics", (Princeton Architectural Press, 2008).
- [4] McClurg, J.D.: "The Principles of Design", URL http://www.digitalweb.com/articles/principles_of_design (last request: 2013-05-08).
- [5] Wheeler, A.Wheeler, A.: "Designing Brand Identity", (John Wiley & Sons, New Jersey, 2013.), pages 118-152.

VISUAL ANALYSIS OF THE TYPEFACE MANAGEMENT IN BRAND IDENTITY

*Irma Puškarević, Uroš Nedeljković, Ivan Pinčjer,
University of Novi Sad, Faculty of Technical Sciences,
Department of Graphic Engineering and Design, Novi Sad, Serbia*

Abstract: Analysing visual communication strategies is of great importance to social, psychological and marketing research. Seeing that communication is the integral part of human interactions we are able to explore the process of visual communication and obtain the information of the relationship between, for example, consumers and advertisers. Rhetorical figures are strategically inserted as persuasive elements in advertisements in order to reinforce advertising effectiveness. It follows that ad content is mainly expressed through rhetorical advertising style. This manner is applied to logo design as well. The style of advertising language, in particular the presence of rhetorical figures, has an important consequence on how the brand image is processed. Judgments of types' perceived appropriateness depends on the meaning consistency between the product and the type itself. This paper explores issues of rhetorical style used in product logo design by confectionery and snacks companies which is based on particular typeface. Our aim is to explore the way rhetorical strategies are used to enhance brand's identity. The results provide a basis for logo design recommendations. The paper concludes that some trends of typeface design are evident in logo design for the above mentioned product companies and points to the opportunities for designers.

Key words: typography, visual rhetoric, logo design,

1. INTRODUCTION

Today's world has become increasingly visually oriented and modern advertisers are coming to rely more on typeface design as a brand marker. Typefaces carry connotations and foster individual recollections. Most type practitioners and communication designers agree that visual communication depends on a typeface connotative characteristics and its appropriate application (Leeuwen, 2006; Mick & Politi, 1989; Morrison, 1986; Tannenbaum, Jacobson, & Norris, 1964). The existing research in the field confirms that the style of lettering i.e. design characteristics of typefaces determine the tone of writing (Brumberger, 2003; Doyle & Bottomley, 2004, 2006; Morrison, 1986; Rowe, 1982). For instance, consumers might associate typefaces with certain attributes such as elegant, friendly, and direct. Consequently, brand names (logo) may also convey certain meaning through the choice of the typeface. This paper examines how a typeface, viewed as a component of brand's visual equity, can enhance a brand's identity and built its market share. The present time introduces the largest choice of brands and products of confectionery and snacks industry. The market has become increasingly competitive attempting to keep pace with the needs of contemporary consumer who became accustomed to faster way of living and continuous "updates" in his surroundings. As a consequence the rhetorical style in advertising text has increased over time. With the advent of technology, advertisers have equipped with tools to visually enhance their products and advertised message more than ever. The ancient practice of persuasion, or the means of directing the communication (Kinross, 1985), is considered the greatest asset of the advertisers in today's marketing world, perfected over time after being used for decades in communication with consumers. Many scholars have explored this notion in regards to advertised language (Deighton, 1985; McQuarrie & Mick, 1996), pictorial elements (Delbaere, McQuarrie, & Phillips, 2011; Tom & Eves, 1999), and some went into deep analytical discussion about the need of theory of visual rhetoric (Scott, 1994). Placing object in the unlikely context attracts the attention of the consumer and becomes an efficient way of communication. The innovative ways of presenting information e.g. visual metaphor can produce completely new meaning of the product or the brand, emphasizing their special qualities and features that make them stand out and, eventually, stimulate purchases. Observing the products in contemporary markets and stores it is evident that food products use striking logo design unlike household appliances where the logo of the company is predominant. The product display through distinguished brand symbol sets in motion a lot of possibilities for analysis considering a brand is used as a link to consumer's emotions.

2. VISUAL IDENTITY AND LOGO DESIGN

One element of the graphic system that largely improves marketing communication is the logo of a company or a product. Numerous studies explored the use of colour and typography in stylization of corporate image. However, use and systematization of rhetorical figures applied to type design in logo representation i.e. branding solutions has been neglected. Basic definition characterizes the brand as a symbol or association that aims to identify and differentiate one brand from another. It carries functional and emotional elements which make the connection between consumer and product or service (Filipović, 2008). According to Eco (Eco, 1973) communication (visual or verbal) is based on a code, a system or an object that takes the meaning or representation of another system or object. One of the earliest schematized models of communication (Shannon & Weaver, 1949) illustrates that the signal which is being sent from a sender to a receiver needs to be coded before it reaches the receiver which will decode it. Once the presence of the code has been ensured both the sender and the receiver must use the same code in order for the effective communication to take place. We can conclude that a code is bound by a convention which assembles the existing elements of the systems involved. However, codes, as do conventions, change overtime due to cultural and time influence, therefore making way for possible further research projects. The codification in marketing and advertising setting is viewed as the process of cryptography that is information transport within these boundaries relies on the coded message (Bašić & Pantović, 2012). Companies use coded elements for their visual identity. These visual codes are known as logo signs which can be represented with a symbol or an icon (picture) or just the name of the company. Also, both of these elements can be used together when coding the identity of the company. Furthermore, the same principle is applied in product logo design which observably relies more on the use of the typeface as a result of the product name prominence.

3. REVIEW OF TYPEFACE DESIGN EFFECTS

Psychologist's insights about the laws of human behaviour "have been called upon in order to draw away from an individual the control of his behaviour and put it into the hands of the advertiser" (Poffenberger & Franken, 1923). To this end great attention has been given to devices that gain and hold attention. One such tool is a typeface, considered by many scholars a tool that affects perception of visual data. Understandably, advertiser's attention is directed toward visual rhetoric and to the role of typography as part of that rhetoric. It is believed that congruity between typeface design characteristics and advertised product (message) will lead to more positive response. One of the first published experimental studies of the appropriateness of typefaces is that of Berliner (Berliner, 1923, cited according to Poffenberger & Franken, 1923). Building on her work, subsequent studies were exploring the effect style of lettering has on viewer's agreement on receiving the message. The scholars of consumer research found the role of typography (typeface in particular) in advertising and consumer context most interesting in the last two decades (Childers & Jass, 2002; Doyle & Bottomley, 2006; Henderson, Giese, & Cote, 2004). Their findings are highly valuable to advertisers for strategically employed impressions, especially when the advertiser's chief field of interest is the meaning that typefaces convey and the congruity of its meaning with that of the product or an object to which they refer to. Emanuel (2010) argues that highly valued aspect of a typeface is the actual shape and appearance of the characters themselves, their visual characteristics such as line thickness, corner smoothness, width, height and so on. Just like our faces, these are the specific traits that give the typeface its personality. Given that these factors all influence the way we perceive a certain shape and form our impression of it, the selection of the typeface is by all means a rhetorical decision. According to Kinross (1988) 'pure' information is non-existent that is information stripped of rhetoric can only exist in a vacuum (or abstract world). Hence, when we choose a typeface there are two aspects of its impressions to be considered. We can talk about typefaces aesthetic meaning and its associated meaning (Wijnholds, 1996). The meaning is expressed through association and it can be that of personality and convention. Association through convention, which is considered to be a subjective trait, leans on shared features of the typeface and the item it represents whereas association through convention results from shared knowledge i.e. an arbitrary link established by frequency of use. The connotations typefaces carry can alter the meaning of the message or the brand. McCarthy and Mothersbaugh (2002) found that consumers look to the text that goes beyond the text's actual content when building up on the semantic connotations of a typeface.

Childers and Jass (2002) showed that congruity of the typeface and advertised content reinforced ad message and enhanced its memorability. In their study Doyle and Bottomley (2004) determined that brand choice was influenced by the perception of the appropriateness of a font. For instance, they found that typical font-product combination people judged to be appropriate was a Snowdrift font for ice cream. Later on they found when font and product shared connotative meaning participants were more likely to choose a brand (Doyle & Bottomley, 2006). Also, their results indicate that a potential confound of congruity are obvious associations which measure the strength of learned or figurative associations (or both).

4. RHETORICAL FIGURATION IN ADVERTISING

The modern system of visual communication in advertising has brought together graphic and typographic designers, psychologists, linguistic scientists and marketing researchers in an attempt to effectively respond to pressing consumer demands. This union has resulted in exchange of tools of the trade and advertisers have come to use ancient art of verbal persuasion we know as figurative speech i.e. rhetorical figures. Similarly to applying schemes and tropes to verbal statements, we can use these operations in visual communication and, considering marketing communication is predominantly visual, we can say that advertising is "the rhetoric of modern age" (Bonsiepe, 1965). Rhetoric provides a system for identifying the most effective form of message representation in any given case. According to rhetoricians the manner in which a message is expressed may be more important than its content (McQuarrie & Mick, 2011). McQuarrie and Mick described how rhetorical figures in advertised language can be integrated conceptually and discuss beneficial effects associated with artful deviation. Moreover, rhetorical style in print ads has expanded over time. Phillips and McQuarrie (2005) found that advertisers switched from using single rhetorical figures to multiple layered figures. It is believed that complex rhetorical figures can increase elaboration (McQuarrie & Mick, 2011) which in turn may increase memorability of the ad (Kardes, 1988; Myzoughi & Abdelhak, 2011). Eventually, it is expected that more complex figuration will influence positive attitude toward the ad. So far rhetoric has been of great value in shaping opinions, determining the attitude of other people and influencing their actions (Bonsiepe, 1965). This being said, we can conclude that stylistic figuration can be used as analytical tool for understanding the ways of directing information – very useful in a competitive market where consumers are saturated with visual communication and this can help them during decision-making process.

5. MATERIALS AND PROCEDURE

5.1 Hypothesis

Following literature review (Doyle & Bottomley, 2006; McQuarrie & Mick, 1996) it is hypothesized that typeface design characteristics in product logo application use stylistic enhancements in following ways:

1. The product logo design for confectionery and snacks use rhetorical figures in a form of schemes and tropes comparatively.
2. The logo design solutions will show evidence of a stylistic trend.

5.2 Method

Data collection required two stages. First, we identified type of product logo design characteristics in regards to typeface impressions and selected a sample of representative design solutions. Second, we applied content analysis on the selected samples to strategically excerpt commonly used rhetorical figures. The phase one: the store avenues were observed for identification of product logo design characteristics. The researchers noted that food product logos displayed the most type forms that deviated from regularity, particularly confectionery and snacks products. After careful study a sample of 45 global brands was chosen. Phase two: the rhetorical handbook by Ehse (1988) had been consulted. The author of the handbook describes principles for generating design concepts by means of rhetorical figures. The content analysis works best at quantifying previously identified ad components; therefore the content assessment preceded the content analyses. The researchers analysed each logo design for the presence of rhetorical figures. If a figure was determined to be present, it was categorized as a scheme or trope.

6. RESULTS

The accumulated data of the implementation of rhetorical figures in product logo design is given in Table 1. The sample consisted of 10 font-based, 17 symbol-based and 18 custom-made logos.

Table 1: Data collection of product logo design trends in confectionery and snacks industry

FORM	TYPE CLASSIFICATION	TROPE	SCHEME
Font	Classical <		

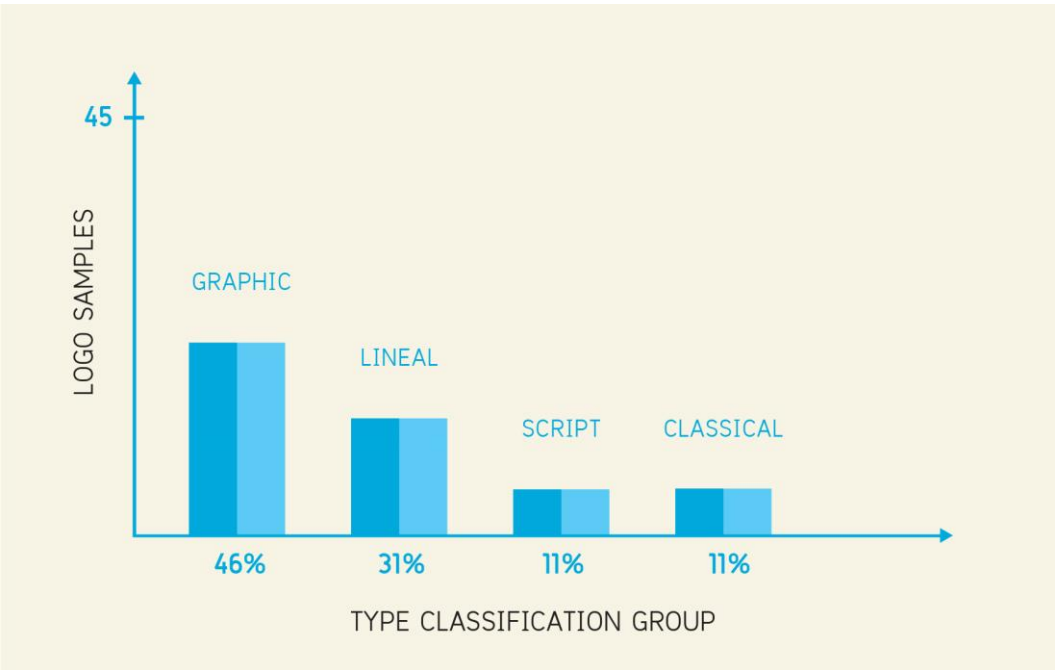


Figure 1: The average representation of the most applied typefaces from the Vox A Typl classification

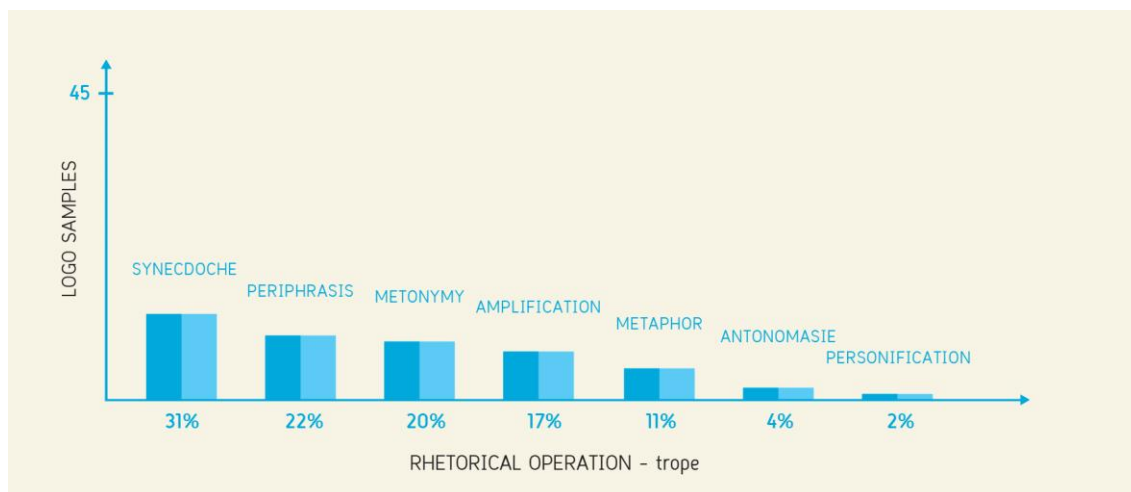


Figure 2: The average representation of the most applied rhetorical figure – trope

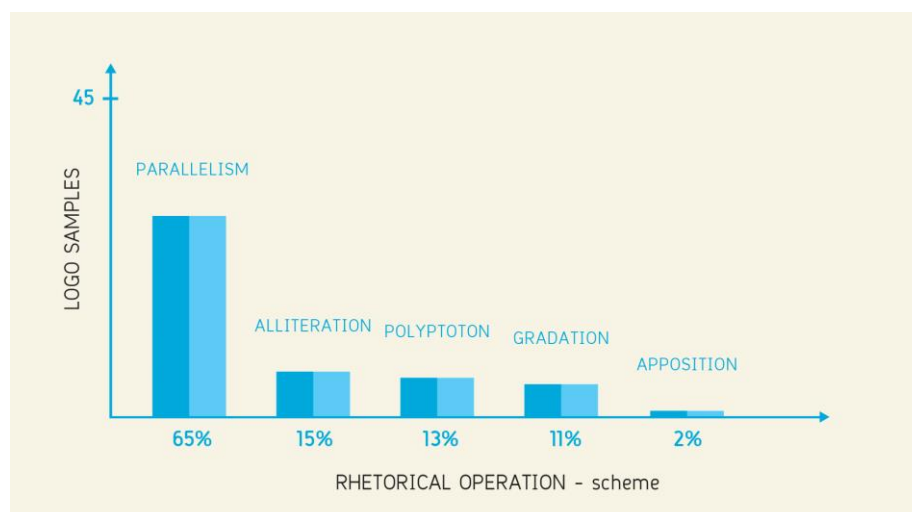


Figure 3: The average representation the most applied rhetorical figure – scheme

7. DISCUSSION

Understanding the function of rhetorical figures requires analytical approach. The content analysis identified layering of many rhetorical figures in logo design, as well as pervasiveness of few of them, which is consistent with previous findings in the field, indicating they are an important stylistic device in advertising. Advertisers increased their usage of the most demanding figures and placed further demands on the consumer by adding tropes to the body copy (Phillips and McQuarrie, 2002). This trend has expanded to other elements of advertiser's agenda. Our results show that product logo design for confectionery and snacks is relying on typeface's associative power and figurative style when it comes to product promotion. In the sample of 45 logos the content analysis revealed that logos can be classified into three groups: (1) the first group is related to logos that use existing typeface, consequently relying on convention and type design characteristics for meaning production, (2) the second group is related to logos that are designed in a way to represent a symbol in close relation to the product they represented, and (3) in the third group logos were custom made. The logos in a form of a symbol present combination of a typeface and a shape that intertwine in a skilful application of rhetorical figure whereas the custom logos use existing fonts from the classification to build on more specific connotations changing the original form of the type characters or making the new forms of the letters. The content assessment showed that the most use typefaces are the ones that are grouped in Vox ATypI classification as classical, lineal, script and graphic. These typefaces are present in all of the three groups we characterized. Previous studies indicate that people perceive classical

typefaces as elegant (the design characteristic's association is one of elegance and style) (Doyle & Bottomley, 2006; Rowe, 1982) which can be explained with convention and tradition of use for such occasions. However, current trends in visual communication bend towards different end and we can see that their use is not as pervasive (11%). The same results are found with script typefaces (11%), nevertheless they present the base for the custom made fonts in most cases which makes them the easy target for designers. The most pervasive typefaces in product logo design found were graphic and lineal group of the classification. The graphic group hosts typefaces with the highest rate of associative power and these typefaces were the most likely choice of designers due to their relevance to the font-congruity aspect.

The schemes and tropes defined by Eshes and Lupton (1988) can be identified in product logo design for confectionery and snacks currently sold in supermarkets (Table 1). Noted is "layering" of figuration, a term coined by scholars to refer to the use of more than one trope in advertising language (Phillips & McQuarrie, 2005). The most prevalent schemes found are parallelism, alliteration and gradation, and the most used tropes are metonymy, synecdoche and periphrasis. The stylistic figures tend to be accompanied with each other. For example, metonymy is paired with amplification, one complex figuration enhanced with the stylization of simpler figure, specifically, the complex trope which uses temporal, spatial or causal connection, an extremely direct way of presenting one term with another, is enhanced additionally with amplification, a figure which expands a topic by listing its particulars.

8. CONCLUSION

Analysing visual communication strategies is of great importance to social, psychology and marketing research. Communication is the integral part of human interactions; therefore exploring the process of communicating visually we are able to investigate the relationship between consumer and advertiser. The typeface as the ubiquitous element in advertising style generates its own connotative meaning which makes it an item of interest to designers and advertisers when it comes to developing an idea for a logo design. The present study links rhetorical figures, typeface associations and product characteristics. The analysis indicates that some trends are evident among the logo design solutions for the above mentioned product companies and these findings may be used by media professionals to help them match typeface connotations through the use of rhetorical figures with desired product or message content connotations on the basis of information rather than intuition. Also, the paper concludes that current package design solutions for confectionery and snacks apply product logo next to the product photograph expanding its effect to the one of the brand where the recognizable symbol (logo) activates positive associations and emotions.

9. ACKNOWLEDGEMENT

This work was supported by the Serbian Ministry of Science and Technological Development, Grant No.:35027 "The development of software model for improvement of knowledge and production in graphic arts industry".

10. REFERENCES

- [1] Bašić, I., & Pantović, B. (2012): "Logo and semiosis: From an icon sign to the Serbian culture symbol", *Glasnik Etnografskog Instituta*, 60 (1), 49–64.
- [2] Bonsiepe, G. (1965): "Visual/verbal rhetoric", *Journal of the Ulm School of Design*, 14/15, 69–82.
- [3] Brumberger, E. (2003): "The rhetoric of typography: The persona of typeface and text", *Technical Communication*, 50 (2), 206–223.
- [4] Childers, T. L., & Jass, J. (2002): "All Dressed Up With Something to Say: Effects of Typeface Semantic Associations on Brand Perceptions and Consumer Memory", *Journal of Consumer Psychology*, 12 (2), 93–106.
- [5] Deighton, J. (1985): "Rhetorical strategies in advertising", *Advances in Consumer Research*, 12, 432–436.
- [6] Delbaere, M., McQuarrie, E. F., & Phillips, B. J. (2011): "Personification in Advertising Using a Visual Metaphor to Trigger Anthropomorphism", *Journal of Advertising*, 40 (1), 121–130.

- [7] Doyle, J. R., & Bottomley, P. a. (2004): "Font appropriateness and brand choice", *Journal of Business Research*, 57(8), 873–880.
- [8] Doyle, J. R., & Bottomley, P. A. (2006): "Dressed for the Occasion: Font-Product Congruity in the Perception of Logotype", *Journal of Consumer Psychology*, 16(2), 112–123.
- [9] Eco, U. (1973): "Kultura, informacija, komunikacija", Nolit, Beograd (Original t.). Beograd: Nolit.
- [10] Ehses, H., & Lupton, E. (1988): "Rhetorical handbook", *Design Papers*, 5, Design Devision, Halifax, Nova Scotia, Canada.
- [11] Emanuel, B. (2010): "Rhetoric in graphic design", Anhalt University of Applied Sciences.
- [12] Filipović, V. (2008): *Brend menadžment* [e-book], Beograd: Univerzitet u Beogradu, Fakultet organizacionih nauka. Univerzitet u Beogradu. Dostupno na: <http://marketing-pr.fon.rs/webroot/uploads/Brand%20Management%20-%20Skripta.pdf>
- [13] Henderson, P. W., Giese, J. L., & Cote, J. A. (2004): "Impression management using typeface design", *Journal of Marketing*, 68, 60–72.
- [14] Kardes, F. R. (1988): "Spontaneous inference processes in advertising: The effects of conclusion omission and involvement on persuasion", *Journal of Consumer Research*, 15, 225–233.
- [15] Kinross, R. (1985): "The rhetoric of neutrality", In Victor Margolin (Ed.), *Design Discourse: History/theory/criticism*, Chicago: University of Chicago Press, 131–143.
- [16] Leeuwen, T. Van. (2006): "Towards a semiotics of typography", *Information Design Journal*, 4 (September 2003), 139–155.
- [17] McCarthy, M. S., & Mothersbaugh, D. L. (2002): "Effects of typographic factors in advertising-based persuasion: A general model and initial empirical tests", *Psychology and Marketing*, 19 (7–8), 663–691.
- [18] McQuarrie, E., & Mick, D. (1996): "Figures of Rhetoric in Advertising Language", *Journal of Consumer Research*, 22(4), 424–438.
- [19] Mick, D. G., & Politi, L. G. (1989): "Consumers' interpretations of advertising imagery: A visit to the hell of connotation", *Interpretive Consumer Research*, Special Vol, 85–96.
- [20] Morrison, G. R. (1986): "Communicability of the emotional connotation of type", *ECTJ*, 34 (4), 235–244.
- [21] Myzoughi, N., & Abdelhak, S. (2011): "The Impact of Visual and Verbal Rhetoric in Advertising on Mental Imagery and Recall", *International Journal of Business and Social Science*, 2 (9), 257–267.
- [22] Phillips, B. J., & McQuarrie, E. F. (2005): "The Development, Change, and Transformation of Rhetorical Style in Magazine Advertisements 1954–1999", *Advertising & Society Review*, 6 (4).
- [23] Poffenberger, A. T., & Franken, R. B. (1923): "A study of the appropriateness of type faces", *Journal of Applied Psychology*, 7 (4), 312–329.
- [24] Rowe, C. L. (1982): "The connotative dimensions of selected display typefaces", *Information Design Journal*, 3 (1), 30–37.
- [25] Scott, L. M. (1994): "Images in Advertising: The Need for a Theory of Visual Rhetoric", *Journal of Consumer Research*, 21 (2), 252–273.
- [26] Shannon, C. E., & Weaver, W. (1949): "The mathematical theory of communication", University of Illinois Press IL.
- [27] Tannenbaum, P. H., Jacobson, H. K., & Norris, E. L. (1964): "An experimental investigation of typeface connotations", *Journalism & Mass Communication Quarterly*, 41 (1), 65–73.
- [28] Tom, G., & Eves, A. (1999): "The use of rhetorical devices in advertising" *Journal of Advertising*, July, 39–43.
- [29] Wijnholds, A. de B. (1996): "Using Type: The Typographer's Craftsmanship and the Ergonomist's Research", Utrecht University, April.

11. ADDITIONAL MATERIAL

The product logos used in the content analyses.



LINEWORK ON CONSUMER PACKAGING CAN HELP TO IMPROVE THE IMAGE OF PORT WINES

Cecilia Tamas-Nyitrai, Emőke Hegedűs

Obuda University, Mediatechnology Institute, RKK-OE, Budapest, Hungary

Abstract: Our objective was to show the step by step design of new, environmentally friendly consumer packaging for a classic product line. The second author's personal Erasmus experience gave the idea to rethink and redesign the appearance of the packaging to the world wide released port wines. The present packaging of the Royal Oporto product line is very simple and classic as the wine itself, and has induced fading its fame and blending into the hypermarket shelves. A gift box of a well selected material like carton or corrugated paperboard from reused paper can solve the problem by not only giving a fashionable vintage and classy feel but being good base for a nice printed surface. The design can be variable, country by country or by seasons.

Our box design is supposed to fit to the original bottle and does not cover its important parts. One of the very useful pieces is the paper trademark on the neck of the bottle which is well known internationally and is an unmistakable sign of original port wines. So we wanted to show it by cutting a triangular hole in the box which is integrated with the printed design. The fonts of the original label were also kept while powerful graphics that can catch attention easily and have serious connection with the product were added. As Port wines travel from Douro valley to Vila Nova de Gaia on the river Douro, and the most famous, very last bridge on the river is the St. Luis bridge, the symbol of the city of Porto, this metal arch construction had been chosen as the additional part for the new design. The bridge has strong, straight lines, an elegant curve and a remarkable silhouette. By night the bridge gets extra attention that we wanted to recall. This is why the base colour of the box is black and the linework of the design is of a bright colour. We believe that using asymmetric composition, sharp lines and triangle shapes gives a different appearance to the box design. It is cutting edge design that takes a leap from the boring grape inspired labels on the market. Hopefully, we can show port wine is more than just a simple wine. For the new graphics, an unusual view of the bridge had been chosen and a photo was taken from below, on the riverbank. From the front, it could not show depth and dimensions, but from this angle it looks like a modern 3D CAD drawing. Using Adobe Illustrator, the photo was transformed to a vector graphic, keeping the most remarkable parts of the construction.

Key words: bridge graphic, corrugated paperboard, design, linework, paper box, port wines

1. INTRODUCTION

In the 21st century we have many chances to get acquainted with the world's beauty easily, via travelling, internet, multinational companies. Our choices became wider but our attention spreads between them. The role of the marketing is increasing: you need sharp business plan to sell your product. The keyword is the attention, you have to be different to people notice your product. In the hypermarkets -lack of shop assistants- the easiest way for that is an eye-catching packaging, which can stand out from the crowd of the products on the shelves.

Port wine is a type of liqueur wine, which made exclusively in Alto-Douro vineyards (Figure 1), and it has to be made in the same special way, with added brandy for the higher alcohol content and sweet taste (Robinson, 2006).



Figure 1: Alto-Douro Valley Vineyards

Wine producing has hundreds years of history: the vineyard has been protected by law since 1756, the liqueur wine is made from the 18th century. The vineyard has a title from UNESCO cultural heritage, because the agriculture does not disturb the balance and the beauty of the nature in the valley of Douro (Unesco, 2014). The climate is mediterranean, usually with hot, dry summers and cold winters and wind from the Atlantic Ocean. The soil is mostly slate.

Port wine is distributed all over the world but unfortunately it has induced fading away its fame. Refreshing the packaging of the product line could hit a new generation of wine consumers and remind the people Port wine still exists and take advantage from the advanced multinational market connections.

1.1 Box design

An elegant paper box can help us to keep the classic packaging and give it a new perspective. The graphic of the box is variable. It can be different by countries or by occasions.

The normal packaging of the wines are only bottles, so a paper box appears instantly different and interesting. If we choose the right graphic it can be more unique.

The box can be easily reused for storage in an environmentally friendly way being aware of the nature at our household.

The printed surface adds the most for the package's appearance. It can broadcast what our product offers: for young people something new, but definitely classic, high quality, mature product. It has to be fashionable to take the product to the 21st century.

2. MATERIALS AND METHODS OF DESIGN

The material of the product (box) is corrugated paperboard with BC flute of 4.0mm the thickness. It is made from 100% recycled paper, which can reduce the environmental impact of its production (Györgyi et al, 2006).

For the box design the Adobe Illustrator program was used. It has many possibilities to make designing easier. It is perfect to create labels, offers good tools for it. With the ESKO packaging plugin, it is also easy to design the shape of the box. And finally it can make our plans alive with applying the graphic to the 3D, freely foldable model of the box (Esko, 2014).

In Adobe graphic programs we work with layers, the contents of the label are easily moveable without having effect on each other. With the occasionally appearing guidelines we can place the elements on symptomatic space.

ESKO plugin is designed to help especially the packaging design works. It contains basic packaging shapes, for example the basic FEFCO boxes.

3. STEP BY STEP DESIGN

The base of our design is the port wine product line of The Real Companhia Velha company. The labels are printed onto the bottles directly with white colour tint (Figure 2). The typography has classic fonts and uppercases make them interesting, it has industrial and vintage feel. The graphic element is just the label of the company, which is very traditional and classic.



Figure 2: Royal Oporto wines in their original packagings

For the ones who know well the product this is enough to recognise it and do not let them to hesitate to purchase it. But the new customers needs something more tempter to catch their attenteion. So we have chosen a simple rectangular box to fit well to the shelves and the logistical packaging (palletisable) and to add extra informations on it.

With the use of ESKO plugin in Adobe Illustrator we could choose the shape of our box, and we set the correct measures to the bottle fit in well. In the 3D editor (Figure 3) we could set the folding by changing the angles.

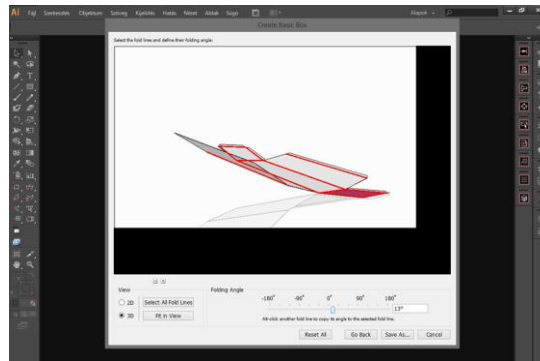


Figure 3: AI ESKO plugin 3D folding

After the layout was ready (Figure 4) we could start designing the graphical appearance of the product.

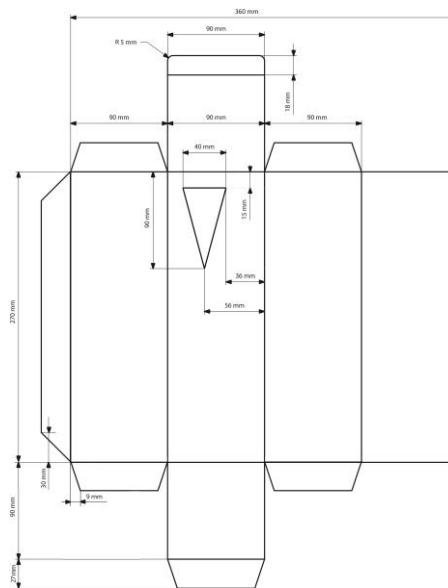


Figure 4: The technical drawing of the box

The speciality of the box is a triangle shaped hole at the top of one side, which will allow to show for the experienced costumers the unique trademark of port wines. The rest of the information was transported from the label to the box.

3.1 Graphic

The printed surface of the box can have the strongest effect on the costumers. It is used to:

- Communicate informations about the product,
- Touch our target audience,

- Classify the product,
- Make product recognisable and memorable.

About port wine the city of Porto is an obvious association. The wine practically made here in the wine cellars of Vila Nova de Gaia. Communicating somehow this connection on the packaging is very useful, it can remind the consumer of its origin, make the product unique and memorable. As one of the symbols of Porto, we had chosen the Dom Luís bridge (Figure 5) to take place on the package. The bridge appears on many pictures about port wines, because the wine cellars are located next to it and the wine transporting boats cruise under it on their way from Alto-Douro to the cellars.



Figure 5: Dom Luís bridge

The bridge has a strong silhouette. It is situated between two hills over the river of Douro, having two floors and a curve between them. Its material is metal, and the basic lines form triangles. To make our graphic a bit unusual and modern, the point of view was down at the riverbank, looking up to the bridge. So the photo was taken from below, on the riverbank in a sharp angle. In Adobe Illustrator the photo was made 50% transparent and a layer was made over it. To the new layer, the silhouette and main lines of the bridge could be transported in vector graphic. The curves were also covered with straight lines. With this technique the photo was transported to an artistic vector graphic.

The base colour is black, connected to the dark, heavy port wines and night which is the best time for drinking them. The colour of the bridge in the graphic shows the difference between the members of product line, the four types of port wine, showing and reminding us for the colour of the wine itself (Figure 6):

- Tawny - brown
- Ruby - red
- White - green
- Extra Dry White - yellow

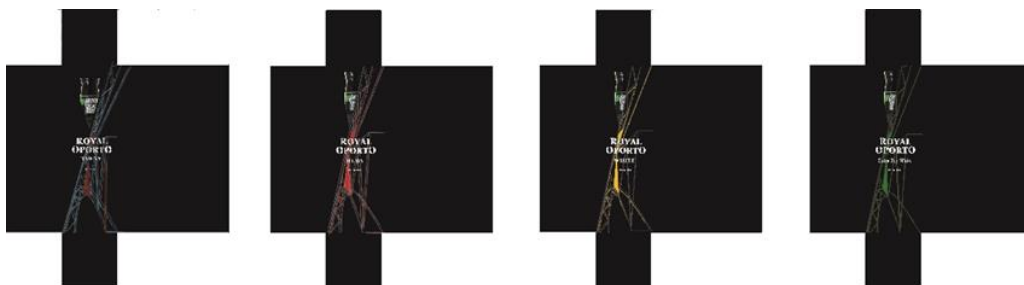


Figure 6: Box outlines with distinctive colour scheme
Tawny – brown, Ruby – red, Extra Dry White – yellow, White – green

With the built-in fonts, we copied the original label from the bottle to the front of the box. To emphasize the text in front of the bridge graphic, black shadows were used.

To the triangle shape of the graphic, the shape of the hole is matching very well. The hole is placed over the bridge, where appears the black and white trademark from the neck of our bottle. Connecting to the triangle theme, some triangle shaped decorations were made on the surface of the box. Finally the information about the wine at the back of the box was also organised to triangle shape, and a photo about Alto-Douro was added to give further information about the origin of the wine (Figure 7).



Figure 7: The printed surface of the box with the information at its back

With the use of ESKO plug-in 3D model window (Figure 8), the graphic on the baselines of the box was applied, and so got the 3D graphic of the designed product. The prototype of the box has also been produced using CAD-CAM systems for cutting.

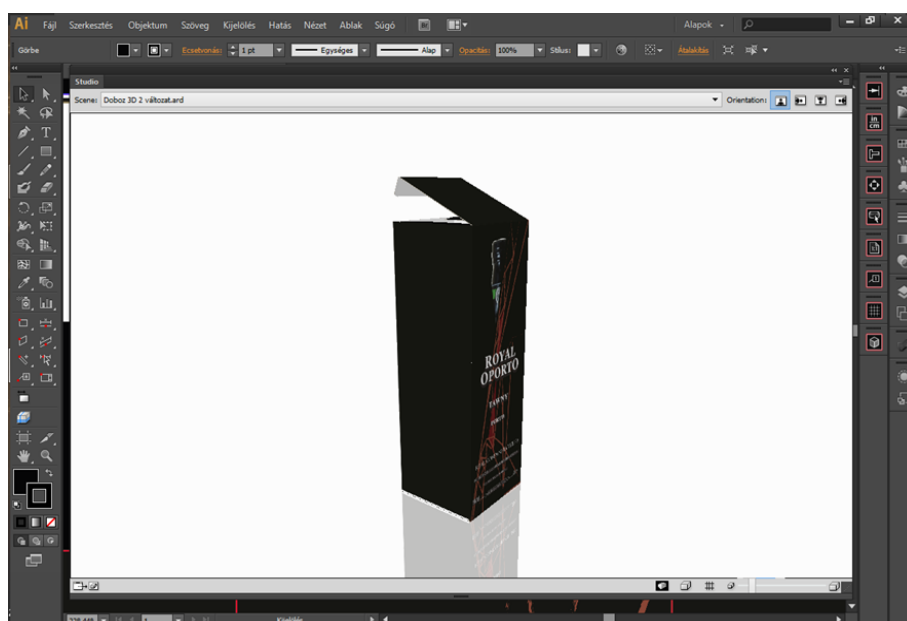


Figure 8: AI ESKO 3D product graphic

4. CONCLUSION

A box design was created to promote the Royal Oporto port wine lines by connecting their members with the same graphic but differentiate between them using the winetype appropriate colour (Figure 9).

The box is supposed to emphasize the product and connect it to the atmosphere of its place of origin, Porto. The place where connects tradition with modern and straight lines with soft curves in nature and culture as well.



Figure 9: The product line in the new packaging

With using a fresh, new design, we could change the appearance of a product. We added new value with the elegant, fashionable design to a box instead of the only bottle. The corrugated paperboard box could stand out on any hypermarket shelves, showing that this product is something more than the most of the wines. It is unique, has history and quality. It intends to talk to the newest generation of wine consumers with a modern graphic design. It also helps customers in decision at purchasing with its attractive appearance and useful information.

To increase the effect of our new packaging, it is an option to print promotion papers to the shopwalls or to displays.

5. ACKNOWLEDGEMENT

Many thanks to my consultant, Cecília Tamás-Nyitrai who helped, motivated and inspired me during the whole work. She shared her professional experiences and gave me useful advices. I thank her for being always available to my project.

I am very thankful for the Erasmus exchange program. Meeting different European culture was very useful experience. I studied another professional point of view in the politechnic from my professors and my classmates. It added new tools and a whole new dimension to my work. Comparing two countries leads to important conclusions, helps observing the world more effectively. This is an experience what everybody should have in their lives.

I want to thank Celia Nunes Barreto, professor of IPT who was my mentor during Erasmus semesters. She supported my studies and integration in politechnic.

6. REFERENCES

- [1] Esko: URL <http://www.esko.com/en/Products/Overview/suite-12/adobe-CS6-compatibility/> (last request: March 2014)
- [2] Györgyi A., Tiefbrunner A., Varga J.: Csomagolástervezés Papír-Press, 2006
- [3] Robinson, J.: "The Oxford Companion to Wine" Third Edition page 231, (Oxford University Press, 2006), ISBN 0198609906
- [4] Unesco: "Alto Douro Wine Region", URL <http://whc.unesco.org/en/list/1046> (last request: Februar 2014)

COMPARING DIFFERENT LETTER SPACING METHODS IN SANS-SERIF TYPEFACE DESIGN

*Bojan Banjanin, Uroš Nedeljković,
University of Novi Sad, Faculty of Technical Sciences,
Department of Graphic Engineering and Design, Novi Sad, Serbia*

Abstract: Designing a typeface does not mean only defining the shape of letters, but also giving an appropriate amount of space around them. The purpose of defining the letter space is to make them visually equally distant from each other within words, sentences and paragraphs creating an even value of grey, without darker or lighter areas. Each letter is formed of black and white parts. The changes of these positive and negative letter elements throughout the text optically mix, creating a visual rhythm which assists the reader. Inter-letter space varies from typeface to typeface and it certainly dictates the amount of space around the characters or their left and right side bearings (Cheng, 2006). Even though defining the letter space is in the final stages of design, depending on designer's eye and craftsmanship, there are some basic rules of spacing related to character shapes and counters that can be defined.

Walter Tracy developed a system for determining letter spacing for Roman alphabets. In 2005, Miguel Sousa developed a reliable spacing method while creating his serif typeface Calouste (Sousa, 2005). Relying on the mentioned spacing methods, Fernando de Mello Vargas compared and applied those methods in determining the letter spacing for serif typeface Minion and sans-serif typeface Myriad. However, Vargas only tested these methods on one serif and one sans-serif font. The aim of this paper is to compare and modify these methods and different approaches in determining letter space in sans-serif typeface Grid Sans developed by the authors in order to broaden these rules and to see which rules are always applicable and which are strictly referring only to certain typeface.

Key words: letter spacing, typeface design, spacing methods, sidebearings

1. INTRODUCTION

Many authors consider the space between letters to be as important as the shape design itself. Designing a typeface does not mean only defining the shape of letters, but also giving an appropriate amount of space around them. The purpose of defining the letter space is to make them visually equally distant from each other within words, sentences and paragraphs creating an even value of grey, without darker or lighter areas. Each letter is formed of black and white parts. Those white parts in certain characters are called "counters" and the space to the left and right of the character are called "sidebearings".

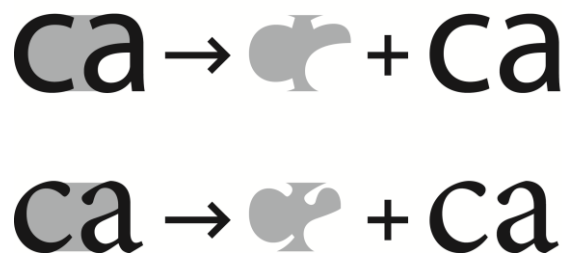


Figure 1: Letters and their inter letter spacing (counter).
Sans serif font (above) and serif font (below)

The changes of these positive and negative letter elements throughout the text optically mix, creating a visual rhythm which assists the reader. Inter-letter space varies from typeface to typeface and it certainly dictates the amount of space around the characters or their left and right sidebearings (Cheng, 2006). Even though defining the letter space is in the final stages of

design, depending on designer's eye and craftsmanship, there are some basic rules of spacing related to character shapes and counters that can be defined.

In the 1940s W. A. Dwiggins wrote in his letter to Rudolph Ruzicka that some rules for letter spacing can be established based on grouping the letters with similar shapes. For example, group with similar shape on one side of letters "n, m, h, b, d, q, k, i", both sides of the letter like "o" which defines amount of space for round shapes (c, e, a) and letters "f, g, r, t," which are hard to fit (Tracy, 2003). In the 1960s, David Kindersley presented a set of rules for spacing letters based on experiments involving transmitted light (Kindersley, 1966). Later on, guided by Dwiggins's hunch for existence of certain rules and with experience based on the principles that he learnt from Harry Smith of Linotype, Tracy developed a system for determining letter spacing for Roman alphabets. In 2005, Miguel Sousa developed a reliable spacing method while creating his serif typeface Calouste (Sousa, 2005).

1.1 Letter spacing methods

Determining a proper amount of letter space can't rely only on strict mathematical formula but rather on fine eye judgements (Vargas, 2007). Figure 2 illustrates differences between same spatial distance of basic geometrical shapes (a) and diverse spatial distance between these same shapes (b). Naturally, better visual results are achieved with different spatial distance (b). Same case is with determining letter spacing.



Figure 2: Equal spatial distance between basic geometrical shapes (a) and diverse distance between basic geometrical shapes (b) (taken from Vargas, 2007)

Similar to white space around these basic shapes, letters have their own amount of white space inside and around them (Figure 1). Finding a proper rhythm between letters and their surrounding space is crucial to good inter-letter spacing. As Lo Celso (Lo Celso, 2005) said: "It seems an obvious assumption that rhythm is a constitutive element in type design, as understood under its sense of pattern and tendency to regularity". Kaech (Kaech, 1956), proposed his method for letter spacing. He took letter "O" as reference letter for arranging the width of all other as well as for their inner spaces. He talks about "golden mean" and defines the quality of rhythm as a result of perfect relations between those measures.

Kindersley also attempted several systems for spacing letters, by defining their "optical centres" through a photo-electric cell device, or by searching their "centre of gravity" by eye. He began with spacing capital letters "O" and "I" in string "OIIIO" and when satisfactory results was achieved, he placed all other characters into the place of second "I" and define their side bearings (Kindersley, 1963).

Harry Carter suggested a method for spacing letters in which counters in letter "m" and ligature "ffi" define an interval between all other strokes. The letters with double upright strokes (n, u, h, fi) should have a wider interval than m, and similarly, the whites of d, o, p are a little wider than the white in "n". Spacing of "m", "n" and "o" are the key to provide a proper spacing for all the other characters (Carter, 1984). In his method, vertical stems, in their condition of acting as units of a pattern, actually are to build up rhythm across the text line (Lo Celso, 2005).

Walter Tracy suggest his method of defining letter spacing taking into consideration inner letter space (counter). He started with capital letter "H", measuring space between two vertical stems and then give the left and right side bearing around quarter of that value (half of counter on letter "H" between two letters with vertical stems; e.g. "HH"). He set value of right and left sidebearing in word "HHHH" and then put letter "O" between them and adjust its sidebearings. When these values are defined (these are called standards) other characters receive their side bearings following scheme (Figure 3).

For small letters he starts with letter "n" defining its left sidebearing value as half of its counter and right sidebearing value as little bit less than left (because of its rounded right corner). Then he adjusted sidebearings for letter "o" in word "nnonn", "nnonon" and "nnoonn". Amount of white space for other characters in alphabet are calculated following scheme on Figure 4.

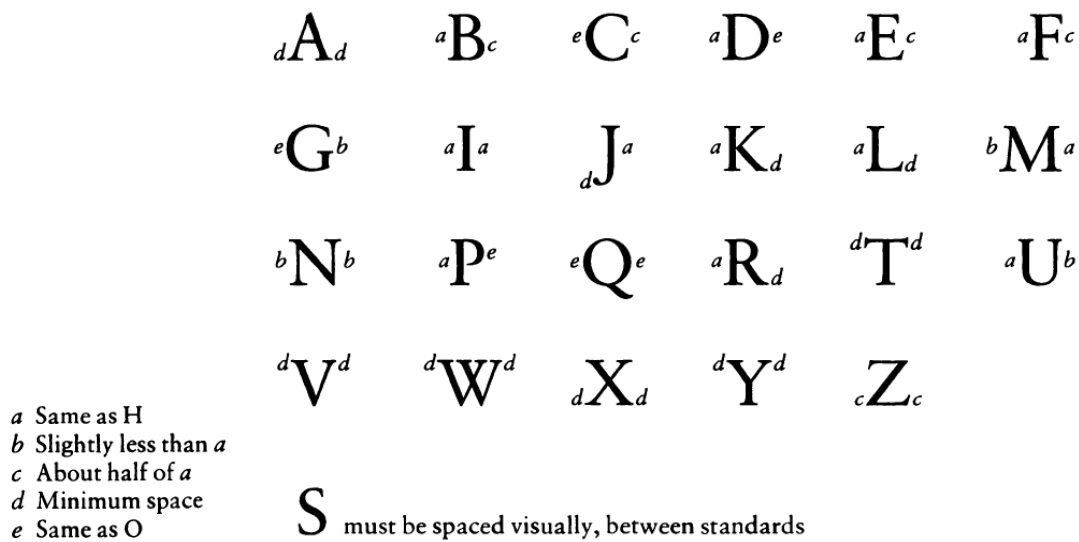


Figure 3: Walter Tracy's method for determining left and right sidebearing values for capital letters (taken from Vargas, 2007)

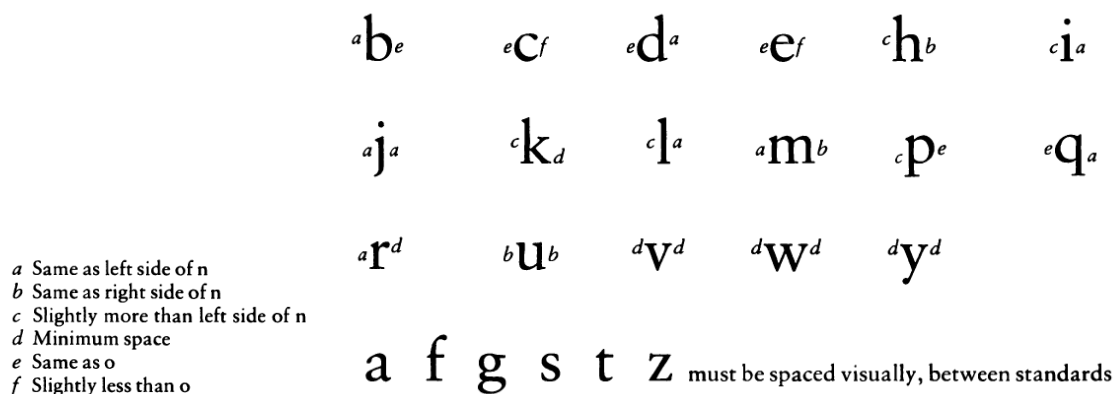


Figure 4: Walter Tracy's method for determining left and right sidebearing values for small letters (taken from Vargas, 2007)

Miguel Sousa starts with defining letter spacing similar as Tracy but he doesn't give any strict "formulas" or values for letter sidebearings. He divides letters in three groups:

- First group: **b,d,h,l,m,n,o,p,q,u** – left and right side of these letters are related to at least one side of letters "n" and "o"
- Second group: **a,c,e,f,j,k,r,t** – letters in this group have one side with similar shapes (and) spaces to letters of the first group
- Third group: **g,s,v,w,x,y,z** – these letters have no direct relation to any other character thus making them hard to space

Consulting values for left and right side bearings of previously set letters "n" and "o" he applied these values to characters that share similar shapes with those in first group. Then he put every character one by one from the second group into first group and set their side bearings through series of testing using his own web based tool *adesiontext* (available at www.adhesiontext.com). Then he repeat this procedure with every letter from the third group until satisfactory results are achieved.

Relying on the mentioned spacing methods, Fernando de Mello Vargas compared and applied those methods in determining the letter spacing for serif typeface Minion and sans-serif typeface Myriad. He concluded that Tracy's method showed better overall results for sans-serif and Sousa's method for serif typeface [Vargas, 2007]. However, Vargas only tested these methods on one serif and one sans-serif font. The aim of this paper is to compare and modify these methods and different approaches in determining letter space in sans-serif typeface Grid Sans developed by the authors in order to broaden these rules and to see which rules are always applicable and which are strictly referring only to certain typeface.

2. METHODS

For the purpose of comparing different methods for letter spacing (font metrics), we used sans-serif typeface Grid Sans developed at Department of Graphic Engineering and Design. First, all previous metrics data were reset. This includes values for left and right sidebearings, as well as kerning values. Kerning values are added or subtracted from side bearing values so they actually represent special cases of letter spacing where metrics can't define proper distances. We focus our research on defining only metrics value for letter sidebearings. After removing all metrics data, propositions of each method for defining letter space was applied. Since these methods in our case are related with process of designing a typeface and not applying them in prepress software (e.g. InDesign, QuarkExpress), measurements were done using font design software FontLab Studio 5. Measurement units for font metrics are given in relative units as to show relation between different methods. These units can be transformed into different measurement systems if needed.

We compared three different methods: Walter Tracy's method (WT), Miguel Sousa's method (MS) and Automatic method (AT) implemented in FontLab's software. With this approach we wanted to compare differences in left and right sidebearings (LSB and RSB) for each character in Latin alphabet. We use theoretical approaches of Tracy and Sousa and strictly mathematical one of automatic algorithm in FontLab. The experiment was conducted with capital and small letters. As a result of this experiment three different variations of Grid Sans typeface were generated each as separate font file.

3. RESULTS

Results of comparison between three different letter spacing methods are shown in Figures 5 and Figure 6 and their values in Table 1-4.

Differences in left and right side bearings of these three methods for capital letters are presented in Figure 5. Their numeric values are shown in Table 1 and Table 2.

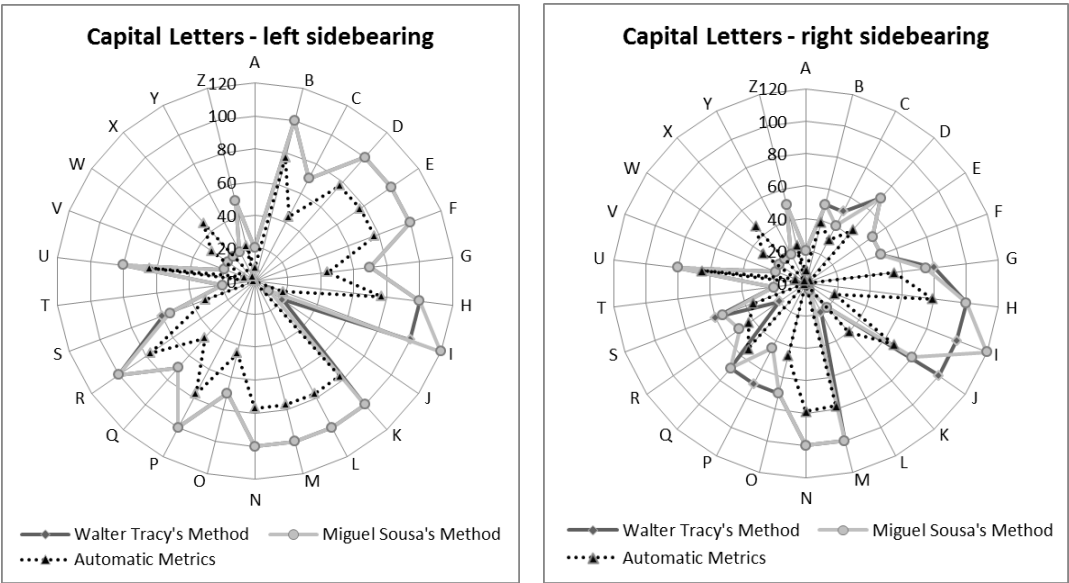


Figure 5: Left and right sidebearing values for capital letters comparing three different spacing methods

Table 1: Numeric values for left side bearings of capital letters obtained with three different spacing methods

Left Side bearing	A	B	C	D	E	F	G	H	I	J	K	L	M
Tracy's Method	20	100	70	100	100	100	70	100	100	20	100	100	100
Sousa's Method	20	100	70	100	100	100	70	100	120	10	100	100	100
Automatic Metrics	8	77	44	77	77	77	44	77	18	0	77	77	77
Left Side bearing	N	O	P	Q	R	S	T	U	V	W	X	Y	Z
Tracy's Method	100	70	100	70	100	60	20	80	20	20	20	20	50
Sousa's Method	100	70	100	70	100	55	20	80	20	20	20	20	50
Automatic Metrics	77	45	77	46	77	32	1	64	7	32	47	3	22

Table 2: Numeric values for right side bearings of capital letters obtained with three different spacing methods

Right Side bearing	A	B	C	D	E	F	G	H	I	J	K	L	M
Tracy's Method	20	50	50	70	50	50	80	100	100	100	20	20	100
Sousa's Method	20	50	40	70	50	50	75	100	120	80	20	5	100
Automatic Metrics	8	39	30	44	3	0	55	79	19	66	40	0	78
Right Side bearing	N	O	P	Q	R	S	T	U	V	W	X	Y	Z
Tracy's Method	100	70	70	70	20	60	20	80	20	20	20	20	50
Sousa's Method	100	70	45	70	50	55	20	80	20	20	20	20	50
Automatic Metrics	79	46	0	54	43	35	1	65	7	32	47	2	24

3.1 Walter Tracy's and Miguel Sousa's methods

Side bearing values for WT and MS methods differ only for 8 characters (three for left side bearings: I, J, S; and eight for right sidebearings: C,G,I,J,L,P,R,S). These values are highlighted in Table 1 and Table 2. These two methods are based on empirical theory of Walter Tracy and Miguel Sousa and they depend on letter shapes and their counters so these values are based on initial value of counter on letter "H" for capital letters, and letter "n" for small letters. Although, both of them starts with defining spacing for letters "H" and "n", and then use those initial values for defining side bearings for rest of alphabet, Walter doesn't give "concrete" but rather descriptive values such as "about half of counter on H" and "slightly less than counter on H". Sousa doesn't give any values at all. He starts with an "H" and "n" and then group letters with similar shapes and spacing and relies on testing letters that don't share any familiarity with them. So in this experiment Sousa's method is derived from Tracy's and then tested and modified to give better visual results.

By Tracy there are strict values for certain letters (e.g. letter H, must have the same side bearing values as letter "I"), but in tested font we have letter "l" with certain stylistic serifs, and length of these serifs should be taken into consideration. The same case is with right side of letter "d" and right side of small letter "l". Letter "l" is expected to get the same amount of space on its right side as letter "d", but in our case letter "l" have certain stylistic terminal on the lower right side so this should be taken in consideration when defining right sidebearing value.

Sidebearings for small letters are shown in Figure 6 and their numeric values are given in Table 3 and Table 4. In case of WT and MS methods, we have 9 characters with different left side bearing values (f,h,i,j,k,l,s,t,u) and 11 characters with different right sidebearing values (a,b,c,f,h,k,l,m,n,r,t). Bolded letters (a,f,s,t) are letters for which Tracy doesn't have any spacing rules. For these letters he said that they must be spaced visually with help of previously established standards. These characters are also elements of the Sousa's second and third group which have little or no shape and letter spacing similarity with characters he put in the first group.

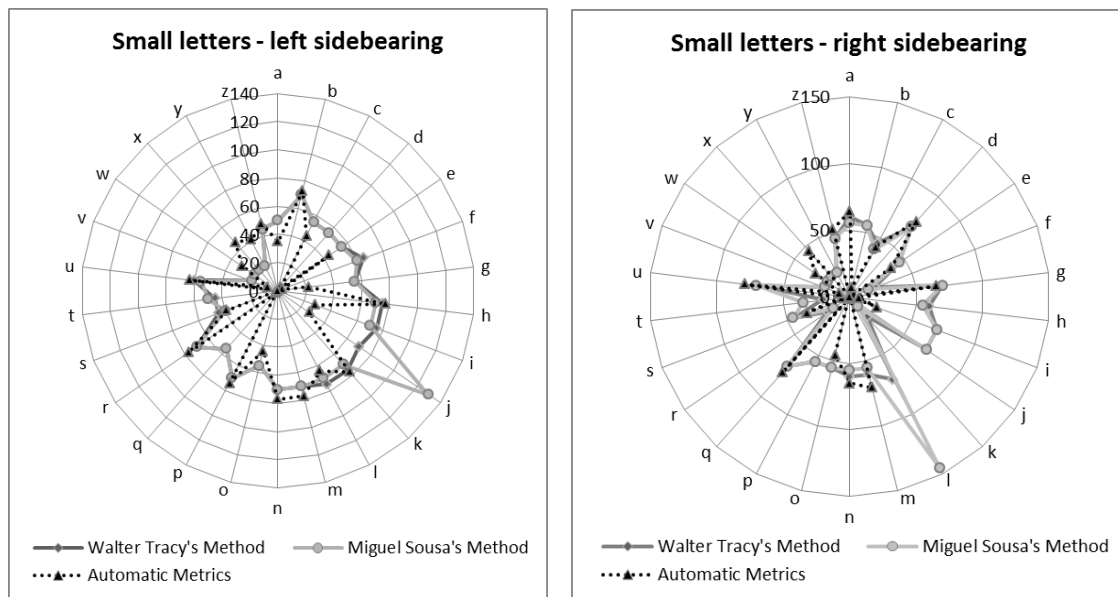


Figure 6: Left and right sidebearing values for small letters comparing three different spacing methods

Table 3: Numeric values for left side bearings of small letters obtained with three different spacing methods

Left Side bearing	a	b	c	d	e	f	g	h	i	j	k	l	m
Tracy's Method	50	70	55	55	55	65	55	75	75	70	75	75	70
Sousa's Method	50	70	55	55	55	60	55	70	70	130	70	70	70
Automatic Metrics	35	73	44	3	44	3	22	77	28	27	77	64	77
Left Side bearing	n	o	p	q	r	s	t	u	v	w	x	y	z
Tracy's Method	70	55	70	55	70	45	45	60	20	20	20	20	45
Sousa's Method	70	55	70	55	70	40	50	55	20	20	20	20	45
Automatic Metrics	77	44	74	2	77	39	0	63	8	31	46	41	49

Table 4: Numeric values for right side bearings of small letters obtained with three different spacing methods

Right Side bearing	a	b	c	d	e	f	g	h	i	j	k	l	m
Tracy's Method	60	55	45	70	45	20	70	60	70	70	20	70	60
Sousa's Method	55	55	40	70	45	15	70	55	70	70	10	145	55
Automatic Metrics	64	7	42	75	38	0	65	7	22	0	0	0	70
Right Side bearing	n	o	p	q	r	s	t	u	v	w	x	y	z
Tracy's Method	60	55	55	70	20	45	20	70	20	20	20	20	45
Sousa's Method	55	55	55	70	15	45	35	70	20	20	20	20	45
Automatic Metrics	65	45	2	76	0	34	6	79	8	31	46	0	52

3.2 Automatic generated letter spacing

Automatic generation of letter spacing which is done using FontLabs letter spacing algorithms, as it was expected doesn't give appropriate side bearing values for certain letters. As it is presented in Tables 1-4 there are certain inconsistencies compared to WT and MS methods. Generally, the same metrics pattern is used in Automatic spacing method as with WT and MS. Wider spacing for letters with straight vertical letter strokes, tighter spacing between straight vertical and curved letter strokes and even tighter spacing between two curved letter strokes (Tracy, 2006; Sousa, 2005; Cabarga, 2008). But letters {b,d,f,h,j,p,q,t,l} have noticeably smaller one or even both sidebearings compared to WT generated metrics. Also letters W,w,X,x,Y,y don't have consistent

spacing values (opposed to Tracy's recommendation - "minimum spacing"). They all have higher than half of "n" spacing. The same case is for Automatic metrics compared to MS method. Same letters have great differences for one or both sidebearing values.

4. DISCUSSION

Walter Tracy's method gives metric proposition only for serif fonts. When applying these side bearing values, serifs are excluded from calculation so spacing is measured from letter stems. When applying these metric values to sans serif font they produce slightly wider letter spacing due to absence of serifs. But applying these basic principles, foundation for further adjustment of letter spacing could be achieved.

Miguel Sousa's method on the other hand takes a little bit different approach. He also begins same as Tracy (with letters "n" and "o") but then he divides all letters from alphabet into three groups. First he begins with letters from the first group defining their left and right sidebearing values from standards (letters "n" and "o"). Then he defines only one side of letters in the second group which is similar with at least one side of letters from the first group. Then he tests every character of that group with the letters from the first group. When satisfied with results he tests every character from the third group with the letters in the first group. Letters from the third group doesn't have any similarity with neither side of letters from the first group. So Miguel Sousa doesn't give any strict rules as Tracy did but rather base his approach on defining side bearings for every character which can be in some way be related to standards (letters "n" and "o") and then constantly test other characters with previously defined one.

Letter spacing defined with FontLab's automatic algorithm follows the similar approach as Tracy's and Sousa's concerning same basic typographic rules but have quite rigid settings when defining metrics. Designer chooses from descriptive list of options whether he want to use very tight or very loose letter spacing settings or something in between. Second option which he can choose is how much shape of letters inflicts the letter spacing. This doesn't give precise control for defining font metrics so additional settings must be taken into consideration. In our experiment we adjust automatic metric settings to values near to WT and MS methods taking spacing of their standards (letters H,O,n,o) as reference values.

5. CONCLUSIONS

Letter spacing as an important factor for proper identification of letter shapes, words and unambiguous smooth reading of text must be conducted carefully. There aren't any strict and universal formula for getting this tedious job right and existing software in this field doesn't reveal their algorithms for calculating font metrics. We can only test and compare their font metrics with some basic guidelines given by type-designers in order to broaden them and to establish some new principles for determining letter spacing.

Walter Tracy's and Miguel Sousa's methods are both intended for serif fonts. Vargas was first to test and publish results for application of their methods for sans serif font Myriad Pro (Vargas, 2007) and he had difficulties to recommend most effective method based on the outcome of his experiments. He concluded that Walter Tracy's method generated an overall spacing more similar to the original adjustment for sans-serif, while Sousa's method had better results for the seriffed font Minion Pro, compared to original letter spacing. But he is also pointing out that it would be necessary to repeat the experiment several times through other typefaces.

Tracy's method, as Varga also concluded, is generally easier to apply because it suggests values for almost all sidebearings. It works like basic formula or foundation for defining letter spacing. But problems that appear working with this method are with characters a,f,g(if double-storey),s,t,z and capital letter "S". Tracy doesn't have any suggestion for these letters so they need to be spaced visually relying on designer's experience and skill. Sousa's method on the other hand doesn't give any "formula" or strict values for sidebearings but pays more attention to design of typeface and therefore gives solution to some characters that have different shape (alterations) that Tracy doesn't predict in his method. Letter spacing generated automatically didn't give satisfactory results because of lack of detailed settings in used software and because it isn't oriented for specific typeface but follows some general principles and algorithms.

So conclusion is that when defining letter space it's recommended to start with same standards (letters H, O, n and o) as Tracy and Sousa and then combine these two methods. For some obvious spacing cases one can use Walter's "formula" but for shapes of typeface that don't match

Tracy's predictions Sousa's method of testing these shapes between standards can give satisfactory results. But for letters that don't share any similarities with others there is still a problem which should be solved. So further research would probably go in direction of defining some basic principles for these problematic letters.

6. ACKNOWLEDGMENTS

This work was supported by the Serbian Ministry of Science and Technological Development, Grant No.:35027 "The development of software model for improvement of knowledge and production in graphic arts industry".

7. REFERENCES

- [1] Cabarga, L.: "Learn Fontlab Fast", 1st Edition, (Iconoclassics Publishing Co., Los Angeles, 2008), pages 71-72.
- [2] Carter, H.: "Optical scale in type founding", Printing Historical Society Bulletin, no.13, pages 144-148, (1984).
- [3] Cheng, K.: "Designing type", 1st Edition, (London: Laurence King, London, 2006), pages 218-223.
- [4] de Mello Vargas, F.: "Approaches to applying spacing methods in serifed and sans-serif typeface designs", Department of Typography and Graphic Communication, The University of Reading, United Kingdom, page 16, (2007).
- [5] Dwiggins, W. A.: "WAD to RR: a letter about designing type", Harvard College Library, Department of Print and Graphic Arts, page 7, (1940).
- [6] Kaech W.: "Rhythm and proportion in lettering / Rhythmus und Proportion in der Schrift", Oltren & Freiburg in Breisgau, Walter Verlag, page 23, (1956)
- [7] Kindersley, D.: "An essay in optical letter spacing and its mechanical application", (Wynkyn de Worde Society, London, 1966), pages 6-12.
- [8] Lo Celso, A.: "Rhythm in type design", University of Reading, United Kingdom, pages 21-34., (2000).
- [9] Sousa, M.: "Spacing method", Typophile, URL <http://typophile.com/node/15794> (last request: 2014-09-25)
- [10] Tracy, W.: "Letters of credit: a view of type design", 2nd Edition, (Boston, David R. Godine, 2003), pages 70-79.

SUBJECTIVE ANALYSIS OF IMAGE QUALITY: EXPERTS AND NAÏVE

*Ivan Pinčjer, Uroš Nedeljković, Srđan Draganov
University of Novi Sad, Faculty of Technical Sciences,
Department of Graphic Engineering and Design, Novi Sad*

Abstract: The paper presents interesting results which are being used to show if there is a justified reasons for raster technique improvement. The professional graphic worker will pay attention to many details in his visual analysis of the print, including the way in which the image was formed, i.e. image halftoning. As the prints are not exclusively meant for professionals only, it begs the question if the naïve will find a new quality in different types of rasterization. By experimental testing and statistical analysis of the mutual relationship between the answers of experts and naïve results were obtained that will reject null hypothesis. Four different images in total, rasterized in four different ways and three sample sizes, will provide enough data in order to make concrete conclusions. Each of the four images contained a strong iconic content with different elements in order to show all of the advantages of both AM and FM halftoning. Data analysis showed correspondence between the answers of both experts and naïve, as well as their estimates of the print quality that was defined by naturalness (more realistic), i.e. the least grainy structure.

Key words: Digital halftoning, subjective print analysis, print fidelity, grainy print structure

1. INTRODUCTION

The comparison between the new and conventional halftoning techniques begins with the appearance of FM halftoning. It can be said that already the first difference slowed down the application of FM technique, in the very beginning. This difference is reflected in the complexity of algorithms that distribute halftone dots over the printing surface. When that difference was overcome by the usage of more advanced computer systems, the other differences started to be explored. In scientific research, so far, there have been perceived and objectively measured many differences between AM and FM raster concerning the colour gamut, ability to reproduce even tones and tonal range or gradient, contrast, sharpness, visible pattern and other characteristics (Pinčjer, Nedeljković, & Papić, 2012). The professional graphic worker will pay attention to many details in his visual analysis of the print, including the way in which the picture was formed, i.e. the way of rasterization. As the prints are not exclusively meant for professionals only, it begs the question if the naïve will find a new quality in different types of rasterization which would be recognized by the experts also. As the naïve are not aware of the term of halftoning, during the creation of tests for the subjects, caution was taken to adapt the questions that will be answered without favorizing any single technique.

Application of FM rasterization implies investment, both of the material funds and time, which is why this paper aims to show if there is a justifiable reason for investment, i.e. if the end user will be able to recognize the quality achieved by the application of new digital halftoning technologies. Digital rasterizing is a process of rendering pictures of continuous – tone with the help of devices (mediums) that do not have the possibility of direct continuous tone interpretation, but instead generate only two levels of grey for every point of device output (Yu & Parker, 1997).

Methods of digital halftoning can be divided according to the distance of raster elements or their characterization in to three groups : conventional amplitude-modular (AM) raster, stochastic frequency-modular (FM) raster and combined, hybrid raster which can be said to be mainly AM raster with the addition of FM elements in some parts of the picture (Gooran, 2005), which makes it convenient for use on less reliable printing systems.

2. ANALYZED RASTER TYPES

Conventional AM raster simulates continuous tones with the help of individual dots whose mutual distance is even. Different levels of mean grey value are obtained exclusively by changing the size of raster dot. The bigger the raster dot is, the greater the coverage, i.e. mean grey value.

With conventional AM rasterization, pixels from the original picture are transformed into binary values, grouped, fill in the raster cells and form raster dots. Concentration of these raster dots, defined as their number by unit of length, is fixed. Difference in tone is achieved by varying the size of each raster dot (Ulichney, 1999).

Classical raster with regular structure has the following characteristics:

1. Halftone frequency: reciprocal value of raster dots or fineness of the screen is called halftone frequency (lines per inch) and represents the number of lines or rows of raster dots per inch (lpi) or per centimeter (l/cm) of the rasterized image. Frequency is dependent upon the resolution of the output device and is limited by the number of grey that is necessary to obtain the image without any perceivable tone jumps. This relationship can be defined by the following equation:

$$\text{halftone screen (lpi)} = \frac{\text{printer resolution (dpi)}}{\sqrt{\text{grey value} - 1}} \quad (1)$$

2. Shape of the raster dot: relates to the specific distribution of pixels inside the halftone cell, which dictates the way in which the dot increases in both directions and shape depending on the tone.
3. Screen angle: orientation of halftone dots in relation to the relative axis. In order to make the illusion of continual tone as convincing as possible, rasterized colour separations are printed over each other under certain angle, most commonly: (Y 0°, C 15°, M 75°, K 45°).

The advantage of AM over FM raster is the possibility of achieving uniform tones, smaller dot gain, greater possibility of colour adjustment during the process of printing, as well as the possibility of achieving larger print runs owing to the stronger presence of halftone dot on the printing plate.

Stochastic raster has gone through several changes from its inception. All of the changes were directed towards obtaining the best possible print quality, both in digital printing and offset technique. First generation of stochastic FM raster simulates continuous tones with the help of raster dots that are constant in size while their mutual distance varies according to tone value. Different tone values are achieved by alternating distribution of same size dots. Smaller distance between the dots will produce darker tones, and, by analogy, greater distance between the dots will produce lighter tones. Second generation of FM raster was developed with a goal to decrease the negative characteristics of the first generation, whose greatest problem is the inability of printing systems to keep the constant isolated dot, i.e. micro dot, whose size starts from 10 µm.

Typical modern resolution of imagesetter 2400 dpi has the size of its laser beam at 10.6µm, and it is capable of producing a micro dot 20.1µm in size. For the purpose of comparison in AM and FM raster dot size, we shall take FM raster with the dot size of 20 µm as an example – it is equivalent to 1% AM raster 150 lpi dot size.

Even though it is not represented in any greater measure in commercial printing, FM raster overcomes many of AM raster problems, such as *Moiré* effect – the appearance of unwanted repeating pattern that is formed by a case of bad overlap between two or more separations with inappropriate angles. Alternative FM raster also removes the need for screen angles and screen frequency, which produces an image with a much less faults, and higher resolution (Dharavath, Bensen, & Gaddam, 2005).

3. AM AND FM RASTER COMPARISON

Comparison of screen types can start with their disadvantages. The fault of AM raster is the appearance of *Moiré* effect, which appears during colour printing, when there is a uncontrolled rotation of one of the colour extracts relative to the others. That is the moment when geometric grid becomes visible to the human eye and continuous tone illusion is lost (Yu & Parker, 1997). It could be said that even the halftone rosette that appears during the AM raster printing is a *Moiré* effect, but is acceptable due to its high frequency.

As said before, FM raster completely removes the problems that appear because of the *Moiré* effect, considering it does not use screen angle, but random dot distribution. Further advantage of FM raster is larger colour range which is explained by its smaller dots, that cover larger

percentage of the printed surface (Pinčjer, Nedeljković, & Nedeljković, 2010). However, this characteristic is not solely dependent upon the halftoning, so it can be concluded that FM enables achievement of larger colour range by its construction.

Another disadvantage of AM raster is relatively lower resolution – by placing raster dots on a fixed grid, most of the time there is a decrease in resolution of the printed image in relation to the resolution of the printing device. Bad reproduction of the brightest and darkest details, as well as the fine details, happens for the same reason. On the other hand, with FM raster micro dots are distributed randomly, depending on their neighbors, which enables higher resolution, as well as the reproduction of a larger number of fine details (Dharavath et al., 2005).

The greatest disadvantage of FM raster is dot gain during printing, which causes lower quality reproduction of middle tones. During raster printing, increase in dot size leads to the decrease of printed tone values, which further causes loss of detail and decrease in contrast and overall quality of image. Also, dot size increase can lead to the clogging of raster and change in the shade. Larger increase in raster dot size relative to AM is caused by the very laws of dot size increase, i.e. it has been determined that it is influenced by the relationship between the perimeter and the surface of the isolated dot (Fung & Chan, 2009). Since it is a characteristic of a phenomenon that is not dependent upon the raster type, it can also be expected to occur with AM raster, especially in the case of higher screen frequencies. Ways of reducing this FM negative characteristic are primarily focused on different ways of halftone design and, in the production process, on the calibration of CTP devices.

Considering the complicated algorithms, FM rastering is, in view of the complexity of calculations, a lot more demanding than AM rastering. However, the daily advancement of technology does greatly to lessen the difference in speed of halftoning between these two techniques so that this difference has a lesser and lesser influence in graphic production.

AM raster is certainly simpler for reproduction, but it implies lesser resolution and a perceivable rosette pattern. Distribution of dots with fixed distance between them, forming the picture, results in loss of detail with AM raster. With FM raster, this loss of detail is minimized, owing to its structure – randomly distributed micro dots, with small mutual distance.

Previously mentioned FM raster characteristic, i.e. random dot distribution, causes problems during the reproduction of even tones. Raster dots distributed according to pattern, as is the case with AM raster, are more pleasing to the eye and it defines them as an even tone (He, 2004).

Since every way of rastering has its advantages and disadvantages, this research will provide an insight into how much the differences between these two types of halftoning are noticeable by experts and non-experts.

4. RESEARCH METHOD

Specific tests were made for the experiment in order to collect relevant results with the help of accepted scientific methods (Cui, 2000). The tests consist of four photographs of different contents, 88x62mm in dimension, reproduced with the help of two conventional (150lpi and 175lpi) and two stochastic (20 μ m and 40 μ m) screens. Photographs were chosen in such a way as to contain strong iconic content.

This experiment compares the frequency of chosen answers for two parameters, the least noticeable grainy structure and the most realistic reproduction, for all images, different in content, in relation to the field of education. Field of education is divided into two groups: one group is represented by subjects that study or work in the field of graphics design and printing industry, while second group is represented by subjects that do not study or work in the field of graphics industry. From the data obtained by this research it can be concluded if the iconic content shown on the used images is more effective (how much of a stronger influence it has on the observer) with the help of stochastic or conventional halftone. This data can be used in the world of printing, advertising and packaging, in order to obtain the best quality reproduction possible which will have a stronger impact on observers/potential consumers, as well as to justify investment into new raster types.

The research was performed on the Faculty of Technical Sciences, University of Novi Sad. The sample in the research numbered 101 subjects. The subjects have a varying degree of experience in the field of graphics: subjects that do not have any experience in the graphic profession (50 subjects) and subjects that study or work in the graphic industry (51 subjects).

The research was executed with the help of four different tests: for each of the four different (in content) photographs a single test was made. So, on each test there are four photographs of the same content, format and different according to raster type. Photographs were chosen in order to be mutually different in the quantity of detail, tone gradient, color and content type. Four photographs were chosen:

- A girl – representation of human face in a close-up;
- Coffee – large quantity of detail, out of focus background;
- Risotto – large quantity of minute details, even colors;
- A car – representation of the front of a car, very little detail, with gradient



Figure 1: Images used in subjective analysis

The subject looks at the same time at all four reproductions, same in content, but different in raster types, and based on psychophysical scaling, or more accurately ranking, evaluates which of the four reproductions shows the best quality related to grainy structure and reproduction realism, writing his answers down into the questionnaire.

Each test is prepared with different halftone image position, so that a single raster type changes its position in different test sheets. This removes the possibility of the subject developing a "habitual knowledge" when the position of a specific raster type is unchanged on different test sheets, and thus automatically chosen by respondent.

The number of subjects is standard for these kind of tests [Engeldrum, 2001], as well as their division into two types, professionals and naïve. Test is designed in a way that it does not require too much time on the part of the subjects to evaluate all the necessary images, in order to avoid making the subjects fatigued.

Tests are shown in the observation booth Agile radiant Controlled Light5 from the Ihara company, in order to facilitate even lighting for all the subjects, which is simulated by a light (color temperature 2700K). Observation distance (distance of the sample – observation tests, from the eyes of the observer) is fixed on the rank of 50cm (which represents standard reading distance) [Pedersen, Bonnier, Hardeberg, & Albrechtsen, 2011].

Reproductions are printed on an Epson Stylus Pro7800 machine for printing test prints. A test print machine was chosen that has the possibility of simulating offset print, in order to obtain printed raster dot in as less steps as possible. Namely, by using Epson Stylus Pro test print machine and Studio Rip software dot-by-dot printing was made possible, which means that the raster dots will look in print exactly as instructed by RIP. Furthermore, by using test print machine further factors that could influence the appearance of the raster dot in print were excluded (for example, printing plate). Before printing the tests, calibration of the test print was performed in order to conform it to ISO standard.

Epson UltraChrome are the inks used in test and Multi-jet M-PHOTO + 255g glossy is the paper on which the test images were printed.

Resolution of the output device (test print machine Epson Stylus Pro) is adjusted to 1.440 dpi, which is the maximum resolution for this printing device, and which enabled reaching the wanted raster dot sizes. ISO Fogra 27 is the colour profile used for all four raster types.

5. DATA ANALYSIS

Goal of this research is to determine the mutual visual relationship and visual effect of AM and FM raster on two groups of subjects, consisting of professional graphic workers and non-professionals. The null hypothesis that is being tested:

There is a statistically significant difference in relation to the least noticeable grainy structure and the most realistic reproduction, considering the field of education.

For this hypothesis, frequency of selection is compared for all the images, considering the field of education. Field of education is divided into two groups: one group is represented by the subjects that study or work in the field of graphic industry, while the other group is represented by the subjects that do not study or work in the field of graphic industry.

Chi-Squared (χ^2) test was used for data processing in order to process discontinuous variables. For each test, depending on the defined degree of freedom, there is a table represented border value for χ^2 . Based on the degree of freedom critical value for 0,05 (95%) is calculated, and then compared to the calculated χ^2 value. Data analysis, shown in the following diagrams, proves that for each given case within the stipulated hypothesis the value of χ^2 implies that the selection of the subjects evaluating the quality was not random. In other words, there is an influence that led to the situation where the subjects choose one type of raster more frequently than the other. By graph analysis it can be determined that the subjects selected 20 μ m raster far more frequently than any other.

6. MEASUREMENT RESULTS

Figure 2 shows numerically the answers by both professionals and naïve for image 1 – a girl. This diagram clearly shows that both groups of subjects convincingly frequently selected 20 μ m FM raster as having the best quality.

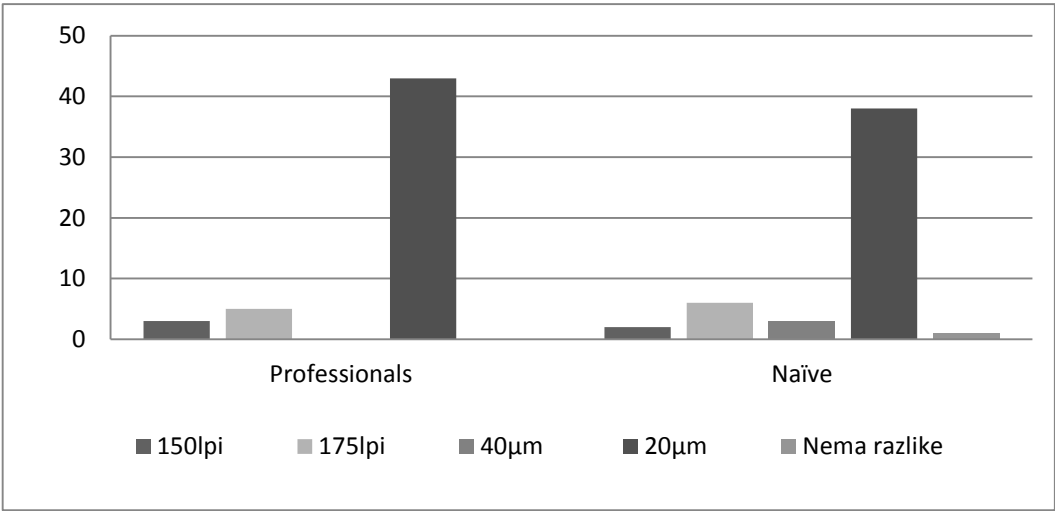


Figure 2. Results for image 1 – a girl

Figure 3 shows numerically the answers by both professionals and naïve for image 2 – coffee. This diagram clearly shows that both groups of subjects convincingly frequently selected 20 μ m FM raster as having the best quality.

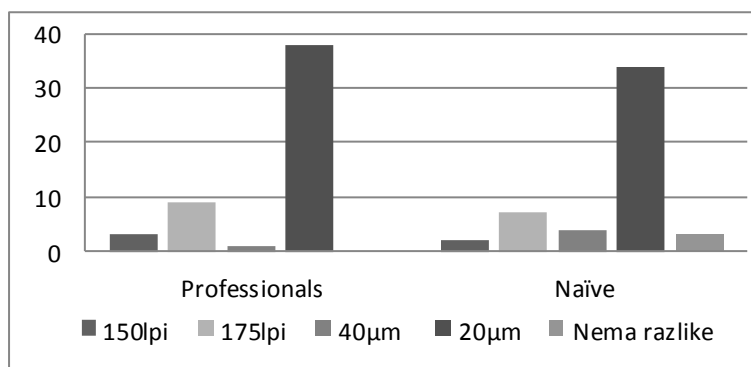


Figure 3. Results for image 2 - a coffee

Figure 4 shows numerically the answers by both professionals and naïve for image 3 – risotto. This diagram clearly shows that both groups of subjects convincingly frequently selected 20µm FM raster as having the best quality.

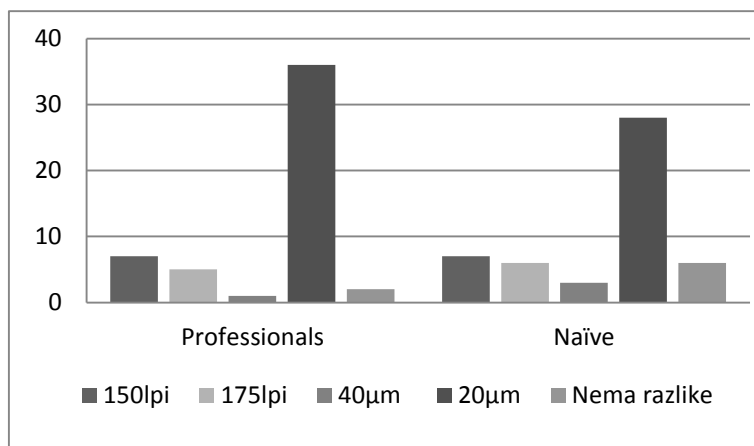


Figure 4. Results for image 3 - a risotto

Figure 5 shows numerically the answers by both professionals and naïve for image 4 – a car. This diagram clearly shows that both groups of subjects convincingly frequently selected 20µm FM raster as having the best quality.

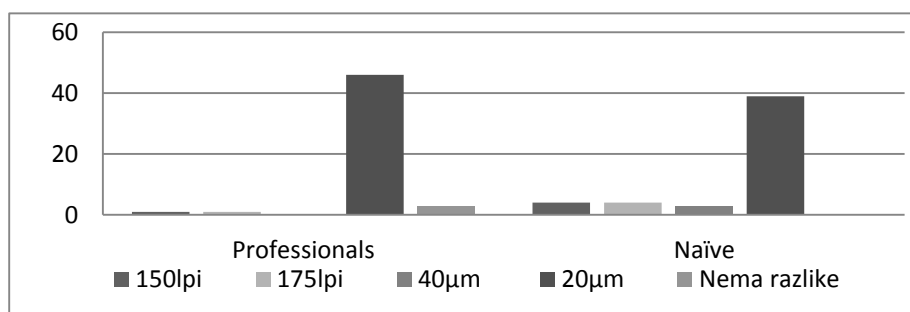


Figure 5. Results for image 4 - a car

After data analysis, it could be said that null hypothesis is rejected. Data analysis for all four images proves that there is no statistically significant difference between the professional and layman answers, which leads to conclusion that both groups perceive and experience FM raster similarly (evenly) – as having the better quality. Furthermore, it can be concluded from the

results that FM raster is not more visually appealing only to the trained eye of the professional, but that any observer can perceive its advantages quite easily.

It is interesting to notice that with all four images, the subjects (regardless of their field of education) most frequently selected 20 μ m raster as having the best quality. From this data it can be concluded that exactly the mentioned raster, regardless of the observer's field of education and the content of the observed image (detail quantity, contrast, colours, gradient...), stands out as having the best quality. It needs to be mentioned here that all parameters that appear in offset printing, and influence the reproduction quality both with AM and FM raster, are excluded from the process. The paper presents the subjects' answer to the algorithm quality, size of raster elements, i.e. graininess and realism of the image.

7. CONCLUSION

FM raster is definitely a technique that needs to be further studied, developed and invested in. From the standpoint of the printing industry, FM raster provides high quality prints. From the standpoint of marketing and advertising industry, that almost ideal reproduction of reality is something which is definitely strived for, in order for the product (object of advertising) to be presented and brought closer to the observer/potential consumer in the best way possible.

Implementation of FM workflow implies certain investment, modern graphic systems with controlled and repeatable printing conditions. That is exactly why printing firms often give up on trying to get to know the FM raster, justifying this choice by a somewhat larger cost of FM raster relative to AM. However, this is certainly a field for further research, and prospective progress and development of FM raster. By comparing the answers from the subjects that study or work within the graphic industry with answers from those that do not, it can be concluded that there is no statistically significant difference in their answers. This means that both subject groups chose their answers evenly, and 20 μ m raster was universally chosen as being of the best quality.

From the given analysis, it can be concluded that better quality raster is perceptually recognized by both people connected to graphic profession and people with no connections to it. Quality of reproductions rastered by 20 μ m raster is perceived by subjects, regardless if they are professionals whose eye is trained and used to observing certain parameters, or naïve without prior raster knowledge.

8. ACKNOWLEDGEMENTS

This work was supported by the Serbian Ministry of Science and Technological Development, Grant No.:35027 „The development of software model for improvement of knowledge and production in graphic arts industry“.

9. REFERENCES

- [1] Cui, C. (2000). Comparison of Two Psychophysical Methods for Image Color Quality Measurement: Paired Comparison and Rank Order. *Color and Imaging Conference, 8th Color and Imaging Conference Final Program and Proceedings* (pp. 222–227). Society for Imaging Science and Technology.
- [2] Dharavath, H., Bensen, T., & Gaddam, B. (2005). Analysis of Print Attributes of Amplitude Modulated (AM) vs. Frequency Modulated (FM) Screening of Multicolor Offset Printing. *Journal of Industrial Technology*, 21(3). Retrieved from [http://scholar.google.com/scholar?hl=en&btnG=Search&q=intitle:Analysis+of+Print+Attributes+of+Amplitude+Modulated+\(AM\)+vs.+Frequency+Modulated+\(FM\)+Screening+of+Multicolor+Offset+Printing#0](http://scholar.google.com/scholar?hl=en&btnG=Search&q=intitle:Analysis+of+Print+Attributes+of+Amplitude+Modulated+(AM)+vs.+Frequency+Modulated+(FM)+Screening+of+Multicolor+Offset+Printing#0)
- [3] Engeldrum, P. (2001). Psychometric Scaling: Avoiding the pitfalls and hazards. *PICS*, 101–107. Retrieved from http://www.imcotek.com/pdf_temp/PICS-27.pdf
- [4] Fung, Y., & Chan, Y. (2009). A Multiscale Error Diffusion Algorithm. *17th European Signal Processing Conference (EUSIPCO 2009) Glasgow*, (pp. 2258–2262). Glasgow.
- [5] Gooran, S. (2005). Hybrid halftoning, a useful method for flexography. *Journal of Imaging Science and Technology*, 49(1), 85–95. Retrieved from <http://www.ingentaconnect.com/content/ist/jist/2005/00000049/00000001/art00011>
- [6] He, Z. (2004). AM/FM halftoning: digital halftoning through simultaneous modulation of dot size and dot density. *Journal of Electronic Imaging*, 13(2), 286. doi:10.1117/1.1669555

- [7] Pedersen, M., Bonnier, N., Hardeberg, J. Y., & Albrechtsen, F. (2011). Image Quality Metrics. (S. P. Farnand & F. Gaykema, Eds.), 7867, 786702–786702–19. doi:10.1117/12.876472
- [8] Pinčjer, I., Nedeljković, U., & Papić, M. (2012). Development of FM screens. *JGED Journal of Graphic Engineering and Design*, 3(1), 1–8.
- [9] Pintier, I., Nedeljković, U., & Nedeljković, S. (2010). Colour gamut of fm screening. *Grid10 Proceedings* (pp. 273–278). FACULTY OF TECHNICAL SCIENCES GRAPHIC ENGINEERING AND DESIGN.
- [10] Ulichney, R. (1999). Review of halftoning techniques. *Electronic Imaging*. Retrieved from <http://proceedings.spiedigitallibrary.org/proceeding.aspx?articleid=920677>
- [11] Yu, Q., & Parker, K. J. (1997). Stochastic Screen Halftoning for Electronic Imaging Devices. *Journal of Visual Communication and Image Representation*, 8(4), 423–440. doi:10.1006/jvci.1997.0363

THE INFLUENCE OF COLOR IN DIGITAL MEDIA ON USER EXPERIENCE

*Lidija Mandić, Domagoj Trojko, Jesenka Pibernik, Jurica Dolić,
University of Zagreb Faculty of Graphic Arts, Zagreb, Croatia*

Abstract: Computers have become a part of everyday life and more and more people, especially younger ones, spend long time watching at the screen of a laptop, tablet or a smartphone. So it's an imperative for web and graphic designers to know how to make a product in digital world to be visually attractive. Color is considered to be one of the most important elements of a graphic user interface. The aim of this research was to examine how users experience colors in user interface and how their perception of colors attracts their attention. This was done with two different online surveys and an experiment where two websites were designed. The results showed that color can be used to control the way websites are used.

Key words: user experience, graphic user interface, color, digital media

1. INTRODUCTION

In this era when the computerization of everyday life takes unexpected proportions and computers, smart phones and tablets have become an indispensable part of modern life, the manufacturers are fighting for each client. One of the strongest weapons is offering a great user experience. There are a number of rules whose knowledge can make a user interface that are both visually and functionally sophisticated, and this may provide a satisfactory user experience. In fact this is not a set of rules, because there are no strict rules and methods that can make a good user interface, it's more a set of guidelines that it is advisable to follow in order to achieve a satisfactory result. This approach of heuristic evaluation is an attempt to describe a number of highly acclaimed experts in the field of interaction between humans and computers like Jill Gerhart-Powalls or Susan Weinschenk and Dean Barker, but the best known and most frequently mentioned guidelines leading man of the area, Jakob Nielsen, who, working together with Rolf Molichom, 1990, for the first time compiled a list of guidelines which was improved and published 1994. in his book "Usability Engineering". It is a set of 10 basic principles that should be followed in designing interfaces in man-machine interaction by Nielsen identified by studying 249 problems in using computer systems (www.nngroup.com, 2013). Thus, the user experience (UX) refers precisely to how the user feels using a system, product, service (Galitz, 2007). Especially in human-computer interaction user experience stands out as one of the key. Therefore, he himself determines whether the product is easy to use, efficient and accurate, depending on the subjective expectations of the user. Because the user experience is subjective, it is also dynamic since the change in circumstances in which the product is used could change the entire user experience. ISO 9241 standard defines ergonomics interaction between people and systems, ie. Section 210 which describe design of interactive systems-oriented man, define user experience as well as perceptions and responses persons arising out of use of the product, system or service. Further explains that the user experience includes the user's feelings, beliefs, attitudes, experiences, physical and psychological responses, behaviors and accomplishments that occur before, during and after use (Smith, 2006). Explanations mentions three factors that affect user experience: the system, the user and the context of use

2. COLOR

The harmony is used to create color balance, and this can create a logical structuring of colors. The tool used in the logical structuring is the color wheel in the way to create relationships among colors in a circle, and made several formulas by which creates pleasing visual experience (Stone, 2006; Lee, 2005). Here are some concepts or relationships between colors, which are widely used by artists and designers.

The concept of complementary pairs - Complementary colors are purple and blue and yellow, green and purple, red and green-blue, and a couple of colors in the color wheel is opposite to one another. Using these pairs of colors obtained the highest contrast and achieves visual vibration that the human visual system operates exciting.

The concept of split complementary pairs - Although this concept was based on the use of complementary colors, since it uses three colors, they are selected in such a way that the primary color is selected and then the other two colors selected by identifying its complementary pair and take two colors that are closest to it, or those on his left and right. This dampens emphasized contrast.

The concept of double complementary pairs- Another concept based on the complementarity of colors, it can choose the four-color or two complementary pairs. The problem occurs when all four colors are used in the same way as the complementary members stress, and the result may well be too jazzy.

The concept of double complementary pairs - Another concept based on the complementarity of colors, it can choose the four-color or two complementary pairs. The problem occurs when all four colors are used in the same way as the complementary members stress, and the result may well be too jazzy.

The concept of analogous colors - Two or more colors in the color wheel that are next to each other and the distance between them is even are used. Then these colors have a wavelength that is close to each other. The result is a color concept which is not conspicuous and does not disturb the visual system.

The triad concept - Triad represents any three colors that are evenly dispersed over the color wheel, with a gap between the colors that are the same. When the triad composed of the primary colors, the result is a garish, therefore secondary and tertiary triad is particularly appropriate since the contrast between them softer.

Monochrome concept - As the name suggests, this is the concept of using only one color. The concept is formed so that one color is changed in the brightness and saturation in order to obtain an acceptable combination of colors that are similar to one another.

3. EXPERIMENT

The aim of research was to investigate the perception of color users of digital media in any graphical user interface, and whether it's using color to focus attention on the desired elements. In order to achieve this goal have been made following steps: survey about the general preference of colors; survey about the colors in the web interface; determining the visibility of graphic elements in the web interface methods by recognizing a focal point of mouse clicks. The survey was conducted via a web browser, using the websites www.surveygizmo.com. For research purposes, made a survey of 20 questions that were divided into three groups. Some results of survey are shown in Figure 1.

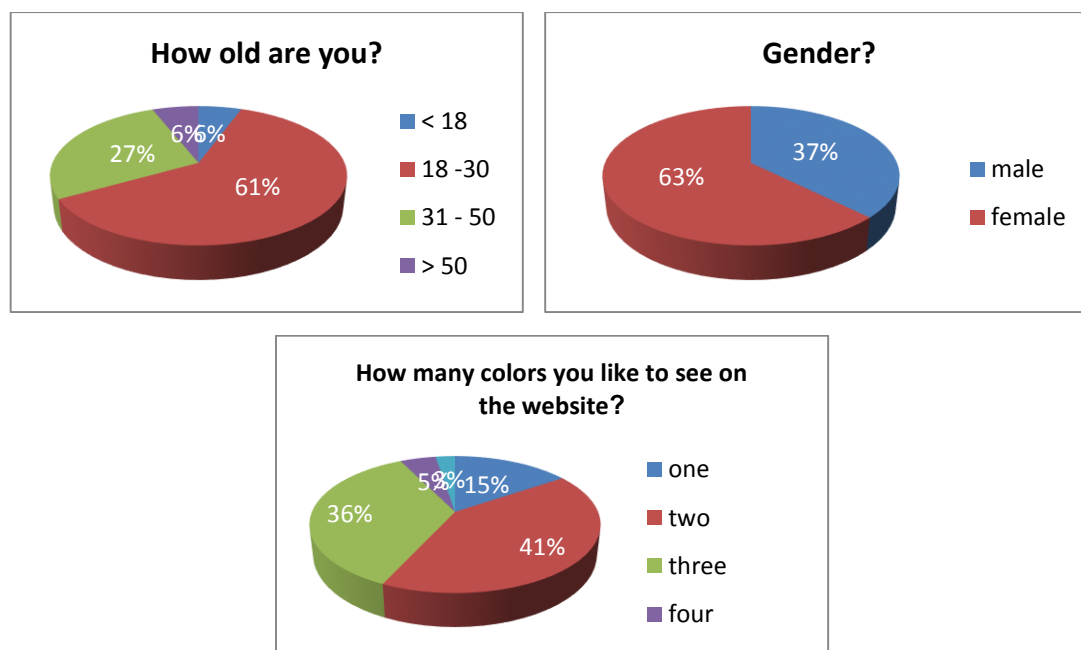


Figure 1: The results of survey

The participants were shown two different websites with two standard types of layout (figure 2). The task was to rank the elements according order noticing. The first element that they noticed was the image that takes up most of the space. Another element that participants noticed was the logo, which occupies the upper left corner, according to many studies, the angle at which most of user first look at any website. They are asked for the same design to distribute elements in order of importance. They first put the logo, and then the image. For the second website, testing was identical to that of the first design. The most visible element was the logo "QR stamp", the second was the text "Enter the code with the brand" and the third logo Croatian Post.

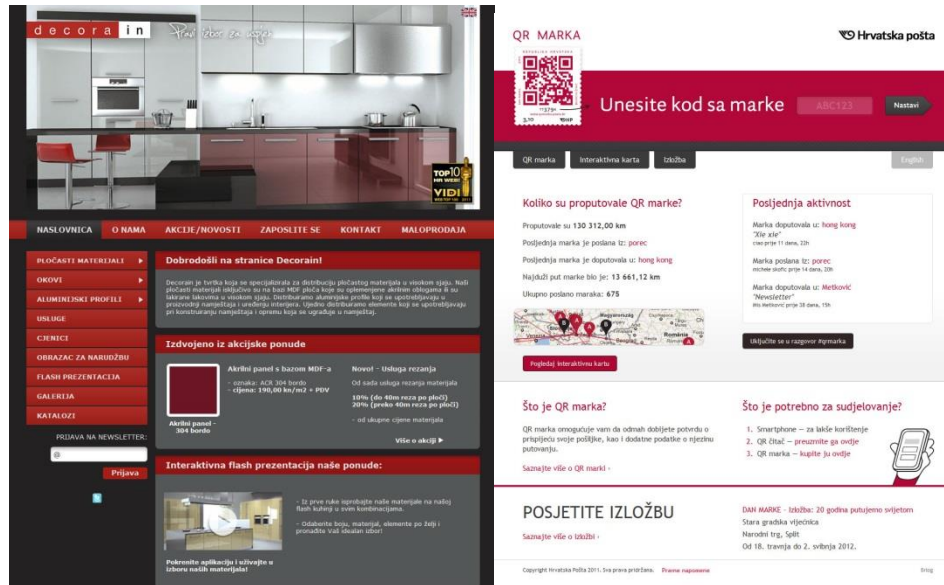


Figure 2: Websites

The last stage of investigation was done via the Internet. The goal was to check whether the changing concepts of harmonic color with simple design web sites will be evident. By changing the settings in the HTML and CSS file for websites, is incorporated a monochromatic color and complementary color concept, and old and new concepts put on an Internet server. For old and new web pages are designed tasks that the participants had to solve. Testing was done using the free tools ClickHeat who saves every mouse click on the page and determines the focal areas in which respondents most frequently clicked the mouse.

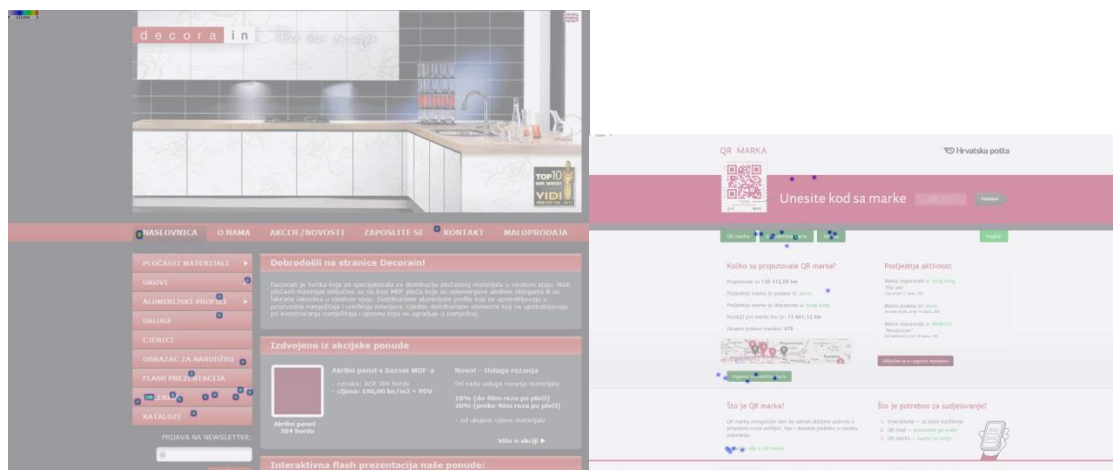


Figure 3: Results of focal areas

In a study where a monochromatic color concept was applied notes are almost identical pattern of mouse clicks, but still it can be seen that the clicks are much less scattered, and it seems that users are finding more precise links to perform tasks.

In a study where the concept of complementary colors was applied, on a test web page notes that respondents were quite accurately using the links so that there are not many clicks outside the scope of these links that were used.

From this study it can be concluded that by changing the use of the concepts of color and creating a larger difference between the colors, whether in color, brightness and saturation, increase the concentration of clicks on certain links and thus increase the visibility of their subjects important elements. This is especially be observed in the use of the concept of complementary colors, it is obvious that the use of complementary colors in the two cases changed the way of accessing a content, while in the third case, the content accessed more precisely, due to the concentration of clicks and it may be concluded that respondents desired finding content quickly.

4. CONCLUSIONS

This paper attempts to demonstrate how color can greatly affect the way you used a specific user interface, and thus the user experience. This influence can be both good and bad. The graphical user interface is one of the most important concepts in today's information technology and it should be in the center of the development of computer programs. It can not rely on a number of rules for the proper production of user interfaces, but these rules should be seen as guidelines that can be used to achieve the main goal when creating a graphical user interface, and a good user experience. User experience is very difficult to achieve because the user experience is personal matter for the individual and depends on many factors. One of the most important factors is the color, the way how the human visual system perceived and interpreted it. The results of surveys showed that all persons have a predetermined relationship to the color that is learned over the years. It is shown how different people have different attitudes towards certain shades of color from the direction of male or female. The results of research shows that it can increase the visibility of certain elements of the user interface concepts using a variety of colors. When using the concept of complementary colors, it is evident that even the subjects changed patterns of behaviour and usage of the website when the design included the complementary color hue that is used as a dominant design. It can be concluded that using complementary colors create a contrast that has worked harmoniously, and that has increased the visibility of the selected graphic elements and thereby facilitate the fulfilment of the tasks of the experiment. Design where monochromatic concept of color is applied, the users were finding ore precise links for the execution of tasks.

5. REFERENCES

- [1] Galitz, W. O.: "The Essential Guide to User Interface Design", (Third Edition, Wiley Computer Publishing, Indianapolis, 2007.)
- [2] Lee, H.C.: "Introduction to Color imaging Science" (Cambridge University Press, Cambridge, 2005.)
- [3] Nielsen, J.: Nielsen Norman Group, 10 Usability Heuristics for User Interface Design, 1995, URL <http://www.nngroup.com/articles/ten-usability-heuristics/>, (last request: 2013-05-17)
- [4] Smith S.: "Color affects our mood: The human reaction", URL http://thaddeussmith.info/uploads/Color_and_Mood_Paper.pdf., (last request: 2013-06-01)
- [5] Stone T. L., Adams S., Morioka N.: "Color design workbook, Rockport publishers, Beverly, 2006.)

THE INFLUENCE OF PACKAGING SHAPE ON PERCEIVED PRODUCT VALUE AND CONSUMER NICHE

Gojko Vladić¹, Darko Avramović¹, Milana Sadžakov¹, Neda Milić¹, Milica Kecman²

¹ University of Novi Sad, Faculty of Technical Sciences,

Department of Graphic Engineering and Design, Novi Sad, Serbia

² Universite Libre de Brussel, Solvay Business School, Marketing and Advertising, Belgium

Abstract: As the products characteristics come closer one to another packaging becomes factor of greater importance in the consumer decision-making process because it communicates to consumers at the precise time of the purchasing decision. Packaging is an important part of the branding process and it offers diverse possibilities for communication. This paper focuses on the influence of packaging shape on perceived product value and consumer niche. Packaging shape can be graded according to shape complexity from primitive geometric shape to very complex shapes. Research hypothesis is that complexity of the packaging has influence on perceived product price, also that consumer niche and type of the product can be determined according to the shape of the packaging.

Key words: Packaging, shape, value

1. INTRODUCTION

Packaging is the first thing that consumer interacts with when faced with any product. Packaging is generally regarded as an essential component of product. Packaging shape has the potential to influence consumer's product-related attitudes and behaviors. Often packaging is the most relevant element of a trademark advertising or communication. Product packaging presents an important opportunity for manufacturers and retailers to communicate with the consumer, both at the point of sale (Rettie, 2000; Silayoi, 2007; Simms, 2010). As the products characteristics come closer one to another packaging becomes factor of greater importance in the consumer decision-making process, because it communicates to consumers at the precise time of the purchasing decision. Packaging is an important part of the branding process and it offers diverse possibilities for communication. Freedom in design, concerning shape of packaging, results in wide range of possible solutions. Packaging shape provides information about product category, 'positioning' it in a certain niche, attracting attention to a product and communicating information regarding brand identity and brand values (Ampuero, 2006; Schoormans, 1997; Creusen, 2005; Bloch, 2003; Schoormans, 2010; Creusen, 2005). To achieve the communication goals effectively and to optimize the potential of packaging, manufacturers must understand consumer response to their packages, and integrate the perceptual processes of the consumer into design (Nancarrow, 1998). Aesthetic qualities of packaging design, such as shape, influence consumers' product attitudes and purchase decisions (Hekkert, 2008; Lindell, 2011).

Shape is a necessary feature of all manufactured objects. As all objects have shape, that shape can be more or less complex, thus giving that object certain characteristics. Complexity of the shape often determines what process may be considered for making it. In the most general sense, rising complexity narrows the range of processes that may be used and increases production cost. A main rule of design is to keep the shape as simple as possible, but if complex shape is adding to perceived value more than it actually increases production cost it can be considered as a useful marketing tool.

There is no universally accepted shape classification system. With increasing spatial complexity, definition of the shape requires additional geometric parameters. A small increment in information content can have significant manufacturing consequences. This paper is dealing with complexity of cardboard box packaging. Complexity of the shape is undoubtedly increasing the production costs. The aim of this research is to determine are those increments in cost reflected in perceived value of the products packaged in the cardboard box. In addition to perceived value the shape can influence the niche of the consumers interested and also products suitable for packaging. There are several ways to achieve gradation of the cardboard packaging complexity. Shape can be manipulated for the basic six sided box shape to very complex shapes by

increasing number of sides od by applying different modification operations such as: slicing, skewing, twisting, squeezing, tapering, etc. Some of the mentioned operations are represented in Figure 1, showing the results of transforming simple six sided cube. All of the operations can be applied in multiple iteration thus achieving more complex shape in gradual manner.

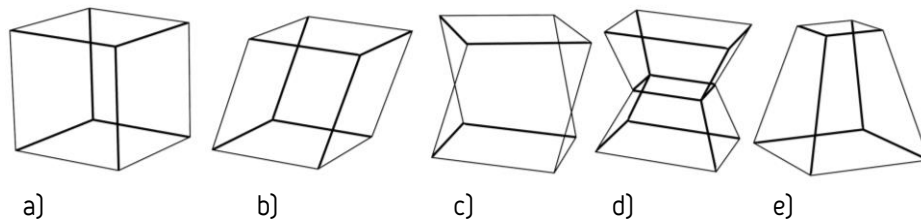


Figure 1: Shape transformation operations: a) basic six sided cube, b) skewing, c) twisting, d) squeezing, e) tapering

2. METHOD

Experiment is conducted in order to deduce influence of the packaging shape on the consumer's perception of value, adequate product type and age group of consumers that shape is suitable for. Web survey was conducted in order to gather data.

2.1 Participants

About hundred participants were asked to take part in the survey, fifty six replayed from witch forty eight participants finished survey successfully. Eight participants did not fill questioner completely or did not submit adequate demographic data and were excluded from further analysis. Twenty seven male and twenty one female participants have successfully finished the survey. Age of the participants was between 22 to 38 years. Participants were chosen by chance or by chaining the survey link to the next participant.

2.2 Stimuli

Using earlier mentioned transformations, variation of cardboard boxes shape were created. Models of boxes were made using CAD software and afterword rendered as animation showing rotating box and lid opening. Each model was designed gradationally increasing the complexity of the packaging. Final stimuli, used in the experiment, gradually increases the complexity from 1 to 6, and is shown in Figure 2.

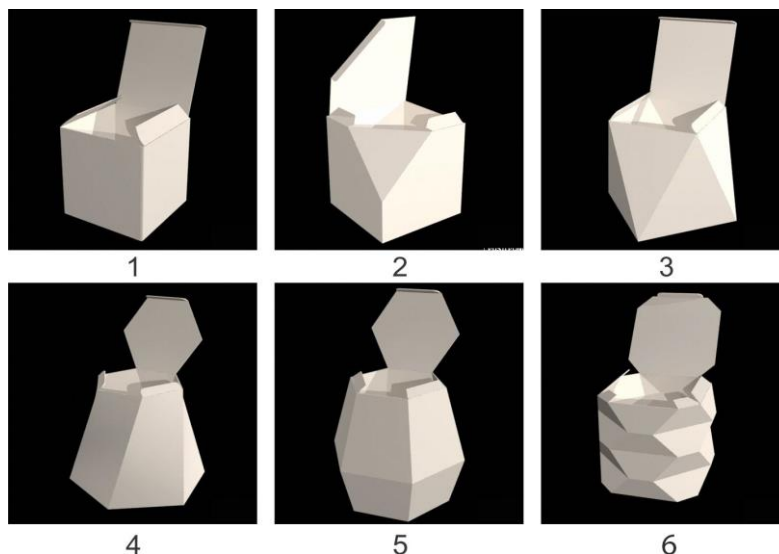


Figure 2: Stimuli, used in the experiment

2.3 Instrument

Survey was conducted by interactive web application, created using Adobe flash Action script, combined with php script. Application is consisted of three parts: explanation of the procedure and demographic data gathering; collecting of experiment data and thank you for participation note; thus enabling users to submit their judgment in interactive and easy procedure. Two main windows of the application are shown in Figure 3.

Dobro došli!

Molimo vas da u zavisnosti od oblika prikazane kutije:

1. Upišete vašu pretpostavku o vrednosti proizvoda koji se pakuje, na skali od 1 do 100.
(1-manje vredni, 100-više vredni)
2. Odaberete vrstu proizvoda za koju je prikazana kutija najadekvatnija.
3. Odaberete starosnu grupu za koju je najadekvatnija prikazana kutija.
(za animirani pregled kutije kliknite na sliku)

U polje ispod teksta upišite svoj pol i godine starosti.
(M26 za muškarca starosti 26 godina ili Z26 za žensku osobu istih godina)

Upravi vrednost proizvoda 1-100

☐ Hemijski ☐ Masiinski ☐ Prehranbeni

☐ Elektronički ☐ Kozmetički

☐ 7-12 god. ☐ 13-19 god. ☐ 20-35 god.

☐ 35-50 god. ☐ 50-70 god. ☐ 70+ god.

Upravi vrednost proizvoda 1-100

☐ Hemijski ☐ Masiinski ☐ Prehranbeni

☐ Elektronički ☐ Kozmetički

☐ 7-12 god. ☐ 13-19 god. ☐ 20-35 god.

☐ 35-50 god. ☐ 50-70 god. ☐ 70+ god.

Upravi vrednost proizvoda 1-100

☐ Hemijski ☐ Masiinski ☐ Prehranbeni

☐ Elektronički ☐ Kozmetički

☐ 7-12 god. ☐ 13-19 god. ☐ 20-35 god.

☐ 35-50 god. ☐ 50-70 god. ☐ 70+ god.

Figure 3: Survey application windows

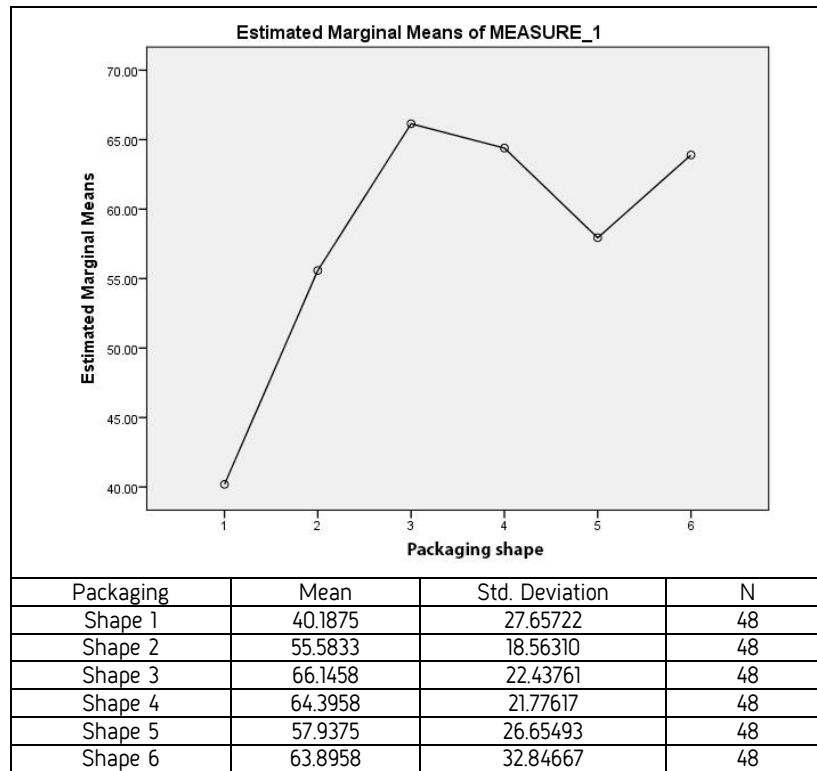
2.4 Procedure

Procedure of the experiment was fairly simple. Participants were asked to give their estimate of the product value suitable for packaging in shown boxes. Non-monetary scale 0 -100 was used. Second question was related to product type suitable for packaging in the shown boxes. Participants were offered five types of products according to the industry: chemical, machine, electronic, food or cosmetic. It was possible to choose only one type of the product. Third question was related to consumer age for which packaging is suitable. Participants could choose one age group from six that were offered. Age groups were created to represent typical demographic groups from children 7 to 12, teenagers 13 to 19, young adults 20 to 35, adults 35 to 50, older adults 50 to 70 and elderly people 70... Results were stored, formatted in to appropriate matrix for statistical analysis and subjected to statistical analysis.

3. RESULTS AND DISCUSSION

Statistical analysis was conducted in order to determine if there is statistically significant difference between perceived values of the product that would be packaged in the differently shaped packaging. IBM SPSS Statistics Data Editor Application and MS Excel were used to perform the analysis. Repeated measures ANOVA was used and post-hoc contrasts were carried out using Fisher's LSD testing procedure. In the statistical analysis, the significance level was set to $p < 0.05$. Descriptive statistics alongside chart of mean values for the product value are presented in Table 1. Although Standard deviation value is high it must be taken in to consideration the very complex nature of the question.

Table 1: Descriptive statistics for the product value



The main effect of the within subjects variable type of product value (Greenhouse-Geisser) is significant using a critical alpha of .05 ($F(5, 48) = 9.146, p = .00$), thus the overall product value are not similar.

Further analysis by post-hoc tests reveals that packaging shape 1 is contributing to observed differences. Other shapes have shown only sporadically statistically significant differences among each other. Results of post-hoc tests are shown in Table 2.

Table 2: Pairwise comparison for packaging shape 1

(I) Shape	(J) Shape	Mean Difference (I-J)	Std. Error	Sig. ^b	95% Confidence Interval for Difference ^b	
					Lower Bound	Upper Bound
1	2	-15.396*	3.735	.000	-22.909	-7.883
	3	-25.958*	5.483	.000	-36.989	-14.928
	4	-24.208*	5.309	.000	-34.889	-13.527
	5	-17.750*	3.689	.000	-25.172	-10.328
	6	-23.708*	5.114	.000	-33.996	-13.420

This indicates that only simple cube box packaging was judged as suitable for cheaper products, while all the other packaging was judged as appropriate for higher value products regardless of the level of complexity.

The suitability of packaging for certain product type, according to manufacturing industry, was analyzed by calculating frequencies for each packaging shape. Calculated frequencies with percentages are shown in Table 3. Interesting fact arouse from the data that simple cube box shape was judged as most suitable for machine industry, while none of the participants chose it as suitable for cosmetics. Other shapes are mainly judged as suitable for cosmetics. Further research should be directed to more detailed division of industries and some more comprehensive data could be gathered.

Table 3: Frequencies of product types according to manufacturing industry

	Shape 1		Shape 2		Shape 3		Shape 4		Shape 5		Shape 6	
Industry	Freq.	Perc. %	Freq.	Perc. %	Freq.	Perc. %	Freq.	Perc. %	Freq.	Perc. %	Freq.	Perc. %
Food	15	31.3	9	18.8	9	18.8	12	25.0	18	37.5	9	18.8
Chemical	4	8.3	2	4.2	4	8.3	6	12.5	8	16.7	2	4.2
Cosmetic	0	0	20	41.7	24	50.0	21	43.8	16	33.3	27	56.3
Electronics	11	22.9	10	20.8	6	12.5	2	4.2	6	12.5	8	16.7
Machine	18	37.5	7	14.6	5	10.4	7	14.6	18	37.5	2	4.2

Assumption of appropriate consumer age according to packaging shape analysis showed once again difference between simple cube packaging and all the other shapes, while there was no significant difference between complex shapes amongst each other. Figure 4 shows the mean values of appropriate consumer age assumption.

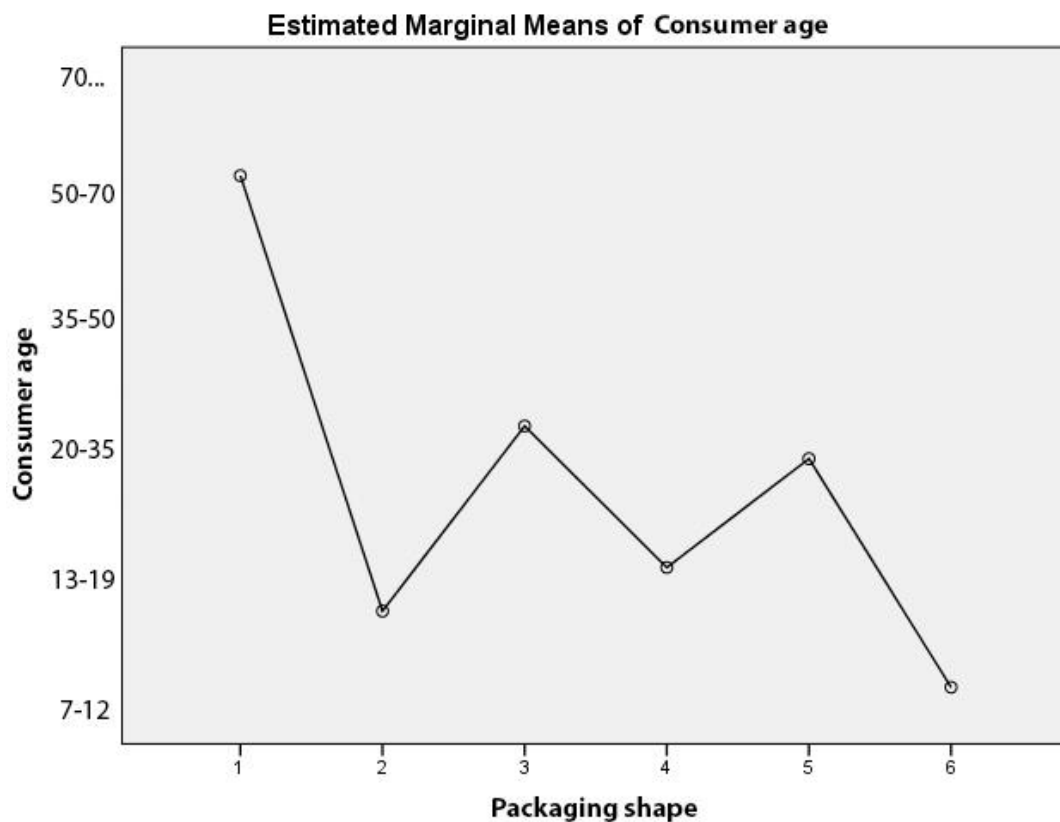


Figure 4: Influence of packaging shape on assumed consumer age

4. CONCLUSION

Results presented in this paper can be viewed as preliminary report considering number of participants. It is important to have in mind that consumers' responses to packaging designs reflect the influence of a complex array of variables that excide those studied in this research, such as color and other design elements. Results of the data analysis supported the hypothesis that packaging shape influences the perceived value of the product, assumption of the packaged product and appropriate of consumers age. Correlation between complexity of the packaging was not observed but significant difference between simple cube shaped packaging and all the others more complex packaging was noted. The simple cube shaped packaging was judged as appropriate for less expensive products, as we as most appropriate for machine industry and for older population of consumers. Further research can be directed towards determining differences resulted from different types of achieving complex shape in order to gain insight in refined differences caused by shape of the packaging.

5. ACKNOWLEDGMENTS

This paper was supported by the Serbian Ministry of Science and Technological Development, Grant No.: 35027 "The development of knowledge and production in graphic arts industry".

6. REFERENCES

- [1] Ampuero, O., Vila, N.: "Consumer perceptions of product packaging", *Journal of Consumer Marketing*, 23(2), pp. 102–114, (2006).
- [2] Bloch, P. H., Brunel, F.H., Arnold, T. J.: "Individual differences in the centrality of visual product aesthetics: Concepts and measurement", *Journal of Consumer Research*, 29, pp. 551–565, (2003).
- [3] Creusen, M. E. H., Schoormans, J. P. L.: "The different roles of product appearance in consumer choice", *Journal of Product Innovation Management*, 22, pp. 63–81, (2005).
- [4] Creusen, M. E. H., Schoormans, J. P. L.: "The different roles of product appearance in consumer choice", *Journal of Product Innovation Management*, 22, pp. 63–81, (2005).
- [5] Hekkert, P., Leder, H.: „Product aesthetics“, In H. N. J. Schifferstein & P. Hekkert (Eds.), *Product Experience*. Amsterdam: Elsevier, (2008).
- [6] Lindell, A. K., & Mueller, J.: „Can science account for taste? Psychological insights into art appreciation“, *Journal of Cognitive Psychology*, 23(4), pp. 453–475, (2011).
- [7] Nancarrow, C., Wright, T.L. and Brace, I.: "Gaining competitive advantage from packaging and labeling in marketing communications", *British Food Journal*, Vol. 100 No. 2, pp. 110–8. (1998).
- [8] Rettie, R., Brewer, C.: "The verbal and visual components of package design", *Journal of Product and Brand Management*, 9(1), pp. 56–70, (2000).
- [9] Schoormans, J. P. L., Robben, H. S. J.: "The effect of new package design on product attention, categorisation and valuation", *Journal of Economic Psychology*, 18, pp. 271–287, (1997).
- [10] Schoormans, J., Eenhuizen-van den Berge, M., van de Laar, van den Berg-Weitzel, L.: „Designing packages that communicate product attributes and brand values: An exploratory method“, *Design Journal*, 13(1), pp. 31–47, (2010).
- [11] Silayoi, P., Speece, M.: "The importance of packaging attributes: A conjoint analysis approach" *European Journal of Marketing*, 41(11–12), pp. 1495–1517. (2007).
- [12] Simms, C., Trott, P. "Packaging development: A conceptual framework for identifying new product opportunities", *Marketing Theory*, 10(4), 397–415, (2010).

NEW AND CREATIVE PRODUCT IDEA GENERATION, ASSOCIATION METHOD

*Siniša Kuzmanović, Gojko Vladić, Milan Rackov,
University of Novi Sad, Faculty of Technical Sciences, Novi Sad, Serbia*

Abstract: This paper presents process of new idea generation for product design methods by association. Main goal is to point out importance and advantages of structured approach to the new and creative product generation. Need for new and fresh product design ideas is more important than ever, as the market is filled with products of equal quality and price. In these conditions design of the product becomes most important characteristic on which consumers make their final decisions about purchase. All of this makes the methodology of new idea generation important subject.

Key words: Idea, product, association

1. INTRODUCTION

Need for new and fresh product design ideas is more important than ever, as the market is filled with products of equal quality and price. In these conditions design of the product becomes most important characteristic on which consumers make their final decisions about purchase. Achieving commercial success through innovation is highly desirable, but difficult to achieve in practice. Typically, out of nine month's product development cycle, only two weeks are devoted to the generation of ideas and creative design - the "front end". Insufficient idea generation and creativity management, or the pre-development phase, can lead to the failure of the product (Bruce, 2000).

2. CREATIVITY IN THE DESIGN PROCESS

Creativity is an extremely important facet of design process and is a feature of many of the tasks in that process. Most authors dealing with creativity regard it as a beneficial process in an organization and it has been said to offer a competitive advantage in the design processes (Cook, 1998). It can occur in a multitude of situations ranging from work to pleasure, from artistic portrayals to technological innovation (Bonnardel, 1999). Creativity is the attribute of bringing into existence a unique concept or thing that would not have occurred or evolved naturally. The creative person combines, mixes, and expands past experiences so that new, nonobvious concepts, variations, or extensions of knowledge are generated (Meredith, 1995).

3. MODEL OF IDEA GENERATION

Synthesized from the earlier creativity models into a unified model of Idea Generation, Problem Preparation and Idea Evaluation, according to Warr and O'Neill (Warr, 2005). This Generic Creative Process model shows the similarities of all previous models and offers one simple model. Although rejected from some author as distinct and limited representation (Lubart, 2001; Eindhoven, 1952; Ghiselin, 1962); this model offers easily understandable idea generation model, Figure 1. From the model of idea generation various methods of idea generation can derive. Structured (formal) idea generation methods can be classified into two major groups: (Figure 2) (Shah, 1998):

- Intuitive and
- Logical.

Further these groups can be divided in to methods for group and individual and in to a specific techniques with strictly defined procedures, as shown in Figure 2.

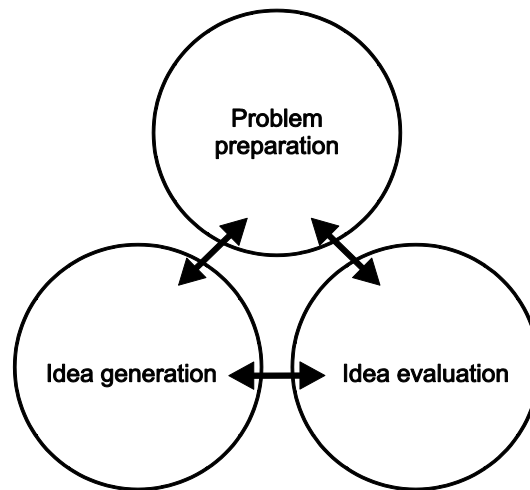


Figure 1: Generic creative process model

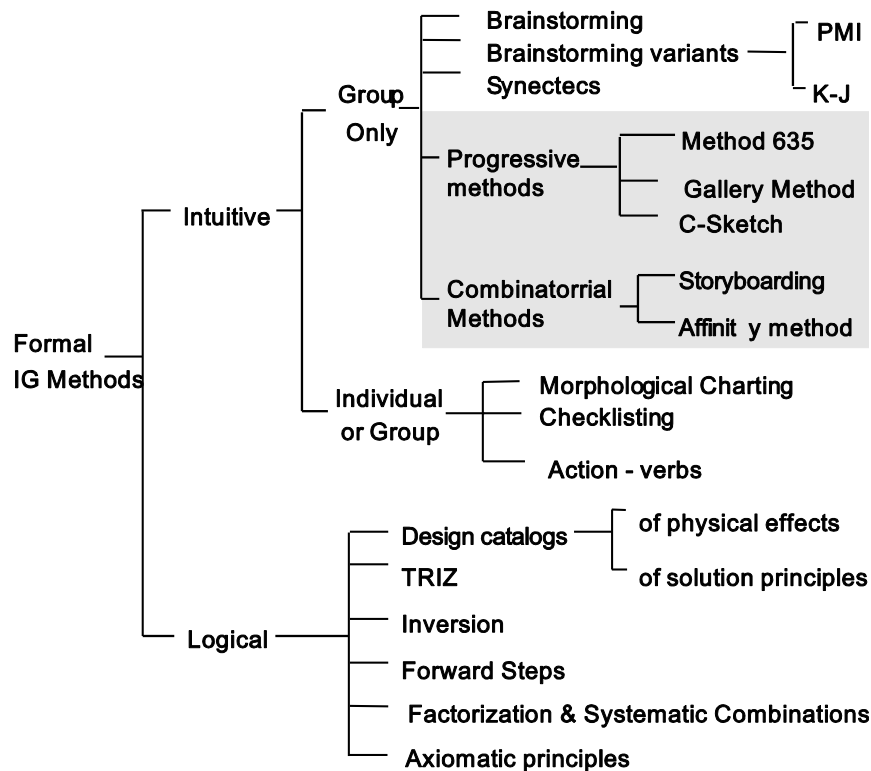


Figure 2: Classification of idea generation methods for design

4. ASSOCIATION OF IDEAS

Creativity most often comes out of association. Association of Ideas, or mental association, as defined by G. C. Robertson refers to explanations about the conditions under which representations arise in consciousness, and also for a principle to account generally for the succession of mental phenomena. One idea was thought to follow another in consciousness if it were associated by some principle. The three commonly asserted principles of association were similarity, contiguity, and contrast (Robertson, 1894).

Association plays important role in all of the idea generation methods (Hill, na; Kuzmanović, 2012), as the new idea can be derived only from earlier experience.

Association as idea generating tool contains elements of several other idea-generating techniques and depends on a mental 'stream of consciousness' and network of associations of which there are two (mycoted.com):

- Serial association, start with a trigger, you record the flow of ideas that come to mind, each idea triggering the next, ultimately reaching a potentially useful one, figure 3a.
- Centered association, (which is close to classical brainstorming) prompts you to generate multiple associations to the original trigger so that you 'delve' into a particular area of associations, Figure 3b.

Two types of association intervene in the creative process so as a rule the serial mode is used to 'travel' until you find an idea that you find of some interest, you then engage the centered mode to 'delve' more deeply around the interesting item. Once you have exhausted the centered investigation, you being to 'travel' again, and so on.

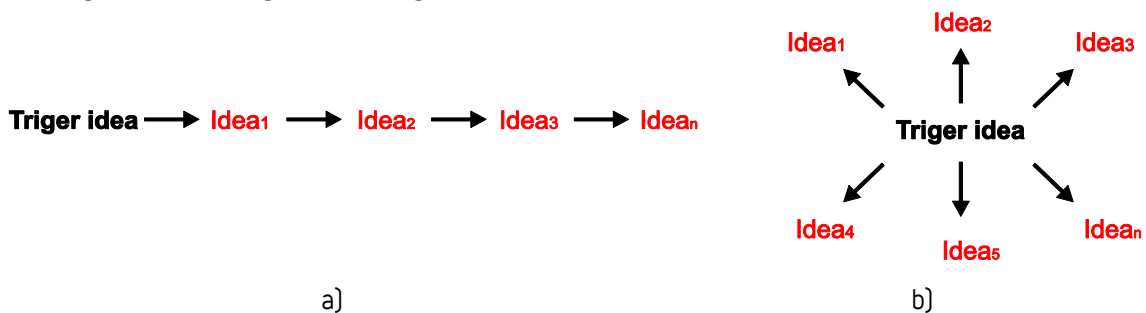


Figure 3: a) Serial association, b) Centered association

4.1 Vertical thinking

Vertical thinking is technique for idea generation highly involved with association it builds on the ideas already generated, or it can look at the different parts of the problem in an effort to generate new ideas. One of the most well-known vertical thinking techniques is Osborn's checklist (Osborn, 1979):

- Put to other uses? As it is? If modified?
- Adapt? Is there anything else like this? What does this tell you?
- Modify? Give it a new angle? Alter the color, sound, meaning, motion, and shape?
- Magnify? Can anything be added, time, frequency, height, length, strength? Can it be duplicated, multiplied or exaggerated?
- Minify? Can anything be taken away? Made smaller? Lowered? Shortened? Lightened? Omitted? Broken up?
- Substitute? Different ingredients used? Other material? Other processes? Other place? Other approach? Other tone of voice? Someone else?
- Rearrange? Swap components? Alter the pattern, sequence or layout? Change the pace or schedule? Transpose cause and effect?
- Reverse? Opposites? Backwards? Reverse roles? Change shoes? Turn tables? Turn other cheek? Transpose '+/-'?
- Combine? Combine units, purposes, appeals or ideas? A blend, alloy, or an ensemble?

The SCAMPER technique, derived from Osborn's checklist, created by Bob Eberle is designed to assist in thinking of changes you can make to an existing product to create a new one via a checklist, these can either be used directly or as starting points for lateral thinking.

The changes SCAMPER stands for are (mycoted.com):

- S - Substitute - components, materials, people
- C - Combine - mix, combine with other assemblies or services, integrate
- A - Adapt - alter, change function, use part of another element
- M - Modify - increase or reduce in scale, change shape, modify attributes (e.g. colour)

- P - Put to another use
- E - Eliminate - remove elements, simplify, reduce to core functionality
- R - Reverse - turn inside out or upside down.

By using SCAMPER product designers are able to identify possible new products. Many of the ideas may be unfeasible or may not suit the equipment used by the manufacturer, but some ideas could be good starting points for discussion of new products.

4.2 Random words and random pictures

On the other side of the spectra from the highly structured SCAMPER technique there is Random words and random pictures are two creativity techniques that push you to think from a different perspective and reach solutions to your problems from new directions. The intention of the technique is to take the designer out of the problem itself; hence, random words and pictures will help in this process. Random pictures may create an association, which help the designer solve a problem or generate ideas for new ways of doing things (slmsc-project.eu).

4.3 Free association

Even less structured is Free association technique that consists of allowing the mind to wander without deliberate direction. The first thing that comes to mind in response to a trigger word, symbol, idea or picture, then use that as a trigger, and so on, quickly repeating the process to produce a stream of associations. The important thing is to avoid justifying the connection between successive ideas. This encourages spontaneity and the emergence of ideas seemingly unrelated to the trigger word. Free association delves deep into the memory, helping the designer to discover remote relationships similar to those uncovered, and using mind maps. To be productive, the ideas need to be recorded, either in writing or on audio tape. This can interfere with the free flow of ideas and therefore requires practice (itseducation.asia/ideas.htm).

5. CONCLUSION

The world surrounding designers offers inspiration and techniques mentioned in this paper are constructed to channel that inspiration towards formulation of idea and ultimately towards implementation of the new idea. It was argued for long period of time by Associationist School that association is base of cognition and consciousness, although these teachings were abandoned, association is still examined as the possible explanation. Association as idea generation method offers possibilities new and creative solutions for the problems and deserves attention as a tool for new and fresh product design ideas.

6. REFERENCES

- [1] A.O.N. Warr, E.: "Understanding Design as a Social Creative Process", Proceedings of the 5th Conference on Creativity & Cognition, pp. 118 – 127, (2005).
- [2] Bruce, M., Cooper, R.: "Creative product design", John Wiley and Sons, (2000).
- [3] Bonnardel, N.: "Creativity in design activities: The role of analogies in a constrained cognitive environment", Creativity and Cognition, pp. 158-165, (1999).
- [4] Cook, P.: "The creativity advantage- is your organization the leader of the pack?" Industrial and Commercial Training 30, pp. 179-184, (1998).
- [5] Creativity and Innovation, Creativity and Innovation Techniques - an A to Z , URL http://www.mycoted.com/Category:Creativity_Techniques, (last request: 22.09.2014.).
- [6] Eindhoven, J.E., Vinacke, W. E.: "Creative processes in painting", Journal of General Psychology 47, pp. 165– 179, (1952).
- [7] Ghiselin, B.: "Automatism, intention, and autonomy in the novelist's production". Daedalus 92, 297–311, (1963).
- [8] Hill, P., "The science of engineering design", Holt, Rinehart and Winston, Inc. New York.
- [9] ITS: The Road to a Solution – Generating Ideas, <http://www.itseducation.asia/ideas.htm>, (last request: 22.09.2014.).
- [10] Kuzmanović, S., "Industrijski dizajn", 1, FTN, Novi Sad, (2012).

- [11] Lubart, T.I.: "Models of the Creative Process: Past, Present and Future", *Creativity Research Journal* 13, pp. 295–308, (2001).
- [12] Meredith J. R., Mantel S. J., Jr.: "Creativity and Idea Generation", University of Cincinnati, John Wiley & Sons, Inc. (1995).
- [13] Osborn, A. F. *Applied imagination*. New York: Charles Scribner's Sons, 1979.
- [14] Robertson, G. C., Bain A., Whittaker T.: "Philosophical remains of George Croom Robertson, with a memoir", London, Great Britain: Williams and Norgate, xxiv, 481 pp. doi: 10.1037/12933-009, pp. 102–118, (1894).
- [15] Shah, J. J.: "Experimental investigation of progressive idea generation techniques in engineering design", *Proceedings of DETC98*, pp. 1–15, (1998).
- [16] SLMSC: Idea generation, http://www.slm-sc-project.eu/en/?page_id=2135, (last request: 22.09.2014.).

ECONOMIC DESIGN OF VOJVODINA (1945-1985): INTRODUCTION TO THE ONE STUDY

Zdravko Rajčetić

Association of Applied Arts Artists and Designers of Vojvodina, Serbia

Abstract: Design in Vojvodina, as an integral part of the post-war design practices in Yugoslavia and Serbia, has also been part of the social events and technological transformations that have appeared on the world stage during the second half of the 20th century. Thus, since the end of World War II, in various fields of economy in Vojvodina, have developed and produced representative examples of industrial design. Due to the above mentioned thesis, four years ago, when I started my research, I relied on the analysis of homology design with social and cultural, and above all, economic factors, by which it is possible to explain the development of design practices in Vojvodina during its socialist development from 1945. to 1985. Among other things, the study bring extract of representative samples of the designed products incurred in accordance with the characteristics of the local economy. This short paper attempts to highlight the basic conceptual elements of the aforementioned studies, which I called the, for obvious reasons "Economic design of Vojvodina (1945-1985)".

Key words: Design, economy, society, culture, Vojvodina, Yugoslavia, socialism.

1. INTRODUCTION

Phenomenon of post-war design in Vojvodina has never before been the subject of systematic and scientific research. In all truth, there were some scope-limited forays that touched on this area in the form of critical comments or descriptions in serial publications and editorials in exhibit catalogues, but without any significant scientific results. It is the opinion of the authors that all of the necessary objective conditions exist at this moment for the realization of a complete study that should valorize more important phenomena of design in Vojvodina, whose temporal context covers forty years of post-war design production, and especially the part that was in direct connection with economy. Due to culturological and ideological content, design has become a significant factor in perception of taste, fashion and totality of thought today, which was closely connected with the process of its global expansion in the other half of 20th century, a period in history during which important political, social and technological transformations gave way one to another in short time intervals. On a global scale, it was the time of realization of a series of social experiments and projects, one of which was being realized in socialist Yugoslavia. During the time the world was locked in the cold war division, in its foreign policy Yugoslavia became the leader of the Non-Aligned Movement, and an active participant in global politics. With its inner-political model of socialist self-management, Yugoslavia was demonstrating a tendency of trying to reconcile two ideologically oposed world views with an intersection of individual and collective aspirations of its citizens at their centre. At the same time, Yugoslavia represented fusion of different national and cultural practices of Central and East European origins, whose traditions decided the fate of design in the limits of its borders.

It is an ireffutable fact that design in Yugoslavia was first accepted and developed as a profession by industrial and cultural centers in the western parts of the joint state, whose historical roots belonged to the Central European tradition of civic culture (Fruht, 1977). They were oriented toward this part of Europe, both on the basis of state organization of cultural policy and the cooperation of Yugoslavia with the rest of the world in the area of culture.

It was in this way that, before all others, Croatian and Slovenian industrialists and cultural workers knew, in a pragmatic way, how to build a structured relationship towards design, which they perceived from the very beginning as both economical and civilizational phenomenon. With strong political power to strengthen their economies, and looking up to their western role models, they used the available space to create image about themselves as being sophisticated communities, sensitive and capable enough to shape esthetic qualities with which they could rival the leading nations in this field, or at least get close enough. Almost all of the more significant Yugoslavian exhibitions, conferences and fair manifestations were organized in these two countries. Furthermore, special professional institutions were being formed where design was

debated and explored in its totality, first study groups were being organized and initiatives were given for the formation of first professional associations. It is in this area that the then contemporary principles of modern design were being pragmatically applied in Yugoslavian industrial production, and where the theoretical awareness of design was being shaped (Galjer, 2014). Under the influence of these trends, but also under strong artistic, conceptual and cultural reflections that were emanating from Belgrade, coming from significant institutions and individuals like the Academy of Applied Arts and The Graphic Collective, at the end of fifties and the beginning of sixties in Vojvodina, many firms, institutions and individuals accept design as an important factor in their business practice, which they developed gradually in accordance with the needs of local economy. Until that time, design existed on this territory in large part as an exclusively intuitive activity, in the sphere of existing product improvement before all else, however, the process of design institutionalization in Vojvodina will unfold systematically through the activity of various economical, socio-political and educational and cultural factors.

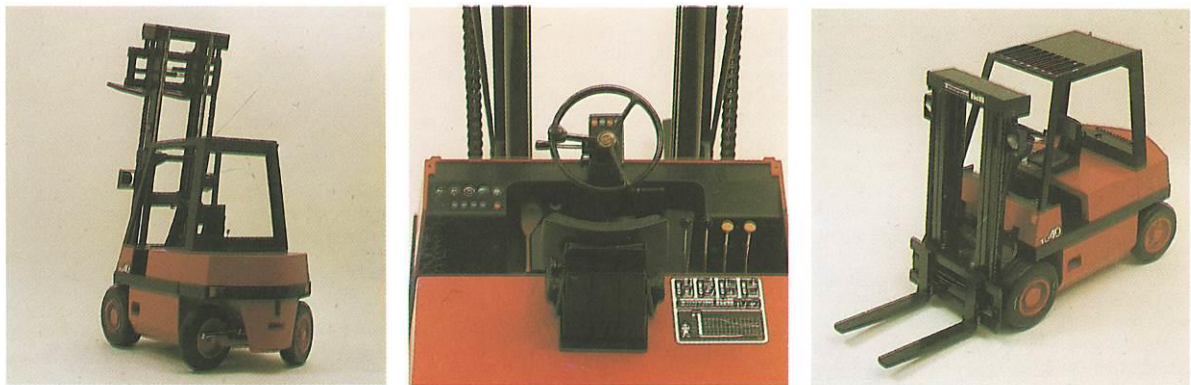


Figure 1: Model of forklift made in Pobeda IMO Novi Sad, Mišo Nikolovski



Figure 2: Danubius product packaging and product catalog, Vojislav Terzić

2. ECONOMIC DESIGN: DEFINITION

What is the reason for framing the study of this type into the context of economic, and not product or industrial design? According to the *Dictionary of Serbian Language*, the very etymology of the word *economic* refers to "that which is in connection with the study of economy" (Matica srpska, 2007). Therefore our reason is easy to understand, since it stems from the intention for this study to cover creativity, creative aspects and concrete products by analysis of economic conditions in Vojvodina after the Second World War. The task that is to be undertaken is impossible to perform without the analysis of economic conditions that contributed to the cumulative development of both the Yugoslavian and the economy of Vojvodina. This refers to technical and technological conditions, labor relations, and the complete industrial and social atmosphere in production collectives, which are often integrally called *economic* in the documents of the time. Furthermore, in the same dictionary the term *economic* refers also to „running the economy“, which directly points to the *character of the economy*, which in the context of this study basically relates to all forms of Yugoslavian post-war economy, with a special focus on the socialistic system of proletariat self-management and decision making in Yugoslavia, with all its historic changes, turbulent phenomena and shapes.

In such a light we also see the economic design in Vojvodina – as a reflection of socialist economic system, where in the territorial sense, Vojvodina represents individual micro world organically connected to the macro world of former Yugoslavia.

3. STUDY STRUCTURE, METHODS, SOURCES

Due to its complexity, research of designer practice in the economy of Vojvodina from 1945 – 1985. is impossible to perform without interdisciplinary connection of knowledge from different scientific areas like: design theory, theory and history of art, general history, cultural history, culturology, ethnology and politicology. The structure of the study is complex, and in its first part it provides the theoretical capacity to the designer practice in Vojvodina. In its second part, a taxative reconstruction of the more important events, institutions, organizations, documents and individuals that played a part in the institutionalization of design on this territory, is realized. In the third part of the study a significant number of good practice examples are presented – relevant economic subjects in whose production reality, completely or partly, principles of designer practice and theory were implemented. Integral part of the study is made up by the essays of the three authors on various areas of economic design.

It should be emphasized that our primary intention is to present designer products in circumstances of immediate production, which consequently means that the study does not deal with analysis of the work and the opus of well-known authors names torn from the context of production and market. Quite the contrary, we analyzed the concrete products and production conditions whose postulates dictated planning, organizational, production and market activities in the limits of Vojvodina economy within the limits of economic and political space of former Yugoslavia.

Methods used in the writing of this study are based on description (descriptive research) of production, economic and socio-political circumstances that were instrumental to the emergence of economic design in Vojvodina. Theoretical considerations on design that existed in Yugoslavia and Vojvodina were interpreted (heuristic method) in the same context. In order to achieve as optimal final scientific result as possible, analytic-synthetic method was also used.

Selection of representative examples was conducted on the basis of several criteria:

1. The presence of a product on the market – commercials in the mass media are excellent indicator, as well as the general information on the popularity of a product;
2. Presence in referential library units (monographs, catalogues, exhibition catalogues, critical reviews and theoretical analysis in professional serial publications);
3. Availability of archive material (photographs, sketches, technical descriptions, projects, models and finished products). With the intention of throwing the light on the role of the design as an inseparable part of the spirit of the time and spirit of the locale of Vojvodina, we used the material from the archives of Museums of Modern Art in Novi Sad and Belgrade, The Historical Archives of Subotica, Novi Sad historical archive, Archive of Vojvodina, Association of Applied Arts Artists and Designers of Vojvodina, Museum of Applied Art in Belgrade, Novi Sad Regional Chamber of Commerce, and City Museum of

Novi Sad. Other important sources of information are materials from archives in the firms that are still active, as well as private archives and collections.

It should be mentioned that extensive archive material disappeared in the vein of economic and political changes in the country and changes in the ownership structure. Due to the society's carelessness towards its technical heritage, considerable part of archive materials has been lost irreplaceably. We know about the existence of this segment of material culture from a series of oral testimonies of then active participants in the designer scene and economic life of Vojvodina.

4. CLOSING CONSIDERATIONS

According to available materials, this study is realized as a chronology (a document), whose trajectory nearly vectorially follows the development of economic design in Vojvodina from the end of the Second World War till the middle of the eighth decade of the previous century, a period of specific and dynamic socio-economic and cultural development of Vojvodina. The time of intensive industrialization, which will start to slow down in the middle of the 1980s under the influence of coming political changes and global economic processes during which the epoch of industrial society gave way to the epoch of post-industrial society.

Results gained from the given analysis imply that design in Vojvodina had a significant political and institutional support, and that it was a part of economic and cultural reality of life in Vojvodina, and even had a certain specific creative characteristic that was formed in accordance with the then current market demands in Yugoslavia. However, theoretical capacity of design in Vojvodina is perceivably weak, which left considerable consequences on its status in the society and economy of today. For that reason, above all else, there is a need to develop educational conditions, and then also a broader academic atmosphere that would include constant reevaluation and dialogue on social, cultural and political aspects of design on the locale of Vojvodina.

5. REFERENCES

- [1] Jasna Galjer: Hrvatski dizajn pedesetih: od utopije do stvarnosti, Horetzky, Zagreb, 2004.
- [2] Miroslav Fruht; Keller Dragoslav: „Razvoj i identitet dizajna u Jugoslaviji“, Industrijsko oblikovanje, Beograd37/38, 1977.
- [3] Rečnik srpskog jezika, Matica srpska, Novi Sad, 2007.

